1.E.1: 1D
Nuclear Physics **34** (1962) 1—324; © *North-Holland Publishing Co., Amsterdam*

ENERGY LEVELS OF LIGHT NUCLEI. III

$Z = 11$ to $Z = 20$

P. M. ENDT and C. VAN DER LEUN
Fysisch Laboratorium der Rijksuniversiteit, Utrecht

Received 20 November 1961

Introduction

MATERIAL

The present compilation of information on the energy levels of nuclei with $Z = 11$ to $Z = 20$ is the third version of an article of which the first and second edition appeared in 1954 (En 54a) and 1957 (En 57). It contains the experimental material received up to October 1, 1961†. In principle, the present version should make the use of the two earlier versions unnecessary. All important data contained in the latter are also given in the present paper. This does not mean that the present bibliography is complete. Papers which only have a historical interest and which are superseded by later, much more detailed work, have been omitted. In those cases a reference is given in the text to the 1954 or 1957 version.

Inevitably the present review has grown in volume compared to En 57 and En 54a. The number of known nuclei in the $Z = 11$–20 region has grown surprisingly little, from 73 in En 54a to 83. The number of known nuclear states in this region, however, has increased from 800 to about 3000 in those seven years, and the number of nuclear states with known spin and parity went up from 70 to 400.

Theoretical articles are quoted only briefly, and the bibliography is certainly incomplete on theoretical subjects. Apart from resonance information, little attention is given to cross section measurements; the reader is referred to the compilations on neutron cross sections (Hu 58) and charged particle cross sections (Sm 61c).

Many-particle reactions, e.g. the spallation reactions, are omitted altogether.

ARRANGEMENT

The nuclei are presented in order of increasing A, and nuclei of the same A in order of increasing Z.

† For more recent information, see Addenda, p. 325.

Generally, each nuclear reaction is treated under the heading of the final nucleus. Exceptions are reactions where resonances have been observed, which are treated under the compound nucleus, and the β decay of unstable nuclei, treated under the parent nucleus, and then as the first reaction. In all other cases, the order of the reactions is determined by the initial nucleus, starting with the lowest-A nuclei and of each group of isobars with the lowest-Z element.

Following the last reaction discussed, for each nucleus a list is given of reactions "Not reported", but which could, if observed, give additional information about the final nucleus. Only those reactions have been included which are in principle feasible with a stable initial nucleus and with a neutron, proton, deuteron, triton, ^{3}He- or alpha-particle as ingoing or outgoing particle.

Discussions on the energy levels of a particular nucleus which do not fit naturally under the heading of a specific reaction leading to that nucleus have been given as "Remarks" at the end of the survey of that nucleus.

PRESENTATION

References are given for all the information given in the text, tables or figures. If the results of one experiment have been published in two or more articles or reports, usually only the most recent or most complete publication is cited. Entries for which no reference to litterature is given generally pertain to conclusions drawn from putting together the data from two or more sources. All electron capture and β decay ft values have been recomputed, using the weighted mean half-lives given in the text and the Q_{m} values (see below) given in the headings of the relevant reactions.

In a few cases in which the use of less familiar symbols, abbrevations or notations was inevitable, their meaning has been explained in the text.

For most of the nuclei a summary and synthesis of the experimental material is given in the first table for each nucleus and in the level diagrams.

FIGURES

The excitation and resonance energies given in the level diagrams are the weighted mean values of all determinations available. All energies are given in MeV; the number of decimals given is limited such that the error is at most five units of the last decimal. Bombarding energies indicated in the level diagrams are given in the laboratory system but plotted to scale in centre-of-mass coordinates. In this way the leaders, indicating resonances, and the corresponding energy levels in the compound nucleus will be found at equal heights.

Doubtful levels or transitions are marked by hatched lines. Uncertain excitation energies and uncertain spin and parity assignments are bracketed.

Reactions leading to a particular nucleus have been indicated in the corresponding level diagram only if experiments on that reaction have been reported. An exception is made for n, p, d, or α-particle binding energies, which are always indicated, unless they exceed the energy range of the diagram.

For seven nuclei an additional figure with the γ decay scheme had to be made since the data could not be included in the standard level diagram.

As a novelty, half-lives of β-unstable nuclei and of a few long-lived isomeric states have been given in the level diagrams. Also E2/M1 amplitude mixing ratios have been indicated. It has not been tried to use a consistent sign convention for mixing ratios, which would require a large amount of work. The signs given here are those published in the original litterature.

MASSES AND Q VALUES

The nuclear mass excesses used throughout this compilation are listed in table 1. The first column gives the mass excesses, $M-A$ in keV, measured in the new scale in which the atomic mass of ^{12}C is equal to 12 units. The other column gives the mass excess in the old ^{16}O scale for comparison with older data.

By far the most of these values have been taken from the table of Everling, König, Mattauch and Wapstra (Ev 60, Ev 61). The mass excesses of new nuclei and a few corrections, mostly due to recent measurements, have been included. The reaction and decay energies used to compute these additions and corrections are listed at the end of the table. New "primary" Q values — essentially those of reactions connecting "central" nuclei — have not been used to correc the masses and errors given in Ev 60. Inclusion of these data would require a lengthy least-squares analysis and would not appreciably improve the precision of the already well-known masses of the central nuclei.

The reaction Q values calculated from the masses in table 1, Q_m, and the binding energies in the compound nucleus of the bombarding particle, E_b, given in the headings of the reactions, are quoted from the Nuclear Data Tables (Ev 61a), except for reactions pertaining to nuclei of which the mass has been corrected in table 1.

For some reactions a difference between the experimental Q value given in the text, and the Q_m value in the heading of the reaction, could be due to the fact that Everling *et al.* recalibrated several reaction energies before using them in the mass computations.

NATURAL ABUNDANCES AND NUCLEAR MOMENTS

The natural abundances of the isotopes in the mass range discussed in this compilation, are listed in table 2 together with the nuclear moments: the spin moment, J, the magnetic dipole moment, μ, and the electric quadrupole moment, q, as found from the hyperfine structure, from optical spectroscopy, nuclear resonance absorption or induction, atomic or molecular beam magnetic resonance, and/or microwave absorption. The values are taken from the "Table of Isotopes" by Strominger, Hollander, and Seaborg (St 58b), except for the annotated additions.

OTHER REVIEW ARTICLES

Much use was made of several recent review articles on more specialized subjects covering the mass range of this compilation; especially of the survey and theoretical discussion of the reduced widths of individual nuclear energy levels obtained from stripping reactions (Ma 60d) and resonance reactions (La 60b). The neutron and charged particle cross section compilations (Hu 58, Sm 61c) have been mentioned above.

A general survey of nuclear reactions, levels, and spectra of light nuclei appeared in the Encyclopedia of Physics (Bu 57c); an exposition of the systematics of nuclei between ^{16}O and ^{40}Ca in the Proceedings of the Kingston Conference (Go 60c).

The experimental data on nuclei between ^{5}He and ^{24}Ne have been compiled by F. Ajzenberg-Selove and T. Lauritsen (Aj 59).

The following theoretical papers, covering a broad range of nuclei have not been quoted at all relevant places in the text: a discussion of nuclear level densities and temperatures in $A = 18$–34 nuclei (Ma 61b); calculations of *ft* values with *jj* and *LS* coupling for $A = 16$–41 nuclei (Wi 57a); a discussion of rotational levels in $A = 16$–25 nuclei (Ra 57): a *jj* coupling calculation of the binding energies of the calcium isotopes (Ta 57).

Finally, the "Nuclear Data Sheets" have been of great benefit in checking and completing the list of references.

We are particularly grateful to the many physicists who sent their results in advance of publication.

The invaluable assistance of Miss Kitty van Bunnik and of H. M. van Zoest in the preparation of the manuscript has been much appreciated.

TABLE 1

Atomic Mass Excesses ($M-A$) in keV

	($^{12}C = 0$)	($^{16}O = 0$)
^{1}n	8071.34 ± 0.41	8367.37
^{1}H	7288.73 ± 0.11	7584.76
^{2}H	13135.26 ± 0.17	13727.42
^{3}H	14949.07 ± 0.36	15837.15
^{3}He	14930.94 ± 0.26	15819.02
^{4}He	2425.11 ± 0.35	3609.22
^{12}C	0	3552.33
^{14}N	2863.60 ± 0.16	7007.98
^{16}O	−4736.43 ± 0.26	0
^{16}F	10904 ± 12[a]	15641
^{17}F	1954.5 ± 2.3	6987.0
^{18}F	884.8 ± 4.0	6213.3
^{19}F	−1486.1 ± 0.7	4138.5
^{20}F	−13.5 ± 3.8	5907.1
^{21}F	−26 ± 25	6191
^{18}Ne	5314 ± 40[b]	10641
^{19}Ne	1762 ± 5	7387
^{20}Ne	−7041.3 ± 0.5	−1120.8
^{21}Ne	−5729.1 ± 1.6	487.5
^{22}Ne	−8024.9 ± 0.6	−1512.3
^{23}Ne	−5146 ± 5	1662
^{24}Ne	−5964 ± 40	1141
^{20}Na	8280 ±300	14200
^{21}Na	−2199 ± 17[c]	4018
^{22}Na	−5183.3 ± 4.6	1329.3
^{23}Na	−9526.2 ± 1.5	−2717.6
^{24}Na	−8413.8 ± 2.7	−1309.2
^{25}Na	−9357 ± 10[aa]	−1956
^{26}Na	−7700 ±300[x]	0
^{22}Mg	−140 ± 80[d]	6370
^{23}Mg	−5448 ± 15[e]	1360
^{24}Mg	−13930.1 ± 1.8	−6825.4
^{25}Mg	−13189.4 ± 1.9	−5788.8
^{26}Mg	−16215.5 ± 2.2	−8518.8
^{27}Mg	−14581.2 ± 3.7	−6588.5
^{28}Mg	−15015 ± 6	−6726
^{24}Al	90 ±300	7190
^{25}Al	−8928 ± 6	−1528
^{26}Al	−12201.5 ± 4.7	−4504.8
^{27}Al	−17199.2 ± 2.0	−9206.4
^{28}Al	−16851.5 ± 3.6	−8562.8
^{29}Al	−18217 ± 6[f]	−9632
^{30}Al	−17150 ±250[bb]	−8270

TABLE 1 *(continued)*

^{26}Si	−7150	± 80[g]	550
^{27}Si	−12384	± 8[h]	−4391
^{28}Si	−21491.0	± 2.9	−13202.3
^{29}Si	−21897.4	± 3.4	−13312.6
^{30}Si	−24410.3	± 4.0	−15559.5
^{31}Si	−22961.1	± 4.6	−13784.3
^{32}Si	−24084	± 15[cc]	−14611
^{28}P	−7690	±300	600
^{29}P	−16949	± 8[i]	−8365
^{30}P	−20192	± 9[j]	−11312
^{31}P	−24437.8	± 1.5	−15261.0
^{32}P	−24303.2	± 2.2	−14830.4
^{33}P	−26334.9	± 3.4[k]	−16566.0
^{34}P	−24830	±200	−14770
^{30}S	−14220	±110[l]	−5340
^{31}S	−18988	± 17[m]	−9812
^{32}S	−26011.7	± 1.0	−16538.8
^{33}S	−26582.9	± 2.8	−16814.0
^{34}S	−29932.4	± 2.9	−19867.4
^{35}S	−28842.9	± 2.6	−18481.9
^{36}S	−30653	± 9	−19996
^{37}S	−26980	± 90	−16020
^{38}S	−26800	±150	−15560
^{32}Cl	−13010	±300	−3540
^{33}Cl	−21008	± 12	−11239
^{34}Cl	−24413	± 21[n]	−14348
^{35}Cl	−29010.2	± 2.6	−18649.2
^{36}Cl	−29516	± 5	−18859
^{37}Cl	−31765.9	± 2.1	−20812.9
^{38}Cl	−29804	± 8	−18555
^{39}Cl	−29803	± 21	−18258
^{40}Cl	−27500	±500	−15700
^{35}Ar	−23040	± 30[o]	−12680
^{36}Ar	−30227.0	± 3.2	−19570.1
^{37}Ar	−30949.9	± 2.5	−19996.9
^{38}Ar	−34719.9	± 2.3	−23470.9
^{39}Ar	−33233	± 6	−21688
^{40}Ar	−35037.3	± 0.8	−23196.2
^{41}Ar	−33058	± 11	−20921
^{42}Ar	−34423	± 40[y]	−21990
^{37}K	−24800	± 50[p]	−13850
^{38}K	−28791	± 11	−17542
^{39}K	−33798.3	± 2.8	−22253.3
^{40}K	−33524.5	± 3.3	−21683.4
^{41}K	−35548.3	± 4.3	−23411.2
^{42}K	−35006	± 20	−22573
^{43}K	−36577	± 11	−23848
^{44}K	−35360	±200	−22330

TABLE 1 *(continued)*

^{39}Ca	−27300 ± 40[q]	−15760
^{40}Ca	−34846.0 ± 3.5	−23004.9
^{41}Ca	−35135 ± 8	−22998
^{42}Ca	−38535.9 ± 4.2	−26102.8
^{43}Ca	−38394.0 ± 4.5	−25664.9
^{44}Ca	−41458.7 ± 4.5	−28433.6
^{45}Ca	−40807.0 ± 4.3	−27485.7
^{46}Ca	−43136 ± 10	−29519
^{47}Ca	−42334 ± 18[r]	−28420
^{48}Ca	−44372 ± 13[s]	−30163
^{49}Ca	−41445 ± 14[t]	−26940
^{40}Sc	−20900 ±200[dd]	−9050
^{41}Sc	−28640 ± 10[u]	−16503
^{42}Sc	−32280 ± 60[z]	−19850
^{43}Sc	−36174 ± 11	−23445
^{44}Sc	−37811 ± 7	−24786
^{45}Sc	−41058.9 ± 4.0	−27737.7
^{46}Sc	−41754 ± 5	−28137
^{47}Sc	−44330 ± 9[v]	−30416
^{48}Sc	−44494 ± 10	−30284
^{49}Sc	−46520 ± 40[w]	−32010
^{50}Sc	−45100 ±500	−30300
^{44}Ti	−37656 ± 12	−24631
^{45}Ti	−39001 ± 6	−25679
^{46}Ti	−44119.2 ± 3.5	−30502.0
^{47}Ti	−44935 ± 7	−31021
^{48}Ti	−48483.6 ± 3.4	−34274.3
^{49}Ti	−48559.1 ± 3.3	−34053.8
^{50}Ti	−51425.7 ± 4.5	−36624.4
^{51}Ti	−49716 ± 20	−34619

a	^{14}N(^{3}He, n)^{16}F	$Q =$ −1181 ± 12 keV	(see Aj 59)
b	^{16}O(^{3}He, n)^{18}Ne	$Q =$ −3190 ± 40 keV	(Aj 60)
c	^{21}Na(β^+)^{21}Ne	$Q =$ 3522 ± 30 keV	(Sc 52)
		$Q =$ 3532 ± 20 keV	(Wa 60a)
d	^{20}Ne(^{3}He, n)^{22}Mg	$Q =$ −40 ± 80 keV	(Aj 61)
e	^{23}Na(p, n)^{23}Mg	$Q =$ −4850 ± 7 keV	(Ki 55a, Go 58f)
	^{23}Mg(β^+)^{23}Na	$Q =$ 4110 ± 10 keV	(Wa 60a)
	^{24}Mg(^{3}He, α)^{23}Mg	$Q =$ 4048 ± 15 keV	(Hi 59a)
f	^{27}Al(t, p)^{29}Al	$Q =$ 8678 ± 6 keV	(Ja 60a)
g	^{24}Mg(^{3}He, n)^{26}Si	$Q =$ 80 ± 80 keV	(Aj 60)
h	^{27}Al(p, n)^{27}Si	$Q =$ −5585 ± 10 keV	(Ki 55a)
		$Q =$ −5607 ± 8 keV	(Ma 55c as corrected in Ev 61)
		$Q =$ −5591 ± 8 keV	(Br 59f)
	^{27}Si(β^+)^{27}Al	$Q =$ 4870 ± 20 keV	(Wa 60a)
	^{28}Si(^{3}He, α)^{27}Si	$Q =$ 3405 ± 15 keV	(Hi 59a)
i	^{28}Si(p, γ)^{29}P	$Q =$ 2760 ± 13 keV	(Ok 60a)
		$Q =$ 2750 ± 20 keV	(Va 60)
	^{28}Si(^{3}He, d)^{29}P	$Q =$ −2731 ± 12 keV	(Hi 60c)
	^{29}P(β^+)^{29}Si	$Q =$ 4960 ± 10 keV	(Li 57b)
		$Q =$ 4982 ± 20 keV	(Wa 60a)

TABLE 1 *(continued)*

j	^{27}Al(α, n)^{30}P	$Q = -2670 \pm 30$ keV	(Ba 59a)
	^{29}Si(p, γ)^{30}P	$Q = 5570 \pm 30$ keV	(Va 58a)
	^{30}Si(p, n)^{30}P	$Q = -5005 \pm 30$ keV	(Br 59f)
	^{32}S(d, α)^{30}P	$Q = 4892 \pm 10$ keV	(En 58 as corrected in Ev 61)
k	^{33}P(β$^-$)^{33}S	$Q = 248 \pm 2$ keV	(see text)
l	^{30}S(β$^+$)^{30}P	$Q = 5930 \pm 150$ keV	(Jo 60)
		$Q = 6010 \pm 150$ keV	(Ro 61a)
m	^{31}P(p, n)^{31}S	$Q = -6253 \pm 20$ keV	(Br 59f)
	^{31}S(β$^+$)^{31}P	$Q = 5440 \pm 30$ keV	(Li 57b)
		$Q = 5410 \pm 30$ keV	(Wa 60a)
n	^{33}S(p, γ)^{34}Cl	$Q = 5120 \pm 30$ keV	(Va 58d)
	^{34}Cl(β$^+$)^{34}S	$Q = 5520 \pm 30$ keV	(Gr 56)
o	^{35}Ar(β$^+$)^{35}Cl	$Q = 5980 \pm 40$ keV	(Ki 56)
		$Q = 5950 \pm 50$ keV	(Wa 60a)
p	^{37}K(β$^+$)^{37}Ar	$Q = 6120 \pm 70$ keV	(Su 58)
		$Q = 6170 \pm 70$ keV	(Wa 60a)
q	^{39}K(p, n)^{39}Ca	$Q = -7044 \pm 70$ keV	(Br 59f)
	^{39}Ca(β$^+$)^{39}K	$Q = 6600 \pm 100$ keV	(Li 57b)
		$Q = 6512 \pm 25$ keV	(Ki 58)
		$Q = 6450 \pm 60$ keV	(Wa 60a)
	^{40}Ca(γ, n)^{39}Ca	$Q = -15800 \pm 100$ keV	(Su 53)
r	^{47}Ca(β$^-$)^{47}Sc	$Q = 1996 \pm 16$ keV	(see discussion of ^{47}Ca decay)
s	^{48}Ca(p, n)^{48}Sc	$Q = -660 \pm 30$ keV	(El 58)
		$Q = -660 \pm 10$ keV	(Jo 60a)
t	^{48}Ca(d, p)^{49}Ca	$Q = 2919 \pm 6$ keV	(Br 56f as corrected in Ev 61)
u	^{40}Ca(^{3}He, d)^{41}Sc	$Q = -4410 \pm 15$ keV	(Hi 60k)
	^{40}Ca(d, n)^{41}Sc	$Q = -1145 \pm 15$ keV	(Ma 61c)
	^{40}Ca(p, γ)^{41}Sc	$Q = 1090 \pm 20$ keV	(Bu 61a)
v	^{47}Sc(β$^-$)^{47}Ti	$Q = 605 \pm 5$ keV	(Li 57b)
w	^{49}Ca(β$^-$)^{49}Sc	$Q = 5080 \pm 60$ keV	(Li 57b)
	^{49}Sc(β$^-$)^{49}Ti	$Q = 2050 \pm 50$ keV	(Ke 56)
x	^{26}Na(β$^-$)^{26}Mg	$Q = 8500 \pm 300$ keV	(Ro 61b)
y	^{40}Ar(t, p)^{42}Ar	$Q = 7046 \pm 40$ keV	(Ja 61d)
z	^{39}K(α, n)^{42}Sc	$Q = -7160 \pm 60$ keV	(Sm 61)
aa	^{23}Na(t, p)^{25}Na	$Q = 7492 \pm 12$ keV	(Hi 61a)
	^{26}Mg(t, α)^{25}Na	$Q = 5664 \pm 10$ keV	(Hi 61a)
bb	^{30}Al(β$^-$)^{30}Si	$Q = 7290 \pm 250$ keV	(Ro 61)
cc	^{30}Si(t, p)^{32}Si	$Q = 7304 \pm 15$ keV	(Hi 61g)
dd	^{40}Sc(β$^+$)^{40}Ca	$Q = 13950 \pm 200$ keV	(Sc 59c)

TABLE 2

Natural Abundances and Nuclear Moments

Isotope	Natural abundance (%)	Nuclear moments J	Nuclear moments μ (nucl. magneton)	Nuclear moments q (10^{-24} cm^2)
^{19}F	100	$\frac{1}{2}$	+2.6275	
^{20}Ne	90.92	0	<0.0002	
^{21}Ne	0.257	$\frac{3}{2}$	−0.66140	+0.09[e]
^{22}Ne	8.82		≈0	
^{22}Na		3	+1.746	
^{23}Na	100	$\frac{3}{2}$	+2.2161	+0.10
^{24}Na		4	+1.69	
^{24}Mg	78.7		≈0	
^{25}Mg	10.1	$\frac{5}{2}$	−0.8547	+0.14[b]
^{26}Mg	11.2		≈0	
^{27}Al	100	$\frac{5}{2}$	+3.6385	+0.149
^{28}Si	92.2			≈0
^{29}Si	4.7	$\frac{1}{2}$	±0.5548	<0.0001
^{30}Si	3.1			≈0
^{31}P	100	$\frac{1}{2}$	+1.1305	
^{32}P		1	−0.2523	
^{32}S	95.0	0		
^{33}S	0.76	$\frac{3}{2}$	+0.6427	−0.064
^{34}S	4.22			<0.002
^{35}S		$\frac{3}{2}$	±1.0	+0.045
^{36}S	0.014			<0.01
^{35}Cl	75.53	$\frac{3}{2}$	+0.82091	−0.0789
^{36}Cl		2	+1.2839	−0.0168
^{37}Cl	24.47	$\frac{3}{2}$	+0.6833	−0.0621
^{36}Ar	0.337		≈0	
^{38}Ar	0.063			
^{40}Ar	99.600		≈0	
^{39}K	93.08	$\frac{3}{2}$	+0.3909	
^{40}K	0.0118	4	−1.2964	−0.07[a]
^{41}K	6.91	$\frac{3}{2}$	+0.2151	±0.1
^{42}K		2	−1.137	
^{43}K		$\frac{3}{2}$[d]	±0.163[d]	
^{40}Ca	96.97		≈0	
^{42}Ca	0.64			
^{43}Ca	0.145	$\frac{7}{2}$	−1.3153	
^{44}Ca	2.06			
^{46}Ca	0.0033			
^{48}Ca	0.185			
^{44}Sc		2[c]		
$^{44}Sc^{m}$		6[c]		
^{45}Sc	100	$\frac{7}{2}$	+4.749	−0.22[f]

TABLE 2 *(continued)*

Isotope	Natural abundance (%)	Nuclear moments		
		J	μ (nucl. magneton)	q (10^{-24} cm^2)
^{46}Ti	7.99			
^{47}Ti	7.32	$\frac{5}{2}$	−0.7871	
^{48}Ti	73.99			
^{49}Ti	5.46	$\frac{7}{2}$	−1.1023	
^{50}Ti	5.25			

[a] Bu 60c.
[b] Bl 61.
[c] Ha 61b.
[d] Pe 59b.
[e] Gr 58d.
[f] Fr 59.

^{20}Na

(Not illustrated)

A. ^{20}Na(β^+)^{20}Ne $\qquad Q_m = 15320 \pm 300$

The half-life is 0.25 sec (Al 50a), 0.23±0.08 sec (Sh 51b), 0.385±0.01 sec (Bi 52a).

The decay, at least partly, proceeds to states of ^{20}Ne between 6.8 and 10.8 MeV which decay by α-particle emission. The possibility that the β^+ decay is super-allowed is discussed in Bo 55.

For a theoretical discussion of the ^{20}Na spin, see De 53a.

B. ^{20}Ne(p, n)^{20}Na $\qquad Q_m = -16100 \pm 300$

The threshold, at $E_p = 16.9$ MeV, has been measured by α-particle detection (Al 50a).

C. Not reported:

^{20}Ne(^{3}He, t)^{20}Na $\qquad Q_m = -15340 \pm 300$

^{21}Na

(Fig. 21.1, p. 12; table 21.1, p. 13)

A. ^{21}Na(β^+)^{21}Ne $\qquad Q_m = 3530 \pm 17$

The weighted average of four half-life measurements is 22.8 ± 0.2 sec (Sc 52, Ph 53, Ar 58, Wa 60a).

The maximum positon energy is 2.50±0.03 MeV (Sc 52), 2.51±0.02 MeV (Wa 60a). A 0.347 MeV γ ray is observed with an intensity of 2.2±0.3 percent (Ta 60c). No γ rays with $E_\gamma > 0.51$ MeV have been found (Sc 52).

The decay is super-allowed (log $ft = 3.6$), indicating that the spin of ^{21}Na is the same as that of its mirror nucleus ^{21}Ne, that is $J^\pi = \frac{3}{2}^+$. For the decay to ^{21}Ne* = 0.35 MeV, log $ft = 5.0$.

B. ^{20}Ne(p, γ)^{21}Na $\qquad Q_m = 2446 \pm 17$

At $E_p = 400$ keV, the cross section is $(2.7 \pm 1.0) \times 10^{-2}$ μb (Pi 57).

One resonance, at $E_p = 1.165$ MeV, is found in the γ-ray yield for protons in the 0.5–1.3 MeV range (Br 47). See fig. 21.1 for the γ decay of the corresponding 3.56 MeV level (Be 61). A $J^\pi = \frac{3}{2}^+$ (or $\frac{5}{2}^+$) assignment follows from the angular distribution of the ground-state transition (Be 61). The level has $\Gamma_p \leq 0.7$ keV (Ta 59), and $(2J+1)\Gamma_p\Gamma_\gamma/\Gamma = 1.13 \pm 0.07$ eV (Th 60). Non-resonant capture has been investigated in the vicinity of this resonance (Ta 59).

Four resonances for the production of annihilation radiation from the decay of ^{21}Na, found for protons in the 1.35–4.4 MeV range, are indicated in table 21.2 (Va 53).

C. ^{20}Ne(p, p′)^{20}Ne $\qquad E_b = 2446 \pm 17$

Elastic scattering studies indicate ten resonances in the range $E_p = 0.2$–4.4

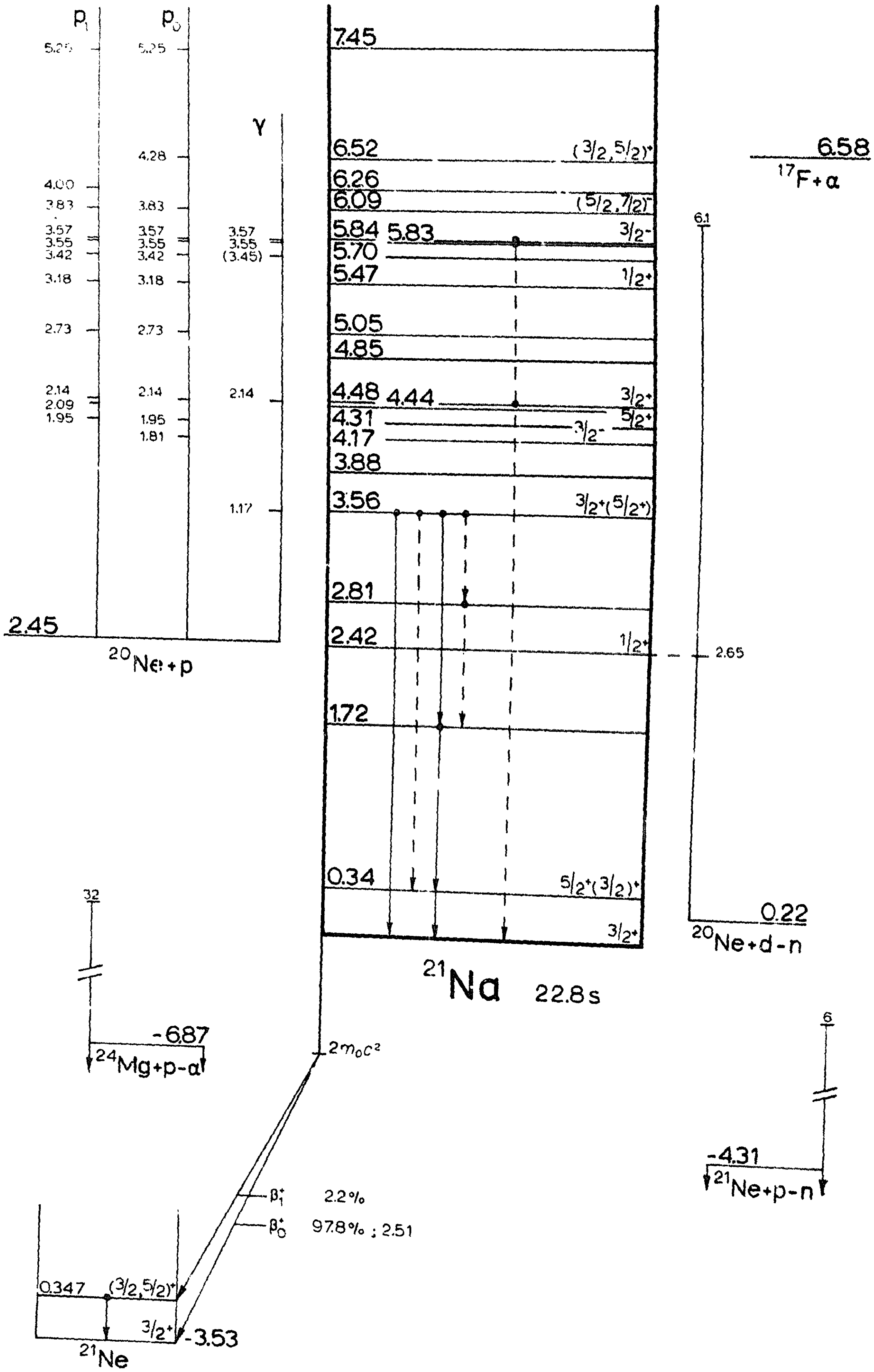

Fig. 21.1. Energy levels of ²¹Na.

TABLE 21.1

Energy levels of ^{21}Na

E_x (MeV)	J^π	$\tau_{\frac{1}{2}}$ or Γ	Decay	Reactions
0	$\frac{3}{2}+$	22.8±0.2 sec	β^+	A, B, D, E, F,
0.34±0.02	$(\frac{3}{2}+)$, $\frac{5}{2}+$		γ	B, D
1.72±0.05			γ	B, D
2.42±0.02	$\frac{1}{2}+$			D
2.81±0.04			(γ)	B, D
3.56	$\frac{3}{2}+$, $(\frac{5}{2}+)$		γ	B, D
3.88±0.05				D
4.17	$\frac{3}{2}-$	121 keV	p	C, D
4.31	$\frac{5}{2}+$	17 keV	p	C, D
4.44			p	C
4.48	$\frac{3}{2}+$	27 keV	γ, p	B, C, D
4.85±0.06				D
5.05		double	p	C, D
5.47	$\frac{1}{2}+$	80 keV	p	C
5.70		≈20 keV	(γ), p	B, C
5.83		≈2 keV	γ, p	B, C
5.84	$\frac{3}{2}-$	25 keV	γ, p	B, C
6.09	$(\frac{5}{2}, \frac{7}{2})-$	6 keV	p	C
6.26			p	C
6.52	$(\frac{3}{2}, \frac{5}{2})+$	150 keV	p	C
7.45			p	C

TABLE 21.2

Resonances in ^{20}Ne+p

E_p (MeV)	^{21}Na* (MeV)	Decay[g]	Γ (keV)	Γ_{p_0}/Γ	J^π[d]
1.165[a]	3.56	γ			
1.81[d]	4.17	p_0	180[d], 121[e]	>0.7[d]	$\frac{3}{2}-$
1.953[d]	4.31	p_0 p_1	6[d], 17[e]	>0.7[d], 0.25[e]	$\frac{5}{2}+$
2.09[b]	4.44	p_1			
2.135[d, c]	4.48	γ p_0 p_1	17[d], 27[e]	>0.7[d], 0.84[e]	$\frac{3}{2}+$
2.73[b]	5.05	p_0 p_1	double[d]		
3.176[d]	5.47	p_0 p_1	110[d], 80[e]	>0.7[d]	$\frac{1}{2}+$
3.42[d, c]	5.70	(γ) p_0 p_1	≈20[d]	<0.1[d]	
3.552[d, c]	5.83	γ p_0 p_1	≈2[d]		
3.566[d, c]	5.84	γ p_0 p_1	25[d]	>0.7[d]	$\frac{3}{2}-$
3.828[d]	6.09	p_0 p_1	6[d]		$\frac{5}{2}-$, $\frac{7}{2}-$
4.00[b]	6.26	p_1			
4.28[d]	6.52	p_0	150[d]	>0.7[d]	$\frac{3}{2}+$, $\frac{5}{2}+$
5.25[f]	7.45	p_0 p_1			

[a] Br 47, Be 61.
[b] Co 54b.
[c] Va 53.
[d] Ha 55a.
[e] Va 60d.
[f] Od 59a.
[g] Resonances in the yield of capture γ rays or in the yield of ^{21}Na β^+ activity are indicated by γ, resonances for elastic scattering by p_0, and resonances in the yield of the 1.63 MeV γ ray from ^{20}Ne(1) by p_1.

MeV; see table 21.2 for energies, widths, spins, and parities (Ha 53, Ha 55a, Va 60d).

The resonances for inelastic proton scattering to ^{20}Ne* = 1.63 MeV generally correspond to those for elastic scattering (Ga 53, Co 54b); two resonances, at E_p = 2.09 and 4.00 MeV, are found from inelastic scattering only (Co 54b). Resonance cross sections are given in Ga 53. See also So 61.

Angular distribution measurements of proton groups to ^{20}Ne(0) and (1) in the E_p = 4.95–5.50 MeV region indicate a resonance at E_p = 5.25 MeV (Od 59a).

See Aj 59 for levels in ^{20}Ne.

D. ^{20}Ne(d, n)^{21}Na $\qquad Q_m = 222 \pm 17$

The ground-state Q value has been measured as 0.22±0.03 MeV (Be 61), and 0.25±0.05 MeV (Gr 61). Excited states have been observed at 0.33±0.03 MeV (Be 61, Gr 61), and at 1.77±0.05, 2.42±0.04, 2.80±0.06, 3.61±0.06 MeV (Be 61). See also Sw 52. From angular distribution measurements l_p = (2,3) (Gr 61) is found for the ground-state transition, $l_p = 2$, $\theta_p^2 = 0.011$ (Be 61; also $l_p = 2$ in Gr 61) for the transition to the 0.33 MeV level, and $l_p = 0$, $\theta_p^2 = 0.17$ (Be 61) for the transition to the 2.42 MeV level.

A slow-neutron threshold has been observed with $Q = -2.201 \pm 0.007$ MeV, corresponding to ^{21}Na* = 2.42 MeV (Ma 56b). An earlier reported threshold with $Q = -1.24 \pm 0.02$ MeV (Ma 56b) has probably to be ascribed to ^{22}Ne(d, n)^{23}Na (Gr 61).

Recent measurements with time-of-flight neutron spectroscopy, at E_d = 2.4, 3.1, 4.6, and 6.1 MeV, yield ^{21}Na levels at 0.36±0.04, 1.68±0.05, 2.82±0.04, 3.88±0.05, 4.85±0.06, and 5.00±0.05 MeV, in addition to the known states at 0, 2.42, 3.56, 4.17, 4.31, and 4.48 MeV (Aj 60a, Aj 61). An assumed Q_0 value of 0.23 MeV instead of 0.22 MeV has been used in Aj 61; the excitation energies given above have already been corrected accordingly.

E. ^{21}Ne(p, n)^{21}Na $\qquad Q_m = -4313 \pm 17$

Observed, Cr 40.

F. ^{24}Mg(p, α)^{21}Na $\qquad Q_m = -6867 \pm 17$

Observed, Br 48, Sc 52, Fu 60.

G. Not reported:

^{19}F(^{3}He, n)^{21}Na	$Q_m = -7573 \pm 17$
^{20}Ne(^{3}He, d)^{21}Na	$Q_m = -3047 \pm 17$
^{20}Ne(α, t)^{21}Na	$Q_m = -17366 \pm 17$
^{21}Ne(^{3}He, t)^{21}Na	$Q_m = -3548 \pm 17$
^{23}Na(p, t)^{21}Na	$Q_m = -14988 \pm 17$

^{22}Na

(Fig. 22.1, p. 16; table 22.1, p. 15)

A. $^{22}Na(\beta^+)^{22}Ne$ $Q_m = 2841.5 \pm 4.6$

The half-life is 2.58 ± 0.03 years (Me 57).

The decay predominantly proceeds by β^+ emission to the 1.27 MeV level of ^{22}Ne. The β^+ end point is 542 ± 5 keV (Ma 50a), 540 ± 5 keV (Wr 53), 545 ± 2 keV (Da 58), 547.4 ± 1.0 keV (Ni 61a); $\log ft = 7.4$.

TABLE 22.1

Energy levels of ^{22}Na

E_x (MeV $\pm$ keV)	$J^\pi; T$	$\tau_{\frac{1}{2}}$ or Γ	Decay	Reactions
0	3^+; 0	2.58 ± 0.03 yr	β^+, EC	many
0.587 ± 4	1^+; 0	$(0.266 \pm 0.010) \times 10^{-6}$ sec	γ	B, D, I, J, K, L, M
0.660 ± 4	0^+; 1	$< 0.35 \times 10^{-9}$ sec	γ	B, D, K, L, M
0.892 ± 3	$(1)^+$		γ	B, D, J, K, L, M
1.532 ± 4	$(\leq 4)^+$		γ	B, D, J, K, L
1.942 ± 5			γ	B, D, K, L
1.949 ± 10			γ	B, D, K, L
1.988 ± 5			γ	B, D, K, L
2.217 ± 5			γ	B, D, E, K, L
2.574 ± 5				D, K, L
2.973 ± 5				D, K, L
3.065 ± 5				D, K, L
3.527 ± 5				D, K, L
3.713 ± 8				D, K, L
3.949 ± 5				K, L
4.073 ± 10				K, L
4.323 ± 8				K, L
4.363 ± 10				K, L
4.473 ± 8				K, L
4.531 ± 10				K, L
4.595 ± 10				K, L
4.732 ± 10				K, L
4.778 ± 10				K, L
7.474 ± 5		≈ 6 keV	γ	E
7.569		< 2 keV	γ	E
7.707			γ	E
7.812			γ	E
7.903			γ	E
7.980			γ	E
8.035			γ	E
12.07			p	C
12.38			p	C

The γ-ray energy has been measured as 1.277 ± 0.004 MeV (Al 49), 1.2736 ± 0.0018 MeV (Si 59g). The internal conversion coefficient of the 1.27 MeV γ ray, $(6.7 \pm 0.7) \times 10^{-6}$, indicates that the transition has E2 character (Le 54).

The Fermi-Kurie plot is linear within the experimental error (Ma 50a,

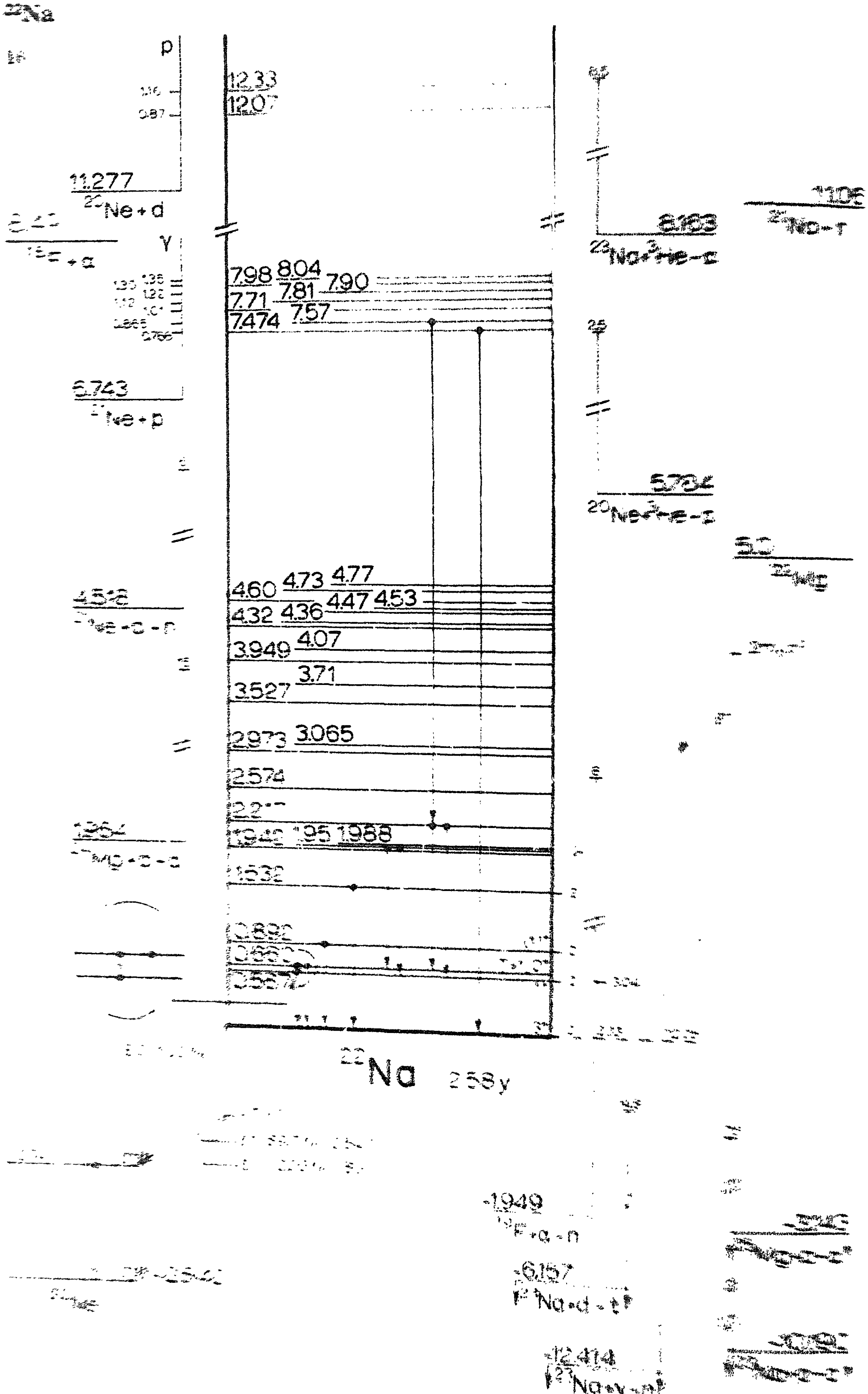

Fig. 22.1 Energy levels of 22Na.

Al 50b, Wo 54, Da 58, Ko 58b, Le 61b). Deviations from linearity, however, are reported in Ha 58c, Ni 61a, and discussed in Ku 59c. A small anisotropy, $A = -0.0027 \pm 0.0004$ (St 59a, St 58a), $-A > 0.026$ (Da 60a), observed in the β–γ angular correlation could be due to higher order effects. For a possible energy dependence of the anisotropy, see Su 61. See also St 51a.

Electron capture also occurs, with an intensity $EC/\beta^+ = 0.114 \pm 0.004$, averaged from 0.124 ± 0.011 (Kr 54), 0.110 ± 0.007 (Sh 54b), 0.122 ± 0.010 (Al 55), 0.109 ± 0.007 (Ko 58b). See also Ho 53b, Ma 54c, Se 54, Ch 55, Di 55. Theory yields 0.1135 (Ko 58b).

A β^+ transition to ^{22}Ne(0) has been observed with an intensity 0.062 ± 0.015 percent of the transition to ^{22}Ne(1). The β^+ end point is 1.83 ± 0.06 MeV; $\log ft = 13.1$ (Wr 53). See also Mo 49.

The asymmetry parameter A of the β–γ circular polarization correlation, $1 + A \langle v/c \rangle \cos \vartheta$, is $A = +0.36 \pm 0.08$ (Ap 59; also Ap 58), $A = +0.35 \pm 0.02$, yielding the relation $C'_A = (1.0 \pm 0.2)\, C_A$ for the axial-vector coupling constants (St 59b).

Longitudinal polarization of positons, Pa 57b.

B. ^{19}F(α, n)^{22}Na $\qquad Q_m = -1949.0 \pm 4.7$

Thresholds for the production of slow neutrons are observed at $E_\alpha = 2.33$ MeV (^{22}Na g.s.) and 3.04 MeV (^{22}Na* = 0.59 MeV) (He 54b). The groundstate Q value has been measured as $Q_0 = -1.950 \pm 0.015$ MeV (Bu 56c, as corrected in Wi 57), -1.959 ± 0.010 MeV (Wi 60). For α particles in the $E_\alpha = 3$–6 MeV range, neutron groups have been observed to the ^{22}Na states indicated in table 22.3 (Ba 59a). See also Qu 56, Sz 60.

Gamma rays observed from this reaction, with relative intensities (at $E_\alpha = 4.9$ MeV) and assignments are listed in table 22.2 (Te 58, Ra 60). Gamma-gamma coincidence experiments indicate a ^{22}Na level at 666 ± 4 keV, decaying

TABLE 22.2

Gamma rays from ^{19}F(α, nγ)^{22}Na

E_γ [a] (MeV ±keV)	E_γ [b] (MeV)	E_γ [c] (MeV ±keV)	Intensity [c] (relative)	Transition in ^{22}Na (E_x in MeV)
0.073 ± 1		0.073 ± 2 [d]		0.66 → 0.59
0.593	0.593	0.586 ± 4 [e]	36	0.59 → 0
		(0.666)	<2	0.66 → 0
0.890 ± 10		0.892 ± 5	25	0.89 → 0
	1.3			1.95 → 0.66 (+0.59)
		1.530 ± 10	6	1.53 → 0
	1.55			2.22 → 0.66 (+0.59)

[a] Te 58; $E_\alpha = 3.9$ MeV.
[b] Te 58; $E_\alpha = 5.7$ MeV; γ rays in this column are coincident with the 73 keV γ ray.
[c] Ra 60; $E_\alpha = 4.9$ MeV; without Doppler correction.
[d] Total internal conversion coefficient, $(4.5 \pm 0.4) \times 10^{-3}$, indicates M1 character (Ra 60).
[e] Total internal conversion coefficient, $(1.14 \pm 0.3) \times 10^{-4}$, indicates E2 or M2 character (Ra 60).

by an $E_\gamma = 73 \pm 1$ keV transition to ^{22}Na(1), which in turn decays to the ground state (Te 58). The $J^\pi = 0^+$, $T = 1$ assignment to the 0.66 MeV level (see reaction L), and the internal conversion coefficient of the 73 keV γ ray (table 22.2) yield $J^\pi = 1^+$ (and thus $T = 0$) for the 0.59 MeV level. These assignments are confirmed by the following data: the conversion coefficient of the 593 keV γ ray indicating E2 or M2 character (Ra 60); the half-life of the 0.59 MeV level, $\tau_{\frac{1}{2}} = 0.266 \pm 0.010$ μsec, ruling out a $J^\pi = 0^+$ (and thus $T = 1$) assignment to this level (Te 58; see also Ho 58b); the half-life of the 0.66 MeV level, $\tau_{\frac{1}{2}} < 0.35 \times 10^{-9}$ sec, supporting a $\Delta T = 1$ assignment to the 73 keV transition (Ho 58b; see also Te 58).

See ^{23}Na for resonances.

C. ^{20}Ne(d, p)^{21}Ne $\qquad Q_m = 4534.4 \pm 1.5 \qquad E_b = 11277.4 \pm 4.6$

The excitation function shows two resonances in the range $E_d = 0.8$–1.1 MeV, corresponding to ^{22}Na levels at 12.07 and 12.13 MeV (Go 55).

See Aj 59 for levels in ^{21}Ne.

D. ^{20}Ne(^{3}He, p)^{22}Na $\qquad Q_m = 5784.2 \pm 4.6$

Nine proton groups have been observed (see table 22.3). A γ ray, with $E_\gamma = 73$ keV, has been observed in coincidence with the proton groups to ^{22}Na* $= 0.66$ and 1.9–2.2 MeV (Te 58).

E. ^{21}Ne(p, γ)^{22}Na $\qquad Q_m = 6743.0 \pm 4.9$

Seven resonances have been reported, at $E_p = 775$ ($\Gamma \approx 6$ keV), 865 ($\Gamma < 2$ keV), 1010, 1120, 1215, 1296, and 1354 keV. At $E_p = 775$ keV, the main capture radiation proceeds to the ground state; at $E_p = 865$ keV, to ^{22}Na* $= 2.25$ MeV (Kr 60).

Other energy determinations of the first resonance give $E_p = 765$ keV (Br 47), 766.1 ± 1.8 keV (Ku 59a).

F. ^{21}Ne(d, n)^{22}Na $\qquad Q_m = 4518.3 \pm 4.9$

Observed, La 37.

G. ^{22}Mg(β^+)^{22}Na $\qquad Q_m = 5040 \pm 80$

See ^{22}Mg.

H. ^{23}Na(γ, n)^{22}Na $\qquad Q_m = -12414.3 \pm 4.9$

The threshold has been measured as 12.05 ± 0.20 MeV (Sh 51a), and 12.47 ± 0.05 MeV (Ch 58). A search for isomeric states in ^{22}Na with half-lives in the 10^{-5}–10^{-1} sec range was unsuccessful (Ve 56).

For yield curve, see Mo 53a.

I. ^{23}Na(p, d)^{22}Na $\qquad Q_m = -10189.3 \pm 4.9$

Differential cross sections of groups to ^{22}Na* $= 0$ and 0.59 MeV, measured at $E_p = 18$ MeV, yield $l_n = 2$ and $\theta_n^2 = 0.021$ for both groups (Be 58g, Ma 60d).

J. ^{23}Na(d, t)^{22}Na $\quad Q_m = -6156.6 \pm 4.9$

At $E_d = 14.8$ MeV, triton groups have been observed to ^{22}Na* = 0, 0.58, 0.89 and 1.53 MeV; $Q_0 = -6.211 \pm 0.040$ MeV. The angular distributions of all four groups are best fitted with $l_n = 2$ (Vo 58). Reduced widths, normalized to that of the ^{23}Na(p, d)^{22}Na ground-state transition (Be 58g), are: $\theta_n{}^2 = 0.021$, 0.007, 0.012 and 0.004, respectively (Vo 58, Ma 60d). For a theoretical discussion, see Ha 60a.

K. ^{23}Na(^{3}He, α)^{22}Na $\quad Q_m = 8162.9 \pm 4.9$

At $E(^3\text{He}) = 8.45$ MeV, 23 α-particle groups have been observed, corresponding to the ground state of ^{22}Na and excited states up to $E_x = 4.78$ MeV (Hi 60f); see table 22.3.

TABLE 22.3

Energy levels in ^{22}Na (in MeV±keV) from ^{19}F(α, n)^{22}Na, ^{20}Ne(^{3}He, p)^{22}Na, ^{23}Na(d, t)^{22}Na, ^{23}Na(^{3}He, α)^{22}Na, ^{24}Mg(d, α)^{22}Na, and ^{25}Mg(p, α)^{22}Na

Hi 60f (^{3}He, α) and (d, α)	Br 59d (d, α)	Br 59d (p, α)	Te 58 (^{3}He, p)	Vo 58 (d, t)	Ba 59a (α, n)
0	0	0	0	0	0
0.582	0.585±5	0.582±6	0.60	0.58	0.59±20
0.656		0.661±8			
0.889	0.893±5	0.891±6	0.90	0.89	0.89±20
1.527	1.533±5		1.55	1.53	1.54±20
1.933	1.944±5				
1.949					
1.980	1.990±5		2.0		1.97±40
2.210	2.219±5				
2.567	2.576±5		2.6		
2.965	2.975±5		3.0		
3.060	3.066±5				
3.532	3.526±5		3.5		
3.712	3.713±8		3.75		
3.951	3.949±5				
4.073					
4.322	4.323±8				
4.363					
4.474	(4.472±8)				
4.531					
4.595					
4.732					
4.778					
all±10 keV					

L. ^{24}Mg(d, α)^{22}Na $\quad Q_m = 1963.5 \pm 4.9$

The α-particle groups, observed at $E_d = 5.0$–7.5 MeV (Br 59d), and $E_d = 5.70$ and 5.90 MeV (Hi 60f) are listed in table 22.3; $Q_0 = 1.954 \pm 0.007$ MeV (Br 59d).

The group to the 0.66 MeV state, with $T = 1$, has an intensity of 1–5 percent of the ground-state group (see also Br 59d). The second $T = 1$ level is expected at $E_x \approx 1.95$ MeV; none of the groups to ^{22}Na* = 1.933, 1.949, and 1.980 MeV, however, is weak (Hi 60f). Angular distribution measurements at $E_d = 15$ MeV, with D. W. B. A. analysis, yield $L = 2$ and 0 for the groups to ^{22}Na* = 0 and 0.89 MeV, respectively (Pe 61). The $L = 0$ assignment to the 0.89 MeV level entails $J^\pi = 1^+$.

For cross section, see Cl 46, Cl 46a.

M. ^{25}Mg(p, α)^{22}Na $\qquad Q_m = -3142.5 \pm 5.0$

At $E_p = 7.5$ MeV, α-particle groups have been observed to the ground state and to the three lowest levels of ^{22}Na, including the 0.66 MeV, $T = 1$ level; see table 22.3 (Br 59d).

For cross section, see Me 51, Ba 54, Co 54a.

N. Not reported:

^{20}Ne(t, n)^{22}Na	$Q_m = 5019.7 \pm 4.7$
^{20}Ne(α, d)^{22}Na	$Q_m = -12568.2 \pm 4.7$
^{21}Ne(^{3}He, d)^{22}Na	$Q_m = 1249.8 \pm 4.9$
^{21}Ne(α, t)^{22}Na	$Q_m = -13069.7 \pm 4.9$
^{22}Ne(p, n)^{22}Na	$Q_m = -3624.2 \pm 4.6$
^{22}Ne(^{3}He, t)^{22}Na	$Q_m = -2859.7 \pm 4.6$
^{24}Mg(n, t)^{22}Na	$Q_m = -15624.5 \pm 4.9$
^{24}Mg(p, ^{3}He)^{22}Na	$Q_m = -16389.0 \pm 4.9$

^{22}Mg

(Fig. 22.2, p. 21)

A. ^{22}Mg(β^+)^{22}Na $\qquad Q_m = 5040 \pm 80$

The decay should proceed to ^{22}Na* = 0.66 MeV, with $J^\pi = 0^+$, $T = 1$. From the well known ft value of this type of super-allowed $0^+ \rightarrow 0^+$ β^+ transitions, and the Q_m value derived from reaction B, a ^{22}Mg half-life of about 4 sec can be estimated.

The 0.13 sec half-life, observed from proton bombardment of natural magnesium with 23 MeV protons, and assigned either to ^{23}Al or to ^{22}Mg (Ty 54), then must be due to ^{23}Al.

B. ^{20}Ne(^{3}He, n)^{22}Mg $\qquad Q_m = -40 \pm 80$

At $E(^3$He$) = 3.4$ and 4.5 MeV, neutron groups have been observed corresponding to ^{22}Mg(0), with $Q_0 = -0.04 \pm 0.08$ MeV, and to ^{22}Mg* = 0.99 ± 0.04 MeV. No other levels with $E_x < 2.5$ MeV have been observed (Aj 61).

C. Not reported:

^{24}Mg(p, t)^{22}Mg $\qquad Q_m = -21450 \pm 80$

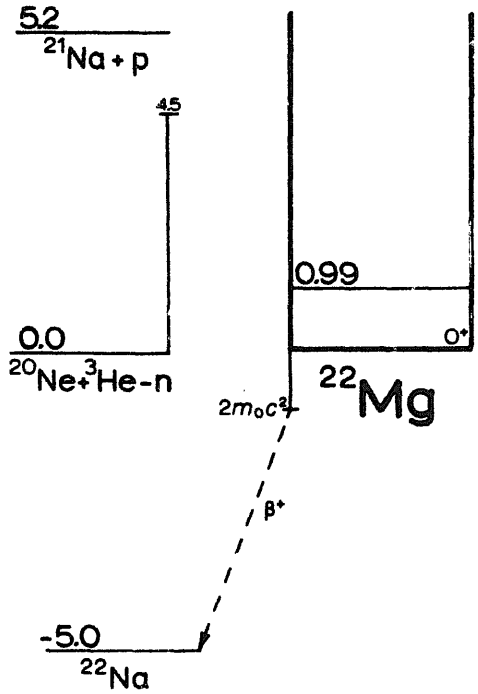

Fig. 22.2. Energy levels of ^{22}Mg.

^{23}Na

(Fig. 23.1, p. 22; table 23.1, p. 23)

A. (a) ^{19}F(α, n)^{22}Na	$Q_m = -1949.0 \pm 4.7$	$E_b = 10465.3 \pm 1.6$
(b) ^{19}F(α, p')^{22}Ne	$Q_m = 1675.2 \pm 0.8$	$E_b = 10465.3 \pm 1.6$
(c) ^{19}F(α, α')^{19}F		$E_b = 10465.3 \pm 1.6$

(a) Fifteen resonances have been found, for α particles in the energy range $E_\alpha = 2.5$–3.5 MeV, by measuring the yield of slow and fast neutrons and the yield of the 590 keV γ ray, from ^{22}Na (1); see table 23.2 for energies, widths, and cross sections (Wi 60; also Wi 57, He 54b).

See ^{22}Na for neutron groups and thresholds.

(b) Resonances in the yield of the 1.27 MeV γ ray, from ^{22}Ne (1), for $E_\alpha = 0.6$–2.8 MeV (Sh 54c), 1.5–3.4 MeV (He 54b), and 2.5–3.5 MeV (Wi 60), are given in table 23.2. See also De 58a.

See Aj 59 for proton groups.

(c) Resonances in the yield of 110 and 198 keV γ rays, from ^{19}F* = 110 and 198 keV, are given in Sh 54c ($E_\alpha = 0.6$–2.8 MeV) and He 54b ($E_\alpha = 1.3$–3.4 MeV); see table 23.2.

See Aj 59 for levels in ^{19}F.

The relative intensities of 18 resonances in the (α, α'), (α, p'), and (α, n') reactions have been reported in He 54b; and of 24 resonances in the (α, α) and (α, p') reactions in Sh 54c.

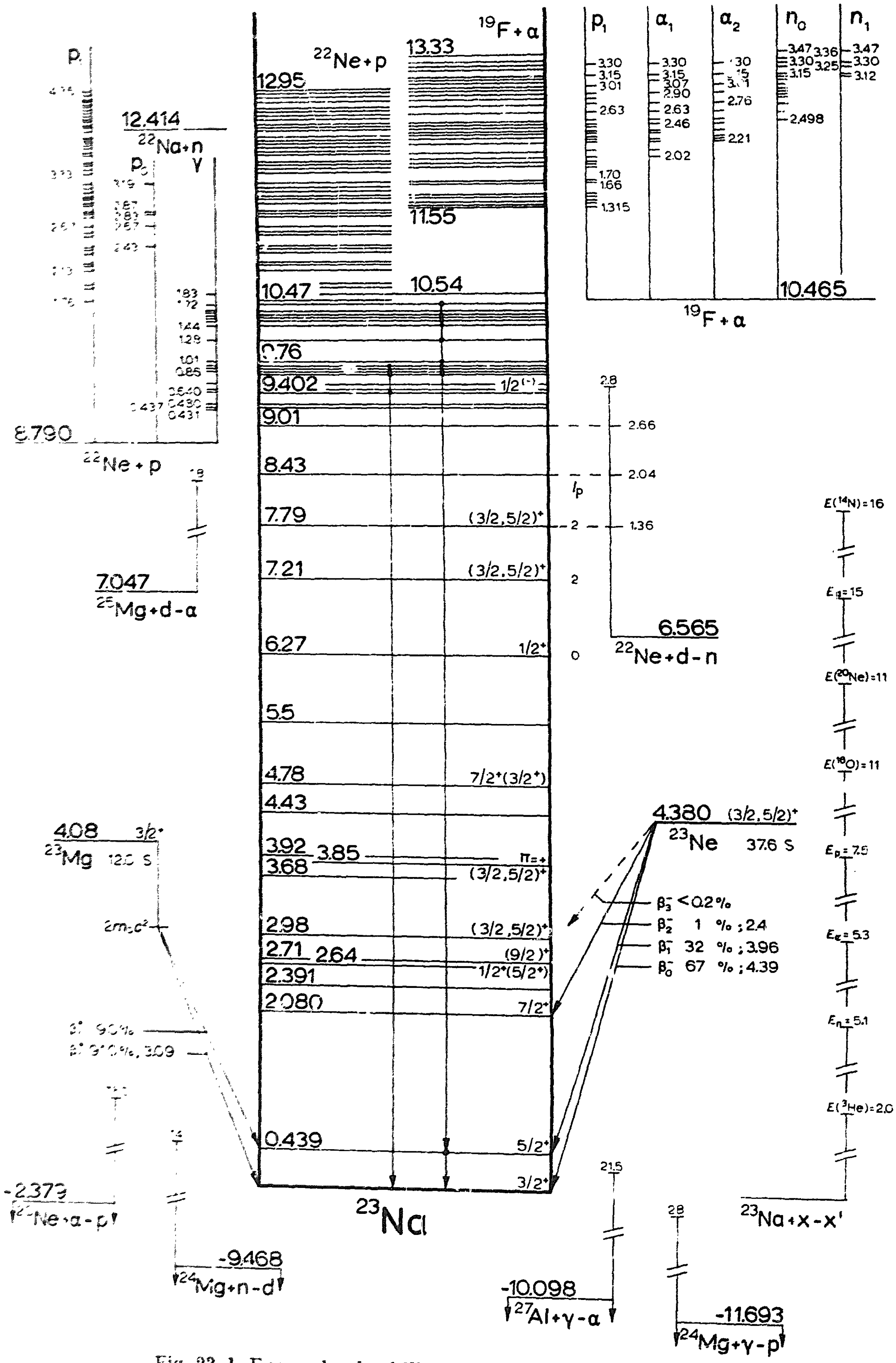

Fig. 23.1. Energy levels of ²³Na; for γ decay, see also fig. 23.2.

B. $^{20}Ne(\alpha, p)^{23}Na$ $Q_m = -2378.7 \pm 1.5$

One proton group, $Q = -2.54 \pm 0.20$ MeV, has been found with ThC′ α particles (Po 37 and Li 37). For the differential cross section, see Ya 60b. See ^{24}Mg for resonances.

C. $^{22}Ne(p, \gamma)^{23}Na$ $Q_m = 8790.1 \pm 1.5$

Resonance energies for $E_p = 0.4$–0.8 MeV (Ku 59a), $E_p = 0.6$–1.8 MeV (Si 59e, also Si 59), and $E_p = 0.6$–0.95 MeV (Th 58) and the main modes of

TABLE 23.1

Energy levels of ^{23}Na

E_x (MeV ± keV)	J^π	τ_m or Γ	Decay	Reactions
0	$\frac{3}{2}^+$		stable	many
0.4392 ± 0.8	$\frac{5}{2}^+$	$(1.6 \pm 0.3) \times 10^{-12}$ sec	γ	C, F, G, H, I, J, K, L, M, O, P
2.080 ± 3	$\frac{7}{2}^+$		γ	C, F, G, H, I, P
2.391 ± 5			γ	C, F, G, H, I
2.640 ± 6	$\frac{1}{2}^+$ $(\frac{5}{2}^+)$		γ	C, F, G, H
2.705 ± 7	$(\frac{9}{2})^+$		γ	C, F, G, H, I
2.984 ± 6	$(\frac{3}{2}, \frac{5}{2})^+$		γ	C, F, G, H, I
3.678 ± 7	$(\frac{3}{2}, \frac{5}{2})^+$		γ	C, H, I
3.850 ± 8	$(\leq\frac{7}{2})^+$		γ	C, H, I
3.915 ±10			γ	C, H, I
4.431 ±10			γ	C, H, I
4.778 ±10	$\frac{7}{2}^+$ $(\frac{3}{2}^+)$		γ	C, H,
5.5				I
6.27 ±50	$\frac{1}{2}^+$			E, I
7.21 ±50	$(\frac{3}{2}, \frac{5}{2})^+$		γ	C, E, I
7.79 ±20	$(\frac{3}{2}, \frac{5}{2})^+$			E
8.431 ±10				E
9.008 ±15				E
9.202 ± 2			γ	C
9.208 ± 2			γ	C
9.249 ± 2			γ	C
9.402 ± 2	$\frac{1}{2}^{(-)}$	$\approx 0.46 \pm 0.36$ keV	γ	C
9.424 ± 2			γ	C
9.484 ± 2			γ	C
9.612–10.543; 15 levels; see table 23.3 and reaction				C
10.470–12.945; 49 levels; see table 23.4 and reaction				D
11.552–13.333; 41 levels; see table 23.2 and reaction				A

decay are summarized in table 23.3. See also Br 47. At $E_p = 640$ keV, the isotropic angular distribution of the ground-state transition γ_0 (Th 58) and its radiative width, $\Gamma_{\gamma_0} = 2.0 \pm 0.5$ eV, favour the assignment $J^\pi = \frac{1}{2}^{(-)}$. A resonance absorption measurement gives $\Gamma_{\gamma_0} = 2.7 \pm 1.1$ eV, and $\Gamma \approx \Gamma_p = 460 \pm 360$ eV (Mo 60). At $E_p = 854$ keV, angular distribution measurements exclude $J = \frac{1}{2}$ for the resonance level (Th 58).

From γ-ray spectra, angular distributions, and γ–γ angular correlations,

TABLE 23.2

Resonances in $^{19}F+\alpha$

E_α (MeV)	$^{23}Na^*$ (MeV)	Outgoing particle[b]	References	E_x (MeV ± keV)	$^{23}Na^*$ (MeV)	Γ (keV)	σ_n (mb)	Outgoing particle[b]	References
1.315	11.552	p_1	c	2.46 ± 10	12.497			$p_1\ \alpha_1\ \alpha_2$	a, c, d
1.362	11.590	p_1	c	2.498 ± 3	12.528	8	3	n_0	a
1.408	11.628	p_1	c	2.53 ± 10	12.555			$p_1\ \alpha_1\ \alpha_2$	a, c, d
1.455	11.667	p_1	c	2.609 ± 3	12.620	11	6	n_0	a
1.501	11.705	p_1	c, d	2.63 ± 10	12.639			$p_1\ \alpha_1\ \alpha_2$	a, c, d
1.662	11.837	p_1	c	2.730 ± 3	12.721	6	14	n_0	a
1.70	11.869	p_1	d	2.738 ± 3	12.728	9		$p_1\ \alpha_1$	a, c
1.879	12.018	p_1	c	2.76	12.745			$p_1\ \alpha_1\ \alpha_2$	c, d
1.914	12.047	p_1	c, d	2.81 ± 10	12.786			p_1	a
1.948	12.074	p_1	c	2.84 ± 10	12.812		16	$p_1\ n_0$	a, d
1.994	12.113	p_1	c, d	2.87 ± 10	12.836		2	n_0	a
2.017	12.130	$p_1\ \alpha_1$	c	2.90 ± 10	12.862		2	$p_1\ \alpha_1\ \alpha_2\ n_0$	a, d
2.083	12.187	p_1	c	2.94 ± 10	12.895		10	n_0	a
2.169	12.206	$p_1\ \alpha_1$	c, d	3.01 ± 10	12.953		3.5	$p_1\ \alpha_2\ n_0$	a, d
2.207	12.288	$p_1\ \alpha_1\ \alpha_2$	c, d	3.07 ± 10	13.002		7	$\alpha_1\ n_0$	a, d
2.257	12.329	U $\alpha_1\ \alpha_2$	c	3.12 ± 10	13.044		3.5	$n_0\ n_1$	a
2.298	12.364	p_1 α_2	c, d	3.15 ± 10	13.067		25	$p_1\ \alpha_1\ \alpha_2\ n_0\ n_1$	a, d
2.337	12.396	U α_1	c	3.25 ± 10	13.151		20	$n_0\ n_1$	a
2.383	12.434	$p_1\ \alpha_1\ \alpha_2$	c, d	3.30 ± 10	13.193		25	$p_1\ \alpha_1\ \alpha_2\ n_0\ n_1$	a, d
2.428	12.471	p_1	c	3.36 ± 10	13.241		25	n_0	a
				3.47 ± 10	13.333		17	$n_0\ n_1$	a

a Wi 60.

b Resonances in the yield of the 1.27 MeV ($^{22}Ne^*$), 0.110 MeV ($^{19}F^*$), and 0.59 MeV ($^{22}Na^*$) γ rays are indicated by p_1, α_1 α_2, and n_1, respectively; U = unresolved.

c Sh 54c. Correction for surface contamination might lower the resonance energies by 10 to 20 keV.

d He 54b.

TABLE 23.3

Resonances in $^{22}Ne(p, \gamma)^{23}Na$

E_p (keV)	$^{23}Na^*$ (MeV ± keV)	Decay[e]	E_p (keV)	$^{23}Na^*$ (MeV)	Decay[e]
431.0 ± 1.3[a]	9.202 ± 2		1010[b]	9.756	γ_1
436.9 ± 1.3[a]	9.208 ± 2		1280[b]	10.014	γ_1
480.1 ± 1.0[a]	9.249 ± 2		1443[b]	10.170	γ_1
639.8 ± 1.6[a, b, c]	9.402 ± 2	γ_0	1500[b]	10.225	γ_1
662.3 ± 1.7[a]	9.424 ± 2		1553[b]	10.276	γ_1
725.5 ± 1.2[a]	9.484 ± 2		1593[b]	10.314	γ_1
859[b, c]	9.612	$\gamma_0\ \gamma_1$	1621[d]	10.340	
904[b, c]	9.655	$\gamma_0\ \gamma_1$	1628[d]	10.347	
933[c]	9.682		1721[b]	10.436	γ_1
(943)[c]	(9.692)		1833[d]	10.543	
954[b]	9.702	$\gamma_0\ \gamma_1$			

a Ku 59a.

b Si 59e.

c Th 58.

d Si 59.

e Si 59e (also Th 58); γ_0 anf γ_1 indicate transitions to $^{23}Na^*$ = 0 and 0.44 MeV, respectively. Cascades through $^{23}Na^*$ = 2.08 and 2.39 MeV have rot been observed.

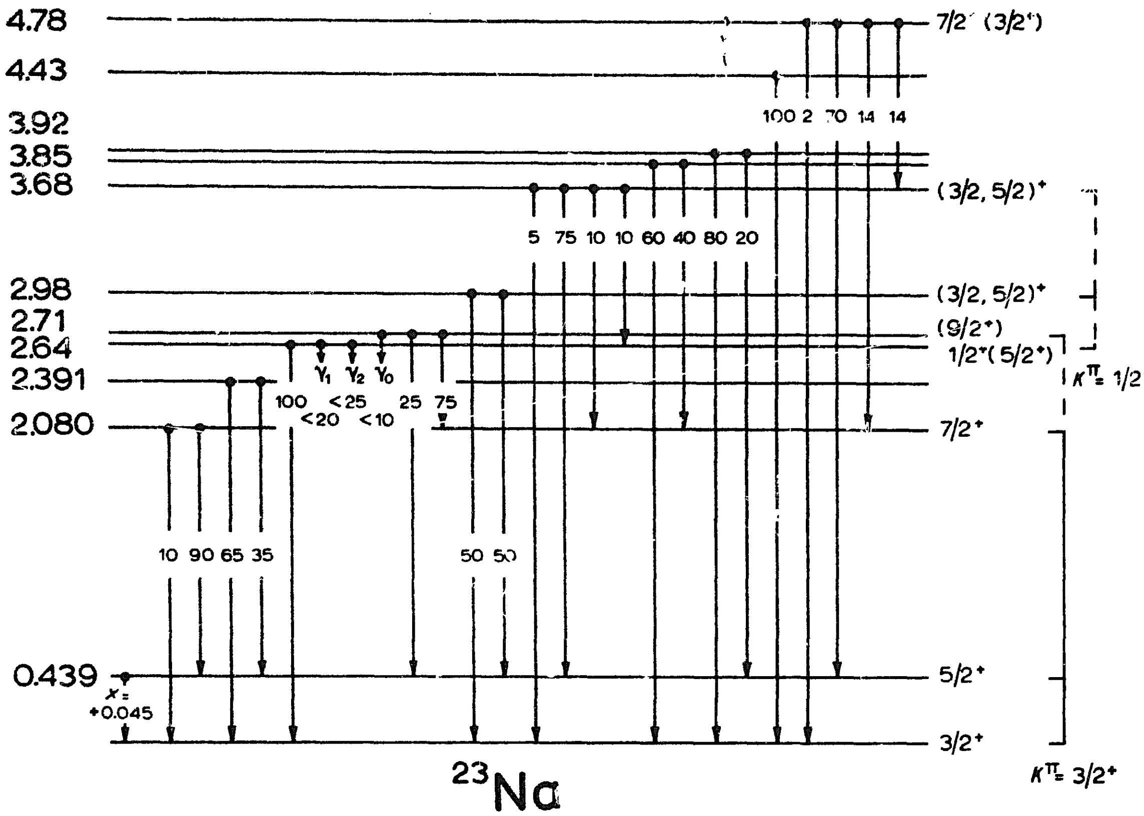

Fig. 23.2. Gamma-ray branchings of ^{23}Na lower levels. Branchings of the 2.08, 2.39, 2.64, and 2.98 MeV levels are averages from values in Go 57b, Fr 58a, Si 59e, Kr 60a, Li 61, Br 61c. At the 2.71 MeV level the Kr 60a results are given; a γ_1 intensity of 100% is reported in Fr 58a and Br 61c. Branchings of levels above 3 MeV are from Br 61c.

at 5 resonances in the $E_p = 600$–1030 keV region, branchings of ^{23}Na lower levels up to $E_x = 5$ MeV, and spins and parities have been determined, as given in fig. 23.2 (Br 61c).

D. ^{22}Ne(p, p')^{22}Ne $\qquad E_b = 8790.1 \pm 1.5$

Resonances both for elastic scattering and for inelastic scattering to ^{22}Ne* = 1.27 MeV have been observed at $E_p = 2.43$, 2.67, 2.83, 2.87, and 3.19 MeV (Ha 53, Ga 53).

Resonances in the yield of the 1.27 MeV γ ray, with relative yields, are listed in table 23.4 (Va 53).

E. ^{22}Ne(d,n)^{23}Na $\qquad Q_m = 6565.4 \pm 1.6$

At $E_d = 2.83$ MeV, neutron groups have been observed to ^{23}Na* = 6.27 ± 0.05, 7.21 ± 0.05, and 7.72 ± 0.05 MeV. Angular distribution measurements yield $l_p = 0$, 2, and 2, and $(2J+1)\theta_p^2 = 0.012$, 0.073, and 0.021, respectively (Gr 61).

Two slow-neutron thresholds, with $Q = -1.866 \pm 0.010$ and -2.443 ± 0.015 MeV, have been observed from deuteron bombardment of natural neon. The assignment to ^{22}Ne is based on the observed intensities (Ma 56b). A threshold with $Q = -1.24 \pm 0.02$ MeV, earlier reported as to be due to ^{20}Ne(d, n)^{21}Na (Ma 56b), has also to be assigned to the ^{22}Ne(d, n)^{23}Na reaction (Gr 61).

F. ^{23}Ne(β^-)^{23}Na $\qquad Q_m = 4380 \pm 5$

The weighted mean of the half-life measurements is 37.6 ± 0.1 sec (Pe 57, Nu 58, Al 59a). Also Br 50d, Ri 58.

TABLE 23.4

Resonances in the yield of $E_\gamma = 1.27$ MeV from ^{22}Ne(p, p'γ)^{22}Ne(Va 53)

E_p (MeV)	^{23}Na* (MeV)	Relative yield	E_p (MeV)	^{23}Na* (MeV)	Relative yield
1.755	10.470		3.435	12.075	70
1.915	10.620		3.470	12.110	120
1.970	10.675		3.560	12.195	270
2.130	10.830	50	3.585	12.220	90
2.190	10.885	22	3.645	12.275	20
2.220	10.915	77	3.685	12.315	30
2.240	10.935	40	3.725	12.355	90
2.355	11.045	10	3.755	12.380	320
2.405	11.090	10	3.800	12.405	45
2.430	11.115	45	3.845	12.470	120
2.565	11.245	40	3.895	12.515	35
2.610	11.285	40	3.920	12.540	370
2.675	11.350	175	3.940	12.560	90
2.795	11.465	40	3.985	12.600	150
2.835	11.500	130	4.035	12.650	130
2.865	11.530	85	4.055	12.670	170
2.940	11.600	30	4.090	12.700	160
2.965	11.625	40	4.125	12.735	290
3.020	11.680	50	4.165	12.775	280
3.055	11.710	160	4.190	12.800	350
3.105	11.760	100	4.235	12.840	120
3.160	11.810		4.255	12.860	210
3.215	11.865	160	4.300	12.905	255
3.330	11.975	35	4.345	12.945	360
3.380	12.025	185			

The β^- branching, with end points, percentages, log *ft* values, and coincident γ rays is given in table 23.5 (Pe 57, Ov 56, Ge 56, Ge 55).

The allowed character of the β transitions to ^{23}Na(0) and (1), with $J^\pi = \frac{3}{2}+$ and $\frac{5}{2}+$, respectively, limits the spin of ^{23}Ne to $J^\pi = \frac{3}{2}+$ or $\frac{5}{2}+$. The same possibilities follow from ^{22}Ne(d, p)^{23}Ne angular distribution measurement (Bu 56d).

The electron-neutrino angular correlation is consistent with pure axial-vector interaction (Al 59a, Bo 59; see, however, Ri 58).

Resonance fluorescence measurements yield $\tau_m = (1.5 \pm 0.3) \times 10^{-10}$ sec (Bo 59), and $\tau_m = (1.5^{+0.3}_{-0.2}) \times 10^{-12}$ sec (Am 61) for ^{23}Na(1). The latter value is in good agreement with the value reported in Ra 59a (see reaction H).

G. ^{23}Na(n, n')^{23}Na

The gamma rays from inelastic neutron scattering, listed in table 23.6, can be fitted into the ^{23}Na level scheme as indicated in the last column of this table (Fr 58a, Mo 56c, Wo 56, Li 61). Gamma rays of 0.15 and 0.61 MeV, observed

TABLE 23.5

The β^- decay of ^{23}Ne

	End point (MeV)	E_γ (MeV±keV)	Branching (%)	log ft[a]	References
β_0^-	4.39±0.05[b]		67 ±3	5.25	Pe 57
β_1^-	3.96±0.04	0.438± 3[c]	32 ±2	5.38	Ge 55, Ge 56, Ov 56, Pe 57
β_2^-	2.4 ±0.1	1.647±16[c, d]	1.00±0.15	5.88	Pe 57
		>2.0	<0.2		Pe 57
		3.0	<0.06		Ov 56, also Ge 55, Ge 56

[a] A super-allowed branch (see Ki 55, Fe 55) does not occur; Pe 57.
[b] This value is in better agreement with Q_m than the results of earlier measurements: 4.21±0.01 MeV (Br 50d), and 3.9±0.3 MeV (Ge 55, Ge 56).
[c] The 0.438 and 1.647 MeV γ rays are coincident; their intensity ratio is 100: (3.0±0.3), Pe 57; see also Go 56. The 0.438 MeV γ ray is coincident with β_1^-, the 1.647 MeV γ ray with β_2^-.
[d] In Ov 56, the 1.63 MeV γ ray is ascribed to the ^{20}F decay on the basis of a half-life measurement and a β-γ coincidence experiment.

TABLE 23.6

Gamma rays (MeV±keV) from ^{23}Na(n, n'γ)^{23}Na

Fr 58 E_n = 0.5–3.7 MeV	Li 61 E_n = 0.5–3.2 MeV	Mo 56c E_n = 5.1 MeV	Wo 56 E_n = 2.5 MeV	Assignment[a]
0.438± 5	0.44	0.439	0.45± 20	0.44 → 0
		0.650		2.71 → 2.08
1.643± 8	1.61	1.63	1.69± 20	2.08 → 0.44
1.954±15	1.90			2.39 → 0.44
2.088±15	2.05	2.07	2.2 ±100	2.08 → 0
2.27 ±20				2.71 → 0.44
2.386±10	2.37			2.39 → 0
2.56 ±20				2.98 → 0.44
2.635±15	2.64			2.64 → 0
2.979±15	2.96	3.01		2.98 → 0

[a] Excitation energies in MeV.

at E_n = 0.8 MeV (Mo 56c), have not been found in other ^{23}Na(n, n')^{23}Na* experiments. See also Le 61a, An 60d.

The branching ratio of the decay to ^{23}Na(0) and (1) is 0.19±0.04 for ^{23}Na*(2.08), 3.0±0.6 for ^{23}Na*(2.39), and ≈ 1 for ^{23}Na*(2.98) (Fr 58a); the values given in Li 61 are 0.11 for ^{23}Na*(2.08) and 13 for ^{23}Na*(2.39); see fig. 23.2.

At E_n = 2.45 MeV, an inelastic neutron group has been observed, corresponding to ^{23}Na* = 0.46±0.05 MeV (Cr 56a). The angular distribution and cross section for inelastic scattering to ^{23}Na*(0.44), at $E_n = 3.49$, 3.75, and 4.00 MeV, is given in Sh 59b; the cross section for scattering to the 0.44, 2.08, 2.39, 2.64 and 2.98 MeV levels is reported in Li 61. Elastic scattering angular distribution, La 57b.

For resonances, see ^{24}Na.

H. ^{23}Na(p, p′)^{23}Na

The levels in ^{23}Na, observed from inelastic proton scattering, are listed in table 23.7. Other values for the excitation energy of ^{23}Na(1) are 439±1 keV (Do 53; electrostatic analysis), 437±5 keV (Sc 56c; magnetic analysis), 444±5 keV (Ne 54; scint. spectrometer), and 450±10 keV (St 54; scint. spectrometer)

TABLE 23.7

Levels in ^{23}Na from ^{23}Na(p, p′)^{23}Na and ^{23}Na(d, d′)^{23}Na

^{23}Na*(MeV ± keV)					l
(p, p′)[a]	(p, p′)[b]	(d, d′)[c]	(d, d′)[d]	(d, d′)[e]	(d, d′)[e]
0.440 ± 3			0.439		
2.078 ± 4	2.10	1.9	2.073	2.07 ± 30	2
2.393 ± 7	2.37		2.400	(2.41 ± 40)	
2.641 ± 7					
2.705 ± 7	2.69	2.6	2.699	2.71 ± 40	2
2.983 ± 7	3.01		2.997	3.00 ± 30	
3.678 ± 7	3.70	3.75	3.689		
3.850 ± 8				3.83 ± 60	2
3.915 ± 10	3.92		3.925		
4.431 ± 10	4.45	4.45	4.457		
4.778 ± 10	all ± 40		all ± 40		
		5.5			
		6.3			
		7.2			

[a] Bu 57 ; $E_p = 7.0$–7.5 MeV, magnetic analysis.
[b] St 52 ; $E_p = 7.26$ MeV, scintillation spectrometer.
[c] Bo 50 ; $E_d = 14$ MeV, Al-absorption.
[d] Vo 58 ; $E_d = 14.8$ MeV, magnetic analysis.
[e] El 56a; $E_d = 8$ MeV, magnetic analysis.

The 0.44 MeV γ transition has been investigated at several resonances. The internal conversion coefficient is $\alpha = (4.9 \pm 0.6) \times 10^{-5}$, indicating that the transition is predominantly dipole (Be 56a). Gamma-ray angular distribution measurements yield $J^\pi = (\frac{3}{2}, \frac{5}{2})^+$ for ^{23}Na* = 0.44 MeV (Ro 56b, Be 56a). The ratio of the Coulomb excitation cross sections for protons and α particles implies E2 excitation, and thus even parity for this level. The Coulomb excitation cross section yields the partial mean life for E2 decay, $\tau_m(\mathrm{E2}) = 4.3 \times 10^{-10}$ sec (Te 56). The mean life of the level, $\tau_m = (1.8^{+0.4}_{-0.3}) \times 10^{-12}$ sec, has been measured in a resonance fluorescence experiment (Ra 59a). See also Kr 56 ($\tau_m = 10^{-12}$–10^{-13} sec), Sw 56 ($\tau_m < 2.5 \times 10^{-11}$ sec). An E2/M1 mixing amplitude $x = \pm 0.056$ follows from these τ_m(E2) and τ_m values. The angular distribution of the fluorescence radiation indicates that $x > 0$ (Ra 59a). Measurement of the angular distribution and polarization of the 440 keV γ ray yields $x = +0.045 \pm 0.015$ (Mi 60a).

The 2.08 MeV level in ^{23}Na is excited at the $E_p = 2.89$ MeV resonance. The branching ratio of the decay to ^{23}Na(1) and (0) is about 20. The ground-state transition is anisotropic, excluding $J = \frac{1}{2}$ for ^{23}Na* = 2.08 MeV (Go 57b).

The decay of ^{23}Na levels up to 4 MeV has been investigated with protons up to 6.4 MeV. The results are summarized in fig. 23.2 (Kr 60a, Fr 58a).

For resonances, see ^{24}Mg.

I. ^{23}Na(d, d')^{23}Na

Deuteron groups corresponding to levels in ^{23}Na are listed in table 23.7 (Bo 50, El 56a, Vo 58). The angular distributions of the groups to ^{23}Na* = 2.08, 2.71, and 3.85 MeV are compatible with $l = 2$, (El 56a). Theory, El 60.

J. ^{23}Na(^{3}He,^{3}He')^{23}Na

The ratio of the radiation yield for ^{3}He -and α-induced Coulomb excitation of the 0.44 MeV level, at $E(^3\text{He}) = 2.00$ MeV and $E_\alpha = 2.23$ MeV, is in agreement with the theoretical value for E2 excitation (Br 59c).

K. ^{23}Na(α, α')^{23}Na

The angular distribution of the 0.44 MeV γ ray following Coulomb excitation with 2.5 MeV α particles eliminates the possibility of a $J^\pi = \frac{3}{2}^+$ assignment to ^{23}Na* = 0.44 MeV. This establishes the $J^\pi = \frac{5}{2}^+$ assignment to this level, $J = \frac{7}{2}$ is ruled out by a comparison of its mean life, τ_m, and its partial mean life τ_m(E2), Te 56; see also reaction H.

For the yield ratio of ^{3}He- and α-induced reactions: see reaction J (Br 59c).

L. ^{23}Na+heavy ions (^{14}N, ^{16}O, ^{20}Ne)

A 0.44 MeV γ ray has been observed from Coulomb excitation by 15.6 MeV ^{14}N (Al 56), 9–11 MeV ^{16}O (Go 60d), and 9–11 MeV ^{20}Ne ions (St 60).

The reduced transition probability B(E2) for excitation of ^{23}Na(1) is $(1.1 \pm 0.2) \times 10^{-50}$ e^{2}cm^4 (St 60), 0.95×10^{-50} e^{2}cm^4 (Go 60d), yielding a partial mean life $\tau_m(\text{E2}) = (6.2 \pm 0.6) \times 10^{-10}$ sec, and 7.2×10^{-10} sec, respectively.

M. ^{23}Mg(β^+)^{23}Na $\qquad Q_m = 4078 \pm 15$

See ^{23}Mg.

N. ^{24}Mg(γ, p)^{23}Na $\qquad Q_m = -11692.6 \pm 2.2$

Cross section for 28 MeV bremsstrahlung, Jo 55. A theoretical discussion of the ratio of (γ, p) and (γ, n) cross sections is given in Mo 55.

O. ^{24}Mg(n, d)^{23}Na $\qquad Q_m = -9467.8 \pm 2.2$

A 0.45 ± 0.02 MeV γ ray observed from a natural Mg target, at $E_n = 14$ MeV, is attributed to this reaction (De 60).

P. ^{25}Mg(d, α)^{23}Na $Q_m = 7047.1 \pm 2.3$

The measured value $Q_0 = 7.019 \pm 0.013$ MeV differs from the value computed from other mass links between ^{23}Na and ^{25}Mg. Levels in ^{23}Na at 0.427 ± 0.018 and 2.073 ± 0.015 MeV have been observed from this reaction (En 52).

Q. ^{27}Al(γ, α)^{23}Na $Q_m = -10098.0 \pm 2.3$

Cross section for 21.5 MeV bremsstrahlung, To 58.

R. Not reported:

^{21}Ne(t, n)^{23}Na	$Q_m = 10674.9 \pm 2.1$
^{21}Ne(^{3}He, p)^{23}Na	$Q_m = 11439.4 \pm 2.0$
^{21}Ne(α, d)^{23}Na	$Q_m = -6913.1 \pm 2.0$
^{22}Ne(^{3}He, d)^{23}Na	$Q_m = 3297.0 \pm 1.5$
^{22}Ne(α, t)^{23}Na	$Q_m = -11022.6 \pm 1.5$
^{24}Mg(d, ^{3}He)^{23}Na	$Q_m = -6199.4 \pm 2.2$
^{24}Mg(t, α)^{23}Na	$Q_m = 8120.1 \pm 2.3$
^{25}Mg(n, t)^{23}Na	$Q_m = -10540.9 \pm 2.4$
^{25}Mg(p, ^{3}He)^{23}Na	$Q_m = -11305.4 \pm 2.3$
^{26}Mg(p, α)^{23}Na	$Q_m = -1825.7 \pm 2.7$

REMARKS

The decay of ^{23}Na levels up to 5 MeV, as summarized in fig. 23.2, is consistent with the results of strong-coupling collective calculations. Proposed rotational bands are indicated in fig. 23.2 (Kr 60a, Br 61c). See also Pa 58a, Li 58c.

^{23}Mg

(Fig. 23.3, p. 31; table 23.8, p. 32)

A. ^{23}Mg(β^+)^{23}Na $Q_m = 4078 \pm 15$

The weighted mean of the reported half-lives is 12.04 ± 0.09 sec (Wh 39, Hu 43, Bo 51, Hu 54, Mi 58, Wa 60a; see also Ba 46, Ed 52).

The decay mainly proceeds to ^{23}Na(0); the β^+ end point is 2.99 ± 0.09 MeV (Bo 51), 2.95 ± 0.07 MeV (Hu 54), 3.09 ± 0.01 MeV (Wa 60a). The decay is super-allowed ($\log ft = 3.7$), determining the spin and parity of ^{23}Mg as $\frac{3}{2}^+$.

Gamma-annihilation coincidence measurements indicate a $(9.1 \pm 0.5)\%$ branch to ^{23}Na* $= 0.44$ MeV (Ta 60c); $\log ft = 4.5$. A $(6.5 \pm 2.5)\%$ intensity is reported in St 59d.

B. ^{23}Na(p, n ^{23}Mg $Q_m = -4861 \pm 15$

A slow-neutron threshold has been observed at $E_p = 5.061 \pm 0.007$ MeV, giving $Q = -4.850$ MeV (Ki 55a, Go 58f).

Cross section, Ta 58. For resonances, see ^{24}Mg.

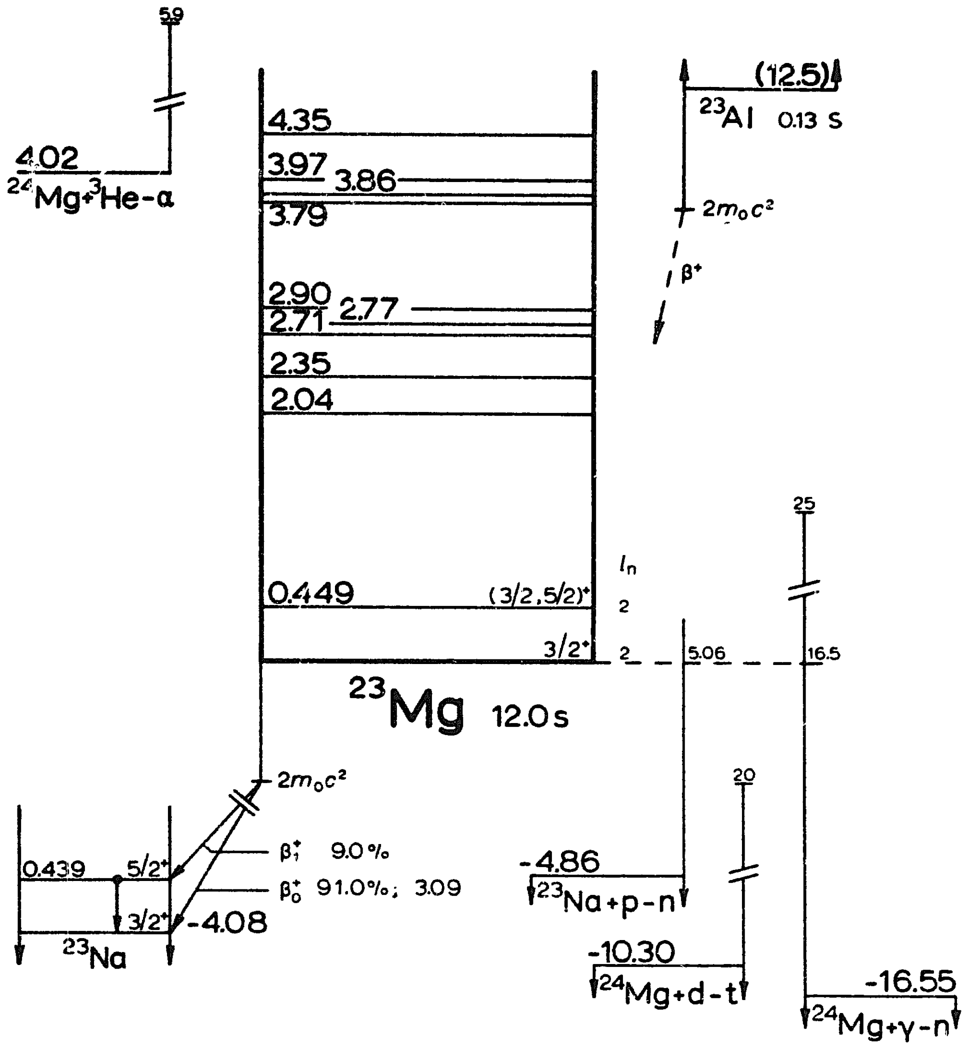

Fig. 23.3. Energy levels of ^{23}Mg.

C. ^{24}Mg(γ, n)^{23}Mg $\qquad Q_m = -16553 \pm 15$

The threshold is measured as 16.4 ± 0.3 MeV (Be 47), 16.2 ± 0.3 MeV (Mc 49), and 16.55 ± 0.25 MeV (Sh 51a).

See ^{24}Mg for yield and resonances.

D. ^{24}Mg(d, t)^{23}Mg $\qquad Q_m = -10296 \pm 15$

Differential cross sections, Vl 61.

E. ^{24}Mg(^{3}He, α)^{23}Mg $\qquad Q_m = 4024 \pm 15$

At $E(^3\mathrm{He}) = 5.7$ and 5.9 MeV, the ground-state Q value has been measured as 4.048 ± 0.015 MeV, and α-particle groups have been observed to ^{23}Mg levels at 0.451 ± 0.010, 2.048 ± 0.010, 2.356 ± 0.015, 2.712 ± 0.010, 2.768 ± 0.010, 2.904 ± 0.010, 3.792 ± 0.010, 3.856 ± 0.010, 3.968 ± 0.010, and 4.353 ± 0.015 MeV (Hi 59a), and at $E(^3\mathrm{He}) = 5.23$ MeV, to levels at 0.449 ± 0.005, 2.038 ± 0.008, and 2.350 ± 0.008 MeV (De 59). At $E(^3\mathrm{He}) = 5.5$ MeV angular distributions have been measured of α-particle groups leading to ^{23}Mg(0) and (1). Interpretation in terms of stripping plus heavy particle pick-up leads to $J^{\pi} = (\frac{3}{2}, \frac{5}{2})^+$ for both states (Pa 61c).

F. Not reported:

^{20}Ne(α, n)^{23}Mg	$Q_m = -\ 7240 \pm 15$
^{21}Ne(^{3}He, n)^{23}Mg	$Q_m = \ 6578 \pm 15$
^{23}Na(^{3}He, t)^{23}Mg	$Q_m = -\ 4097 \pm 15$
^{24}Mg(p, d)^{23}Mg	$Q_m = -14328 \pm 15$
^{25}Mg(p, t)^{23}Mg	$Q_m = -15402 \pm 15$

TABLE 23.8

Energy levels of ^{23}Mg

E_x (MeV ± keV)	J^{π}	$\tau_{\frac{1}{2}}$	Decay	Reactions
0	$\frac{3}{2}^+$	12.04 ± 0.09 sec	β^+	A, B, C, D, E
0.449 ± 4	$(\frac{3}{2}, \frac{5}{2})^+$			D, E
2.042 ± 6				D, E
2.351 ± 7				D, E
2.712 ± 10				D, E
2.768 ± 10				D, E
2.904 ± 10				E
3.792 ± 10				E
3.856 ± 10				E
3.968 ± 10				E
4.353 ± 15				E

^{23}Al

(Not illustrated)

A 0.13 sec half-life, observed from bombardment of natural magnesium with 23 MeV protons, might be assigned to ^{23}Al; see Ty 54 and ^{22}Mg, reaction A.

Coulomb energy systematics yield an estimated ^{23}Al$-$^{23}Mg mass difference of 12.5 MeV. The ^{23}Al half-life calculated from this mass difference and from the log ft values found for the analog ^{23}Ne(β^-)^{23}Na decay, is in reasonable agreement with the experimental half-life, if the possibility of ^{23}Al decay to higher excited ^{23}Mg states is taken into account.

^{24}Na

(Fig. 24.1, p. 34; table 24.1, p. 33)

A. (a) ^{24}Na(β^-)^{24}Mg $\qquad Q_m = 5516.3 \pm 2.7$

The weighted mean of fourteen half-life determinations is 14.968 ± 0.009 hr (Wi 49, as corrected in Sr 51, So 50, Co 50a, Si 51, Sr 51, Bl 52, Lo 53, To 55c, Ru 56a, Wr 57, Ca 58a, Da 58, Po 59, Wo 60).

The decay predominantly proceeds to the 4.12 MeV level of ^{24}Mg followed by two γ rays in cascade through the 1.37 MeV level. The β^- end point is 1.391±0.002 MeV (averaged from Si 46, Po 57, Da 58); log $ft = 6.1$. The allowed character of the decay has been confirmed experimentally by the linearity of the Fermi-Kurie plot (Si 46, Po 57; a small deviation from linearity

TABLE 24.1

Energy levels of ^{24}Na

E_x (MeV±keV)	J^π	$\tau_{\frac{1}{2}}$	Decay	Reactions
0	4+	14.968±0.009 hr	β^-	many
0.473± 3	1+	19.6 ±0.4 msec	(β^-) γ	C, F, G, K
0.564± 8	(2)+		γ	C, F, G
1.347± 4	1+		γ	C, F, G
1.844± 8	(1, 2)+		γ	C, F
1.884± 8	(≤4)+		γ	C, F
2.464± 8	(≤3)−		γ	C, F
2.561± 8	(≤4)+		γ	C, F
2.98 ±20	(≤4)+			F
3.22 ±20	(≤6)+			F
3.37 ±20	(≤3)−			F
3.409± 8			γ	C, F
3.582± 9	(1, 2)+		(γ)	C, F
3.623± 9	(≤4)+		γ	C, F
3.648± 9			(γ)	C, F
3.738± 8				F
3.850± 8			γ	C, F
3.899± 8			(γ)	C, F
3.929± 8	(≤3)−		(γ)	C, F
3.97 ±20				F
4.184± 8			(γ)	C, F
4.202± 8	(≤3)−		(γ)	C, F
4.219± 8			(γ)	C, F
4.44 ±20	(≤3)−		γ	C, F
4.53 ±20	(≤3)−			F
4.558± 9			γ	C, F
4.62 ±20	(≤3)−			F
4.69 ±20	(≤3)−			F
4.75 ±20	(≤3)−		γ	C, F
4.95 ±20	(1, 2)+			F
5.13 ±80			γ	C, F
6.930± 4	2+			D
6.962– 7.78; 230 levels, see reactions				D, C
11.95 –14.40; 12 levels, see reaction				E

is reported in Da 58), and by the isotropy of the β–γ angular correlation (Be 50, St 51a, St 58a, St 59a). A Compton-spectrometer determination of the γ-ray energies (Mo 59c) yields 2.7527±0.0001 MeV (also He 52: 2.7535±0.0010 MeV, and Kn 59: 2.750±0.003 MeV), and 1.3676±0.0002 MeV (also He 52: 1.3630±0.0010 MeV, and Kn 59: 1.368±0.001 MeV). The intensity

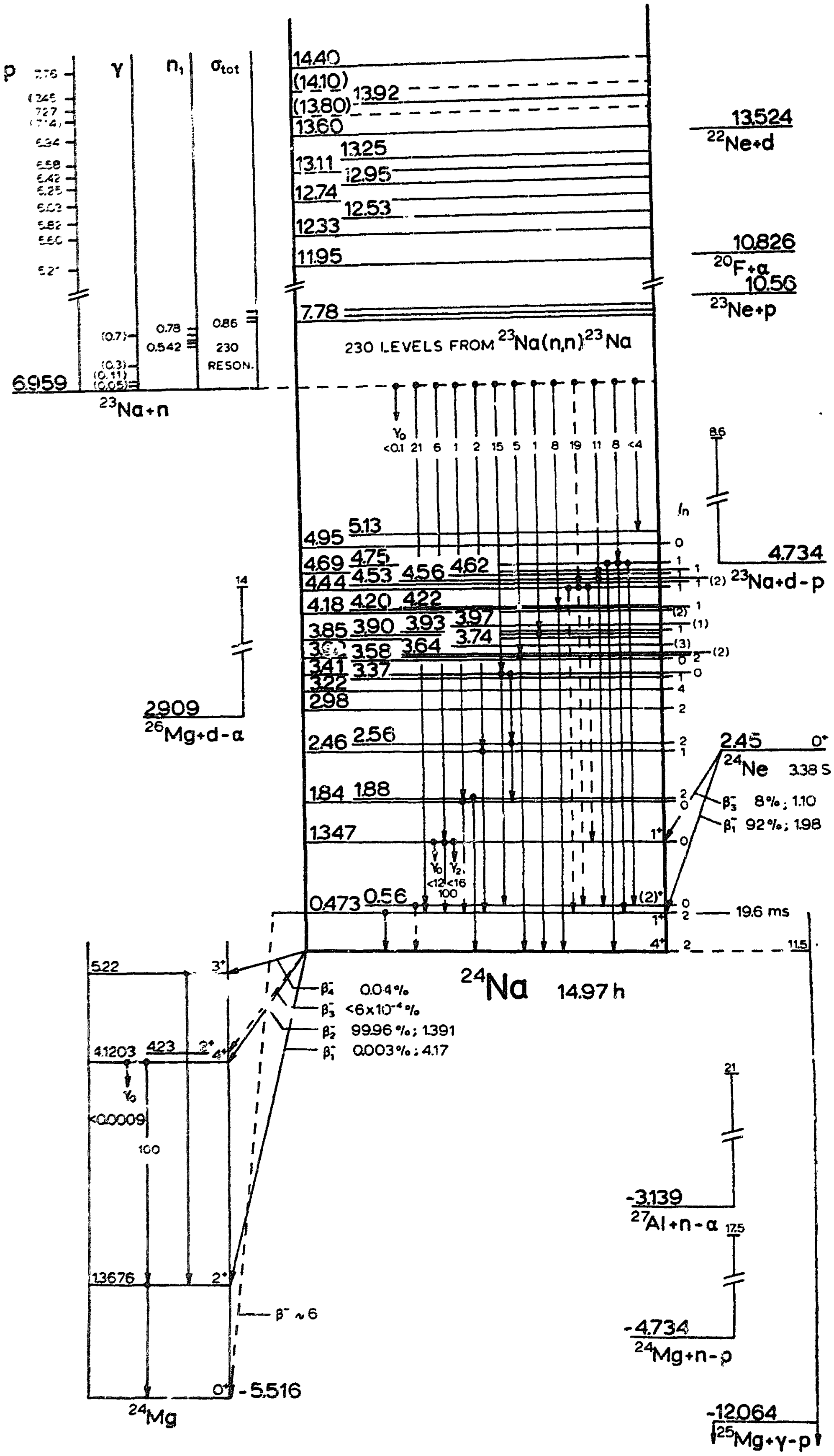

Fig. 24.1. Energy levels of ^{24}Na.

of a 4.12 MeV cross-over γ ray is $\leq 9 \times 10^{-4}$ percent (Gu 58a; also Bi 50).

A 3.85 ± 0.04 MeV γ ray with a 0.09 ± 0.02 percent intensity indicates a β^- transition to the 5.22 MeV level of ^{24}Mg. The intensity of a 5.22 MeV γ ray to the ground state is $< 2 \times 10^{-5}$ percent (Ar 60; also Gu 58a, Tu 51, Be 51, To 55b). Log $ft = 6.6$.

A 0.003 percent high-energy β^- component, proceeding to the 1.37 MeV level (end point 4.17 MeV) has been reported (Tu 51; also Gr 50a). Log $ft = 12.7$.

The intensity of the 4.24 MeV γ ray, following the β^- decay to ^{24}Mg* $= 4.24$ MeV, is $(1.5 \pm 0.5) \times 10^{-3}$ percent per disintegration (Ar 60). Log $ft = 10.7$.

Both the 2.75 and 1.37 MeV γ rays have E2 character. This follows from the polarization-direction correlation of the two γ rays (Es 56), the γ–γ angular correlation (Wa 41, Br 50c, Ch 50), and the internal pair-formation coefficients: $(7.1 \pm 0.2) \times 10^{-4}$ for $E_\gamma = 2.75$ MeV (Bl 52; also Ra 49, Mi 50a, Cl 51, Sl 52) and $(0.6 \pm 0.1) \times 10^{-4}$ for $E_\gamma = 1.37$ MeV (Bl 52, also Sl 52). The E2 character of $E_\gamma = 2.75$ MeV is also consistent with the shape of the internal pair spectrum (Bl 52), the angular correlation between e$^+$ and e$^-$ (Si 52), and the internal conversion coefficient $\alpha = 3 \times 10^{-6}$ (Si 50). The E2 character of $E_\gamma = 1.37$ MeV is confirmed by measurements of the mean life of ^{24}Mg(1); the results from different methods are compared in table 24.9. The experimental results summarized above and the $J^\pi = 4^+$ value (St 58b, table 2) of the ^{24}Na ground state uniquely determine the spin sequence $J^\pi = 0^+, 2^+, 4^+$ for ^{24}Mg* $= $, 1.37 and 4.12 MeV. The same spin assignments can be obtained from the γ–γ angular correlation measurements alone.

Measurements of the β–γ circular polarization correlation (Sc 57, Bo 58, Ma 59, St 59b, Bl 61c), and of the electron-neutrino angular correlation (Bu 59a) are consistent with pure axial vector interaction. For longitudinal polarization measurements, see So 61a.

Theory, see Ga 57, Be 58d, Bo 59b, Bo 60b.

(b) ^{24}Na^m $(\beta^-)^{24}$Mg: see reaction G.

B. ^{22}Ne(d, γ)^{24}Na $\qquad Q_m = 13\,524.3 \pm 2.7$

At $E_d = 1.6$ MeV, no ^{24}Na activity has been observed from deuteron bombardment of natural neon; $\sigma < 0.4$ μb (Al 55b).

C. ^{23}Na(n, γ)^{24}Na $\qquad Q_m = 6\,958.9 \pm 2.6$

Two thermal neutron capture cross section measurements are reported yielding 505 ± 10 mb, 536 ± 10 mb (see Hu 58); a recent measurement gives 531 ± 8 mb (Wo 60). Capture cross sections at different energies, ranging from $E_n = 25$ keV to 14.5 MeV, are given in Hu 58, Bo 58b, Ko 58d, Ly 59a. Incompletely resolved resonances have been found in the range $E_n = 20$–1000 keV (Ba 59).

TABLE 24.2

Gamma rays from thermal neutron capture in ^{23}Na

Gr 58c[a]		Ki 51[b]		Mo 56a[c]		Bu 56e[b]		Gr 58c
E_γ (MeV ± keV)	I_γ[e]	E_γ (MeV ± keV)	I_γ[e, f]	E_γ (MeV ± keV)	I_γ[e]	E_γ (MeV ± keV)	I_γ[e]	Assignment[g]
6.96	< 0.1							
6.400 ± 15	22	6.41 ± 30	13			6.42 ± 30	21	C → 0.56
5.61 ± 20	6	5.61 ± 30	5			5.62 ± 30	5.7	C → 1.35
						(5.35 ± 50)	(0.5)	
(5.12 ± 50)	0.8	5.13 ± 30	1			(5.08 ± 50)	(1.2)	C → 1.84
(4.90 ± 50)	1.2					(4.91 ± 70)	(1.3)	
(4.70 ± 50)	0.9					(4.72 ± 50)	(1.3)	4.75 → 0
4.56 ± 40	2.1					(4.54 ± 50)	(1.3)	C → 2.46
(4.30 ± 50)	0.5					(4.29 ± 50)	(0.7)	4.75 → 0.47
4.18 ± 40	2.1							4.20 → 0; 4.75 → 0.56
3.985 ± [illegible]	17.2	3.96 ± 30	8			4.03 ± 50	14.6	4.44 → 0.47; 4.56 → 0.56
3.86 ± 40	5.9	3.85 ± 30	5					3.90 → 0; 4.44 → 0.56
(3.68 ± 50)	1.3							
3.617 ± 20 3.56 ± 30	18	3.60 ± 30 3.56 ± 20	7 8	3.590 ± 25	18	3.64 ± 50	13.2	C → 3.41; 3.62 → 0
						3.40 ± 50	(2.3)	
3.30 ± 20	5					(3.31 ± 70)	(5)	C → 3.62
3.10 ± 20	9.5			3.070 ± 20	7	(3.11 ± 50)	(8.2)	C → 3.90; 4.44 → 1.35
		Br 56e[d]						
2.84 ± 20	7							3.41 → 0.56
2.68 ± 20	8.5							C → 4.20
2.52 ± 20	21	2.53 ± 30	19	2.510 ± 20	≈15			C → 4.44
2.41 ± 30	10.5					(2.36 ± 50)	(13.5)	C → 4.56
2.21 ± 30	7.5			2.210 ± 15	8	(2.20 ± 50)	(22.6)	C → 4.75
2.020 ± 15	11.5	2.02 ± 30	12	2.030 ± 10	13			
(1.95 ± 30)	4							2.46 → 0.47
(1.87 ± 30)	5.5			1.900 ± 20	≈3			C → 5.13; 1.88 → 0
1.66 ± 10	7.5	1.66 ± 50	5	1.630 ± 8	10			
1.35 ± 10	6.5	1.35 ± 30	6					1.84 → 0.47
0.875 ± 10	44	0.86 ± 20	34	0.877 ± 5	30 ± 10			1.35 → 0.47
(0.790 ± 15)	4.3							1.35 → 0.56
(0.710 ± 15)	5							2.56 → 1.84
0.475 ± 10	74	0.48 ± 20	60	0.473 ± 4	50 ± 10			0.47 → 0
				≈0.090				0.56 → 0.47

[a] Magnetic Compton spectrometer.
[b] Magnetic pair spectrometer.
[c] Magnetic lens spectrometer.
[d] Two-crystal scintillation spectrometer.
[e] Intensities in gammas per 100 captures.
[f] As revised in Ba 58c.
[g] The capturing state is indicated by C; excitation energies are in MeV.

The observed thermal neutron capture γ rays are listed in table 24.2, together with the intensities and the ^{24}Na levels between which they presumedly occur (Gr 58c, Ki 51, Bu 56e, Br 56e, Mo 56a). The 6.96 MeV ground-state transition has not been observed; its intensity is < 0.1 per 100 captures. Notable is the absence of the 0.56 MeV γ ray. The upper limit for its intensity is 3 per 100 captures. The 0.56 MeV level decays through the 0.47 MeV level (Gr 55a). A level at 4.44 MeV is proposed in addition to the levels known from ^{23}Na(d, p)^{24}Na; most of the observed γ rays can then be fitted in the ^{24}Na level scheme (Gr 58c). Later measurements on the ^{23}Na(d, p)^{24}Na reaction confirm the existence of a level at 4.44 ± 0.02 MeV (Da 61a). The 1.34 MeV level is not de-excited to the ground state; this would conflict with the spin assignments found from reaction G. For assignments see also Mo 56a.

The new levels recently found from the ^{23}Na(d, p)^{24}Na reaction (Da 61a) indicate that a revision of the Gr 58c γ-ray assignments would be desirable. In particular, it is probable that the strong 3.59 MeV γ ray excites, not the 3.41 MeV level, but the new odd-parity level at 3.37 MeV.

D. ^{23}Na(n, n)^{23}Na $E_b = 6958.9 \pm 2.6$

For cross section, see Hu 58, La 60a.

With high resolution ($\Delta E_n \leq 0.5$ keV) 230 resonances in the total cross section have been found for $E_n < 860$ keV. The energies and probable values of J, Γ_n, and l_n are listed in Hi 60b (86 resonances with $E_n < 350$ keV), Hi 61b (71 resonances in the range $E_n = 350$–630 keV), and Hi 61i (73 resonances in the range $E_n = 630$–860 keV). Below 250 keV, most of the levels are p-wave levels. Above 250 keV, the analysis shows a few s-wave levels, a small number of p-wave levels and a large number of d- and f-wave levels. A plot of the number of resonances with energies $\leq E_n$ as a function of the neutron energy shows an essentially linear distribution up to $E_n = 860$ keV. The reduced neutron widths and the strength function are discussed (Hi 60b, Hi 61b, Hi 61i).

Only one resonance has been found for $E_n < 50$ keV. The shape of this resonance, with a peak cross section $\sigma = 600$ b, is best fitted with the parameters $E_n = 2.95$ keV, $\Gamma_n = 0.22$ keV, $J = 2$, and $l_n = 0$, if strong interference is assumed with a bound level located at $E_n = -30$ keV, with $J = 2$, $l_n = 0$ (Hi 60b). Earlier lower resolution experiments indicated $J^\pi = 1^+$, a lower cross section, a larger width, and $E_n = 2.85 \pm 0.04$ keV (Ly 58, Go 58a, Bl 58a); $\Gamma_\gamma < 0.34 \pm 0.01$ eV (Ly 58). The second resonance, at $E_n = 54.1$ keV, has $J = 3$, $l_n = 1$ and $\Gamma_n = 0.75$ keV (Hi 60b, Me 59a, Bl 58b, Cr 57).

In the energy range $E_n = 0.44$–0.80 MeV, the inelastic scattering cross section shows resonances at $E_n = 542$, 602, 633, 710, and 780 keV (Ha 56). See ^{23}Na for γ rays from inelastic scattering.

E. ^{23}Na(n, p)^{23}Ne $Q_m = -3597 \pm 5$ $E_b = 6958.9 \pm 2.6$

The cross section in the range $E_n = 3.3$–8.2 MeV shows poorly resolved resonances at $E_n = 5.21$, 5.60, 5.82, 6.03, 6.25, 6.42, 6.58, 6.94, (7.14), 7.27, (7.45), and 7.76 MeV, corresponding to ^{24}Na* = 11.95, 12.33, 12.53, 12.74, 12.95, 13.11, 13.25, 13.60, (13.80), 13.92, (14.10), 14.40, all ± 0.05 MeV (Wi 58, Bo 57a). Cross section in the range $E_n = 5.7$–20.4 MeV (Bu 61b), and at $E_n = 14$ MeV (Al 61).

F. ^{23}Na(d, p)^{24}Na $\qquad Q_m = 4734.2 \pm 2.6$

The ground-state Q value is 4.731 ± 0.007 MeV (Sp 52), 4.723 ± 0.008 MeV (Mi 52), 4.731 ± 0.010 MeV (Pi 60), 4.736 ± 0.005 MeV (Te 61). At $E_d = 1.5$–2.2 MeV, nineteen levels in ^{24}Na have been found by magnetic analysis (Sp 52). Additional levels have been reported in Da 61a, El 60c; see table 24.3, also

TABLE 24.3

Levels in ^{24}Na from ^{23}Na(d, p)^{24}Na

^{24}Na* [a] (MeV ± keV)	l_n	$(2J+1)\theta_n^2$ [k] × 10^3	^{24}Na* [a] (MeV ± keV)	l_n	$(2J+1)\theta_n^2$ [k] × 10^3
0	2[b, c, e, f, g, h]	320	3.850 ± 8[j, l]		
0.472 ± 8[l]	2[b, h; also f, g, d]	210	3.899 ± 8[j]		
0.564 ± 8[l]	0[b, d, h; also f, g]	80	3.929 ± 8	1[h, b]	50
1.341 ± 8[l]	0[b, c, f, g, h]	270	3.97 ± 20	(1)[h]	(14)
1.844 ± 8[l]	0[h]	220	4.184 ± 8[l]	(2)[h]	(100)
1.884 ± 8[l]	2[h]	160	4.202 ± 8[l]	1[h, b]	90
2.464 ± 8	1[h]	10–25	4.219 ± 8[j]		
2.561 ± 8[i, l]	2[h]	55	4.44 ± 20	1[h]	25
2.98 ± 20	2[h]	260	4.53 ± 20	1[h]	40
3.22 ± 20	4[h]	190	4.558 ± 9	(2)[h], 1[b]	(50)
3.37 ± 20	1[h(b)]	250	4.62 ± 20	1[h]	14
3.409 ± 8	0[h]	400	4.69 ± 20	1[h]	22
3.582 ± 9	0[h]	120	4.75 ± 20	1[h, b]	95
3.623 ± 9	2[h]	150	4.95 ± 20	0[h]	22
3.648 ± 9	(2)[h]	(90)	5.13 ± 80[b]		
3.738 ± 8	(3)[h]	(230)			

[a] Excitation energies with 8–9 keV error are from Sp 52 ($E_d = 1.5$–2.2 MeV); with 20 keV error from Da 61a ($E_d = 7.77$ MeV).
[b] El 60c; $E_d = 8.6$ MeV.
[c] Vo 58; $E_d = 14.8$ MeV.
[d] Di 58; $E_d = 2.95$ MeV.
[e] Ta 53; $E_d = 1.15$ MeV.
[f] Sh 54; $E_d = 3$ MeV.
[g] Br 54c; $E_d = 10$ MeV.
[h] Da 61a; $E_d = 7.77$ MeV (preliminary).
[i] In Da 61a the excitation energy is given as 2.52 ± 0.02 MeV.
[j] Levels at 3.850, 3.899, and 4.219 MeV have not been reported in Da 61a.
[k] The ground-state reduced width has been given in Vo 58, Ma 60 d. The relative reduced widths reported in Da 61a have been normalized to this value.
[l] Recently reported excitation energies (in MeV ± keV): 0.472 ± 6, 0.568 ± 4, 1.347 ± 4, 1.847 ± 8, 1.893 ± 8, 2.563 ± 10, 3.754 ± 8, 4.191 ± 10, 4.210 ± 8 (Ja 61a).

for l_n values and reduced widths (Sc 61a, Da 61a, El 60c, Vo 58, Di 58, Br 54c, Sh 54, Ta 53). Recently reported excitation energies (Ja 61a) are given in a note of table 24.3.

Absorption measurements, En 54a.

G. ^{24}Ne(β^-)^{24}Na $\qquad Q_m = 2450 \pm 40$

The half-life of ^{24}Ne, produced in the ^{22}Ne(t, p)^{24}Ne reaction, is 3.38 ± 0.02 sec.

The $(92\pm2)\%$ branch to ^{24}Na*(0.473), with end point 1.98 ± 0.05 MeV, and the $(8\pm2)\%$ branch to ^{24}Na*(1.35), with end point 1.10 ± 0.05 MeV are allowed; both have $\log ft = 4.4$, and show linear Fermi plots (Dr 56).

The first level in ^{24}Na, de-excited by a 472 ± 5 keV (100%) γ ray is isomeric (Dr 56). Its half-life is 18.3 ± 0.6 msec (Gl 61c), 19.9 ± 0.3 msec (Sc 61b), 20 ± 1 msec (Al 60a), 20 ± 2 msec (Ca 59), establishing the character of $E_\gamma =$ 473 keV as octupole (see also Dr 56, Po 59a). The allowed character of the β decay then gives $J^\pi(0.473) = 1^+$. The observed weak β^- branch, with end point ≈ 6 MeV, may be explained as a transition from this state to ^{24}Mg(0).

A 878 ± 9 keV $(8\pm2)\%$ γ ray de-excites the 1.35 MeV level to ^{24}Na*(0.47). Upper limits of γ branchings to ^{24}Na* = 0 and 0.56 MeV are 1% and 0.5%, respectively. The decay is in agreement with a $J^\pi = 1^+$ assignment to this level following from the allowed character of the β decay ($J^\pi = 0^+$ or 1^+), and the ^{23}Na(d, p)^{24}Na angular distribution measurements ($J^\pi = 1^+$ or 2^+) (Dr 56).

The 0.56 MeV level probably has $J^\pi = 2^+$, since ^{23}Na(d, p)^{24}Na angular distribution measurements yield $J^\pi = 1^+$ or 2^+, whereas a $J^\pi = 1^+$ assignment would imply an allowed β^- transition to this level.

H. ^{24}Mg(n, p)^{24}Na $\qquad Q_m = -4733.7\pm2.8$

At $E_n = 14$ MeV proton groups, corresponding to groups of levels in ^{24}Na, have been observed; angular distributions have been measured (Co 59c, Co 60b). For a comparison between the ^{23}Na(d, p)^{24}Na and ^{24}Mg(n, p)^{24}Na proton spectra, see Bl 57a.

For cross section, see Hu 58, Ke 59, De 60a, Ga 60b, Ha 61. Differential cross section, Ve 57, Za 59, Ha 61.

I. ^{25}Mg(γ, p)^{24}Na $\qquad Q_m = -12064.4\pm3.1$

The threshold has been measured as 11.5 ± 1.0 MeV (Mc 49). Cross section, Ka 54, To 51.

J. ^{26}Mg(d, α)^{24}Na $\qquad Q_m = 2908.6\pm3.5$

Cross section for E_d up to 14 MeV, Cl 46, Cl 46a.

K. ^{27}Al(n, α)^{24}Na $\qquad Q_m = -3139.1\pm2.9$

The cross section has been measured at several neutron energies in the range $E_n = 6$–21 MeV; Hu 58, and Ku 57, Ke 59, Ke 59b, Kh 59a, Po 59, Ce 60, De 60a, Ma 60b, Sc 61, Ba 61b.

L. Not reported:

^{21}Ne(α, p)^{24}Na	$Q_m = -2178.9\pm3.1$
^{22}Ne(t, n)^{24}Na	$Q_m = 7266.7\pm2.8$
^{22}Ne(^{3}He, p)^{24}Na	$Q_m = 8031.2\pm2.7$
^{22}Ne(α, d)^{24}Na	$Q_m = -10321.3\pm2.7$

^{23}Na(t, d)^{24}Na	$Q_m = 701.3 \pm 2.6$
^{23}Na(α, ^{3}He)^{24}Na	$Q_m = -13618.2 \pm 2.6$
^{24}Mg(t, ^{3}He)^{24}Na	$Q_m = -5498.1 \pm 2.7$
^{25}Mg(n, d)^{24}Na	$Q_m = -9839.6 \pm 3.1$
^{25}Mg(d, ^{3}He)^{24}Na	$Q_m = -6571.2 \pm 3.1$
^{25}Mg(t, α)^{24}Na	$Q_m = 7748.3 \pm 3.1$
^{26}Mg(n, t)^{24}Na	$Q_m = -14679.4 \pm 3.5$
^{26}Mg(p, ^{3}He)^{24}Na	$Q_m = -15443.9 \pm 3.5$

REMARKS

A theoretical discussion of the ^{24}Na spin is given in De 53a, In 53, Hi 54, Sc 54c.

^{24}Mg

(Fig. 24.2, p. 41; table 24.4, p. 42)

A. (a)	^{12}C(^{12}C, γ)^{24}Mg	$Q_m = 13930.1 \pm 1.8$	
(b)	^{12}C(^{12}C, n)^{23}Mg	$Q_m = -2623 \pm 15$	$E_b = 13930.1 \pm 1.8$
(c)	^{12}C(^{12}C, p)^{23}Na	$Q_m = 2237.5 \pm 1.5$	$E_b = 13930.1 \pm 1.8$
(d)	^{12}C(^{12}C, α)^{20}Ne	$Q_m = 4616.2 \pm 0.6$	$E_b = 13930.1 \pm 1.8$
(e)	^{12}C(^{12}C, ^{12}C)^{12}C		$E_b = 13930.1 \pm 1.8$

The yields of these reactions have been measured in the $E(^{12}\text{C}) = 9$–27 MeV range at several angles. Elastic scattering angular distributions were measured at several energies. The elastic scattering cross section and angular distribution are in accordance with Mott scattering up to $E(^{12}\text{C}) = 11$ MeV. Sharp resonances ($\Gamma_{\text{lab}} \approx 260$ keV) are observed at $E(^{12}\text{C}) = 11.30$, 11.96, 12.64, and 13.00 MeV, corresponding to ^{24}Mg* = 19.58, 19.91, 20.25, and 20.43 MeV (Al 60, Al 60c, Br 60g, Br 60h). Analysis of the cross section, yields (8$^+$) and (4$^+$) for the 19.58 and 19.91 MeV states, respectively (Ku 60f). For the theoretical meaning of these quasi-molecular states, see Vo 60.

B. ^{12}C(^{16}O, α)^{24}Mg $Q_m = 6768.6 \pm 1.8$

From magnetic analysis at $E(^{16}\text{O}) = 24$ MeV, new levels, not found from the ^{23}Na(^{3}He, d)^{24}Mg reaction (Hi 60i), have been observed at ^{24}Mg* $= 6.44 \pm 0.02$, 11.08 ± 0.03, and 11.73 ± 0.03 MeV (Hi 61). The angular distribution of the groups leading to the eight lowest ^{24}Mg states has been measured. Application of the rule stating that $\sigma(0°)$ must be zero for final states of anomalous parity, yields natural parity for all states up to $E_x = 7.35$ MeV except for the 5.22 MeV 3$^+$ level (Hi 61f).

C. ^{20}Ne(α, p)^{23}Na $Q_m = -2378.7 \pm 1.5$ $E_b = 9313.9 \pm 1.9$

Has been observed at the $E_\alpha = 3.923$ MeV resonance (table 24.5). At the other

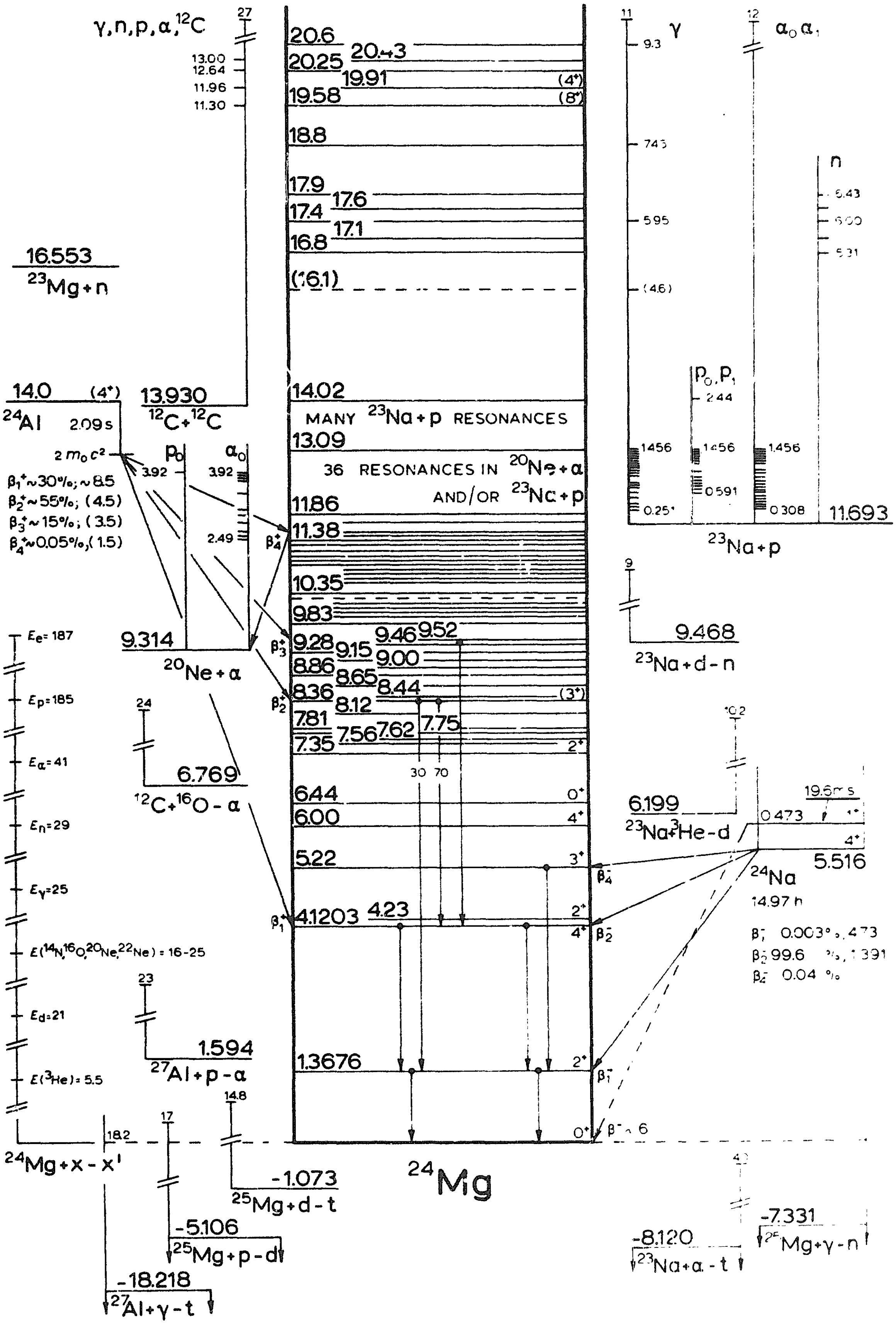

Fig. 24.2. Energy levels of ^{24}Mg; for γ decay, see also fig. 24.3.

TABLE 24.4

Energy levels of ^{24}Mg

E_x (MeV ± keV)	J^π	$\tau_{\frac{1}{2}}$ or Γ	Decay	Reactions
0	0+		stable	many
1.3676 ± 0.2	2+	(1.2±0.2) × 10⁻¹² sec	γ	many
4.1203 ± 0.2	4+		γ	many
4.232 ± 8	2+		γ	B, E, G, H, I, O, P, R, V, W, Y
5.224 ± 8	3+		γ	B, E, G, H, I, J, N, O, P, W
6.005 ± 8	4+		γ	B, E, H, O, W
6.44 ±20	0+		γ	B, E, G, O, P
7.350 ± 8	2+		γ	B, E, H, W
7.561 ±10				H, W
7.620 ±10			γ	E, H, W
7.746 ±10			γ	E, H
7.808 ±10				H
8.120 ±10				H
8.357 ±10	(3+)		γ	H, T
8.439 ±10			γ	E, H
8.654 ±10			γ	E, H
8.864 ±10			γ	E, H
9.004 ±12			γ	E, H
9.148 ±12				H
9.282 ±12				H
9.456 ±12			(γ)	H, T
9.517 ±12			(γ)	H, T
9.826 ±12			γ	E, H
9.960 ±15			γ	E, H
10.025 ±15			γ	E, H
10.055 ±15			γ	E, H
10.161 ±15			(γ)	H, K
(10.30 ±50)				H
10.353 ±20			γ	E, H
10.577 ±20				H
10.661 ±20			γ	E, H
10.723 ±20				H
10.822 ±20				H
10.916 ±20				H
11.010 ±20				H
11.08 ±30				B
11.188 ±25				H
11.313 ±25				H
11.379 ± 5	1−		α	D, H
11.450 ± 5	0+		α	D, H
11.516 ± 5	2+		α	D, H
11.725 ± 5	0+	10 ±2 keV	α	B, D
11.857 ± 5	1−	8 ±2 keV	α	D, H
11.933 ± 2			γ	E
11.968 ± 3	2+		α	D, E
11.988 ± 2	2+		γ, α	E
12.017 ± 3			γ, α	E
12.051 ± 2			γ	E
12.183 ± 2	1		γ	E

TABLE 24.4 *(continued)*

E_x (MeV ± keV)	J^π	$\tau_{\frac{1}{2}}$ or Γ	Decay	Reactions
12.259 ± 2	(2+, 3−)		γ, p, α	D, E
12.340 ± 2	3+		γ, p	E
12.388	0−	7 ±2 keV	p	E
12.400 ± 2			γ, p, α	E
12.405 ± 2			γ, p, α	E
12.455 ± 5	1−	5 ±2 keV	p, α	D, E
12.472 ± 5	2+	4 ±1 keV	p, α	D, E
12.504 ± 5	4+		p, α	D, E
12.528 ± 2		7.5 ±1.0 keV	γ, p, α	E
12.574 ± 5	2+	4 ±1 keV	p, α	C, D, E
12.638 ± 2	4		γ	E
12.657 ± 2			γ, (p)	E
12.659 ± 2	3−		(p), α	E
12.669 ± 2	2−	5 ±1 keV	γ, p, α	E
12.732 ± 2			γ, p, α	E
12.737 ± 2		5 ±1 keV	p, α	E
12.779	0+	30 ±5 keV	α	E
12.805 ± 2	2+	1.2 ±0.2 keV	γ, p, α	E
12.816 ± 2	1+	3.5 ±0.7 keV	γ, p, α	E
12.844 ± 2	(2−)	0.3 ±0.1 keV	γ, p, α	E
12.850 ± 2	(3+)	0.4 ±0.1 keV	p, α	E
12.893 ± 2	1+	0.4 ±0.2 keV	p, α	E
12.920 ± 2	1−	5.2 ±0.4 keV	γ, p, α	E
12.954 ± 2	3+	1.5 ±0.3 keV	γ, p, α	E
12.963 ± 2		2.8 ±0.6 keV	p, α	E
12.967 ± 2		3.0 ±1.0 keV	p	E
12.997 ± 2	(0−)	0.8 ±0.4 keV	p	E
13.027 ± 2	3+	0.75±0.3 keV	γ, p, α	E
13.049 ± 2	4+		γ, p, α	E
13.088 ± 2	3−	7.5 ±1.0 keV	γ, p, α	E
For higher levels, see reactions				A, E, F, L

^{20}Ne(α, α)^{20}Ne resonances in table 24.5 the proton width is smaller than 1% of the α-particle width (Go 54c).

For non-resonance data, see ^{23}Na.

D. ^{20}Ne(α, α)^{20}Ne $E_b = 9313.9 \pm 1.9$

Thirteen sharp resonances have been observed in the neon elastic cross section at four different scattering angles for E_α = 2–4 MeV. Eleven resonances are assigned to ^{20}Ne (table 24.5) and two to ^{22}Ne. The widths for α-particle emission to ^{20}Ne(1) and for proton emission to ^{23}Na(0) and (1) are smaller than 1% of the width for ground-state α-particle emission (except at the E_α = 3.923 MeV resonance, see reaction C). Reduced widths, spins, and parities in table 24.5 follow from partial wave analysis (Go 54c).

Spin and parity assignments from ^{20}Ne+α are generally in good agreement

TABLE 24.5

Resonance levels in ^{24}Mg as observed from the ^{20}Ne(α, α)^{20}Ne reaction (Go 54c)

E_α (MeV)	^{24}Mg* (MeV)	Γ (keV)	θ^2_α	J^π
2.488	11.387	(0.5)	(0.06)	1⁻
2.573	11.458	(1)	(0.06)	0⁺
2.652	11.524	(0.5)	(0.08)	2⁺
2.903	11.733	10±2	0.16	0⁺
3.062	11.865	8±2	0.14	1⁻
3.184	11.967	(0.5)	(0.01)	2⁺
3.548	12.270	(1)	(0.03)	3⁻
3.780	12.463	7±2	0.02	1⁻
3.801	12.481	5±1	0.03	2⁺
3.839	12.513	(1)	(0.08)	4⁺
3.923	12.583	6±1	0.03	2⁺
all ±0.005				

with those from ^{23}Na+p (table 24.6); ^{24}Mg excitation energies from ^{20}Ne+α are on the average about 8 keV high.

E. (a) ^{23}Na(p, γ)^{24}Mg $Q_m = 11692.6 \pm 2.2$
(b) ^{23}Na(p, p)^{23}Na $E_b = 11692.6 \pm 2.2$
(c) ^{23}Na(p, α)^{20}Ne $Q_m = 2378.7 \pm 1.5$ $E_b = 11692.6 \pm 2.2$

Resonances in these reactions, and in the yields of 0.44 MeV and 1.63 MeV γ rays from the ^{23}Na(p, p')^{23}Na(1) and ^{23}Na(p, α')^{20}Ne(1) reactions, are given in table 24.6. The table covers the region up to $E_p = 1.5$ MeV. For resonances in the $E_p = 1.5$–2.5 MeV region, see St 54. The yield of γ_0 and γ_1 has been measured in the $E_p = 4.0$–11.0 MeV region. Broad but pronounced resonances appear at $E_p = (4.6)$, 5.95, and 7.45 MeV (Ge 59), and 6.0 and 9.3 MeV; the latter shows considerable fine structure (Go 61b). The α-particle yield has been measured up to $E_p = 12$ MeV (Ad 61a).

For relative γ-ray yields, see references below table 24.6; also Te 54a, Ny 55.

The γ-ray branching of the 308, 511, 591, 676, 738, and 743 keV resonances and of nineteen ^{24}Mg lower levels (Gl 61a) is shown in fig. 24.3. For other measurements of the γ spectrum at the 308 keV resonance, see Ca 53, Tu 53, Ca 54a, Hi 54a, Gr 55e, Lo 59. For spectra at other resonances, see also Gr 55e, Ne 54, Pr 56.

The spin and parity assignments at the 308, 511, 594, and 675 keV resonances (Gr 55e), and at the 1392 keV resonance (Ne 54) are based on measurements of γ-ray spectra, angular distributions, γ–γ angular correlations, and partial widths. See also Si 59b, Si 59c. These investigations yield $J^\pi = 2^+$ for the 4.23 MeV ^{24}Mg level and $J = 3$ for the 5.22 MeV level. The spin and parity assignments given in St 54a are based on α_0 angular distribution measurements, those in Ba 56 mainly on p_0 and some on γ angular distribution measurements.

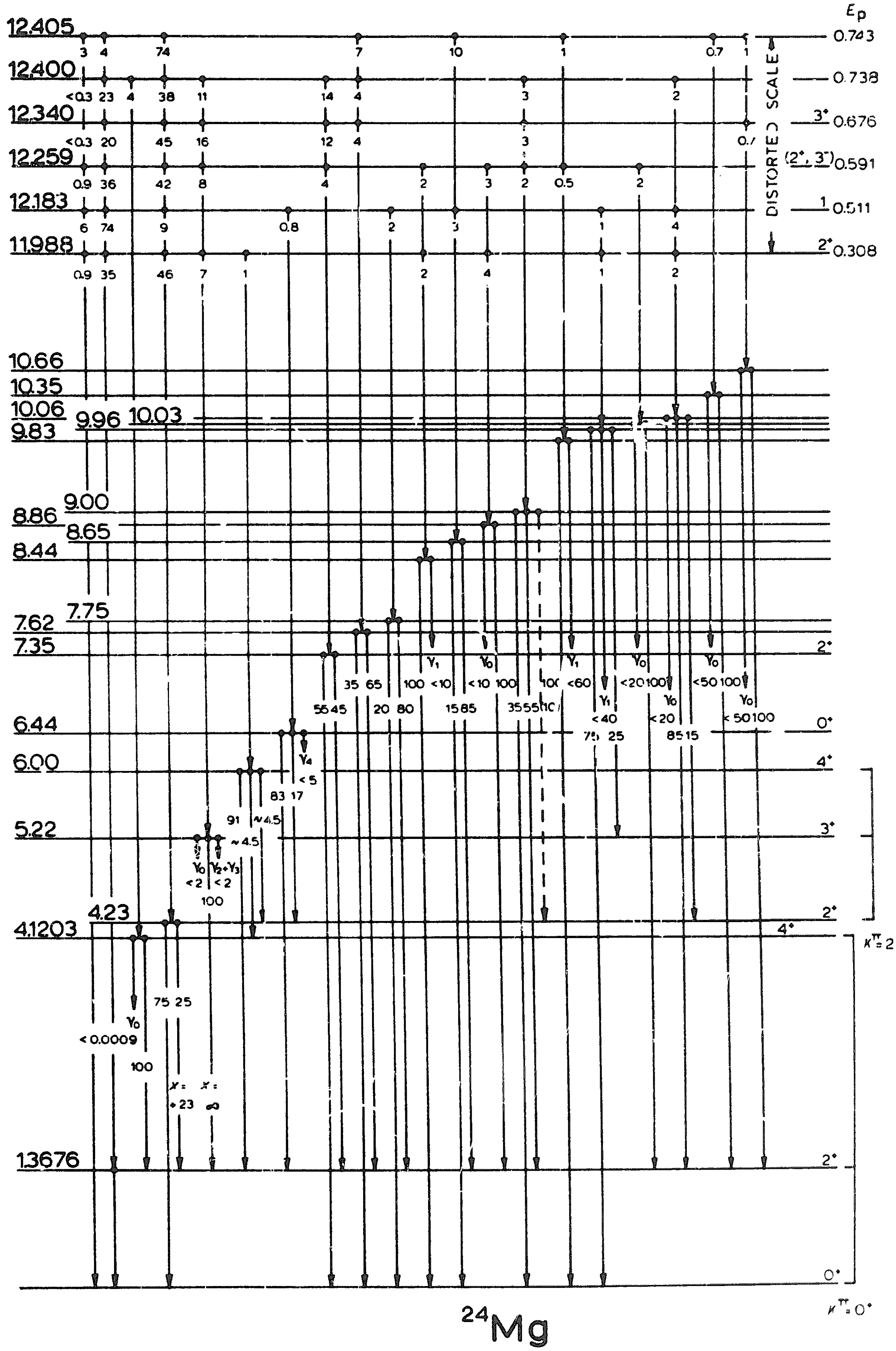

Fig. 24.3. Gamma-ray branchings of ^{24}Mg levels. The γ_0 upper limit at the 4.12 MeV level has been established from the ^{24}Na(β^-)^{24}Mg decay. The branching of the 4.23 MeV level is an average of values given by many authors, e.g. Gl 61a, Ba 60, Mi 59b, Co 61d. The branchings of the 6.00 and 6.44 MeV levels are from Co 61d. Branchings of the 5.22 MeV level and of all higher levels are from Gl 61a.

TABLE 24.6

Resonances in ^{23}Na+p

E_p (keV)	E_x (MeV)	Γ (keV)	Partial $\omega\gamma$ in eV: γ[n]	p_0[f]	p_1	α_0	α_1	J^π
250.7±0.2[a, c]	11.933	<0.02[c]	0.003[i]					
287 ±1.5[d]	11.968[k]		< 0.005[l]			0.2[l]		
308.2±0.2[a, b, c]	11.988	<0.02[c]	0.36[h]			< 0.02[l]	0.04[h]	2−[p]
338 ±1.5[d]	12.017		< 0.01[l]			0.17[l]		
373.6±0.3[a, b, c]	12.051	< 0.02[c]	0.010[i]					
511.4±0.3[a, b, c]	12.183	< 0.05[c]	0.30[h]			< 0.08[l]	< 0.003[h]	1+[p]
591.3±0.4[b, c]	12.259[k]	< 0.06[c]	0.7[h]	×		170[l]	0.14[h]	2−[p], 3−[f]
676.0±0.5[b, c]	12.340	< 0.07[c]	2.0[h]	×		<0.3[l]	< 0.01[h]	3+[p]
725[f]	12.388	7 ±2[f]		×				0−[f]
738.1±0.4[b, c, e]	12.400	< 0.09[c]	0.34[h]	×	0.05[h]		0.26[h]	
743.3±0.4[b, c, e]	12.405	< 0.1[c]	0.45[h]		0.05[h]		0.06[h]	
795[f, g]	12.455[k]	5 ±2[f]		×		110[m]		1−[f]
813[f, g]	12.472[k]	4 ±1[f]		×		60[m]		2+[f]
846[f, g]	12.504[k]	< 1[f]		×				4+[f]
871.5±0.6[e]	12.528	7.5 ±1.0[e]	13[j]	×	< 0.2[j]		≈ 1[j]	1+[f]
919[f, g]	12.574[k]	4 ±1[f]		×		150[m]		2+[f]
986.0±0.6[e]	12.638	< 0.4[e]	4.6[j]		< 1.5[j]		< 0.4[j]	4±[f]
1006.5±0.5[e]	12.657	< 0.35[e]	3[j, f]		140[j, f]			
1008.0±1.0[e]	12.659	< 0.7[e]				500[m]	80[j, f]	3−[g]
1019.0±0.6[e]	12.669	5.0 ±1.0[e]	18[j]	×	130[j]		weak[f]	2−[f]
1084.8±0.6[e]	12.732	< 0.55[e]	1[j]				4[j]	
1089.7±0.5[e]	12.737	5.0 ±1.0[e]	< 0.8[j]		60[j]	700[m]	30[j]	
1133[f, g]	12.779	30 ±5[f]				≈500[m]		0+[g]
1161.0±1.0[e]	12.805	1.2 ±0.2[e]	2.7[j]		180[j]	400[m]	170[j]	2+[f, g]
1172.4±0.5[e]	12.816	3.5 ±0.7[e]	13[j]	×	9[j]		weak[f]	1+[f]
1201.8±1.0[e]	12.844	0.3 ±0.1[f]	6.4[j]	×	weak[f]		weak[f]	(2−)[f]
1207.6±1.0[e]	12.850	0.4 ±0.1[f]	< 1[j]	×	130[j]		110[j]	(3+)[f]
1252.4±0.6[e]	12.893	0.4 ±0.2[e]	< 1[j]	×	100[j]		80[j]	1+[f, r]
1281.0±1.0[e]	12.920	5.2 ±0.4[e]	8[j]	×	1300[j]	750[m]	9[j]	1−[f, g]
1316.7±0.7[e]	12.954	1.5 ±0.3[e]	54[j]	×	weak[f]		weak[f]	3+[f]
1326.2±1.0[e]	12.963	2.8 ±0.6[e]	< 3[j]	×	1700[j]		34[j, k]	
1329.7±1.0[e]	12.967	3.0 ±1.0[e]		×				
1360.8±0.7[e]	12.997	0.8 ±0.4[e]	< 3[j]	×	100[j]		< 2[j]	(0−)[f]
1392.0±1.0[e]	13.027	0.75±0.3[e]	20[j]	×	150[j]		weak[f]	3+[f, j]
1415.1±0.8[e]	13.049	< 0.2[e]	70[j]	×	80[j]	100[m]	weak[f]	4+[f]
1456.3±0.8[e]	13.088	7.5 ±1.0[e]	10[j]	×	3000[j]	400[m]	50[j]	3−[f]

[a] Ha 55c. [b] Ku 59a. [c] Wa 60. [d] Fl 54.

[e] An 61. All energies relative to E_p = 990.8 keV for ^{27}Al(p, γ)^{28}Si resonance.

[f] Ba 56, Pr 56. The × in the p_0 column indicates that proton elastic scattering has been observed.

[g] Corrected for a systematic difference (as observed at neighbouring resonances) with the more accurate values given in An 61.

[h] Gl 61a.

[i] From relative yields in Ha 55c and Wa 60 normalized to 0.36 eV at E_p = 308 keV.

[j] Ne 54. The quoted yields might be too large by a factor of ≈ 5 compared to those given in Gl 61a; see relative yield curve in Pr 56, also Gl 61b.

[k] Levels also observed from ^{20}Ne+α elastic scattering (see table 24.5).

[l] From relative yields in Fl 54 normalized to the absolute yields in Gl 61a.

[m] From relative yield curve in Ba 56, normalized to 170 eV at E_p = 591 keV.

[n] At the 308, 511, 591, 743, 871, 1161, 1172, and (1317) keV resonances ground-state γ transitions have been observed (Gl 61a, Ne 54).

[p] Gr 55e. [q] St 54a. [r] Se 53.

The 1^+ assignment to the 1252 keV resonance in Se 53 follows from an $\alpha-\gamma$ angular correlation measurement. The odd parity assigned to the 591 keV resonance is in agreement with a polarization measurement of 10.8 MeV capture radiation (Hu 56). The angular distribution and internal conversion coefficient of the 0.44 MeV γ ray from ^{23}Na(p, p')^{23}Na have been measured at the 1281 and 1456 keV resonances (Be 56a, see ^{23}Na). For p_0 angular distribution measurements at the 871 and 919 keV resonances, see also De 56.

For non-resonance data, see Aj 59 (for ^{20}Ne) and ^{23}Na.

F. ^{23}Na(p, n)^{23}Mg $Q_m = -4861 \pm 15$ $E_b = 11692.6 \pm 2.2$

Broad resonances in the ^{23}Mg activity yield have been observed at $E_p = 5.31$, 5.61, 6.00, 6.20, and 6.43 MeV (Bl 51). For threshold determinations, see ^{23}Mg.

G. ^{23}Na(d, n)^{24}Mg $Q_m = 9467.9 \pm 2.2$

For results from angular distribution measurements, see table 24.7.

TABLE 24.7

Neutron groups from ^{23}Na(d, n)^{24}Mg

^{24}Mg* (MeV)	l_p [a]	$(2J+1)\theta_p^2$ [c] absolute	l_p [b]	$(2J+1)\theta_p^2$ [c] relative
0	–	weak		
1.37	–	weak		
4.12, 4.23	2+0	0.044, 0.012	2+0	9, 1.7
5.22	–	weak		
6.3	–	isotropic		
7.4	0 (2)	0.03 (0.07)	0	5.4
8.4	0	0.038	0 (+2)	10.1
10.5			0	32

[a] Ca 55; $E_d = 7.75$ MeV; neutron detection with nuclear emulsions.
[b] El 57; $E_d = 9.02$ MeV; neutron detection with a triple ionization chamber.
[c] As computed in Ma 60d from Ca 55 and El 57, respectively. See also Ma 60d for theoretical comments.

At $E_d = 5$ MeV, γ rays from the deuteron bombardment of sodium have been observed with a magnetic pair spectrometer at $E_\gamma = 6.42 \pm 0.04$, 7.12 ± 0.03, 7.34 ± 0.03, 7.50 ± 0.03, (7.9 ± 0.1), 8.50 ± 0.03, 8.64 ± 0.04, (8.77 ± 0.04), 9.02 ± 0.04, 9.40 ± 0.04, 9.86 ± 0.04, (10.0 ± 0.1), (10.4 ± 0.1), and 10.72 ± 0.04 MeV. Most of these might result from the ^{23}Na(d, n)^{24}Mg reaction de-exciting known ^{24}Mg levels to the ground or first excited state (Ek 60).

H. ^{23}Na(^{3}He, d)^{24}Mg $\quad Q_m = 6199.4 \pm 2.2$

The best survey of ^{24}Mg levels up to $E_x = 11.9$ MeV has been performed with this reaction. See table 24.8. The levels above 11.35 MeV check well with levels found from ^{20}Ne$+\alpha$ elastic scattering (see table 24.5).

I. ^{23}Na(α, t)^{24}Mg $\quad Q_m = -8120.1 \pm 2.3$

Angular distributions of several groups have been measured at $E_\alpha = 40$ MeV. The group to ^{24}Mg(1) is strong and has $l_p = 2$ (Vl 60).

J. ^{24}Na(β^-)^{24}Mg $\quad Q_m = 5516.3 \pm 2.7$

See ^{24}Na.

K. ^{24}Mg(γ, γ)^{24}Mg

In the fluorescence radiation from a Mg sample irradiated by betatron bremsstrahlung a γ ray is observed with $E_\gamma = 10.15 \pm 0.06$ MeV (To 60), 10.5$\pm$0.14 MeV (Bu 60; see also Bu 60b), and 10.5 MeV (Se 60). From self-absorption measurements the radiation width is determined as 4.8$\pm$1.5 eV (To 60), and 180$\pm$50 eV (Bu 60b), and the total width as 1.7$\pm$0.4 keV (Bu 60b). The angular distribution points to dipole absorption (Bu 60).

TABLE 24.8

Levels in ^{24}Mg (E_x in MeV$\pm$keV) from ^{23}Na(^{3}He, d)^{24}Mg[a]

	7.620$\pm$10	9.004 $\pm$12	10.055$\pm$15	10.916$\pm$20
	7.745$\pm$10	9.148 $\pm$12	10.161$\pm$15	11.010$\pm$20
4.122 Datum	7.808$\pm$10	9.292[b]$\pm$12	(10.30 $\pm$50)	11.188$\pm$25
4.232$\pm$ 8	8.120$\pm$10	9.456 $\pm$12	10.353$\pm$20	11.313$\pm$25
5.224$\pm$ 8	8.357$\pm$10	9.517 $\pm$12	10.577$\pm$20	11.380$\pm$25
6.005$\pm$ 8	8.439$\pm$10	9.826 $\pm$12	10.661$\pm$20	11.446$\pm$25
7.350$\pm$ 8	8.654$\pm$10	9.960 $\pm$15	10.723$\pm$20	11.511$\pm$25
7.561$\pm$10	8.864$\pm$10	10.025 $\pm$15	10.822$\pm$20	11.861$\pm$25

[a] Hi 60i. High resolution magnetic analysis at five angles; E(^{3}He) = 8.47 and 10.19 MeV.
[b] Possibly a doublet.

For other ^{24}Mg(γ, γ)^{24}Mg experiments, see ^{24}Na, reaction A, and ^{24}Mg, reaction O.

L. ^{24}Mg(γ, n)^{23}Mg $\quad Q_m = -16553 \pm 15$

Two peaks in the activation cross section have been observed at $E_\gamma = 17.2 \pm 0.2$ and 19.2$\pm$0.2 MeV (Ki 60; see also Ka 54). They check with peaks in the ^{23}Na(p, γ)^{24}Mg cross section (Ge 59).

For theory on giant-resonance splitting, see Gl 61e.

M. ^{24}Mg(e, e')^{24}Mg

From the differential cross section for inelastic scattering of 187 MeV electrons the radiation width of ^{24}Mg(1) has been determined as $\Gamma_\gamma = 0.34 \pm 0.03$ meV (He 56). For comparison with other results, see table 24.9.

N. ^{24}Mg(n, n')^{24}Mg

At $E_n = 2.56$ MeV, only one γ ray ($E_\gamma = 1.368 \pm 0.010$ MeV) from inelastic neutron scattering on Mg can be assigned to ^{24}Mg (Da 56c). See also Sc 54d, Ra 55, Pa 58b, An 60d, Le 61a. At $E_n = 14$ MeV many more γ rays are observed of which $E_\gamma = 2.78 \pm 0.02$ MeV ($E_x = 4.12 \rightarrow 1.37$ MeV) and $E_\gamma \approx 3.9$ MeV ($E_x = 5.22 \rightarrow 1.37$ MeV) may be attributed to ^{24}Mg(n, n')^{24}Mg (De 60).

The differential and integral cross section for elastic scattering (La 57b, Th 58b, Be 59) and for inelastic scattering (Cr 56a, Ma 57, Hu 58, Ma 58f, Th 58b, Cr 59, Ma 59a, Bo 61c, Cl 60a) has been measured at several neutron energies. For theoretical work on ^{24}Mg+n scattering, see Cu 56, Ma 59f.

The elastic scattering of polarized neutrons has been investigated at $E_n = 3.1$ MeV (Mc 57). The n'–γ ($E_\gamma = 1.37$ MeV) angular correlation has been measured at $E_n = 3.45$ MeV (Br 60f, Pr 60a).

For older references, see En 54a.

For resonances, see ^{25}Mg.

O. ^{24}Mg(p, p')^{24}Mg

By electrostatic analysis the first level in ^{24}Mg has been determined at $E_x = 1.371 \pm 0.002$ MeV (Do 53); by magnetic analysis the second and third level at $E_x = 4.13 \pm 0.02$ and 4.24 ± 0.02 MeV, respectively (Ha 52). See also Od 60, Ty 58.

From ^{24}Mg(p, p'γ)^{24}Mg γ-ray angular distribution and γ–γ angular correlation measurements it follows that the ^{24}Mg levels at 4.23, 5.22, 6.00, and 6.44 MeV have $J^\pi = 2^+, 3^+$, 4, and 0, respectively. The branching percentages of the 4.23 MeV level to ^{24}Mg(0) and ^{24}Mg(1) are 74% and 26%, respectively (same branching ratio given in Mi 59b; 77% and 23% in Co 61d). The latter transition ($2^+ \rightarrow 2^+$) has an E2/M1 amplitude mixing ratio of $x = +23 \pm 9$. The decay of the 5.22 MeV level to ^{24}Mg(1) is pure quadrupole (Ba 60, Br 60e, Go 60c, Br 61b, Br 61d). The branchings of the 6.00 and 6.44 MeV levels, reported in Co 61d, are shown in fig. 24.3. See also Li 58b, Wa 60c.

From resonant scattering and self-absorption of 1.37 MeV γ rays the width of ^{24}Mg(1) has been determined as $\Gamma = 0.42 \pm 0.15$ meV (Me 60b). For comparison with other results, see table 24.9. For the theory of this process, see Va 59.

The differential cross section for elastic scattering and for inelastic scattering leading to ^{24}Mg(1) has been measured at many different proton energies (Ki 56a, Co 57a, Gr 57b, Ya 58, Ya 58a, Ne 60, Ne 60b, Od 60, Hi 61c). For the theory of these reactions see Me 57a, Sa 58a, Ma 59f, Ro 61d. The p'–γ ($E_\gamma = 1.37$ MeV) angular correlation (La 59, Se 59a, Yo 60, Br 61), and the polarization of elastically scattered protons (Ro 60, Sa 60a, Ya 60a, Ro 61c) have also been investigated.

For older references, see En 57, En 54a.

For resonances, see ^{25}Al.

P. ^{24}Mg(d, d')^{24}Mg

For elastic and inelastic differential cross-section measurements, see Ho 49, Gr 55, Ha 56c, Hi 57b, Sl 59, Bl 60b, Gr 60, Ne 60, Ne 60b, Ta 60e, Ba 61d, Bl 61a, Fr 61, Is 61, Ig 61, Ja 61c. For theoretical considerations, see Ko 58c, Sa 58a, Ed 60, El 60.

Q. ^{24}Mg(^{3}He, ^{3}He)^{24}Mg

For a measurement of the elastic differential cross section at $E(^{3}\text{He}) = 5.5$ MeV, see Pa 61a.

R. ^{24}Mg(α, α')^{24}Mg

For elastic and inelastic differential cross section measurements, see Bl 60b, Sh 59, Wa 56a, Gu 56. For the theory of this reaction, see Bu 57a, Ro 60b. See also Bl 59a, Co 61.

For resonances, see ^{28}Si.

S. ^{24}Mg — heavy ions (^{14}N, ^{16}O, ^{20}Ne, ^{22}Ne)

From heavy ion Coulomb excitation the width of ^{24}Mg(1) has been measured as 0.25 meV (Go 60d), and 0.30 ± 0.15 meV (An 60).

T. ^{24}Al(β^{+})^{24}Mg $Q_m = 14020 \pm 300$

See ^{24}Al.

U. ^{25}Mg(γ, n)^{24}Mg $Q_m = -7330.7 \pm 2.1$

For threshold and yield measurements, see Ka 54, Na 55, Mo 55, Ye 56, En 54a.

V. ^{25}Mg(p, d)^{24}Mg $Q_m = -5106.0 \pm 2.1$

The differential cross section of deuteron groups to ^{24}Mg(0), (1), and (2—3) has been measured at $E_p = 17$ MeV. From stripping analysis $l_n = 2$ is found for these groups, and reduced widths of $\theta_n^2 = 0.0079$, 0.022, and 0.012, respectively (Be 61b, Ma 60d). See also Bl 58.

W. ^{25}Mg(d, t)^{24}Mg $Q_m = -1073.1 \pm 2.1$

From magnetic analysis at $E_d = 14.5$ MeV, triton groups to all ^{24}Mg states up to $E_x = 7.60$ MeV (except to $E_x = 6.44$ MeV) were observed. From stripping analysis of the differential cross sections $l_n = 2$ is found for groups to ^{24}Mg(0) through (3) with $\theta_n^2 = 5.5$, 17, 2.5, and 0.75, all $\times 10^{-3}$, respectively (Ha 60c, Ma 60d). See also Ha 60a, Vl 61.

X. ^{27}Al(γ, t)^{24}Mg $Q_m = -18218.2 \pm 1.1$

For threshold and yield, see Wa 56.

Y. ^{27}Al(p, α)^{24}Mg $Q_m = 1594.5 \pm 1.1$

The Q value has been determined by electrostatic analysis as 1.594 ± 0.002 MeV

(Do 53), and by magnetic analysis as 1.585±0.015 MeV (Fr 50b), 1.595±0.007 MeV (Va 52a), 1.596±0.006 MeV (Va 57d), 1.603±0.007 MeV (Ma 60e).

The first level in ^{24}Mg is found at 1.366±0.004 MeV (Do 53), 1.366±0.006 MeV (Va 57d). The internal conversion coefficient of the 1.37 MeV γ ray has been determined as $\alpha = (1.3 \pm 0.3) \times 10^{-5}$ (Ra 58). Transitions to ^{24}Mg(2) and (3) have also been observed (Re 52).

For measurements of differential and integral cross section, see Fi 58, Fu 58, Ku 59, Fu 60, Og 60, Ad 61a.

For resonances, see ^{28}Si

Z. Not reported:

^{21}Ne(α, n)^{24}Mg	$Q_m = 2554.8 \pm 2.4$
^{22}Ne(^{3}He, n)^{24}Mg	$Q_m = 12764.8 \pm 1.9$
^{25}Mg(^{3}He, α)^{24}Mg	$Q_m = 13246.5 \pm 2.1$
^{26}Mg(p, t)^{24}Mg	$Q_m = -9945.8 \pm 2.7$

REMARKS

The lowest $T = 1$ state ($J^{\pi} = 4^{+}$) in ^{24}Mg has not yet been located. A comparison of Coulomb energies of neighbouring nuclides shows that both the 9.46 MeV and the 9.52 MeV states are acceptable candidates.

For rotation bands in ^{24}Mg, see Pe 57a, Co 61d. The $K^{\pi} = 0^{+}$ and 2^{+} bands are shown in fig. 24.3.

Results of ^{24}Mg(1) mean-life measurements are compared in table 24.9. Most

TABLE 24.9

Mean life determinations of ^{24}Mg* = 1.37 MeV

Method	$\tau_m(10^{-12}$ sec)	Reference
β-γ coincidence	< 3000	En 53
β-γ coincidence	36 ±25	Co 55c
e scatt. cross section	1.9 ± 0.2	He 56
res. fluorescence	0.26 ± 0.02	Bu 59a
res. fluorescence	1.7 ± 0.4	De 58, De 58b
res. fluorescence	$0.9^{+5.1}_{-0.4}$	Ar 59
res. fluorescence	1.1 ± 0.4	Of 59
Coul. excit. ^{14}N, ^{16}O, ^{20,22}Ne	1.3 ± 0.4	An 60
Coul. excit. ^{16}O	2.5	Go 60d
res. fluorescence	$1.6^{+0.8}_{-0.4}$	Me 60b

results are in agreement with an average of $\tau_m = (1.7 \pm 0.2) \times 10^{-12}$ sec, with the values given in Co 55c and Bu 59a deviating appreciably.

The J^{π} assignments to the 6.00 and 6.44 MeV levels follow from combining the data found from reactions B and O. The 2^{+} assignment to the 7.35 MeV level follows from the experimental facts: a) that it shows a ground-state γ transition, b) that it is excited from the 3^+ 12.340 MeV level (see fig. 24.3), and c) that it has natural parity (reaction B).

The parity of the 11.988 MeV level should be even and not odd (table 24.6) because it de-excites to 0^+ and 4^+ states (fig. 24.3).

The 12.259 MeV level, finally, should have $J^\pi = 2^+$ because it de-excites to 0^+ and 3^+ states (fig. 24.3) and emits α particles. This is in conflict with a γ-ray polarization measurement (Hu 56), yielding odd parity, and with the ^{20}Ne$+\alpha$ elastic scattering experiment (reaction D), yielding $J^\pi = 3^-$.

^{24}Al

(Not illustrated; see fig. 24.2, p. 41)

A. ^{24}Al$(\beta^+)^{24}$Mg $\qquad Q_m = 14020 \pm 300$

The half-life is 2.09 ± 0.04 sec (weighted mean of Bi 52, Gl 55, Br 54a).

Positons with an end point of $\approx$ 8.5 MeV, and the γ rays listed in table 24.10, have been reported. One per several thousand disintegrations proceeds through an excited state in ^{24}Mg which emits α particles with $E_\alpha \approx 2$ MeV (Gl 55).

The β^+ decay seems to be best explained by assuming a 30% branch to ^{24}Mg(4.12); a 55% branch to the 8.36 MeV level, with probably $J^\pi = 3^+$, de-exciting to the 1.37 MeV ($J^\pi = 2^+$) and 4.12 MeV ($J^\pi = 4^+$) levels, through

TABLE 24.10

Gamma rays from the ^{24}Al$(\beta^+)^{24}$Mg decay

E_γ [a] (MeV)	Rel. intensity [a]	E_γ [b] (MeV)	Transition in ^{24}Mg (E_x in MeV)
1.39 ± 0.03	40	1.38 ± 0.04	1.37 → 0
2.73 ± 0.06	32	2.70 ± 0.06	4.12 → 1.37
4.22 ± 0.10	15	4.21 ± 0.12	8.36 → 4.12
5.35 ± 0.10	6	5.37 ± 0.14	9.5 → 4.12
		(5.66 ± 0.18)	
7.12 ± 0.10	7	7.02 ± 0.20	8.36 → 1.37

[a] Gl 55.
[b] Br 54a.

7.12 and 4.22 MeV γ rays; a 15% branch to a 9.5 MeV level, de-exciting to the 4.12 MeV level through a 5.35 MeV γ ray; and finally a weak transition to a level at $\approx$ 11 MeV, de-exciting through α emission (Gl 55).

The $T = 0$ member of the $T = 1$ triplet to which the ^{24}Na and ^{24}Al ground states also belong, is expected at about 9.5 MeV (see ^{24}Mg, "Remarks"). The γ-ray intensities indicate log $ft = 3.8$ for the β^+ transition to the 9.5 MeV level (Gl 55), which is consistent with the expected favoured character of this transition (Bo 55, Wi 56a). A possible β–γ directional correlation in the ^{24}Al decay, as a consequence of a conserved vector current, is discussed in Be 58d.

B. $^{24}Mg(p, n)^{24}Al$ $Q_m = -14800 \pm 300$

The threshold is at 15.4 ± 0.3 MeV (Bi 52). Cross sections at $E_p = 18$ and 32 MeV, Ta 58. Neutron angular distribution at $E_p = 23$ MeV, Co 55b. Also Ty 54.

C. Not reported:

$^{24}Mg(^3He, t)^{24}Al$ $Q_m = -14040 \pm 300$

^{25}Na

(Fig. 25.1, p. 54; table 25.1, p. 53)

A. $^{25}Na(\beta^-)^{25}Mg$ $Q_m = 3832 \pm 10$

The weighted mean of the reported half-life measurements is 59.6 ± 0.7 sec (Hu 44, Ri 44, Bl 47, Iw 55, Na 56; see also Ba 46, Pe 48a).

The main branch (65%, Go 56, Ma 55; 50%, Na 54b, Bl 47) proceeding to ^{25}Mg(0) has an end point of 3.7 ± 0.3 MeV (Bl 47), 3.65 ± 0.25 MeV (Na 54b), 4.0 ± 0.2 MeV (Ma 55).

TABLE 25.1

Energy levels of ^{25}Na

E_x (MeV)	J^π	$\tau_{\frac{1}{2}}$ (sec)	Decay	Reactions
0	$\frac{5}{2}^+$	59.6 ± 0.7	β^-	A, B, C, D, E, F
0.090–5.746; 29 levels, see table 25.4 and reactions				C, F

TABLE 25.2

Gamma rays following the β^- decay of ^{25}Na[a]

Iw 55	Ma 55	Na 56	Go 56	Assignment
410	384 ± 10 (44 ± 4)	370 ± 10 (108)	400 (95 ± 4)	^{25}Mg(2) → (1)
590	576 ± 10 (59 ± 7)	580 ± 10 (135)	580 (89 ± 5)	^{25}Mg(1) → (0)
980	978 ± 15 (100 ± 15)	975 (100)	980 (100 ± 3)	^{25}Mg(2) → (0)
	1603 ± 20 (40 ± 7)		1610 (33 ± 3)	^{25}Mg(3) → (0)
			1960 (<2.4)	^{25}Mg(4) → (0)

[a] Energies in keV; relative intensities bracketed (980 keV γ ray normalized to 100).

From the analysis of the γ spectrum (see table 25.2) and the β–γ coincidence spectrum 3.5%, 25%, and 6.5% branches have been found to $^{25}Mg^* = 0.59$, 0.98, and 1.62 MeV, respectively (Ma 55). Investigation of the γ spectrum with a large NaI crystal shows, however, that the β^- branching to the 0.59 MeV level is probably less than 1% (Go 56). See table 25.3 for branchings, log ft values, spins, and parities.

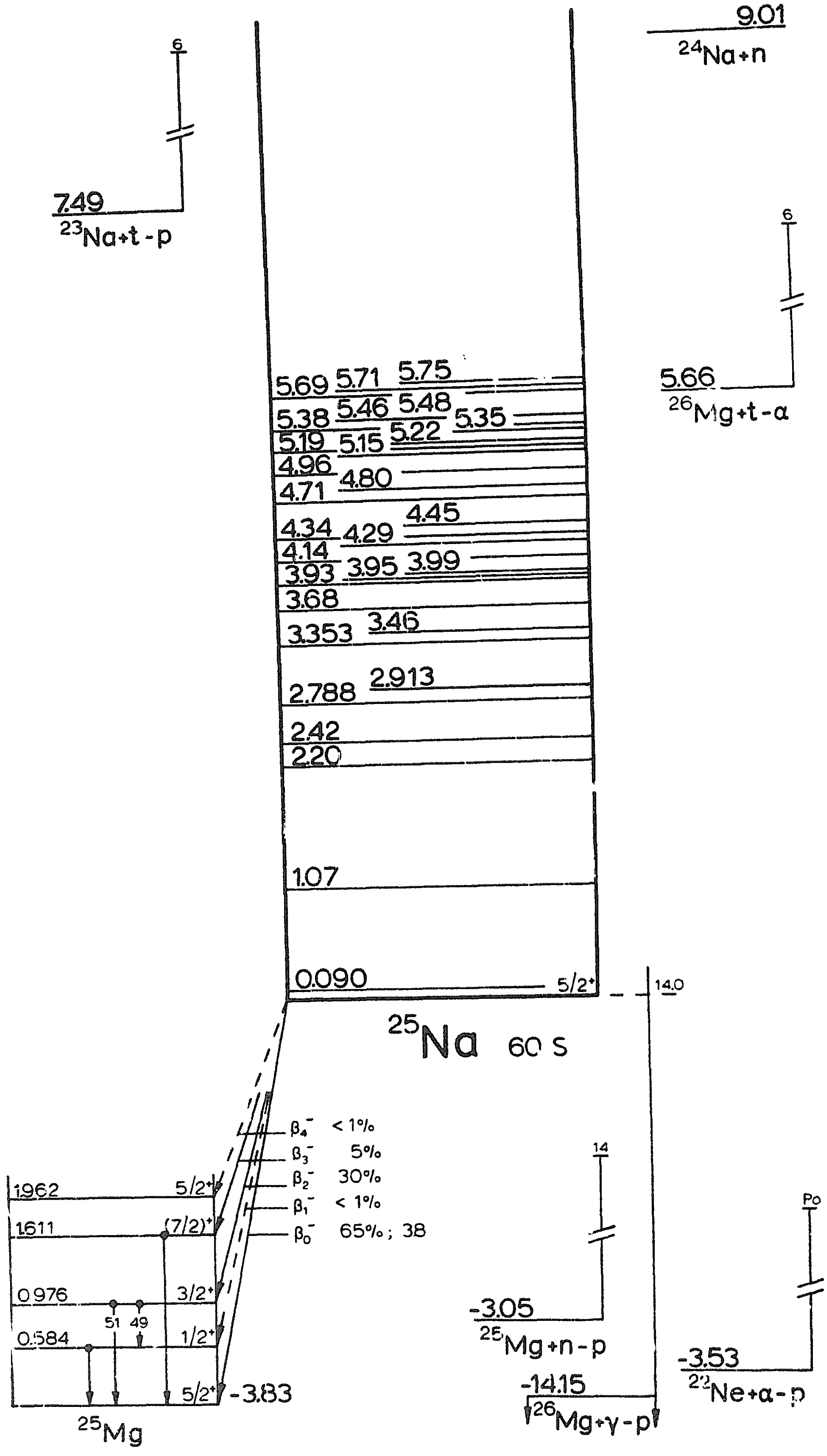

Fig. 25.1. Energy levels of ^{25}Na.

TABLE 25.3

The β^- decay of ^{25}Na

^{25}Mg* (MeV)	J^π	Branching ratio (%)				Log ft (Go 56)
		(Bl 47)	(Na 54b)	(Ma 55)	(Go 56)	
0	$\frac{5}{2}+$	≈ 55	≈ 50	65	65	5.2
0.58	$\frac{1}{2}+$			3.5	< 1	> 6.9
0.98	$\frac{3}{2}+$	≈ 45	≈ 50	25	30	5.2
1.61	$(\frac{7}{2})+$			6.5	5	5.6
1.96	$\frac{5}{2}+$				< 1	> 5.9

The absence of a measurable transition to ^{25}Mg(1), with $J^\pi = \frac{1}{2}^+$, and the allowed character of the transitions to ^{25}Mg(0) and (2), with $J^\pi = \frac{5}{2}^+$ and $\frac{3}{2}^+$, respectively, imply a $J^\pi = \frac{5}{2}^+$ assignment to ^{25}Na(0) (Go 56).

A discussion of the possibility of favoured transitions is given in Ki 55, Fe 55. Beta branchings computed from the ^{25}Mg rotational band structure are discussed in Li 58c.

B. ^{22}Ne(α, p)^{25}Na $\qquad Q_m = -3532 \pm 10$

Observed (Ol 51).

C. ^{23}Na(t, p)^{25}Na $\qquad Q_m = 7491 \pm 10$

Thirty proton groups have been observed at $E_t \approx 6$ MeV. For the excitation energy of ^{25}Na levels, see table 25.4; $Q_0 = 7.492 \pm 0.012$ MeV (Hi 61a).

D. ^{25}Mg(n, p)^{25}Na $\qquad Q_m = -3049 \pm 10$

For cross section at $E_n \approx 14$ MeV, see Pa 53, Al 61. See also Hu 44, Ri 44.

TABLE 25.4

Energy levels of ^{25}Na (E_x in MeV±keV) from ^{23}Na(t, p)^{25}Na and ^{26}Mg(t, α)^{25}Na (Hi 61a)

(t, p)	(t, α)	Average	(t, p)	(t, α)	Average
0	0	0	4.339	4.340	4.340±7
0.090	0.091	0.090±5	4.448	4.451	4.450±10
1.069	1.067	1.068±7	4.709	4.712	4.710±10
2.200	2.207	2.204±7	4.797	4.804	4.800±10
2.418	2.417	2.418±7	4.964	4.960	4.962±10
2.787	2.788	2.788±5	5.144	5.149	5.146±10
2.912	2.914	2.913±5	5.185	5.194	5.190±10
3.351	3.355	3.353±5	5.223	5.223	5.223±10
3.456	3.457	3.456±7	5.344	5.350	5.347±10
3.685	3.684	3.685±7	5.378	5.378	5.378±10
3.925	3.930	3.928±7	5.463	5.467	5.465±10
3.952	3.953	3.952±7	5.484		5.484±12
3.996	3.995	3.995±7	5.691	5.689	5.690±12
4.137	4.136	4.136±7	5.714	5.712	5.713±12
4.285	4.288	4.286±7	5.749	5.744	5.746±12

E. ^{26}Mg(γ, p)^{25}Na $Q_m = -14148 \pm 10$

The threshold is at $E_\gamma = 14.0 \pm 1.0$ MeV (Mc 49). For yield curves and cross sections, see Ba 49, Mc 49, Ed 52, Ka 54. Discussion of relative (γ, p) and (γ, n) cross sections, Mo 55.

F. ^{26}Mg(t, α)^{25}Na $Q_m = 5665 \pm 10$

Magnetic analysis of the α-particle groups at $E_t \approx 6$ MeV yields the ^{25}Na levels listed in table 25.4; $Q_0 = 5.664 \pm 0.010$ MeV (Hi 61a).

G. Not reported:

^{25}Mg(t, ^{3}He)^{25}Na	$Q_m = -\ 3814 \pm 10$
^{26}Mg(n, d)^{25}Na	$Q_m = -11923 \pm 10$
^{26}Mg(d, ^{3}He)^{25}Na	$Q_m = -\ 8655 \pm 10$
^{27}Al(n, ^{3}He)^{25}Na	$Q_m = -14702 \pm 10$

^{25}Mg

(Fig. 25.2, p. 57; table 25.5, p. 58)

A. ^{22}Ne(α, n)^{25}Mg $Q_m = -481.6 \pm 2.0$

In the range $E_\alpha = 2.2$–3 MeV, a 0.58 MeV γ ray has been found in coincidence with neutrons (De 61c). See also Ol 51. For resonances, see ^{26}Mg.

B. ^{24}Mg(n, γ)^{25}Mg $Q_m = 7330.7 \pm 2.1$

The thermal neutron capture cross section of natural magnesium is 63 ± 3 mb; those of ^{24}Mg, ^{25}Mg, and ^{26}Mg are 34 ± 10, 280 ± 90, and 27 ± 5 mb, and the abundances 78.6, 10.1, and 11.3%, respectively. Approximately 45% of the thermal neutron capture in natural magnesium should thus occur in ^{24}Mg (Hu 58).

Gamma rays from capture of thermal neutrons in natural magnesium are listed in table 25.6 with intensities and probable assignments (Ca 57b, Gr 58c, Br 56e, Ma 59c; see also Ki 51, Ki 53a).

The intensity of the γ rays feeding ^{25}Mg*(3.41) and the branching of the de-excitation γ rays lead to the assignment $J^\pi = \frac{3}{2}^-$ to this level (Ki 54a). The angular correlations of two cascades through the 3.41 MeV level corroborate this assignment (Ma 59c). The comparatively large intensities of the γ rays feeding and de-exciting ^{25}Mg* = 4.28 MeV, suggest that this level is the analogue of ^{25}Al* = 3.85 MeV, with $J^\pi = \frac{1}{2}^-$. This assignment would be in agreement with the (d, p) stripping results which indicate $l_n = 1$ (Ca 57b; reaction D).

Theoretical discussion on the relative yields of the (n, γ) and (d, p) reactions, Gr 58b, Bo 59a.

Cross section at higher E_n, Hu 58, Be 58e.

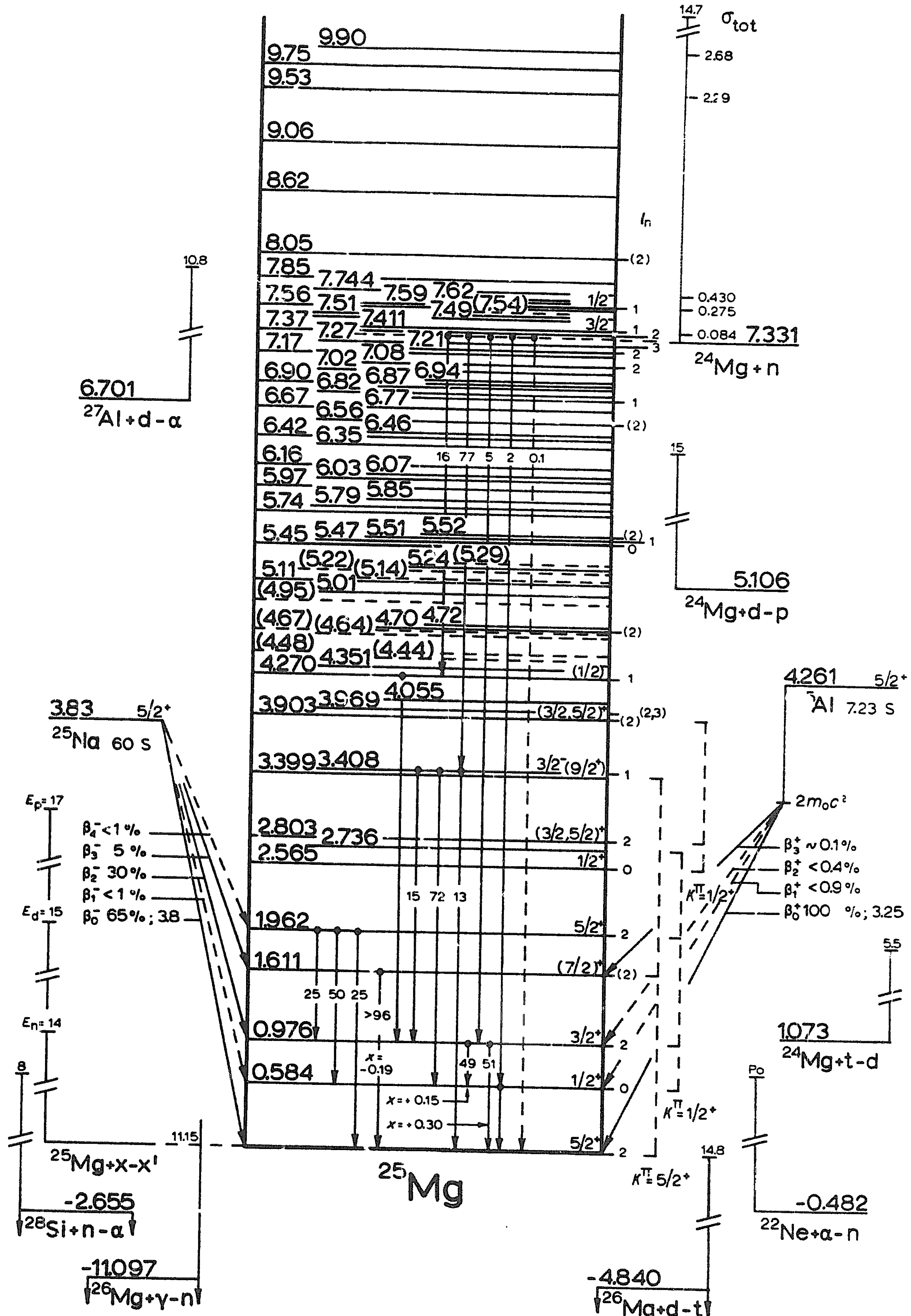

Fig. 25.2. Energy levels of 25Mg.

TABLE 25.5

Energy levels of ^{25}Mg

E_x (MeV ± keV)	J^π	$\tau_{\frac{1}{2}}$ or Γ	Decay	Reactions
0	$\frac{5}{2}^+$		stable	many
0.584 ± 4	$\frac{1}{2}^+$	$(3.4 \pm 0.3) \times 10^{-9}$ sec	γ	many
0.976 ± 4	$\frac{3}{2}^+$	$< 10^{-10}$ sec	γ	many
1.611 ± 4	$(\frac{7}{2})^+$	$(1.7 \pm 0.4) \times 10^{-14}$ sec	γ	many
1.962 ± 4	$\frac{5}{2}^+$		γ	D, F, G, H, M, N
2.565 ± 4	$\frac{1}{2}^+$			D, H, M, N
2.736 ± 4				D, H, M, N
2.803 ± 4	$(\frac{3}{2}, \frac{5}{2})^+$			D, M, N
3.399 ± 4	$(\frac{9}{2}^+)$			D, H, I, N
3.408 ± 4	$\frac{3}{2}^-$		γ	B, D, H, I, N
3.903 ± 5	$(\frac{3}{2}, \frac{5}{2})^+$			D, H, N
3.969 ± 5				D, N
4.055 ± 5				D, N
4.270 ± 5	$(\frac{1}{2})^-$		γ	B, D, N
4.351 ± 6				D, N
(4.436 ± 10)				D
(4.482 ± 10)				D
(4.639 ± 10)				D
(4.666 ± 10)				D
4.704 ± 10				D, N
4.717 ± 7				D, N
(4.946 ± 10)				D
5.010 ± 7			(γ)	B, D, N
5.113 ± 7			(γ)	B, D, N
(5.140 ± 10)				D
(5.217 ± 10)				D
5.244 ± 10				D, N
(5.287 ± 10)				D
5.455 ± 10				D, N
5.470 ± 7	$\frac{1}{2}^-$			D, N
5.512 ± 10	$(\frac{3}{2}, \frac{1}{2})^-$			B, I, N
5.523–7.365, 24 levels, see table 25.9 and reactions				D, N
7.411 ± 4	$\frac{1}{2}^-$	7.8 ± 0.5 keV	n	C, D, N
7.486 ± 10				D, N
7.512 ± 10				D, N
7.538 ± 10				D, N
7.564 ± 10				D, N
7.595 ± 4	$\frac{1}{2}^-$	80 ± 20 keV	n	C, D, N
7.623 ± 10				D, N
7.640 ± 10				D, N
7.744 ± 5	$(\frac{1}{2}^-)$	30 ± 10 keV	n	C, D, N
7.85–11.39, 9 levels, see tables 25.7 and 25.9 and reactions				C, D, N

C. ^{24}Mg(n, n)^{24}Mg $E_b = 7330.7 \pm 2.1$

Total cross-section measurements at neutron energies up to 82 MeV, Hu 58, Pe 60. Differential scattering cross section at $E_n = 14.7$ MeV, Be 58b, Cr 60. Resonances in the ^{24}Mg + n total cross section are listed in table 25.7. A large

TABLE 25.6
Gamma rays from capture of thermal neutrons in natural Mg

E_γ[a] (MeV ± keV)	I_γ[a]	E_γ[b] (MeV ± keV)	I_γ[b]	Final nucleus	Probable transition[f]
11.089 ± 25	0.03			^{26}Mg	C → 0
10.08 ± 20	0.04			^{26}Mg	
9.282 ± 13	0.5	9.27 ± 30	1	^{26}Mg	C → 1.81
8.93 ± 20	0.06			^{26}Mg	
8.55 ± 20	0.06			^{26}Mg	
8.149 ± 10	3	8.14 ± 30	3.5	^{26}Mg	C → 2.94
7.36 ± 30	0.06			(^{25}Mg)	(C → 0)
7.16 ± 30	0.11			^{26}Mg	C → 3.94
6.735 ± 15	1.2			^{25}Mg	C → 0.58
6.440 ± 8	0.9			^{27}Mg	C → 0
6.358 ± 8	2.4	6.36 ± 30	2	^{25}Mg	C → 0.98
5.76 ± 20	0.6				
5.51 ± 20	0.6			(^{25}Mg)	(5.51 → 0)
5.442 ± 12	3			^{27}Mg	C → 0.99
5.05 ± 20	1.7				
4.93 ± 20	2.7	4.93 ± 30	3		
4.77 ± 30	0.6				
4.21 ± 20	2.5				
3.918 ± 4	47	3.92 ± 20	30	^{25}Mg	C → 3.41
3.552 ± 14	8	3.58 ± 30	3	(^{27}Mg)	3.56 → 0
3.408 ± 15	5	3.41 ± 20	4	^{25}Mg	3.41 → 0
3.290 ± 10	9	3.31 ± 20	7	^{25}Mg	4.27 → 0.98
3.054 ± 12	9	3.06 ± 20	7	^{25}Mg	C → 4.27
2.816 ± 15	24	2.82 ± 20[c]	24; 49[d]	^{25}Mg	3.41 → 0.58
		2.43 ± 20	5	^{25}Mg	3.41 → 0.98
		1.83 ± 20[c]	11; 22[d]	^{26}Mg	1.81 → 0
		1.14[e]	13[d]	^{26}Mg	2.94 → 1.81[e]
		1.0[e]		^{26}Mg	(3.94 → 2.94)[e]

[a] Ca 57b; magnetic pair spectrometer. Intensities in gammas per 100 captures.
[b] Gr 58c; Compton spectrometer. Intensities in gammas per 100 captures.
[c] See also Br 56e.
[d] Br 56e; two-crystal scintillation spectrometer.
[e] Coincident with $E_\gamma \approx 7$ MeV (Ma 59c).
[f] Excitation energies in MeV; C is the capturing state.

value for the left-right asymmetry in the scattering of polarized neutrons has been found at the 257 keV resonance (El 60b). For non-resonance information, see ^{24}Mg.

D. ^{24}Mg(d, p)^{25}Mg $\qquad Q_m = 5106.0 \pm 2.1$

Sixty levels, with excitation energies up to $E_x = 7.64$ MeV, have been found from high resolution magnetic analysis. For energies, widths, and l_n values, see tables 25.8a and 25.9 (En 52b, En 54b, Hi 58, Hi 61d, Hi 61h, Mi 61a, Pa 61); $Q_0 = 5.097 \pm 0.007$ MeV (En 52b, En 54b), 5.112 ± 0.012 MeV (Ma 60e), 5.096 ± 0.012 MeV (Hi 61h). For a discussion of the doublet character of the 3.41 MeV level, see reaction N (Hi 61d). Earlier low-resolution measure-

TABLE 25.7

Resonances in ^{24}Mg+n total cross section

E_n (keV)	^{25}Mg* (MeV)	σ_{peak} (barns)	Γ (keV)	J^π	References
84± 3	7.411	≈ 65	7.8± 0.5	$\frac{3}{2}^-$	a, b, c, (f)
275± 8	7.595		80 ±20	$\frac{1}{2}^-$	a, b, f
430± 5	7.744		30 ±10	$(\frac{3}{2}^-)$	a, f
2290±10	9.530	3.8			d, (e)
2680±10	9.900	5.53			d, (e)

[a] Hu 58.
[b] Ne 59c.
[c] Bl 58b.
[d] Br 58e.
[e] De 58c.
[f] Fi 51.

ments (Kr 55, Ho 53, Al 49a, Am 52) are generally in good agreement with the results summarized in these tables.

Proton-gamma coincidence experiments indicate transitions from the first four excited states of ^{25}Mg to ^{25}Mg(0), and from ^{25}Mg(2) and (4) to ^{25}Mg(1) (Mu 58b). For conclusions about J^π values from γ branching ratios, see reaction H.

The angular distribution of the proton group to ^{25}Mg* = 3.41 MeV, and the angular correlation between the proton and the resulting de-excitation γ rays, measured at E_d = 2 to 4 MeV, yields $J^\pi = \frac{3}{2}^-$ for the 3.41 MeV level (Co 57b). At E_d = 15 MeV, the angular distribution is in good agreement with the distorted-wave stripping theory (Ma 60a). The polarization of the proton group to ^{25}Mg* = 3.41 MeV is in agreement with the magnitude predicted from (d, pγ) angular correlation measurements (Jo 61, Is 61a).

For a discussion of the spins and reduced widths of the 3.90 and 3.97 MeV levels, see Mi 61a.

For a discussion of the reduced widths in ^{25}Mg and ^{25}Al found from (d, p), (p, p), (n, γ), and (d, n) reactions, see Gr 58b, Bo 59a, Ma 60d, Mi 61a; also Ne 59b.

E. ^{24}Mg(t, d)^{25}Mg $Q_m = 1073.1\pm2.1$

At E_d = 5.5 MeV, the angular distributions of the deuteron groups to ^{25}Mg* = 0 and 0.59 MeV yield l_n = 2 and 0, respectively (De 61b).

F. ^{25}Na(β^-)^{25}Mg $Q_m = 3832\pm10$

See ^{25}Na.

G. ^{25}Mg(n, n')^{25}Mg

At neutron energies of about 3 MeV, γ rays have been observed of 0.38±0.02, 0.59±0.02 (Sc 54d), 0.95±0.025 (Pa 58b), 1.616±0.016 (Da 56c), and

TABLE 25.8a

Levels of ^{25}Mg, with $E_x < 4.4$ MeV, from $^{24}Mg(d, p)^{25}Mg$

E_x [a] (MeV)	E_x [b] (MeV ± keV)	E_x [c] (Mev ± keV)	l_n	$(2J+1)\theta_n^2$ [d] $\times 10^3$
0	0	0	2 [e, f, g, h, i, m, n]	57
0.579	0.595±4	0.582± 6	0 [e, f, i, m, n]	42
0.973	0.983±4	0.976± 6	2 [e, f, m, n]	29
1.609	1.620±4	1.612± 6	(2) [m]	
1.962	1.977±5	1.957± 6	2 [e, f, g, h, i, m, n]	26
2.564	2.572±5	2.565± 6	0 [e, m, n]	19
2.737		2.742± 8	isotropic [m]	
2.800	2.815±8	2.806± 7	2 [e, m, n]	48
3.398 [o]				
3.407 [o]		3.405± 7	1 [e, f, i, j, m, n]	76
3.900	3.915±4	3.899± 8	2 [g], (1,2) [m]	40
3.965	3.977±4	3.972±10	(2, 3) [m, n, k]	53 or 80
4.054	4.053±4	(4.052±10)		
4.268	4.282±4	(4.265± 7)	1 [e, m, n]	22
4.351	4.352±4			
all±10 keV				

[a] Hi 61h; $E_d = 5.5$–6.0 MeV.

[b] Ja 61a.

[c] En 52b, En 54b; $E_d = 1.8$ MeV.

[d] Ma 60d, Hi 58; the relative reduced widths given in Mi 61a are in accordance with all values given in this column, except for the 2.56 MeV level, where 29 is found instead of 19. The 3.90 MeV level is not considered in Mi 61a to be formed by stripping; if it has $l_n = 2$, then $(2J+1)\theta_n^2 \leq 0.007$.The absolute widths for $^{25}Mg(0)$ and (4) in Ha 60c are in good agreement with those tabulated.

[e] Hi 58.

[f] Ho 53.

[g] Ri 59a.

[h] Ha 60c.

[i] Co 57b.

[j] Ma 60a.

[k] Stripping analysis favours the $l_n = 2$ rather than the $l_n = 3$ assignment. The total cross section of the $^{27}Al(d, \alpha)^{25}Mg$ α-particle group to this level favours $J = \frac{5}{2}$ (Mi 61a). This is in contradiction with the suggestion that this level is the analogue of the 3.72 MeV, $J^\pi = \frac{7}{2}^-$ level in ^{25}Al (Go 57d).Very recent D.W.B.A. analysis of the Mi 61a results, however, has shown that the 3.96 MeV level has $l_n = 3$, and not $l_n = 2$ (Dr. Hinds, Aldermaston, private communication).

[m] Pa 61 (preliminary).

[n] Mi 61a.

[o] Hi 61d; doublet at 3.398±0.007 and 3.407±0.007 MeV, distance 9±2 keV. Observed at $E_d = 6.0$ MeV from the $^{24}Mg(d, p)^{25}Mg$ and $^{27}Al(d, \alpha)^{25}Mg$ reactions.

1.92±0.04 MeV (Pa 58b). See also Pa 55, Ra 55, Ho 59a, Le 61a. At $E_n = 14$ MeV, a 1.60±0.01 MeV γ ray has been observed (De 60).

Cross section, Da 56c.

Resonances, see ^{26}Mg.

TABLE 25.8b

Levels of ^{25}Mg, with E_x < 4.4 MeV, from ^{27}Al(d, α)^{25}Mg

E_x [a] (MeV)	E_x [b] (MeV)	E_x [c] (MeV±keV)	E_x [d] (MeV±keV)
0	0	0	0
0.583	0.586	0.584± 6	0.584± 6
0.979	0.975	0.977±10	0.976±10
1.609	1.608	1.610±10	1.616±10
1.958	1.963	1.958±10	1.973±10
2.564	2.568	2.558±10	2.572±10
2.731	2.741	2.729±10	2.741±15
2.795	2.806	2.791±15	2.815±10
3.398 [e] 3.407 [e]	3.404	3.404±12	
3.902	3.915	3.896±15	
3.966	3.975	3.960±15	
4.057	4.061	4.057±15	
4.269	4.280		
4.350	all ± ≈ 7 keV		
all ± 10 keV			

[a] Hi 61h; E_d = 5.5–6.0 MeV.
[b] Sh 59c; E_d = 7.5 and 8.6 MeV.
[c] En 52b, En 54b; E_d = 2.1 MeV.
[d] Ja 61a.
[e] Hi 61d; doublet at 3.398±0.007 and 3.407±0.007 MeV, found from the ^{27}Al(d, α)^{25}Mg and ^{24}Mg(d, p)^{25}Mg reactions.

H. ^{25}Mg(p, p')^{25}Mg

Observed inelastic proton groups are shown in table 25.10 (Ha 52, Sc 59a; also Fi 54).

Yields of the 1.96, 1.61, 0.98, and (0.40+0.58) MeV γ radiation have been measured as functions of the proton energy in the 1.5 to 3.0 MeV range (Go 56). See also Mi 59b, E_p = 4.0–5.4 MeV. By comparing the γ spectra at different resonances, and by measuring γ–γ coincidences, branching ratios of the levels at 0.98, 1.61, and 1.96 MeV have been obtained (see fig. 25.2). Spins and parities of the lower levels agree with these branching ratios, hyperfine-structure measurements, (d, p) angular distributions, log *ft* values in the decay of ^{25}Na and ^{25}Al, shell model predictions, and classification of corresponding levels in the mirror nucleus ^{25}Al (Go 56). Angular distribution and linear polarization measurements, at the E_p = 1.91 and 2.41 MeV resonances, yield the E2/M1 amplitude mixing ratios $x = +0.30\pm0.15$ and $+0.15\pm0.05$ for the 0.98 → 0 and 0.98 → 0.58 transitions, respectively (Mc 61a). A theoretical discussion of the rotational bands in ^{25}Mg has been given in Li 58c; see also ^{25}Al, "Remarks".

The first level, de-excited by a 588±5 keV γ ray (Ka 55), has a half-life $\tau_{\frac{1}{2}} = (3.5\pm0.2)\times10^{-9}$ sec (Fe 60a), $(2.1\pm0.7)\times10^{-9}$ sec (Bi 59a). The reduced

TABLE 25.9

Levels of ^{25}Mg, with $E_x > 4.4$ MeV, from ^{24}Mg(d, p)^{25}Mg and ^{27}Al(d, α)^{25}Mg

E_x[a] (MeV ± keV)	E_x[b] (MeV)	l_n(d, p)	$(2J+1)\theta_n^2$[c] × 10^3	E_x[b] (MeV ± keV)	l_n(d, p)	$(2J-1)\theta_n^2$[c] × 10^3
4.436 ± 9				6.558 ± 10	(2,[d]	
4.482 ± 4				6.668 ± 10		
4.639 ± 9				6.768 ± 10	1[e, i]	7.2
4.666 ± 6				6.825 ± 10	> 1[e]	
	4.704	(2)[d]		6.872 ± 10		
4.727 ± 4	4.712	x[k]		6.901 ± 10		
4.946 ± 4				6.944 ± 10		
5.020 ± 4	5.005			7.025 ± 10		
5.123 ± 4	5.108			7.076 ± 10	2[i]	4.9
5.140 ± 4				7.171 ± 10		
5.217 ± 9				7.215 ± 10	2[i]	22
	5.244	x[k]		7.270 ± 10	3[i]	98
5.287 ± 4				7.365 ± 10	2[i]	4.2
	5.454			7.400 ± 10[g]	1[e, i]	48[j]
5.479 ± 4	5.465	0[e, i]	71	7.486 ± 10		
	5.512	1[d]		7.512 ± 10		
	5.523	(2)[d]		(7.538 ± 10)		
	5.738			7.564 ± 10		
	5.785	x[k]		7.57 ± 20[h]	1[e]	(42)[j]
	5.851			7.623 ± 10		
	5.967			7.640 ± 10		
	6.032			7.85 ± 40[f]		
	6.074			8.05[e]	2 (1)[e]	(32)[j]
	6.159			8.62 ± 50[f]		
	6.350			9.06 ± 40[f]		
	6.423			9.75 ± 40[f]		
	6.457			10.78 ± 40[f]		
	all ± 10 keV			11.89 ± 50[f]		

[a] Ja 61a; ^{24}Mg(d, p)^{25}Mg.
[b] Hi 61h; ^{24}Mg(d, p)^{25}Mg and ^{27}Al(d, α)^{25}Mg, $E_d = 5.5$–6.0 MeV.
[c] Relative reduced widths given in Mi 61a, adjusted to the value $(2J+1)\theta_n^2 = 0.048$ given in Ma 60d for the 7.40 MeV level.
[d] Pa 61 (preliminary).
[e] Hi 58; low resolution; level assignment not obvious in all cases.
[f] To 52; ^{27}Al(d, α)^{25}Mg, $E_d = 10.8$ MeV.
[g] $\Gamma = 13 \pm 3$ keV (Hi 61h), see also table 25.7.
[h] $\Gamma = 80 \pm 20$ keV (Hi 61h), see also table 25.7.
[i] Mi 61a.
[j] Ma 60d, Hi 58.
[k] The stripping states at 4.72, 5.27, and 5.79 MeV, reported in Hi 58, were not confirmed (Mi 61a).

transition probabilities of ^{25}Mg(1) and ^{25}Al(1) differ by a factor of 7; this is discussed in Fe 60a. The half-life of ^{25}Mg*(0.98) is less than 10^{-9} sec (Fe 60a). Resonance fluorescence experiments yield a mean life $\tau_m = 2.5^{+0.6}_{-0.4} \times 10^{-14}$ sec for ^{25}Mg* = 1.61 MeV, assuming $J = \frac{7}{2}$. The angular distribution of scattered radiation yields an E2/M1 amplitude ratio $x = -0.19 \pm 0.015$ and $B(E2)/B(E2)_{s.p} = 6.5$ (Ra 61a).

For resonances, see ^{26}Al.

TABLE 25.10

Levels in ^{25}Mg from ^{25}Mg(p, p')^{25}Mg and ^{25}Mg(d, d')^{25}Mg

E_x [a] (MeV)	E_x [b] (MeV)	E_x [c] (MeV)
0.61±0 02		0.58
		0.98
1.62±0.02	1.6	1.61
1.98±0.02		
2.56±0.02		
2.76±0.02	2.8	
3.41±0.02	3.4	3.40
3.91±0.02	4.0	

[a] (p, p'); E_p = 8 MeV (Ha 52).
[b] (p, p'); E_p = 17 MeV (Sc 59a).
[c] (d, d'); E_d = 15 MeV (Bl 61a).

I. ^{25}Mg(d, d')^{25}Mg

Observed inelastic deuteron groups are listed in table 25.10. The only strong groups are those corresponding with levels at 1.61 and 3.40 MeV. It is suggested that this last group mainly excites, not the 3.409 MeV, $J^\pi = \frac{3}{2}^-$ level, but a $J^\pi = \frac{9}{2}^+$ ground-state rotational-band level which should appear at approximately this excitation energy (Bl 61a).

J. ^{25}Mg(^{14}N, ^{14}N')^{25}Mg

By Coulomb excitation with 12.2, 16.8, 18.0, and 21.5 MeV ^{14}N ions the partial E2 mean lives of ^{25}Mg(1), (2), and (3) have been measured as $(6.9\pm1.7)\times10^{-9}$, $(1.7\pm0.4)\times10^{-10}$, and $(9.0\pm1.6)\times10^{-13}$ sec, respectively (An 61f).

K. ^{25}Al(β^+)^{25}Mg $Q_m = 4261\pm6$

See ^{25}Al.

L. ^{26}Mg(γ, n)^{25}Mg $Q_m = -11097.4\pm2.7$

The threshold has been measured as 11.15±0.20 MeV (Sh 51a). The cross section shows a maximum at $E_\gamma \approx 17$ MeV ($\Gamma \approx 2.5$ MeV) (Ka 54). See, however, Na 55, Ye 56. Theoretical discussion of the observed cross section, Mo 55.

M. ^{26}Mg(d, t)^{25}Mg $Q_m = -4839.8\pm2.7$

Triton groups observed at $E_d = 14.8$ MeV, the results of angular distribution analysis, and the extracted reduced widths are listed in table 25.11. From a comparison of the experimental widths to the predictions of the rotational model, an admixture of higher rotational bands was found in the ^{26}Mg ground-state wave function (Ha 60c, Ma 60d). See also Vl 61.

TABLE 25.11

Levels in ^{25}Mg from ^{26}Mg(d, t)^{25}Mg (Ha 60c, Ma 60d)

E_x (MeV)	l_n	$\theta_n^2 \times 10^3$
0	2	31
0.58	0	2.5
0.98	2	0.4
1.61	(4)	
1.96	2	1.8
2.57	0	0.7
2.74		
2.80	2	0.9

N. ^{27}Al(d, α)^{25}Mg $Q_m = 6700.5 \pm 2.2$

Observed levels are listed in tables 25.8b and 25.9 (Hi 61h, Hi 61d, Sh 59c, En 54b, En 52b, To 52, Sc 50; see also Sh 61a). The ground-state Q value has been measured as $Q_0 = 6.694 \pm 0.010$ MeV (En 52b, En 54b), 6.718 ± 0.005 MeV (Ma 60e), 6.687 ± 0.010 MeV (Sh 59c), 6.691 ± 0.012 MeV (Hi 61h). For excitation energies below 7.6 MeV, the results of low-resolution experiments have not been listed (see En 54a).

A detailed investigation of the 3.40 MeV level proves that this is a doublet of 9 ± 2 keV separation. The higher member is the well known $l_n = 1$ state observed in the ^{24}Mg(d, p)^{25}Mg reaction. A $J^\pi = \frac{9}{2}^+$ assignment for the lower member, suggested by mirror nucleus arguments, is supported by the observed relative intensities of the α-particle groups (Hi 61d).

Angular distributions of 44 α-particle groups, measured at $E_\alpha = 10$ MeV, yield total cross sections. For the states of known spin, the proportionality of the total cross section of the individual groups and $(2J+1)$, is obeyed surprisingly well (Hi 61e). Gamma rays from deuteron bombardment of aluminium, see Be 55. Cross section measurements, Ci 61.

O. ^{28}Si(n, α)^{25}Mg $Q_m = -2655.4 \pm 3.4$

From the bombardment of a silicon surface barrier counter with $E_n = 5$–8 MeV neutrons, α-particle groups have been observed to the four known lowest states in ^{25}Mg (De 61d).

P. Not reported:

^{23}Na(t, n)^{25}Mg	$Q_m = 10540.9 \pm 2.4$
^{23}Na(^{3}He, p)^{25}Mg	$Q_m = 11305.4 \pm 2.3$
^{23}Na(α, d)^{25}Mg	$Q_m = -7047.0 \pm 2.4$
^{24}Mg(α, ^{3}He)^{25}Mg	$Q_m = -13246.5 \pm 2.1$
^{26}Mg(p, d)^{25}Mg	$Q_m = -8872.7 \pm 2.7$
^{26}Mg(^{3}He, α)^{25}Mg	$Q_m = 9479.8 \pm 2.7$
^{27}Al(n, t)^{25}Mg	$Q_m = -10887.5 \pm 2.3$
^{27}Al(p, ^{3}He)^{25}Mg	$Q_m = -11651.9 \pm 2.3$

^{25}Al

(Fig. 25.3, p. 67; table 25.12, p. 66)

A. ^{25}Al(β^+)^{25}Mg $\qquad Q_m = 4261 \pm 6$

The half-life is 7.23 ± 0.03 sec (weighted mean of Ja 60a, Wa 60a, Mu 58, Ar 58; the value given in Hu 54b, 7.62 ± 0.13 sec, deviates appreciably; see also Br 48, Gr 54).

The decay almost entirely proceeds to the ^{25}Mg ground state; end point

TABLE 25.12

Energy levels of ^{25}Al

E_x (MeV $\pm$ keV)	J^π	$\tau_{\frac{1}{2}}$ or Γ	Decay	Reactions
0	$\frac{5}{2}^+$	7.23 ± 0.03 sec	β^+	A, B, D, E, F, G
0.455 ± 2	$\frac{1}{2}^+$	$(1.88 \pm 0.10) \times 10^{-9}$ sec	γ	B, D
0.949 ± 3	$\frac{3}{2}^+$		γ	B, D
1.610 ± 20	$(\frac{7}{2})^+$		γ	B
1.810 ± 20	$\frac{5}{2}^+$		γ	B, D
2.502 ± 6	$\frac{1}{2}^+$	< 1.0 keV	γ	B, D
2.689 ± 6	$\frac{3}{2}^+$	< 0.4 keV	γ	B, D
2.739 ± 10			γ	B
3.077 ± 6	$\frac{3}{2}^-$	1.3 ± 0.4 keV	γ, p	B, C, D
(3.424 ± 7)			γ	B
3.439 ± 6	$(\frac{9}{2}^+)$	< 10 keV	γ	B
3.72	$\frac{7}{2}^-$	0.3 keV	γ, p	B, C
3.84	$\frac{1}{2}^-$	36 keV	γ, p	B, C
3.88	$\frac{5}{2}^+$	0.1 keV	γ, p	B, C
4.047 ± 9	$(\frac{5}{2}, \frac{3}{2})^+$	< 10 keV	γ	B
4.22	$\frac{3}{2}^+$	> 0.12 keV	γ, p	B, C
4.59	$\frac{5}{2}^+$	> 0.47 keV	γ, p	B, C
4.90	$\geqslant \frac{5}{2}$	< 10 keV	p	C
5.06	$\frac{1}{2}, (\frac{3}{2}^+)$	< 16 keV	p	C
(5.09)			p	C
5.10	$(\frac{5}{2}^+)$	≈ 50 keV	p	C
5.30	$\frac{3}{2}^-$	200 keV	p	C
5.80	$\frac{3}{2}^-$		p	C
6.13	$\frac{1}{2}, (\frac{3}{2}^+)$		p	C
6.70			p	C
7.14	$(\frac{3}{2})$		p	C
7.32		100 ± 20 keV	p	C
(7.5)			p	C
7.78	$(\frac{3}{2})$	340 ± 50 keV	p	C

3.24 ± 0.03 MeV (El 55), 3.27 ± 0.03 MeV (Wa 60a; also Hu 54c); $\log ft = 3.6$. A weak 1.58 ± 0.03 MeV γ ray has been detected, indicating that about 0.1% of the β^+ transitions go to ^{25}Mg$^* = 1.61$ MeV (Ma 55). For this transition $\log ft \approx 5.3$. Upper limits for transitions to ^{25}Mg$^* = 0.98$ and 0.58 MeV are

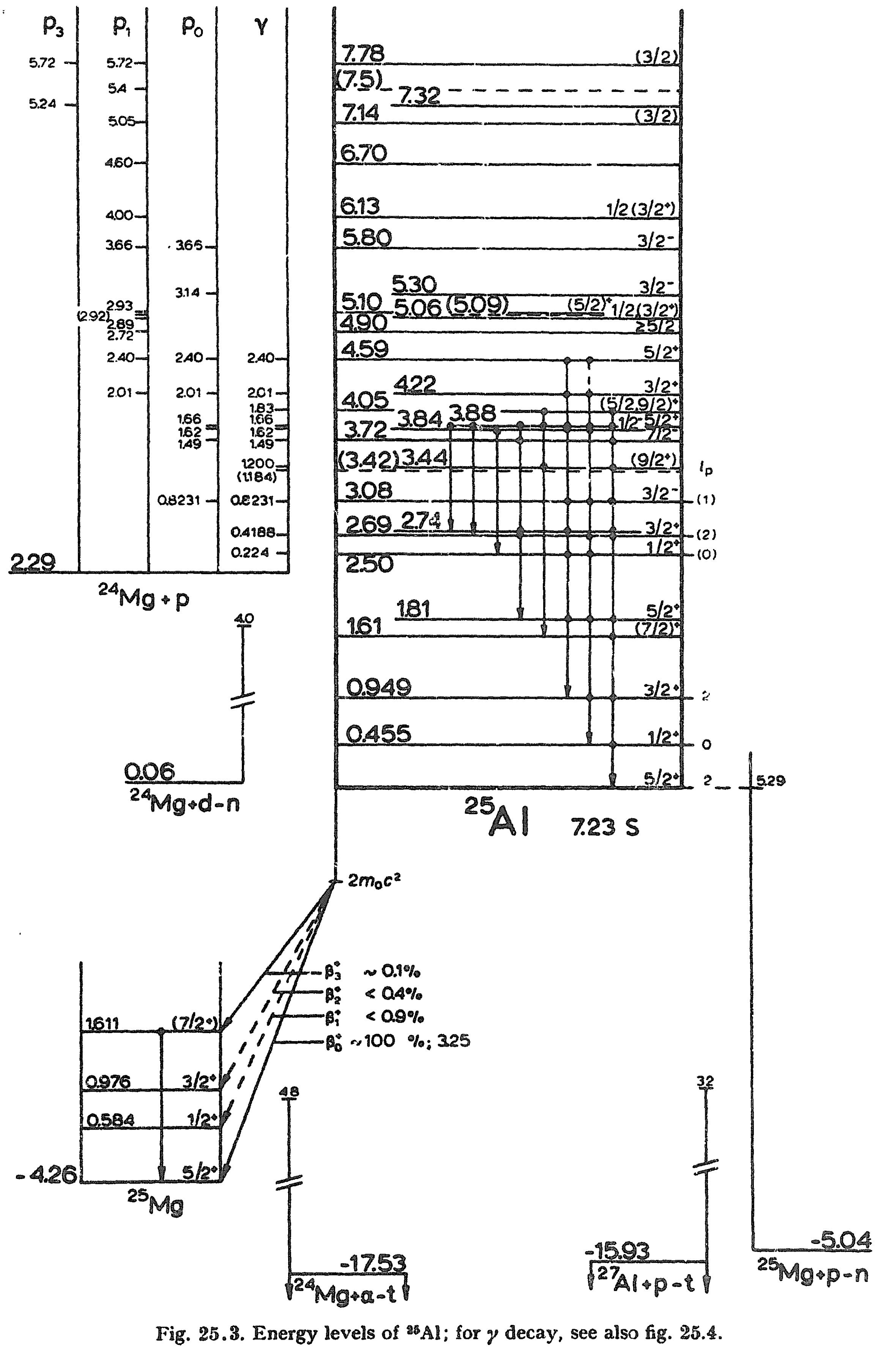

Fig. 25.3. Energy levels of ^{25}Al; for γ decay, see also fig. 25.4.

0.4% (Ma 55; also St 56, Ta 60c) and 0.9% (Ta 60c), respectively. See also El 55, Ch 56, Va 56b.

Longitudinal β^+ polarization measurements, Pr 58.

B. ^{24}Mg(p, γ)^{25}Al $\qquad Q_m = 2287 \pm 6$

Ten resonances in the γ-ray yield are listed in table 25.13. The listed energies of the lowest three resonances are weighted mean values of several precision measurements.

Measurements of γ-ray spectra, angular distributions, coincidence spectra, γ–γ angular correlations, and γ-ray polarizations, yield decay modes, partial

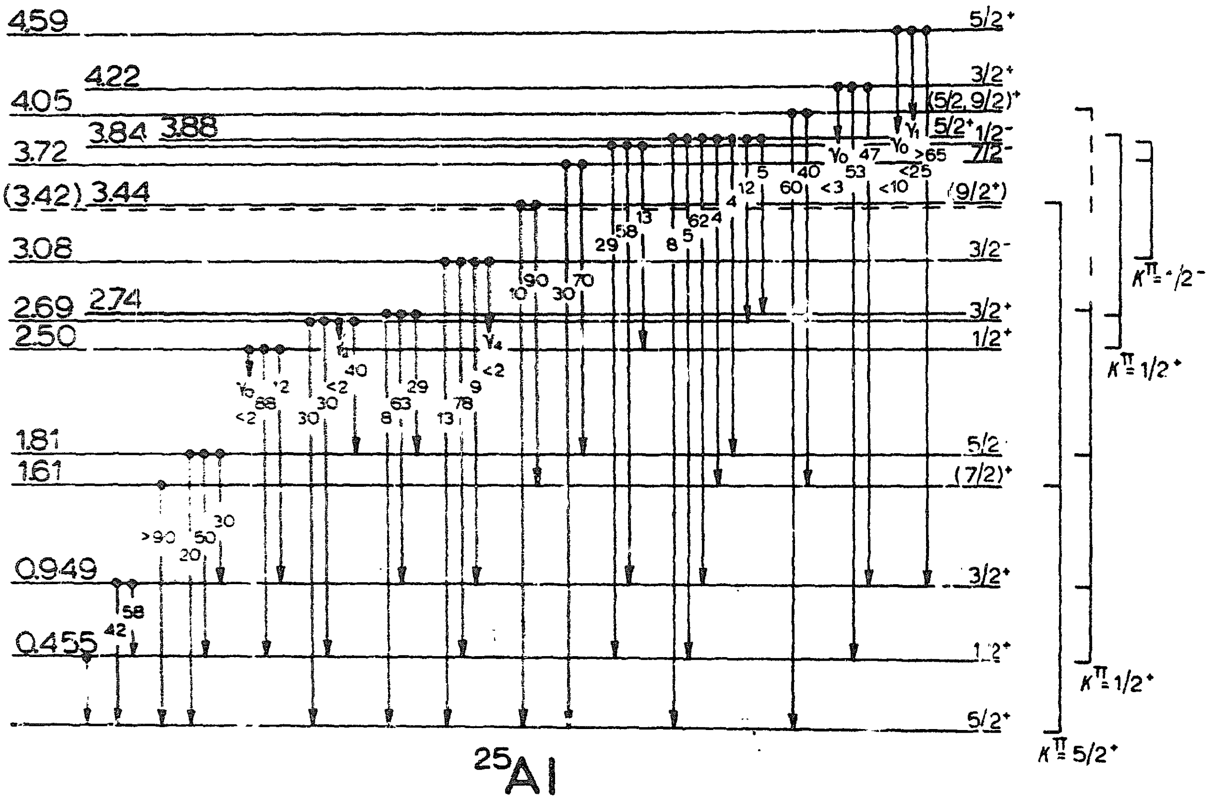

Fig 25.4. Gamma-ray branchings in ^{25}Al (Li 56a, Go 58e, Li 59a).

widths, spins, and parities of the resonance levels (values and references in table 25.13; branching ratios in fig. 25.4). Levels below the proton binding energy have been found at 455 ± 2 keV (Cr 56, Va 56b, Ag 56, Go 58e), 949 ± 3 keV (Go 58e), 1610 ± 20 keV, and 1810 ± 20 keV (Li 56a); for J^π values and branching ratios, see fig. 25.4. Delayed γ–γ coincidence measurements yield a half-life $\tau_{\frac{1}{2}} = (1.88 \pm 0.10) \times 10^{-9}$ sec for ^{25}Al* $= 0.455$ MeV (Go 60f). The resonance corresponding to the level at 2739 ± 10 keV has not been found; $(2J+1)\, \Gamma_\gamma \Gamma_p / \Gamma < 0.6$ meV. This level could be the fourth term ($J^\pi = \frac{7}{2}^+$) of the $K = \frac{1}{2}$ band on the first excited state (Go 58e); also "Remarks".

TABLE 25.13

Resonances in ^{24}Mg+p

E_p (keV)	^{25}Al* (MeV)	Decay[a]	Γ (keV)	$\Gamma_\gamma\Gamma_p/\Gamma$[d] (meV)	$(2J+1)\,\Gamma_p\Gamma_{p_1}/\Gamma$[d] (eV)	J^π
223.8 ± 0.8[b, p, r]	2.502	γ[c, g, h, i, j]	< 1.0[m, q]	13.7		$\frac{1}{2}^-$[i]
418.8 ± 0.2[b, p, q, r]	2.689	γ[c, d, s]	< 0.4[q]	14 ± 7		$\frac{3}{2}^+$[d, s, v]
823.1 ± 0.5[p, q]	3.077	γ[c, d, l] p_0[e]	1.3 ± 0.4[q]	110 ± 20		$\frac{3}{2}^-$[d, l, n, v]
(1184 ± 3)[q]	(3.424)	γ[q]				
1200 ± 1[q]	3.439	γ[d]	< 10[d]	5.5 ± 1.1		$(\frac{9}{2}^+)$[d]
1490[e]	3.72	γ[d] p_0[e]	0.3[n]	12 ± 2		$\frac{7}{2}^-$[d, n]
1620[e]	3.84	γ[d] p_0[e]	36[n]	520 ± 100		$\frac{1}{2}^-$[d, n]
1660[e]	3.88	γ[t] p_0[e]	0.1[n]	45 ± 9		$\frac{5}{2}^+$[d, n, t]
1833 ± 7[u]	4.047	γ[u]	< 10[u]	≈ 1[u]		$(\frac{5}{2}, \frac{9}{2})^+$[u]
2010[d, e]	4.22	γ[d] p_0[e] p_1[d, f]	> 0.12[d]	340 ± 70	120	$\frac{3}{2}^+$[d, f]
2400[d, e]	4.59	γ[d] p_0[e] p_1[d, f]	> 0.47[d]	60 ± 12	700	$\frac{5}{2}^-$[d, f]
2720[d]	4.90	p_1[d]	< 10[d]		40	$\geq\frac{5}{2}$[d]
2890[d]	5.06	p_1[d, f]	< 10[d]		370	$\frac{1}{2}, (\frac{3}{2}^+)$[f]
(2920)[d]	(5.09)	p_1[d]				
2930[d]	5.10	p_1[d, f]	≈ 50[d]		6700	$(\frac{5}{2}^+)$[d, i]
3140[e]	5.30	p_0[e]	200[n]			$\frac{3}{2}^-$[n]
3660[e]	5.80	p_0[e] p_1[f]				$\frac{3}{2}^-$[f]
4000[o]	6.13	p_1[f, o]				$\frac{1}{2}, (\frac{3}{2}^+)$[f]
4600[o]	6.70	p_1[o]				
5050[o]	7.14	p_1[o]				$(\frac{3}{2})$[o]
5240[w]	7.32	p_3[w]	100 ± 20[w]			
≈ 5400[o]	≈ 7.5	p_1[o]				
5720[w]	7.78	(p_1)[o] p_3[o, w]	340 ± 50[w]			$(\frac{3}{2})$[w]

[a] The symbols γ, p_0, p_1, and p_3 refer to proton capture, elastic proton scattering, and inelastic scattering to ^{24}Mg* = 1.37 and 4.24 MeV, respectively.

[b] Hu 55.
[c] Ag 56.
[d] Li 56a.
[e] Mo 51.
[f] Le 56a.
[g] Ca 53.
[h] Cr 56.
[i] Va 56b.
[j] Ch 56.
[l] Gr 55c.
[m] Ta 46.
[n] Ko 52.
[o] Mi 59b.
[p] Ku 59a.
[q] An 59b.
[r] Wa 59a.
[s] Va 58.
[t] Go 58e.
[u] Li 59a.
[v] Su 60c.
[w] Ba 60.

C. ^{24}Mg(p, p')^{24}Mg $\qquad E_b = 2287 \pm 6$

Elastic proton scattering shows eight resonances in the energy range $E_p = 0.4$ to 3.9 MeV (Mo 51); partial-wave analysis (Ko 52) yields widths and J^π values of the corresponding levels; see table 25.13.

Eleven resonances for inelastic proton scattering to ^{24}Mg*(1.37) have been observed for protons in the energy range $E_p = 2$ to 5.5 MeV (Li 56a, Le 56a, Mi 59b). Yield curve up to $E_p = 7.0$ MeV, Se 59a. The angular distribution of $E_\gamma = 1.37$ MeV, measured at $E_p \approx 5.05$ MeV, yields $J = (\frac{3}{2})$ for the resonance level. Resonances in the yield of $E_\gamma \approx 4.23$ MeV, de-exciting ^{24}Mg(3), have been found at $E_p = 5.24$ and 5.72 MeV (Ba 60; also Mi 59b); see table 25.13.

For non-resonance data, see ^{24}Mg.

D. ^{24}Mg(d, n)^{25}Al $Q_m = 62 \pm 6$

At $E_d = 4.0$ MeV, neutron groups have been observed to ^{25}Al* = 0 ($l_p = 2$, $\theta_p^2 = 2.8 \times 10^{-3}$), 0.45 ± 0.03 ($l_p = 0$, $\theta_p^2 = 7.3 \times 10^{-3}$), 0.95 ± 0.03 ($l_p = 2$, $\theta_p^2 = 3.0 \times 10^{-3}$), 1.81 ± 0.04, (1.94), 2.51 ± 0.05, 2.70 ± 0.05, (2.92), and 3.09 ± 0.06 MeV ($l_p = 1$) (Go 53, Ma 60d). The ground-state Q value is 0.07 ± 0.06 MeV (Go 53).

E. ^{24}Mg(α, t)^{25}Al $Q_m = -17526 \pm 6$

Cross-section measurement at $E_\alpha = 48$ MeV, Go 60e.

F. ^{25}Mg(p, n)^{25}Al $Q_m = -5044 \pm 6$

Threshold measured as $E_p = 5.1$ MeV (Bl 51), 5.25 ± 0.1 MeV (Sc 54b), and 5.289 ± 0.025 MeV (Ki 55a). For resonances, see ^{26}Al.

G. ^{27}Al(p, t)^{25}Al $Q_m = -15931 \pm 6$

Cross-section measurement at $E_p = 32$ MeV, Go 60e.

H. Not reported:

^{24}Mg(^{3}He,d)^{25}Al	$Q_m = -3206 \pm 6$
^{25}Mg(^{3}He, t)^{25}Al	$Q_m = -4279 \pm 6$
^{28}Si(p, α)^{25}Al	$Q_m = -7699 \pm 7$

REMARKS

The striking similarity of the excitation energies, γ-branching ratios, spins and parities of the low-lying levels in the mirror nuclei ^{25}Mg and ^{25}Al has been discussed in Li 56a, Go 56, Go 57d, Li 58c. The experimental γ-branching ratios in ^{25}Al agree with collective-model calculations if it is assumed that the levels below 4 MeV belong to four rotational bands with $K^\pi = \frac{5}{2}^+, \frac{1}{2}^+, \frac{1}{2}^+$, and $\frac{1}{2}^-$, as given in fig. 25.4. Ground-state M1 transitions from levels of the $K^\pi = \frac{1}{2}^+$ bands are attenuated by factors of approximately 20 as compared to M1 transitions between levels in the same bands. In Bi 60 a modification of the Nilsson calculations has been discussed which in the case of ^{25}Mg appears to lead to a better agreement with the observed decay scheme. A discussion concerning the half-life of the first excited state of ^{25}Mg relative to that of ^{25}Al has been given in Fe 60a.

Relations connecting the strenghts of γ transitions between corresponding states in mirror nuclei are derived in Mo 59a, and compared with the experimental data on the decay of ^{25}Mg and ^{25}Al states.

^{26}Na

(Not illustrated; see fig. 26.1, p. 72)

A. ^{26}Na(β^-)^{26}Mg $Q_m = 8500 \pm 300$

At $E_n = 14.8$ MeV and $E_n = 24$ MeV, ^{26}Na has been produced in the reaction ^{26}Mg(n, p)^{26}Na. The half-life is 1.04 ± 0.03 sec (Nu 58), 1.03 ± 0.06 sec (Ro 61b). It decays by β^- emission to ^{26}Mg*(1.83); the end point, 6.7 ± 0.3 MeV, yields a ^{26}Na mass excess of -7700 ± 300 keV; log $ft = 4.4$. The intensities of β^- transitions to ^{26}Mg* = 0 and 2.97 MeV are less than 10% of the main branch (Ro 61b). The forbidden character of the β^- transition to the ^{26}Mg ground-state, together with the allowed character of the transition to the 2^+ first excited state, suggests $J^\pi(^{26}\text{Na}) = (2,3)^+$.

B. ^{26}Mg(n, p)^{26}Na $Q_m = -7700 \pm 300$

Observed, see reaction A.
Cross section at $E_n = 14$ MeV, Al 61.

C. Not observed:

^{26}Mg(t, ^{3}He)^{26}Na $Q_m = -8500 \pm 300$

^{26}Mg

(Fig. 26.1, p. 72; table 26.1, p. 73)

A. ^{22}Ne(α, n)^{25}Mg $Q_m = -481.6 \pm 2.0$ $E_b = 10615.8 \pm 2.3$

In the 2.2–3.0 MeV range, one resonance has been found at $E_\alpha = 2.88$ MeV (De 61c). See also ^{25}Mg.

B. ^{22}Ne(α, α)^{22}Ne $E_b = 10615.8 \pm 2.3$

Thirteen sharp resonances in the neon elastic scattering cross section have been observed at four angles for $E_\alpha = 2$ to 4 MeV. Two of these resonances, at $E_\alpha = 3.245$ MeV ($\Gamma = 2.5 \pm 0.5$ keV) and 3.418 MeV ($\Gamma = 3.2 \pm 0.5$ keV), can be assigned to ^{22}Ne. Partial wave analysis yields $J^\pi = 3^-$ for the corresponding ^{26}Mg levels at 13.362 and 13.507 MeV (Go 54c).

C. ^{23}Na(α, p)^{26}Mg $Q_m = 1825.7 \pm 2.7$

Conflicting experimental evidence for several low lying ^{26}Mg levels, as found with Al absorption and nuclear emulsion techniques, has been summarized in En 54a.

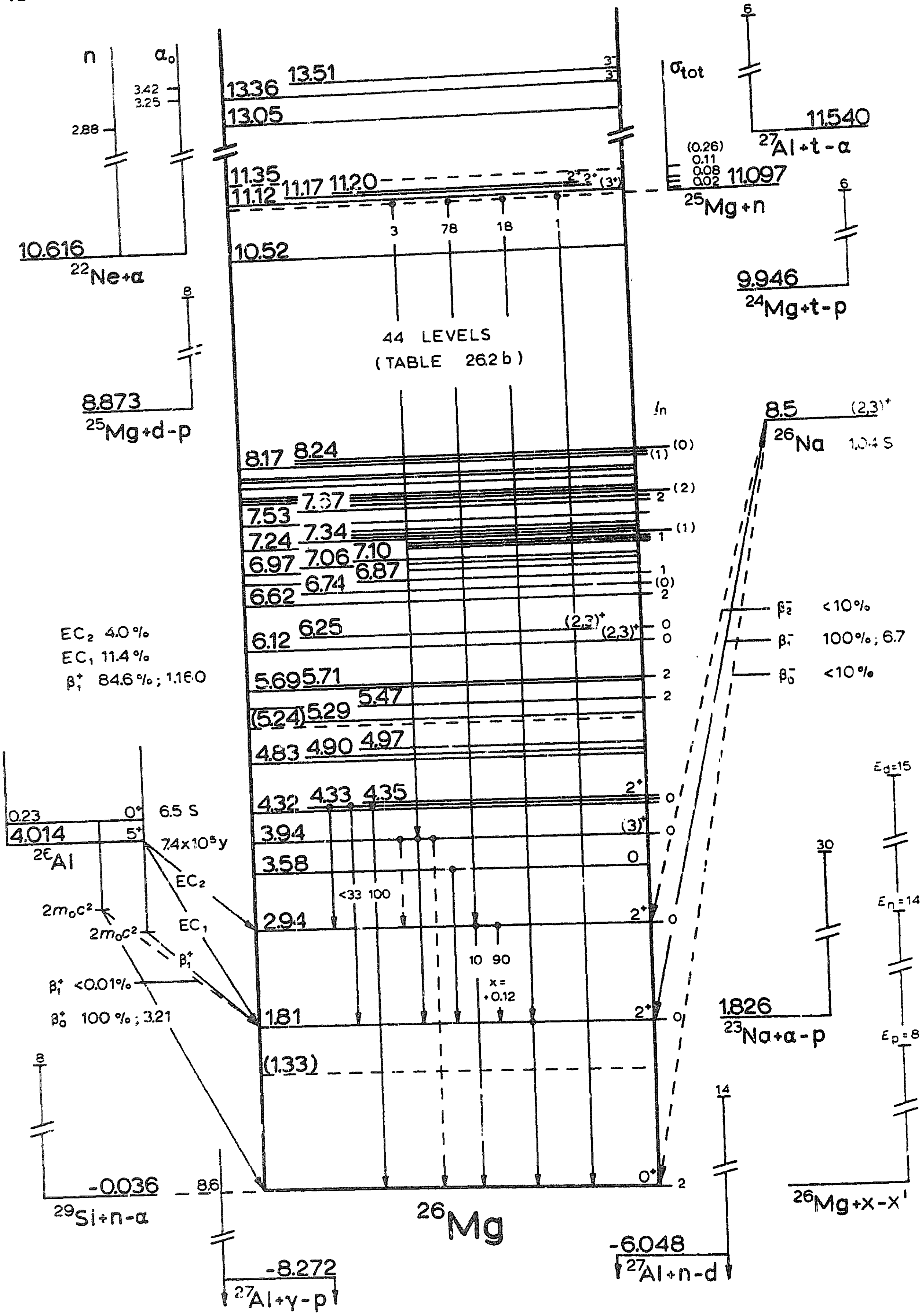

Fig. 26.1. Energy levels of ^{26}Mg.

TABLE 26.1

Energy levels of ^{26}Mg

E_x (MeV±keV)	J^π	τ_m or Γ	Decay	Reactions
0	0+		stable	many
(1.33 ±20)				Q
1.805±10	2+	(6.0±1.3) × 10^{-13} sec	γ	many
2.941±10	2+		γ	many
3.584±10	0		γ	D, G, J, K, O, P
3.943±10	(3)+		γ	C, D, E, G, J, K, P
4.319±10				D, G, P
4.331±10	2+		γ	C, D, G, J, K
4.350±10				D, G
4.830±10				D, G, K, P
4.896±10				D, G, K, P
4.970±10				D, G, P
(5.240±11)				G
5.287±10				D, G, K, P
5.472±10	(≦5)+			D, G, K, P
5.686±10				D, G, P
5.710±10	(≦5)+			D, G, P
6.120±10	(2, 3)+			D, G, P
6.253±10	(2, 3)+			D, G, P
6.616±10	(≦5)+			D, G, P
6.737±10				D, G, P
6.870±10	(≦4)−			D, G, P
6.970±10				D, G, P
7.055–10.515; 66 levels, see tables 26.2a and b and reactions				D, G, P
11.117	(3+)	1.6±0.3 keV	n	F
11.174	2+	12 ±3 keV	n	F
11.198	2+	10 ±2 keV	n	F
(11.347)			n	F
13.05			n	A
13.362	3−	2.5±0.5 keV	α	B
13.507	3−	3.2±0.5 keV	α	B

At E_α = 7.8 MeV, p–γ coincidence measurements yield the γ-decay modes of four of the lowest ^{26}Mg levels. The 2.94 MeV level decays to ^{26}Mg* = 0 and 1.81 MeV; intensity ratio 1:6; the 3.94 MeV level decays to the same two states, and the 4.33 MeV level to ^{26}Mg* = 2.94 MeV (Ma 53b; also Al 48a, Br 55b).

The differential cross section for groups to the low lying states has been measured at E_α = 19 MeV (Pl 60, Pl 61), and E_α = 30.4 MeV (Hu 59a).

For resonances, see ^{27}Al.

D. ^{24}Mg(t, p)^{26}Mg Q_m = 9945.8±2.7

From magnetic analysis at E_t = 5–6 MeV, levels in ^{26}Mg have been observed up to E_x = 9.37 MeV, see tables 26.2a and b; Q_0 = 9.930±0.012 MeV (Hi 61h).

E. ^{25}Mg(n, γ)^{26}Mg $Q_m = 11097.4 \pm 2.7$

The thermal neutron capture cross section is 280 ± 90 mb (Hu 58). From the neutron binding energies of ^{25}Mg, ^{26}Mg, and ^{27}Mg it follows that all thermal neutron capture γ rays in natural Mg with $E_\gamma > 7.4$ MeV, and those coincident with these high energy γ rays, must be assigned to ^{26}Mg. The observed γ-ray energies, intensities, and the proposed assignments are listed in table 25.6. The decay of the capturing state of ^{26}Mg mostly proceeds by multiple cascade transitions (Ca 57b, Gr 58c, Br 56e, Ma 59c).

F. ^{25}Mg(n, n)^{25}Mg $E_b = 11097.4 \pm 2.7$

Resonances in the total cross section of samples enriched in ^{25}Mg have been found at $E_n = 20$ keV ($\Gamma_n = 1.6 \pm 0.3$ keV; $J^\pi = (3^+)$), 80 keV ($\Gamma_n = 12 \pm 3$ keV; $J^\pi = 2^+$), 105 keV ($\Gamma_n = 10 \pm 2$ keV; $J^\pi = 2^+$), and probably at 260 keV (Ne 59c).

For non-resonance data, see ^{25}Mg.

G. ^{25}Mg(d, p)^{26}Mg $Q_m = 8872.7 \pm 2.7$

The ground-state Q value has been measured as 8.880 ± 0.012 MeV (En 52), 8.876 ± 0.012 MeV (Ma 60e), 8.861 ± 0.012 MeV (Hi 61h).

Proton groups to ^{26}Mg levels with excitation energies up to 8.62 MeV have been observed at $E_d \approx 6$ MeV (Hi 61h). The excitation energies of the ^{26}Mg levels below 5.5 MeV, found from magnetic analysis at $E_d = 1.8$ MeV (En 52), show a systematic difference of about 25 keV with those reported in Hi 61h. The excitation energies reported in Ja 61a are in agreement with the values from Hi 61h for $E_x < 4$ MeV. At higher energies, however, a systematic difference of ≈ 15 keV exists. See also Am 52.

The level energies (Ja 61a, Hi 61h, En 52), the l_n values from angular distribution measurements (Pa 61, Ho 53), and the reduced widths as given in Ma 60d (computed from the data in Ho 53), are listed in tables 26.2a and b. Theory, Sa 58.

Resonances, see ^{27}Al.

H. ^{26}Na(β^-)^{26}Mg $Q_m = 3500 \pm 300$

See ^{26}Na.

I. ^{26}Mg(n, n')^{26}Mg*

Inelastic scattering of 2.56 and 14 MeV neutrons on natural Mg gives a 1.820 ± 0.015 MeV γ ray which must be assigned to ^{26}Mg (De 60, Da 56c). See also Le 61a.

For resonances, see ^{27}Mg.

J. ^{26}Mg(p, p')^{26}Mg*

Magnetic analysis at $E_p = 8$ MeV gives levels at 1.83 ± 0.02 and 2.96 ± 0.02 MeV (Ha 52).

TABLE 26.2a

Levels in ^{26}Mg (MeV±keV) from ^{25}Mg(d, p)^{26}Mg, ^{27}Al(t, α)^{26}Mg, and ^{24}Mg(t, p)^{26}Mg; $E_x < 7.3$ MeV

^{25}Mg(d, p)^{26}Mg			^{27}Al(t, α)^{26}Mg	^{24}Mg(t, p)^{26}Mg	l_n (d, p)		$(2J+1)\theta_n^2 \times 10^3$
En 52	Ja 61a	Hi 61h	Hi 61h		Ho 53	Pa 61	Ho 53, Ma 60d
E_d = 1.8 MeV		E_d = 5–6 MeV	E_t = 5–6 MeV		E_d = 8 MeV		
0	0	0	0	0	(2)	2	40
1.825±15	1.804±12	1.807	1.800	1.803	0+2	0	19, 210
2.972±10	2.935±12	2.941	2.938	2.944	0		170
		3.591[a]	3.571[a]	3.588[a]			
3.969±10	3.941±12	3.945	3.944	3.938	0	0	170
		4.321	4.316	4.318			
4.353±10	4.344±12	4.331		4.332	0		190
		4.353		4.348			
4.863±11	4.852±12	4.829	4.834	4.828			
4.924±11	4.906±12	4.896	4.900	4.892			
		4.968	4.976	4.966			
5.270±11							
5.322±11	5.302±12	5.287	5.290	5.285			
5.502±11	5.487±12	5.474	5.471	5.468		2	
		5.687	5.684	5.686			
		5.711	5.709	5.711		2	
6.147±11	6.134±12	6.121	6.120	6.118	0	0	(120)
		6.252	6.259	6.249		0	
		6.617	6.617	6.614		2	
		6.738	6.740	6.734		(0)	
		6.866	6.871	6.872		1	
		6.967	6.971	6.972			
		7.053	7.058	7.055			
		7.096	7.092	7.097			
		7.237	7.241	7.238			
		7.251	7.252	7.249		1	
		7.273		7.270			
		all ±15 keV	all ±15 keV	all ±15 keV			

[a] This level has also been observed from ^{26}Mg(d, d′)^{26}Mg and ^{25}Mg(d, p)^{26}Mg at E_d = 15 MeV, Bl 61a.

At three resonant proton energies ($E_p \approx 5$ MeV), ground-state γ transitions have been observed from ^{26}Mg* = 1.81, 2.94, (3.94), 4.33, and (4.83) MeV (Mi 59b), and transitions to the 1.81 MeV state from ^{26}Mg* = 2.94, 3.58, 3.94, and 4.33 MeV (Mi 59b, Br 60e). The branching ratio of the decay to the ground state and first excited state is 11:89 for the 2.94 MeV level and > 3 for the 4.33 MeV level (Mi 59b). Gamma-gamma angular correlations yield $J = 2$ and 0 for ^{26}Mg* = 2.94 and 3.58 MeV, respectively. The 2.94 → 1.81, 2 → 2^+ transition has a quadrupole/dipole amplitude ratio of $x = +0.12 \pm 0.02$ (Br 61d). A resonance fluorescence experiment yields $\tau_m = (7 \pm 3) \times 10^{-13}$ sec for ^{26}Mg* = 1.81 MeV (Ra 61a).

For resonances, see ^{27}Al.

TABLE 26.2b

Levels in ^{26}Mg (MeV±keV) from ^{25}Mg(d, p)^{26}Mg, ^{27}Al(t, α)^{26}Mg, and ^{24}Mg(t, p)^{26}Mg; $E_x > 7.3$ MeV

^{25}Mg(d, p)^{26}Mg	^{27}Al(t, α)^{26}Mg	^{24}Mg(t, p)^{26}Mg	l_n(d, p)
	Hi 61h		Pa 61
E_d = 5–6 MeV	E_t = 5–6 MeV		E_d = 7.8 MeV
7.338	7.338	7.341	(1)
	7.352	7.364	
7.383	7.377	7.383	
7.414	7.40	7.417	
7.528	7.531	7.535	1
7.668	7.670	7.667	} 2
		7.680	
7.714	7.716	7.712	(2)
7.761	7.762	7.761	
7.808	7.816	7.807	
7.842		7.834	
7.945	7.948	7.940	
8.020	8.030	8.022	
8.040			
8.175		8.169	} (1)
	8.189	(8.186)	
		(8.215)	
8.243	8.233	(8.235)	(0)
8.388	8.384	8.386	
8.451	8.448	8.446	
8.494	8.488	8.491	
8.524	8.518	8.521	
8.565	8.566	8.576	
8.617	8.611	8.615	
	all ± 15 keV		

^{27}Al(t, α)^{26}Mg	^{24}Mg(t, p)^{26}Mg
Hi 61h	
E_t = 5–6 MeV	
8.660	8.658
8.694	8.694
8.849	8.853
8.889	8.891
8.917	8.920
	8.950
9.031	9.034
	9.045
9.101	9.102
9.157	9.155
9.225	9.224
9.242	9.246
9.294	9.296
9.366	9.370

^{27}Al(t, α)^{26}Mg (Hi 61h)		
9.415	9.814	10.213
9.461	9.841	10.272
9.528	9.895	10.316
9.564	9.931	10.358
9.615	9.970	10.40
9.674	10.028	10.419
9.707	10.090	10.483
9.760	10.118	10.515
	all ± 15 keV	

K. ^{26}Mg(d, d')^{26}Mg

At $E_d = 15$ MeV a level at 3.614±0.020 MeV has been observed in addition to the levels from ^{25}Mg(d, p)^{26}Mg reported in En 52. The differential inelastic scattering cross section for levels up to 5.50 MeV has been measured (Bl 61a).

L. ^{26}Mg+heavy ions (^{14}N, ^{20}Ne)

From Coulomb excitation with 16.8 and 18.0 MeV ^{14}N ions, and 25.8 MeV ^{20}Ne ions the ^{26}Mg(1) mean life has been measured as $(5.7 \pm 1.4) \times 10^{-13}$ sec (An 61f).

M. ^{26}Al(β^+)^{26}Mg $\qquad Q_m = 4014.0 \pm 4.9$

See ^{26}Al.

N. ^{27}Al(γ, p)^{26}Mg $\qquad Q_m = -8272.4 \pm 2.8$

Threshold reported at $E_\gamma = 8.6 \pm 0.5$ MeV (Di 50). Cross section, Di 50, Ha 51b, Ba 57a, Ch 60a. Angular distribution measurements, Da 56d, Mi 57, Ba 58a.

At $E_\gamma = 21.2 \pm 0.5$ MeV, the cross section shows a maximum with a half width of 5.4 ± 0.5 MeV (Ha 51b).

Discussion of relative (γ, p) and (γ, n) cross sections, Mo 55.

O. ^{27}Al(n, d)^{26}Mg $\qquad Q_m = -6047.7 \pm 2.8$

At $E_n = 14$ MeV, deuteron groups have been observed to the ^{26}Mg ground state and some known excited states (Ma 58g, Co 59b). A 1.80 ± 0.03 MeV γ ray has been observed (De 60).

Angular distributions of the deuteron groups to ^{26}Mg* = 0, 1.81, and 3.58 MeV yield $l_p = 2$, 2, and 2(+0), and reduced widths $\theta_p^2 = 0.011$, 0.024, and 0.045, respectively (Gl 61).

P. ^{27}Al(t, α)^{26}Mg $\qquad Q_m = 11540.3 \pm 2.8$

Alpha-particle groups, corresponding to ^{26}Mg levels with excitation energies up to 10.515 MeV have been reported, see table 26.2a and b; $Q_0 = 11.541 \pm 0.012$ MeV (Hi 61h).

Q. ^{29}Si(n, α)^{26}Mg $\qquad Q_m = -35.7 \pm 4.0$

From the bombardment of a silicon surface barrier counter with $E_n = 5$–8 MeV neutrons, α-particle groups have been observed to the two known lowest states in ^{26}Mg. A third group leads to a ^{26}Mg level at $E_x = 1.33 \pm 0.02$ MeV, not observed from any other reaction (De 61d).

R. Not reported:

^{25}Mg(t, d)^{26}Mg	$Q_m = 4839.8 \pm 2.7$
^{25}Mg(α, ^{3}He)^{26}Mg	$Q_m = -9479.8 \pm 2.7$
^{27}Al(d, ^{3}He)^{26}Mg	$Q_m = -2779.2 \pm 2.8$
^{28}Si(n, ^{3}He)^{26}Mg	$Q_m = -12135.1 \pm 3.5$

REMARKS

Angular distribution measurements of protons from the ^{25}Mg(d, p)^{26}Mg reaction limit the spin and parity of the 2.94 and 3.94 MeV levels to 2^+ or 3^+. These levels belong to the same isobaric spin triplets as the 3.16 and 4.18 MeV levels of ^{26}Al, with $J^\pi = 2^+$ and 3^+, respectively. The $J^\pi = 2^+$ assignment to ^{26}Mg* = 2.94 MeV is strengthened by the observation of a ground-state γ transition.

The $J^\pi = 2^+$ assignment to ^{26}Mg*(1.81), found from the unique second-forbidden character of the ^{26}Al(β^+) transition to this level (see ^{26}Al, reaction A (a)), is in accordance with the $J^\pi = 2^+$ assignment to the analogous level at 2.07 MeV in ^{26}Al.

For a jj-coupling computation of the excitation energy of the first ^{26}Mg level, see Th 56.

^{26}Al

(Fig. 26.2, p. 79; table 26.3, p. 80)

A. (a) $^{26}Al(\beta^+)^{26}Mg$ $Q_m = 4014.0 \pm 4.9$

Measurements of the specific activity of bombarded magnesium samples, with mass-spectroscopic analysis, yield a half-life of $(7.38 \pm 0.29) \times 10^5$ yr (Ri 58b), $(8 \pm 2) \times 10^5$ yr (Fi 58a), in agreement with earlier less accurate estimates of the half-life following from the ^{25}Mg(d, n)^{26}Al yield (Si 54), the comparison of the ^{26}Al and ^{22}Na yields from deuteron bombardment of Mg, and from the same comparison for proton bombardment (Ri 58b).

The β^+ branching fraction of the ^{26}Al decay is (84.6 ± 1.8)%. The β^+ decay entirely proceeds to $^{26}\text{Mg}^* = 1.81$ MeV (Ri 59). Scintillation-spectrometer determinations of the β^+ end point yield: 1.160 ± 0.008 MeV (Fe 58a), 1.17 ± 0.05 MeV (La 55); $\log ft = 14.17$. The unique second forbidden shape of the β^+ spectrum (La 55, Jo 57, Fi 58a; Fe 58a) determines $J^\pi = 2^+$ for $^{26}\text{Mg}^* = 1.81$ MeV ($J^\pi = 2^+$ or 3^+ follows from ^{25}Mg(d, p)^{26}Mg angular distribution measurements), and $J^\pi = 5^+$ for ^{26}Al(0) ($J \leq 5$ and even parity follow from shell model considerations). The energy of the γ ray de-exciting ^{26}Mg*(1.81) is 1.76 ± 0.10 MeV (La 55), 1.82 MeV (Ha 55b), 1.84 ± 0.01 MeV (Fe 58a), 1.83 ± 0.03 MeV (Ri 59); this γ ray is coincident with positons (Fe 58a).

The electron-capture branching fraction is (15.4 ± 1.8)% of which (11.4 ± 1.9)% to ^{26}Mg*(1.81) and (4.0 ± 0.3)% to ^{26}Mg*(2.94). The EC branch to ^{26}Mg*(1.81) has $\log ft = 13.33$ (Ri 59; see also Ja 61, Fe 58a), and the branch to ^{26}Mg(2.94), $\log ft = 13.0$.

The 2.94 MeV level mainly (91%) decays to ^{26}Mg*(1.81) by a 1.12 ± 0.03 MeV (Ri 59), 1.10 ± 0.05 MeV (Fe 58a) γ ray. The 9% direct ground-state transition has $E_\gamma = 2.96 \pm 0.05$ MeV (Ri 59). An observed 0.7 MeV γ ray (Ha 55b, Jo 57, Fe 58a) is instrumental (Fe 58a).

(b) $^{26}Al^m(\beta^+)^{26}Mg$ $Q_m = 4243 \pm 6$

Eight half-life determinations, ranging from 6.28 ± 0.04 sec to 6.74 ± 0.03 sec, yield a weighted mean $\tau_{\frac{1}{2}} = 6.47 \pm 0.06$ sec (Ka 51, Ha 54a, Hu 54b, Ar 58, Cl 58, Mi 58, Mu 58, Ja 60a).

The β^+ spectrum is simple and the Fermi plot is straight (Ka 55, El 55). The β^+ end point is 3.20 ± 0.05 MeV (Ka 55), 3.21 ± 0.03 MeV (El 55), 3.2 ± 0.1 MeV (Ha 54a); $\log ft = 3.3$. The ft value of this super-allowed $0^+ \rightarrow 0^+$ transition has been used to determine the vector-interaction constant C_v (En 54c, Ka 55, Va 58d; corrections Ge 58a, Du 60).

An upper limit of 0.01% is given for a potential branch to $^{26}\text{Mg}^* = 1.81$ MeV (Ma 55).

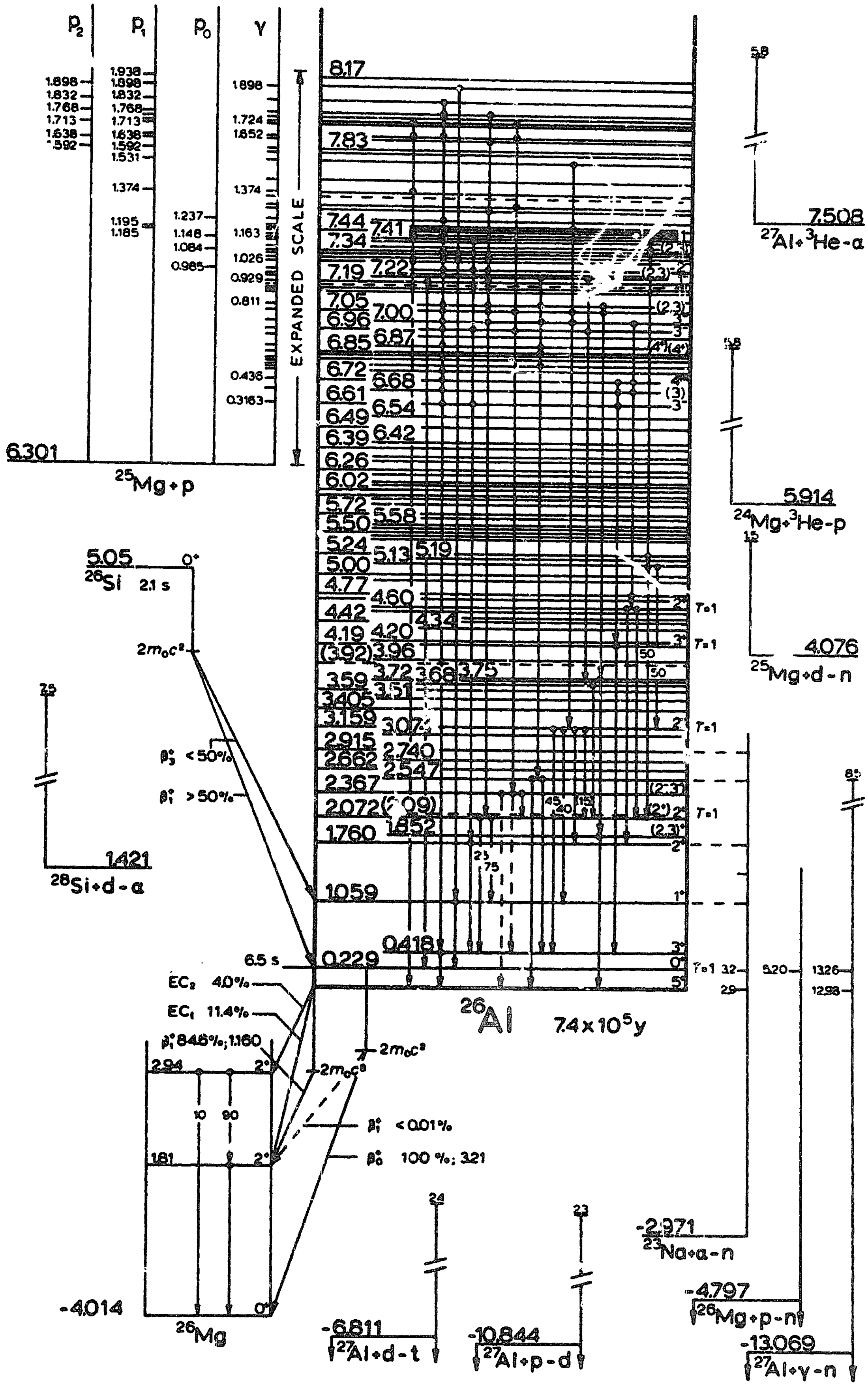

Fig. 26.2. Energy levels of ^{26}Al.

TABLE 26.3

Energy levels of ^{26}Al

E_x (MeV ± keV)	J^π; T	$\tau_{\frac{1}{2}}$	Decay	Reactions
0	5+; 0	(7.38 ± 0.29) × 10^5 yr	β^+, EC	many
0.229 ± 3	0+; 1	6.47 ± 0.06 sec	β^+	many
0.4186 ± 1.4	3+; 0	(1.23 ± 0.05) × 10^{-9} sec	γ	B, C, D, K, L, M, N
1.059 ± 2	1+; 0		γ	B, C, D, I, L, M, N
1.760 ± 3	2+; 0		γ	B, C, D, M, N
1.852 ± 3	(2,3)+		γ	B, C, D, M, N
2.072 ± 3	2+		γ	C, D, G, L, M, N
(2.09 ± 30)	2+; 1		γ	D
2.367 ± 3	(2, 3)−; 0		γ	B, C, D, M, N
2.547 ± 4			γ	B, C, D, L, M, N
2.662 ± 4				B, C, M, N
2.740 ± 5				B, C, M, N
2.915 ± 5				B, C, M, N
3.074 ± 5				B, C, M, N
3.159 ± 5	2+; 1		γ	C, D, M, N
3.405 ± 5				C, M, N
3.507 ± 7				C, M, N
3.594 ± 7				C, M, N
3.675 ± 10			γ	C, D, G, M
3.719 ± 10				C, M
3.746 ± 10			γ	C, D, M
(3.918 ± 15)				C, M
3.962 ± 10				C, M
4.191 ± 10	3+; 1		γ	C, D, M
4.202 ± 10				C, M
4.342 ± 10				C, M
4.424 ± 10				C, M
4.477 ± 10				C, M
4.541 ± 10				C, M
4.595 ± 10	2+; 1		γ	C, D, M
4.613 ± 10				C, M
4.699 ± 10				C, L, M
4.766 ± 10				C, M
4.935 ± 10				C, M
5.002 ± 10				C, M
5.126 ± 10			γ	C, D, G, M
5.193 ± 10			(γ)	C, D, M
5.238 ± 10			(γ)	C, D, M
5.390–6.544; 27 levels, see table 26.5 and reactions				C, M
6.605 ± 5	3−		γ	C, D, M
6.676 ± 5	(3)		γ	C, D, M
6.720 ± 5	4(+)		γ	C, D, M
6.778 ± 5			γ	C, D, M
6.783 ± 5			γ	C, D, M
6.797 ± 5			γ	D
6.812 ± 5			γ	C, D, M
6.815 ± 5			γ	D
6.836 ± 5			γ	D
6.845 ± 5	(4+)		γ	C, D, M
6.849 ± 5			γ	C, D, M
6.869 ± 5	(4+)		γ	C, D, M
6.931–8.165; 42 levels, see tables 26.4a and b and reactions				D, F

B. ^{23}Na(α, n)^{26}Al $Q_m = -2971 \pm 5$

The angle cut-off of neutrons at the $E_\alpha = 3492 \pm 3$ keV resonance yields $Q_0 = -2969 \pm 4$ keV (Wi 60). The threshold for slow neutrons, $Q = -2.9 \pm 0.2$ MeV, and for β^+ emission, $Q = -3.2$ MeV, indicate that the 0.23 MeV level is a β^+ emitter. Thresholds for slow neutrons, and the energies of neutron groups indicate ^{26}Al levels at 0.3, 1.0, 1.4, 1.8, 2.5, and 2.9 MeV, all ± 0.2 MeV (Do 56).

See ^{27}Al for resonances.

C. ^{24}Mg(^{3}He, p)^{26}Al $Q_m = 5914 \pm 5$

Magnetic analysis at $E(^3\text{He}) = 5.8$ MeV yields the excitation energy of about 70 levels, see table 26.5; $Q_0 = 5.928 \pm 0.015$ MeV. A level at 2.09 MeV (see reaction D) has not been found (Hi 59b).

D. ^{25}Mg(p, γ)^{26}Al $Q_m = 6301 \pm 5$

Resonances observed in the γ and/or β^+ yield and the resonance strengths as found from the thick target γ-ray yields are listed in tables 26.4a and 26.4b (enriched targets: Pr 61, Ba 59b, Ku 59a, Wa 59a, Bi 58a, Va 58d, Gr 56e, Hu 55, Kl 54; also Ny 60, Ka 55, Ta 54b; natural Mg targets: An 59b; also Sm 57, Ta 46, Cu 39). The branching of the γ decay to the ^{26}Al ground state and first excited state varies from resonance to resonance with corresponding large variation of the β^+/γ ratio; no β^+ emission has been observed at the 436 and 956 keV resonances. The excitation energies of the corresponding ^{26}Al levels (tables 26.4) have been calculated using the weighted mean values of the resonance energies. The resonances of which the γ decay has been analyzed are indicated (with references) in the last column of the tables 26.4. Prominent modes of decay of both resonance levels and lower lying states of ^{26}Al are given in fig. 26.2. Strong direct transitions to the ^{26}Al ground state have been observed at the 436, 1026, 1046, 1086, 1150, 1163, 1374, 1589, 1652, and 1724 keV resonances (Kl 54, Bi 58a, Mu 60, Pr 61). The first level at 0.23 MeV is fed directly at the 929 keV resonance only (Gr 56e).

The existence of several levels proposed to explain the decay spectra of ^{26}Al resonance levels (Kl 54, Gr 56e, Br 56i, Bi 58a, Mu 60), has been confirmed in the experiments listed in table 26.5 (Br 59a, Hi 59b, Ta 60b). The proposed doublet character of the 2.07 MeV level (Gr 56e), however, has not been confirmed. It has been shown that this doublet character is not strictly necessary to explain the observed γ-ray spectra. An alternate solution could be: direct transitions to $^{26}\text{Al}^* = 5.196 \pm 0.025$, 5.27 ± 0.03, and 5.606 ± 0.025 MeV at the 811 and 956 keV resonances (Ba 60b). In the excitation range of the proposed levels at 2.32 MeV (decaying to the ground state, Gr 56e) and 2.39 MeV (not decaying to the ground state, Bi 58a), only one level has been found: $^{26}\text{Al}^*_6 =$ 2.367 MeV (see table 26.5).

TABLE 26.4a

Resonances in $^{25}Mg(p, \gamma)^{26}Al$ ($E_p < 980$ keV)

E_p (keV)					$^{26}Al^*$	Γ	$(2J+1)\ \Gamma_p\Gamma_\gamma/\Gamma$ (eV); J^π		References
Hu 55	Wa 59a	Ku 59a	An 59b	Average	(MeV)	(keV)	Va 58d	Mu 60	γ-decay
316.7 ± 0.7	316.1 ± 0.5	316.4 ± 1.6	312	316.3 ± 0.4	6.605[h]	< 2.0	0.3; (3⁻)	0.36 ± 0.07; 3⁻	a, f
391.5 ± 0.5	389.3 ± 0.7	389.3 ± 1.7	390.2 ± 0.6	390.5 ± 0.5	6.676[h]	< 1.0	0.7; (3⁻)	0.64 ± 0.13; (2, 3)⁺	a, f
436.5 ± 0.4	434.6 ± 0.8	435.2 ± 1.3		436.0 ± 0.5	6.720[h]		1.5; 4(+)	0.69 ± 0.14; (4)	a, d, f
495.6 ± 0.6	496.5 ± 0.8	495.6 ± 1.4	495.2 ± 1.0	495.8 ± 0.4	6.778(h)	< 1	1.2		a, d
		501.4 ± 1.4	501.1 ± 1.0	501.2 ± 0.8	6.782(h)	< 2			
513.4 ± 0.7	514.8 ± 0.8	513.4 ± 1.5	513.3 ± 1.0	513.8 ± 0.4	6.797	< 2	1.2		
530.4 ± 0.7		532.4 ± 0.6	532.0 ± 1.0	531.6 ± 0.6	6.812[h]	< 2			
			535.0 ± 1.0	535.0 ± 1.0	6.815	< 2			
			556.0 ± 2.0	556.0 ± 2.0	6.836	< 3			
	567.2 ± 0.7	564.6 ± 1.5	565.4 ± 0.5	565.9 ± 0.7	6.845(h)	< 0.5	2.7; (4⁺)		a, d
			570.0 ± 1.5	570.0 ± 1.5	6.849(h)	< 3			
	591.9 ± 0.7	592.3 ± 1.6	590.7 ± 0.5	591.2 ± 0.4	6.869[h]	< 0.5	1.9; (4⁺)		a, d
								Gr 56e	
		655.5 ± 0.9	654.0 ± 1.5	655.1 ± 0.8	6.931	< 2	0.6		
	685.2 ± 1.0	684.7 ± 0.9	682.6 ± 0.5	683.4 ± 0.8	6.958	< 2	3.4	3.5; 3⁻	b, c
		722.9 ± 1.8	723.2 ± 0.5	723.2 ± 0.5	6.996	< 2		2.8; 3⁻	b, c
		774.7 ± 1.8	777.7 ± 0.5	777.5 ± 0.7	7.049	< 2		1.9; (2, 3)⁻	b
		811.2 ± 1.3	811.0 ± 0.8	811.0 ± 0.7	7.081	< 2		1.2; $\pi = -$	b, g
			870 ± 3		7.138				
			882.4 ± 0.7		7.149				
			890 ± 1.5		7.157				
Pr 61	Ba 59b	Ny 60	(902 ± 4)		(7.168)				
	929 ± 3		928.6 ± 0.6		7.194			1.5; 1⁻	b
956	957 ± 3	956	955 ± 4	956 ± 2	7.220			3.8; (2, 3)⁻	b, c, e, g, i
		970	969 ± 2		7.233				

[a] Kl 54, En 54c; single spectra, relative intensities.
[b] Gr 56e; single spectra, coincidence spectra, relative intensities, angular distributions.
[c] Ka 55; single and coincidence spectra.
[d] Br 56i; single spectra.
[e] Ny 60; single spectra.
[f] Mu 60; single and coincidence spectra, angular distributions.
[g] Ba 60b; single, coincidence, and sum-coincidence spectra, intensities.
[h] These levels have probably also been seen from the $^{24}Mg(^3He, p)^{26}Al$ and $^{27}Al(^3He, \alpha)^{26}Al$ reactions, see table 26.5.
[i] Pr 61.

TABLE 26.4b

Resonances in ^{25}Mg+p (E_p > 980 keV)

E_p (keV) An 59b	Ba 59b	Pr 61	^{26}Al* (MeV)	Relative intensity[g]	Γ[c] (keV)	J^{π}[c]	Decay[a]	References γ-decay
(985 ±1)	986 ±3	987	7.248	18	3.8	2⁻	γ p_0	b, d, e, f
1026 ±1	1029[h]	1028	7.287				γ	d, f
1042.6±0.6	1045 ±3	1046	7.304	22			γ	b, d, f
1070 ±3			7.330				γ	
1084 ±2	1085 ±3	1086	7.343	18	(2.4, 1.7)	(2, 3)⁻	γ p_0	b, d, f
1104.7±1.3	1100 ±3	1105	7.362				γ	d, f
1136.1±1.0	1137[h]	1138	7.393				γ	d, f
1148 ±3	1148 ±3	1150	7.405	23	1.9	1⁻	γ p_0	d, f
1163 ±2	1166[h]	1166	7.419				γ	d, f
(1184 ±3)	1185[h]		7.439				(γ)p_1	d
1195.2±0.7	1196 ±3	1197	7.450	17			γ p_1	d, f
	1208[h]	1207	7.462				γ	d, f
1236.9±0.8	1241 ±3	1240	7.491	25			γ p_0	d, f
1283.4±0.6	1288 ±3	1285	7.537	20			γ	d, f
1303.9±0.5	1310 ±3		7.555	35			γ	d
(1352 ±3)			(7.601)				γ	
1373.5±2.5	1377 ±3	1377	7.622	48			γ p_1	d, f
	1432 ±5		7.678	9			γ	
	1531 ±4	1527	7.771	10			γ p_1	d, f
	1573 ±4		7.814	42			γ	
	1592 ±5	1589	7.831	24			γ p_1 p_2	d, f
	1638 ±4	1634	7.874	33			γ p_1 p_2	d, f
	1652 ±4	1652	7.889	1			γ p_1	d, f
		1701	7.936				γ	f
	1713 ±4	1717	7.946	100			γ p_1 p_2	d, f
	1724 ±4		7.959	100			γ p_1	d
	1748 ±5		7.982	40			γ p_1	d
	1768 ±4		8.001	90			γ p_1 p_2	d
	1832 ±5		8.063	130			γ p_1 p_2	d
	1898 ±5		8.126	600			γ p_1 p_2	d
	1938 ±5		8.165	1200			p_1	d

[a] Resonances in the yield of capture γ rays or β^+ activity are indicated by γ; resonances for elastic scattering by p_0, and resonances in the yield of the 0.58 and 0.98 MeV γ rays by p_1 and p_2, respectively.

[b] Ka 55.

[c] Pr 60.

[d] Bi 58a.

[e] Ny 60.

[f] Pr 61.

[g] Ba 59b.

[h] Bi 58a; these resonances have not been reported in Ba 59b.

Some γ-ray energies, measured with an accuracy comparable to that of the level differences from other reactions have been used in calculating the excitation energies given in table 26.3: $E_\gamma = 418 \pm 2$ keV and 827 ± 6 keV for the transitions (2) → (0) and (3) → (1), respectively (weighted mean of En 54c, Ka 55, Mu 60).

Most of the spins of ^{26}Al excited states, as given in fig. 26.2 and table 26.3, have been found from γ-ray angular distribution measurements (Gr 56e, Mu 60). Spin and parity assignments to ^{26}Al* = 1.06 and 2.37 MeV, probably $J^\pi = 1^+$ and $(2,3)^-$, respectively, from intensity considerations. Isobaric-spin assignments from comparison with the ^{26}Mg level scheme. The odd parity resonances predominantly decay either to $T = 0$ or to $T = 1$ levels, in accordance with the E1 isobaric spin selection rule for self-conjugate nuclei, $\Delta T = \pm 1$ (Gr 56e). From delayed γ–γ coincidence measurements the half-life of ^{26}Al* = 0.42 MeV has been determined as $\tau_{\frac{1}{2}} = (1.23 \pm 0.05) \times 10^{-9}$ sec (Go 60f).

E. ^{25}Mg(p, n)^{25}Al $Q_m = -5044 \pm 6$ $E_b = 6301 \pm 5$

Resonances have been observed at $E_p = 5.47$, 5.80, 6.02, 6.31, and 6.49 MeV. They might, however, also be assigned to ^{26}Mg(p, n)^{26}Al^m (Bl 51).

See ^{25}Al for threshold measurements.

F. ^{25}Mg(p, p)^{25}Mg $E_b = 6301 \pm 5$

The differential cross section for elastic scattering, measured at three resonances, yields the J^π values and widths given in table 26.4b (Pr 60).

Inelastic proton scattering to ^{25}Mg* = 0.58 and 0.98 MeV, observed by γ-ray detection, shows 15 resonances in the range $E_p = 1.184$–2.0 MeV; see table 26.4b (Bi 58a). At the 1185 keV resonance, the decay proceeds by at least 99% through the ^{25}Mg(p, p')^{25}Mg reaction to ^{25}Mg*(0.58), but positons have also been observed (Ka 55).

In the range $E_p = 1.5$–3.0 MeV, the inelastic scattering cross section shows more than 20 resonances (not tabulated). For $E_p > 2.3$ MeV, several resonances for inelastic scattering to ^{25}Mg* = 1.61 and 1.96 MeV have been found (Go 56).

For non-resonance data, see ^{25}Mg.

G. ^{25}Mg(d, n)^{26}Al $Q_m = 4076 \pm 5$

Observed, Sw 50.

For resonances, see ^{27}Al.

H. ^{26}Mg(p, n)^{26}Al $Q_m = -4796.7 \pm 4.9$
^{26}Mg(p, n)^{26}Al^m $Q_m = -5026 \pm 6$

A slow-neutron threshold has been observed at $E_p = 5.200 \pm 0.010$ MeV (also: $5.2? \pm 0.01$ MeV, Sc 54b), corresponding to $Q = -5.006 \pm 0.010$ MeV. The threshold corresponding to the ^{26}Al ground state has not been found (Ki 55a).

Resonances, see ^{27}Al.

I. ^{26}Si(β^+)^{26}Al $Q_m = 5050 \pm 80$

See ^{26}Si.

J. ^{27}Al(γ, n)^{26}Al $Q_m = -13069 \pm 5$

The threshold for neutron emission has been measured as 12.98 ± 0.08 MeV

(Ch 58), 12.75±0.20 MeV (Sh 51a). The threshold for production of $^{26}Al^m$ activity as 13.26±0.07 MeV (Ge 60a; see also Mc 49, Ha 54a).

Excitation curves have been measured up to $E_\gamma = 85$ MeV (Ba 61a, Pr 61a, Ch 60a, Fe 58, Mi 59, Ha 54a, En 54a; also Mo 55, theory). Neutron groups have been observed at $E_\gamma = 24$ and 30 MeV (Co 59d). Neutron angular distribution, Ku 59b.

K. ^{27}Al(p, d)^{26}Al $\qquad Q_m = -10844 \pm 5$

At $E_p = 18$ MeV, the angular distribution of deuterons proceeding to one or more of the three lowest ^{26}Al states, corresponds to $l_n = 2$ (Re 56, also Se 56). Deuteron energy spectra at various angles at $E_p = 23$ MeV, Co 59.

L. ^{27}Al(d, t)^{26}Al $\qquad Q_m = -6811 \pm 5$

At $E_d = 20$ MeV, the angular distributions of partly resolved triton groups yield the l_n values listed in table 26.5 (Vl 59; see also Go 60e).

M. ^{27}Al(^{3}He, α)^{26}Al $\qquad Q_m = 7508 \pm 5$

Magnetic analysis at $E(^3\text{He}) = 5.8$ MeV yields seventy ^{26}Al levels, listed in table 26.5; $Q_0 = 7.523 \pm 0.015$ MeV. The 2.09 MeV level (Ka 55, Gr 56e) has not been found; if the members of the 2.07–2.09 MeV doublet are equally excited the spacing would have to be less than 4 keV (Hi 59b).

At $E(^3\text{He}) = 5.2$ MeV, angular distribution measurements yield l_n values for the ground state and nine lowest excited states (see table 26.5); $Q_0 = 7.519 \pm 0.015$ MeV (Ta 60b).

N. ^{28}Si(d, α)^{26}Al $\qquad Q_m = 1420.7 \pm 4.2$

Measurements at several deuteron energies in the range $E_d = 5.5$–7.5 MeV, yield the excitation energies of 16 levels, see table 26.5; $Q_0 = 1.428 \pm 0.004$ MeV (see also Ma 60e, $Q_0 = 1.410 \pm 0.012$ MeV). The angular distributions of the groups leading to ^{26}Al(0), (1), and (2) were obtained at $E_d = 7.03$ MeV. At this energy the total yield of the isobaric-spin forbidden reaction leading to ^{26}Al(1) is 10% of the yield to ^{26}Al(0). The second $T = 1$ level could not be observed; the group to the 2.07 MeV level is strong (Br 59a).

For resonances, see ^{30}P.

O. Not reported:

^{24}Mg(α, d)^{26}Al	$Q_m = -12438.9 \pm 5.0$
^{25}Mg(^{3}He, d)^{26}Al	$Q_m = 808 \pm 5$
^{25}Mg(α, t)^{26}Al	$Q_m = -13512 \pm 5$
^{26}Mg(^{3}He, t)^{26}Al	$Q_m = -4032.2 \pm 4.9$
^{28}Si(n, t)^{26}Al	$Q_m = -16167.3 \pm 4.3$
^{28}Si(p, ^{3}He)^{26}Al	$Q_m = -16931.8 \pm 4.2$
^{29}Si(p, α)^{26}Al	$Q_m = -4832 \pm 5$

TABLE 26.5

Levels in ^{26}Al from ^{25}Mg(^{3}He, p)^{26}Al, ^{27}Al(d, t)^{26}Al, ^{27}Al(^{3}He, α)^{26}Al, and ^{28}Si(d, α)^{26}Al

E_x (MeV ± keV) Dr 59a[b]	E_x (MeV ± keV) Hi 59b[a]	E_x (MeV ± keV) Ta 60b[c]	l_n Ta 60b[c]	l_n Vl 59[d]
0	0	0	2	2
0.229 ± 3	0.229	0.234	2	(2, bracketed with above)
0.418 ± 2	0.416	0.422	0	0
1.060 ± 2	1.052	1.059	2	2
1.762 ± 3	1.755	1.741	2	
1.853 ± 3	1.846	1.844	0	
2.073 ± 3	2.067	2.064	2	(2)
2.368 ± 3	2.362	all ± 10		
2.548 ± 4	2.542			(1)
2.663 ± 4	2.659			
2.741 ± 5	2.738			
2.916 ± 6	2.910			
3.075 ± 6	3.072			
3.160 ± 6	3.155			
3.407 ± 6	3.398			
3.510 ± 10	3.504			
3.596 ± 10	3.593			
	3.675			
	3.719			
	3.746			
	3.918			
	3.962			
	4.194			
	4.202			
	all ± 10			

E_x (MeV ± keV) Hi 59b[a]	E_x (MeV ± keV) Hi 59b[a]
4.342	5.842
4.424	5.875
4.477	5.910
4.541	5.942
4.595	6.020
4.613	6.080
4.699	6.112
4.766	6.188
4.935	6.236
5.002	6.260
5.126	6.335
5.193	6.351
5.238	6.388
5.390	6.424
5.424	6.487
5.450	6.544
5.485	6.593[e]
5.506	6.670[e]
5.536	6.715[e]
5.558	6.776[e]
5.580	6.805[e]
5.665	6.842[e]
5.690	6.865[e]
5.715	all ± 10
all ± 10	

[a] ^{25}Mg(^{3}He, p)^{26}Al and ^{27}Al(^{3}He, α)^{26}Al: $E(^{3}\mathrm{He}) = 5.8$ MeV.
[b] ^{28}Si(d, α)^{26}Al, $E_d = 5.5$–7.5 MeV.
[c] ^{27}Al(^{3}He, α)^{26}Al; $E_d = 5.2$ MeV.
[d] ^{27}Al(d, t)^{26}Al: $E_d = 20$ MeV.
[e] These levels probably have also been seen as resonances in the ^{25}Mg(p, γ)^{26}Al reaction; see table 26.4a.

^{26}Si

(Fig. 26.3, p. 87)

A. ^{26}Si(β^+)^{26}Al $\qquad Q_m = 5050 \pm 80$

The half-life is 2.1 ± 0.3 sec (Ro 60a). A 1.7 sec half-life has been observed from bombardment of Al with 23 MeV protons; this might be attributed to ^{26}Si produced through the ^{27}Al(p, 2p) reaction (Ty 54).

A 824 ± 15 keV γ ray indicates a β^+ transition to ^{26}Al(1.06). A more intense β^+ branch proceeds to ^{26}Al(0.23); the end point of this transition is larger than 3.5 MeV (Ro 60a).

Observation of the transition to ^{26}Al(1.06) (log $ft > 3.2$), in competition with the super-allowed β^+ transition to ^{26}Al(0.23) (log $ft < 3.7$) yields $J^\pi = (0,1)^+$ for the 1.06 MeV level. De-excitation of this level to the $J^\pi = 0^+$, 0.23 MeV level then uniquely determines $J^\pi = 1^+$ for ^{26}Al* = 1.06 MeV.

B. ^{24}Mg(^{3}He, n)^{26}Si $\qquad Q_m = 80 \pm 80$

At $E(^3\text{He}) = 5.52$ MeV, three neutron groups have been observed, corresponding to $Q_0 = 0.08 \pm 0.08$ MeV, and to ^{26}Si* = 1.78 ± 0.06 and 2.79 ± 0.08 MeV. The angular distribution is peaked in the forward direction for the neutron groups to ^{26}Si* = 0 and 1.78 MeV, and is isotropic for the group to ^{26}Si* = 2.79 MeV (Aj 60).

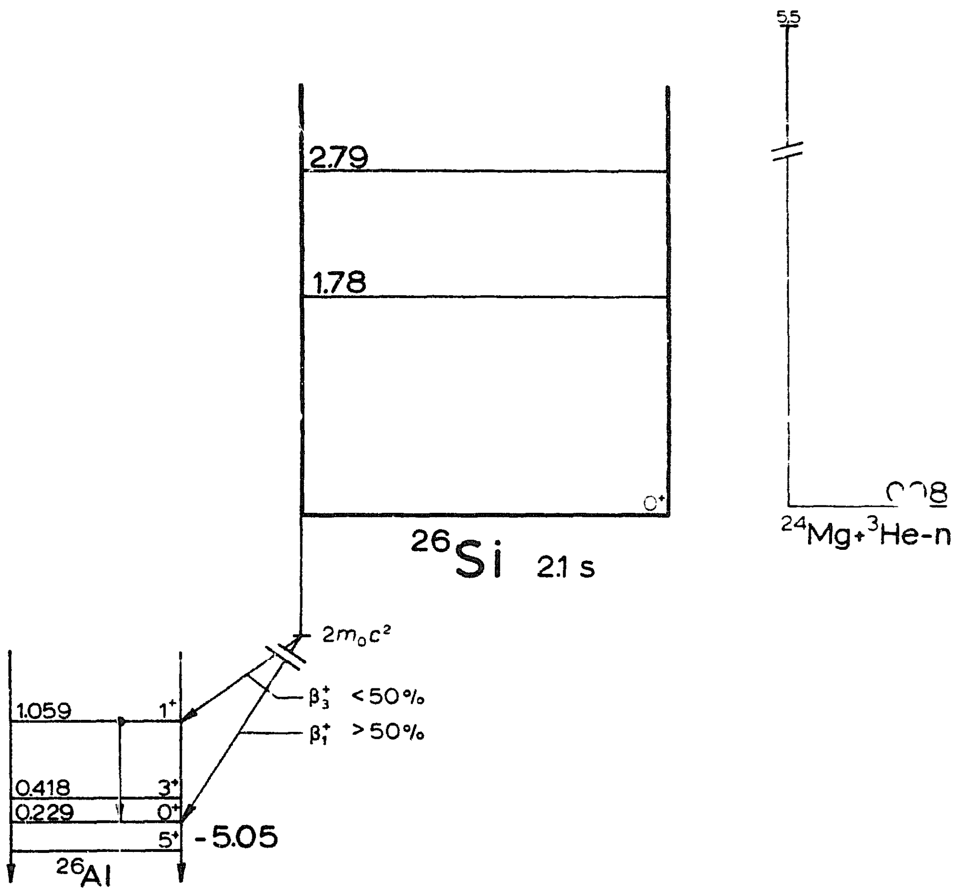

Fig. 26.3. Energy levels of ^{26}Si.

C. Not reported:

^{28}Si(p, t)^{26}Si $\qquad Q_m = -22000 \pm 80$

REMARKS

The close correspondence of the excitation energies of ^{26}Si* = 1.78 and 2.79 MeV with those of the lowest two levels of the mirror nucleus ^{26}Mg (1.81 and 2.94 MeV) suggests a $J^\pi = 2^+$ assignment to both levels (Aj 60).

^{27}Mg

(Fig. 27.1, p. 88; table 27.1, p. 89)

A. $^{27}Mg(\beta^-)^{27}Al$ $Q_m = 2617.9 \pm 4.0$

The weighted mean half-life is 9.46 ± 0.02 min (Ek 43, Sa 53, Da 53, Lo 53 Po 59).

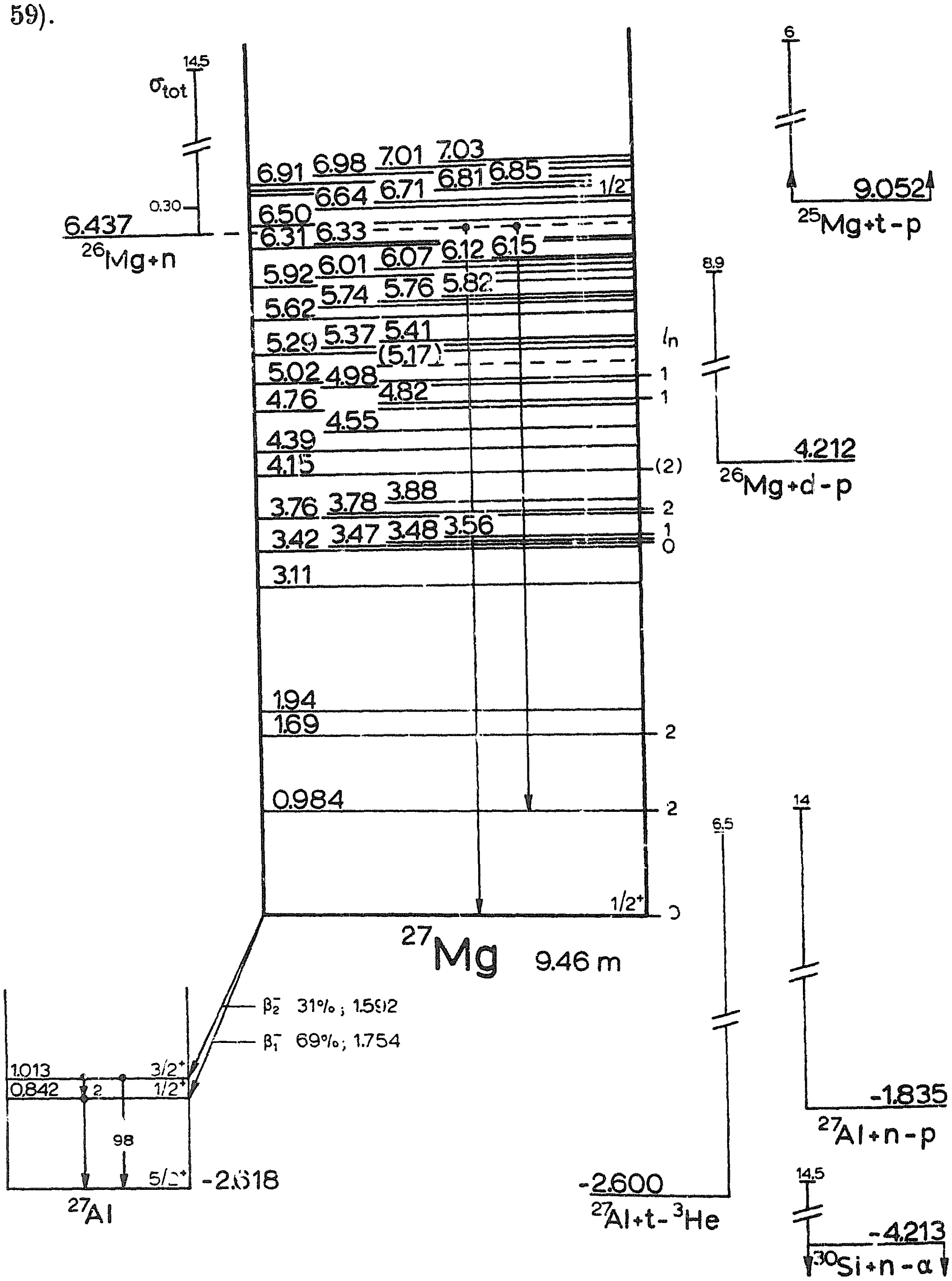

Fig. 27.1. Energy levels of ^{27}Mg.

A 58% (see, however, below) branch, end point 1.754±0.011 MeV, proceeds to ^{27}Al(0.842); the energy of the coincident γ ray has been measured as 834±8 keV; log ft = 4.75. A 42% branch, end point 1.592±0.022 MeV, to ^{27}Al(1.013), is coincident with a 1015±7 keV γ ray; log ft = 4.87 (Da 54a; see also Ma 54a).

The branching ratio reported above, is inconsistent with two independent measurements of the relative intensities of the 842 and 1015 keV γ rays, 70:30 (Ly 56, Mo 61). A 175±15 keV γ ray has been observed (relative intensity

TABLE 27.1

Energy levels of ^{27}Mg

E_x (MeV±keV)	J^π	$\tau_{\frac{1}{2}}$ or Γ	Decay	Reactions
0	$\frac{1}{2}^+$	9.46±0.02 min	β^-	A, B, C, E, F, G, H
0.984± 5	$(\frac{3}{2}, \frac{5}{2})^+$			B, C, E, F
1.692±10	$(\frac{3}{2}, \frac{5}{2})^+$			B, E, F
1.936±10				B, E, F
3.109±10				B, E, F
3.423±10				B, E, F
3.470±10				B, E, F
3.484±10	$\frac{1}{2}^+$			B, E, F
3.555±10	$(\frac{1}{2}, \frac{3}{2})^-$			B, E, F
3.757±10	$(\frac{3}{2}, \frac{5}{2})^+$			B, E
3.782±10				B, E
3.880±10				B, E
4.146±10				B, E
4.394±10				B, E
4.549±10				B, E
4.763±10				B, E
4.816±10	$(\frac{1}{2}, \frac{3}{2})^-$			B, E
4.982±10				B, E
5.017±10	$(\frac{1}{2}, \frac{3}{2})^-$			B, E
5.169–6.643; 17 levels, see table 27.2 and reaction				B
6.712±10	$\frac{1}{2}^-$	> 75 keV	n	B, D
6.807–7.031; 6 levels, see table 27.2 and reaction				B

0.66%), indicating a 2.2% decay of the 1.013 MeV level to the 0.842 MeV level in ^{27}Al (Ly 56; see also ^{27}Al). These γ ray measurements imply a (69±2)% β^- branch to ^{27}Al(1) and a (31±2)% branch to ^{27}Al(2).

A reported β^- branch to the ^{27}Al ground state (Da 53) has later been shown to be absent (Da 54a, Ma 54a, Ko 54a).

Calculation of the matrix elements of the observed β^- transitions, Fe 55.

B. ^{25}Mg(t, p)^{27}Mg $\qquad Q_m = 9052.1 \pm 4.0$

By magnetic analysis at E_t = 5–6 MeV, levels in ^{27}Mg have been observed up to E_x = 7.03 MeV, see table 27.2; Q_0 = 9.045±0.012 MeV (Hi 61h).

C. ^{26}Mg(n, γ)^{27}Mg $\qquad Q_m = 6437.1 \pm 3.1$

The thermal neutron capture cross section is 27 ± 5 mb (Hu 58). For the cross section at higher E_n, see Hu 58.

Gamma rays from thermal neutron capture in natural Mg are listed in table 25.4. The ^{27}Mg capturing state decays to ^{27}Mg* = 0 and 0.98 MeV (Ca 57b, Gr 58c).

At $E_n = 14.5$ MeV, the 0.85 ± 0.01 and 1.01 ± 0.02 MeV γ rays of ^{27}Al have

TABLE 27.2

Levels in ^{27}Mg from the ^{26}Mg(d, p)^{27}Mg and ^{25}Mg(t, p)^{27}Mg reactions

^{26}Mg(d, p)^{27}Mg Hi 61h E_d = 5–6 (MeV)	^{25}Mg(t, p)^{27}Mg Hi 61h E_t = 5–6 (MeV)	l_n(d, p) Ho 53 E_d = 8	l_n(d, p) Hi 58 8.9	l_n(d, p) Pa 61 7.8 MeV	$(2J+1)\theta_n^2 \times 10^3$ [a] Hi 58	$(2J+1)\theta_n^2 \times 10^3$ [a] Pa 61	^{25}Mg(t, p)^{27}Mg Hi 61h E_t = 5–6 (MeV)	
0	0	0	0	0	45	47	(5.169)	6.846
0.982 [b]	0.981	2	2	2	48	43	5.292	6.912
1.694	1.690			2		26	5.365	6.978
1.939	1.934						5.405	7.007
3.106	3.112						5.618	7.031
3.420	3.426						5.742	
3.470	3.471		} 0	0	40	44	5.762	
3.485	3.483		}				5.817	
3.556	3.554		1	1	140	65	5.922	
3.756	3.758		} 2	2 (+0)	90	55	6.005	
3.782	3.782		}				6.074 [c]	
3.879	3.880						6.122	
4.147	4.145			(2)		6	6.152	
4.391	4.398						6.306	
4.548	4.550						6.327	
4.759	4.767						6.499	
4.817	4.816		(1)	1		21	6.643	
4.982	4.982						6.712	
5.017	5.016			1		1.3	6.807	
all ± 10 keV							all ± 15 keV	

[a] The Hi 58 angular distribution measurements have been analyzed in Ma 60d. The relative reduced widths given in Pa 61 have been normalized by making the average value of the widths at the 0, 0.98, and 3.47+3.48 MeV states equal to that in Hi 58, Ma 60d.

[b] Also 0.987 ± 0.006 MeV (En 52), 0.978 ± 0.012 MeV (Ja 61a).

[c] With $l_n = 2$, $\theta_n^2 = 0.026$ (Pa 61).

been observed from bombardment of natural Mg, indicating capture in ^{26}Mg (De 60).

D. ^{26}Mg(n, n)^{26}Mg $\qquad E_b = 6437.1 \pm 3.1$

A resonance has been found at $E_n \approx 300$ keV; $\Gamma > 75$ keV; $J^\pi = \frac{1}{2}^-$ (Ne 59c). For non-resonance data, see ^{26}Mg.

E. ^{26}Mg(d, p)^{27}Mg $Q_m = 4212.3 \pm 3.1$

The ground state Q value has been measured as $Q_0 = 4.207 \pm 0.006$ MeV (En 52), 4.215 ± 0.010 MeV (Ma 60e), 4.213 ± 0.012 MeV (Hi 61h).

Magnetic analysis at $E_d = 5$–6 MeV, yields 19 proton groups; see table 27.2 (Hi 61h). See also Am 52.

Angular distribution analysis yields the l_n values and reduced widths listed in table 27.2 (Pa 61, Hi 58; also Ho 53). For a theoretical discussion of the reduced widths given in Hi 58 and Ho 53, see Ma 60d.

Discussion of the ratio of stripping to compound nucleus formation, Ne 56.

F. ^{27}Al(n, p)^{27}Mg $Q_m = -1835.3 \pm 4.0$

At neutron energies of about 14 MeV, proton groups have been observed to ^{27}Mg* = 0 and 1.66 MeV (Ja 60); to 0, 1.0, 1.6, 2.1, 2.8, and 3.5 MeV (Ov 59), and to 0, 1.0, 1.6, 3.5, 5.7, and 7.0 MeV (Ha 57a). The angular distributions of these groups have been measured (Ha 57a, Ov 59). See also Gl 61, Ha 61, Na 61, St 60a, Ma 58g, Co 59c, Co 58e, Co 57d, Br 57e, Al 57a.

For cross section and resonances, see ^{28}Al.

G. ^{27}Al(t, ^{3}He)^{27}Mg $Q_m = -2599.8 \pm 4.0$

Observed at $E_t = 6.5$ MeV (Po 52b).

H. ^{30}Si(n, α)^{27}Mg $Q_m = -4213 \pm 5$

Cross section at $E_n = 14.5$ MeV, Pa 53.

I. Not reported:

^{26}Mg(t, d)^{27}Mg	$Q_m = 179.4 \pm 3.1$
^{26}Mg(α, ^{3}He)^{27}Mg	$Q_m = -14140.1 \pm 3.1$
^{29}Si(n, ^{3}He) ^{27}Mg	$Q_m = -14175.8 \pm 4.9$

REMARKS

For a theoretical discussion of the ^{27}Mg level scheme in terms of the Nilsson model, Bi 60.

^{27}Al

(Fig. 27.2, p. 94; table 27.3, p. 92)

A. ^{23}Na(α, n)^{26}Al $Q_m = -2971 \pm 5$ $E_b = 10098.0 \pm 2.3$

Resonances have been observed at $E_\alpha = 3492 \pm 3$ keV ($\Gamma < 1$ keV), 3536, 3583, 3607, 3655, 3787, and 3832 keV, all ± 5 keV, corresponding to ^{27}Al levels at 13.073, 13.110, 13.150, 13.171, 13.212, 13.324, and 13.362 MeV (Wi 60). See also An 60c.

For Q value and ^{26}Al levels, see ^{26}Al.

B. ^{23}Na(α, p)^{26}Mg $Q_m = 1825.7 \pm 2.7$ $E_b = 10098.0 \pm 2.3$

Partially resolved resonances in the 1.81 MeV γ-ray yield, observed in the

TABLE 27.3

Energy levels of ^{27}Al

E_x (MeV $\pm$ keV)	J^π	τ_m	Decay	Reactions
0	$\frac{5}{2}^+$		stable	many
0.8424 $\pm$ 1.4	$\frac{1}{2}^+$	$(3.2\pm1.0)\times10^{-11}$ sec	γ	many
1.013 $\pm$ 2	$\frac{3}{2}^+$	$(2.0\pm0.8)\times10^{-12}$ sec	γ	many
2.212 $\pm$ 3	$(\frac{7}{2}^+)$	$(4.5\pm0.7)\times10^{-15}\,(2J+1)$ sec	γ	many
2.731 $\pm$ 3	$\frac{5}{2}^+$		γ	many
2.976 $\pm$ 3	$\frac{3}{2}^+$		γ	E, L, M, O, S
3.000 $\pm$ 3			γ	E, L, M, O
3.674 $\pm$ 5	$\frac{1}{2}$		γ	E, G, L, S
3.951 $\pm$ 5			γ	E, L, S
4.052 $\pm$ 5	$\frac{1}{2}$		γ	E, L, S
4.403 $\pm$ 6				G, L
4.504 $\pm$ 5				L, S
4.576 $\pm$ 6				L
4.805 $\pm$ 6				L, O
5.149 $\pm$ 5				L, S
5.240 $\pm$ 5				G, L, S
5.410 $\pm$ 6				G, L
5.424 $\pm$ 5				L, S
5.491 $\pm$ 6				L
5.543 $\pm$ 5				L, S
5.659 $\pm$ 6				L
5.745 $\pm$12				S
5.821 $\pm$ 5				G, L, S
5.951 $\pm$ 5				L, S
6.074 $\pm$12				S
6.154 $\pm$12				S
6.264 $\pm$12				S
6.527 $\pm$12				S
6.596 $\pm$12				S
6.764 $\pm$12				S
6.812 $\pm$12				G, S
6.989 $\pm$12				S
8.2	$(\frac{1}{2}, \frac{3}{2})^-$			G
8.554–10.102; 28 levels, see table 27.4, reaction				E (and G)
11.1			p	F
11.75			p	B
11.91			p	B, F
12.07			p	B
12.23			p	B
12.27			p	B
12.34			p	B
12.46			p	B
12.68			p	B, F
12.71			p	B
12.78			p	B
12.84			p	B
12.87			p	B
12.99			p	B
13.073 $\pm$ 6			p	B, F
			n, p	A, B

TABLE 27.3 *(Continued)*

E_x (MeV ± keV)	J^π	τ_m	Decay	Reactions
13.110 ± 6			n	A
13.150 ± 6			n, p	A, B
13.171 ± 6			n	A
13.212 ± 6			n	A
13.324 ± 6			n	A
13.362 ± 6			n	A
13.5			p	F
(18.07)			n	D

E_α = 1.8–3.7 MeV range, correspond to ^{27}Al* = 11.75, 11.91, 12.07, 12.23, 12.27, 12.34, 12.46, 12.68, 12.71, 12.78, 12.84, 12.87, 12.99, 13.07, and 13.14 MeV (Te 54).

For non-resonance information, see ^{26}Mg.

C. ^{24}Mg(α, p)^{27}Al $\qquad Q_m = -1594.5 \pm 1.1$

At E_α = 8.4 MeV, proton groups have been observed to ^{27}Al* = 0, 0.85 ± 0.04, 1.06 ± 0.04, 2.17 ± 0.04, and 2.64 ± 0.10 MeV (Gr 57; see also Br 55b).

For resonances, see ^{28}Si.

D. ^{25}Mg(d, n)^{26}Al $\qquad Q_m = 4076 \pm 5 \qquad E_b = 17145.1 \pm 2.2$

^{25}Mg(d, p)^{26}Mg $\qquad Q_m = 8872.7 \pm 2.7 \qquad E_b = 17145.1 \pm 2.2$

A resonance at E_d = 0.965 ± 0.015 MeV has been observed from natural Mg target bombardments. Assignment to ^{25}Mg yields ^{27}Al* = 18.07 MeV (Al 48a). Assignment to ^{24}Mg, however, seems more probable.

For non-resonance data, see ^{26}Al and ^{26}Mg.

E. ^{26}Mg(p, γ)^{27}Al $\qquad Q_m = 8272.4 \pm 2.8$

Resonances in the γ-ray yield are listed in table 27.4 (enriched targets: Ru 54a, Hu 55, Ba 59b, Ku 59a, Wa 59a; natural Mg targets: An 59b; see also Sm 54). The corresponding ^{27}Al excitation energies have been computed using the weighted mean values of the resonant proton energies. In the range E_p = 0.8–2.36 MeV, 35 resonances (not tabulated) have been observed (Al 57).

The decay scheme of the 338, 454, 661, and 719 keV resonances is given in fig 27.2. Measurements of the γ-ray spectra, angular distributions, and γ–γ coincidences yield the strenghts of these resonances, the spin of the resonance levels (table 27.4), and of the following lower levels: ^{27}Al* = 0.842 MeV, $J = \frac{1}{2}$; 2.212 MeV, $J = (\frac{3}{2})$; 2.731 MeV, $J = \frac{5}{2}$; 2.976 and/or 3.000 MeV, $J = \frac{3}{2}$; 3.674 MeV, $J = \frac{1}{2}$; 4.052 MeV, $J = \frac{1}{2}$. The energies of the γ rays de-exciting ^{27}Al(1) and (2), are 840 ± 6 keV, and 1012 ± 8 keV, respectively (Va 56d).

The 648 keV resonance decays to ^{27}Al(0) and, indirectly, to ^{27}Al(1); $J^\pi = (\frac{5}{2}^-)$ (No 61a). At the 809 keV resonance, angular distribution measurements of

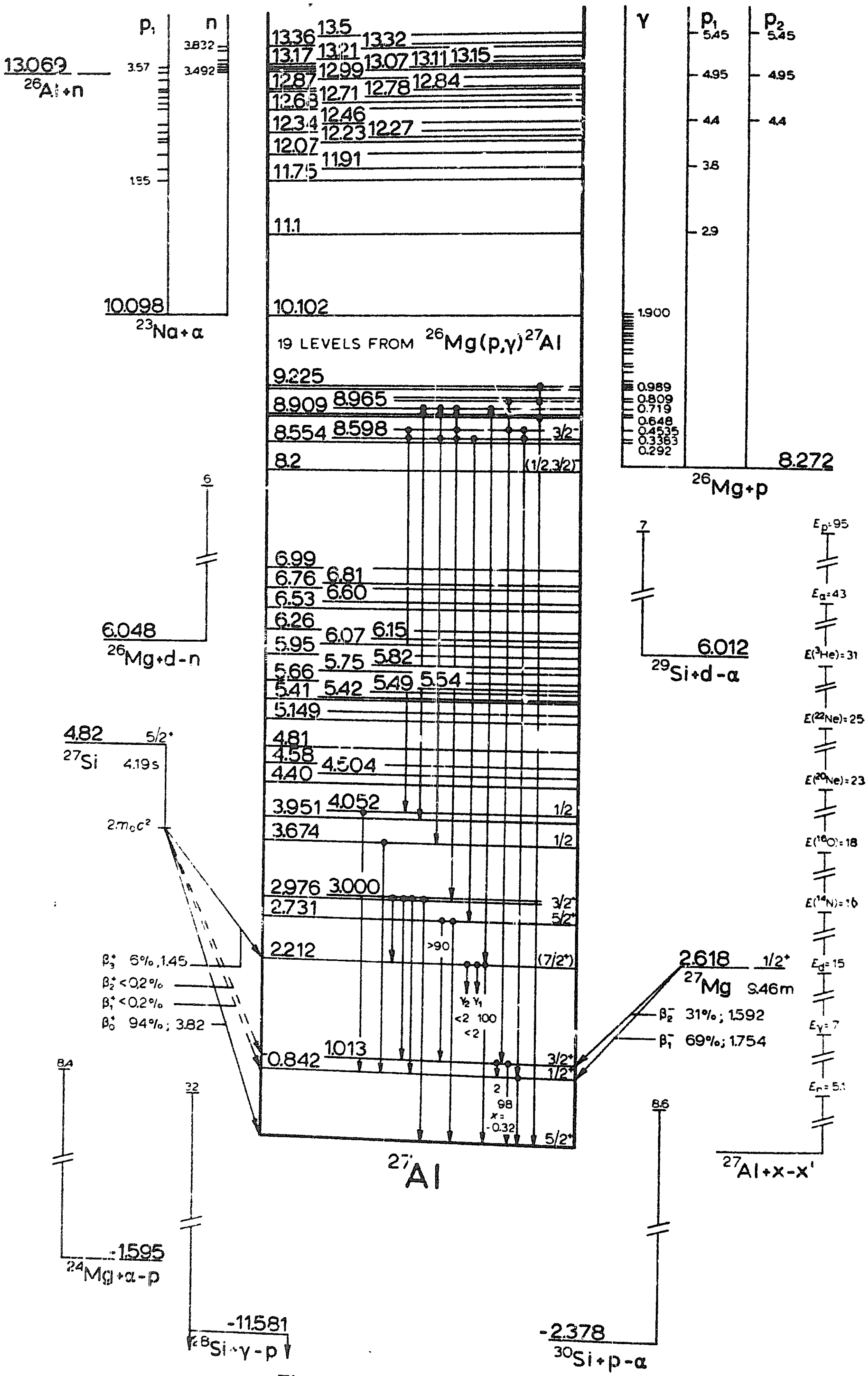

Fig. 27.2. Energy levels of ^{27}Al.

TABLE 27.4

Resonances in ^{26}Mg(p, γ)^{27}Al

E_p [a] (keV)	^{27}Al* (MeV)	J^π	$\Gamma_p\Gamma_\gamma/\Gamma$ (eV)	E_p [a] (keV)	^{27}Al* (MeV)	Intensity [h] (relative)
292.3 ± 0.7 [c, d]	8.554			1251 ± 4 [f, h]	9.477	10
338.3 ± 0.1 [b, c, d, e, f]	8.598	$\frac{3}{2}^-$ [i, j]	0.4 ± 0.1 [m]	1289 ± 4 [f, h]	9.514	70
453.5 ± 0.1 [b, c, d, e, f]	8.709	$\frac{1}{2}(-)$ [j]	1.4 ± 0.3 [m]	1417 ± 4 [f, h]	9.637	140
647.5 ± 0.8 [b]	8.896	$\frac{5}{2}(-)$ [k]	[k]	1452 ± 4 [f, h]	9.671	70
661.1 ± 0.4 [b, c, d, f]	8.909	$\frac{1}{2}(+)$ [j]	0.7 ± 0.2 [m]	1554 ± 4 [h]	9.769	140
718.5 ± 1.2 [c, f]	8.965	$\frac{3}{2}(+)$ [j]	0.21 ± 0.05 [m]	1588 ± 4 [h]	9.803	7.5
809.0 ± 0.4 [b, c, f]	9.051	$\frac{5}{2}$ [l]	[l]	1615 ± 4 [h]	9.828	110
838.8 ± 0.5 [b, c, f]	9.080			1637 ± 4 [h]	9.849	50
954 ± 10 [f]	9.191			1725 ± 4 [h]	9.933	95
989 ± 7 [f, g]	9.225	$(\frac{7}{2})^+$ [g]		1735 ± 4 [h]	9.943	95
1015 ± 10 [f]	9.250			1759 ± 4 [h]	9.966	190
1056 ± 10 [f]	9.289			1786 ± 5 [h]	9.992	110
1172 ± 10 [f]	9.401			1823 ± 5 [h]	10.028	145
				1882 ± 5 [h]	10.085	135
				1900 ± 5 [h]	10.102	180

[a] Weighted mean values. For $E_p < 840$ keV the energies from four precision measurements (An 59a, Ku 59a, Wa 59a, Hu 55) are in excellent agreement.
[b] An 59a.
[c] Ku 59a.
[d] Wa 59a.
[e] Hu 55.
[f] Ru 54a.
[g] Al 57.
[h] Ba 59b.
[i] The odd parity follows from the E1 character of the γ ray de-exciting the 338 keV resonance to ^{27}Al(1), as determined by a polarization measurement (Hu 56).
[j] Parity assignments based on intensity considerations only (Va 58d).
[k] No 61a; the γ-ray yield is about 10% of that at the 661 keV resonance.
[l] Sm 59; $\Gamma_{\gamma_0} \leq 0.15$ eV, resonance absorption measurement.
[m] Va 56d.

the transitions to ^{27}Al(0) and (2) give $J = \frac{5}{2}$ for the resonance level (Sm 59).

Angular distribution measurements at some unspecified resonances yield $J = \frac{3}{2}$ for ^{27}Al(2), and very probably, $J = \frac{1}{2}$ for ^{27}Al(1). The 2.731 MeV level mainly (> 90%) decays to ^{27}Al(2). Angular correlations measured at the 989 keV resonance are in agreement with $J^\pi = \frac{7}{2}^+$ or $\frac{3}{2}^+$ for the resonance level and $J^\pi = \frac{5}{2}^+$ for the 2.731 MeV level. The $\frac{7}{2}^+$ assignment to the resonance is favoured because no direct transitions to ^{27}Al(1) and (2) have been observed; their intensity is at most 3% of the ground-state transition (Al 57).

F. (a) ^{26}Mg(p, p')^{26}Mg $E_b = 8272.4 \pm 2.8$

(b) ^{26}Mg(p, n)^{26}Al^m $Q_m = -5026 \pm 6$ $E_b = 8272.4 \pm 2.8$

(a) At $E_p = 2.9$ and 3.8 MeV, resonances have been observed in the yield of the 1.81 MeV γ ray, and at $E_p = 4.4$, 4.95 and 5.45 MeV in the yield of the 1.13 and 1.81 MeV γ rays (Mi 59b).

For non-resonance data, see ^{26}Mg.

(b) Resonances at $E_p = 5.47$, 5.80, 6.02, 6.31, and 6.49 MeV, observed from the ^{25}Mg(p, n)^{25}Al reaction, might also be assigned to the ^{26}Mg(p, n)^{26}Al^m reaction (Bl 51).

For threshold measurements, see ^{26}Al.

G. ^{26}Mg(d, n)^{27}Al $\quad Q_m = 6047.7 \pm 2.8$

Nuclear emulsion work at $E_d = 1.47$ MeV gives ^{27}Al levels at 0.88, 1.92, 2.75, 3.65, 4.33, 5.32, and 5.81 MeV, all ± 0.07 MeV (Sw 50). At $E_d = 1.0$ and 6.0 MeV, levels have been found at 1.0, 2.3, 2.9, 6.8, 8.2, 9.5, and 10.0 MeV. Angular distribution measurements yield $l_p = 0$ and 1 for the 6.8 and 8.2 MeV levels, respectively (Tr 56).

H. ^{27}Mg(β^-)^{27}Al $\quad Q_m = 2617.9 \pm 4.0$

See ^{27}Mg.

I. ^{27}Al(γ, γ)^{27}Al

Resonance absorption measurements yield a mean life $\tau_m = (4.1^{+2.9}_{-1.6}) \times 10^{-14}$ sec for ^{27}Al* = 1.013 MeV (Va 60a; see, however, reaction L, Me 60b), and $\tau_m = 3.5 \times 10^{-14}\ g_2/g_1$ sec for ^{27}Al* = 2.21 MeV, where g_1 and g_2 are the statistical weights of the ground state and the 2.21 MeV level (Bo 61).

J. ^{27}Al(γ, p)^{26}Mg $\quad Q_m = -\ 8272.4 \pm 2.8$

^{27}Al(γ, n)^{26}Al $\quad Q_m = -13069 \quad \pm 5$

The total absorption cross section in the range $E_\gamma = 10$–30 MeV does not show a resonance fine structure. The peak cross section, at $E_\gamma = 20$ MeV, is larger than the sum of the (γ, n) and (γ, p) cross sections (Zi 60; see also Mi 59). No resonance structure has been found at $E_\gamma = 20$–20.5 MeV (Ca 60).

K. ^{27}Al(n, n′)^{27}Al*

Gamma-ray energies and intensities from inelastic neutron scattering have been measured by scintillation counter. The weighted mean values of the reported γ-ray energies are $E_\gamma = 0.166 \pm 0.003$, 0.842 ± 0.005, 1.021 ± 0.006, 1.727 ± 0.015, and 2.209 ± 0.007 MeV (Da 56c, Ro 55a, Ho 59a, De 60, Mi 59c, Pa 58b, Cr 56a, Gr 55d, Ki 54, Sc 54d; see also As 61, Mo 56c, Ra 55, Pa 55, Ga 53a). The three first mentioned γ rays are ground-state transitions since the production thresholds are equal to the γ-ray energies (Ki 54). The 0.166 and 1.73 MeV gammas correspond to the 1.01 → 0.84 and 2.73 → 1.01 MeV transitions, respectively. Gamma rays of 1.19 MeV (Sc 54d, De 30), 1.33 MeV (De 60), 1.40 MeV (Mo 56c), and 1.91 MeV (Ro 55a) have not been found in other experiments. At higher neutron energies γ rays of 2.72 MeV (Mo 56c) and 3.10 ± 0.08 MeV (Gr 55d) have been reported. See also Ra 55a, An 60d, As 61.

Cross section for inelastic scattering, Hu 58, Ma 57, Ma 58f, To 59. Elastic scattering angular distribution, Li 55a, Be 56, Do 56a, La 57b, Na 57, Be 58b, Co 58b, Hi 58a, An 59a, St 59, St 59c, Yu 59, Lo 60.

For resonances, see ^{28}Al.

L. $^{27}Al(p, p')^{27}Al$

Levels derived from the observation of proton groups are listed in table 27.5 (Do 53, Br 54b, Va 57d, De 59a; also Sh 51, Re 52, St 52, Ba 52).

Elastic scattering angulı distribution, Wi 41, Rh 50, Bu 51, Ba 52, Gu 52, Da 54, Hi 55, Da 56a, Ge 56a, Ki 56a, Sh 56, Wa 57, Gr 59, Ho 61a, Jo 61b, Ta 61a; theory, Gl 57, Me 57a. Angular dependence of the polarization of elastically scattered protons, Wa 59, Sa 60a, Ho 61a, Ya 60a, Ro 61c. Inelastic proton angular distributions at $E_p = 5$ MeV, De 59a, and at 6.6 MeV, Va 61a.

TABLE 27.5

Levels of ^{27}Al (MeV±keV) from the $^{27}Al(p, p')^{27}Al$ and $^{29}Si(d, \alpha)^{27}Al$ reactions

(p, p')[a]	(p, p')[b]	(p, p')[c]	(p, p'γ)[d]	(p, p')[e]	(d, α)[f]	(p, p')[b]	(d, α)[g]
0.842±3	0 842	0.843±2	0.845± 5	0.840±4	0.837±16	5.425	5.419
1.013±3	1.013		1.014± 7	1.010±4	1.007±13	5.491	
2.205±4	2.213	(d, α)[g]	2.216±10	2.219±4	2.21 ±30	5.5[illegible]	5.537
2.727±4	2.732	2.729	2.736±12	2.736±6	2.74 ±20	5.659	
2.975±4	2.977	2.971		2.980±6			5.745
2.998±4	3.001		2.992±15	3.002±6		5.821	[illegible].820
	3.677	3.663				5.951	5.953
	3.954	3.940				all±6	6.074
	4.054	4.044					6.154
	4.403						6.264
	4.505	4.499					6.527
	4.576						6 596
	4.807						6.764
	5.150	5.145					6.812
	5.242	5.232					6.989
	5.410						all±12
	all±6	all±12					

[a] Va 57d; $E_p = 2$–4 MeV; magn. anal.
[b] Br 54b; $E_p = 5.6$–8.4 MeV; magn. anal.
[c] Do 53; $E_p = 2.3$ MeV; electrost. anal.
[d] Ra 58; $E_p = 2.4$–4.4 MeV; γ energies, lens spectrom.
[e] De 59a; $E_p = 5$ MeV; magn. anal.
[f] Va 52; $E_d = 1.8$–2.0 MeV; magn. anal.
[g] Br 59a; $E_d = 7.0$ MeV; magn. anal.

Direct interaction analysis applied to the results in Va 61a, yields $l = 2$ for transitions to the 0.84, 1.01, 2.74, and 3.00 MeV states, and $l = 3$ for transitions to the 2.21 MeV state. See also Ty 58, Gu 54.

The yield of the 0.84 and 1.01 MeV γ rays from inelastic proton scattering shows 23 resonances in the range $E_p = 1.7$–2.8 MeV; see ^{28}Si. Angular distribution measurements at 15 resonances yield $J = \frac{1}{2}$ for ^{27}Al(1) and $J > \frac{1}{2}$ for ^{27}Al(2). Proton-gamma coincidence experiments indicate that the 1.01 MeV level also de-excites via a 0.170 ± 0.007 MeV γ ray to the 0.84 MeV level; intensity (2.4 ± 1.0)% (Al 60b). Angular distribution and linear polarization measurements of the 1.01 MeV γ ray, at the $E_\text{p} = 1.74$ and 2.13 MeV resonances yield the E2/M1 amplitude mixing ratio $x = -0.32 \pm 0.14$ or -1.1 ± 0.5 (Mc 61a).

Doppler corrected energies of the ground-state transitions from ^{27}Al* = 0.84, 1.01, 2.21, (2.73), and 2.98+3.00 MeV, and the $E_\gamma = 1.722 \pm 0.010$ MeV ^{27}Al(4) → (2) transition, yield the excitation energies listed in table 27.5, column 4. Measurement of the internal conversion coefficients yields E2 for the (1) → (0) transition, M1 for the (2) → (0) transition, and favours M1 for (4) → (2), and E1 for (3) → (0) (Ra 58).

Self absorption and resonance scattering studies yield partial widths Γ_γ for the ground-state γ transitions from ^{27}Al(2): $\Gamma_0 = (3.9 \pm 1.6) \times 10^{-4}$ eV, and from ^{27}Al(3): $\Gamma_0 = (g_1/g_2)(2.4 \pm 0.3) \times 10^{-2}$ eV, where g_1 and g_2 are the statistical weights of ^{27}Al(0) and (3), respectively. The angular distribution of the 2.21 MeV radiation, and the observed partial width rule out $J = \frac{1}{2}$ and $J^\pi = \frac{1}{2}^-$ assignments to ^{27}Al(3). This level branches for less than 2% to ^{27}Al(1) and/or (2). Comparison of the width of the 1.01 MeV level with its partial E2 width (see reaction P) yields an E2/M1 intensity ratio $x^2 = 0.1 \pm 0.05$ (Me 60b, Ra 61a).

For resonances, see ^{28}Si.

M. ^{27}Al(d, d')^{27}Al

Inelastically scattered deuterons to ^{27}Al* = 0.84, 1.01, 2.21, 2.73 MeV, and the 2.98/3.00 MeV doublet have been observed at various deuteron energies between 5 and 15 MeV (Hi 56b, Ha 56c, Gr 49, Ho 49, Ke 51, En 54b). The angular momentum transfer $l = 2$ connected with the transitions to ^{27}Al* = 2.21, 2.73, and 2.98/3.00 MeV, determines the parity of these levels as even (Hi 56b). See also Ha 56c, Do 60, El 60.

Elastic scattering angular distribution, Sl 59, Ci 60, Ci 60a, Ta 60e, Go 61, Ba 61d, Ig 61.

N. ^{27}Al(^{3}He, ^{3}He)^{27}Al

Elastic scattering angular distribution at $E(^3\text{He}) = 31$ MeV, Ig 60; 29 MeV, Gr 61a; 5.5 MeV, Pa 61a.

O. ^{27}Al(α, α')^{27}Al

Elastic scattering angular distributions, Bl 55a, Ig 56, Bl 56a, Ga 58, Ko 61a.

Inelastic scattering has been observed to the first two ^{27}Al levels (unresolved) at $E_\alpha = 19$ MeV, to ^{27}Al* = 2.69, 4.80, and 6.87 MeV at $E_\alpha = 30$ MeV (Cr 60a) and 43 MeV (Yn 60), and to ^{27}Al* = (0.84+1.01), 2.21, and (2.73+3.00) MeV at

$E_\alpha = 22$ MeV (Be 61c). Inelastic scattering angular distributions at $E_\alpha = 40.2$ MeV, Ig 57.

Alpha-gamma coincidence experiments at $E_\alpha = 22$ MeV, establish a strong $3.0 \rightarrow 2.21$ MeV transition. This result is in accordance with the suggestion that one of the 3.0 MeV states and the 2.21 MeV state are the $J^\pi = \frac{9}{2}^+$ and $\frac{7}{2}^+$ members of a $K^\pi = \frac{5}{2}^+$ rotational band on the ground state. Ground-state transitions have been observed from ^{27}Al* = 1.01, 2.21, 2.73, and 2.98 and/or 3.00 MeV. The 2.73 MeV level mainly decays to ^{27}Al(2); a 10% transition to ^{27}Al(1) is not excluded (Be 61c).

P. ^{27}Al+heavy ions (^{14}N, ^{16}O, ^{20}Ne, ^{22}Ne)

Coulomb excitation with heavy ions at $E(^{14}\text{N}) = 16.3$ MeV, $E(^{16}\text{O}) = 18.2$ MeV, $E(^{20}\text{Ne}) = 23.1$ MeV, $E(^{22}\text{Ne}) = 25.2$ MeV, yields partial mean lives $\tau_m(\text{E2}) = (3.2 \pm 1.0) \times 10^{-11}$ sec and $(1.3 \pm 0.4) \times 10^{-11}$ sec for ^{27}Al* = 0.84 and 1.01 MeV, respectively (Al 59b). Also Go 60d: $\tau_m(\text{E2}) = 5.3 \times 10^{-11}$ sec and 2.4×10^{-11} sec, respectively.

Q. ^{27}Si(β^+)^{27}Al $Q_m = 4815 \pm 8$

See ^{27}Si.

R. ^{28}Si(γ, p)^{27}Al $Q_m = -11580.6 \pm 3.3$

Cross section for 28 and 32 MeV bremsstrahlung, Jo 55, Cu 59; also Mo 55a, Sh 61b. No activity with a half-life in the μsec or msec range has been found from the bombardment of natural silicon with 22 MeV bremsstrahlung (Ve 56a).

S. ^{29}Si(d, α)^{27}Al $Q_m = 6012.0 \pm 3.6$

Magnetic analysis of α-particle groups yields ^{27}Al levels listed in table 27.5 (Va 52, Br 59a); $Q_0 = 5.994 \pm 0.011$ MeV (Va 52), 5.994 ± 0.012 MeV (Ma 60e).

T. ^{30}Si(p, α)^{27}Al $Q_m = -2377.6 \pm 4.1$

Magnetic analysis at $E_p = 8.0$ and 8.6 MeV yields $Q_0 = -2.366 \pm 0.010$ MeV (Wh 60).

U. Not reported:

^{25}Mg(t, n)^{27}Al	$Q_m = 10887.5 \pm 2.3$
^{25}Mg(^{3}He, p)^{27}Al	$Q_m = 11651.9 \pm 2.3$
^{25}Mg(α, d)^{27}Al	$Q_m = -6700.5 \pm 2.2$
^{26}Mg(^{3}He, d)^{27}Al	$Q_m = 2779.2 \pm 2.8$
^{26}Mg(α, t)^{27}Al	$Q_m = -11540.3 \pm 2.8$
^{28}Si(n, d)^{27}Al	$Q_m = -9355.9 \pm 3.3$
^{28}Si(d, ^{3}He)^{27}Al	$Q_m = -6087.5 \pm 3.3$
^{28}Si(t, α)^{27}Al	$Q_m = 8232.1 \pm 3.4$
^{29}Si(n, t)^{27}Al	$Q_m = -11576.0 \pm 3.6$
^{29}Si(p, ^{3}He)^{27}Al	$Q_m = -12340.5 \pm 3.5$

REMARKS

The rotational collective model, with a prolate distortion for ^{27}Al, gives a good qualitative description of many of the properties of the low lying levels of ^{27}Al with the exception of the excitation energies. The 0.84, 1.01, and 2.73 MeV levels, with $J^\pi = \frac{1}{2}^+, \frac{3}{2}^+$, and $\frac{5}{2}^+$, respectively, are the lowest three members of the $K^\pi = \frac{1}{2}^+$ rotational band derived from the $s_{\frac{1}{2}}$ shell model state. The 2.21 MeV level is a likely candidate for the second member of the $K^\pi = \frac{5}{2}^+$ rotational band based on the ^{27}Al ground state; the required $J^\pi = \frac{7}{2}^+$ assignment, however, conflicts with some of the experimental data (Al 60b). Odd parity for the 2.21 MeV level follows from angular distribution measurements of inelastically scattered protons (De 59a, Va 61a). The internal conversion coefficient of the 2.21 MeV γ ray favours an E1 assignment to this γ ray and thus odd parity for the 2.21 MeV level, but M1 character is not completely excluded (Ra 58). The angular distribution of the 2.21 MeV γ ray from the $^{27}Al(p, p'\gamma)^{27}Al$ reaction excludes $J^\pi = \frac{1}{2}^\pm, \frac{3}{2}^-$ (Me 60b). The intensity of the γ transitions to the 2.21 MeV level at two $^{26}Mg(p, \gamma)^{27}Al$ resonances suggests $J = \frac{7}{2}$ (Va 56d). Even parity for the 2.21 MeV level follows from the angular momentum transfer in inelastic deuteron scattering (Hi 56b), and from the allowed character of the $^{27}Si(\beta^+)$ decay to $^{27}Al^* = 2.21$ MeV. The strong $3.0 \rightarrow 2.21$ MeV γ transition, observed from inelastic α-particle scattering, is in accordance with the suggestion that one of the 3.0 MeV states and the 2.21 MeV state are the $J^\pi = \frac{9}{2}^+$ and $\frac{7}{2}^+$ members of the $K^\pi = \frac{5}{2}^+$ band on the ground state. Finally, a $J^\pi = \frac{7}{2}^+$ assignment to the 2.21 MeV level would explain the small γ branching ($< 2\%$) to $^{27}Al(1)$ and (2) (Me 60b). See also Bi 60.

^{27}Si

(Fig. 27.3, p. 101; table 27.6, p. 102)

A. $^{27}Si(\beta^-)^{27}Al$ $\qquad Q_m = 4815 \pm 8$

The weighted mean value of the half-life measurements, which are in rather bad agreement, is $\tau_{\frac{1}{2}} = 4.19 \pm 0.05$ sec (Su 53, Hu 54, Cl 58, Wa 60a, Ku 57a, Mi 58, Va 60f). The β^- decay proceeding to the ^{27}Al ground state, with end point 3.82 ± 0.05 MeV (Ba 40, Bo 51, Hu 54, Wa 60a; see also Va 60f), is super-allowed ($\log ft = 3.6$), determining $J^\pi = \frac{5}{2}^+$ for $^{27}Si(0)$. A 10% branch, with end point 1.45 ± 0.10 MeV proceeding to $^{27}Al^* = 2.21$ MeV has been reported (Va 60f); the intensity of the 2.21 MeV γ ray leads to a branching of $(6 \pm 3)\%$ (Pa 61d). This intensity, however, would give $\log ft = 3.3$.

The intensity of potential branches to $^{27}Al(1)$ or (2) is less than 0.2% (Ta 60c).

B. $^{24}Mg(\alpha, n)^{27}Si$ $\qquad Q_m = -7193 \pm 8$

Observed at $E_\alpha = 15$ MeV (El 41).

C. ^{27}Al(p, n)^{27}Si $\qquad Q_m = -5598 \pm 8$

Recent measurements of the threshold give $E_p = 5.792 \pm 0.010$ MeV (Ki 55a), 5.798 ± 0.008 MeV (Ma 55c), 5.800 ± 0.008 MeV (Br 59f); the weighted average yields $Q_0 = -5.590 \pm 0.005$ MeV.

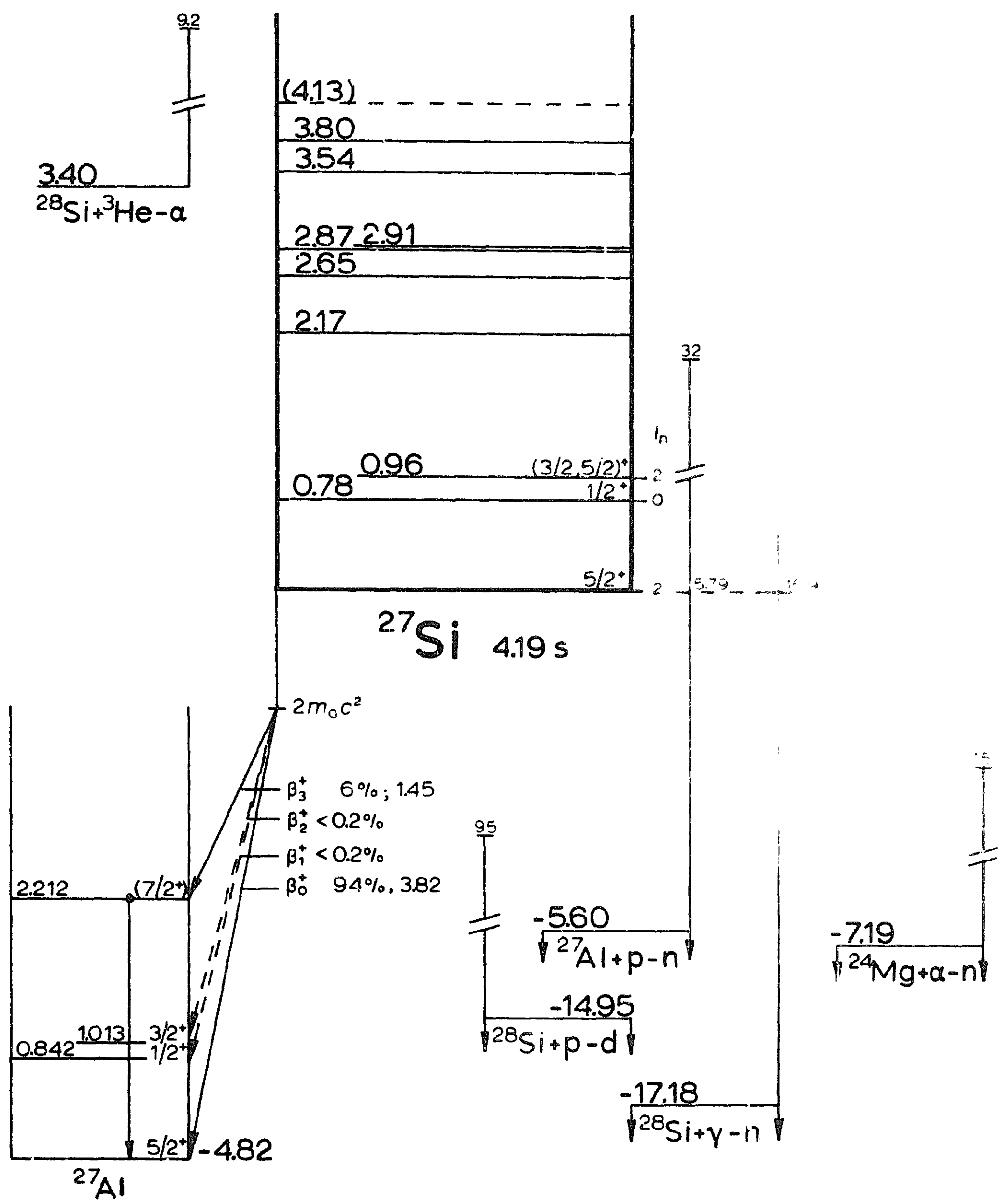

Fig. 27.3. Energy levels of ^{27}Si.

Angular distribution at $E_p = 23$ MeV, Co 55b; at $E_p = 14$ MeV, Hi 601. Cross section, Ta 58, Al 61b. See also Ad 61.

For resonances, see ^{28}Si.

TABLE 27.6

Energy levels of ^{27}Si

E_x (MeV±keV)	J^π	$\tau_{\frac{1}{2}}$	Decay	Reactions
0	$\frac{5}{2}^+$	4.19±0.05 sec	β^+	A, B, C, D, E, F
0.782±10	$\frac{1}{2}^+$			F
0.958±10	$(\frac{3}{2}, \frac{5}{2})^+$			F
2.165±10				F
2.651±10				F
2.866±10				F
2.908±10				F
3.540±10				F
3.800±15				F
(4.13 ±20)				F

D. ^{28}Si(γ, n)^{27}Si $Q_m = -17179 \pm 9$

The threshold has been determined as 16.8±0.4 MeV (Mc 49) and 16.9±0.2 MeV (Su 53). Cross section, Ka 54. See also Wa 48, Mo 55a (theory). No activity in the μsec or msec range has been observed from bombardment of natural silicon with 22 MeV bremsstrahlung (Ve 56a).

E. ^{28}Si(p, d)^{27}Si $Q_m = -14954 \pm 9$

Cross section, Se 56.

F. ^{28}Si(^{3}He, α)^{27}Si $Q_m = 3399 \pm 9$

At $E(^3\text{He}) = 5.7$ and 5.9 MeV, α-particle groups have been observed to the nine excited states listed in table 25.7; $Q_0 = 3.405 \pm 0.015$ MeV (Hi 59a). At $E(^3\text{He}) = 9.16$ MeV the angular distributions of the groups to $^{27}\text{Si}^* = 0$, 0.78, and 0.96 MeV yield $l_n = 2$, 0, and 2, respectively (Hi 60c).

G. Not reported:

^{25}Mg(^{3}He, n)^{27}Si $Q_m = 6054 \pm 8$
^{27}Al(^{3}He, t)^{27}Si $Q_m = -4834 \pm 8$
^{28}Si(d, t)^{27}Si $Q_m = -10921 \pm 9$
^{29}Si(p, t)^{27}Si $Q_m = -17174 \pm 8$

^{28}Mg

(Fig. 28.1, p. 103; table 28.1, p. 104)

A. ^{28}Mg(β^-)^{28}Al $Q_m = 1837 \pm 5$

The weighted mean of six half-life determinations is 21.43±0.16 hr (Sh 54d, Li 53a, Ma 53a, Jo 53, Iw 53, Wa 53).

The β^- spectrum is simple and has the allowed shape (Ma 53a, Ol 54). The end point as measured by Al absorption is 0.40±0.06 MeV (Sh 54d), 0.3 MeV

(Jo 53), 0.39±0.05 MeV (Wa 53); magnetic spectrometer determinations give: 0.418±0.010 MeV (Ma 53a) and 0.459±0.002 MeV (Ol 54). Log ft = 4.4.

The energies and intensities (in photons per disintegration) of observed γ rays are listed in table 28.2. The γ rays γ_2, γ_3, and γ_4 are coincident with γ_1; and γ_2

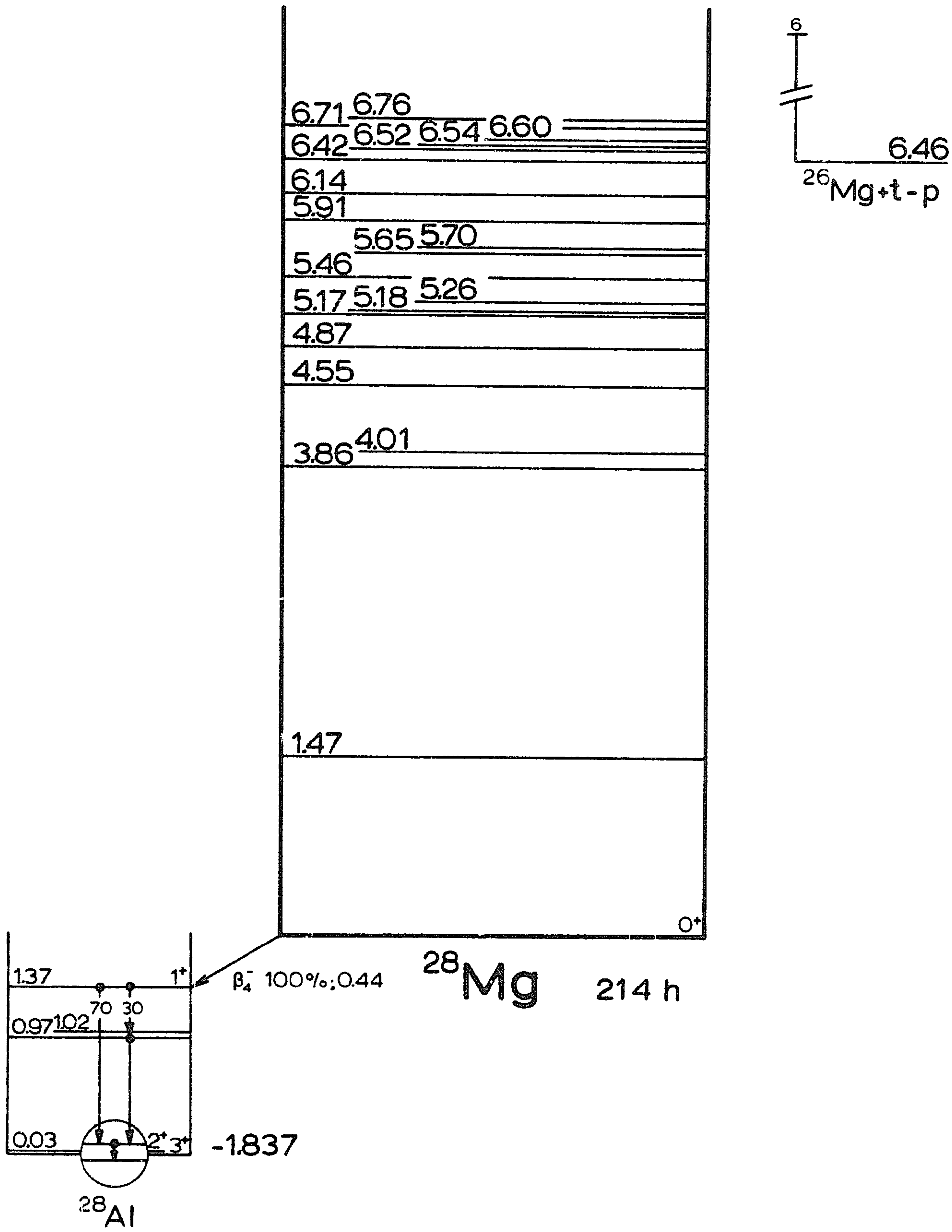

Fig. 28.1. Energy levels of ^{28}Mg.

with γ_3. The delay between γ_4 and γ_1 is quite small ($\tau_m < 2 \times 10^{-9}$ sec). The conversion coefficient of γ_1, $\alpha_K = 0.032 \pm 0.066$, confirms the M1 character of γ_1 (Sh 54d).

Gamma-ray energy and coincidence measurements indicate that the β^--decay proceeds to the 1.37 MeV level in ^{28} Al, which in turn decays through

^{28}Al* = 0.97 and 0.03 MeV. The isobaric-spin selection rule, excluding $\Delta T = \pm 1$ $0^+ \to 0^+$ β^- transitions, determines $J^\pi = 1^+$ for ^{28}Al* = 1.37 MeV. Assuming $J^\pi = 3^-$ for the ^{28}Al ground state and $J^\pi = 2^+$ for ^{28}Al* = 0.03 MeV, then leaves the possibilities $J^\pi = 0^+$ and 2^+ for the 0.97 MeV level to explain the absence of β^- decay to this level and the observed γ-ray branching from the 1.37 MeV level.

TABLE 28.1

Energy levels of ^{28}Mg

E_x MeV ± keV	J^π	$\tau_{\frac{1}{2}}$	Decay	Reactions
0	0^+	21.43 ± 0.16 hr	β^-	A, B
1 464 ± 12				B
3 861 ± 12				B
4 014 ± 12				B
4 553 ± 12				B
4 874 ± 15				B
5 166 ± 15				B
5 177 ± 15				B
5 264 ± 15				B
5 663 ± 15				B
5 682 ± 15				B
5 865 ± 15				B
5 936 ± 15				B
6 135 ± 15				B
6 418 ± 15				B
6 516 ± 15				B
6 559 ± 15				B
6 589 ± 15				B
6 746 ± 15				B
6 799 ± 15				B

TABLE 28.2

Gamma rays from ^{28}Mg$(\beta^-)^{28}$Al

	Sh 54d		Wa 53		Iw 53	Probable
	E (MeV)	Rel int.	E_γ (MeV)	Rel. int.	E_γ (MeV)	assignment
γ_1	0.0319 ± 0.001	0.96	0.0322	(≈ 0.70)		^{28}Al(1) → (0)
γ_2	0.400 ± 0.01	0.31			0.391 ± 0.005	^{28}Al(4) → (2)
γ_3	0.949 ± 0.01	0.29			0 95	^{28}Al(2) → (1)
γ_4	1.346 ± 0.01	0.70			1.35	^{28}Al(4) → (1)

B. ^{26}Mg(t, p)^{28}Mg $\qquad Q_m = 6459 \pm 7$

At $E_t = 6.0$ MeV, proton groups have been observed to the levels listed in table 28.1 (Hi 61h).

C. Not reported:

^{30}Si(n, ^{3}He)^{28}Mg $\qquad Q_m = -16285 \pm 7$

^{28}Al

(Fig. 28.2, p. 106; table 28.3, p. 107)

A. ^{28}Al(β^-)^{28}Si $\qquad Q_m = 4639.5 \pm 4.2$

The half-life is 2.28 ± 0.02 min (weighted mean of Ba 53a, Ek 43, Co 56, Va 58f).

The β^- spectrum is simple with allowed shape; end point 2.865 ± 0.010 MeV (Mo 52), 2.878 ± 0.014 MeV (Ol 54). Log $ft = 4.9$. See also Va 58f. Each β^- particle is followed by one γ quantum. Determinations of the γ-ray energy with lowest stated error: 1.782 ± 0.010 (Mo 52), 1.769 ± 0.010 MeV (Sh 54d). References to less accurate determinations of half-life, end point, and γ-ray energy, En 54a, Na 54a. See also Ma 54a.

Resonance fluorescence yields $\tau_m = (7.3 \pm 2.2) \times 10^{-13}$ sec for ^{28}Si(1) (Of 59). For comparison with other measurements, see table 28.17.

B. ^{25}Mg(α, p)^{28}Al $\qquad Q_m = -1201.5 \pm 3.9$

At $E_\alpha = 8.41$ MeV, proton groups have been observed to ^{28}Al* $= 1.00 \pm 0.04$, 1.57 ± 0.04, 2.18 ± 0.04, 2.54 ± 0.06, and 2.96 ± 0.06 MeV; $Q_0 = -1.29 \pm 0.04$ MeV (Gr 57).

For resonances, see ^{29}Si.

C. ^{27}Al(n, γ)^{28}Al $\qquad Q_m = 7723.7 \pm 3.4$

The thermal neutron absorption cross section is 230 ± 5 mb (Hu 58). For the cross section at higher E_n, see Hu 58, Be 58e, Ko 58d, Ve 59.

A resonance in the ^{28}Al yield has been found at $E_n = 40$ keV, and many more partly resolved resonances in the range $E_n = 0.1$–4.0 MeV (see Hu 58). Comparison of (n, γ) and (d, p) yields and reduced widths, Gr 58b, Bo 59a.

Thermal neutron capture γ rays are listed in table 28.4. The last column gives the ^{28}Al levels between which the transitions possibly occur The strong 7.724 ± 0.006 MeV γ ray represents the ground-state transition. Its great intensity is a notable exception to the rule that only E1 ground-state transitions are intense (Ki 52b). It is impossible to fit the γ rays uniquely into the complicated ^{28}Al level scheme. From the ^{27}Al(d, p)^{28}Al reaction, odd parity has been assigned to ^{28}Al* $= 3.46$, 3.59, 3.88, 4.03, 4.69, 4.77, 4.85, 4.91, and 5.14 MeV; see table 28.6. All but the two weakest γ rays in the energy range from 2.61 to 5.14 MeV can be explained as E1 transitions to and from eight of these nine levels (En 56). The two remaining γ rays ($E_\gamma = 4.43$ and 3.30 MeV) could form a cascade through ^{28}Al* $= 3.29$ MeV. Another odd parity state at 5.45 MeV (Ne 56b) could be used to explain an $E_\gamma = 2.28$ and 5.45 MeV cascade. The γ rays with energies of 5.21 MeV and higher, and with intensities above 1.5% could be explained as transitions from the capturing state to known low lying ^{28}Al levels.

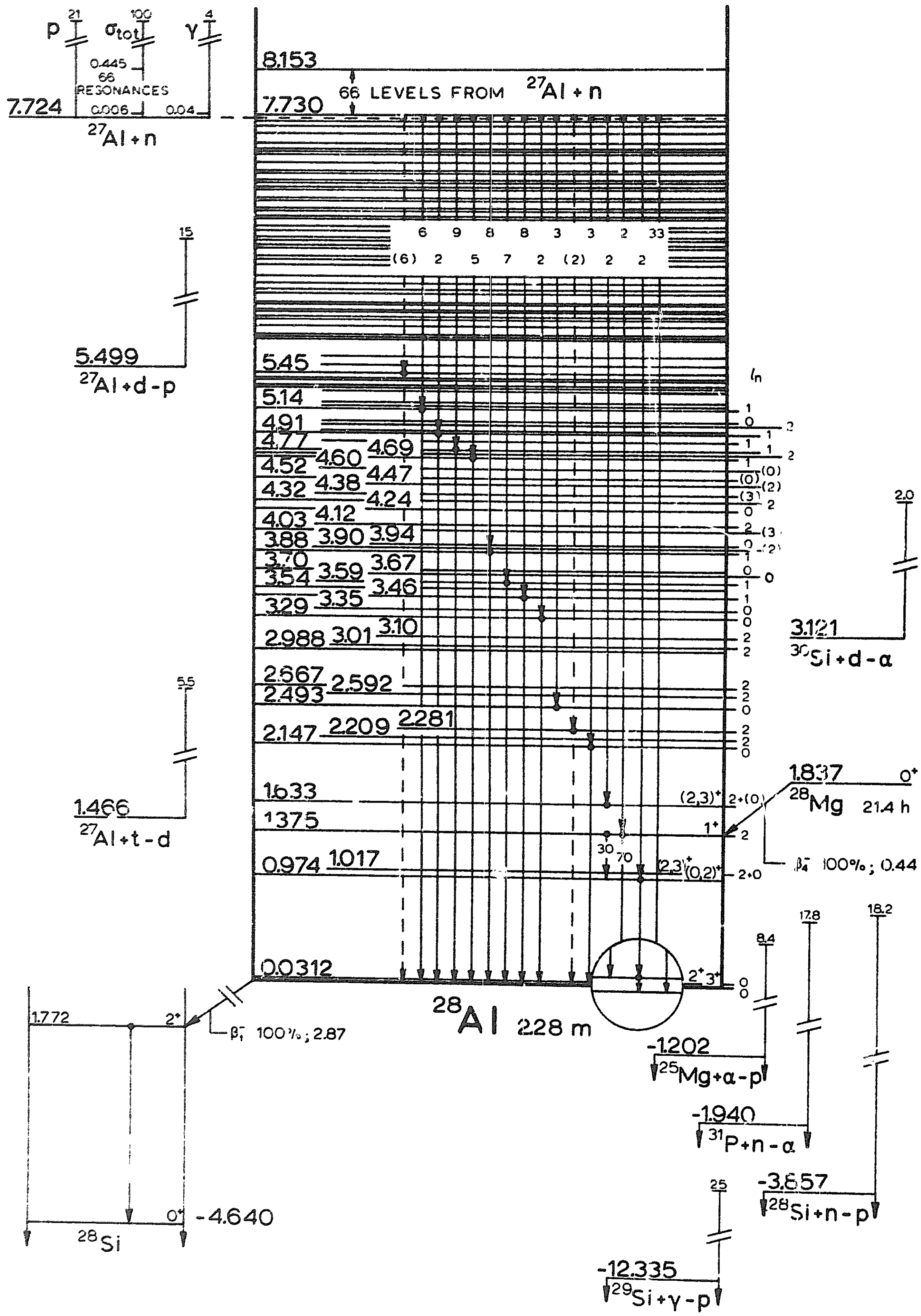

Fig. 28.2. Energy levels of ^{28}Al.

TABLE 28.3

Energy levels of ^{28}Al

E_x (MeV ± keV)	J^π	$\tau_{\frac{1}{2}}$	Decay	Reactions
0	3^+	2.28 ± 0.02 min	β^-	many
0.0312 ± 0.4	2^+	(2.2 ± 0.2) × 10^{-9} sec	γ	B, C, F, G, H, I, K
0.974 ± 4	$(0^+, 2^+)$		γ	B, C. F, H, I
1.017 ± 4	$(2, 3)^+$			B, F, G, I
1.375 ± 4	1^+		γ	C, F, G, H, I
1.633 ± 4	$(2, 3)^+$			B, C, F, I
2.147 ± 4	$(2, 3)^+$		γ	B, C, F, G, I
2.209 ± 4	$(\leq 5)^+$			B, F, G
2.281 ± 4	$(\leq 5)^+$		γ	C, F, G
2.493 ± 4	$(2, 3)^+$			B, C, F, G
2.592 ± 4	$(\leq 5)^+$			B, F
2.667 ± 4	$(\leq 5)^+$			F, G
2.988 ± 5				B, F
3.011 ± 6	$(\leq 5)^+$			B, F
3.102	$(\leq 5)^+$			F
3.294	$(2, 3)^+$		γ	C, F
3.347	$(2, 3)^+$			F
3.461	$(\leq 4)^-$		γ	C, F
3.537				F
3.591	$(\leq 4)^-$		γ	C, F
3.669	$(2, 3)^+$			F
3.704	$(2, 3)^+$			F
3.878	$(\leq 4)^-$		γ	C, F
3.900				F
3.935	$(2, 3)^+$			F
4.030			γ	C, F
4.115	$(\leq 5)^+$			F
4.243	$(2, 3)^+$			F
4.315	$(\leq 5)^+$			F
4.383				F
4.466				F
4.518				F
4.595				F
4.685	$(\leq 4)^-$		γ	C, F
4.741	$(\leq 5)^+$			F
4.767	$(\leq 4)^-$		γ	C, F
4.845	$(\leq 4)^-$			F
4.906	$(\leq 4)^-$		γ	C, F
4.928				F
4.999	$(\leq 5)^+$			F
5.019	$(2, 3)^+$			F
5.138	$(\leq 4)^-$		γ	C, F
5.168–7.700; 57 levels, see table 28.6 and reaction				F
7.730 ± 4			n	D, F
7.757–8.153; 65 levels, see table 28.5 and reaction				D

TABLE 28.4

Gamma rays from $^{27}Al(n, \gamma)^{28}Al$

Ki 51, Ki 53c, Ba 58c[c]		Gr 57c[d]		En 56, Gr 58c
E_γ (MeV ± keV)	I_γ[a]	E_γ (MeV ± keV)	I_γ[a]	Assignment[b]
7.724 ± 6	20	7.730 ± 15	24	C → 0
7.34 ± 40	0.45			
6.98 ± 40	0.5			
6.77 ± 20	0.8	6.76 ± 20	1.7	C → 0.97
6.61 ± 30	0.23			
6.50 ± 30	0.3			
6.33 ± 20	0.9	6.35 ± 20	2.3	C → 1.33
6.22 ± 30	0.3			
6.13 ± 20	1.5	6.13 ± 20	3	C → 1.63
6.01 ± 50	0.44			
5.89 ± 40	0.5	(5.88 ± 30)	0.8	
5.78 ± 30	0.8			
5.60 ± 20	1.2			C → 2.15
5.41 ± 30	1.2	5.45 ± 30	1.6	(C → 2.28) (5.45 → 0)
5.32 ± 30	0.55			
5.21 ± 20	1.5			C → 2.49
		5.140 ± 15	3.9	5.14 → 0
4.94 ± 50	0.8	4.91 ± 20	2.4	4.91 → 0
4.79 ± 20	4.3	4.730 ± 15	8	4.77 → 0
4.66 ± 50	2.5	4.66 ± 20	5	4.69 → 0
4.45 ± 20	1.4	4.42 ± 20	1	C → 3.29
4.29 ± 20	4.3	4.260 ± 15	6.1	C → 3.46
4.16 ± 20	3	4.13 ± 20	6	C → 3.59
4.06 ± 40	2			4.03 → 0
3.88 ± 20	4.4	3.88 ± 20	6	C → 3.88 → 0
		(3.30 ± 30)	1.3	
3.62 ± 20	2.5	3.600 ± 15	4.5	3.59 → 0
3.46 ± 20	1.5	3.470 ± 15	5.2	3.46 → 0
3.29 ± 20	2	(3.32 ± 30)	0.6	3.29 → 0
3.02 ± 50	10	3.04 ± 10	5.1	C → 4.69
		2.960 ± 15	8	C → 4.77
2.84 ± 30	4.6	2.82 ± 20	≈ 2	C → 4.91
Br 56e[e]		2.61 ± 10	5	C → 5.14
2.26 ± 30	14	2.28 ± 10	5.1	(2.28 → 0) (C → 5.45)
		2.12 ± 20	3	2.15 → 0
0.97 ± 30	10			0.97 → 0.03

[a] Intensity in gammas per 100 captures.
[b] The capturing state is indicated by C; excitation energies are in MeV; 0 generally stands for ground state or 0.03 MeV level.
[c] Magnetic pair spectrometer.
[d] Magnetic Compton spectrometer.
[e] Two-crystal scintillation spectrometer.

Delayed coincidences yield a half-life $\tau_{\frac{1}{2}} = (2.3 \pm 0.2) \times 10^{-9}$ sec for $^{28}Al^* = 0.03$ MeV (Du 61).

The circular polarization of the 7.72 MeV γ ray produced by capture of polarized thermal neutrons has been measured (Ve 61).

D. ^{27}Al(n, n)^{27}Al $E_b = 7723.7 \pm 3.4$

Sixty-six resonances in the total cross section for E_n = 1–450 keV have been observed in a high resolution experiment; see table 28.5 for energies, spins, and widths (Hi 59; see also Hu 58, Bl 58b, Go 58a, Cr 57, To 55a). Cross section at higher energies, Hu 58, Mc 60b, Pe 60. Theory, Lu 61.

For non-resonance data, see ^{27}Al.

E. ^{27}Al(n, p)^{27}Mg $Q_m = -1835.3 \pm 4.0$ $E_b = 7723.7 \pm 3.4$

In the energy range E_n = 3–7.5 MeV, several resonances have been observed

TABLE 28.5

Resonances in the ^{27}Al+n total cross section[a]

E_n (keV)	^{28}Al* (MeV)	Γ_n (keV)	l_n	J	E_n (keV)	^{28}Al* (MeV)	Γ_n (keV)	l_n	J
5.6[b]	7.729	0.0[illegible][b]	1[b]		250.5	7.965	3	2	0
35	7.757	1.7	0	3	257	7.972	5	1	1
84	7.805	5	1	1	266	7.981	1.5	2	0
86.6	7.807	2.4	0	3	271	7.986	1.5	2	0
89	7.810	2	1	1	278	7.993	5	0	3
91.5	7.812	4	0	2	284	7.998	2.5	1	1
120	7.839	3	1	2	288	8.002	3	1	2
140	7.859	5	1	1	292	8.006	1.5	2	1
143.3	7.862	3.5	0	3	294.5	8.008	2	1	2
149	7.867	3	1	2	300	8.013	4	1	2
152	7.870	[illegible]	1	1	305.5	8.018	2	1	2
158	7.876	4	1	4	309	8.022	2	1	2
163	7.881	2	1	1	311.8	8.024	4	0	3
166.5	7.885	1.8	1	1	316.5	8.029	1.5	2	0
169	7.887	2.5	2	0	329.5	8.041	1.5	2	0
172	7.890	2	1	1	342	8.053	1.5	2	0
175.5	7.893	3	2	0	349.5	8.061	1.5	2	0
179	7.897	2	1	1	366	8.077	5	1	4
182	7.899	2	2	0	370	8.081	2	2	1
185.5	7.903	2.5	2	0	374	8.085	3.5	1	2
190.5	7.908	3	2	0	384.8	8.096	4	0	2
195	7.912	2	2	0	404.5	8.114	[illegible]	2	1
204	7.921	7	1	2	407.5	8.117	2	2	1
209	7.926	1.8	1	1	411	8.120	2	2	3
212	7.929	2	1	2	416.5	8.125	3.5	1	3
217	7.934	1.5	1	2	420.5	8.129	1.5	2	3
223	7.939	3	1	2	423	8.132	1.5	2	2
229	7.945	2	1	1	426	8.135	2.5	2	2
233	7.948	2	1	1	433	8.141	4	1	4
237.5	7.953	1.5	1	1	437.5	8.146	1.5	2	2
240.5	7.956	1.5	1	1	439.5	8.148	1.4	2	2
243	7.958	1	2	1	442	8.150	1.5	2	3
245.5	7.960	1.5	1	1	445	8.153	1.5	2	3

[a] The parameters Γ_n, l_n, and J are probable values, obtained as best fit to the data (Hi 59).
[b] Go 58a.

(Hu 58; see also Cu 61). Cross section in the range $E_n = 12$–21 MeV, Ma 60b, Ke 59b, Hu 59, St 60a, De 60a, Kh 59a, Po 59, Al 61, Ka 61, Mu 61, Po 61.

For non-resonance data, see ^{27}Mg.

F. ^{27}Al(d, p)^{28}Al $Q_m = 5499.0 \pm 3.4$

The ground-state Q value is 5.511 ± 0.005 MeV (Ma 60e), 5.502 ± 0.010 MeV (Bu 56), 5.494 ± 0.008 MeV (En 52a, En 54b).

One hundred ^{28}Al levels have been observed in a region of excitation up to the neutron threshold (table 28.6). See also Kr 55, Be 55. For a comparison of (d, p) and (n, p) energy spectra, see Bl 57a.

Results of angular distribution measurements are also given in table 28.6. See also Ne 56a, Ha 61a. Theory, Sa 58, Bo 59a, Ma 60d.

The ground-state doublet has the ($d_{\frac{5}{2}}$, $s_{\frac{1}{2}}$) configuration. For equal reduced widths the intensity ratio should be 1.4; experiment yields 1.95 (table 28.6), En 54b, En 54, En 56.

A 31.4 ± 1.0 keV γ ray has been observed by proportional counter and scintillation spectrometer (Sm 51). With a recoil method the mean life of ^{28}Al(1) has been measured as $(3.0 \pm 0.5) \times 10^{-9}$ sec (Se 56a).

The proton polarization of the unresolved groups leading to ^{28}Al(0) and (1) has been measured at $E_d = 15$ MeV (Is 61a).

G. ^{27}Al(t, d) ^{28}Al $Q_m = 1466.1 \pm 3.4$

Angular distributions of deuteron groups to nine ^{28}Al levels have been observed at $E_t = 5.5$ MeV. The l_n values and peak cross sections are listed in table 28.7 (De 61b).

H. ^{28}Mg(β^-)^{28}Al $Q_m = 1837 \pm 5$

See ^{28}Mg.

I. ^{28}Si(n, p)^{28}Al $Q_m = -3856.9 \pm 4.2$

For cross section, see Hu 58, Ke 59, Al 61. Proton groups, Co 59c, De 61d, Bl 57a (theory). Angular distribution measurements, Ha 61, Co 61c.

For resonances, see ^{29}Si.

J. ^{29}Si(γ, p)^{28}Al $Q_m = -12334.6 \pm 4.4$

The cross section has a maximum at $E_\gamma = 20.5$ MeV with a half-width of 7.9 MeV (Ka 54).

K. ^{30}Si(d, α)^{28}Al $Q_m = 3121.4 \pm 4.3$

At $E_d = 1.8$ MeV, magnetic analysis yields $Q_0 = 3.120 \pm 0.010$ MeV (St 51). An α-particle group leading to ^{28}Al(1) has been observed at several deuteron energies up to $E_d = 2.0$ MeV (En 54b).

L. $^{31}P(n, \alpha)^{28}Al$ $Q_m = -1940.1 \pm 3.8$

Cross section at $E_n = 3$–5 MeV, Cu 61a; at $E_n = 14$ MeV, Pa 53; and at 12.4–17.8 MeV, Ke 59b, Ga 61.

TABLE 28.6

Levels in ^{28}Al from the ^{27}Al(d, p)^{28}Al reaction

^{28}Al* (MeV ± keV)		l_n		$(2J+1)\theta_n^2 \times 10^3$	
Bu 56[a]	Ja 61a	En 56, En 56a, En 57d[b]	Ti 61[c]	Ma 60d[d]	Ti 61[c]
0	0	0	0	150	160
0.0312	0.032	0	0	80	83
0.973	0.976				
1.017	1.018	2+0	2+(0)	130, 16	110, (14)
1.372	1.378	2	2		17
1.633	1.632	0	2+(0)		24, (5.4)
2.143	2.152	0	0	50	5
2.207	2.212	2	2	40	39
2.279	2.284	2	2	110	89
2.490	2.496	0+(2)	0	10	6.3
2.589	2.596		2		36
2.663	2.672	2	2	110	100
2.988	2.988				
3.011	all ± 5 keV	2	2		6
3.102		2	2		11
3.294		0+(2)	0	5	6.1
3.347		0	0	4	5.2
3.461		1+(3)	1	80	57
3.537					
3.591		1+(3)	1	130	
3.669		0	0	2	
3.704		0	0	8	
3.878		1	(1)	30	
3.900		(2)			
3.935		0+2	0		
4.030		(3)	(2 or 3)		
4.115		2	(2 or 3)		
4.243		0	0	4	
4.315		2	(2 or 3)	30	
4.383			(3)		
4.466		(2)	(1 or 2)		
4.518		(0)			
4.595		(0)	(1 or 2)		
4.685		1	1	150	
4.741		2			
4.767		1+(3)	1	120	
4.845		1			
4.906		1	1	80	
4.928					
4.999		2	(2)		
5.019		0			
5.138		1		80	

TABLE 28.6 *(Continued)*

Levels (E_x in MeV) in ^{28}Al above E_x = 5.15 MeV (Bu 56)[a]

5.168	5.596	6.027	6.569	6.970	7.444
5.179	5.746	6.067	6.591	7.025	7.460
5.191	5.766	6.073	6.626	7.090	7.505
5.289	5.802	6.163	6.657	7.121	7.596
5.331	5.867	6.201	6.719	7.149	7.655
5.346	5.909	6.247	6.760	7.180	7.669
5.377	5.931	6.322	6.835	7.247	7.700
5.405	5.960	6.424	6.856	7.274	7.731
5.445	5.989	6.446	6.896	7.345	
5.525	6.012	6.485	6.934	7.408	

[a] The error is 0.5 keV for the 31.2 keV level, and then ranges from 5 keV for the 0.973 MeV level to 10 keV for the highest levels. The corresponding Q values all have 10 keV errors.

[b] E_d = 6.0 MeV. Angular distributions cover the $\vartheta = 5^0$–60^0 region. Possible $l_n = 3$ distributions or admixtures are uncertain because of this limited angular range.

[c] E_d = 7.8 MeV; preliminary results.

[d] The absolute reduced widths tabulated in Ma 60d have been obtained by normalizing the relative widths given in En 56, En 56a, En 57d, with the aid of the absolute widths of three ^{28}Al levels given in Ho 53e.

TABLE 28.7

Levels in ^{28}Al from ^{27}Al(t, d)^{28}Al (De 61b)

E_x (MeV)	l_n	Differential cross section (mb/sr) at c.m. angle shown
0	0	13.6(12°)
0.030	0	8.7(12°)
1.020	2	1.7(33°)
1.370	2	2.7(33°)
2.138	0	2.0(12°)
2.203	2	0.7(23°)
2.279	2	1.1(16°)
2.489	0	0.3(16°)
2.664	2	1.1(17°)

M. Not reported:

^{26}Mg(t, n)^{28}Al	Q_m = 7513.7 ± 4.2
^{26}Mg(^{3}He, p)^{28}Al	Q_m = 8278.2 ± 4.2
^{26}Mg(α, d)^{28}Al	Q_m = −10074.2 ± 4.2
^{27}Al(α, ^{3}He)^{28}Al	Q_m = −12853.5 ± 3.4
^{28}Si(t, ^{3}He)^{28}Al	Q_m = − 4621.4 ± 4.2
^{29}Si(t, d)^{28}Al	Q_m = −10109.9 ± 4.4
^{29}Si(d, ^{3}He)^{28}Al	Q_m = − 6841.5 ± 4.4
^{29}Si(t, α)^{28}Al	Q_m = 7478.1 ± 4.4
^{30}Si(n, t)^{28}Al	Q_m = −14466.5 ± 4.3
^{30}Si(p, ^{3}He)^{28}Al	Q_m = −15231.0 ± 4.3

REMARKS

A discussion of the ^{28}Al levels up to 2.3 MeV in terms of the rotational model has been given in Sh 56a. Herein it is assumed that the $1d_{\frac{3}{2}}$ orbits make no significant contribution. The observed reduced widths, however, indicate that such an assumption is unjustified (Ma 60d).

Theoretical discussion of the ground-state doublet, In 53, Bi 60a, Ba 61c, Pa 61b.

^{28}Si

(Fig. 28.3, p. 116; table 28.8, p. 114)

A. (a) ^{12}C(^{16}O, γ)^{28}Si $\quad Q_m = 16754.6 \pm 2.9$
(b) ^{12}C(^{16}O, ^{16}O)^{12}C

The yield of these reactions has been measured up to $E(^{16}\text{O}) = 36$ MeV. The elastic scattering yield follows Mott scattering up to $E(^{16}\text{O}) = 22$ MeV. Some, not very pronounced, resonance structure is observed at higher energies in both reactions (Al 60c, Br 60h).

B. ^{14}N(^{14}N, γ)^{28}Si $\quad Q_m = 27218.2 \pm 2.9$

One resonance has been observed at $E(^{14}\text{N}) = 15.0$ MeV, corresponding to $^{28}\text{Si}^* = 34.7$ MeV (Al 60c).

C. ^{24}Mg(α, γ)^{28}Si $\quad Q_m = 9986.1 \pm 3.3$

Resonances observed in this reaction for $E_\alpha < 3.25$ MeV are given in table 28.9. Spin and parity determinations are from γ-ray angular distribution and γ–γ angular correlation measurements. Most resonances above $E_\alpha = 2.2$ MeV (except for the resonances at $E_\alpha = 2.38$ and 2.57 MeV) correspond to resonances in the ^{27}Al(p, α)^{24}Mg and/or ^{27}Al(p, γ)^{28}Si reactions (see tables 28.11 and 28.12). The ^{28}Si excitation energies found from the ^{24}Mg(α, γ)^{28}Si reaction are 11–19 keV higher. Apparently, all strong resonances have $J^\pi = 2^+$ or 4^+; they decay by pure or at least relatively strong E2 transitions (Sm 60a, Sm 61a).

D. (a) ^{24}Mg(α, p)^{27}Al $\quad Q_m = -1594.5 \pm 1.1 \quad E_b = 9986.1 \pm 3.3$
(b) ^{24}Mg(α, α)^{24}Mg $\quad E_b = 9986.1 \pm 3.3$

The yield of these reactions has been measured in the region $E_\alpha = 3.1$–4.0 MeV. Data on observed resonances are given in table 28.10. The spin and parity assignments follow from the observed ratio of maximum and minimum (α, α) cross section to Rutherford cross section ($\vartheta = 164°$). On the average, the observed ^{28}Si excitation energies are ≈ 20 keV high; from a comparison of ^{24}Mg(α, p)^{27}Al and ^{27}Al(p, α)^{24}Mg (Sh 51) resonance energies, a Q value of 1.613 ± 0.010 MeV is found for the latter reaction. The ^{24}Mg(α, p)^{27}Al yields are proportional to those at corresponding ^{27}Al(p, α)^{24}Mg resonances as required by the principle of detailed balancing (Ka 52).

For non-resonance information from these reactions, see ^{27}Al, ^{24}Mg.

TABLE 28.8

Energy levels of ^{28}Si

E_x (MeV ± keV)	J^π, T	τ_m or Γ	Decay	Reactions
0	0^+		stable	many
1.772 ± 5	2^+	$(6.0 \pm 1.1) \times 10^{-13}$ sec	γ	many
4.614 ± 6	4^+		γ	F, K, Q, T, V
4.975 ± 6	0		γ	K, Q
6.272 ± 6	3^+		γ	F, J, K, Q, T
6.880 ± 8			γ	F, J, K, Q
6.889 ± 8			γ	F, J, K
7.382 ± 8	$(1^\pm, 2^+)$		γ	F, K, Q
7.415 ± 8	2^+		γ	F, K, Q
7.798 ± 8	$(2, 3)^+$			K
7.932 ± 8	2^+		γ	F, J, K
8.260 ± 8				J, K
8.328 ± 8	$(1^\pm, 2^+)$		γ	F, J, K
8.411 ± 8			γ	F, K
8.543 ± 8				K
8.587 ± 8	3^+		γ	F, K, T
8.902 ± 10				K, T
8.941 ± 10				K
9.167 ± 10				K
9.314 ± 10	(3^+) $T = 1$		γ	F, J, K, T
9.379 ± 10	2^+ $T = 1$		γ	F, J, K, T
9.41 ± 14				K
9.491 ± 10	$(1^\pm, 2^+)$		γ	F, K
9.700 ± 10				K
9.762 ± 10	$(1^\pm, 2^+)$		γ	F, K
9.932 ± 20				K
10.180 ± 20				K
10.273 ± 20				K
10.308 ± 20				K
10.375 ± 20			γ	F, K
10.60 ± 50			γ	F
10.71 ± 20	$(1^+, T = 1)$		γ	F
10.91 ± 20	$(1^\pm, 2^+)$		γ	C
11.13 ± 20			γ	F
11.29 ± 10	1^-		γ	C, N, O
11.40 ± 20			γ	F
11.51 ± 10	2^+		γ	C
11.58 ± 10	3^-		γ	C
11.65 ± 10	2^+		γ	C
11.66 ± 10	2^+		γ	C
11.78 ± 10			γ	C
11.797 ± 3			γ	F
11.864 ± 3			γ	F
11.895 ± 3	4^+		γ	C, F
11.971 ± 3	4^+		γ	C, F
12.007 ± 4			γ	F
12.018 ± 6			γ	C
12.067 ± 3	2^+		γ, α	C, F, I
12.069 ± 3	(1^+)		γ	F
12.171 ± 3	4^+		γ	F

TABLE 28.8 *(Continued)*

E_x (MeV ± keV)	J^π, T	τ_m or Γ	Decay	Reactions
12.179 ± 7	1⁻		γ	C
12.190 ± 3	3⁻		γ	C, F, I
12.212 ± 3	2		γ	F
12.234 ± 3	(3, 4)⁺		γ	C, F
12.285 ± 3	2⁺		γ, α	C, F, I
12.290 ± 3	3⁺		γ	F
12.296 ± 3	2⁺		γ	C, F
12.313 ± 3	2⁺		γ	F
12.320 ± 3	4⁺		γ	F
12.326 ± 3	1⁺	9.0 ± 0.8 eV	γ	F
12.434 ± 4	2⁺		γ, α	C, F, I
12.469 ± 3	4⁺		γ, α	C, F, I
12.484 ± 3	3⁻	340 ± 110 eV	γ, α	F, I
12.536 ± 3	3⁺	80 ± 40 eV	γ	F
12.546 ± 3	4⁺		γ, α	C, F, I
12.568 ± 3			γ	F
12.630 ± 3			γ	F
12.638 ± 3			γ	F
12.658 ± 3		800 ± 80 eV	γ	F
12.710 ± 3			γ	F
12.721 ± 3	2⁺	710 ± 130 eV	γ, p, α	C, D, F, I
12.736 ± 3		6.3 ± 0.4 keV	γ	F
12.749 ± 3			γ, α	F, I
12.796 ± 3			γ, α	F,
12.809 ± 4	0⁺		γ, p, α	D, F, I
12.849 ± 3	4⁺		γ, α	F, I
12.860 ± 3			γ	F
12.894 ± 3			γ	F
12.895 ± 3	2⁺	≈ 1.1 keV	γ, p, α	D, F, I
12.911 ± 3		700 ± 50 eV	γ	F
12.918 ± 3	(2⁺, 3⁻)	290 ± 70 eV	γ, p, α	D, F, I
12.97	0⁺		p, α	D
13.04–13.25; 7 levels, see table 28.10 and reaction				D
13.26–14.26; 15 levels, see reaction				H
For higher levels, see reactions				B, F, G, H, I, O

E. ^{25}Mg(α, n)^{28}Si $\qquad Q_m = 2655.4 \pm 3.4$

See Na 53a, Cs 61.

F. ^{27}Al(p, γ)^{28}Si $\qquad Q_m = 11580.6 \pm 3.3$

Precision measurements (0.2% or better) of resonance energies are given in Br 47a (E_p = 500–1400 keV), Hu 53 (E_p < 600 keV), Ku 59a (E_p < 800 keV), An 59 (E_p = 500–1400 keV), Da 60b (six selected resonances in the E_p = 600–1300 keV region). Selected "best" values are presented in table 28.11.

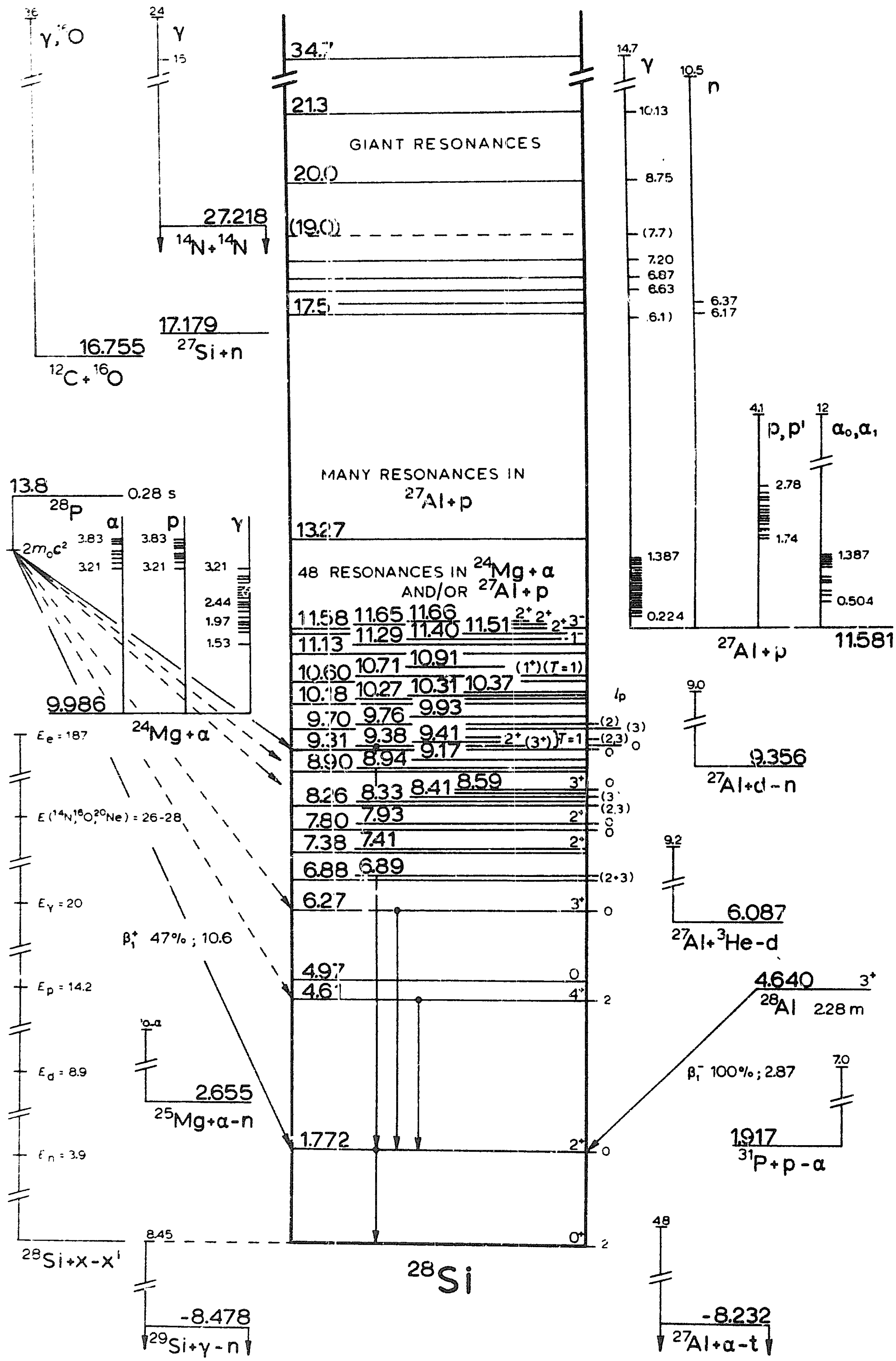

Fig. 28.3. Energy levels of ^{28}Si; for γ decay see also fig. 28.4.

TABLE 28.9

Levels in ^{28}Si from the ^{24}Mg(α, γ)^{28}Si reaction (Sm 60a, Sm 61a)

E_α (MeV ± keV)	^{28}Si* (MeV)	E_p (keV) of corresponding ^{27}Al+p resonance	$(2J+1)\Gamma_\alpha\Gamma_\gamma/\Gamma^a$ (eV)	$\Gamma_{\gamma_0}/\Gamma_{\gamma_1}$	(E2/M1) ampl. ratio for γ_1	J^π
1.534±3	11.301		0.11	2.5		1$^-$
1.791±4	11.521		0.065	< 0.05	−3.2 ±0.5	2$^+$
1.871±4	11.590		0.05	< 0.05		3$^-$
1.956±4	11.663		0.075	0.5		2$^+$
1.971±4	11.675		0.30	< 0.08	0.53±0.05	2$^+$
2.100±5	11.786		0.045	< 0.05		
2.241±5	11.907	326	0.025			
2.329±5	11.982	405	0.05			
2.384±5	12.029		0.035			
2.442±5	12.079	504	0.40	6		2$^+$
2.572±6	12.191		0.09			1$^-$
2.586±6	12.202	632	0.18	< 0.10		3$^-$
2.641±6	12.250	(678)	0.38	< 0.05		4$^+$
2.698±6	12.299	731	0.05	< 0.15	0.60±0.05	2$^+$
2.711±6	12.309	(742)	0.035	< 0.20		
2.876±6	12.451	884	1.25	10		2$^+$
2.916±6	12.486	922	2.0	< 0.07		4$^+$
3.008±7	12.564	1001	0.68	< 0.05		4$^+$
3.213±7	12.740	1183	5.3	3		2$^+$

[a] If the $\Gamma_{\gamma_0}/\Gamma_{\gamma_1}$ ratio is indicated, the radiation width in column four is taken equal to $\Gamma_{\gamma_0}+\Gamma_{\gamma_1}$. At the E_α = 2.24 and 2.33 MeV resonances, however, the main decay proceeds to the 4.61 MeV ^{28}Si level; at the 2.38 MeV resonance it proceeds to the 6.88–6.89 MeV doublet; only those transitions are included in Γ_γ. At the 2.57 MeV resonance, γ_1 is obscured by a strong cascade through a new 10.91±0.02 MeV level; γ_0 and this cascade are included in Γ_γ.

TABLE 28.10

Resonances in the ^{24}Mg(α, p)^{27}Al and ^{24}Mg(α, α)^{24}Mg reactions (Ka 52)

E_α (MeV)	^{28}Si* (MeV)	Reaction		J^π
		(α, p)	(α, α)	
3.214	12.741	yes	yes	
3.31	12.83	weak	yes	0$^+$
3.420	12.917	yes	yes	2$^+$
3.448	12.941	yes		
3.502	12.988	yes	yes	0$^+$
3.58	13.06		yes	(double ?)
3.65[a]	13.11	weak		
3.660	13.123	yes		
3.737	13.189		weak	
3.75[a]	13.20	weak		
3.80	13.24		yes	(double)
3.827	13.266	yes	yes	

[a] Estimated from published yield curve.

The Br 47a values are low compared to An 59, by an amount increasing from 2.5 keV at $E_p = 600$ keV to 7.5 keV at $E_p = 1400$ keV. The values in Ku 59a agree well with those in Hu 53 (except at the 442 keV resonance where the difference is 7.7 keV), and very well with those in An 59. The values in Da 60b agree very well with those in An 59 if the calibration energy in An 59 is changed from 990.8 keV to 992.0 keV (see below). See also An 57.

The strong and narrow resonance at 992 keV is particularly suited for generator energy calibrations. The weighted mean of five precision measurements is 992.0 ± 0.5 keV (Ma 61d). Recent measurements yield 992.2 ± 0.5 keV (Be 61f), 991.86 ± 0.10 keV (Ry 61), in good agreement with the Ma 61d average.

The spin and parity assignments in table 28.11 are all from γ-ray spectra, γ-ray angular distribution, and γ–γ angular correlation measurements. The parity of the 654 keV resonance has been determined as odd by a γ-ray polarization measurement (Hu 56). For the γ spectrum at the $E_p = 992$ keV resonance see Go 57; also Ha 55, Br 59b, An 61d.

At the $E_p = 504$ and 773 keV resonances γ-ray resonant absorption measurements have been performed. The measured widths of the ground-state transitions are ≤ 0.35 eV (Sm 59) and 5.2 ± 0.5 eV (Sm 58) respectively; the recent increase in the (p, γ) yield values (No 61b) should also increase these numbers.

The γ-ray branching of fifteen ^{28}Si lower levels and of sixteen resonance levels is given in fig. 28.4. The data mainly are from En 60 and Ok 60, in good agreement with data in Ru 54.

At the 1117 keV resonance, the γ decay occurs (intensity $> 60\%$) to new ^{28}Si levels at 10.60 ± 0.05, 11.13 ± 0.02, and 11.40 ± 0.02 MeV (No 60). From the γ decay at the 742 keV resonance a new level has been found at 10.71 ± 0.02 MeV (En 60).

From γ-ray angular distribution and γ–γ angular correlation measurements some J^π values of lower levels have been determined. To the levels at 4.61 MeV, the doublet at 6.88 MeV, and the 8.59 MeV level, $J^\pi = 4^{(+)}$, ($2^\pm$ or 4^+), and 3^+ were assigned, respectively (Ok 60). The 4^+ and 3^+ assignments to the 4.61 and 8.59 MeV levels, respectively, are also given in Va 61c. In En 60, He 61, the 4^+ assignment to the 4.61 MeV level is confirmed, and 3^+, 2^+, 2^+, and 2^- is assigned to the levels at 6.27, 7.42, 7.93, and 9.38 MeV, respectively.

Seventeen (p, γ) resonances in the $E_p = 1.4$–2.6 MeV region are given in Pl 40. A γ-ray yield curve up to $E_p = 4.1$ MeV is given in Sh 51; resonance energies for 64 resonances in the $E_p = 1.4$–4.1 MeV region have been computed from this curve (Al 50, En 54a). See also Go 54, Pa 54, Ma 57a. The yields of γ_0 and γ_1 have also been measured in the $E_p = 5$–7.7 MeV region. They show broad but pronounced resonances at $E_p = (6.1)$, 6.63, 6.87 (strong), 7.20, and (7.7) MeV (Ge 59). They have also been measured in the $E_p = 4.0$–10.4 MeV region (Go 61b), in the 5–13 MeV region (Ga 61b), and in the 7.5–14.7 MeV region (Ki 61).

TABLE 28.11
Levels in ^{28}Si from ^{27}Al(p, γ)^{28}Si

E_p[a] (keV)	^{28}Si* (MeV)	Γ[b] (eV)	$(2J+1)\Gamma_p\Gamma_\gamma/\Gamma$[c] (eV)	J^π
224.5±0.7	11.797		0.00094	
294.1±0.4	11.864		0.0042	(4−)[i]
326.0±0.4	11.895		0.028	4(−)[d, i]
404.9±0.4	11.971		0.15	4−[d, f, i]
442 ±4	12.007		≈0.04	
504.5±0.3	12.067	< 200	0.95	2+[e, f, g]
506.5±0.3	12.069	< 170	0.95	(1+)[e, g]
612.4±1.0	12.171	< 1000	0.11	4+[e]
632.3±0.3	12.190	< 60	5.4	3−[e, f, i]
654.3±0.3	12.212	< 60	3.2	2+[e], (2−)[f]
677.6±1.0	12.234	< 1000	1.0	3+[e, f]
730.6±0.3	12.285	< 160	4.0	2+[e]
735.6±0.3	12.290	< 90	4.3	3+[e]
741.7±0.7	12.296	< 1000	0.4	2+[e]
759.4±0.3	12.313	< 60	3.5	2+[e]
766.3±0.3	12.320	< 80	4.1	4+[e]
772.8±0.3	12.326	9.0± 0.8[j]	10.2±3.0	1+[e]
884 ±2	12.434	< 1000	1.0	
921.7±0.3	12.469	< 190	4.3	
936.3±0.3	12.484	340 ±110	4	
992.0±0.5	12.536	80 ± 40	40	3+[h]
1001.5±0.5	12.546	< 1000	1.0	
1023.9±0.3	12.568	< 240	9	
1088.6±0.3	12.630	< 110	1.0	
1096.4±0.5	12.638	< 1000	1.0	
1117.2±0.3	12.658	800 ± 80	6.5	
1170.6±0.4	12.710	< 250	2	
1182.6±0.4	12.721	710 ±130	4.7±1.5	
1198.0±0.6	12.736	6300 ±400	9	
1211.6±0.4	12.749	< 210	10	
1260.7±0.4	12.796	< 200	10	
1274 ±2	12.809	< 1000	1.0	
1315.2±0.4	12.849	< 160	10	
1326.6±0.4	12.860	< 160	10	
1362.0±0.4	12.894	< 120	10	
1363.2±0.4	12.895	≈ 1100	≈0.2	
1379.6±0.4	12.911	700 ± 50	65	
1386.7±0.4	12.918	290 ± 70	50	

[a] Weighted average of values in Hu 53 and Ku 59a for $E_p < 500$ keV; An 59 for $E_p > 500$ keV, except for $E_p = 992$ keV (Ma 61d, see text), and $E_p = 1363$ keV (An 61a). For An 59 energy calibration, see text.

[b] All widths from An 59, except for the resonances at 773 keV (Sm 58), 991 keV (see Ma 61d), and 1363 keV (An 61a).

[c] For $E_p = 224$, 294, 326, and 405 keV absolute yields given in Ok 60; for $E_p = 442$ keV relative yields in Ta 46, Br 47a, matched to 1.9 eV for the 504+506 keV resonances; for $E_p = 500$–800 keV relative yields in En 60, matched to absolute yield at $E_p = 773$ keV given in Sm 58 and recently corrected in No 61b; for $E_p > 800$ keV from relative yields in No 61 matched to 10.2 eV at $E_p = 773$ keV, except for the absolute yield at $E_p = 1183$ keV in No 61b.

[d] Ok 60. [e] En 60, [illegible]e 61. [f] Ru 54. [g] Sm 60. [h] Go 57. [i] Va 61c.

[j] The recent correction (No 61b) to the Sm 58 yield measurement should also increase this number.

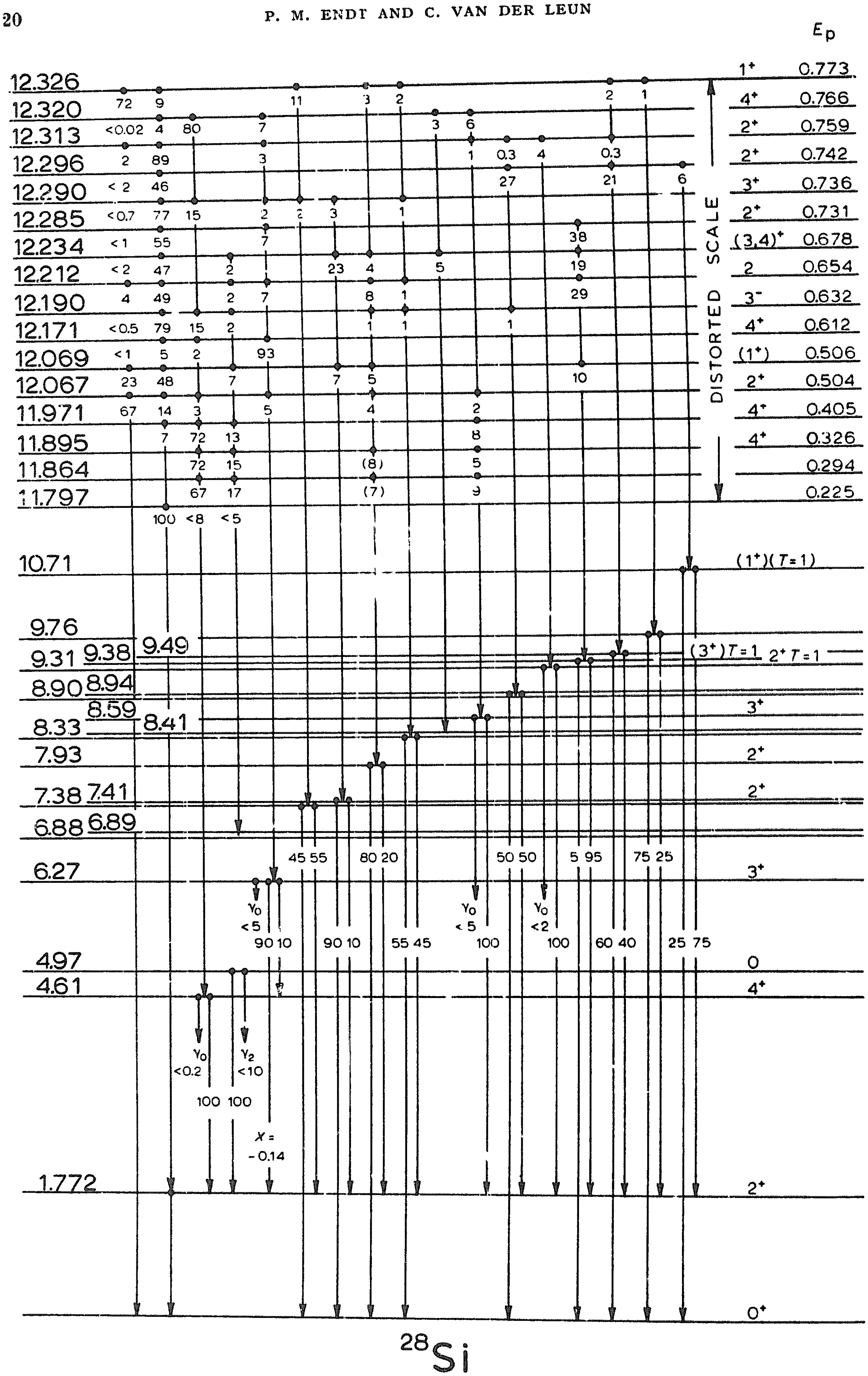

Fig. 28.4. Gamma-ray branchings of ^{28}Si levels. The data are from En 60, except for the branching at the 4.97 MeV level (Co 61d), the mixing ratio of the 6.27 → 1.77 MeV transition (Br 61d), and the branching of the four resonances in the E_p = 225–405 keV region (Ok 60).

In the latter work indications are found for giant resonance peaks at $E_p = 8.75$ and 10.13 MeV. Observation of giant resonance splitting, also in Ok 60b.

G. ^{27}Al(p, n)^{27}Si $Q_m = -5598 \pm 8$ $E_b = 11580.6 \pm 3.3$

Sharp resonances in the neutron yield have been observed up to several MeV above the threshold (Br 59f, Go 61b). Broad resonances in the ^{27}Si activity yield were found at $E_p = 6.17$ and 6.37 MeV (Bl 51).

For threshold determinations, see ^{27}Si.

H. ^{27}Al(p, p')^{27}Al $E_b = 11580.6 \pm 3.3$

Yield curves for elastic scattering in the $E_p = 1.4$–4.1 MeV region, and for inelastic scattering to the ^{27}Al 0.84 and 1.01 MeV levels in the $E_p = 2.3$–2.6 MeV region are given in Sh 51.

The $I(90°)/I(0°)$ yield ratio of the 0.84 and 1.01 MeV γ rays has been measured at the $E_p = 1.74$, 1.77, 1.82, 1.94, 1.99, 2.13, 2.34, 2.39. 2.43, 2.47, 2.51, 2.56, 2.60, 2.70, and 2.78 MeV resonances (Al 60b). See also Me 60c. For non-resonance information, see ^{27}Al.

I. ^{27}Al(p, α)^{24}Mg $Q_m = 1594.5 \pm 1.1$ $E_b = 11580.6 \pm 3.3$

Yields measured in the $E_p = 500$–1400 keV region are given in table 28.12. The spin assignments in An 61a are from α-particle angular distribution measurements. See also Ru 53 for the $E_p = 500$–800 keV region. Yield curves for the $E_p = 0.6$–4.1 MeV region, both for α_0 and for α_1, are given in Sh 51. Yield curves up to $E_p = 12$ MeV, Ad 61a.

For non-resonance data, see ^{24}Mg.

TABLE 28.12

Levels in ^{28}Si from the ^{27}Al(p, α_0)^{24}Mg reaction

E_p (keV)	^{28}Si* (MeV)	$(2J+1)\,\Gamma_p\Gamma_\alpha/\Gamma$ (eV)		J^π
		Ku 60g	An 61a	An 61a
504	12.067	0.8		
632	12.190	2.6		
731	12.285	3.1	5.9	
884	12.434		10	
922	12.469		4	
936	12.484		65	3−
1001	12.546		2.4	
1183	12.721		940	2+
1212	12.749		4.4	
1261	12.796		1.7	
1274	12.809		3.4	
1315	12.849		35	4+
1363	12.895		1640	(2+, 3−)
1387	12.918		206	(2+, 3−)

J. ^{27}Al(d, n)^{28}Si $Q_m = 9355.9 \pm 3.3$

Results from angular distribution measurements are given in table 28.13.

At $E_d = 4.6$ MeV, the following γ-ray energies have been measured with a magnetic pair spectrometer: $E_\gamma = 6.9 \pm 0.1$, 7.41 ± 0.05, 7.58 ± 0.05. 7.94 ± 0.03, 8.31 ± 0.03, 8.78 ± 0.03, 9.11 ± 0.03, 9.49 ± 0.07, 9.91 ± 0.07, and 10.8 ± 0.2 MeV. The assignment to the ^{27}Al(d, n)^{28}Si reaction is not certain (Be 55). See also Ek 60.

TABLE 28.13

Levels in ^{28}Si from the ^{27}Al(d, n)^{28}Si reaction

^{28}Si*[a] (MeV)	l_p[b]	$(2J+1)\theta_p^2$[b] $\times 10^3$	l_p[c]	$(2J+1)\theta_p^2$[c] relative
0	2	39	2	1
1.77	0	6	0	0.37
6.27	} 0		0	0.35
6.88			} 1	0.30
6.89				
7.93	0	28	0	0.36
8.26	} 0		} (0)	
8.33				
8.54				
8.59				
9.31	} 0	310	} 0	1.25
9.38				

[a] Excitation energies are from table 28.8. The identification of neutron groups given in Ca 55 may be in doubt. See also Ru 56.

[b] Ca 55, Ma 60d; $E_d = 9.0$ MeV; neutron detection with a triple ionization chamber.

[c] Ru 57, Ma 60d; $E_d = 2.2$ and 6.0 MeV; neutron detection with nuclear emulsions. More groups have been observed, which had either bad statistics, or could not be fitted with any l_p value in stripping analysis.

K. ^{27}Al(^{3}He, d)^{28}Si $Q_m = 6087.5 \pm 3.3$

Results from angular distribution measurements are given in table 28.14. This reaction has provided the most complete survey of ^{28}Si levels below $E_x = 10.4$ MeV.

L. ^{27}Al(α, t)^{28}Si $Q_m = -8232.1 \pm 3.4$

The differential cross section has been measured for groups t_0 and t_1 at $E_\alpha = 43$ MeV (Wa 57a, Go 60a, Go 60e).

M. ^{28}Al(β^-)^{28}Si $Q_m = 4639.5 \pm 4.2$

See ^{28}Al.

N. ^{28}Si(γ, γ)^{28}Si

Discrete γ rays have been observed in the scattered radiation from Si samples irradiated with betatron or linear accelerator bremsstrahlung; see table 28.15. The threshold determination (To 60) proves that the two γ rays

TABLE 28.14

Levels in ^{28}Si from the ^{27}Al(^{3}He, d)^{28}Si reaction

Hi 60d[a]			Fo 60[b]	
$E_x(^{28}Si)$ (MeV ± keV)	l_p	$(2J+1)\theta_p^2 \times 10^3$	$E_x(^{28}Si)$ (MeV ± keV)	l_p
4.617 (datum)	2	15	4.617 (datum)	
4.975 ± 8			4.979 ± 15	
6.276 ± 8	0	21	6.272 ± 15	0
6.880 ± 8	} 2 or 3		6.880 ± 15	3
6.889 ± 8	} or 2+3			
7.382 ± 8			7.392 ± 15	
7.415 ± 8				
7.798 ± 8	0	26	7.807 ± 15	3
7.932 ± 8	0	24	7.948 ± 15	
8.260 ± 8	(2 or 3)			
8.328 ± 8				
8.411 ± 8	(3)	(14)		
8.545 ± 8	weak			
8.587 ± 8	0	140		
8.902 ± 10				
8.941 ± 10				
9.167 ± 10	weak			
9.314 ± 10	0	220[c]		
9.379 ± 10	0	91[c]		
9.41 ± 14				
9.491 ± 10	(2 or 3)			
9.700 ± 10	(3)	(22)		
9.762 ± 10	(2)	(13)		
9.932 ± 20				
10.180 ± 20				
10.273 ± 20				
10.308 ± 20				
10.375 ± 20				

[a] $E(^{3}$He $= 5.7$ and 9.2 MeV; magnetic analysis.
[b] $E(^{3}\text{He}) = 5.2$ MeV; magnetic analysis.
[c] Comparison with reduced widths observed in the ^{27}Al(d, p)^{28}Al reaction makes it probable that the 9.31 and 9.38 MeV states are the $T_z = 0$, $T = 1$ analogs of the ^{28}Al ground-state doublet, with $J = 3^+$ and 2^+, respectively.

TABLE 28.15

Nuclear fluorescence radiation from the ^{28}Si(γ, γ)^{28}Si reaction

	Bu 61c	Se 60	To 60
E_{γ_0} (MeV)	11.2 ± 0.05[d]	11.2	11.40 ± 0.06[a]
E_{γ_1} (MeV)		9.4	
Γ_{γ_0} (eV)	115 ± 30[b]		2.9 ± 0.9[c]
Γ_{γ_1} (eV)	65 ± 30[b]		
Γ (eV)	330 ± 70[b]		

[a] From a threshold determination.
[b] From self-absorption measurements.
[c] From self-absorption measurements, assuming $\Gamma_{\gamma_0} = \Gamma$.
[d] The γ_0 angular distribution is consistent with dipole radiation.

are transitions to ^{28}Si(0) and (1) from an 11.3 MeV ^{28}Si level. Energy, spin, and branching ratio suggest that the level can be identified with the 11.29 MeV 1- state observed from the ^{24}Mg(α, γ)^{28}Si reaction (table 28.9). For this level, see also reaction O.

With the same method the mean life of ^{28}Si(1) has been measured as 1.3×10^{-12} sec (Bo 61); the results from different methods are compared in table 28.17.

For other (γ, γ) work see also ^{28}Al, reaction A, and ^{28}Si, reaction F.

O. ^{28}Si(e, e')^{28}Si

From a measurement of the differential cross section for inelastic scattering of 187 MeV electrons the mean life of ^{28}Si(1) has been determined as $(6 \pm 1.5) \times 10^{-13}$ sec (He 56); see table 28.17 for comparison with other measurements.

At $E_e = 40$ MeV the spectra of inelastically scattered electrons at $\vartheta = 132°$ and 160° show a peak corresponding to $E_x = 11.6$ MeV, and a broad peak corresponding to the giant resonance at $E_x = 20$ MeV. The 11.6 MeV level has $\Gamma_\gamma = 1030^{+310}_{-210}$ eV (for E1 excitation) or 47^{+14}_{-9} eV (for M1 excitation) (Ba 60g). For this level, see also reaction N.

P. ^{28}Si(n, n')^{28}Si

The only γ ray from inelastic neutron scattering (E_n up to 3.9 MeV) on natural Si, which can be assigned to ^{28}Si has an energy of $E_\gamma = 1.78 \pm 0.02$ MeV (Ro 55a, An 60d, Li 61). For the theory of inelastic neutron scattering on ^{28}Si, see Ma 59f.

Elastic scattering, La 61.

For resonances, see ^{29}Si.

Q. ^{28}Si(p, p')^{28}Si

Levels in ^{28}Si observed by magnetic analysis of inelastically scattered protons are given in table 28.16. See also Ty 58.

The γ decay of the levels at 4.61, 4.97, and 6.27 MeV mainly occurs through ^{28}Si(1), except for a (8 ± 4)% 6.27 → 4.61 MeV branch (Co 61d, see fig. 28.4).

TABLE 28.16

Levels in ^{28}Si from the ^{28}Si(p, p')^{28}Si reaction

Reference: E_p (MeV):	Br 54b 5.6–8.4	Wh 60a 7.5–8.6	Co 61b 10.0–12.3
E_x (MeV ± keV):	1.777 ± 10	1.775 ± 6	1.761 ± 9
		4.614 ± 6	4.602 ± 16
		4.975 ± 6	4.960 ± 17
		6.270 ± 6	6.242 ± 21
			6.867 ± 23
			7.359 ± 25
			7.390 ± 24

From γ–γ angular correlation measurements spins are determined as $J = 4$, 0, and 3, respectively. The 6.27 → 1.77 MeV $3 \rightarrow 2^+$ decay has a quadrupole/dipole amplitude ratio of $x = -0.14 \pm 0.07$ (Br 60e, Go 60c, Br 61d).

Differential cross sections for elastic and inelastic scattering have been measured at many proton energies in the $E_p = 2.2$–14.2 MeV range, Co 57a, Gr 58a, Ok 58, Ya 58a, Od 59, Od 60, Ta 61. The p′–γ ($E_\gamma = 1.77$ MeV) angular correlation (Bo 60e, Ha 60b, Ta 61), and the polarization of elastically scattered protons (So 58) have also been measured. For theoretical remarks, see Mc 57a, Ma 59f. See also Sh 58, Wa 60c.

For resonances, see ^{29}P

R. $^{28}Si(d, d')^{28}Si$

For the differential cross section of 8.9 MeV deuterons, see Hi 57b. For theoretical remarks, El 60.

S. ^{28}Si + heavy ions (^{14}N, ^{16}O, ^{20}Ne)

From heavy ion Coulomb excitation the mean life of $^{28}Si(1)$ has been measured as 9.4×10^{-13} sec (Go 60d), and $(5 \pm 2) \times 10^{-13}$ sec (An 60). For a comparison with the results from other methods, see table 28.17.

TABLE 28.17

Mean life determinations of $^{28}Si^* = 1.77$ MeV

Method	$\tau_m(10^{-13}$ sec)	Reference
e scatt. cross section	6 ±1.5	He 56
res. fluorescence	7.3±2.2	Of 59
Coul. excit. (^{14}N, ^{20}Ne)	5 ±2	An 60
Coul. excit. (^{16}O)	9.4	Go 60d
res. fluorescence	13	Bo 61

T. $^{28}P(\beta^+)^{28}Si$ $\quad Q_m = 13800 \pm 300$

See ^{28}P.

U. $^{29}Si(\gamma, n)^{28}Si$ $\quad Q_m = -8477.7 \pm 3.4$

For threshold and cross section, see Sh 51a, Ka 54.

V. $^{31}P(p, \alpha)^{28}Si$ $\quad Q_m = 1916.8 \pm 2.8$

The ground-state Q value has been measured as 1.909 ± 0.010 MeV (Va 52a), 1.911 ± 0.005 MeV (Va 56), and 1.909 ± 0.010 MeV (En 57a). Levels in ^{28}Si have been observed at 1.771 ± 0.008 and 4.617 ± 0.008 MeV (En 57a).

For resonances, see ^{32}S.

W. Not reported:

$^{26}Mg(^3He, n)^{28}Si$ $\quad Q_m = 12135.1 \pm 3.5$

$^{29}Si(p, d)^{28}Si$ $\quad Q_m = -6253.0 \pm 3.4$

^{29}Si(d, t)^{28}Si $Q_m = -\ 2220.1 \pm 3.4$
^{29}Si(^{3}He, α)^{28}Si $Q_m = 12099.5 \pm 3.4$
^{30}Si(p, t)^{28}Si $Q_m = -10609.6 \pm 4.5$

REMARKS

For a computation of the excitation energy of ^{28}Si(1) from those of the lowest three ^{29}Si states, see La 57a.

^{28}P

(Not illustrated; see fig. 28.3, p. 116)

A. ^{28}P(β^+)^{28}Si $Q_m = 13800 \pm 300$

The half-life, averaged from two measurements (Gl 55, Br 54a) in good mutual agreement, is 0.285 ± 0.007 sec.

The β^+ decay is complicated. The highest energy branch proceeds to ^{28}Si(1) with an end point of 10.6 ± 0.4 MeV, intensity $(47 \pm 15)\%$, log $ft = 4.9$. No delayed α particles have been found (Gl 55). Observed γ rays are given in table 28.18. Most of the high energy γ rays cannot be fitted uniquely. Some of the β^+ decay might occur to the 9.31–9.38 MeV doublet in ^{28}Si, which is then de-excited through ^{28}Si(1). The super-allowed character of such a β^+ transition (log ft = 3.4–3.7) would be in accordance with the $T = 1$ assignment to this doublet (Bo 55, Wi 56a, Hi 60d).

B. ^{28}Si(p, n)^{28}P $Q_m = -14580 \pm 300$

From ^{28}P yield measurements the threshold has been determined at

TABLE 28.18

Gamma rays from the ^{28}P(β^+)^{28}Si decay

Gl 55		Br 54a	Probable transition in ^{28}Si
E_γ (MeV)	Rel. int.	E_γ (MeV)	(E_x in MeV)
1.79 ± 0.02	0.75	1.78 ± 0.04	$1.77 \rightarrow 0$
$(2.6\ \pm 0.2)$		2.67 ± 0.08	$4.61 \rightarrow 1.77$
		(3.01 ± 0.07)	
		(4.26 ± 0.12)	
4.44 ± 0.05	0.10	4.63 ± 0.10	$6.27 \rightarrow 1.77$
(4.93 ± 0.08)		4.89 ± 0.09	
		(5.16 ± 0.12)	
		(5.46 ± 0.10)	
6.14 ± 0.10	0.10		
6.70 ± 0.12	0.10	6.65 ± 0.11	$8.59 \rightarrow 1.77$
7.04 ± 0.08	0.10	7.10 ± 0.12	$8.90 \rightarrow 1.77$
7.59 ± 0.15	0.05	(7.44 ± 0.14)	$9.31 \rightarrow 1.77$
		(7.73 ± 0.14)	
		(8.12 ± 0.21)	

E_p = 15.6±0.3 MeV (Gl 55), 15.4±0.5 MeV (Br 54a). For the cross section at E_p = 18 and 32 MeV, see Ta 58.

C. Not reported:

^{28}Si(^{3}He, t)^{28}P $Q_m = -13820 \pm 300$

^{29}Al

(Fig. 29.1, p. 128; table 29.1, p. 127)

A. ^{29}Al(β^-)^{29}Si $Q_m = 3680 \pm 7$

Measurements of the half-life yield an average of 6.52±0.05 min (He 39, Se 49; see also En 54a).

The β^- decay proceeds to ^{29}Si(1) and (3) which levels in turn de-excite by γ transitions to ^{29}Si(0); a ^{29}Si(3) → (1) γ transition has not been observed (< 11%). The intensity of a potential 2.03 MeV γ ray, ^{29}Si(2) → (0), is less than 2% (Ro 55, Br 57, Na 54c, Se 49). The energies and relative intensities of the β^- branches and γ rays are listed in table 29.2. Log ft = 4.9, > 6.0, and 4.9 for transitions to ^{29}Si(1), (2), and (3), respectively (Br 57).

TABLE 29.1

Energy levels of ^{29}Al

E_x (MeV)	J^π	$\tau_{\frac{1}{2}}$	Decay	Reactions
0	$\frac{5}{2}$+	6.52±0.05 min	β^-	A, B, C, D, E
1.402				C
1.762				B, C
2.334				C
2.875				C
3.071				C
3.191				C
3.434				C
3.584	$(\leq\frac{9}{2})^+$			C
3.646–6.840; 33 levels, see table 29.3 and reaction				C

TABLE 29.2

The ^{29}Al(β^-)^{29}Si decay

Reference	E_{β_1} (MeV)	E_{β_3} (MeV)	E_{γ_1} (MeV)	E_{γ_3} (MeV)
Se 49	2.5; 70%	1.4; 30%	1.25±0.2	2.35±0.5
Na 54c		1.55±0.1	1.31±0.05	2.42±0.05
Ro 55			1.28; (89±3.4)%	2.43; (9.4±2.1)%
Br 57			1.28; 93.8%	2.43; (6.2±0.6)%

B. ^{26}Mg(α, p)^{29}Al $Q_m = -2862 \pm 6$

At E_α = 8 MeV, proton groups have been observed to ^{29}Al(0) and to a level at 1.69±0.10 MeV; Q_0 = −2.90±0.04 MeV (Gr 57; see also Br 55b).

For resonances, see ^{30}Si.

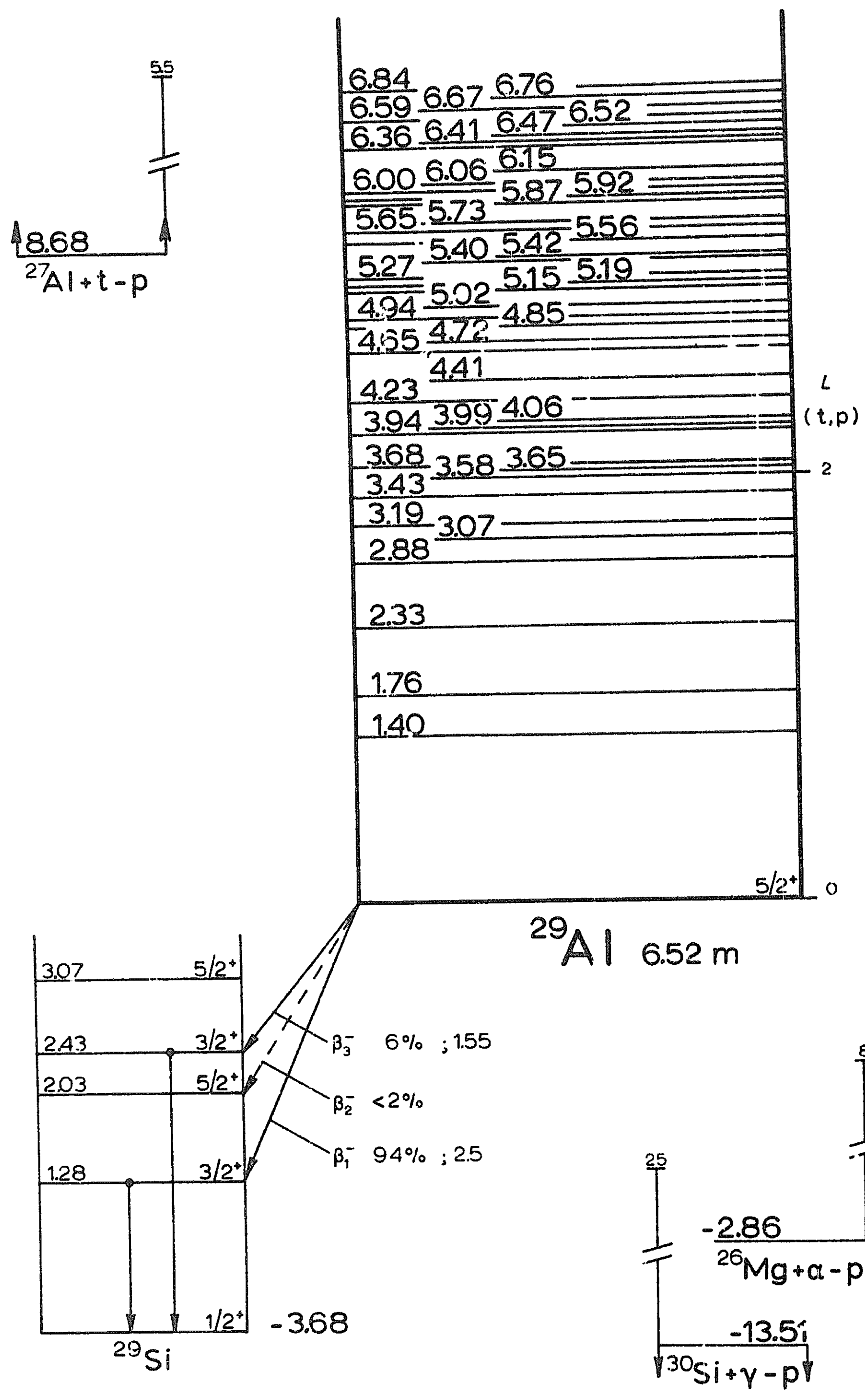

Fig. 29.1. Energy levels of ²⁹Al.

C. $^{27}Al(t, p)^{29}Al$ $Q_m = 8678 \pm 6$

Forty-two proton groups have been observed by magnetic analysis at $E_t = 5.5$ MeV and at five different angles; $Q_0 = 8.678 \pm 0.006$ MeV. The excitation energies of the levels are listed in table 29.3. Angular distribution analysis

TABLE 29.3

Energy levels (E_x in MeV) in ^{29}Al from ^{27}Al(t, p)^{29}Al (Ja 60b)

1.402	3.584	4.411	5.190	5.869	6.469
1.762	3.646	4.646[a]	5.267	5.916	6.517
2.334	3.676	4.716	5.395	6.002	6.588
2.875	3.941	4.846	5.424	6.063	6.674
3.071	3.993	4.939[a]	5.561[a]	6.152	6.753
3.191	4.064	5.024	5.654	6.358	6.840
3.434	4.228	5.154	5.732	6.412	

[a] Possibly double.

yields $L = 0$ for the group to ^{29}Al(0), thus $J^\pi = \frac{5}{2}^+$ for ^{29}Al(0), and $L = 2$ for the group to ^{29}Al* = 3.584 MeV, thus even parity for this level (Ja 60b).

D. ^{29}Si(n, p)^{29}Al $Q_m = -2898 \pm 7$

Cross section, Pa 53.

E. ^{30}Si(γ, p)^{29}Al $Q_m = -13512 \pm 7$

Cross section, Ka 54, Hi 47.

F. Not reported:

^{29}Si(t, ^{3}He)^{29}Al	$Q_m = -3662 \pm 7$
^{30}Si(n, d)^{29}Al	$Q_m = -11287 \pm 7$
^{30}Si(d, ^{3}He)^{29}Al	$Q_m = -8019 \pm 7$
^{30}Si(t, α)^{29}Al	$Q_m = 6301 \pm 7$
^{31}P(n, ^{3}He)^{29}Al	$Q_m = -13080 \pm 6$

^{29}Si

(Fig. 29.2, p. 130; table 29.4, p. 131)

A. ^{25}Mg(α, p)^{28}Al $Q_m = -1201.5 \pm 3.9$ $E_b = 11133.1 \pm 3.7$

Resonances in the yield of ^{28}Al activity have been found at $E_\alpha = 5.4$, 6.1, and 6.9 MeV (Ch 37, Me 37, Fa 35).

For proton groups, see ^{28}Al.

B. ^{26}Mg(α, n)^{29}Si $Q_m = 35.7 \pm 4.0$

Analysis of γ-ray spectra at $E_\alpha = 4.5$–5.5 MeV yields ground-state transitions from ^{29}Si(1), (2), and (3). The 3.07 MeV level decays to ^{29}Si(2) and (1); intensity ratio as measured by sum-coincidence method, 25:70, with a ground-state transition $< 5\%$, indicating $J^\pi = \frac{5}{2}^+$ for the 3.07 MeV level. The 3.62 MeV level decays to ^{29}Si(2) (Li 58a).

At $E_\alpha = 4.5$–5.0 MeV, n–γ angular correlation measurements yield E2/M1 amplitude ratios of the ground-state transitions from ^{29}Si(1), ($x = +0.25 \pm 0.05$

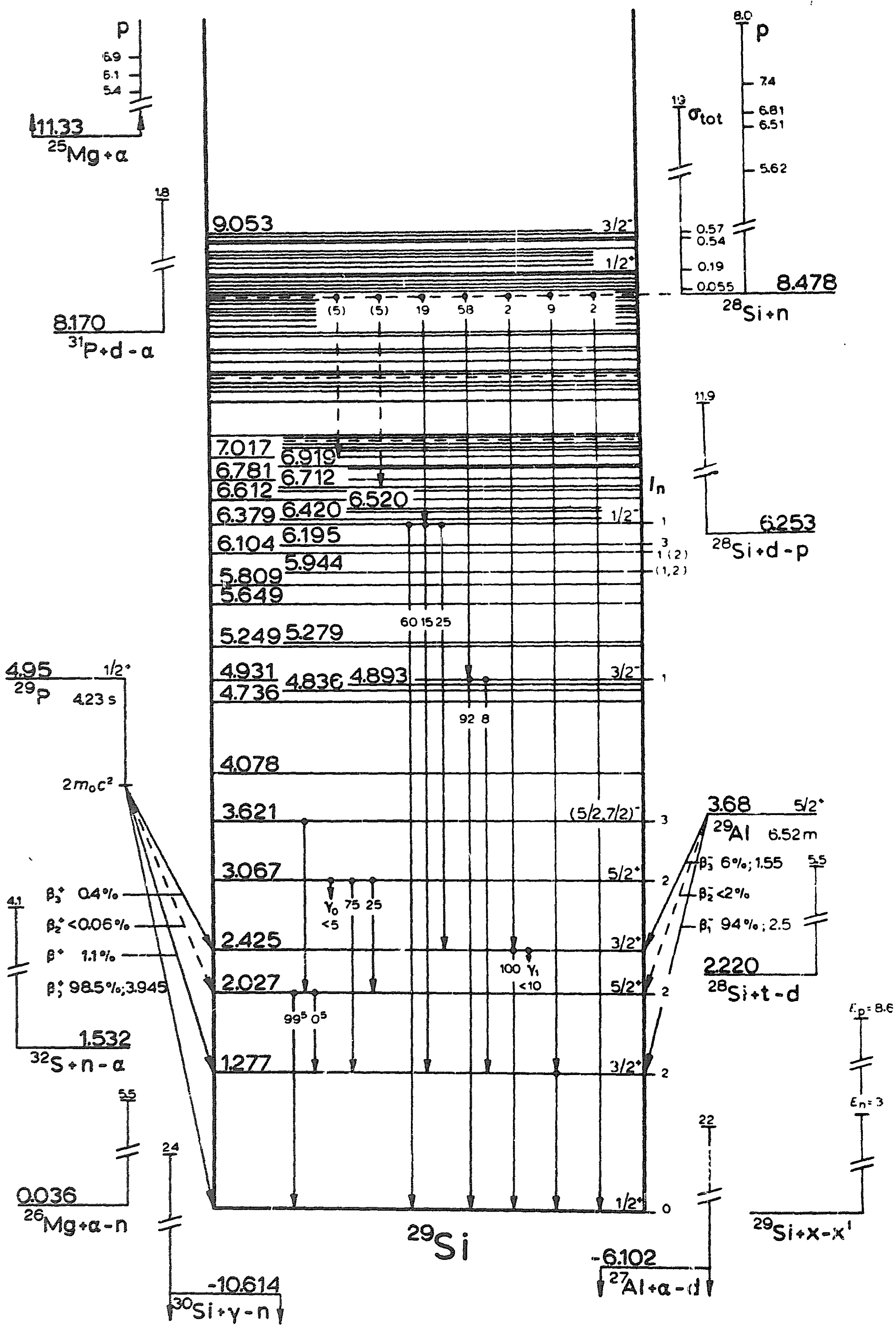

Fig. 29.2. Energy levels of ²⁹Si.

TABLE 29.4

Energy levels of ^{29}Si

E_x (MeV ± keV)	J^π	Γ	Decay	Reactions
0	$\frac{1}{2}^+$		stable	many
1.277 ± 4	$\frac{3}{2}^+$		γ	many
2.027 ± 4	$\frac{5}{2}^+$		γ	B, C, G, I, J, K, L, N, O
2.425 ± 4	$\frac{3}{2}^+$		γ	B, D, G, I, J, K, L, N
3.067 ± 4	$\frac{5}{2}^+$		γ	B, G, H, K, N
3.621 ± 3	$(\frac{5}{2}, \frac{7}{2})^-$		γ	B, G, H, K, N
4.078 ± 3				G, K, N
4.736 ± 4				G, K
4.836 ± 3				G, K
4.893 ± 3				G, K
4.931 ± 3	$\frac{3}{2}^-$		γ	D, G, H, K, N
5.249 ± 4				G, K
5.279 ± 4				G, K
6.649 ± 4				G, K
5.809 ± 4				G, K
5.944 ± 4				G, K
6.104 ± 4				G, K
6.195 ± 4	$(\frac{5}{2}, \frac{7}{2})^-$			G, K
6.379 ± 4	$\frac{1}{2}^-$		γ	D, G, K
6.420 ± 5				G
6.491 ± 6				G, K
6.520 ± 4				G, K
6.612 ± 4				G, K
6.695 ± 4				G, K
6.712 ± 5				D, G
6.781 ± 5				G
6.906 ± 5				G
6.919 ± 5				G
7.017 ± 5				D, G
7.058–8.526; 27 levels, see table 29.6 and reaction				G
8.539 ± 5			n	E, G
8.556 ± 5				G
8.601 ± 5				G
8.609 ± 8				G
(8.644 ± 8)				G
8.669 ± 5	$\frac{1}{2}^+$		n	E, G
8.760 ± 5				G
8.814 ± 5				G
8.848 ± 5				G
8.860 ± 5				G
8.908 ± 5				G
8.936 ± 5				G
(9.013 ± 5)			n	E, G
9.040 ± 8	$\frac{3}{2}^-$		n	E, G
9.053 ± 5				G
13.91 ± 50			p	F
14.77 ± 50			p	F
15.05 ± 50			p	F
15.7 ± 100		300 keV	p	A, F
16.4			p	A
17.1			p	A

[illegible]

or −1.4 ±0.5 (^{28}Si(2) pure E2) and ^{28}Si(3) (x = −0.26 ± 0.06 or −1.10 ± 0.15 [illegible]).

See also [illegible] 61, Br 56h, [illegible].

[illegible] ^{27}Al(t, n)^{29}Si $Q_m = -6612.0 \pm 3.6$

At E_t = [illegible] MeV, 1.28 and 2.03 MeV γ rays have been observed, probably from this reaction (Be 61c).

[illegible] ^{28}Si(n, γ)^{29}Si $Q_m = 8477.7 \pm 3.4$

The thermal neutron capture cross section of natural silicon is 160 ± 20 mb; the isotopic cross sections of ^{28}Si, ^{29}Si, and ^{30}Si are 80 ± 30, 280 ± 90, and [illegible] mb, and their abundances 92.27, 4.68, and 3.05%, respectively (Hu 58). Approximately 30% of the thermal-neutron captures in natural silicon should thus occur in ^{29}Si.

Energies and intensities of γ rays from capture of thermal neutrons in natural silicon are listed in table 29.5 (Ki 51, Ki 53c, Ad 56a, Br 56e, Ba 58c). The assignment of most γ transitions is based on comparison of the γ-ray energy with binding energies and excitation energies in ^{29}Si, ^{30}Si, and ^{31}Si, as measured by magnetic analysis of charged-particle reaction products. The γ-ray spectrum of the ^{28}Si(n, γ)^{29}Si reaction is dominated by cascades via ^{29}Si* = 4.93 and 6.38 MeV. Gamma-gamma angular correlations of the 3.54–4.93 MeV and 2.09–6.38 MeV cascades are in agreement with pure dipole radiation for both transitions and $J^\pi = \frac{3}{2}^-$ and $\frac{1}{2}^-$ for ^{29}Si* = 4.93 and 6.38 MeV, respectively. The same experiment yields the E2/M1 mixing ratio of the 7.19 MeV γ ray (Ma 59c).

The branching percentages of the capturing state, as given in fig. 29.2, are averaged from Ki 51 (as corrected in Ba 58c), Br 56e, and Ad 56a. The branching ratios of the 4.93 and 6.38 MeV levels follow from the intensities and assignments in Ad 56a.

Comparison of (d, p) and (n, γ) reduced widths, Bo 59a, Gr 58b; see "Remarks".

[illegible] ^{28}Si(n, n)^{28}Si $E_b = 8477.7 \pm 3.4$

Total neutron cross section of natural Si, Hu 58, Pe 60. The resonances at E_n = 55, 190 ($J^\pi = \frac{1}{2}^-$), 540, and 570 keV ($J^\pi = \frac{3}{2}^-$) are assigned to ^{28}Si (La 61, Ne 56c, Fi 51; Hu 58).

For resonances in the inelastic scattering to ^{28}Si(1), see Li 61.

For non-resonance data, see ^{28}Si.

[illegible] ^{28}Si(n, p)^{28}Al $Q_m = -3856.9 \pm 4.2$ $E_b = 8477.7 \pm 3.4$

In the range E_n = 4.4–8.0 MeV, broad resonances have been found at E_n = 5.62, 6.51, and 6.81 ± 0.05 MeV ($\Gamma \leq 0.1$ MeV), and at E_n = 7.45 ± 0.1 MeV (Γ = 0.3 MeV), Hu 58.

For non-resonance information, see ^{28}Al.

TABLE 29.5

Gamma rays from thermal neutron capture in natural silicon

E_γ[a] (MeV ±keV)	I_γ[b]	E_γ[c] (MeV ±keV)	I_γ[c]	Final nucleus	Probable transition[d]
10.601±11	0.2	10.59 ±30	0.2	^{30}Si	C → 0
8.468± 8[g]	2	8.482±15	1.6	^{29}Si	C → 0
7.79 ±50	0.8				
7.36 ±80	0.7	(7.38 ±30)	0.5	^{30}Si	
7.18 ±30	8	7.22 ±30	6.1	^{29}Si	C → 1.28
6.88 ±30	0.4				
6.76 ±40	1.5	6.758±20	1.4	^{30}Si	C → 3.79
6.40 ±30	11	6.354±15	9.2	^{29}Si	6.38 → 0
6.11 ±50	2.5	6.04 ±50	1	^{29}Si	C → 2.43
5.70 ±40	1				
5.52 ±50	1				
		5.24 ±30	0.8	(^{30}Si)	5.25 → 0
5.11 ±40	8	5.113±15	2.3	^{29}Si	6.38 → 1.28
4.933± 5[g]	75	4.930±10	37.4	^{29}Si	4.93 → 0
4.60 ±80	2.5				
4.20 ±30	10	(4.30 ±50)	2		
		3.976±20	4.2	^{29}Si	6.38 → 2.43
		≈ 3.8	≈ 3	^{30}Si	3.79 → 0
		3.667±20	3.2	^{29}Si	4.93 → 1.28
3.540± 6[g]	60[f]	3.547±10	36.5	^{29}Si	C → 4.93
2.65 ±30[e]	11[e]		< 1[h]		
2.13 ±30[e]	19[e]	2.10 ±10	12.8	^{29}Si	C → 6.38
		1.95 ±20	3.4		
		≈ 1.7	≈ 3	^{29}Si	(C → 6.71)
		≈ 1.5	≈ 3	^{29}Si	(C → 7.02)
1.26 ±30[e]	14[e]	1.28 ±10	16	^{29}Si	1.28 → 0

[a] Ki 51, unless marked otherwise.
[b] Intensity in photons per 100 captures in natural silicon, Ba 58c.
[c] Ad 56a; intensity in photons per 100 captures in natural silicon.
[d] The capturing state is indicated by C; excitation energies are in MeV.
[e] Br 56e.
[f] Br 56e reports 49 per 100 captures
[g] Ki 53c.
[h] See Gr 58c.

G. ^{28}Si(d, p)^{29}Si $\qquad Q_m = 6253.0 \pm 3.4$

Magnetic analysis at $E_d = 7.0$ MeV and at several angles yields seventy proton groups, corresponding to levels with excitation energies up to 9.1 MeV (Br 60d; also Ja 61a), see table 29.6; $Q_0 = 6.246 \pm 0.010$ MeV (Va 52), 6.252 ± 0.010 MeV (Te 61). For earlier work at $E_d = 1.8$–4.4 MeV, see Va 52, Mo 50, Kr 55, Ne 56b. The excitation energies are in excellent agreement with those found from (d, α), (t, d), and (p, p′) reactions.

Angular distributions of the most prominent proton groups yield the l_n values listed in table 29.6 (Ho 53a, Ho 53d, Te 58a, Za 59a, Bl 61b). Discussion of the reaction mechanism, Ku 60e, Bu 61; of reduced widths Bl 61b, Ma 60d, Ku 60e,

TABLE 29.6

Energy levels (MeV ± keV) of ^{29}Si from ^{28}Si(d, p)^{29}Si and ^{29}Si(p, p')^{29}Si

(p, p')[a]	(d, p)[b]	(d, p)[c]	(d, p)[d]	l_n (d, p)	$(2J+1)\theta_n^2$ [e] × 10^3
0	0	0		0[e, i, j, k, h]	42
1.278 ± 6	1.276 ± 10	1.278 ± 7		2[e, i, j, k, h]	56
2.027 ± 6	2.034 ± 10	2.027 ± 7		2[e, i]	20
2.424 ± 6	2.429 ± 15	2.426 ± 7		isotropic[e, i]	< 1.2
3.064 ± 6	3.076 ± 10	3.070 ± 7		2[e, i]	22
3.620 ± 6	3.635 ± 10	3.623 ± 7	3.621	3[e, i, j]	100
4.079 ± 6	4.089 ± 15	4.078 ± 8	4.078	isotropic[e, m]	
4.735 ± 6			4.737		
4.833 ± 6	4.848 ± 10	4.840 ± 8	4.836		
4.891 ± 6	4.907 ± 15	4.897 ± 8	4.893		
4.930 ± 6	4.943 ± 10	4.934 ± 8	4.931	1[e, i, m]	130
5.244 ± 6			5.252		
5.274 ± 7			5.282		
5.346 ± 7			5.650		
5.804 ± 7			5.812		
5.937 ± 7	5.960 ± 10	5.946 ±	5.947	2[e], 1[m]	6
6.098 ± 7	6.115 ± 10	6.105 ± 9	6.107	1 (2)[m]	
6.189 ± 7			6.198	3[e]	43
6.380 ± 7	6.399 ± 10	6.380 ± 9	6.378[g]	1[e, i, m]	62
[f]			6.420		
6.482 ± 7			6.495		
6.515 ± 7			6.522		
6.609 ± 7			6.614		
6.695 ± 7			6.695		
			all ± 5 keV		

(d, p)[d]	
6.712	8.270
6.781	8.331
6.906	8.347
6.919	8.368
7.017	8.418
7.058	8.479
7.074	8.504
7.140	8.526
(7.164)	8.539
7.183	8.556
7.192	8.601
7.523	8.609[g]
7.622	(8.644)[g]
7.648	8.669
7.693	8.760
(7.735)[g]	8.814
7.766	8.848
7.787	8.860
7.892	8.908
7.986	8.986
7.995	(9.013)
8.135	9.040[g]
8.159	9.053
8.208	all ± 5 keV

[a] ^{29}Si(p, p')^{29}Si: E_p = 7.5, 8.0, and 8.6 MeV; Wh 60a.
[b] ^{28}Si(d, p)^{29}Si: Ja 61a.
[c] ^{28}Si(d, p)^{29}Si: E_d = 1.8 MeV, Va 52.
[d] ^{28}Si(d, p)^{29}Si: E_d = 7.03 MeV; Br 60d.
[e] Bl 61b: E_d = 15 MeV; reduced widths in good agreement with Ho 53d, Ma 60d.
[f] A 6.414 MeV level is not excluded.
[g] ± 8 keV.
[h] Bl 53, E_d = 14.3 MeV.
[i] Ho 53d: E_d = 8 MeV.
[j] Za 59a: E_d = 3–5 MeV.
[k] To 58a: E_d = 4 MeV.
[m] Al 60d: E_d = 6.3 MeV.

Bo 59a, Ca 56a, Fu 54; of l_n values and neutron capture probabilities, Ho 53a, Ho 53d, Al 60d.

Direct ground-state γ transitions have been observed from ^{29}Si* = 1.28, 2.03, 2.43, 3.07, 4.93, and 6.38 MeV (Al 49a, Th 54, Go 58). The 2.03 MeV level decays almost entirely (99.5%) to the ground state; at the 2.43 MeV level the ground-state branch is > 40%. Angular correlations of protons and γ rays corresponding to ^{29}Si(1) and (2), Ku 60d, Hi 58c, Al 56a. The polarization of the p_0 group (Is 61a), and of protons leading to the p-states at 4.93 and 6.38 MeV (Ju 58) has been measured.

For resonances, see ^{30}P.

H. ^{28}Si(t, d)^{29}Si $\quad Q_m = 2220.1 \pm 3.4$

Angular distributions of deuteron groups to ^{29}Si* = 0, 1.271, 3.071, 3.630, and 4.936 MeV, yield l_n = 0, 2, 2, 3, and 1, respectively, in agreement with the l_n values found from reaction G; peak cross sections, De 61b.

I. ^{29}Al(β^-)^{29}Si $\quad Q_m = 3680 \pm 7$

See ^{29}Al.

J. ^{29}Si(n, n'γ)^{29}Si

Gamma rays with E_γ = 1.28, 2.02, and 2.41 MeV, corresponding to ground-state transitions from the three lowest excited states have been observed from inelastic scattering of neutrons with E_n up to 3 MeV (Li 61).

K. ^{29}Si(p, p')^{29}Si

Magnetic analysis at E_p = 7.5–8.6 MeV, yields twenty-two levels in ^{29}Si; see table 29.6 (Wh 60a).

Gamma rays of 1.28, 2.03, and 2.43 MeV have been observed from inelastic proton scattering. Angular distributions of the 2.03 MeV γ ray, measured at E_p = 2.798 and 2.934 MeV, yield P_4 terms, indicating that ^{29}Si(2) has $J^\pi = \frac{5}{2}^+$. About 0.5% of the decay of this level proceeds through ^{29}Si(1). Angular distributions of the 1.28 MeV γ ray at E_p = 2.798 and 2.922 MeV are consistent with the assignment $J^\pi = \frac{3}{2}^+$ to ^{29}Si(1) (Br 57). An E2/M1 amplitude mixing ratio $x = +0.21 \pm 0.03$ or -4.7 ± 0.6 follows from angular distribution and linear polarization measurements at the E_p = 2.80 MeV resonance (Mc 61a).

For resonances, see ^{30}P.

L. ^{29}P(β^+)^{29}Si $\quad Q_m = 4948 \pm 9$

See ^{29}P.

M. ^{30}Si(γ, n)^{29}Si $\quad Q_m = -10614.3 \pm 4.3$

Cross section, Ka 54.

N. ^{31}P(d, α)^{29}Si $\quad Q_m = 8169.8 \pm 3.3$

Magnetic analysis at E_d = 1.8 MeV yields Q_0 = 8.170±0.020 MeV, and seven α-particle groups corresponding to ^{29}Si* = 0, 1.274±0.010, 2.032±0.014, 2.431±0.015, 3.072±0.016, 3.619±0.017, 4.078±0.018, and 4.937±0.020 MeV (En 51a). Remeasurement gives Q_0 = 8.158±0.011 MeV (Va 52a). The excitation energies of the ^{29}Si levels given above have been corrected accordingly. See also Be 55.

Angular distribution of ground-state group, Hu 60a.

O. ^{32}S(n, α)^{29}Si $\qquad Q_m = 1532.0 \pm 3.5$

At $E_n = 3.7$ MeV, α groups have been observed to ^{29}Si* = 0, 1.28, and 2.03 MeV (Bu 55); $Q_0 = 1.8 \pm 0.4$ MeV (Mu 58a). The thermal neutron cross section is 1.8 ± 1.0 mb (Hu 58). Cross section for $E_t = 1.4$–4.1 MeV, Hu 58, Sc 58.

For resonances, see ^{33}S.

P. Not reported:

^{27}Al(t, n)^{29}Si	$Q_m = 11576.0 \pm 3.6$
^{27}Al(^{3}He, p)^{29}Si	$Q_m = 12340.5 \pm 3.5$
^{28}Si(α, ^{3}He)^{29}Si	$Q_m = -12099.5 \pm 3.4$
^{30}Si(p, d)^{29}Si	$Q_m = -8389.6 \pm 4.2$
^{30}Si(d, t)^{29}Si	$Q_m = -4356.6 \pm 4.2$
^{30}Si(^{3}He, α)^{29}Si	$Q_m = 9962.9 \pm 4.2$
^{31}P(n, t)^{29}Si	$Q_m = -9418.1 \pm 3.3$
^{31}P(p, ^{3}He)^{29}Si	$Q_m = -10182.6 \pm 3.3$

REMARKS

The ^{29}Si ground state has $J^\pi = \frac{1}{2}^+$ (Ho 53d). Two possible J^π values for several excited states follow from (d, p) angular distributions. Selection of one of these two values is possible from angular correlation measurements for ^{29}Si* = 1.28, 2.03, 4.93, and 6.93 MeV; see reactions B, D, and K. Gamma branching selects $J^\pi = \frac{5}{2}^+$ for ^{29}Si = 3.07 MeV. The level at 2.43 MeV has $J^\pi = \frac{3}{2}^+$ since the β^+ and β^- transitions from the ground states of ^{29}P ($J^\pi = \frac{1}{2}^+$) and ^{29}Al ($J^\pi = \frac{5}{2}^+$), respectively, are both allowed.

There is little doubt that in the ^{28}Si(d, p)^{29}Si reaction the strong $l_n = 3$, 1, and 1 transitions to the levels at 3.62, 4.93, and 6.38 MeV reveal relatively pure single-particle $1f_{\frac{7}{2}}$, $2p_{\frac{3}{2}}$, and $2p_{\frac{1}{2}}$ states, respectively (Ma 60d). The strong excitation of the 4.93 and 6.38 MeV levels in the ^{28}Si(n, γ)^{29}Si reaction is in agreement with this assumption.

A good over-all picture of both excitation energies and reduced widths of ^{29}Si levels below 3.5 MeV has been obtained by application of the collective model. Agreement with the experimental reduced widths cannot be obtained without taking account of the interaction between the two $1d_{\frac{5}{2}}$ bands (Ma 60d; see also Br 57c, Kh 59).

See also In 53.

^{29}P

(Fig. 29.3, p. 137; table 29.7, p. 138)

A. ^{29}P(β^+)^{29}Si $\qquad Q_m = 4948 \pm 9$

The weighted mean of four half-life determinations, which are in rather bad agreement, is 4.23 ± 0.05 sec (Ja 60a, Wa 60a, Ro 55, Wh 41).

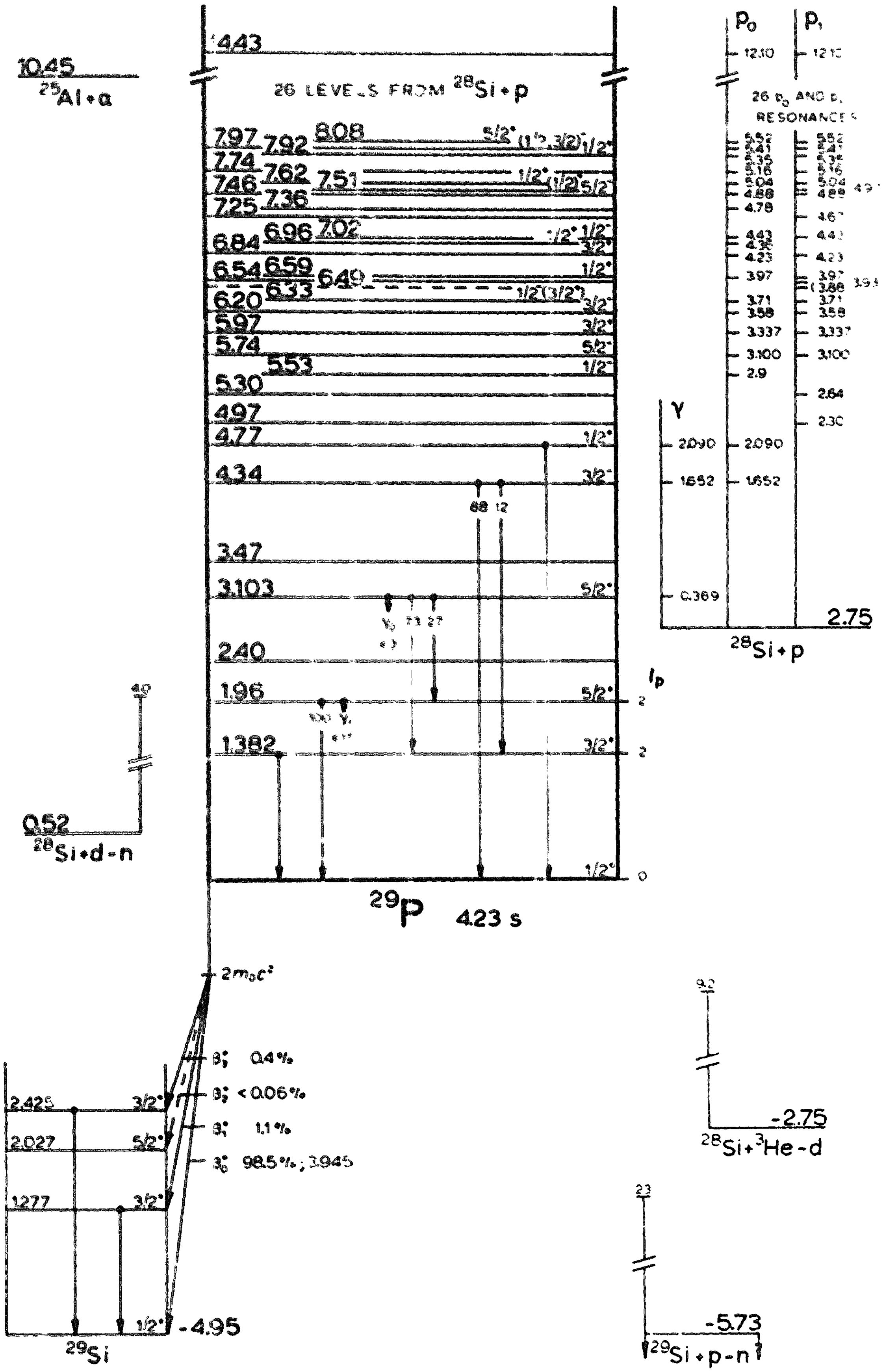

Fig. 29.3. Energy levels of ^{29}P.

TABLE 29.7

Energy levels of ^{29}P

E_x (MeV ± keV)	J^{π}	$\tau_{\frac{1}{2}}$ or Γ	Decay	Reactions
0	$\frac{1}{2}^+$	4.23 ± 0.05 sec	β^+	A, B, D, E, F
1.382 ± 5	$\frac{3}{2}^+$		γ	B, D, E
1.955 ± 6	$\frac{5}{2}^+$		γ	B, D, E
2.40 ± 30				D
3.103 ± 5	$\frac{5}{2}^+$		γ	B, D
3.47 ± 20				D
4.342 ± 8	$\frac{3}{2}^-$	53 ± 3 keV	γ, p	B, C
4.765 ± 10	$\frac{1}{2}^+$	15.5 ± 1.0 keV	γ, p	B, C
4.968 ± 18		< 4 keV	p	C
5.30			p	C
5.53 ± 20	$\frac{1}{2}^-$	425 ± 50 keV	p	C
5.740 ± 9	$\frac{5}{2}^-$	12.5 ± 0.7 keV	p	C
5.968 ± 9	$\frac{3}{2}^+$	9.5 ± 1.5 keV	p	C
6.195 ± 10	$\frac{3}{2}^-$	95 ± 6 keV	p	C
6.329 ± 10	$(\frac{3}{2}^+)$, $\frac{1}{2}^-$	73 ± 5 keV	p	C
(6.49)			p	C
6.54			p	C
6.590 ± 10	$\frac{1}{2}^+$	200 ± 20 keV	p	C
6.836 ± 14	$\frac{3}{2}^+$	4.9 ± 0.4 keV	p	C
6.956 ± 14	$\frac{1}{2}^+$	120 ± 10 keV	p	C
7.024 ± 14	$\frac{1}{2}^-$	100 ± 8 keV	p	C
7.25			p	C
7.362 ± 14			p	C
7.463 ± 14	$\frac{5}{2}^-$	8.4 ± 0.7 keV	p	C
7.513 ± 14	$(\frac{1}{2})^+$	7 ± 3 keV	p	C
7.62 ± 15	$\frac{1}{2}^+$	165 ± 25 keV	p	C
7.74 ± 15	$(\leq\frac{5}{2})^+$	< 2 keV	p	C
7.92 ± 15	$\frac{1}{2}^+$	14 ± 4 keV	p	C
7.97 ± 15	$(\frac{1}{2}, \frac{3}{2})^-$	125 ± 25 keV	p	C
8.08 ± 15	$\frac{5}{2}^+$	36 ± 10 keV	p	C
8.20–14.43; 25 levels, see table 29.8b and reaction				C

A (98.8 ± 0.4)% β^+ branch proceeds to ^{29}Si(0), with end point 3.945 ± 0.005 MeV (Ro 55, see also Wa 60a). A (98.5 ± 0.2)% intensity is given in Lo 61; log ft = 3.73. Gamma rays of 1.28 and 2.43 MeV have been observed in coincidence with positons. Branching ratios of transitions to ^{29}Si* = 1.28, 2.03, and 2.43 MeV are (1.09 ± 0.10)%, ≲ 0.06%, and (0.35 ± 0.07)% respectively. Log ft = 4.94, ≥ 5.5, and 4.3, respectively (Lo 61; see also Ro 55).

The 2.43 MeV level of ^{29}Si mainly decays to ^{29}Si(0). Transitions to ^{29}Si(1) and (2) have an intensity less than 60 and 17% of the ground-state transition, respectively (Lo 61).

Longitudinal polarization measurement, Pr 58.

Theoretical discussion of β^+– and γ–transition probabilities, Go 56b.

B. ^{28}Si(p, γ)^{29}P $Q_m = 2747 \pm 9$

Proton capture has been observed at the lowest three resonances listed in table 29.8 (Ku 59a, Va 61, Ok 60a, Ne 60d, Ol 60, Se 60a, Oh 61). Fourteen resonances observed for $E_p = 1100$–1650 keV from proton bombardment of natural silicon targets and presumed to be due to the ^{28}Si + p reaction (Se 60a) have not been observed in other experiments (Oh 61, Ts 56). Two resonances are expected in the range of excitation between the lowest two resonances of table 29.8 from comparison with the ^{29}Si level scheme; see also reaction D. A search for these resonances between 700 and 1200 keV yields $(2J+1)\Gamma_\gamma\Gamma_p/\Gamma < 5$ meV (Ch 61). Two measurements of the decay scheme of the 369 keV resonance level are in excellent agreement (Va 61, Ok 60a; also Ol 60); see fig 29.3. Gamma-ray energies and angular distributions yield the following excitation energies (weighted mean values) and spins and parities: ^{29}P* = 0, 1.380 ± 0.006, 1.953 ± 0.007, and 3.102 ± 0.006 MeV, with $J^\pi = \frac{1}{2}^+, \frac{3}{2}^+, \frac{5}{2}^+$, and $\frac{5}{2}^+$, respectively (Ok 60a, Va 61, Ol 60). For E2/M1 mixing ratios, see Ok 60a.

The γ decay of the 1652 keV resonance proceeds to ^{29}P(0) (88%) and to ^{29}P(1) (12%) (Va 60). Gamma-ray energy and angular distribution measurements yield $E_x = 4.341 \pm 0.012$ MeV, and $J^\pi = \frac{3}{2}^-$ for the resonance level (Ne 60d, Va 60). The strength of this resonance is limited by the radiative width; $\Gamma_\gamma = 1.85 \pm 0.40$ eV (Va 60), $\Gamma_{\gamma_0} = 1.75 \pm 0.35$ eV (Ne 60d). The total width is $\Gamma = 44 \pm 4$ keV (Va 61), 55.2 ± 2 keV (Ne 60d), 55 ± 8 keV (Vo 59a), 48 keV (Va 58g), 60 keV (Ru 59). The reduced widths listed in table 29.8 are from Vo 59a; see reaction C.

The 4.765 MeV level, corresponding to the 2090 ± 4 keV resonance, decays to ^{29}P(0) with a 4.74 ± 0.03 MeV γ ray (Va 60, Ne 60d). The resonance strength $\Gamma_\gamma\Gamma_p/\Gamma \approx \Gamma_\gamma = 0.43 \pm 0.08$ eV (Va 61), 0.45 ± 0.20 eV (Ne 60d). The total width $\Gamma \approx \Gamma_p = 15 \pm 3$ keV (Va 60), 18 ± 4 keV (Vo 59a), 14 ± 2 keV (Ne 60d), 13.5 keV (Va 58g), 30 keV (Ru 59), 16.2 keV (Be 61a).

A collective-model discussion of these results is given in Va 60.

C. ^{28}Si(p, p')^{28}Si $E_b = 2747 \pm 9$

Differential cross sections for elastic scattering and inelastic scattering to ^{28}Si(1) measured at four angles for proton energies between 1.4 and 3.8 MeV, show seven resonances for elastic scattering and four for inelastic scattering. Analysis of these data yields spins, parities, elastic, and inelastic scattering widths of seven resonance levels (Vo 59a). Similar work in the range $E_p = 2$–5 MeV yields eleven resonances with spins, parities, and widths (Be 61a). See table 29.8a. Except for the spin of the 6.33 MeV level, the results given in these two reports are in good agreement. At the 1.65 and 2.09 MeV resonances the results agree with those of Va 58g and of reaction B; see also Ru 59. The large reduced elastic scattering widths of the 4.34 ($J^\pi = \frac{3}{2}^-$) and 5.53 MeV ($J^\pi = \frac{1}{2}^-$) levels indicate that these levels are single particle $2p_{\frac{3}{2}}$ and $2p_{\frac{1}{2}}$ levels (Vo 59a,

TABLE 29.8a

Resonances in $^{28}Si+p$ ($E_p < 5$ MeV)

E_p (MeV ± keV)	$^{29}P^*$ (MeV)	J^π	Decay	Γ (keV)	$\Gamma_p\Gamma_\gamma/\Gamma$ (meV)	Γ_{p_0}[r] (keV)	Γ_{p_1}[r] (keV)	$\theta_{p_0}^2$[r] $\times 10^3$	$\theta_{p_1}^2$[r] $\times 10^3$
0.3689 ± 0.7[a, b, c, d, g]	3.103	$\frac{5}{2}^+$[a, b, g]	γ		0.8 ± 0.1[a, b]			> 1.2[a]	
1.652 ± 4[a, c, f, g, h, i, j]	4.342	$\frac{3}{2}^-$[a, c, f, i]	γ p_0	53 ± 3[a, c, f, i, j]	1800 ± 300[a, f]	53 ± 3[s]		300[s]	
2.090 ± 4[a, c, f, i, j, p]	4.765	$\frac{1}{2}^+$[c, f, i, p]	γ p_0	15.5 ± 1.0[a, c, f, i, j, p]	430 ± 80[a, f]	15.5 ± 1.0[s]		15[s]	
2.30 ± 15[f]	4.968		p_1	<4[f]					
2.641[l]	5.30		p_1	narrow[l]					
2.880 ± 20[e, l, p]	5.53	$\frac{1}{2}^-$[e, p]	p_0	425 ± 50[e, p]		425[e, p]		250[e, p]	
3.100 ± 2[e, l, m, p]	5.740	$\frac{5}{2}^-$[e, p]	p_0 p_1	12.5 ± 0.7[e, m, p]		3.9[t]	9.0[t]	20	≈ 1000
3.337 ± 2[e, m, p]	5.968	$\frac{3}{2}^+$[e, p]	p_0 p_1	9.5 ± 1.5[e, m, p]		6.4[t]	2.0[u]	6.3	170
3.571 ± 5[e, m, p]	6.195	$\frac{3}{2}^-$[e, p]	p_0 p_1	95 ± 6[e, m, p]		20[u]	78[t]	6.7	≈ 1000
3.710 ± 5[e, m, p]	6.329	$\frac{1}{2}^-$[p], $(\frac{3}{2}^+)$[e]	p_0 p_1	73 ± 5[e, m, p]		18[u]	56[t]	5.6	800
(3.88)[l, o]	(6.49)		p_1	narrow[l]					
3.93[l]	6.54		p_1	narrow[l]					
3.980 ± 5[l, p]	6.590	$\frac{1}{2}^+$[p]	$p_0(p_1)$	200 ± 20[p]		200		41	
4.235 ± 10[m, p]	6.836	$\frac{3}{2}^+$[p]	p_0 p_1	4.9 ± 0.4[p, v]		2.9	2.0	1.6	4
4.36 ± 10[p]	6.956	$\frac{1}{2}^+$[p]	p_0	120 ± 10[p]		120		22	
4.43 ± 10[m, p]	7.024	$\frac{1}{2}^-$[p]	p_0 p_1	100 ± 8[m, p]		30	70	6.8	100
	7.25[m]		p_1						
4.78 ± 10[p]	7.362		p_0 p_1			(small)	(small)		
4.884 ± 10[p, q, m]	7.463	$\frac{5}{2}^-$[p]	p_0 p_1	8.4 ± 0.7[p]		2.9	5.5	3.5	90
4.936 ± 10[l, p, q]	7.513		p_1			(no)	(small)		

[a] Va 60, also Va 61.
[b] Ok 60a.
[c] Ku 59a.
[d] Se 60a.
[e] Vo 59a.
[f] Ne 60d.
[g] Ol 60.
[h] Oh 61.
[i] Va 58g.
[j] Ru 59.
[l] Wi 56.
[m] Co 55a.
[o] Ba 61.
[p] Be 61a.
[q] See also table 29.8b.
[r] Be 61a, unless indicated otherwise.
[s] For references, see column Γ.
[t] Widths given in Vo 59a are in essential agreement with these values.
[u] Widths given in Vo 59a are about a factor of two lower.
[v] Co 55a gives 22 keV.

TABLE 29.8b

Proton scattering resonances on ^{28}Si (E_p > 4.8 MeV)

E_p (MeV)	^{29}P* [a] (MeV)	Γ [a] (keV)	l_p [a]	E_p [b] (MeV)	^{29}P* (MeV)	Γ [b] (keV)
4.85 [e]	7.43	12 ± 3	3	8.77 [c]	11.22 [c]	≈ 100 [c]
4.92 [e]	7.50	7 ± 3	0, (2)	10.25	12.64	30
5.04	7.62	165 ± 25	0	10.32	12.71	30
5.17	7.74	⩽ 2	2, (0)	10.40	12.79	40
5.35	7.92	14 ± 4	0	10.61	12.99	130
5.41	7.97	125 ± 25	1	10.88	13.28	150
5.52	8.08 [d]	36 ± 10	2	11.28	13.64	120
5.64	8.20	20 ± 4	2, (0)	11.56	13.91	80
5.71	8.26	40		11.73	14.05	80
5.95	8.49	36 ± 10		12.10	14.43	50
5.97	8.51	25 ± 7	2, (0)			
6.08	8.62	10				
6.13	8.67	120 ± 30	0			
6.22	8.76	14 ± 3	0			
6.32	8.85	9 ± 3	0			
6.36	8.89	33 ± 6	0, (2)			
6.44	8.97	50				
6.54	9.06	23 ± 5	0			
6.76	9.28	7 ± 3				
6.83	9.34					
6.86	9.37	13 ± 5	0, (2)			
6.93	9.44	20 ± 5	0			
all ± 15 keV						

[a] Br 61a; yield measured of p_0 and p_1.
[b] Co 61b; yield measured of p_1.
[c] Od 60; yield measured of p_1.
[d] See also Ok 58, Ya 58a; $J^\pi = \frac{3}{2}^+$.
[e] See also table 29.8a.

Va 58g, Ne 60d). Magnetic analysis of the proton groups to ^{28}Si(0) and (1) in the range E_p = 4.8–7.0 MeV yields 22 levels in ^{29}P with excitation energies from 7.43 to 9.44 MeV, with widths and l_p values. See table 29.8b.

Resonances in the yield of the 1.77 MeV γ ray from ^{28}Si(1) have been reported in Co 55a, Wi 56, Ok 58, Od 59, Ne 60d, Od 60, Co 61b; see also Ya 58a. See tables 29.8a and b for energies and widths. The 3.88 MeV resonance could be due to ^{30}Si(p, p'γ), Ba 61. In the high energy range, E_p = 10.0–12.3 MeV, it is not certain that the compound-nuclear process predominates. Peaks could be due to interference between direct interaction and compound nucleus formation (Co 61b).

For non-resonance data, see ^{28}Si.

D. ^{28}Si(d, n)^{29}P $\qquad Q_m = 522 \pm 9$

Six neutron groups have been observed. For corresponding excitation energies, l_p values from angular distribution measurements, and reduced widths, see

TABLE 29.9

Levels in ^{29}P from $^{28}Si(d, n)^{29}P$ and $^{28}Si(^3He, d)^{29}P$

E_x [a] (MeV)	E_x [b] (MeV)	l_p [b]	θ_p [a d] $\times 10^3$	E_x [e] (MeV)	l_p [e]
0	0	0	17	0	0
1.36±0.04	1.30	2	9	1.386±0.010	2
1.94±0.04	1.92	2	5	1.960±0.010	(2)
2.40±0.03	2.5[c]				
3.11±0.02	2.9[c]				
3.47±0.02	3.5				

[a] Ma 60; $^{28}Si(d, n)^{29}P$, $E_d = 3.4$ and 4.0 MeV; excitation energies calculated with an assumed $Q_0 = 0.54 \pm 0.02$ MeV (cf. reaction E).
[b] Ca 57; $^{28}Si(d, n)^{29}P$, $E_d = 9$ MeV.
[c] Also Gr 55f; $^{28}Si(d, n)^{29}P$.
[d] Ca 57, Ma 60d.
[e] Hi 60c; $^{28}Si(^3He, d)^{29}P$, $E(^3He) = 9.16$ MeV.

table 29.9 (Ma 60, Ma 60d, Ca 57, Gr 55f); $Q_0 = 0.63 \pm 0.06$ MeV (Ma 60), 0.6 ± 0.1 MeV (Ca 57), 0.29 ± 0.04 MeV (Ma 52).

E. $^{28}Si(^3He, d)^{29}P$ $Q_m = -2746 \pm 9$

Magnetic analysis at $E_d = 9.16$ MeV, yields three deuteron groups. For corresponding excitation energies and l_p values, see table 29.9; $Q_0 = -2.731 \pm 0.012$ MeV (Hi 60c).

F. $^{29}Si(p, n)^{29}P$ $Q_m = -5731 \pm 9$

Observed, Wh 41, Ty 54. See also Sa 56a.

G. Not reported:

$^{27}Al(^3He, n)^{29}P$	$Q_m = 6610 \pm 8$
$^{28}Si(\alpha, t)^{29}P$	$Q_m = -17066 \pm 9$
$^{29}Si(^3He, t)^{29}P$	$Q_m = -4966 \pm 9$
$^{31}P(p, t)^{29}P$	$Q_m = -15149 \pm 8$
$^{32}S(p, \alpha)^{29}P$	$Q_m = -4199 \pm 8$

^{30}Al

(Not illustrated; see fig. 30.1, p. 144)

A. $^{30}Al(\beta^-)^{30}Si$ $Q_m = 7290 \pm 250$

A 3.27 ± 0.20 sec activity from fast neutron bombardment of natural silicon has been assigned to ^{30}Al. Gamma rays with energies of 2.26 ± 0.03 MeV (rel. int. 100) and 3.52 ± 0.03 MeV (rel. int. 64 ± 6) have been observed. The end point of the β^- spectrum is 5.05 ± 0.25 MeV; the intensity of a potential branch with a 7.29 MeV end point is $< 2\%$. Nuclear mass systematics make it probable that the observed end point corresponds to a β^- transition to $^{30}Si(1)$.

From the known γ branching of ^{30}Si(2) (see ^{30}Si) and from the observed γ intensities, the relative intensities of β^- branches to ^{30}Si(1) and (2) are computed as $\approx$ 16% and $\approx$ 84%, yielding log *ft* values of 5.2 and 3.9, respectively (Ro 61).

B. ^{30}Si(n, p)^{30}Al $\qquad Q_m = -6510 \pm 250$

See reaction A.

C. Not reported:

^{30}Si(t, ^{3}He)^{30}Al $\qquad Q_m = -7270 \pm 250$

^{30}Si

(Fig. 30.1, p. 144; table 30.1, p. 145)

A. ^{26}Mg(α, p)^{29}Al $\qquad Q_m = -2862 \pm 6 \qquad E_b = 10649.9 \pm 4.5$

With RaC′ α particles and natural Mg targets, resonances in the ^{29}Al yield have been observed at $E_\alpha = 5.3$ and 6.0 MeV (Me 37).

For proton groups, see ^{30}Si.

B. ^{27}Al(α, p)^{30}Si $\qquad Q_m = 2377.6 \pm 4.1$

At $E_\alpha = 8$ MeV, nuclear emulsion work yields the ten levels listed in table 30.2; $Q_0 = 2.38 \pm 0.03$ MeV (Ha 56e). At $E_\alpha = 10.4$, 13.7, and 14.7 MeV, the same ten levels have been found, plus groups to ^{30}Si* = 5.70, 7.76, 8.44, 8.80, 9.38, (9.70), 9.96, 10.60, and 11.06 MeV, all ±0.08–0.10 MeV (Ro 60c). At $E_\alpha = 22$ MeV, Al absorption measurements yield levels at 5.61, 7.35, 8.37, 9.43, 10.04, and 11.03 MeV (Br 49).

Magnetic analysis at $E_\alpha = 5$ MeV yields the excitation energies of four levels with small errors. Some of these values, however, are in disagreement with other accurate measurements; $Q_0 = 2.373 \pm 0.008$ MeV (De 59a; table 30.2). See also Hu 59a, Sw 61.

Angular distributions of the p_0 and p_1 groups, Vo 57a ($E_\alpha = 8$ MeV), Ko 61 ($E_\alpha = 22$ MeV), Hu 59a ($E_\alpha = 30.4$ MeV), Sw 61 (theory). Angular distribution of p_0 at $E_\alpha = 19$ MeV, Pl 61. Much of the older work on this reaction has been done with radioactive α-particle sources; for a summary, see En 54a.

Proton-gamma coincidence measurements yield ground-state γ transitions from ^{30}Si* = 2.23 and (3.51+3.77+3.79) MeV. One of the levels at 4.8 MeV is probably de-excited (with a 1.28±0.06 MeV γ ray) through the 3.51 MeV level, and for less than 15% through ^{30}Si(1) (Al 51, La 51). See also Be 48, Br 55b.

For resonances, see ^{31}P.

C. ^{28}Si(t, p)^{30}Si $\qquad Q_m = 10609.6 \pm 4.5$

Levels found from magnetic analysis at $E_t = 5.97$ MeV are listed in table 30.2; $Q_0 = 10.586 \pm 0.015$ MeV (Hi 61g).

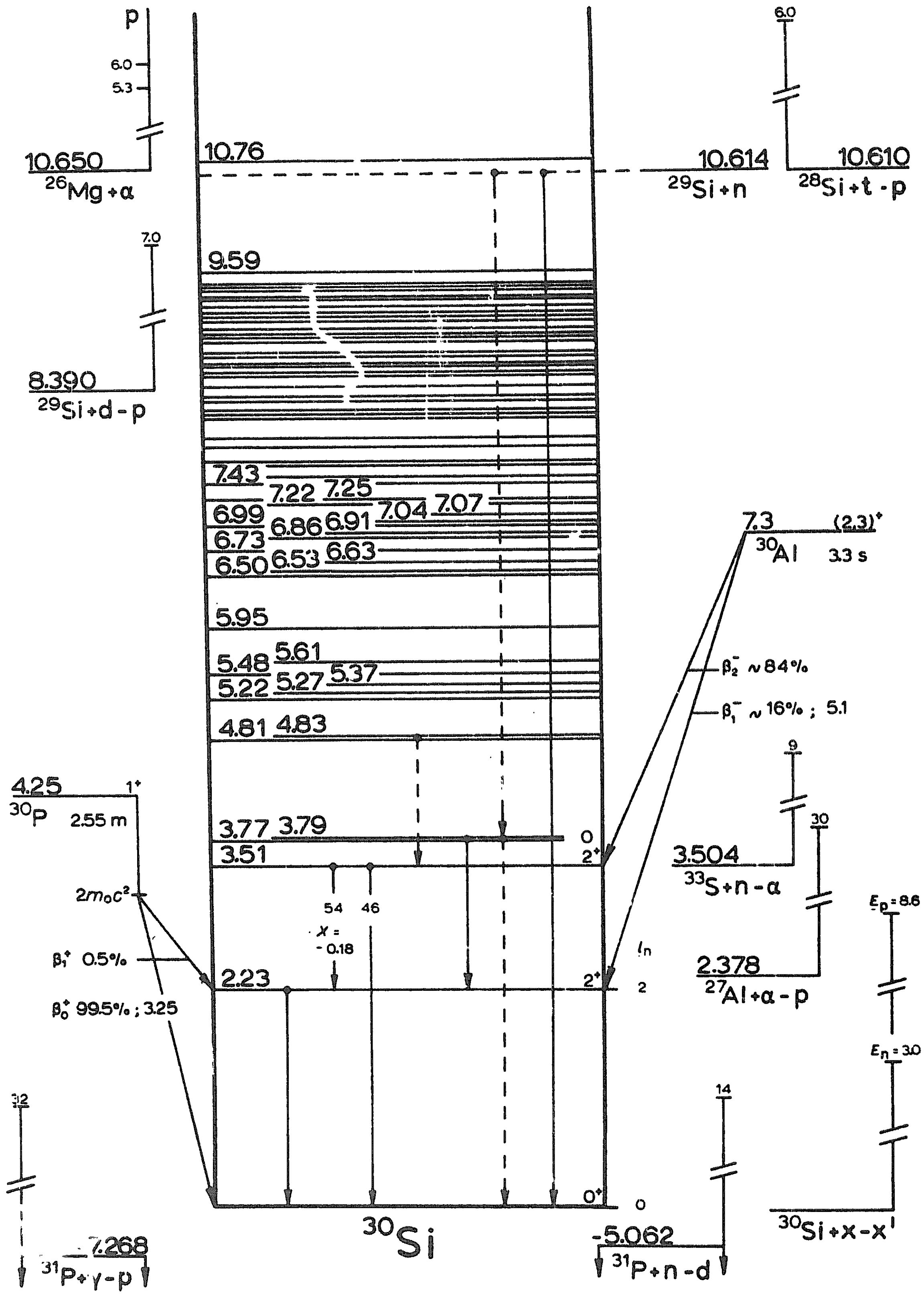

Fig. 30.1. Energy levels of ^{30}Si.

TABLE 30.1

Energy levels of ^{30}Si

E_x (MeV ± keV)	J^π	Decay	Reactions
0	0^+	stable	many
2.232 ± 6	2^+	γ	B, C, E, F, G, H, I, K
3.507 ± 6	2^+	γ	B, C, E, F, H, K
3.767 ± 6	} 0	γ	C, H
3.786 ± 6		γ	B, C, D, E, H, K
4.808 ± 6		γ	C, H
4.826 ± 6		γ	B, C, H
5.222 ± 7		(γ)	C, D, H
5.274 ± 10			B, C
5.366 ± 7			C, H
5.480 ± 7			B, C, E, H
5.611 ± 7			B, C, E, H
5.948 ± 10			B, C
6.496 ± 5			C, E
6.528 ± 10			B, C
6.630 ± 5			C, E
6.735 ± 5			C, E
6.860 ± 10			C
6.908 ± 10			C
6.993 ± 10			C
7.039 ± 10			C
7.070 ± 10			B, C
7.216 ± 10			C
7.248 ± 10			C
7.435 ± 10			B, C
7.497–10.760	32 levels, see table 30.2 and reactions B, C, F		

D. ^{29}Si(n, γ)^{30}Si $\qquad Q_m = 10614.3 \pm 4.3$

The thermal neutron absorption cross section is 0.28 ± 0.09 b (Hu 58).

Thermal neutron capture γ rays are listed in table 29.5. The assignments to the ^{29}Si(n, γ)^{30}Si reaction are uncertain, except for the 10.599 ± 0.011 MeV ground-state transition (Ki 53c, Ad 56a).

E. ^{29}Si(d, p)^{30}Si $\qquad Q_m = 8389.6 \pm 4.2$

Magnetic analysis at $E_d = 2.1$ MeV (Va 52) and 7.0 MeV (Br 60d) yields the levels listed in table 30.2; $Q_0 = 8.388 \pm 0.013$ MeV (Va 52), 8.413 ± 0.010 MeV (Ma 60e). The excitation energies of the three lowest levels are reported as 2.249, 3.520, and 3.790 MeV, all ±12 keV (Ja 61a). For Al-absorption work at $E_d = 3.7$ MeV, see Mo 50.

Angular distributions of the groups to ^{30}Si(0) and (1), yield $l_n = 0$ and 2, and $\theta_n^2 = 0.29$ and 0.19, respectively (Su 59b, as corrected in Su 60).

F. ^{30}Al(β^-)^{30}Si $\qquad Q_m = 7290 \pm 250$

See ^{30}Al.

TABLE 30.2

Levels in ^{30}Si (in MeV ± keV) from the reactions ^{27}Al(α, p)^{30}Si, ^{28}Si(t, p)^{30}Si, ^{29}Si(d, p)^{30}Si, and ^{30}Si(p, p')^{30}Si

a	b	c	d	e	a	f
0	0	0	0	0	7.800 ± 10	
2.232	2.23 ± 20	2.258 ± 6	2.232 ± 6	2.239 ± 20	7.899 ± 10	
3.510	3.52 ± 20	3.518 ± 7	3.493 ± 6	3.515 ± 16	8.094 ± 10	8.093
3.769			(3.765 ± 6)		8.145 ± 10	8.143
3.788	3.80 ± 40	3.798 ± 9	3.785 ± 6	3.786 ± 20	8.177 ± 10	
4.813			4.805 ± 6		8.279 ± 10	
4.825	4.83 ± 20	4.85 ± 10	4.827 ± 6		8.319 ± 10	
5.225			(5.220 ± 7)		8.430 ± 10	
5.274	5.28 ± 20				8.539 ± 10	
5.367			5.365 ± 7		8.584 ± 10	8.571
5.483	5.52 ± 30		5.477 ± 7	(5.497 ± 15)	8.632 ± 10	
5.612			5.610 ± 7	(5.622 ± 15)	8.661 ± 10	
5.948	5.94 ± 40			f	8.720 ± 20	
6.502				6.494	8.785 ± 10	8.790
6.528	6.52 ± 30				8.881 ± 10	8.890
6.632				6.630	8.927 ± 10	
6.739				6.734	8.950 ± 20	(8.947)
6.860					9.021 ± 10	
6.908					9.092 ± 10	9.098
6.993					9.120 ± 20	
7.039					9.152 ± 10	
7.070	7.10 ± 30				9.241 ± 10	9.246
7.216					9.296 ± 10	
7.248					9.338 ± 10	
7.435	7.38 ± 30				9.396 ± 10	
7.500				7.497	9.418 ± 20	
7.610				(7.613)	9.457 ± 10	
7.660				7.658		9.590
all ± 10 keV				all ± 5 keV		10.760
						all ± 5 keV

a Hi 61g: ^{28}Si(t, p)^{30}Si — E_t = 5.97 MeV; magn. anal.
b Ha 56e: ^{27}Al(α, p)^{30}Si — $E_α$ = 8 MeV; nucl. emulsions.
c De 59a: ^{27}Al(α, p)^{30}Si — $E_α$ = 5 MeV; magn. anal.
d Wh 60a: ^{30}Si(p, p')^{30}Si — E_p = 7.5, 8.0, 8.6 MeV; magn. anal.
e Va 52: ^{29}Si(d, p)^{30}Si — E_d = 2.1 MeV; magn. anal.
f Br 60d: ^{29}Si(d, p)^{30}Si — E_d = 7.03 MeV; magn. anal.

G. ^{30}Si(n, n')^{30}Si

The yield of 2.23 MeV γ rays from natural Si targets has been measured up to $E_n = 3.0$ MeV (Li 61).

H. ^{30}Si(p, p')^{30}Si

Magnetic analysis at $E_p = 7.5$, 8.0, and 8.6 MeV, yields the levels listed in table 30.2; a level at 5.075 MeV (Va 52) has not been observed (Wh 60a).

Angular distribution measurements of the 2.23 MeV γ ray yield $J^π = 2^+$

for ^{30}Si(1) (Br 60e, Ba 61). Gamma rays of 1.27 and 1.55 MeV have been observed in coincidence with the 2.23 MeV γ ray. A direct ground-state transition has been observed from the 3.51 MeV level, intensity $(46\pm5)\%$, but not from the 3.78 MeV doublet (Br 60b, Go 61a). Gamma-gamma angular correlations and angular distributions give $J^\pi = 2^+$ for ^{30}Si(2), and $J = 0$ for one of the components of the 3.78 MeV doublet. The E2/M1 amplitude ratio of the ^{30}Si(2) $\rightarrow$ (1) transition amounts to $x = -0.18\pm0.05$, Br 60e, Go 60c, Br 61d. See also Ok 58.

For resonances, see ^{31}P.

I. ^{30}P(β^+)^{30}Si $\qquad Q_m = 4248\pm10$

See ^{30}P.

J. ^{31}P(γ, p)^{30}Si $\qquad Q_m = -7286.2\pm4.0$

Energy spectrum and angular distribution of photoprotons from phosphorus irradiated with 32 MeV bremsstrahlung, Cu 59.

K. ^{31}P(n, d)^{30}Si $\qquad Q_m = -5061.5\pm4.0$

The angular distribution of the deuteron group to ^{30}Si(0) yields $l_p = 0$ (Ve 60a, Co 60a, Ha 59a: $\theta_p^2 = 0.012$ and $Q_0 = -5.2\pm0.2$ MeV. Groups to ^{30}Si* = 2.23 and (3.5+3.8) MeV have been observed (Ve 60a).

See also Za 61.

L. ^{33}S(n, α)^{30}Si $\qquad Q_m = 3503.7\pm4.9$

Cross section, Mu 58a.

M. Not reported:

^{29}Si(t, d)^{30}Si	$Q_m = 4356.6\pm4.2$
^{29}Si(α, ^{3}He)^{30}Si	$Q_m = -9962.9\pm4.2$
^{31}P(d, ^{3}He)^{30}Si	$Q_m = -1793.1\pm4.0$
^{31}P(t, α)^{30}Si	$Q_m = 12526.5\pm4.0$
^{32}S(n, ^{3}He)^{30}Si	$Q_m = -8430.9\pm4.1$

REMARKS

Collective model interpretation of ^{30}Si, Su 60. Prediction of a $(d_{\frac{3}{2}})^2$ level with $J^\pi = 0^+$ at $E_x \approx 2$ MeV, La 58a.

^{30}P

(Fig. 30.2, p. 148; table 30.3, p. 149)

A. ^{30}P(β^+)^{30}Si $\qquad Q_m = 4248\pm10$

The half-life is 2.55 ± 0.02 min (weighted mean of Ko 54a, Mi 55, Ar 58, Cl 58; see also Ba 52a, St 53b, Gr 56, En 54a).

A magnetic spectrometer determination of the β^+ end point of the main branch to ^{30}Si(0), yields 3.24 ± 0.04 MeV (Gr 56), in good agreement with values

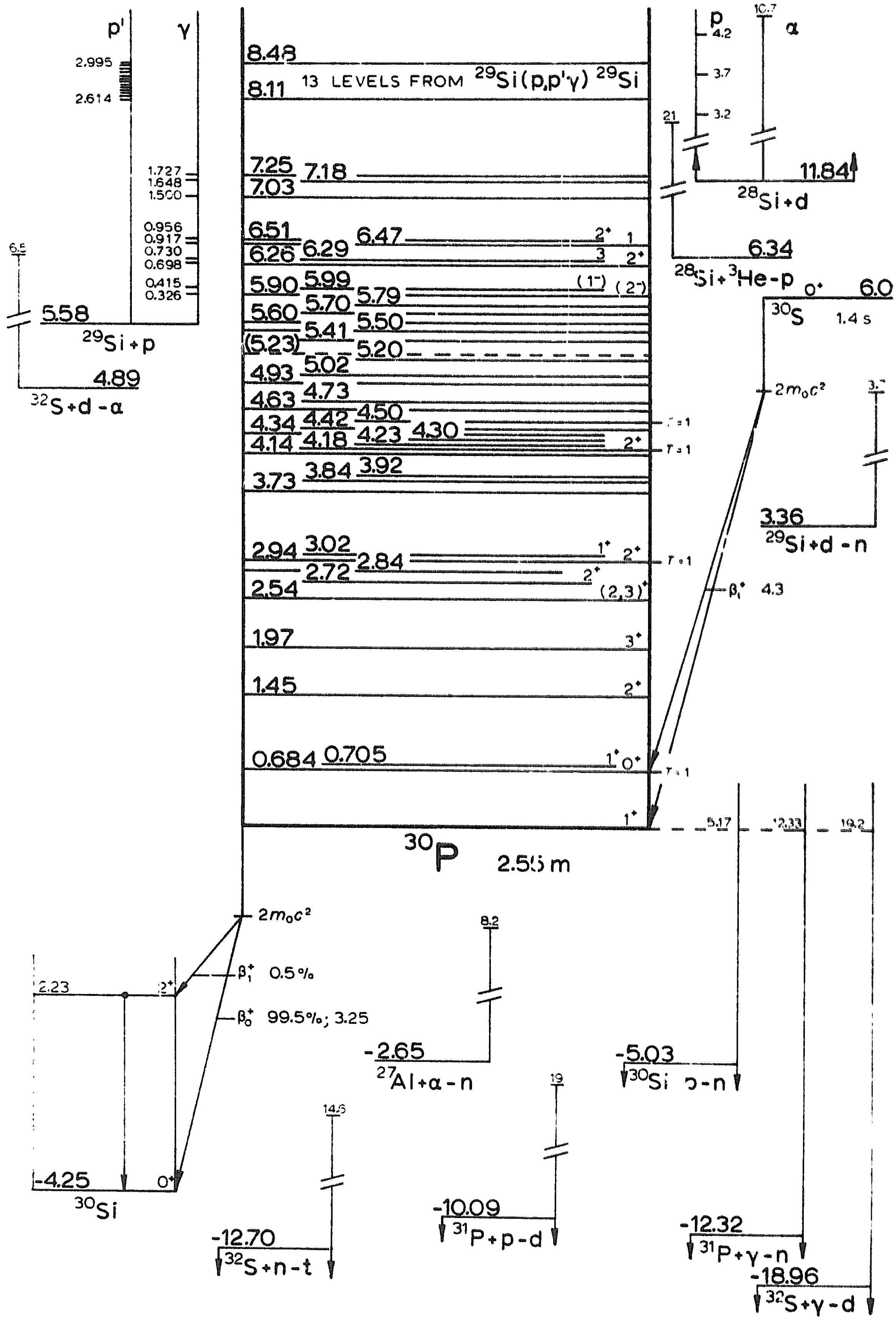

Fig. 30.2. Energy levels of ^{30}P; for γ decay see fig. 30.3.

TABLE 30.3

Energy levels in ^{30}P

E_x (MeV ± keV)	$J^\pi; T$	$\tau_{\frac{1}{2}}$	Decay	Reactions
0	$1^+; 0$	2.55±0.02 min	β^+	many
0.684 ± 3	$0^+; 1$		γ	B, E, I, K, N
0.705 ± 3	$1^+; 0$		γ	B, E, G, K, N
1.451 ± 10	2^+		γ	B, E, G, N
1.972 ± 10	3^+		γ	E, G, N
2.538 ± 10	$(2, 3)^+$		γ	E, N
2.723 ± 10	2^+		γ	E, N
2.839 ± 10			γ	E, N
2.937 ± 10	$2^+; 1$		γ	E, N
3.018 ± 10	1^+		γ	E, N
3.734 ± 10				N
3.836 ± 10				N
3.926 ± 10				N
4.141 ± 10				N
4.181 ± 10	$2^+; 1$		γ	E, N
4.230 ± 10				N
4.296 ± 10				N
4.342 ± 10				N
4.421 ± 10				N
4.501 ± 10	; 1		γ	E, N
4.625 ± 10				N
4.734 ± 10				N
4.929 ± 10				N
5.024 ± 10				N
5.200 ± 10				N
(5.233 ± 10)				N
5.412 ± 10				N
5.504 ± 10				N
5.598 ± 10				N
5.700 ± 10				N
5.790 ± 10				N
5.900–7.253; 11 levels, see table 30.4 and reaction				E
8.11–8.48; 13 levels, see table 30.4 and reaction				F
14.8			p	C
15.3			p	C
15.7			p	C

of 3.31±0.07 MeV (Hu 54a; scintillation spectrometer) and 3.23±0.07 MeV (Ko 54a; Al absorption). Log ft = 4.84.

Although absence of γ rays in the ^{30}P decay is reported in St 53b, Ko 54a, and Gr 56, later a 2.24 MeV γ ray has been observed with 0.5% intensity (Mo 56d); log ft = 4.9. This uniquely fixes $J^\pi = 1^+$ for ^{30}P(0), since ^{30}Si(1) has $J^\pi = 2^+$.

B. ^{27}Al(α, n)^{30}P $\qquad Q_m = -2653 \pm 9$

At E_α = 3–6 MeV, neutron groups have been observed to ^{30}P* = 0, 0.70±0.03, and 1.45 ± 0.03 MeV; $Q_0 = -2.67 \pm 0.03$ MeV (Ba 59a), $\geqslant -2.662 \pm 0.005$ MeV (Wi 60). See also Ya 60, Pe 48.

For resonances, see ^{31}P.

C. (a) ^{28}Si(d, α)^{26}Al $Q_m = 1420.7 \pm 4.2$ $E_b = 11837 \pm 9$
(b) ^{28}Si(d, p)^{29}Si $Q_m = 6253.0 \pm 3.4$ $E_b = 11837 \pm 9$

Strong resonance structure in the α-particle and proton yield has been observed for $E_d = 5.5$–10.7 MeV, corresponding to ^{30}P excitation energies between 17.1 and 21.9 MeV (Br 59a, Ku 60e). At lower energies, the resonant character of the (d, p) reaction indicates ^{30}P levels at 14.8, 15.3, and 15.7 MeV (Ne 56b; see also Co 57b).

For non-resonance data, see ^{26}Al and ^{29}Si.

D. ^{28}Si(^{3}He, p)^{30}P $Q_m = 6344 \pm 9$

Observed, Po 52b, Po 53.

E. ^{29}Si(p, γ)^{30}P $Q_m = 5584 \pm 10$

With targets enriched in ^{29}Si, the assignment to the ^{29}Si(p, γ)^{30}P reaction was established of the resonances listed in table 30.4, with corresponding ^{30}P excitation energies, spins, parities, isobaric spins, and resonance strengths (Ba 60f, Oh 60, Ku 59a, Si 59d, Va 58a, Gr 57a, Ts 56, Mi 55, Ta 46; see also Se 60a, Se 55).

The γ-ray energies measured at the four lowest resonances lead to $Q_0 = 5.57 \pm 0.03$ MeV (Va 58a). Results of the analysis of γ-ray spectra, γ–γ coincidences, and angular distributions at the four lowest resonances (Va 58a), and at the six lowest resonances (Ba 60f), are in excellent agreement. See also Mi 55, Si 59d. Branching ratios of the resonance states and lower lying levels, and spins, parities, and isobaric spins found from this work are summarized in fig. 30.3 (Ba 60f). The 1307.5 keV resonance de-excites predominantly to ^{30}P* = 0.68 MeV; the 1331.5 keV resonance to ^{30}P(0) (Oh 61). The doublet character of the 700 keV level was demonstrated by measurement of γ-ray energies: 686 ± 4 and 686 ± 6 keV at the 415 and 730 keV resonances, and 703 ± 6 and 705 ± 5 keV at the 326 and 698 keV resonances (Va 58a). In Si 59d $E_\gamma = 690 \pm 5$ keV is reported at $E_p = 415$, 730, and 917 keV, and $E_\gamma = 708 \pm 5$ keV at $E_p = 698$ keV; see also Si 59f. Angular distribution measurements yield $J^\pi = 0^+$ and 1^- for the 684 and 705 keV levels, respectively; the first is the $T = 1$ analogue of ^{30}Si(0) (Va 58a, Si 59d, Ba 60f).

At the four lowest resonances some evidence is found for the operation of an E1 isobaric spin selection rule (Va 58a). Description of this nucleus in terms of a strong coupling version of the unified model is probably difficult (Ba 60f).

TABLE 30.4

Resonances in ^{29}Si+p

E_p (keV)	^{30}P* (MeV)	J^π	Decay	$(2J+1)\,\Gamma_p\Gamma_\gamma/\Gamma$ (eV)
326.4±1.2[a, d, e, l]	5.900	2^-[g]; 1^+, $2^\pm$[h]	γ	0.07±0.02[g]
415.3±1.3[a, d, e, l]	5.986	1^-[g]; 1^- (1^+)[h]	γ	0.23±0.06[g]; 0.23[l]
697.5±0.7[a, e, l]	6.258	(3^+)[f]; 2^+[h]	γ	0.18±0.05[g]; 0.11[l]
730.1±1.2[a, e, l]	6.290	3^-[g]; 3^+ (3^-)[h]	γ	0.15±0.04[g]; 0.11[l]
916.5±0.5[b, e, l]	6.470	1^+ (1^-)[b]	γ	
956 ±1[b, e, l]	6.508	2^+[h]	γ	
1307.5±3[l]	6.848		γ	
1331.5±3[l]	6.871		γ	
1500[c]	7.034		γ	
1648[c, b]	7.177		γ	
1727[c]	7.253		γ	
2614[k]	8.11		p_1	
2678[k]	8.17		p_1, p_2	
2700[k]	8.19		p_1, p_2	
2720[k]	8.21		p_1	
2760[k]	8.25		p_1	
2798[k]	8.29		p_1, p_2	
2843[k]	8.33		p_1	
2876[k]	8.36		p_1, p_2	
2922[k]	8.41		p_1	
2934[k]	8.42		p_1, p_2	
2958[k]	8.44		p_1, p_2	
2982[k]	8.47		p_1, p_3	
2995[k]	8.48		p_1	

[a] Ku 59a.
[b] Ts 56.
[c] Gr 57a.
[d] Ta 46.
[e] Mi 55.
[f] Va 58d.
[g] Va 58a.
[h] Ba 60f.
[i] Br 56h.
[k] Br 57.
[l] Oh 61.

F. ^{29}Si(p, p′)^{29}Si* $E_b = 5584 \pm 10$

In the range $E_p = 2.5$–3.0 MeV, resonances in the yield of 1.28, 2.03, and 2.43 MeV γ rays have been observed; see table 30.4 (Br 57).

For non-resonance data, see ^{29}Si.

G. ^{29}Si(d, n)^{30}P $Q_m = 3359 \pm 10$

With enriched ^{29}Si targets, groups to ^{30}P* = 0, 0.75±0.06, 1.46±0.06, and 2.00±0.06 MeV have been found at $E_d = 1.4$ MeV; $Q_0 = 3.27 \pm 0.04$ MeV (Ma 52; see also Pe 48).

H. ^{30}Si(p, n)^{30}P $\qquad Q_m = -5031 \pm 10$

Threshold measured at $E_p = 5.174 \pm 0.030$ MeV, yielding $Q_0 = -5.005 \pm 0.030$ MeV (Br 59f).

For resonances, see ^{31}P.

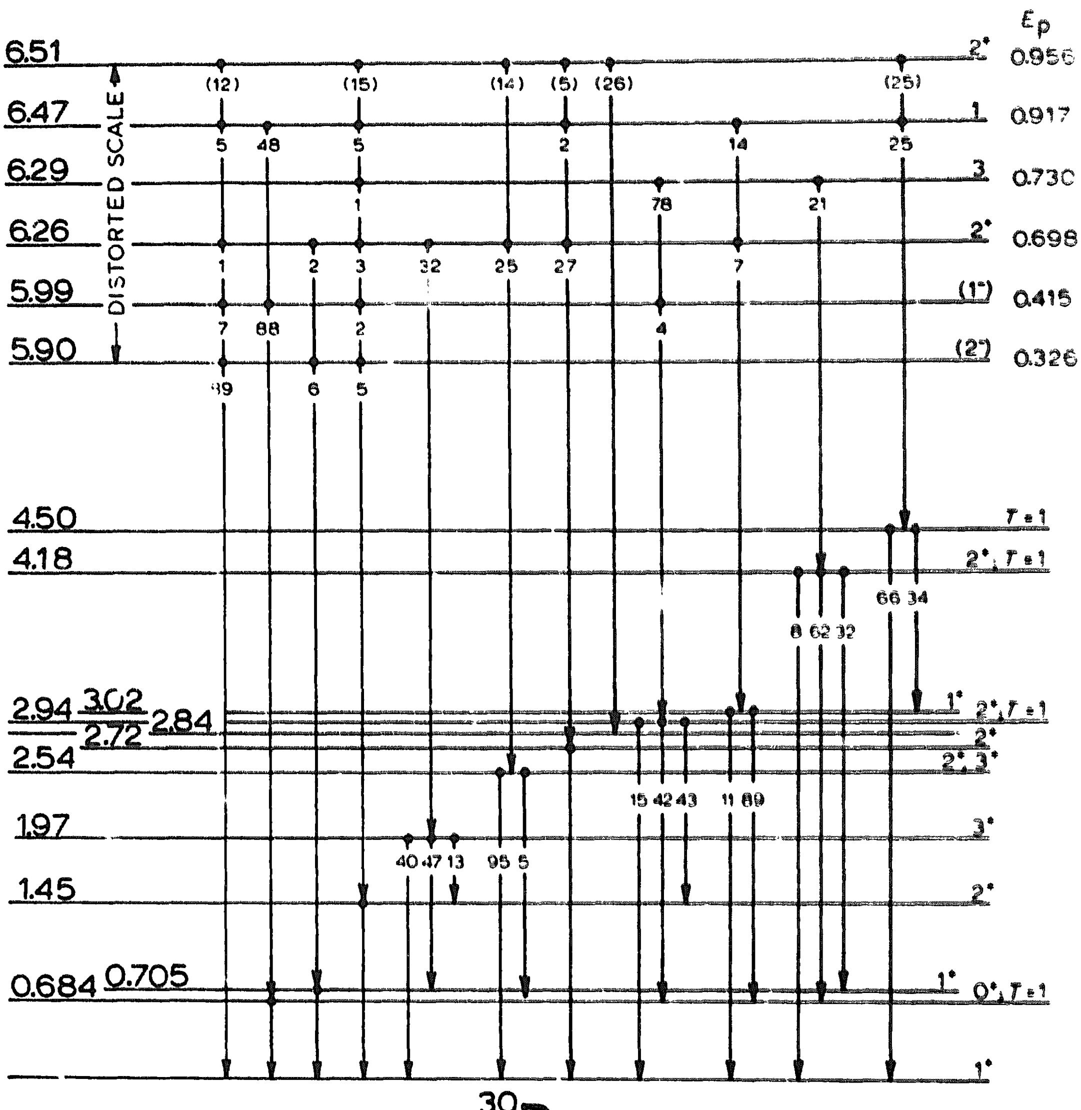

Fig. 30.3. Gamma-ray branchings of ^{30}P states (Ba 60f).

I. ^{30}S(β^+)^{30}P $\qquad Q_m = 5970 \pm 110$

See ^{30}S.

J. ^{31}P(γ, n)^{30}P $\qquad Q_m = -12317 \pm 9$

Recent threshold measurements give 12.33 ± 0.05 MeV (Ba 57b), 12.50 ± 0.05 MeV (Ch 58), $< 12.391 \pm 0.026$ MeV (Ge 60a), and 12.23 ± 0.04 MeV (Sa 61). See also Mc 49, Ka 51a, Sh 51a.

For breaks, see ^{31}P.

Cross section measurements, see En 54a, Na 54.

K. $^{31}P(p, d)^{30}P$ $Q_m = -10092 \pm 9$

At $E_p = 18.6$ MeV, angular distribution analysis yields $l_n = 0$ for the deuteron groups to the ground state and the 700 keV doublet; reduced width $\theta_n^2 = 0.013$ for the ground state, and $\frac{1}{3}\theta^2_{J=0} + \theta^2_{J=1} = 0.012$ for the 700 keV doublet (Be 61b, Ma 60d).

L. $^{32}S(\gamma, d)^{30}P$ $Q_m = -18955 \pm 9$

Threshold reported at $E_\gamma = 19.15 \pm 0.20$ MeV (Ka 51a). For yield measurements, see Fo 61, Fe 60, Fa 59, Go 58d, Ri 55, Ka 51c.

M. $^{32}S(n, t)^{30}P$ $Q_m = -12697 \pm 9$

Cross section at $E_n = 14.6$ MeV, Ba 61f.

N. $^{32}S(d, \alpha)^{30}P$ $Q_m = 4891 \pm 9$

Magnetic analysis, at $E_d = 6.0$ and 6.5 MeV and at several angles, yields $Q_0 = 4.887 \pm 0.010$ MeV, and levels at $^{30}P^* = 0.680 \pm 0.010$, 0.708 ± 0.008, 1.451, 1.972, 2.538, 2.723, 2.839, 2.937, 3.018, 3.734, 3.836, 3.926, 4.141, 4.181, 4.230, 4.296, 4.342, 4.421, 4.501, 4.625, 4.734, 4.929, 5.024, 5.200, (5.233), 5.412, 5.504, 5.598, 5.700, 5.790, all ± 0.010 MeV. The intensity of the group to the 0.68 MeV level, relative to that to the 0.71 MeV level, at $\vartheta = 130°$, is 0.20 at $E_d = 6.0$ MeV and 0.02 at $E_d = 6.5$ MeV, indicating that the 0.68 MeV level should be identified with the $J^\pi = 0^+$, $T = 1$ state at 686 keV found from the $^{29}Si(p, \gamma)^{30}P$ reaction. The violation of the isobaric-spin selection rule is more pronounced for the higher $T = 1$ levels, presumably at 2.937, 4.181, and 4.501 MeV. The intensities of the α-particle groups to these levels are about 50% of neighbouring groups corresponding to $T = 0$ final states (En 58). See also Le 56b.

In Ja 61a, groups are reported to $^{30}P^* = 0.711 \pm 0.008$, and 1.459 ± 0.012 MeV; $Q_0 = 4.888 \pm 0.010$ MeV (Ma 60e).

O. Not reported:

$^{28}Si(t, n)^{30}P$	$Q_m = 5579 \pm 9$
$^{28}Si(\alpha, d)^{30}P$	$Q_m = -12009 \pm 9$
$^{29}Si(^3He, d)^{30}P$	$Q_m = 91 \pm 10$
$^{29}Si(\alpha, t)^{30}P$	$Q_m = -14229 \pm 10$
$^{30}Si(^3He, t)^{30}P$	$Q_m = -4266 \pm 10$
$^{31}P(d, t)^{30}P$	$Q_m = -6059 \pm 9$
$^{31}P(^3He, \alpha)^{30}P$	$Q_m = 8260 \pm 9$
$^{32}S(p, ^3He)^{30}P$	$Q_m = -13461 \pm 9$
$^{33}S(p, \alpha)^{30}P$	$Q_m = -1527 \pm 9$

^{30}S

(Not illustrated; see fig. 30.2 p. 148)

A. $^{30}S(\beta^+)^{30}P$ $\qquad Q_m = 5970 \pm 110$

The half-life is 1.5 ± 0.1 sec (Jo 60), 1.35 ± 0.10 sec (Ro 61a). Coincidence measurements indicate that the β^+ decay mainly proceeds to ^{30}P(1). The β^+ end point is 4.22 ± 0.15 MeV (Jo 60), 4.30 ± 0.15 MeV (Ro 61a); the γ-ray energy is 676 ± 8 keV (Jo 60), 677 ± 10 keV (Ro 61a); log $ft = 3.6$.

A β^+ branch to ^{30}P(0) has also been observed. The calculated branching percentage (19%; log $ft = 4.7$) is not inconsistent with very crude estimates. No evidence has been found for a transition to ^{30}P*(0.704); $< 25\%$ (Ro 61a).

B. $^{28}Si(^3He, n)^{30}S$ $\qquad Q_m = -410 \pm 110$

At $E(^3He) = 3$ and 8 MeV, ^{30}S has been produced (Jo 60, Ro 61a).

C. Not reported:

$^{32}S(p, t)^{30}S$ $\qquad Q_m = -19450 \pm 110$

^{31}Si

(Fig. 31.1, p. 155; table 31.1, p. 156)

A. $^{31}Si(\beta^-)^{31}P$ $\qquad Q_m = 1476.7 \pm 4.6$

The weighted mean value of the half-life is 157.3 ± 0.4 min (Ci 38, Lu 50, We 51, De 52, Mo 52a, Gu 58b).

The β^- spectrum is simple and has the allowed shape. The end point has been measured as 1.471 ± 0.008 MeV (Mo 52a) and 1.486 ± 0.012 MeV (Wa 52); log $ft = 5.5$. A 1.26 MeV γ ray (intensity 0.07%) has been detected by scintillation spectrometer. The corresponding β^- transition is allowed (log $ft = 5.2$), Ly 54.

The allowed character of the β^- branch to ^{31}P(0) with $J^\pi = \frac{1}{2}^+$ yields $J^\pi = \frac{1}{2}^+$ or $\frac{3}{2}^+$ for ^{31}Si(0), of which the first value is excluded by ^{30}Si(d, p)^{31}Si angular distribution measurements (see reaction C).

Theoretical remarks concerning the ^{31}Si decay, Go 56b.

B. $^{29}Si(t, p)^{31}Si$ $\qquad Q_m = 8724 \pm 5$

By magnetic analysis at $E_t = 5$–6 MeV, levels in ^{31}Si have been observed at $E_x = 0.754$, 1.692, 2.314, 2.799, 3.141, 3.534, 3.877, 4.264, 4.386, 4.688, 4.716, 4.940, 4.964, 5.272, 5.312, 5.439, 5.594, 5.605, 5.655, 5.675, 5.730, 5.816, 5.868, 5.955, 5.982, 6.068, 6.107, 6.248, 6.340, 6.450, 6.468, 6.576, 6.650, 6.810, 6.874, all ± 0.010 MeV; $Q_0 = 8.715 \pm 0.015$ MeV (Hi 61g).

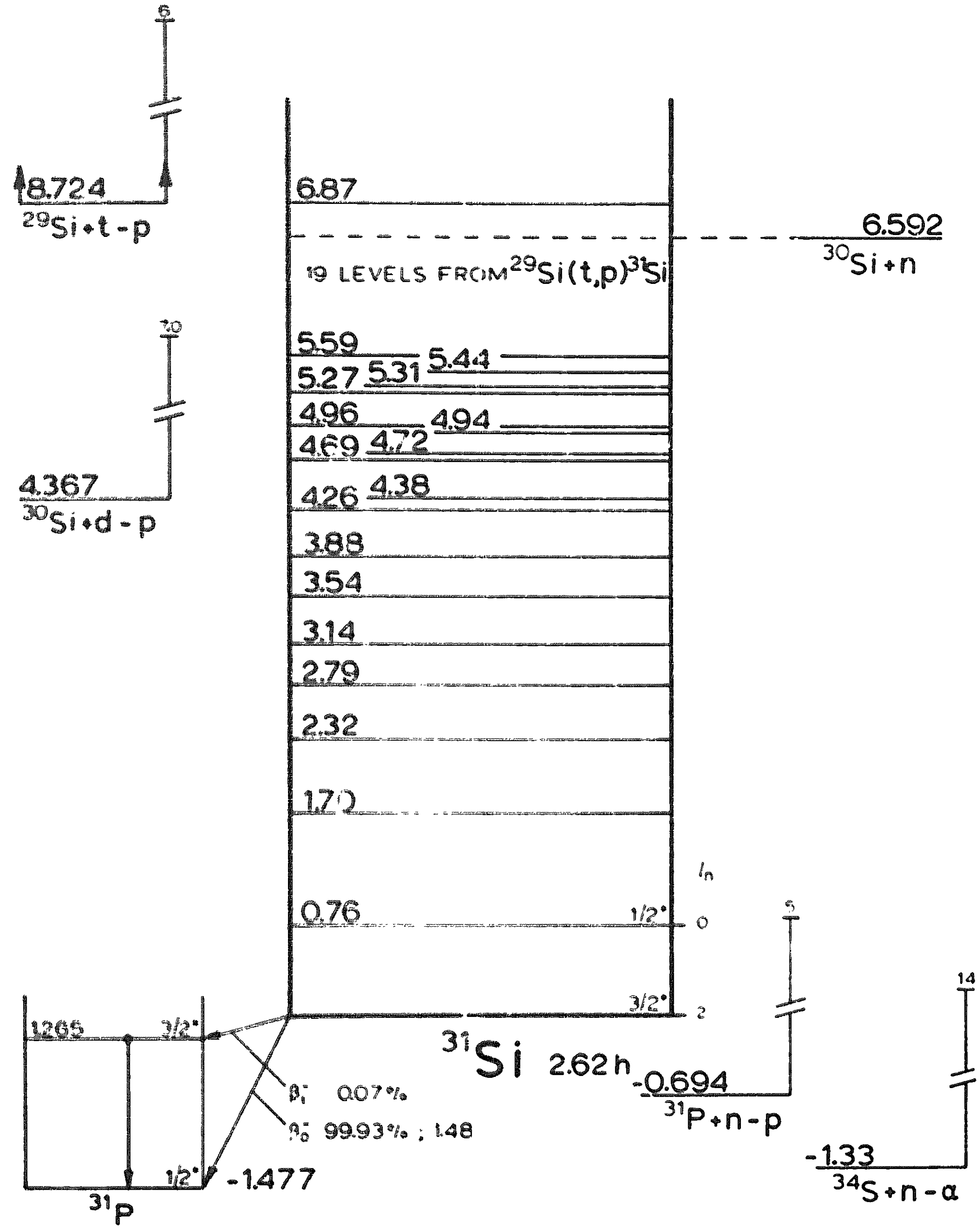

Fig. 31.1. Energy levels of ^{31}Si.

C. ^{30}Si(n, γ)^{31}Si $\qquad Q_n = 6592.1 \pm 3.8$

The thermal neutron capture cross section is 110 ± 10 mb (Hu 58). For the cross section at higher E_n, see Hu 58, Bo 58b, Ko 58d.

D. ^{30}Si(d, p)^{31}Si $\qquad Q_m = 4367.4 \pm 3.7$

By magnetic analysis at deuteron energies up to 2.1 MeV, proton groups have been found to ^{31}Si* = 0, 0.757 ± 0.007, 1.699 ± 0.007, 2.319, 2.791, 3.140, 3.539, and 4.384 MeV, all ± 0.008 MeV; $Q_0 = 4.364 \pm 0.007$ MeV (Va 52), 4.364 ± 0.010 MeV (Ma 60e). At $E_d = 7.0$ MeV, magnetic analysis yields groups

TABLE 31.1

Energy levels of ^{31}Si

E_x (MeV ± keV)	J^π	$\tau_{\frac{1}{2}}$	Decay	Reactions
0	$\frac{3}{2}^+$	157.3 ± 0.4 min	β^-	A, B, D, E, F
0.756 ± 6	$\frac{1}{2}^+$			B, D, E
1.697 ± 6				B, D
2.319 ± 5				B, D
2.791 ± 5				B, D
3.139 ± 5				B, D
3.536 ± 5				B, D
3.877 ± 10				B
4.264 ± 10				B
4.385 ± 5				B, D
4.688 ± 10				B
4.722 ± 6				B, D
4.940 ± 10				B
4.964 ± 10				B
5.272 ± 10				B
5.312 ± 10				B
5.444 ± 6				B, D
5.594–6.874; 19 levels, see reaction				B

to $^{31}Si^*$ = 2.322, 2.788, 3.137, 3.535, 4.386, 4.725, and 5.447 MeV, all ±0.006 MeV (Br 60d).

Angular distribution analysis of the groups to $^{31}Si(0)$ and (1) gives $l_n = 2$ and 0, and thus $J^\pi = (\frac{3}{2}, \frac{5}{2})^+$ and $\frac{1}{2}^+$, respectively. The reduced widths are $\theta_n^2 = 0.11$ ($J^\pi = \frac{3}{2}^+$; see reaction A) and 0.06, respectively (Su 59b, as corrected in Su 60; Ho 53d).

E. $^{31}P(n, p)^{31}Si$ $Q_m = -694.1 \pm 4.6$

With D(d, n) neutrons, a ^{31}Si level at 0.7 MeV has been found; $Q_0 = -0.97 \pm 0.13$ MeV (Me 48).

For cross section and resonances, see ^{32}P.

F. $^{34}S(n, \alpha)^{31}Si$ $Q_m = -1325 \pm 6$

Cross section, Hu 58.

G. Not reported:

$^{30}Si(t, d)^{31}Si$	$Q_m = 334.5 \pm 3.7$
$^{30}Si(\alpha, {}^3He)^{31}Si$	$Q_m = -13985.0 \pm 3.8$
$^{31}P(t, {}^3He)^{31}Si$	$Q_m = -1458.6 \pm 4.6$
$^{33}S(n, {}^3He)^{31}Si$	$Q_m = -10481 \pm 5$

REMARKS

For a collective model interpretation of the ^{31}Si level scheme, see Su 60.

^{31}P

(Fig. 31.2, p. 158; table 31.2, p. 159)

A. ^{27}Al(α, n)^{30}P $Q_m = -2653 \pm 9$ $E_b = 9663.8 \pm 2.4$

Resonances in the ^{30}P activity have been observed at E_α = 3.42, 3.58, 3.68, 3.72, 3.76, 3.81, 3.90 (Wi 60), 3.95, 4.53, 4.70, 4.84, 5.12, and 5.3 MeV (Sz 39). With natural α-particle sources, 13 resonances have been found for E_α = 5.29 to 8.62 MeV (Fu 38). See also En 54a.

For Q value and neutron groups, see ^{30}P.

B. ^{27}Al(α, p)^{30}Si $Q_m = 2377.6 \pm 4.1$ $E_b = 9663.8 \pm 2.4$

With natural α-particle sources, resonances have been found at E_α = 4.0, 4.44, 4.86, 5.25, 5.75, and 6.6 MeV; for references, see En 54a.

For Q value and proton groups, see ^{30}Si.

C. ^{28}Si(α, p)^{31}P $Q_m = -1916.8 \pm 2.8$

At E_α = 19 MeV, the angular distributions of the p_0, p_1, p_2 groups indicate l = 0, 2, and 2, respectively (Pl 60, Pl 61). The same result has been obtained at E_α = 22 MeV (Ko 61).

D. (a) ^{30}Si(p, γ)^{31}P $Q_m = 7286.2 \pm 4.0$

(b) ^{30}Si(p, p$'\gamma$)^{30}Si $E_b = 7286.2 \pm 4.0$

Capture resonances for $E_p \lesssim 1$ MeV, with strengths, spins, parities, and the excitation energies of the corresponding ^{31}P levels are listed in table 31.3a. The resonance energies listed are those reported in Ku 59a and Oh 61. Other less accurate measurements are in good agreement with these values (Ta 46, Ts 56, Tu 57, Br 58c, Ho 58c; see also Se 55, Se 60a). Resonances at E_p = 367 keV (Ta 46), and at E_p = 717, 800, and 895 keV (Ts 56) have not been observed in other work.

Investigation of the γ-ray spectra, γ–γ coincidences (including sum-coincidence measurements), angular distributions, and γ–γ angular correlations at the lowest five resonances of table 31.3a (Ho 58c), and at all ten resonances of this table (Br 58c), yields branching ratios, spins, and parities of the resonances and lower lying levels. In addition to the levels known from reaction K, levels at 6.55, 6.43, 6.25 (or 5.26), and (6.05) MeV are necessary to explain the observed γ-ray spectra (Br 58c).

The branching ratios reported in Br 58c and Ho 58c are in good agreement; the averages are given in fig. 31.3; the few discrepancies are mentioned in the figure caption.

Spins and parities of the resonance levels are listed in table 31.3a. Spin and parity assignments $J^\pi = \frac{1}{2}^+, \frac{3}{2}^+, \frac{5}{2}^+, \frac{3}{2}^+, \frac{5}{2}^+, \frac{3}{2}^+$, and $\frac{5}{2}^+$, to ^{31}P* = 0, 1.27, 2.23, 3.13, 3.29, 3.51, and 4.19 MeV, respectively, follow from angular distributio

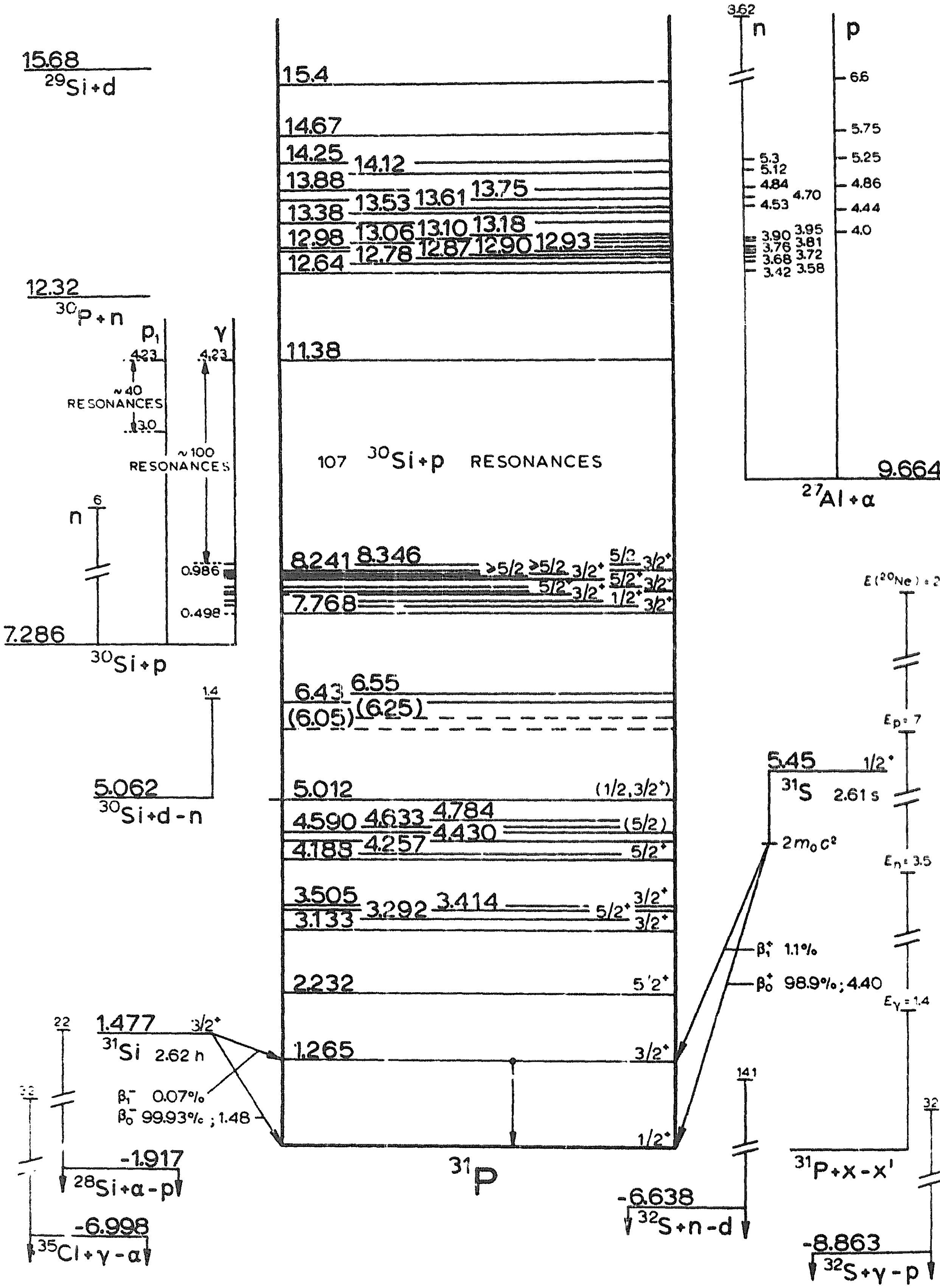

Fig. 31.2. Energy levels of ³¹P; for γ decay see fig. 31.3.

TABLE 31.2

Energy levels of ^{31}P

E_x (MeV ± keV)	J^π	τ_m or Γ	Decay	Reactions
0	$\frac{1}{2}^+$		stable	many
1.265 ± 3	$\frac{3}{2}^+$	$(4.6 \pm 2.3) \times 10^{-13}$ sec	γ	many
2.232 ± 4	$\frac{5}{2}^+$		γ	C, D, F, J, K
3.133 ± 4	$\frac{3}{2}^+$		γ	D, K
3.292 ± 4	$\frac{5}{2}^+$		γ	D, K
3.414 ± 5				F, K
3.505 ± 5	$\frac{3}{2}^+$		γ	D, K
4.188 ± 5	$\frac{5}{2}^+$		γ	D, K
4.257 ± 5				K
4.430 ± 5				K
4.590 ± 5	$(\frac{5}{2})$		γ	D, K
4.633 ± 5				K
4.784 ± 5			γ	K
5.012 ± 5	$(\frac{1}{2}, \frac{3}{2}^+)$		γ	D, K
(6.05)			γ	D
(6.25)			γ	D
6.43			γ	D
6.55			γ	D
7.768 ± 4	$\frac{3}{2}^+$		γ	D
7.886 ± 4	$\frac{1}{2}^+$	40 ± 7 eV	γ	D
7.934 ± 4	$\frac{3}{2}^+$		γ	D
8.021 ± 4	$\frac{5}{2}^+$		γ	D
8.038 ± 4	$\frac{3}{2}^+$		γ	D
8.093 ± 4	$\frac{5}{2}^+$		γ	D
8.201 ± 5	$\frac{3}{2}^+$		γ	D
8.217 ± 5	$\geq \frac{5}{2}$		γ	D
8.236 ± 5	$\geq \frac{3}{2}$		γ	D
8.241 ± 5	$\frac{3}{2}^+$		γ	D
8.346–11.381; 107 γ- and/or p-emitting levels; see tables 31.3b and c and reaction				D
12.58–17.17; 24 n-emitting levels; see reactions				A, E, I
13.2–15.4; 6 p-emitting levels; see reaction				B

and correlation measurements (Br 58c). The assignments reported in Ho 58c, as far as these are unique, agree with these values; in addition $J^\pi = (\frac{5}{2})$ and $(\frac{1}{2}, \frac{3}{2}^+)$ are given for $^{31}P^* = 4.59$ and 5.01 MeV, respectively. See also Si 59a, Si 59b. The E2/M1 mixing ratios of the γ rays de-exciting the resonance levels (all with $\pi = +$), and of a few lower energy γ rays are given in Br 58c, Ho 58c.

For protons with $E_p > 1$ MeV, 107 (p, γ) and (p, p'γ) resonances have been found in the proton energy range up to 4.25 MeV, corresponding to ^{31}P levels up to 11.4 MeV; see tables 31.3b and c (Ba 61, On 61, Sm 61b, Va 61d; see also Pa 56, Gr 57a, Se 60a). For $E_p = 3.0$–4.3 MeV, inelastic proton scattering to ^{30}Si(1) is more prominent than the competing proton capture (Ba 61). The γ decay of some resonances up to $E_p = 1.52$ MeV is given in fig. 31.3.

TABLE 31.3a

Resonances in ^{30}Si(p, γ)^{31}P ($E_p \leqq 1000$ keV)

E_p [a] (keV)	E_p [b] (keV)	^{31}P* (MeV)	J^π	$\Gamma_p\Gamma_\gamma/\Gamma$ [h] (meV)	Γ [i] (eV)	Γ_{γ_0} [i] (meV)
498.3±1.0	501	7.768	$\frac{3}{2}^+$ [c, d]	45± 4		
619.6±1.2	620	7.886	$\frac{1}{2}^+$ [c, d, e]	1610±120	40±7	1520±120
669.8±1.0	670	7.934	$\frac{3}{2}^+$ [d]	32± 3		
759.3±0.9	759	8.021	$\frac{5}{2}^+$ [c, d]	24± 3		
776.4±1.0	776	8.038	$\frac{3}{2}^+$ [c, d, f]	182± 16		140± 40
834.2±1.3	835.5	8.093	$\frac{5}{2}^+$ [c]			
	945	8.201	$\frac{3}{2}^+$ [c, g]			
	961.5	8.217	$\geqq \frac{5}{2}$ [c]			
	982	8.236	$\geqq \frac{5}{2}$ [c]			
	986.5	8.241	$\frac{3}{2}^+$ [c]			
	all±3					

[a] Ku 59a.
[b] Oh 61.
[c] Br 58c.
[d] Ho 58c.
[e] Angular distribution measurements (Br 58c, Ho 58c) yield $J^\pi = \frac{1}{2}\pm$; the partial widths as found from resonance absorption measurements make even parity most probable (Sm 58a).
[f] A γ polarization measurement indicates that the ground-state transition is predominantly E2 (Su 60c).
[g] Spin assignment from angular distribution measurement; parity from γ polarization (Tu 57).
[h] Ho 58c; obtained by standardizing on the value $\Gamma_p\Gamma_\gamma/\Gamma = 1610\pm120$ meV for the 620 keV resonance (Sm 58a).
[i] Sm 58a, Sm 59; resonance absorption measurements.

Spins and parities of resonance levels, and the methods of investigation, are listed in tables 31.3b and c. Angular correlation measurements give $J^\pi = \frac{5}{2}^+$ and $\frac{3}{2}^+$ for ^{31}P(2) and (1), respectively. The 2.23 MeV level predominantly (> 97%) decays to the ground state (Li 59, Pa 56).

E. ^{30}Si(p, n)^{30}P $\quad Q_m = -5031\pm10 \quad E_b = 7286.2\pm4.0$

The cross section above the threshold shows resonance structure (Br 59f). For threshold, see ^{30}P.

F. ^{30}Si(d, n)^{31}P $\quad Q_m = 5061.5\pm4.0$

At $E_d = 1.4$ MeV, neutron groups have been observed to ^{31}P* = 0, 0.33, 1.19, 2.22, and 3.41 MeV, all±0.04 MeV, Ma 52. See also Pe 48.

G. ^{31}Si(β^-)^{31}P $\quad Q_m = 1476.7\pm4.6$

See ^{31}Si.

H. ^{31}P(γ, γ)^{31}P

Resonance fluorescence measurements yield $\tau_m = (4.6\pm2.3)\times10^{-13}$ sec for ^{31}P(1) (Bo 60f).

TABLE 31.3b

Resonances in ^{30}Si(p, γ)^{31}P (1000 keV $< E_p <$ 1825 keV)

E_p[a] (keV)	E_p[b] (keV)	E_p[c] (keV)	E_p[d] (keV)	^{31}P* (MeV)	Relative intensity[d]	J^π
1103	1094		1096	8.346	0.7	$\frac{5}{2}$[a, d]
1186	1179.5	1177	1178	8.426	0.2	$\frac{7}{2}(-)$[a]
1212	1209.5	1204	1205	8.453	0.7	$\frac{5}{2}(+)$[a, d]
1294	1290.5		1292	8.536	0.1	$\frac{1}{2}+$[a]
1304	1300			8.544		$\frac{1}{2}+$[a]
1307	1302	1302	1302	8.546	0.3	$(\frac{3}{2})$[a]
1328	1324.5	1322	1326	8.567	2.5	$\frac{5}{2}$[a, d]
1339				8.578		$\frac{5}{2}$[a]
1397	1394.5	1387	1393	8.633	2.1	$\frac{5}{2}$[a, d]
1406	1403	1396	1402	8.642	2.5	$\frac{3}{2}$[a, d]
1483	all ± 3	1476	1482	8.719	2.5	$\frac{3}{2}+$[a, d]
1492		1487	1491	8.728	1.7	$\frac{3}{2}$[a]
1516		1507	1516	8.751	1.9	$\frac{5}{2}+$[a]
1524			1516	8.759		$(\frac{1}{2}, \frac{3}{2})$[a, d]
all ± 3		1591	1599	8.830	0.3	
		1657	1665	8.893	0.4	
		1665	1672	8.901	0.6	
		1693	1697	8.926	1.3	$\frac{3}{2}+$[e]
		1768	1774	9.000	2.0	
		1806	1811	9.037	1.1	$\frac{3}{2}(+)$[f]
		1815	1820	9.046	1.1	$\frac{3}{2}(+)$[f]

[a] Sm 61b; J^π assignments from γ-ray angular distributions and γ–γ angular correlations.
[b] Oh 61.
[c] Ba 61; a qualitative indication of the γ decay at most resonances is also given.
[d] Va 61d; J^π assignments from γ-ray angular distributions.
[e] Li 59.
[f] Pa 56.

I. ^{31}P(γ, n)^{30}P $\qquad Q_m = -12317 \pm 9$

Breaks in the ^{30}P yield curve, not corresponding to known levels in ^{30}P, have been observed at $E_\gamma = 12.58 \pm 0.07$, 12.75 ± 0.08, 12.90 ± 0.08, 13.18 ± 0.10, and 13.38 ± 0.10 MeV (Ba 57b), and at 12.37, 12.47, 12.68, 12.78, 12.83, 12.98, 13.18, and 13.32 MeV, all ± 0.04 MeV (Sa 61). For a possible correspondence of these breaks with strong ^{30}Si(n, p)^{30}P resonances, see Sa 61. The ^{31}P excited state, corresponding to a break at about 12.59 MeV has a width $\Gamma \approx 80$ keV (Ge 60a).

For cross section and threshold measurements, see ^{30}P.

J. ^{31}P(n, n')^{31}P

At several neutron energies between 2.45 and 3.5 MeV, γ rays have been observed from the first two excited states in ^{31}P, with $E_\gamma = 1.266 \pm 0.011$ and 2.23 ± 0.03 MeV (weighted average of Mi 59c, Bo 53a, Cr 56a). See also Sc 54d, An 60d. No γ rays have been observed at $E_n = 1.2$ MeV (Va 56a). From

TABLE 31.3c

Resonances in the ^{30}Si+p γ-ray yield (E_p > 1825 keV)[a]

E_p[b] (keV)	E_p[c] (keV)	Rel. int.[c]	^{31}P* (MeV)	E_p[b] (keV)	E_p[c] (keV)	Rel. int.[c]	^{31}P* (MeV)
1828	1835	2.2	9.059	2311	2317	1.5	9.525
1874	1881	4.0	9.103	2350	2355	1.3	9.563
1888			9.117		2362	1.0	9.570
1892	1898	1.0	9.121		2378	1.1	9.585
1917	1925	1.4	9.145	2390	2394	0.5	9.601
1939	1945	0.7	9.165	2510	2506	3.1	9.713
1970	1977[d]	0.4	9.196		2545	2.0	9.751
1990	1997	0.3	9.216	2552	2550	5.5	9.755
2004	2011	1.2	9.229		2554	1.5	9.758
2019	2024	0.9	9.243		2590	1.1	9.792
2057			9.280		2610	1.3	9.812
2087	2093	0.5	9.309	2616	2615	1.0	9.817
	2125	0.4	9.340		2620	1.1	9.822
2129	2136	1.0	9.350		2630	1.1	9.831
2183	2187	6.0	9.400	2633	2635	2.6	9.835
	2193	1.2	9.406	2647			9.848
2215	2217	1.0	9.430		2660	1.1	9.860
	2225	2.2	9.438	2668	2665	1.0	9.866
2300	2305	1.9	9.515		2701	4.0	9.871

E_p[b] (keV)	^{31}P* (MeV)	E_p[b] (keV)	^{31}P* (MeV)	J^π[b]	E_p[b] (keV)	^{31}P* (MeV)	E_p[b] (keV)	^{31}P* (MeV)
2730	9.928	3154	10.338	$(\frac{3}{2}^-, \frac{7}{2}^+)$	3558	10.729	3886	11.046
2753	9.950	3204	10.387		3606	10.776	3920	11.079
2828	10.023	3223	10.405		3634	10.803	3980	11.137
2856	10.050	3267	10.477	$\frac{5}{2}^-$	3667	10.835	4012	11.168
2883	10.076	3307	10.486	$\frac{3}{2}^-$	3677	10.844	4055	11.210
2901	10.093	3323	10.502	$\frac{5}{2}^-$	3689	10.856	4090	11.244
2910	10.102	3348	10.526	$(\frac{3}{2}, \frac{5}{2})^-$	3714	10.880	4110	11.263
2926	10.117	3434	10.609	$\frac{3}{2}^-$	3740	10.905	4121	11.274
2952	10.143	3453	10.627	$(\frac{5}{2}^-)$	3772	10.936	4143	11.295
3006	10.195	3467	10.641	$\frac{3}{2}^-$	3820	10.983	4172	11.323
3022	10.211	3500	10.673	$(\frac{5}{2}, \frac{5}{2})^-$	3846	11.008	4184	11.335
		3525	10.697	$(\frac{3}{2}, \frac{5}{2})^-$	3869	11.030	4202	11.354
							4232	11.381

[a] Below E_p = 2.5 MeV all resonances are from ^{30}Si(p, γ)^{31}P; above E_p = 3.0 MeV the ^{30}Si(p, p$'\gamma$)^{30}Si, E_γ = 2.23 MeV γ ray is predominant.

[b] Ba 61; J^π assignments from angular distributions of the inelastic scattering 2.23 MeV γ ray. A qualitative indication is given of the γ decay of some resonances below E_p = 2.4 MeV.

[c] Va 61d.

[d] In Va 61d E_p = 1987 keV is given for this resonance; examination of the yield curves in Ba 61 and Va 61d makes E_p = 1977 keV more probable.

coincidence measurements it is concluded that ^{31}P(2) has a 40% ground-state transition (Bo 58a); see, however, reaction D.

Elastic scattering angular distributions, La 57b.

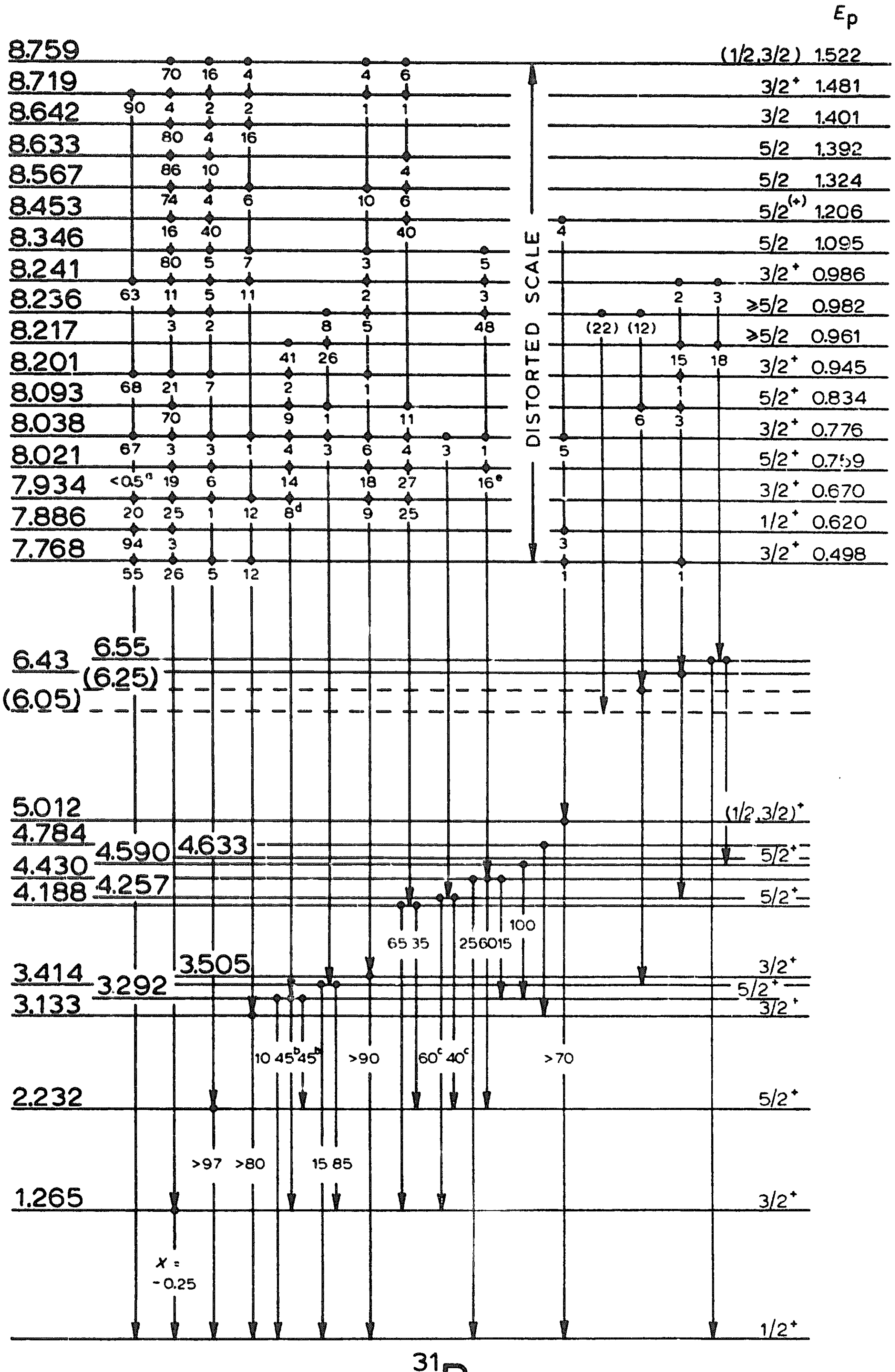

Fig. 31.3. Gamma decay of ^{31}P levels. The branchings of all levels below $E_x = 8.3$ MeV are average values from Br 58c and Ho 58c, except for the following annotated transitions: $^a \approx 3\%$ (Br 58c); $^b > 85\%$ to 1.27 MeV level (Ho 58c); ^{c} de-excitation to 2.23 MeV level only (Br 58c); ^{d} this branch proceeds to the 3.41 MeV level (Br 58c); ^{e} de-excitation to 3.41 MeV level in Br 58c. The mixing ratio of the 1.27 MeV γ ray is from Mc 61a; the 4.78 → 3.13 MeV transition is from Wa 60d. Branchings of levels above $E_x = 8.3$ MeV are from Va 61d.

For cross section, see Hu 58, Ri 60, Cu 60b.

For resonances, see ^{32}S.

K. $^{31}P(p, p')^{31}P$

Levels found from this reaction are listed in table 31.4 (En 57a, Va 57a). In addition to γ rays observed from the $^{30}Si(p, \gamma)^{31}P$ reaction, an intense 1.65 MeV γ ray has been observed, corresponding to a 4.78 → 3.13 MeV transition (Wa 60d).

From angular distribution and linear polarization measurements of the $E_\gamma = 1.26$ MeV γ ray, at the $E_p = 2.70$ and 2.87 MeV resonances, the E2/M1 amplitude mixing ratio has been determined as $x = -0.25 \pm 0.15$ or $+6 \pm 4$ (Mc 61a). For elastic scattering differential cross-section measurements, see Ki 55a; for calculations, Me 57a.

For resonances, see ^{32}S.

TABLE 31.4

Levels in ^{31}P from $^{31}P(p, p')^{31}P$

E_x [a] (MeV ± keV)	E_x [b] (MeV ± keV)	E_x [b] (MeV ± keV)
1.264 ± 4	1.267	4.257
2.230 ± 5	2.234	4.430
3.134 ± 6	3.133	4.590
3.292 ± 5	3.293	4.633
	3.414	4.784
	3.505	5.012
	4.188	all ± 5
	all ± 5	

[a] Va 57a, E_p = 3.72 and 4.62 MeV.
[b] En 57a E_p = 7.04 MeV.

L. $^{31}P(^{20}Ne, ^{20}Ne)^{31}P$

By Coulomb excitation at $E(^{20}Ne) = 28$ MeV the partial mean life for E2 emission of $^{31}P(1)$ has been determined as $\tau_m(E2) = (4.8 \pm 1.4) \times 10^{-12}$ sec (An 61e).

M. $^{31}S(\beta^-)^{31}P$ $\qquad Q_m = 5450 \pm 17$

See ^{31}S.

N. $^{32}S(\gamma, p)^{31}P$ $\qquad Q_m = -8862.6 \pm 1.6$

Cross section, Jo 55, Ri 55, Mo 55a, Go 56c, Cu 59, Fo 61.

O. $^{32}S(n, d)^{31}P$ $\qquad Q_m = -6637.8 \pm 1.7$

Differential cross section Ha 59a. Angular distribution of ground-state group yields $l_p = 0$ (Co 60a) and $\theta_p^2 = 0.011$ (Ve 60a). See also Za 61.

P. $^{35}Cl(\gamma, \alpha)^{31}P$ $\qquad Q_m = -6997.5 \pm 2.9$

Cross section for 32 MeV bremsstrahlung, Er 57.

Q. Not reported:

$^{29}Si(t, n)^{31}P$	$Q_m = 9418.1 \pm 3.3$
$^{29}Si(^3He, p)^{31}P$	$Q_m = 10182.6 \pm 3.3$
$^{29}Si(\alpha, d)^{31}P$	$Q_m = -8169.8 \pm 3.3$
$^{30}Si(^3He, d)^{31}P$	$Q_m = 1793.1 \pm 4.0$
$^{30}Si(\alpha, t)^{31}P$	$Q_m = -12526.5 \pm 4.0$
$^{32}S(d, ^3He)^{31}P$	$Q_m = -3369.4 \pm 1.6$
$^{32}S(t, \alpha)^{31}P$	$Q_m = 10950.1 \pm 1.7$
$^{33}S(n, t)^{31}P$	$Q_m = -9022.8 \pm 3.1$
$^{33}S(p, ^3He)^{31}P$	$Q_m = -9787.2 \pm 3.1$
$^{33}S(d, \alpha)^{31}P$	$Q_m = 8565.2 \pm 3.1$
$^{34}S(p, \alpha)^{31}P$	$Q_m = -630.9 \pm 3.3$

REMARKS

A possible interpretation of the ^{31}P level scheme in terms of the unified model is discussed in Br 59. With oblate deformation a reasonable interpretation of the spins and positions of the first six excited states can be obtained. The branching ratios and E2/M1 mixing ratios predicted by the Nilsson wave functions which would be required by this interpretation are at variance with experimental values (Br 59). Also, Th 60a. For a discussion of the energy level spacing, see Gr 61b.

There is a striking resemblance between the properties and decay of the low lying levels in ^{31}P and ^{29}Si (Ho 58c).

^{31}S

(Fig. 31.4, p. 166; table 31.5, p. 166)

A. $^{31}S(\beta^+)^{31}P$ $Q_m = 5450 \pm 17$

The weighted mean of seven half-life determinations is 2.61 ± 0.03 sec (Ha 52a, Hu 54, Cl 58, Mi 58, Ja 60a, Li 60a, Wa 60a).

The decay mainly (99%) proceeds to $^{31}P(0)$; end point 4.50 ± 0.10 MeV (Hu 54), 4.39 ± 0.03 MeV (Wa 60a). See also Wh 41, El 41. The transition is super-allowed ($\log ft = 3.7$), giving $J^\pi = \frac{1}{2}^+$ for ^{31}S.

A (1.1 ± 0.1)% branch to $^{31}P(1)$ has been found by detection of the 1.27 MeV γ ray (Ta 60c); $\log ft = 5.0$.

B. $^{28}Si(\alpha, n)^{31}S$ $Q_m = -8149 \pm 17$

Threshold, see Ne 61.

C. $^{31}P(p, n)^{31}S$ $Q_m = -6232 \pm 17$

At $E_p = 17.2$ MeV, neutron groups have been observed to $^{31}S^* = 0$, 1.15 ± 0.15, 2.28 ± 0.20, 3.35 ± 0.20, 4.51 ± 0.15, 5.94 ± 0.30, and 6.41 ± 0.20 MeV;

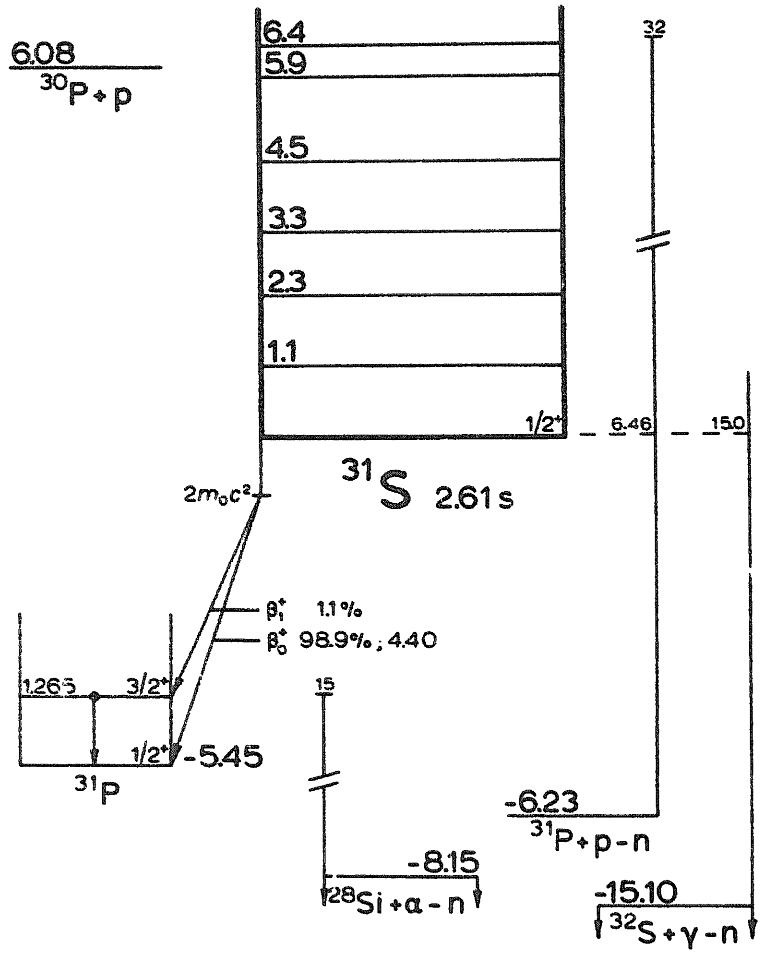

Fig. 31.4 Energy levels of ^{31}S.

TABLE 31.5
Energy levels of ^{31}S

E_x (MeV)	J^π	$\tau_{\frac{1}{2}}$	Decay	Reactions
0	$\frac{1}{2}^-$	2.61 ± 0.03 sec	β^+	A, B, C, D
1.15 ± 0.15				C
2.28 ± 0.20				C
3.35 ± 0.20				C
4.51 ± 0.15				C
5.94 ± 0.30				C
6.41 ± 0.20				C

$Q_0 = -6.06 \pm 0.20$ MeV (Ru 56b). The threshold, at 6.456 ± 0.020 MeV, yields $Q_0 = -6.253 \pm 0.020$ MeV (Br 59f).

Cross section at $E_p = 18$ and 32 MeV, Ta 58.

D. $^{32}S(\gamma, n)^{31}S$ $\qquad Q_m = -15095 \pm 17$

The threshold has been measured as 15.0 ± 0.1 MeV (Ha 52a; also Mc 49. Be 47). Cross section, Fe 60, Fa 59, Mo 55a; for references to older work, En 54a,

E. Not reported:

$^{29}Si(^3He, n)^{31}S$	$Q_m = 3951 \pm 17$
$^{31}P(^3He, t)^{31}S$	$Q_m = -5468 \pm 17$
$^{32}S(p, d)^{31}S$	$Q_m = -12870 \pm 17$
$^{32}S(d, t)^{31}S$	$Q_m = -8837 \pm 17$
$^{32}S(^3He, \alpha)^{31}S$	$Q_m = 5483 \pm 17$
$^{33}S(p, t)^{31}S$	$Q_m = -15254 \pm 17$

^{32}Si

(Fig. 32.1, p. 167)

A. $^{32}Si(\beta^-)^{32}P$ $Q_m = 219 \pm 15$

Radioactive ^{32}Si has been produced from the reaction $^{37}Cl(p, \alpha\, 2p)^{32}Si$ at $E_p = 340$ MeV. From the measured activity and estimated reaction cross

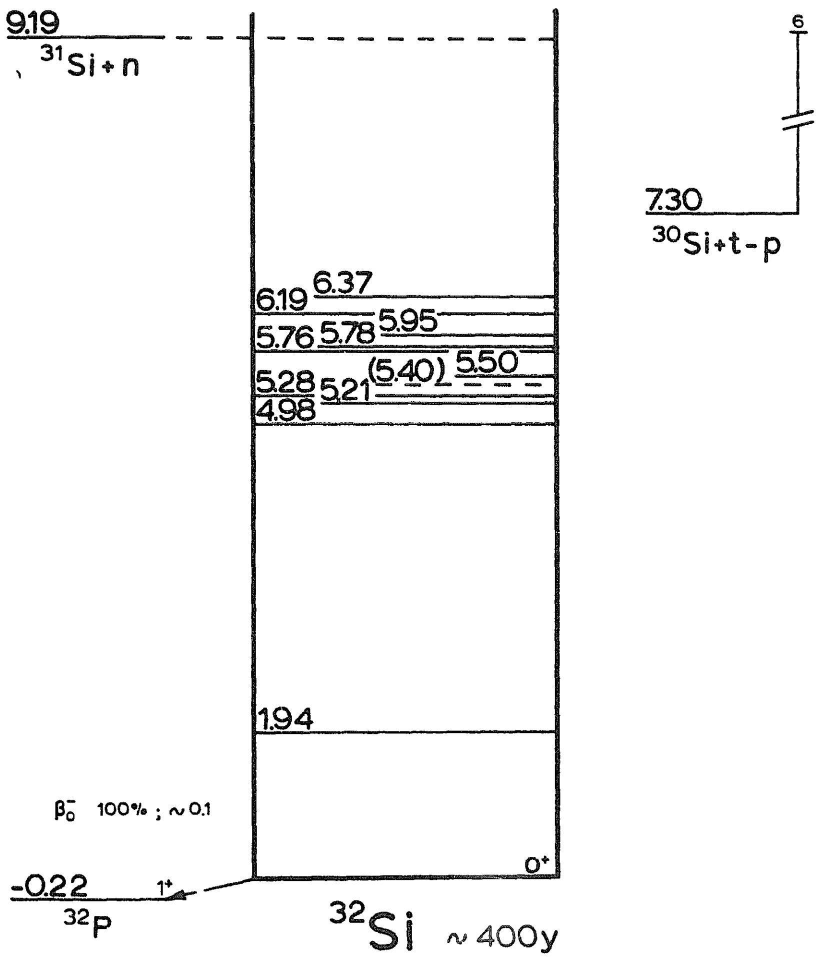

Fig. 32.1. Energy levels of ^{32}Si.

section, a half-life is calculated between 100 and 710 years. The β^- spectrum end point is $\approx$ 100 keV. There are no γ rays (Li 53a). See also Li 53. Log *ft* between 8.0 and 8.8, which is even higher than for ^{32}P.

B. ^{31}Si(n, γ)^{32}Si $Q_m = 9194 \pm 15$

Neutron capture in ^{31}Si in a high-flux reactor has also produced ^{32}Si. From the yield, the half-life (in years) is computed as 600 times the cross section (in barns) (Tu 54). Observation of ^{32}Si produced by cosmic rays is reported in La 59a.

C. ^{30}Si(t, p)^{32}Si $Q_m = 7304 \pm 15$

From magnetic analysis at $E_t = 5$–6 MeV, levels in ^{32}Si have been observed at 1.941, 4.981, 5.212, 5.279, (5.405), 5.499, 5.763, 5.782, 5.949, 6.186, 6.375, all ± 0.010 MeV; $Q_0 = 7.304 \pm 0.015$ MeV (Hi 61g).

D. Not reported:

^{34}S(n, ^{3}He)^{32}Si $Q_m = -12708 \pm 15$

^{32}P

(Fig. 32.2, p. 169; table 32.1, p. 170)

A. ^{32}P(β^-)^{32}S $Q_m = 1708.4 \pm 2.0$

The weighted mean of nine half-life determinations is 14.32 ± 0.02 days (Ro 59, Gu 58b, An 57a, Lo 53, Si 51, Kl 48, Mu 40, Ca 38, Si 36).

Determinations of the β^- end point by magnetic spectrometer, collected in table 32.2, are in good agreement and yield an average of 1.7088 ± 0.0014 MeV. The average β^- energy per disintegration is 694 ± 25 keV (Br 53b), 693 ± 22 keV (Sh 57b). No discrete γ rays have been observed (La 54, Go 54b). The ft value ($\log ft = 7.9$) is very large for an allowed transition (Po 56, An 54a, Je 52, Si 46); this can be explained by l-forbiddenness. Small deviations from the allowed shape have been reported (Po 57, Da 58, Jo 58a, Br 60j, Ni 61) and theoretically discussed (Ca 57a, Ib 58, Ku 59c, Ge 60). The effect of "weak magnetism" is discussed in Be 58d.

Measurements of the degree of longitudinal polarization are in agreement with the predicted value $-v/c$ (Sp 61, Ul 61, Cu 60a, Sp 60a, Ke 59c, Mi 59a, Bo 58, Ge 58b, Fr 57; see also De 57b, Du 57). For recently reported energy dependence of the polarization and/or small deviations from the $-v/c$ value, see Sp 61, Bi 60b, Ga 61a.

The internal bremsstrahlung spectrum is in agreement with theory (Su 59, Pe 59a, Re 57, Mi 54a, Go 54b; En 54a for references to older work); disagreement, however, has been found especially at higher energies (Li 55, Su 59, Ko 60). Theory, Le 57a. Circular polarization of internal bremsstrahlung, Ga 61a, Bo 58.

For internal pair formation, see Mc 54, We 54, Mi 56, Gr 56b, Hu 56a; for effects involving the atomic electron cloud, Ch 54, Ch 55a, Re 55, Re 57, Su 59, Du 61a.

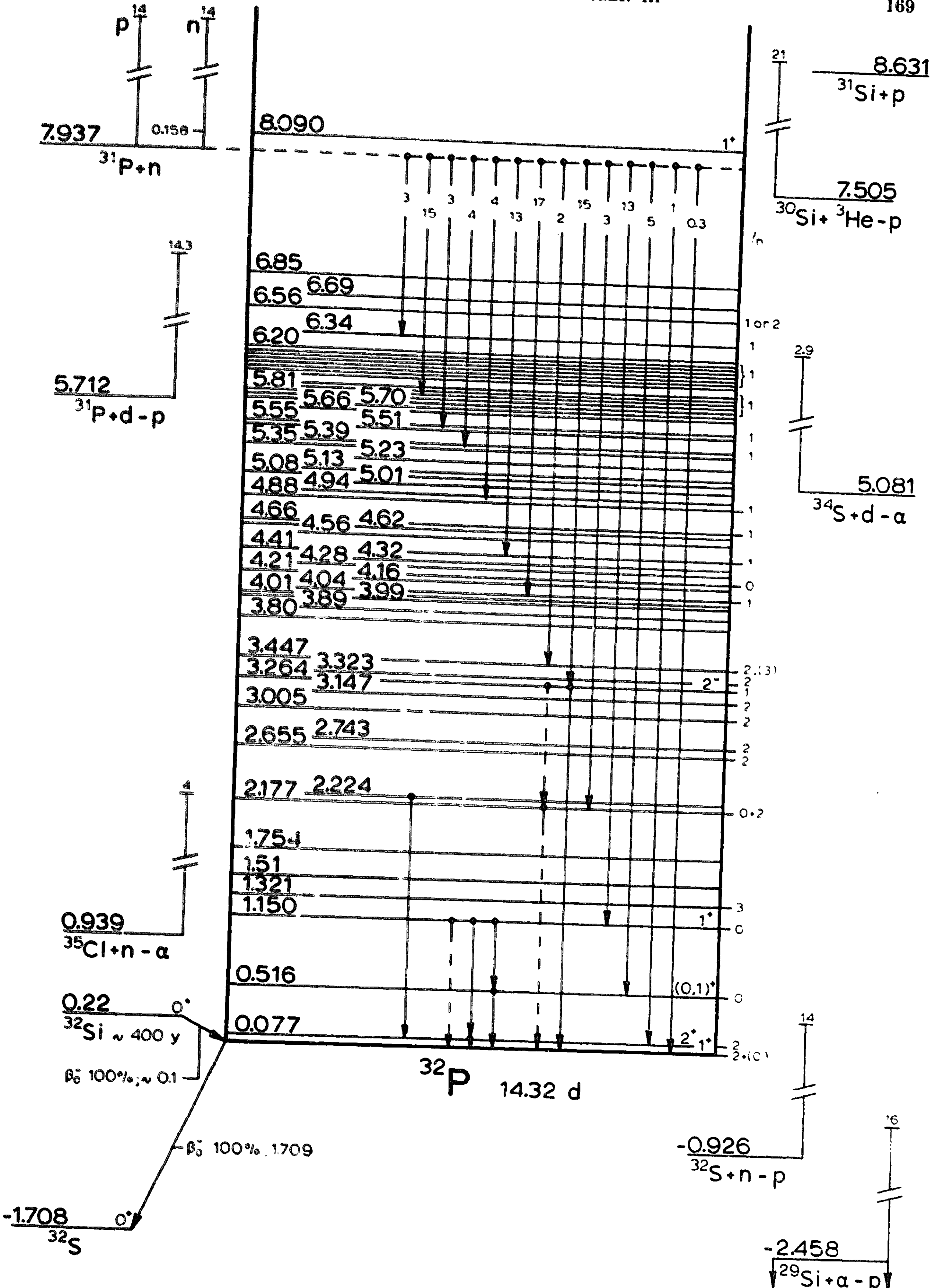

Fig. 32.2. Energy levels of 32P.

TABLE 32.1

Energy levels of ^{32}P

E_x (MeV ± keV)	J^π	$\tau_{\frac{1}{2}}$ or Γ	Decay	Reactions
0	1^+	14.32 ± 0.02 days	β^-	many
0.0770 ± 0.3	2^+	$\leqq 3 \times 10^{-8}$ sec	γ	D, G, I
0.516 ± 3	$(0, 1)^+$		γ	D, G
1.150 ± 3	1^+		γ	D, G
1.321 ± 3	$(\leqq 4)^-$			G
1.51 ± 20				G
1.754 ± 4				G
2.177 ± 4	$(0, 1)^+$		γ	D, G
2.224 ± 4			γ	D, G
2.655 ± 4	$(\leqq 3)^+$			G
2.743 ± 4	$(\leqq 3)^+$			G
3.005 ± 4	$(\leqq 3)^+$			G
3.147 ± 5	$(\leqq 3)^+$			G
3.264 ± 4	2^-		γ	D, G
3.323 ± 4	$(\leqq 3)^+$			G
3.447 ± 5			γ	D, G
3.798 ± 6				G
3.890 ± 6				G
3.994 ± 6				G
4.010 ± 6				G
4.038 ± 5	$(\leqq 2)^-$		γ	D, G
4.158 ± 6				G
4.209 ± 6	$(0, 1)^+$			G
4.280 ± 6				G
4.316 ± 6				G
4.412 ± 6	$(\leqq 2)^-$		γ	D, G
4.560–6.85; 32 levels, see table 32.4 and reactions				D, G
8.090 ± 3	1^+	1.1 ± 0.2 keV	n	E

TABLE 32.2

Magnetic spectrometer determinations of the ^{32}P(β^-)^{32}S end point

Reference	End point (keV)	Reference	End point (keV)	Reference	End point (keV)
Ly 37	1690 ± 30	Ag 50	1718 ± 10	Wo 54	1714 ± 8
La 39a	1720 ± 10	Wa 50	1708 ± 8	An 54a	1712 ± 8
Wi 41a	1750 ± 20	Sh 51c	1695 ± 5	Po 56	1712 ± 4
Si 46	1712 ± 8	Je 52	1704 ± 8	Po 57	1711 ± 2
La 49	1689 ± 10	Mo 52a	1697 ± 10	Da 58	1705 ± 4

B. ^{29}Si(α, p)^{32}P $\qquad Q_m = -2457.8 \pm 4.0$

At $E_\alpha = 16$ MeV, ^{32}P has been produced from this reaction (Ki 39a).

C. ^{30}Si(^{3}He, p)^{32}P $\qquad Q_m = 7505.1 \pm 4.5$

Radioactive ^{32}P has been found from this reaction at $E(^3\text{He}) = 13$ and 21 MeV (Po 52b, Po 53).

TABLE 32.3

Gamma rays from thermal neutron capture in phosphorus

E_γ[a] (MeV ± keV)	I_γ[b, g]	E_γ[c] (MeV ± keV)	I_γ[c, g]	Probable transition in ^{32}P[f]
7.94 ± 30	0.3			C → 0
7.85 ± 50	0.9			C → 0.08
7.62 ± 30	1			
7.42 ± 30	4			C → 0.52
6.76 ± 30	14	6.79 ± 20	10	C → 1.15[e]
6.33 ± 30	0.6			6.34 → 0
6.14 ± 30	0.9			
6.02 ± 40	1	5.96 ± 30	1	6.09 → 0.08
		5.87 ± 30	0.6	5.82 → 0
5.71 ± 30	3	5.73 ± 20	3.3	C → 2.18
		5.57 ± 30	1.2	5.53 → 0
5.41 ± 30	1	(5.41 ± 30)	0.8	5.37 → 0
5.27 ± 30	5.5	5.30 ± 30	3	5.82 → 0.52
4.92 ± 30	3	4.90 ± 20	2	4.90 → 0
4.68 ± 30	17	4.660 ± 15	10	C → 3.26[e]
4.49 ± 30	3	4.44 ± 30	1.3	C → 3.45
4.38 ± 30	8	4.34 ± 20	4	4.41 → 0.08
4.20 ± 30	5	4.16 ± 30	2	5.37 → 1.15
3.92 ± 30	16	3.900 ± 15	14	C → 4.04
3.55 ± 30	16	3.510 ± 15	8	4.04 → 0.52; C → 4.41
3.28 ± 40	8	3.27 ± 20	3.8	3.26 → 0[e]
3.04 ± 40	5	3.05 ± 20	2.7	C → 4.90
E_γ[d] (MeV ± keV)	I_γ[d, g]	E_γ[e] (MeV ± keV)		
		2.93 ± 20	2.2	3.45 → 0.52
		2.87 ± 20	3.4	4.04 → 1.15
		2.60 ± 20	3.6	C → 5.37
		2.46 ± 20	2.7	C → 5.53
2.19 ± 30	41			(2.18 → 0)[e]; 2.22 → 0.08[e]
		2.10 ± 30	13	C → 5.82; 3.26 → 1.15
		1.95 ± 20	4.5	
		1.72 ± 20	5	
		1.60 ± 20	3	C → 6.34
1.13 ± 30	14	1.07 ± 20	1.07 ± 20	20	1.15 → 0.08[e]; (3.26 → 2.18)[e]
			(0.93 ± 30)	8	
		0.64 ± 20			1.15 → 0.52[e]
0.51 ± 20	28		0.51 ± 20		0.52 → 0[e]
			0.43 ± 20	70	
		0.08 ± 10			0.08 → 0[e]

[a] Ki 52; magnetic pair spectrometer.
[b] Ki 52, as corrected in Ba 58c.
[c] Gr 58c; magnetic Compton spectrometer.
[d] Br 56e; two-crystal scintillation spectrometer.
[e] Ma 59c; assignments based on coincidence experiments.
[f] Gr 58c; the capturing state is indicated by C; excitation energies are in MeV. The transitions marked [e] are confirmed by coincidence experiments.
[g] Intensities in gamma quanta per 100 captures.

D. ^{31}P(n, γ)^{32}P $Q_m = 7936.8 \pm 2.5$

The thermal neutron capture cross section is 190 ± 10 mb (Hu 58). Capture gamma rays are listed in table 32.3, with the observed intensities and the levels between which they probably occur (Ki 52, Br 56e, Ba 58c, Gr 58c, Ma 59c). Most of these γ rays can be regarded as transitions between known levels in ^{32}P. The intensities, however, of the γ rays feeding and de-exciting a level, may differ appreciably, indicating that the decay scheme may be more complicated.

The results of coincidence measurements are also indicated in table 32.3.

The mean life of ^{32}P(1) is less than 4×10^{-8} sec. This is consistent with the conclusion that the 0.08 MeV γ ray is mainly M1 (Ma 59c).

Gamma-gamma angular correlation measurements yield $J^\pi = 1^+$ and 2^- for ^{32}P* = 1.15 and 3.26 MeV, respectively (Ma 59c).

For a comparison of the (n, γ) and (d, p) yields, see Gr 58b, Bo 59a.

E. ^{31}P(n, n)^{31}P $E_b = 7936.8 \pm 2.5$

A resonance has been observed at $E_n = 158 \pm 2$ keV, with $J = 1$, $l = 0$, and $\Gamma_n = 1.1 \pm 0.2$ keV (Hu 58; also Pa 55b). Partly resolved resonances for $E_n = 0.1$–0.8 MeV, Ha 53b; for $E_n = 1.9$–5.0 MeV, Ri 51, Cu 60b.

For non-resonance information, see ^{31}P.

F. ^{31}P(n, p)^{31}Si $Q_m = -694.1 \pm 4.6$ $E_b = 7936.8 \pm 2.5$

Several unresolved resonances have been observed in the range $E_n = 1.9$–5.0 MeV (Ri 51, Ni 52, Cu 60).

For cross section and angular distribution, see Hu 58, Al 61, Ha 61.

Measurements of Q value, see ^{31}Si.

G. ^{31}P(d, p)^{32}P $Q_m = 5712.0 \pm 2.4$

Levels in ^{32}P found by magnetic analysis are listed in table 32.4 (Pi 60, Da 57, Va 52b, Ho 61) together with the l_n values (Ho 61, Pa 58, Te 58a, Da 57, Te 56b, Bl 53) and the reduced widths (Ho 61, see also Ma 60d), deduced from the angular distributions of the proton groups. Several of the groups to higher excited states consist of unresolved components (Pi 60). The ground-state Q value has been measured as $Q_0 = 5.709 \pm 0.010$ MeV (Pi 60), 5.704 ± 0.008 MeV (Va 52b).

The relative intensities of the groups to ^{32}P(1) and (0) are expected to be in the ratio $2J+1$, or 1.67, for $J = 2$ and 1, respectively (En 54). The experimentally determined ratios at $E_d = 6.0$ MeV are: 1.61 at 30°, 1.52 at 50°, 1.44 at 70°, and 1.41 at 90° (Pi 60); at $E_d = 1.8$ and 2.0 MeV and 90° the ratios are 1.7 and 1.2, respectively (Va 52b).

For a discussion of the yields and relative reduced widths, see Gr 58b, Bo 59a, Ma 60d.

See ^{32}S, reaction F, for γ rays from ^{31}P+d reactions.

TABLE 32.4

Levels in ^{32}P from the $^{31}P(d, p)^{32}P$ reaction

$^{32}P^*$ [a] (MeV ± keV)	$^{32}P^*$ [b] (MeV ± keV)	l_n	$(2J+1)\theta_n^2$ [d, i] (relative)	$^{32}P^*$ [a] (MeV ± keV)	$^{32}P^*$ [c] (MeV ± keV)	l_n [c, i]
0	0	2+(0)[c, d, e, g, h]	3 (0.15)	5.010±7		
0.077±3	0.077± 2	2[c, d, e, f, g, h]	4.4	5.077±7	5.11±100	
0.516±3	0.515± 5	0[c, d, f]	0.65	5.129±7		
1.149±3	1.154± 7	0[c, d, f]	1.2	5.232±7		
1.322±3	1.316± 8	3[f]		5.346±7	5.37± 70	1
	1.51 ± 20[d]			5.394±7		
1.755±4	1.750± 9			5.510±8	5.53± 70	1
2.177±4	2.177± 9	0+2[d]	(0.32) (1.1)	5.550±8		
2.223±4	2.227± 9			5.657±8		
2.657±5	2.650± 8	2[d]	0.30	5.700±8		
2.743±5	2.742± 8	2[d]	0.10	5.724±8		
3.007±5	2.999± 10	2[d]	0.33	5.775±8	5.75±100	
3.148±5	(3.141± 12)	2[d]	0.15	5.813±8		
3.265±5	3.259± 9	1[c, d]	4.6	5.835±8		
3.324±5	3.318± 9	2[d]	2.0	5.858±8	5.82± 70	1
3.447±5	3.45 ±100[c]	2[d] (3)[c]	3.7	5.964±8		
3.798±6				5.989±8		
3.890±6				6.024±8		
3.994±6				6.062±8		
4.010±6				6.096±8	6.09± 70	1
4.040±6	4.032± 9	1[c, d]	3.3	6.131±8		
4.158±6				6.160±8		
4.209±6	4.207± 10	0[c, d]	0.50	6.196±8	6.20±100	
4.280±6					6.34±100	1
4.316±6					6.56±100	1 or 2
4.412±6	4.43 ±100[c]	1[c, d]	0.21		6.69±100	
4.560±7					6.85±100	
4.615±7						
4.664±7	4.66 ±100[c]	1[d]	1.6			
4.878±7	4.90 ± 70[c]	1[c, d]	2.0			
4.944±7						

[a] Pi 60, E_d = 6.0 MeV.
[b] Va 52b, E_d = 1.8 and 2.0 MeV.
[c] Da 57, E_d = 8.9 MeV.
[d] Ho 61, E_d = 7.77 MeV (preliminary).
[e] Pa 58, E_d = 7.8 MeV.
[f] Te 56b, E_d = 4.0 MeV.
[g] Bl 53, E_d = 14.3 MeV.
[h] Te 58a, E_d = 4.0 MeV.
[i] For relative reduced widths calculated from the experiments reported in Da 57, see Ma 60d.

H. $^{32}Si(\beta^-)^{32}P$ $\quad Q_m = 219 \pm 15$

See ^{32}Si.

I. $^{32}S(n, p)^{32}P$ $\quad Q_m = -925.8 \pm 2.1$

An ionization chamber measurement yields $Q_0 = -0.93 \pm 0.1$ MeV (Hu 41). At $E_n = 2.56$ MeV, a 77 ± 2 keV γ ray has been observed (Da 56c).

For cross section, see Hu 58, Al 61. See also Eu 58, Co 57d, Co 59c (proton spectra at $E_n = 14$ MeV), Co 60b, Ha 61 (angular distribution at $E_n = 14$ MeV).

J. ^{34}S(d, α)^{32}P $Q_m = 5081.1 \pm 3.7$

With enriched ^{34}S targets, magnetic analysis at $E_d = 1.6$–2.9 MeV yields $Q_0 = 5.04 \pm 0.02$ MeV (Le 56b).

Cross section, An 60b.

K. ^{35}Cl(n, α)^{32}P $Q_m = 939.3 \pm 3.3$

Ionization chamber pulse-height analysis yields $Q_0 = 1.07 \pm 0.15$ MeV (Fo 52), 0.97 ± 0.16 MeV (Ad 53). For cross section, see Ad 53, Pa 53, Le 57b.

L. Not reported:

^{30}Si(t, n)^{32}P	$Q_m = 6740.6 \pm 4.5$
^{30}Si(α, d)^{32}P	$Q_m = -10847.4 \pm 4.5$
^{31}P(t, d)^{32}P	$Q_m = 1679.1 \pm 2.4$
^{31}P(α, ^{3}He)^{32}P	$Q_m = -12604.4 \pm 2.5$
^{32}S(t, ^{3}He)^{32}P	$Q_m = -1690.3 \pm 2.0$
^{33}S(n, d)^{32}P	$Q_m = -7343.6 \pm 3.5$
^{33}S(d, ^{3}He)^{32}P	$Q_m = -4075.2 \pm 3.4$
^{33}S(t, α)^{32}P	$Q_m = 10244.4 \pm 3.5$
^{34}S(n, t)^{32}P	$Q_m = -12506.8 \pm 3.7$
^{34}S(p, ^{3}He)^{32}P	$Q_m = -13271.3 \pm 3.7$

REMARKS

For theoretical discussions regarding doublet levels in ^{32}P, see In 53, Pa 57d, Bi 60a, Ba 61c, Pa 61b.

^{32}S

(Fig. 32.3, p. 175; table 32.5, p. 176)

A. ^{28}Si(α, γ)^{32}S $Q_m = 6945.7 \pm 3.1$

Results obtained from this reaction for $E_\alpha < 3.0$ MeV are given in table 32.6. The J^π values result from γ-ray angular distribution and γ–γ angular correlation measurements. The two highest energy resonances probably correspond to the ^{31}P(p, γ)^{32}S resonances at $E_p = 618$ and 641 keV, respectively. The observed ^{32}S excitation energies are 11 and 12 keV higher than those found from the ^{31}P(p, γ)^{32}S reaction (Sm 61a).

B. ^{29}Si(α, n)^{32}S $Q_m = -1532.0 \pm 3.5$

For resonances, see ^{33}S.

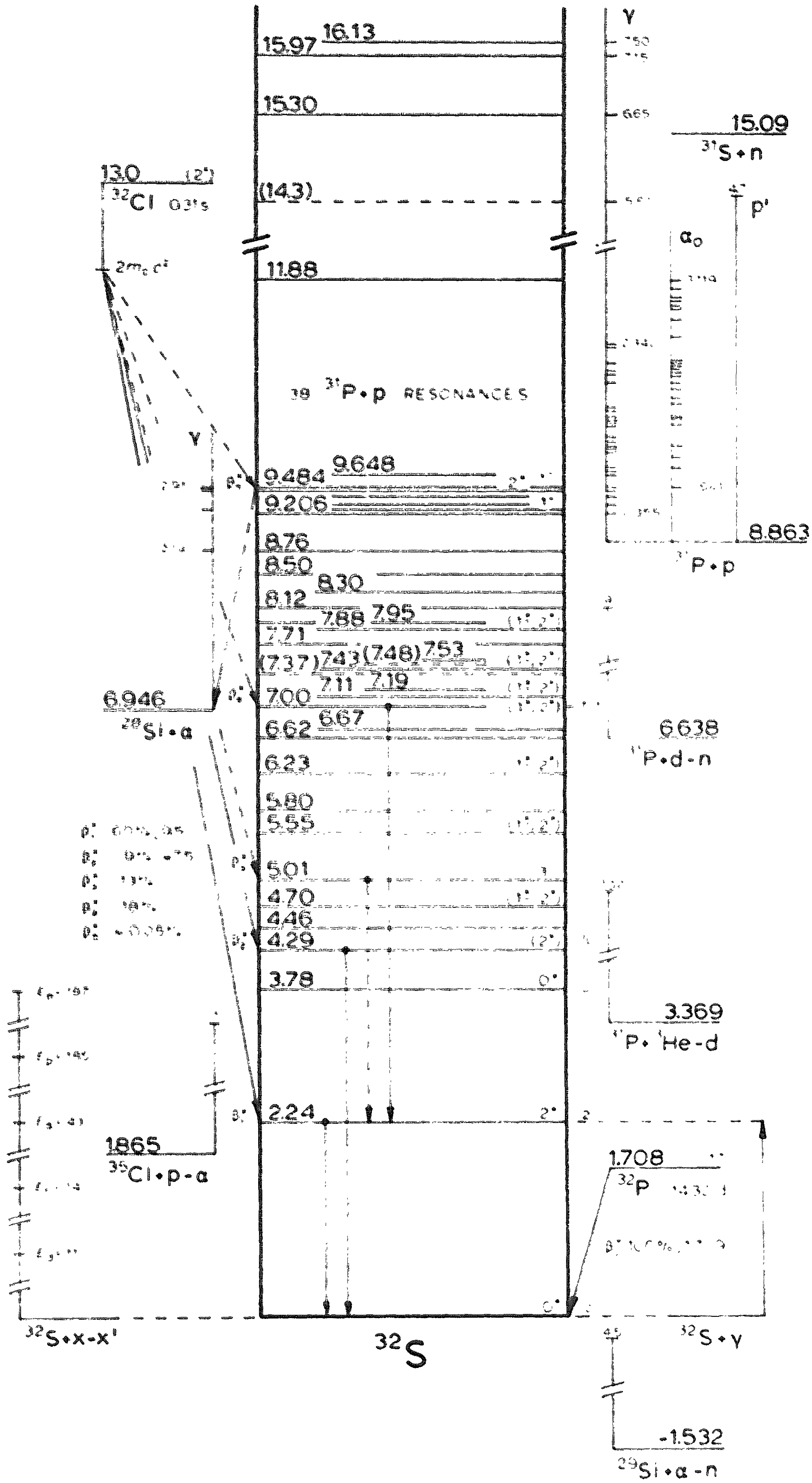

Fig. 32.3. Energy levels of ^{32}S; for γ decay, see also fig. 32.4.

TABLE 32.5

Energy levels of ³²S

E_x MeV ± keV	J^π; T	τ_m	Decay	Reactions
0	0+		stable	many
2.236 ± 8	2+	(2.8 ± 0.3) × 10⁻¹³ sec	γ	many
3.786 ± 8	0+		γ	F, G, J, L, P
4.288 ± 8	2+		γ	C, F, G, L, O, P
4.465 ± 20			γ	C, F, G, L, P
4.699 ± 20	1±, 2+		γ	C, F, G, L, P
5.012 ± 8	3		γ	C, F, G, K, L, O
5.[illegible] ± 8	1±, 2+		γ	C, G
5.[illegible] ± 8	≤ 3			F, G, J, L
6.226 ± 8	1±, 2+		γ	C, F, G
6.[illegible] ± 8			γ	C, G, J
6.[illegible] ± 8				G
7.002 ± 8	1±, 2+; T = 1		γ	G, O
7.[illegible] ± 8	1±, 2+		γ	C, G
7.[illegible] ± 20				F, G
7.[illegible] ± 20				G
7.[illegible] ± 10	1±, 2+		γ	C, G
7.[illegible] ± 20			γ	G
7.[illegible] ± 12				G
7.[illegible] ± 12	1±, 2+		γ	C, G
7.[illegible] ± 12				G
7.[illegible] ± 12		possibly a doublet		G
8.[illegible] ± 17				G
8.[illegible] ± 15				F, G
8.[illegible] ± 17				G
8.[illegible] ± 6			γ	A
9.[illegible] ± 2			γ	C
9.[illegible] ± 6	1−		γ	A
9.[illegible] ± 2			γ	C
9.[illegible] ± 2			γ	C
9.[illegible] ± 2	2+		γ	A, C
9.[illegible] ± 2	[illegible]		γ, α	A, C, E
9.[illegible] – 11.884: 38 levels, see tables 32.7 and 32.8 and reactions				C, D, E
[illegible]			γ	C
[illegible]			γ	C
[illegible]			γ	C
[illegible]			γ	C

TABLE 32.6

Levels of ³²S from the ²⁸Si(α, γ)³²S reaction (Sm 61a)

E_x MeV ± keV	E_α MeV	Decay	Γ_γ/Γ	$(2J+1)\Gamma_\alpha\Gamma_\gamma/\Gamma$ eV	J^π
[illegible]	[illegible]	[illegible]		0.02	
[illegible]	[illegible]	[illegible]	~ 0.1	0.8	1−
[illegible]	[illegible]	[illegible]	1.5	0.4	[illegible]
[illegible]	[illegible]	[illegible]	~ 3	0.7	1−

[a] [illegible] are included in [illegible]

C. $^{31}P(p, \gamma)^{32}S$ $Q_m = 8862.6 \pm 1.6$

Resonances observed in this reaction are given in table 32.7; see also Ta 46, Gr 51, Sm 54, Ke 56a. All spins in table 32.7 follow from γ-ray angular distribution measurements. The parity of the $E_p = 641$, 1892, 2027, and 2120 keV resonances follows from the fact that these states are also resonant for the $^{31}P(p, \alpha_0)^{32}S$ reaction (see table 32.8).

TABLE 32.7

Levels in ^{32}S from the $^{31}P(p, \gamma)^{32}S$ reaction

E_p (keV)	$^{32}S^*$ (MeV)	Γ (keV)	$(2J+1)\,\Gamma_p\Gamma_\gamma/\Gamma$ (eV)	J^π	Main decay
354.8±0.7[a]	9.206				$\gamma_0+\gamma_1$[e]
438.7±0.9[a]	9.288				$\gamma_0+\gamma_1$[e]
540.9±1.1[a]	9.387				
618.2±1.0[b]	9.462		0.003[b]		$\gamma_0+\gamma_1$[b]
641.3±0.8[a]	9.484		0.19[b]	1^-[b]	γ_0[b]
811.8±0.5[c]	9.648	< 0.45[c]	1.8[d]		γ_1[d]
820.0±1.0[a]	9.657		0.36[d]	1[d]	γ_0[d]
892.0±0.5[c]	9.727	< 0.35[c]			
1052.6±0.5[c]	9.882	< 0.30[c]			
1088.0±0.5[c]	9.917	< 0.30[c]			
1116.2±0.5[c]	9.944	< 0.15[c]	1.9[d]	1[d]	γ_0[d]
1147.0±0.5[c]	9.974	< 0.16[c]	2.2[d]		γ_1[d, f]
1246.5±0.6[c]	10.070	1.5±0.3[c]	3.9[d]	2[d]	$(\gamma_0+)\gamma_1$[d, f]
1396.0±0.7[c]	10.215	< 0.30[c]			} [f]
1398.7±0.7[c]	10.218	< 0.35[c]			
1436.3±0.7[c]	10.254	< 0.20[c]			[f]
1468.6±0.7[c]	10.285	< 0.25[c]			[f]
1553.9±0.8[c]	10.368	< 0.40[c]			[f]
1581.5±0.8[c]	10.395	< 0.55[c]			[f]
1892[d]	10.696	24[d]	37[h]	1^-[d]	γ_0[d]
1985[d]	10.786	10[d]	13[d]	1[d]	γ_0[d]
2027[d]	10.826	24[d]	26[d]	1^-[d]	γ_0[d]
2120[d]	10.917	5[d]	4.0[d]	1^-[d]	γ_0[d]
2320[d]	11.111	8[d]	20[d]	1[d]	γ_0[d]
2340[d]	11.131	8[d]	64[d]	1[d]	γ_0[d]

[a] Ku 59a.
[b] Sm 61a.
[c] An 61.
[d] Pa 55a; in the reported yields Γ_γ only includes transitions to $^{32}S(0)$ and (1).
[e] Sc 61c.
[f] See fig. 32.4 for more details on decay.

The γ-ray branching of the resonance levels in the $E_p = 1140$–1590 keV region and of many lower levels (An 61b) are presented in fig. 32.4. See also Sm 54, Ke 56a.

The yields of γ_0 and γ_1 have also been measured in the $E_p = 5.0$–7.7 MeV region. Pronounced resonance structure has been observed, with maxima at

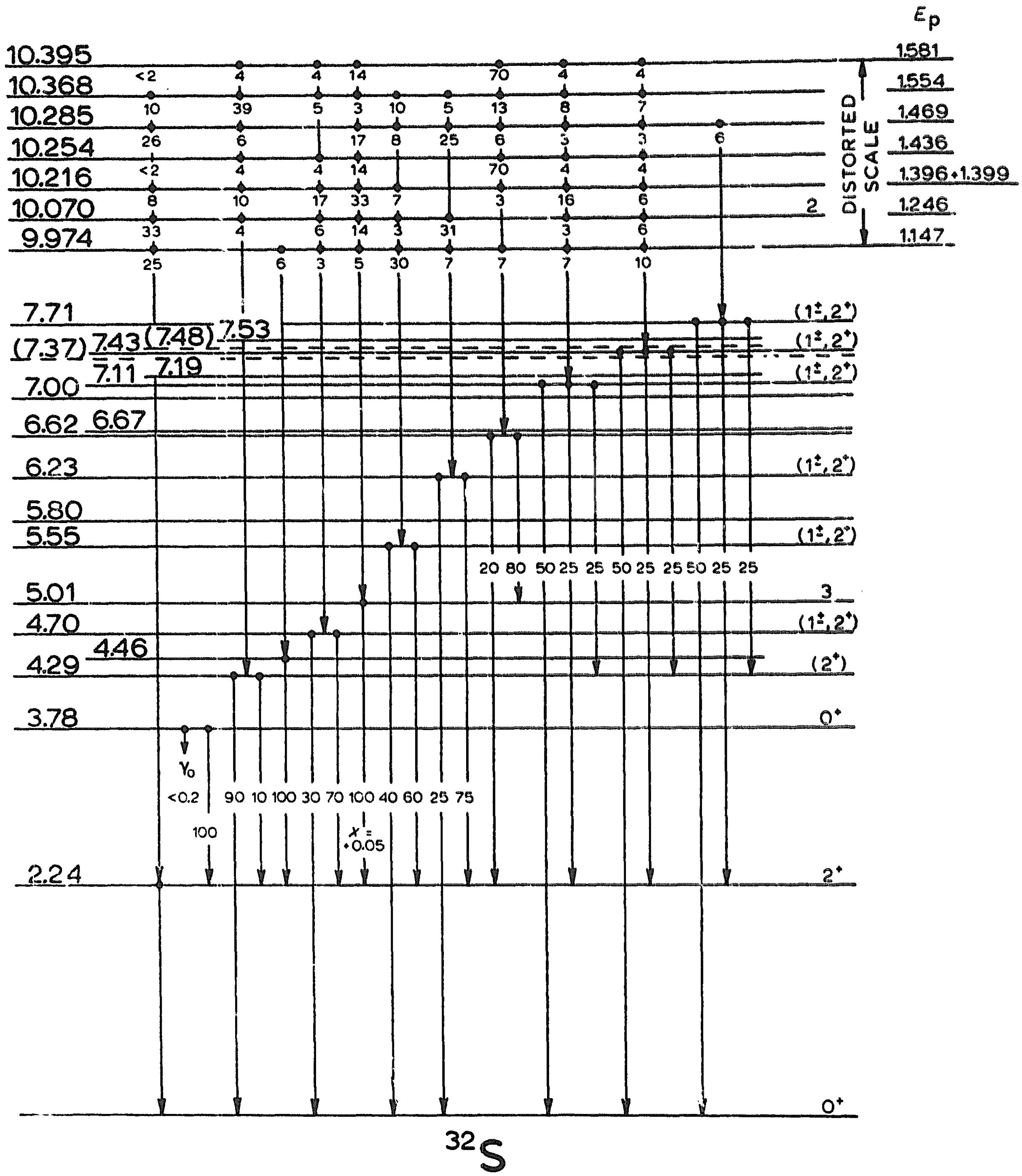

Fig. 32.4. Gamma-ray branchings of ^{32}S levels. The data are from An 61b, except for the γ_0 upper limit at the 3.78 MeV level (Wa 60b), and for the mixing ratio of the 5.01 → 2.24 MeV transition (Br 61d).

E_p = (5.6), 6.65, 7.15, and 7.50 MeV, corresponding to ^{32}S levels at (14.3), 15.30, 15.97, and 16.13 MeV (Ge 59).

D. ^{31}P(p, p'γ)^{31}P $\quad E_b = 8862.6 \pm 1.6$

At 21 resonances (not tabulated) in the E_p = 2.3–3.4 MeV region a

1.26±0.015 MeV γ ray has been observed (Ol 55). A yield curve of the same γ ray has been given in the $E_p = 2.2$–2.95 MeV region; the angular distribution has been measured at the $E_p = 2.70$, 2.78, and 2.87 MeV resonances (Al 61a). Yield curves of proton groups leading to the four lowest ^{31}P excited states have been measured in the 3.57–4.00 MeV and 4.55–4.70 MeV region. Considerable resonance structure is found (Va 56, Va 57a).

For non-resonance data, see ^{31}P.

TABLE 32.8

Levels in ^{32}S from the $^{31}P(p, \alpha_0)^{28}Si$ reaction

E_p (keV)	$^{32}S^*$ (MeV)	Γ (keV)	$(2J+1)\,\Gamma_p\Gamma_{\alpha_0}/\Gamma$ (eV)
641	9.484		4.6
900	9.735		
1024±10	9.854	≲ 3	100
1161±10	9.988	≈ 4	24
1404±10	10.223	≈ 6	130
1474±10	10.290	≲ 2.4	34
1514±10	10.330	7	3100
1640±10	10.452	≈ 4.2	230
1710±10	10.520	≲ 5.5	36
1811±10	10.618	≈ 4.7	100
1892±10	10.696	27	2900
1976±10	10.777	≲ 2.8	68
1990±10	10.791	≲ 3.6	120
2018±10	10.818	≲ 3	92
2029±10	10.828	18	1800
2031±10	10.830	≈ 6	480
2041±10	10.840	≈ 6	80
2109±10	10.906	≲ 4	5.2
2434±10	11.221	17	1600
2644±10	11.424	≈ 5	92
2779±10	11.555	8	480
2805±10	11.580	17	540
2874±10	11.647	≈ 5	88
2922±10	11.694	10	1100
3008±10	11.777	75	5000
3119±10	11.884	20	560

All data are from Cl 60, except those at $E_p = 641$ keV (Ku 60g) and $E_p = 900$ keV (Fr 51). Upper limits of 0.08, 0.15, 1.6, and 1.6 eV are given for the (p, α_0) yields at the 439, 541, 812, and 820 keV $^{31}P(p, \gamma)^{32}S$ resonances (Ku 60g).

E. $^{31}P(p, \alpha)^{28}Si$ $Q_m = 1916.8 \pm 2.8$ $E_b = 8862.6 \pm 1.6$

Resonances observed in the α_0 yield are given in table 32.8. See also Va 56.

In the $E_p = 2.47$–3.36 MeV region a 1.8 MeV γ ray has been observed, presumably following the transition to $^{28}Si(1)$ (Ol 55).

For non-resonance data, see ^{28}Si.

F. ^{31}P(d, n)^{32}S $Q_m = 6637.8 \pm 1.7$

Results from angular distribution measurements are given in table 32.9. For a theoretical discussion of the results, see Hu 55b, Ma 60d. With nuclear emulsions the ground-state Q value has been measured as 6.63 ± 0.08 MeV; transitions have also been observed to states at 6.29, 7.28, and 8.33 MeV, all ± 0.10 MeV (El 55a).

TABLE 32.9

Levels in ^{32}S from the ^{31}P(d, n)^{32}S reaction

^{32}S*[a]	Ca 55; E_d = 9 MeV; Ma 60d		El 55a; E_d = 8 MeV
(MeV)	l_p	$\theta_p{}^2$	l_p
0	0	6×10^{-3}	0
2.24	2	0.3×10^{-3}	2
3.78	}		0
4.29	} 0		
4.46	}		
4.70	} –		
5.01	}		
5.80	2		

[a] The excitation energies are taken from table 32.5.

TABLE 32.10

Levels in ^{32}S (MeV±keV) from the ^{31}P(^{3}He, d)^{32}S reaction (Hi 60i)

2.235[a]	5.553 ± 8	7.114 ± 8	7.707 ± 12
3.780[a]	5.799 ± 8	7.194 ± 10	7.881 ± 12
4.289[a]	6.226 ± 8	(7.371 ± 20)	7.951 ± 12[b]
4.465[a]	6.621 ± 8	7.429 ± 10	8.125 ± 15
4.701[a]	6.671 ± 8	(7.479 ± 20)	8.298 ± 15
5.012 ± 8	7.002 ± 8	7.523 ± 12	8.496 ± 15

[a] The ground-state deuteron group was outside the range of the magnetic spectrograph. Its position was computed by choosing the average excitation energy of the lowest five levels equal to that found from the ^{35}Cl(p, α)^{32}S reaction (En 56c).
[b] Possibly a doublet.

The following γ rays have been observed with a magnetic pair spectrometer at $E_d = 4.6$ MeV: $E_\gamma = 4.43 \pm 0.03$, 4.73 ± 0.03, 4.95 ± 0.03, 5.31 ± 0.03, 5.81 ± 0.03, 6.13 ± 0.03, 6.86 ± 0.03, 7.49 ± 0.07, 8.19 ± 0.03, and 8.56 ± 0.03 MeV. The assignment is uncertain (Be 55).

G. ^{31}P(^{3}He, d)^{32}S $Q_m = 3369.4 \pm 1.6$

Results from magnetic analysis at several angles and at $E(^3\text{He}) = 10.19$ MeV are given in table 32.10 (Hi 60i).

H. ^{32}P(β^-)^{32}S $Q_m = 1708.4 \pm 2.0$

See ^{32}P.

I. $^{32}S(\gamma, \gamma)^{32}S$

By bremsstrahlung resonance fluorescence the mean life of $^{32}S(1)$ has been determined as $\tau_m = 4 \times 10^{-13}$ sec (Bo 61).

J. $^{32}S(e, e')^{32}S$

The differential cross section has been measured for elastic scattering of 187 MeV electrons, and for inelastic scattering to the 2.24, 3.78, 5.80 MeV levels, and to a 6.6 MeV level. For $^{32}S(1)$, $J^{\pi} = (2^+)$ is found and a mean life of $\tau_m = (1.6 \pm 0.2) \times 10^{-13}$ sec (He 56).

K. $^{32}S(n, n')^{32}S$

The only γ ray found from inelastic neutron scattering has $E_\gamma = 2.23 \pm 0.02$ MeV (Da 56c), 2.25 ± 0.03 MeV (Ro 55a). See also An 60d. At $E_n = 14$ MeV a neutron group has been found by time-of-flight spectroscopy leading to a, possibly double, level at 5.2 ± 0.3 MeV (Cl 60a). For elastic and inelastic total and differential cross sections, see Li 55a, El 56, La 57b, Ma 57, Ma 59b, St 59c, Cl 60a, Bo 61b, La 61. Elastic scattering of polarized neutrons, Co 60.

For resonances, see ^{33}S.

L. $^{32}S(p, p')^{32}S$

By magnetic analysis, at $E_p = 8$ MeV, levels in ^{32}S have been observed at 2.25, 3.81, 4.32, 4.50, 474, 5.04, and 5.83 MeV, all ± 0.02 MeV (Ar 52; see also Od 60). At $E_p = 185$ MeV a transition is seen to $E_x = 4.7 \pm 0.2$ MeV (Ty 58).

The γ decay from the 3.78 MeV level proceeds to $^{32}S(1)$ (intensity of $E_\gamma = 3.78$ MeV $< 0.2\%$) (Wa 60b). From γ-γ angular correlation measurements $J = 0$ is found for this level (Wa 60b, Go 60c, Br 60e, Br 61d). With the same technique $J^{\pi} = (2^+)$ is obtained for the 4.29 MeV level, decaying to $^{32}S(0)$ and (1), and $J = 3$ for the 5.01 MeV level, decaying only to $^{32}S(1)$. The quadrupole/dipole amplitude ratio of the 5.01 $\rightarrow$ 2.24 MeV $3 \rightarrow 2^+$ transition amounts to $x = +0.05 \pm 0.04$ (Go 60c, Br 60e, Br 61d).

For elastic and inelastic differential cross section, see Old 59, Od 60. For a p′–γ angular correlation measurement, Ha 60. For a polarization measurement of elastically scattered protons, Ro 61c. For optical model calculations on elastic scattering, Me 57a.

Resonances, see ^{33}Cl.

M. $^{32}S(d, d)^{32}S$

Elastic differential cross section, Ta 60e, Ba 61d.

N. $^{32}S(\alpha, \alpha')^{32}S$

For elastic and inelastic differential cross sections, see Fa 57, Co 59. See also Bl 59a.

O. ^{32}Cl(β^+)^{32}S $Q_m = 13000 \pm 300$

See ^{32}Cl.

P. ^{35}Cl(p, α)^{32}S $Q_m = 1865.1 \pm 2.6$

By magnetic analysis the Q value has been measured as 1.860 ± 0.005 MeV (Va 57d), 1.863 ± 0.008 MeV (En 56c), 1.865 ± 0.015 MeV (Cl 60).

Levels in ^{32}S are observed at 2.237, 3.780, 4.287 MeV, all ± 0.008 MeV, 4.465 ± 0.010, and 4.698 ± 0.010 MeV (En 56c).

For resonances, see ^{36}Ar.

Q. Not reported:

^{30}Si(^{3}He, n)^{32}S	$Q_m = 8430.9 \pm 4.1$
^{31}P(α, t)^{32}S	$Q_m = -10950.1 \pm 1.7$
^{33}S(γ, n)^{32}S	$Q_m = -8642.5 \pm 2.8$
^{33}S(p, d)^{32}S	$Q_m = -6417.8 \pm 2.8$
^{33}S(^{3}He, α)^{32}S	$Q_m = 11934.6 \pm 2.8$
^{34}S(p, t)^{32}S	$Q_m = -11581.0 \pm 3.1$

^{32}Cl

(Not illustrated; see fig. 32.3, p. 175; table 32.11, p. 182)

A. ^{32}Cl(β^+)^{32}S $Q_m = 13000 \pm 300$

The half-life has been measured as 0.306 ± 0.004 sec (Gl 55), 0.32 ± 0.01 sec (Be 54a), 0.28 sec (Ty 54).

The maximum β^+ energy is 9.5 ± 0.4 MeV, indicating a β^+ transition to ^{32}S(1). This branch has an intensity of (48 ± 15)%. A weaker branch with ≈ 7.5 MeV end point has also been observed. In one per several thousand disintegrations the β^+ decay proceeds to an α-unstable level in ^{32}S; $E_\alpha = 2$–3 MeV (Gl 55).

TABLE 32.11

Energy levels of ^{32}Cl

E_x (MeV)	J^π	$\tau_{\frac{1}{2}}$	Decay	Reactions
0	(2)$^+$	0.308 ± 0.04 sec	β^+	A, B
1.0				B
1.4				B
2.0				B

Energies, intensities, and probable assignments of γ rays observed in the decay of ^{32}Cl are listed in table 32.12; see fig. 32.3. From the γ ray intensities, branchings of 60, 9, 13, and 18% are computed for β^+ transitions to ^{32}S* = 2.24, 4.29, 5.01, and 7.00 MeV, yielding log ft = 4.6, 5.0, 4.6, and 3.8, respectively.

TABLE 32.12

Gamma-ray energies (in MeV) and intensities from $^{32}Cl(\beta^+)^{32}S$

Gl 55		Br 54a	Assignment[a]
2.21 ± 0.03	70%	2.25 ± 0.04	$2.24 \to 0$
2.77 or 3.79 ± 0.08	10%	(3.79 ± 0.08)	$(5.01 \to 2.24)$
4.27 ± 0.08	7%	4.33 ± 0.09	$4.29 \to 0$
4.77 ± 0.04	14%	4.82 ± 0.08	$(7.00 \to 2.24)$

[a] Excitation energies in ^{32}S in MeV.

The super-allowed character of the transition to $^{32}S^* = 7.00$ MeV, expected for the β^+ branch to the $T = 1$ analog of the ^{32}Cl ground state (Bo 55), indicates that this level has $T = 1$; in good agreement with the 7.0 MeV excitation energy estimated in Wi 56a.

B. $^{32}S(p, n)^{32}Cl$ $Q_m = -13780 \pm 300$

Threshold measurements yield 14.3 ± 0.5 MeV (Gl 55) and 14.5 ± 0.6 MeV (Br 54a).

At $E_p = 17.5$ MeV, neutron groups have been observed to $^{32}Cl^* = 1.0$, 1.4, and 2.0 MeV (Aj 55). For cross section at $E_p = 18$ and 32 MeV, see Ta 58.

C. Not reported:

$^{32}S(^3He, t)^{32}Cl$ $Q_m = -13020 \pm 300$

^{33}P

(Not illustrated)

A. $^{33}P(\beta^-)^{33}S$ $Q_m = 248 \pm 2$

The half-life is 24.6 ± 0.2 days (weighted mean of Sh 51c, Je 52, We 52, Ni 54, Ru 58, Fo 60b; see also An 60b). The β^- end point is 248 ± 2 keV (average of Sh 51c, Je 52, We 52, El 54, Ni 54, Ru 58). The transition is allowed ($\log ft = 5.0$), but l-forbidden. Gamma rays have not been found (We 52, also La 54).

B. $^{33}S(n, p)^{33}P$ $Q_m = 534 \pm 2$

The thermal neutron cross section is 15 ± 10 mb (Hu 58). See also Je 52, Ni 54.

C. $^{34}S(\gamma, p)^{33}P$ $Q_m = -10886 \pm 5$

Production of ^{33}P, Sh 51c, Je 52.

D. $^{37}Cl(\gamma, \alpha)^{33}P$ $Q_m = -7856 \pm 4$

Cross section measurement, Er 57. See also Sh 51c, Je 52.

E. Not reported:

$^{30}Si(\alpha, p)^{33}P$ $Q_m = -2969 \pm 5$

$^{31}P(t, p)^{33}P$ $Q_m = 9557 \pm 4$

^{33}S(t, ^{3}He)^{33}P	$Q_m = -\ \ 230 \pm\ 2$
^{34}S(n, d)^{33}P	$Q_m = -8662 \pm\ 5$
^{34}S(d, ^{3}He)^{33}P	$Q_m = -5393 \pm\ 5$
^{34}S(t, α)^{33}P	$Q_m = \ \ 8927 \pm\ 5$
^{35}Cl(n, ^{3}He)^{33}P	$Q_m = -9535 \pm\ 5$
^{36}S(p, α)^{33}P	$Q_m = \ \ 545 \pm 10$

^{33}S

(Fig. 33.1, p. 185; table 33.1, p. 186)

A. ^{29}Si(α, n)^{32}S $Q_m = -1532.9 \pm 3.5$ $E_b = 7110.5 \pm 4.4$

Cross section for $E_\alpha = 2.1$–4.5 MeV shows many partly resolved resonances, Gi 59.

B. ^{32}S(n, γ)^{33}S $Q_m = 8642.5 \pm 2.8$

Cross sections and abundances of sulphur isotopes indicate that probably most of the thermal neutron captures in natural sulphur occur in ^{32}S (Ki 52, Hu 58). The thermal neutron absorption cross section of natural sulphur is 0.52 ± 0.02 b (Hu 58).

Gamma rays from thermal neutron capture in natural sulphur with intensities in photons per 100 captures are listed in table 33.2 (Ki 52, Br 56e, Gr 58e). Remarkable are the strong El transitions to and from the p states in ^{33}S at 3.22 and 5.71 MeV (cf. the large intensity of the proton groups to these levels from the ^{32}S(d, p)^{33}S reaction; En 58).

Measurement of the circular polarization of the strong 5.43 MeV γ ray (C $\rightarrow$ 3.22) reveals its El character; ^{33}S* = 3.22 MeV has $J^\pi = \frac{3}{2}^-$ (Tr 57, Ve 61). Angular correlations between the 5.43 MeV γ ray and the 3.22, 2.38, and 0.84 MeV γ rays yield $J^\pi = \frac{3}{2}^-$ and $\frac{1}{2}^+$ for ^{33}S* = 3.22 and 0.84 MeV, respectively (Ma 59c). Several of the weaker γ rays of table 33.2 might also be explained as transitions to or from known levels in ^{33}S, but their assignment is less certain. Sum-coincidence measurements confirm the cascades through ^{33}S* = 0.84, (1.97), 3.22, (4.05), and 7.42 MeV. In addition to they γ rays listed in table 33.2, a 1.21 MeV γ ray has been observed. A probable 1.64–7.02 MeV cascade through ^{33}S* = 7.02 MeV is also indicated (Bu 59b).

See Bo 59a for a discussion of the (n, γ) and (d, p) reduced widths. Cross section at higher E_n, Hu 58, Be 58e.

C. ^{32}S(n, n)^{32}S $E_b = 8642.5 \pm 2.8$

For cross section, see Hu 58, Ri 60, Cu 60b.

Fifteen resolved resonances have been observed below $E_n = 1.1$ MeV. The characteristics of the nine lowest-energy resonances are given in table 33.3 (Hu 58). The angular distribution of elastically scattered neutrons has been

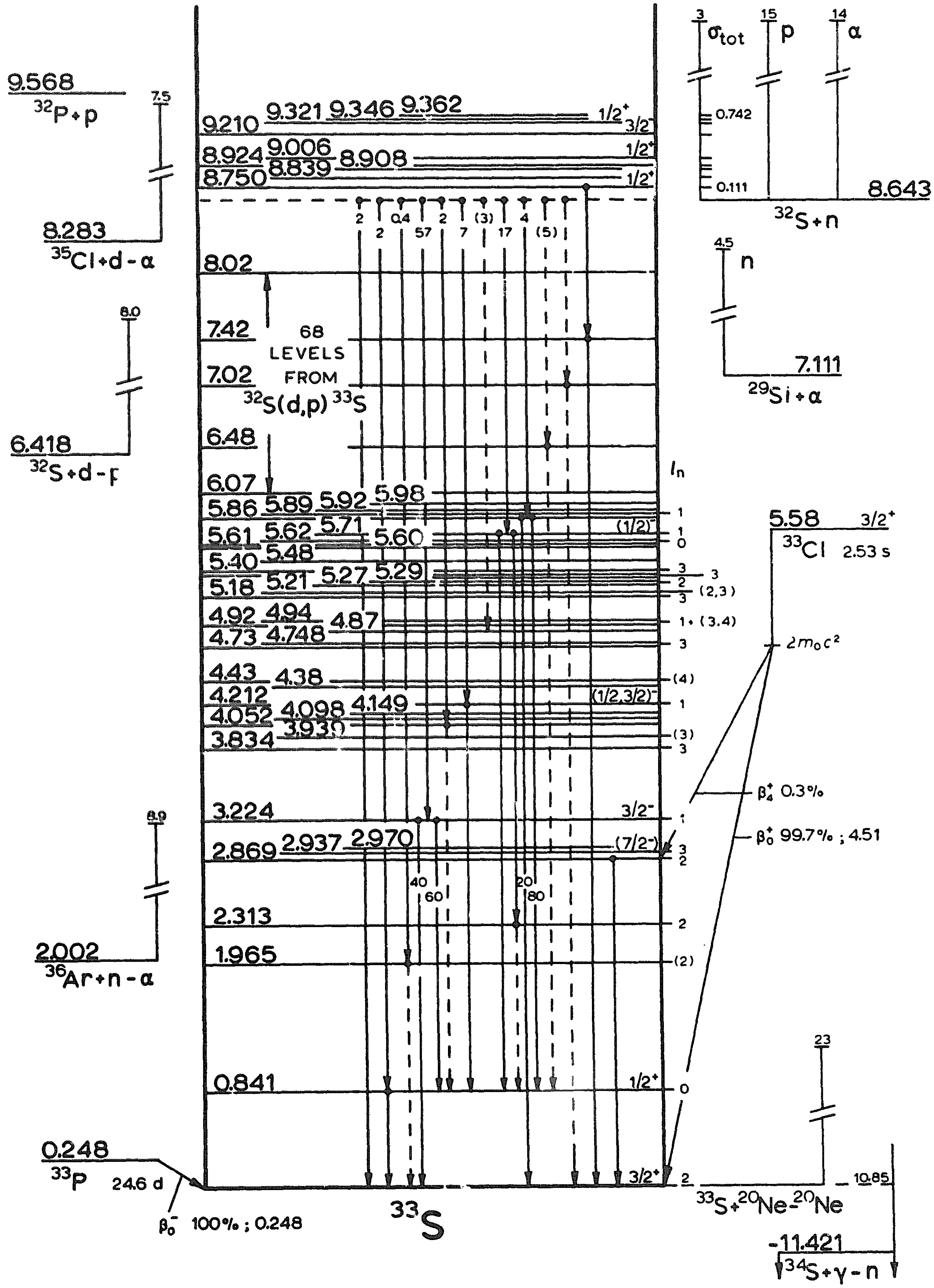

Fig. 33 1. Energy levels of ^{33}S.

TABLE 33.1
Energy levels of ^{33}S

E_x (MeV ± keV)	J^π	Γ (keV)	Decay	Reactions
0	$\frac{3}{2}^+$		stable	many
0.841 ± 4	$\frac{1}{2}^+$		γ	B, E, G, J, K
1.965 ± 5			γ	B, E, J, K
2.313 ± 5	$(\frac{3}{2}, \frac{5}{2})^+$		(γ)	B, E, J, K
2.869 ± 5	$(\frac{3}{2}, \frac{5}{2})^+$		γ	E, G, H, J, K
2.937 ± 5	$(\frac{7}{2})^-$			E, J, K
2.970 ± 5				E, J, K
3.224 ± 5	$\frac{3}{2}^-$		γ	B, E, J
3.834 ± 5	$(\frac{5}{2}, \frac{7}{2})^-$			E, J
3.939 ± 5				E, J
4.052 ± 5			(γ)	B, E, J
4.098 ± 5				E, J
4.149 ± 5				E, J
4.212 ± 5	$(\frac{1}{2}, \frac{3}{2})^-$		γ	B, E, J
4.377 ± 6				E
4.425 ± 6				E
4.732 ± 6				E
4.748 ± 6				E, J
4.869 ± 6				B, E
4.919 ± 6				E
4.941 ± 6				E
5.177 ± 6	$(\frac{5}{2}, \frac{7}{2})^-$			E
5.210 ± 6				E
5.272 ± 6				E
5.287 ± 6				E
5.340 ± 6				E
5.351 ± 6				E
5.399 ± 6	$(\frac{5}{2}, \frac{7}{2})^-$			E
5.479 ± 6				E
5.597 ± 6				E
5.613 ± 6				E
5.622 ± 6				E
5.711 ± 6	$(\frac{1}{2})^-$		γ	B, E
5.864 ± 6			γ	B, E
5.888 ± 6	$(\frac{1}{2}, \frac{3}{2})^-$			E
5.915–8.015; 70 levels, see table 33.4 and reaction				E (and B)
8.750 ± 3	$\frac{1}{2}^+$	18 ± 3	n	C
8.839 ± 3		< 2	n	C
8.908 ± 3		< 3	n	C
8.924 ± 3		< 3	n	C
9.006 ± 4	$\frac{1}{2}^+$	12 ± 2	n	C
9.210 ± 4		1.4 ± 0.5	n	C
9.321 ± 5	$\frac{1}{2}^+$	14 ± 3	n	C
9.346			n	C
9.362			n	C

measured at the $E_n = 585$ keV resonance (La 61). For many unresolved resonances with neutron energies up to 5 MeV, see Hu 58, Cu 60b.

For non-resonance data, see ^{32}S.

TABLE 33.2

Gamma rays from thermal-neutron capture in sulphur

Gr 55a, Gr 58c[a]		Ki 52, Ba 58c[b]		Probable transition in ^{33}S[d]
E_γ (MeV ± keV)	I_γ[c]	E_γ (MeV ± keV)	I_γ[c]	
8.63 ± 40	1.8	8.64 ± 20	1.2	C → 0
7.80 ± 40	2.6	7.78 ± 30	1.6	C → 0.84
7.42 ± 30	0.6	7.42 ± 30	0.3	7.42 → 0
7.20 ± 50	0.5	7.19 ± 30	0.25	
6.62 ± 50	0.5	6.64 ± 30	0.25	C → 1.97
5.88 ± 50	0.4	5.97 ± 60	0.8	5.86 → 0
5.44 ± 20	48	5.43 ± 20	60	C → 3.22; (6.48 → 0.84)
5.07 ± 30	3.5	5.03 ± 60	2.7	5.86 → 0.84
4.87 ± 20	12	4.84 ± 60	11	5.71 → 0.84
4.58 ± 30	1.2	4.60 ± 60	2.7	C → 4.05
4.40 ± 20	6	4.38 ± 30	7	C → 4.21
3.66 ± 50	2	3.69 ± 50	4	(C → 4.87)
3.41 ± 30	7.1	3.36 ± 50	7	4.21 → 0.84; 5.71 → 2.31
3.27 ± 30	19	3.21 ± 30	20	3.22 → 0; (4.05 → 0.84)
3.10 ± 30	2			
2.97 ± 30	13	2.94 ± 50	20	C → 5.71
2.82 ± 30	4	Br 56e		C → 5.86
2.70 ± 50	2			
2.55 ± 30	4.4			
2.41 ± 30	30	2.34 ± 30	37	3.22 → 0.84
2.29 ± 30	5			(C → 6.48)
2.00 ± 20	3			(1.96 → 0)
		1.52 ± 50	1	(2.31 → 0.84)
0.84 ± 10	47	0.84 ± 20	56	0.84 → 0

[a] Magnetic Compton spectrometer.
[b] Magnetic pair spectrometer.
[c] Intensities in photons per 100 captures in natural sulphur.
[d] The capturing state is denoted by C; all transitions are assumed to result from $^{32}S(n, \gamma)^{33}S$.

TABLE 33.3

Resonances in the sulphur total neutron cross section (Hu 58)

E_n (keV)	$^{33}S^*$ (MeV)	J^π	l_n	Γ_n (keV)
111 ± 2	8.750	$\frac{1}{2}^+$	0	18 ± 3
203 ± 2	8.839		⩾ 1	< 2
274 ± 2	8.908		⩾ 1	< 3
290 ± 2	8.924		⩾ 1	< 3
375 ± 3	9.006	$\frac{1}{2}^+$	0	12 ± 2
585 ± 3	9.210	$\frac{3}{2}^{-}$[a]	1[a]	1.4 ± 0.5
700 ± 4	9.321	$\frac{1}{2}^+$	0	14 ± 3
725	9.346			
742	9.362			

[a] Also $J \geq \frac{5}{2}$, $l_n \geqslant 2$ (La 56a).

D. (a) $^{32}S(n, p)^{32}P$ $Q_m = -925.8 \pm 2.1$ $E_b = 8642.5 \pm 2.8$
(b) $^{32}S(n, \alpha)^{29}Si$ $Q_m = 1532.0 \pm 3.5$ $E_b = 8642.5 \pm 2.8$

Unresolved resonances, Hu 58.

For Q-value measurements, cross section, and particle groups, see ^{32}P and ^{29}Si, respectively.

E. $^{32}S(d, p)^{33}S$ $Q_m = 6417.8 \pm 2.8$

Magnetic analysis yields $Q_0 = 6.422 \pm 0.011$ MeV (St 61), 6.408 ± 0.020 MeV (Le 56b), 6.413 ± 0.006 MeV (En 58), 6.420 ± 0.005 MeV (Ma 60e).

High-resolution magnetic analysis, at $E_d = 6.0$ and 6.5 MeV and at several angles, yields the 104 levels listed in table 33.4 (En 58), together with l_n values from angular distribution measurements (Ja 61b, Ho 53a, Ho 53d, Te 57, Te 58a) and the relative reduced widths (Ja 61b, Ma 60d). The excitation energies of the seven lowest levels, reported in Ja 61a, $^{33}S^* = 0.846 \pm 0.005$, 1.986 ± 0.006, 2.328 ± 0.009, 2.887 ± 0.009, 2.957 ± 0.012, 2.995 ± 0.012, and 3.238 ± 0.012 MeV, are 15–20 keV higher than those reported in En 58 and Pa 55c. See also Kr 56a.

The high intensity of the proton groups leading to the 2.937, 3.224, and 5.711 MeV levels, together with the stripping distributions of these groups, and the intensities of the γ rays to the last two of these levels in the $^{32}S(n, \gamma)^{33}S$ reaction, leads to the identification of these levels with the expected $1f_{\frac{7}{2}}$, $2p_{\frac{3}{2}}$, and $2p_{\frac{1}{2}}$ single-particle states, respectively. Other strong groups lead to the levels at 4.212, 5.888, 6.427, 6.676, and 6.689 MeV (En 58). For a discussion of the (n, γ) and (d, p) reduced widths, see Bo 59a. For γ rays observed from this reaction, see Ch 58a.

F. $^{33}P(\beta^-)^{33}S$ $Q_m = 248 \pm 2$

See ^{33}P.

G. $^{33}S(^{20}Ne, ^{20}Ne)^{33}S$

From Coulomb excitation at $E(^{20}Ne) = 23$ MeV, the E2 partial mean life of $^{33}S(1)$ has been found as 5.2×10^{-11} sec (An 61e).

H. $^{33}Cl(\beta^+)^{33}S$ $Q_m = 5575 \pm 12$

See ^{33}Cl.

$^{34}S(\gamma, n)^{33}S$ $Q_m = -11420.8 \pm 4.0$

Threshold measurement yields 10.85 ± 0.20 MeV (Sh 51a). For cross section, see Mo 53a.

J. $^{35}Cl(d, \alpha)^{33}S$ $Q_m = 8282.9 \pm 3.6$

Magnetic analysis of the α-particle groups from bombardment of targets containing natural Cl with deuterons of several energies between 3.0 and 7.5 MeV

TABLE 33.4

Levels in ^{33}S from the $^{32}S(d, p)^{33}S$ reaction

E_x[a] (MeV)	l_n[b]	$(2J+1)\theta_n^2$[b] (relative	E_x[a] (MeV)	E_x[a] (MeV)
0	2[c, d, g]	4.0[f]	5.915	7.330
0.839[e]	0[e, d, g]	1.1[f]	5.982	(7.335)
1.965	(2)	(0.4)	6.067	7.353
2.314	2	0.8	(6.079)	7.359
2.869	2	1.2	6.101	7.369
2.936	3[c]	9.1[f]	6.131	7.401
2.971	w		6.234	7.413
3.222	1[c]	8.1[f]	6.261	7.452
3.832	3	0.7	6.310	7.460
3.935	w (3)	(0.3	6.326	7.475
4.049	w		6.360	7.482
4.095	w		6.372	7.487
4.145	w		6.416	7.503
4.211	1[c]	0.9[f]	6.427	(7.560)
4.377	w		6.487	(7.579)
4.425	(4)	(1.5)	6.513	(7.589)
4.732	} 3	1.5	6.526	(7.595)
4.747			6.559	(7.601)
4.869	w		6.616	7.615
4.919	1[c] and	0.2[f]	6.676	7.629
4.941	3 or 4	0.8 or 1.1	6.689	7.658
5.177	3	0.6	6.710	7.693
5.210	3 or 2	0.5 or 0.2	6.720	7.711
5.272	} 2	0.4	6.788	7.749
5.287			6.892	7.766
5.340	} 3	0.6	6.903	7.779
5.351			6.965	7.797
5.399	3	0.6	6.999	7.828
5.479	w		7.017	7.840
5.597	w		7.037	7.862
5.613	} 0	0.3	7.133	7.892
5.622			7.164	7.906
5.711	1[c]	3.5[f]	7.183	7.983
5.864			7.190	7.991
5.888	1	1.2	7.254	8.015
all ±0.006			all ±0.006	all ±0.006

[a] En 58; E_d = 6.0 and 6.5 MeV.

[b] Ja 61b (preliminary), E_d = 7.77 MeV; w means "weak and/or isotropic": intensity at $\vartheta = 30°$ is $\leqslant 7\%$ of the ground-state transition.

[c] Also Ho 53a, Ho 53d; E_d = 8.0 MeV.

[d] Also Te 57, Te 58a; E_d = 1.3, 1.8, 2.2, 3.8 and 4.0 MeV.

[e] ±0.005 MeV.

[f] For these levels relative reduced widths are also given in Ho 53a, Ho 53d, as discussed in Ma 60d.

[g] Also Bl 53, E_d = 14.3 MeV.

yields ^{33}S levels at 0.844±0.006, 1.966±0.007, 2.312, 2.869, 2.938, 2.969, 3.227, all ±0.008, 3.840, 3.947, 4.060, 4.105, 4.159, 4.224, all ±0.009, and 4.749±0.010 MeV; Q_0 = 8.277±0.010 MeV (Pa 55c). An earlier reported level at 3.365 MeV does not exist. Alpha-particle groups leading to 4.38 and 4.43 MeV levels, observed from the ^{32}S(d, p)^{33}S reaction, may have been present, but were weak or obscured by contaminant groups (En 58).

K. ^{36}Ar(n, α)^{33}S Q_m = 2002.1±4.1

Ionization chamber measurements at E_n = 2.15–4.40 MeV yield a ^{33}S level at 0.9±0.1 MeV; Q_0 = 2.0±0.1 MeV (To 53). At E_n = 1.32–8.94 MeV, the cross sections for transitions to the ^{33}S ground state and six lowest excited states have been measured; Q_0 = 1.96±0.04 MeV (Da 60, Da 61b). See also Gr 46.

Resonances, see ^{37}Ar.

L. Not reported:

^{31}P(t, n)^{33}S	Q_m = 9022.8±3.1
^{31}P(^{3}He, p)^{33}S	Q_m = 9787.2±3.1
^{31}P(α, d)^{33}S	Q_m = − 8565.2±3.1
^{32}S(t, d)^{33}S	Q_m = 2384.9±2.8
^{32}S(α, ^{3}He)^{33}S	Q_m = −11934.6±2.8
^{34}S(p, d)^{33}S	Q_m = − 9196.1±4.0
^{34}S(d, t)^{33}S	Q_m = − 5163.2±4.0
^{34}S(^{3}He, α)^{33}S	Q_m = 9156.3±4.0
^{35}Cl(n, t)^{33}S	Q_m = − 9305.1±3.6
^{35}Cl(p, ^{3}He)^{33}S	Q_m = −10069.6±3.6

REMARKS

For a theoretical discussion of collective model predictions pertaining to ^{33}S, see Bi 60.

^{33}Cl

(Fig. 33.2, p. 191; table 33.5, p. 192)

A. ^{33}Cl($β^+$)^{33}S Q_m = 5575±12

The weighted mean half-life is 2.53±0.04 sec (Mu 58, Ja 60a, Wa 60a; see also Ho 40, Sc 48). Other determinations (Wh 41, Bo 51) are in doubt as possibly a mixture of ^{33}Cl and ^{34}Cl has been studied (St 53).

Possible confusion with short-lived ^{34}Cl also sheds doubt on measurements of the $β^+$ end point (Wh 41, Bo 51, Na 53). A recent measurement yields 4.51±0.05 MeV (Wa 60a). Log *ft* = 3.7.

A γ ray of 2.85 MeV with an intensity of 0.3% per disintegration (log *ft* = 4.3) has been observed (Me 54).

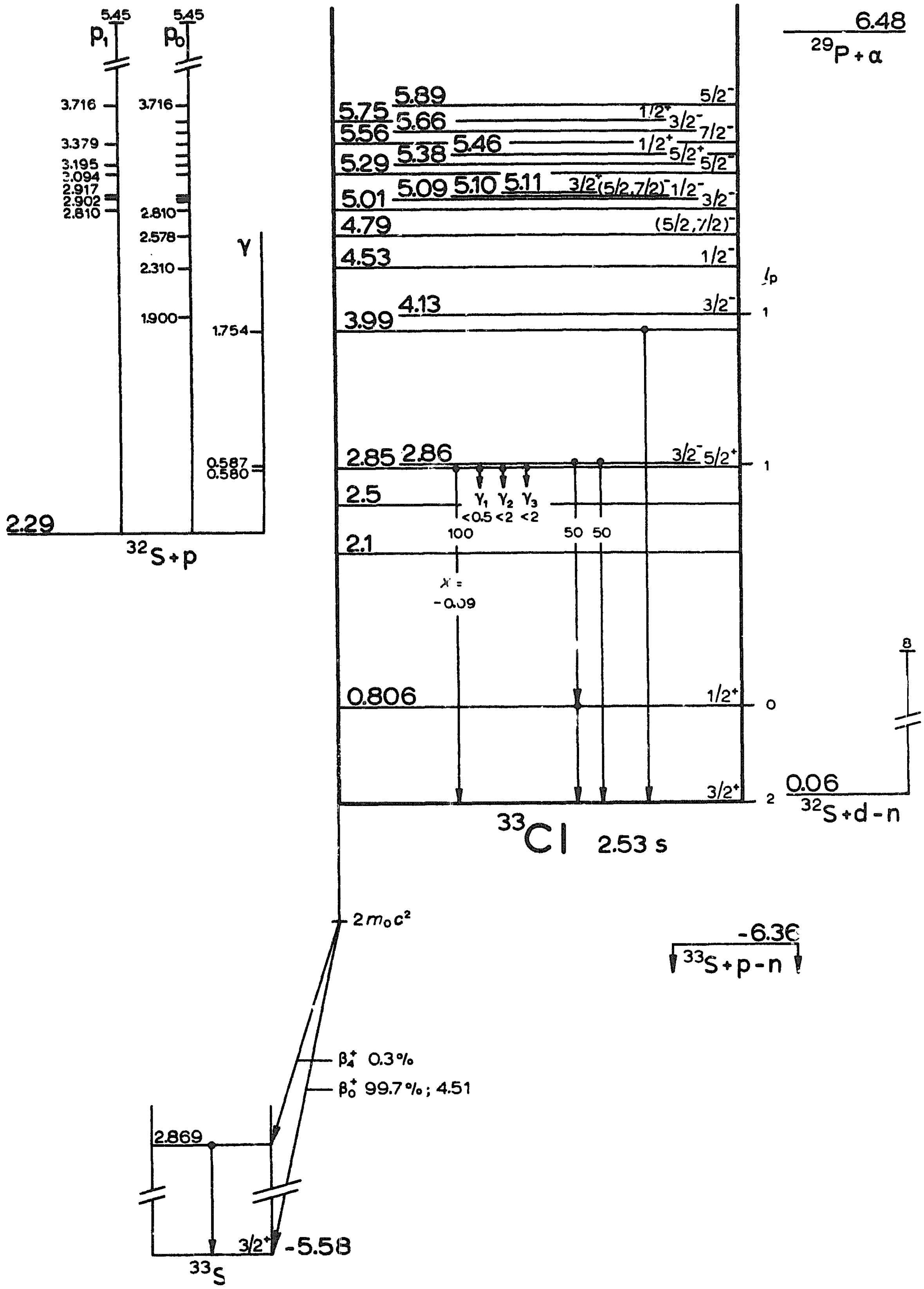

Fig. 33.2. Energy levels of 33Cl.

TABLE 33.3

Energy levels of ^{33}Cl

E_x (MeV ± keV)	J^π	τ_m or Γ	Decay	Reactions
0	[illegible]	2.8[illegible] ± 0.06 sec	β^+	[illegible]
0.806 ± 4	[illegible]		γ	[illegible]
2.1[illegible] ± 30				[illegible]
2.3[illegible] ± 30				[illegible]
2.84[illegible] ± 1[illegible]	[illegible]		γ	[illegible]
2.85[illegible] ± 1[illegible]	[illegible]		γ	[illegible]
3.98[illegible] ± 1[illegible]		1.[illegible] ± 0.4 keV	γ	[illegible]
4.1[illegible] ± 1[illegible]	[illegible]	4.[illegible] ± [illegible] keV	γ, p	[illegible]
4.53[illegible] ± 1[illegible]	[illegible]	35 ± [illegible] keV	p	[illegible]
4.78[illegible] ± 1[illegible]	[illegible]	0.27 ± 0.05 keV	p	[illegible]
5.01[illegible] ± 1[illegible]	[illegible]	4 ± 2 keV	p	[illegible]
5.09 ± 30	[illegible]	300 ± 60 keV	p	[illegible]
5.09[illegible] ± 1[illegible]	[illegible]	~1.5 keV	p	[illegible]
5.11[illegible] ± 1[illegible]	[illegible]	[illegible] ± 1.5 keV	p	[illegible]
5.2[illegible] ± 1[illegible]	[illegible]	0.34 ± 0.06 keV	p	[illegible]
5.38[illegible] ± 1[illegible]	[illegible]	0.54 ± 0.08 keV	p	[illegible]
5.45[illegible] ± 1[illegible]	[illegible]	32 ± 6 keV	p	[illegible]
5.56[illegible] ± 1[illegible]	[illegible]	1.06 ± 0.20 keV	p	[illegible]
5.66[illegible] ± 1[illegible]	[illegible]	100 ± 17 keV	p	[illegible]
5.7[illegible] ± 1[illegible]	[illegible]	40 ± 7 keV	p	[illegible]
5.8[illegible] ± 1[illegible]	[illegible]	1.50 ± 0.30 keV	p	[illegible]

TABLE 33.4

Levels in ^{33}Cl from the $^{32}S(p, \gamma)^{33}Cl$ reaction

E_p (keV)	$^{33}Cl^*$ (MeV)	J^π	$(2J+1)\Gamma_p\Gamma_\gamma/\Gamma$ (meV)	Γ (keV)	Reference
57[illegible] ± 1.[illegible]	2.84[illegible]	[illegible]	2[illegible] ± [illegible]		Va 58a, [illegible]
579.[illegible] ± [illegible]					[illegible]
58[illegible] ± 0.[illegible]		[illegible]			Va 58a
58[illegible] ± 1.[illegible]	2.85[illegible]	[illegible]	100 ± 40		Va 58a, [illegible]
58[illegible] ± [illegible]					[illegible]
59[illegible] ± 0.[illegible]		[illegible]			Va 58a
17[illegible] ± 0.[illegible]	3.9[illegible]		75 ± 25	[illegible] ± 0.[illegible]	[illegible]
1[illegible]	4.1[illegible]		[illegible] ± 40		[illegible]

E. $^{32}S(p, \gamma)^{33}Cl$ Q_m = [illegible] ± [illegible]

Resonant energies, corresponding ^{33}Cl states, spins, parities, and resonance strengths found from measurements of the γ-ray spectra, sum-coincidence and angular distributions are listed in table 33.4. The decay scheme is shown in fig. 33.2. The J^π = [illegible] and [illegible] assignments to $^{33}Cl^*$ = 0 and 0.81 MeV, respectively, are confirmed by these measurements (Va 58a, Va 58b). The strength of an additional resonance occurring in the E_p = 500–8[illegible] keV range is less than [illegible] meV (Va 58a).

At $E_p = 580$ keV, the decay almost entirely ($> 96\%$) proceeds to ^{33}Cl (0). The intensity of a cascade through ^{33}Cl(1) is less than 0.5% (Va 58e); in Va 59a, however, 10% is reported. Polarization measurements (Su 60c) of the ground-state γ ray confirm the $J^\pi = \frac{3}{2}^+$ assignment to the resonance level, and select the small value for the E2/M1 amplitude ratio, $x = -0.09 \pm 0.03$, out of the two possibilities found from angular distribution measurements (Va 58e, Va 59a).

At $E_p = 587$ keV, the γ decay about equally proceeds to ^{33}Cl(0) and (1); the γ-ray energies are $E_\gamma = 2.862 \pm 0.015$, 2.053 ± 0.015, and 0.806 ± 0.004 MeV (Va 58e, Va 59a). Polarization measurements prove the odd parity of this resonance, and confirm the $J^\pi = \frac{1}{2}^+$ assignment to ^{33}Cl(1) (Su 60c).

The reaction energy, computed from the resonance and γ-ray energies amounts to $Q = 2.289 \pm 0.011$ MeV (Va 58e).

The resonance at 1890 keV probably corresponds with the lowest (p, p) resonance listed in table 33.7.

C. ^{32}S(p, p')^{32}S $E_b = 2285 \pm 12$

Resonances observed in the elastic and inelastic (to ^{32}S* = 2.24 MeV) scattering cross sections at five different angles and at proton energies up to 3.8 MeV, are listed in table 33.7, with corresponding excitation energies in ^{33}Cl, spins,

TABLE 33.7

Resonances for proton scattering from ^{32}S (Ol 58)

E_p (MeV ± keV)	^{33}Cl* (MeV)	J^π	Γ (keV)	Γ_{p_0} (keV)	Γ_{p_1} (keV)	$\theta_{p_0}^2 \times 10^3$	$\theta_{p_1}^2 \times 10^3$
1.900 ± 2	4.127	$\frac{3}{2}^-$	8.5 ± 1.5	a		43	
2.310 ± 4	4.525	$\frac{1}{2}^-$	55 ± 5	a		118	
2.578 ± 3	4.785	$(\frac{5}{2}, \frac{7}{2})^-$	0.25 ± 0.05	a		9	
2.810 ± 2	5.010	$\frac{3}{2}^-$	6 ± 2	a	≈ 0.0015	6	≈ 500
2.895 ± 30	5.092	$\frac{1}{2}^-$	360 ± 60	a		336	
2.902 ± 2	5.099	$(\frac{5}{2}^-, \frac{7}{2}^-)$	< 0.5	a	≈ 0.010	< 9	≈ 9
2.917 ± 2	5.114	$\frac{3}{2}^+$	1.5 ± 0.5	a	≈ 0.0018	4	≈ 1.6
3.094 ± 2	5.285	$\frac{5}{2}^-$	0.34 ± 0.06	0.29	0.05	4	101
3.195 ± 2	5.383	$\frac{5}{2}^+$	0.44 ± 0.08	0.43	0.01	0.8	2.3
3.273 ± 4	5.459	$\frac{1}{2}^+$	32 ± 4	a	(< 0.01)	12.8	(< 9.4)
3.379 ± 2	5.562	$\frac{7}{2}^-$	1.00 ± 0.20	0.40	0.60	3.0	106
3.480 ± 10	5.660	$\frac{3}{2}^-$	100 ± 15	a	(< 0.08)	54.7	(< 8)
3.570 ± 5	5.747	$\frac{1}{2}^+$	40 ± 5	a	(< 0.01)	13.1	(< 0.9)
3.716 ± 2	5.888	$\frac{5}{2}^-$	1.50 ± 0.30	0.84	0.66	4.2	19

[a] No measurable difference between Γ_{p_0} and Γ.

parities, partial widths, and reduced widths. No capture γ rays have been found except, probably, at the 1900 keV resonance (see reaction B). The difference in the reported level densities of ^{33}Cl and ^{33}S is discussed in Ol 58. Essentially the same results at the 1.90 and 2.31 MeV resonances are given in Fe 53. For cross sections in the $E_p = 4.95$–5.45 MeV range, see Od 59.

For non-resonance data, see ^{32}S.

D. ^{32}S(d, n)^{33}Cl $Q_m = 60 \pm 12$

With nuclear emulsions, at $E_d = 8$ MeV, neutron groups have been found to ^{33}Cl* $= 0, 0.76 \pm 0.07, 2.84 \pm 0.06$, and 4.22 ± 0.08 MeV. Angular distribution measurements yield $l_p = 2$, 0, 1, and 1, giving $J^\pi = (\frac{3}{2}, \frac{5}{2})^+, \frac{1}{2}^+, (\frac{1}{2}, \frac{3}{2})^-$, and $(\frac{1}{2}, \frac{3}{2})^-$, respectively. Groups to several more closely spaced levels above 4.22 MeV have been found. A doubtful level at 1.89 MeV is reported (Mi 53). The relative reduced widths of the transitions to ^{33}Cl* = 0, 0.76, and 4.12 MeV, are 1, 3.0, and (5.5), respectively (Mi 53, Ma 60d). Time-of-flight measurements, at $E_d = 3.5$, 3.9, and 4.2 MeV, yield levels at 0.88 ± 0.07, 2.11 ± 0.06, 2.53 ± 0.06, and 2.82 ± 0.06 MeV; $Q_0 = 0.10 \pm 0.05$ MeV (Ma 60).

E. ^{33}S(p, n)^{33}Cl $Q_m = -6358 \pm 12$

Observed, Wh 41.

F. Not reported:

^{31}P(^{3}He, n)^{33}Cl	$Q_m = 3430 \pm 12$
^{32}S(^{3}He, d)^{33}Cl	$Q_m = -3208 \pm 12$
^{32}S(α, t)^{33}Cl	$Q_m = -17528 \pm 12$
^{33}S(^{3}He, t)^{33}Cl	$Q_m = -5593 \pm 12$
^{35}Cl(p, t) ^{33}Cl	$Q_m = -15663 \pm 12$
^{36}Ar(p, α)^{33}Cl	$Q_m = -4355 \pm 12$

^{34}P

(Not illustrated; see fig. 34.1, p. 196)

A. ^{34}P(β^-)^{34}S $Q_m = 5100 \pm 200$

The half-life is 12.40 ± 0.12 sec (Bl 46; see also Co 40, Hu 45). The β^- decay predominantly proceeds to ^{34}S(0) and (1) (Bl 46); in addition, a 4.0 MeV γ ray, with a 0.2% intensity, reveals a weak β^- branch to a 4.0 MeV level (Mo 56d). For end points, branching ratios, and log *ft* values, see table 34.1. A discussion of the β^- transition probabilities is given in De 53b.

The allowed character of the transitions to ^{34}S(0) and (1) with $J^\pi = 0^+$ and 2^+, respectively, yields $J^\pi = 1^+$ for ^{34}P(0).

TABLE 34.1

The ^{34}P(β^-)^{34}S decay

Final ^{34}S state (MeV)	E_{β^-} (MeV)	Branching ratio (%)	log *ft*	Reference
0	5.1 ± 0.2	75	5.1	Bl 46
2.13	3.2 ± 0.2	25	4.7	Bl 46
3.30			> 5.6	Mo 56d
4.0		$\geqslant 0.2$	$\leqslant 4.9$	Mo 56d

B. ^{33}P(n, γ)^{34}P $Q_m = 6570 \pm 200$

Perhaps observed, see Ya 51 and Je 52.

C. ^{34}S(n, p)^{34}P $Q_m = -4320 \pm 200$

Cross section at $E_n = 14.5$ MeV, Pa 53.

D. ^{37}Cl(n, α)^{34}P $Q_m = -1290 \pm 200$

Cross section, Pa 53, Le 57b.

E. Not reported:

^{34}S(t, ^{3}He)^{34}P	$Q_m = -5080 \pm 200$
^{36}S(n, t)^{34}P	$Q_m = -12700 \pm 200$
^{36}S(p, ^{3}He)^{34}P	$Q_m = -13460 \pm 200$
^{36}S(d, α)^{34}P	$Q_m = 4890 \pm 200$

^{34}S

(Fig. 34.1, p. 196; table 34.2, p. 197)

A. ^{31}P(α, p)^{34}S $Q_m = 630.9 \pm 3.3$

Scintillation spectrometer measurements of proton and γ-ray energies and coincidences yield levels at ^{34}S* $= 2.13 \pm 0.02$, 3.33 ± 0.05, 4.3 ± 0.1, and 4.8 ± 0.1 MeV; $Q_0 = 0.7 \pm 0.1$ MeV. The 3.30 MeV level decays by γ emission to ^{34}S(1), $(73 \pm 4)\%$, and to ^{34}S(0), $(27 \pm 4)\%$ (St 56b); see, however, ^{34}Cl, reaction A. Differential cross sections for transitions to ^{34}S(0) and (1) at $E_\alpha = 7.0$ and 8.1 MeV (Vo 57a), and to ^{34}S(0) at $E_\alpha = 30.4$ MeV (Hu 59a), are in fair agreement with direct-interaction calculations.

B. ^{33}S(d, p)^{34}S $Q_m = 9196.1 \pm 4.0$

At $E_d = 6.0$ MeV, with enriched targets, proton groups have been observed to ^{34}S levels at 0, 2.123, 3.305, 4.125, (4.26), 4.630, (4.70), 4.886, (5.38), 5.691, (5.85), 6.173, 6.252, 6.348, 6.482, 6.64, 7.110, 7.632, 7.78, 7.914, (8.12), 8.30, and (8.62) MeV; $Q_0 = 9.194$ MeV. Groups have been seen at different angles unless the corresponding excitation energy has been put in brackets (Br 61e). See also Da 49a.

C. ^{34}P(β^-)^{34}S $Q_m = 5100 \pm 200$

See ^{34}P and remarks.

D. ^{34}Cl(β^+)^{34}S $Q_m = 5519 \pm 21$

See ^{34}Cl and remarks.

E. ^{37}Cl(p, α)^{34}S $Q_m = 3030.1 \pm 3.1$

Magnetic analysis yields $Q_0 = 3.023 \pm 0.006$ MeV (Va 57d), 3.026 ± 0.008 MeV

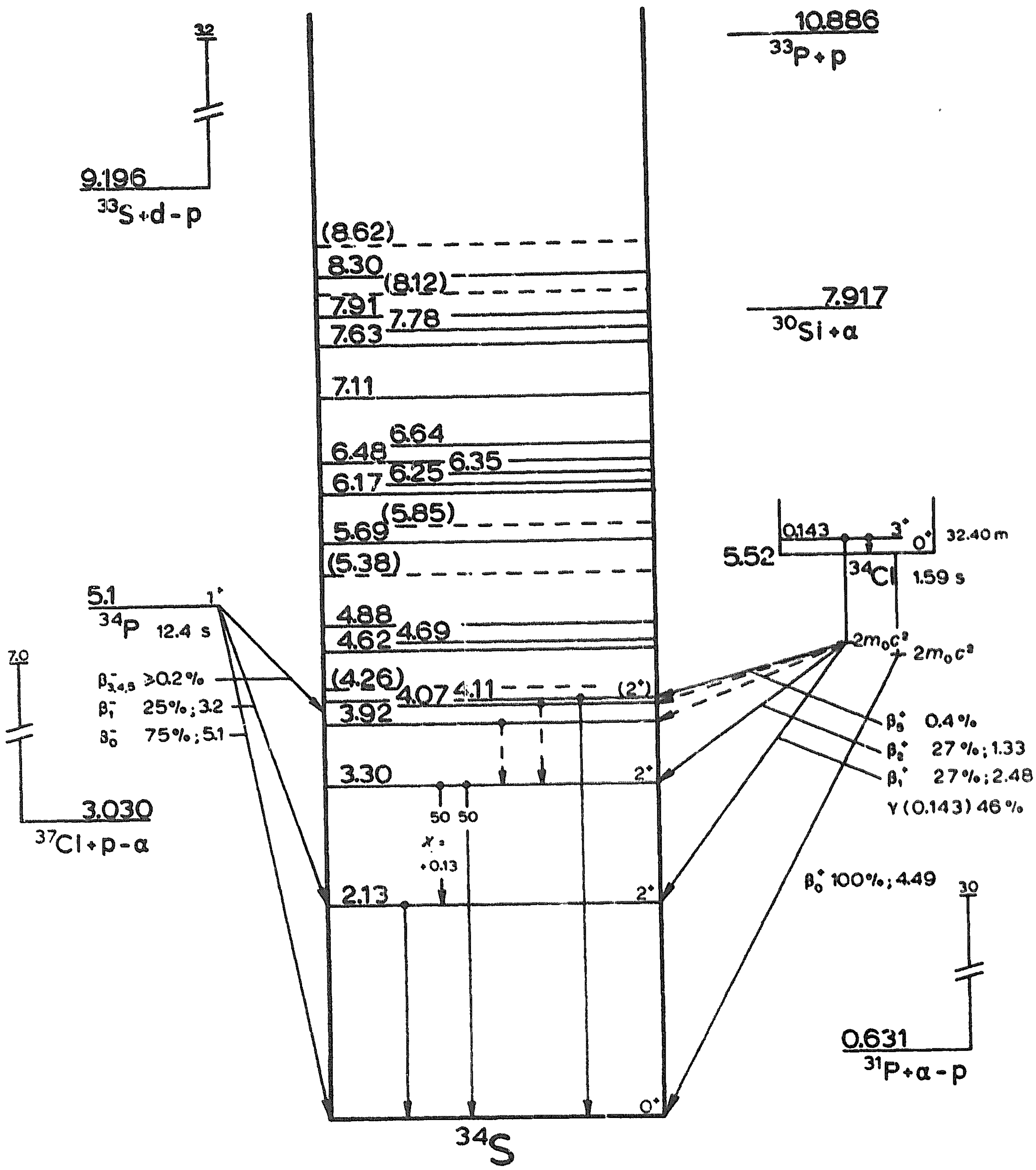

Fig. 34.1. Energy levels of ^{34}S.

(En 56c), and 3.015 ± 0.015 MeV (Cl 60). At E_p = 1.8–4.0 MeV, a level has been found at 2.129 ± 0.014 MeV (Va 56), and at E_p = 7.0 MeV levels at 2.127, 3.302, 3.915, 4.073, 4.114, 4.621, 4.685, and 4.876, all ± 0.008 MeV (En 56c).

For the excitation function of the α_0 group, see ^{38}Ar.

TABLE 34.2

Energy levels of ^{34}S

E_x (MeV ± keV)	J^π	Decay	Reactions
0	0^+	stable	A, B, C, D, E
2.127 ± 7	2^+	γ	A, B, C, D, E
3.302 ± 8	2^+	γ	A, B, D, E
3.915 ± 8		(γ)	C, D, E
4.073 ± 8		(γ)	C, D, E
4.114 ± 8	(2^+)	γ	B, C, D, E
(4.26)			A, B
4.621 ± 8			B, E
4.685 ± 8			B, E
4.876 ± 8			A, B, E
5.38-8.62; 15 levels, see reaction			B

F. Not reported:

^{32}S(t, p)^{34}S	$Q_m = 11581.0 \pm 3.1$
^{33}S(n, γ)^{34}S	$Q_m = 11420.8 \pm 4.0$
^{33}S(t, d)^{34}S	$Q_m = 5163.2 \pm 4.0$
^{33}S(α, ^{3}He)^{34}S	$Q_m = -9156.3 \pm 4.0$
^{35}Cl(n, d)^{34}S	$Q_m = -4141.9 \pm 3.8$
^{35}Cl(d, ^{3}He)^{34}S	$Q_m = -873.4 \pm 3.7$
^{35}Cl(t, α)^{34}S	$Q_m = 13446.1 \pm 3.7$
^{36}S(p, t)^{34}S	$Q_m = -8381 \pm 9$
^{36}Ar(n, ^{3}He)^{34}S	$Q_m = -7154.3 \pm 4.2$

REMARKS

The assignments $J^\pi = 1^+$ to ^{34}P(0) and $J^\pi = 2^+$ to ^{34}S(1) follow from the allowed character of both the ^{34}P β^- decay to ^{34}S(0) and (1), and the ^{34}Cl^m ($J^\pi = 3^+$) β^+ decay to ^{34}S(1).

For a discussion of the $J^\pi = 2^+$ assignment to ^{34}S* = 3.30 and 4.11 MeV, see ^{34}Cl, reaction A.

For a theoretical discussion of the excitation energy of the lowest 2^+ states, see Th 56.

^{34}Cl

(Fig. 34.2, p. 198; table 34.3, p. 199)

A. (a) ^{34}Cl(β^+)^{34}S $\qquad Q_m = 5519 \pm 21$

The weighted mean half-life is 1.588±0.014 sec (St 53b, Kl 54b, Mi 58, Ja 60a). The decay proceeds to ^{34}S(0); end point 4.50±0.03 MeV (Gr 56), 4.45±0.11 MeV (Ru 51), 4.45±0.10 MeV (Hu 54a). The log *ft* value is 3.5, indicating that ^{34}Cl(0) is the $T = 1$ analog of ^{34}S(0) (see also Qu 56). A theoretical

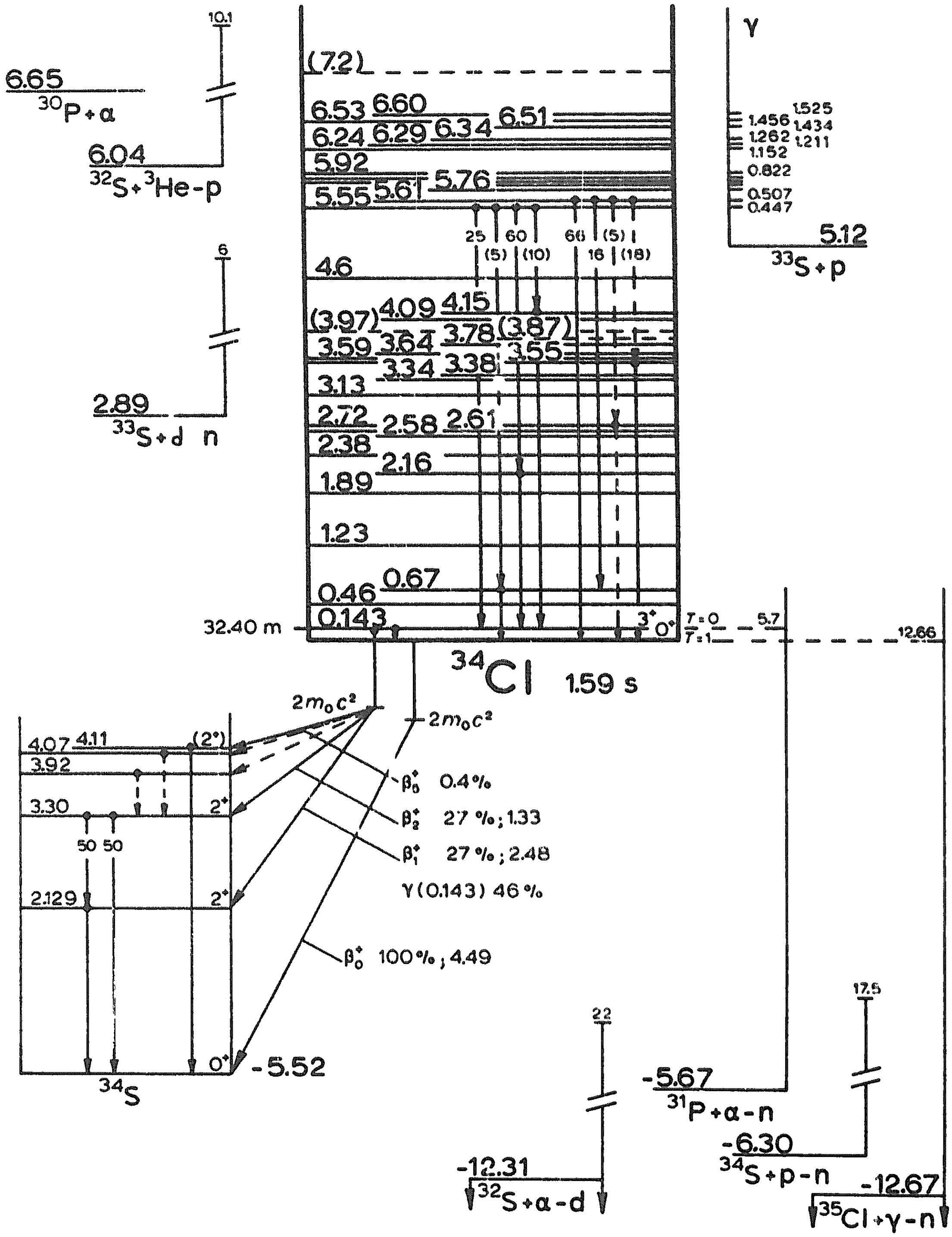

Fig. 34.2. Energy levels of ^{34}Cl.

discussion of corrections to ft-values of $0^+ \to 0^+$ transitions is given in Ma 58e, Du 60.

Longitudinal polarization measurements, De 57a.

(b) ^{34}Cl$^m(\beta^+)^{34}$S $\qquad Q_m = 5662 \pm 21$

The half-life of the 143 keV isomeric state is 32.40 ± 0.04 min (Gr 56; see also

TABLE 34.3

Energy levels of ^{34}Cl

E_x (MeV ± keV)	J^π; T	$\tau_{\frac{1}{2}}$	Decay	Reactions
0	0^+; 1	1.588±0.014 sec	β^+	many
0.143± 2	3^+; 0	32.40 ±0.04 min	β^+, γ	A, B, C, E, H
0.46 ±20				C
0.67 ±10	($1^\pm$, 2^+)		γ	C, E
1.23 ±20				C, G
1.89 ±20				C, G
2.16 ±20			γ	C, E
2.38 ±20				C
2.58 ±20				C
2.61 ±20				C
2.72 ±20			γ	C, E, G
3.13 ±20				C
3.34 ±20				C
3.38 ±20				C
3.55 ±20			γ	C, E
3.59 ±20				C
3.64 ±20				C, G
3.78 ±20				C, G
(3.87 ±20)				C
(3.97 ±20)				C
4.09 ±20				C
4.15 ±20				C, E
4.6				G
5.552 ±21			γ	E
5.611 ±21	($1^\pm$, 2^+)		γ	E, G
5.76–6.60: 11 levels, see reaction				E
(7.2)				G

Hi 52a, Pe 48a, Hu 43, Ri 37). The decay proceeds by γ emission (46%) to ^{34}Cl(0) (Gr 56, St 53, Ru 51), and with about equal intensities by β^+ emission to ^{34}S* = 2.13 MeV ($E_{\beta^+\max} = 2.48\pm0.07$ MeV) and 3.30 MeV ($E_{\beta^+\max} = 1.33 \pm0.10$ MeV); log ft = 6.1 and 4.9, respectively (Gr 56, Ru 51). From the conversion coefficient of the 145±3 keV γ ray, $\alpha = 0.14\pm0.04$, it follows that this transition has M3 character (St 53). Hence the isomeric state has $J^\pi = 3^+$.

Measurement of single γ-ray spectra (see table 34.4) and of coincidences confirms the β^- branches to ^{34}S* = 2.13 and 3.30 MeV, and indicates a weak ($\approx$ 0.4%) β^+ branch to ^{34}S* = 4.11 MeV, with log ft = 5.4. The latter state decays to ^{34}S(0) with $E_\gamma = 4.10\pm0.02$ MeV; it should thus have $J^\pi = 2^+$. The 0.64 and 0.77 MeV γ rays possibly indicate weak β^+ transitions to ^{34}S* = 3.92 and 4.07 MeV, respectively (To 60a; also Mo 56d).

The angular correlation of the 1.17 and 2.13 MeV γ rays indicates that both the 2.13 and 3.30 MeV levels have $J^\pi = 2^+$ (Ha 56d, Fi 57, Sh 58a). The E2/M1 amplitude ratio of the 1.17 MeV γ ray is $x = +0.13$ (Ha 56d), $+0.12$ (Fi 57),

TABLE 34.4

Energies (in MeV) and relative intensities of γ rays in the β^+ decay of ^{34}Cl^m

Ru 51	Ti 51	Mo 56d	To 60a	Transition
0.145 ± 0.003				^{34}Cl(0.14) → ^{34}Cl(0)
			0.64 (weak)	^{34}S(3.92) → ^{34}S(3.30)
			0.77 (weak)	^{34}S(4.07) → ^{34}S(3.30)
	1.16 ± 0.03	1.14	1.17 ± 0.02 (32)	^{34}S(3.30) → ^{34}S(2.13)
2.13 ± 0.12	2.10 ± 0.03	2.10	2.14 ± 0.02 (100)	^{34}S(2.13) → ^{34}S(0)
3.30 ± 0.14	3.22 ± 0.03	3.22	3.32 ± 0.02 (32)	^{34}S(3.30) → ^{34}S(0)
		4.0 (0.2%)	4.10 ± 0.02 (1)	^{34}S(4.11) → ^{34}S(0)

± 0.126 (Sh 58a). Angular correlation polarization experiments confirm the spin assignments (Sh 58a).

B. ^{31}P(α, n)^{34}Cl $\quad Q_m = -5671 \pm 21$

Threshold measurements yield $Q_0 = -5.7 \pm 0.2$ MeV. This corresponds to the threshold for slow neutron production as well as for production of the 1.59 sec ground-state activity (Qu 56).

C. ^{32}S(^{3}He, p)^{34}Cl $\quad Q_m = 6044 \pm 21$

At $E(^3$He$) = 9.82$ and 10.10 MeV, proton groups have been observed to ^{34}Cl* = 0, 0.15, 0.46, 0.67, 1.23, 1.89, 2.16, 2.38, 2.58, 2.61, 2.72, 3.13, 3.31, 3.38, 3.55, 3.59, 3.84, 3.78, (3.87), (3.97), 4.09, and 4.15 MeV, all ± 0.02 MeV (Hi 60f).

D. ^{32}S(α, d)^{34}Cl $\quad Q_m = -12309 \pm 21$

Probably observed, Sh 40.

E. ^{33}S(p, γ)^{34}Cl $\quad Q_m = 5119 \pm 21$

In the range $E_p = 200$–850 keV, resonances have been observed at 446.5 ± 3.5 and 507.1 ± 1.0 keV, with strengths $(2J+1)\,\Gamma_p \Gamma_\gamma / \Gamma = 0.06$ and 0.10 eV, respectively (Va 58d, Ku 59a); and at $E_p = 446$, 507, 662, 682, 730, 778, and 822 keV, all ± 2 keV (Gl 61b); in the range $E_p = 1100$–1550 keV, resonances have been found at 1152, 1211, 1262, 1434, 1456, and 1525 keV (Ga 59).

Most of the γ rays observed at the 447 and 507 keV resonances (Va 58d, Gl 61b) can be assigned to transitions in ^{34}Cl using the excitation energies found from reaction C (see fig. 34.2). A reaction Q value of 5.12 ± 0.03 MeV follows from these measurements (Va 58d).

F. ^{33}S(d, n)^{34}Cl $\quad Q_m = 2893 \pm 21$

Observed, Sa 36.

G. ^{34}S(p, n)^{34}Cl $\quad Q_m = -6302 \pm 21$

At $E_p = 17.5$ MeV, neutron groups have been observed to ^{34}Cl* = 0, 1.1, 1.9, 2.7, 3.7, 4.6, (5.7), and (7.2) MeV, if it is assumed that the highest Q value measured ($Q = -6.1$ MeV), corresponds to $^{34}Cl(0)$ (Aj 55).

H. $^{35}Cl(\gamma, n)^{34}Cl$ $\quad Q_m = -12668 \pm 21$

The Q value for the transition to $^{34}Cl^m$ is -12.35 ± 0.35 MeV (De 55). The ground-state Q value is -12.79 ± 0.07 MeV (Ba 57b), -12.66 ± 0.04 MeV (Sa 61).

Cross section, Fe 59a, Ba 57b, Go 54a, Ed 52, Wa 48.

For "breaks" in the excitation curve, see ^{35}Cl.

I. Not reported:

$^{32}S(t, n)^{34}Cl$	$Q_m = 5279 \pm 21$
$^{33}S(^3He, d)^{34}Cl$	$Q_m = -374 \pm 21$
$^{33}S(\alpha, t)^{34}Cl$	$Q_m = -14693 \pm 21$
$^{34}S(^3He, t)^{34}Cl$	$Q_m = -5537 \pm 21$
$^{35}Cl(p, d)^{34}Cl$	$Q_m = -10443 \pm 21$
$^{35}Cl(d, t)^{34}Cl$	$Q_m = -6411 \pm 21$
$^{35}Cl(^3He, \alpha)^{34}Cl$	$Q_m = 7909 \pm 21$
$^{36}Ar(n, t)^{34}Cl$	$Q_m = -12691 \pm 21$
$^{36}Ar(p, ^3He)^{34}Cl$	$Q_m = -13456 \pm 21$
$^{36}Ar(d, \alpha)^{34}Cl$	$Q_m = 4897 \pm 21$

REMARKS

Positions of the lowest $T = 0$ and $T = 1$ states, St 53a, St 53b, Pe 53, Mo 54, Wi 56a, Va 58d.

^{35}S

(Fig. 35.1, p. 202; table 35.1, p. 202)

A. $^{35}S(\beta^-)^{35}Cl$ $\quad Q_m = 167.34 \pm 0.19$

The half-life is 86.73 ± 0.27 days (weighted average, He 43, Se 58b, Ca 59a, Co 59e); the end point is 167.6 ± 0.3 keV (Co 57c, Fe 54a, La 50, Gr 50b, Co 48, Be 48b). The spectrum has the allowed shape, at least down to 2 keV (Al 48c, Be 48b, Co 48, La 50, Gr 50b, He 51, Mi 53a, Fe 54a, Mo 54a, Di 55, Co 57c). Log $ft = 5.0$. For computation of the β^- matrix element, see Gr 56c.

The longitudinal β^- polarization is equal to $-v/c$ (La 58).

For inner bremsstrahlung, see St 55, Ch 59, Le 57a (theory). For effects involving the atomic electron cloud, see Du 61a, Ch 59, Ru 54b.

B. $^{34}S(n, \gamma)^{35}S$ $\quad Q_m = 6981.8 \pm 3.8$

The thermal neutron capture cross section is 0.26 ± 0.05 b, Hu 58.

C. $^{34}S(d, p)^{35}S$ $Q_m = 4757.1 \pm 3.7$

Magnetic analysis of charged particles from na.ural sulphur targets bombarded with deuterons of 6.0 and 6.5 MeV, gives weak proton groups to $^{35}S^* = 0$,

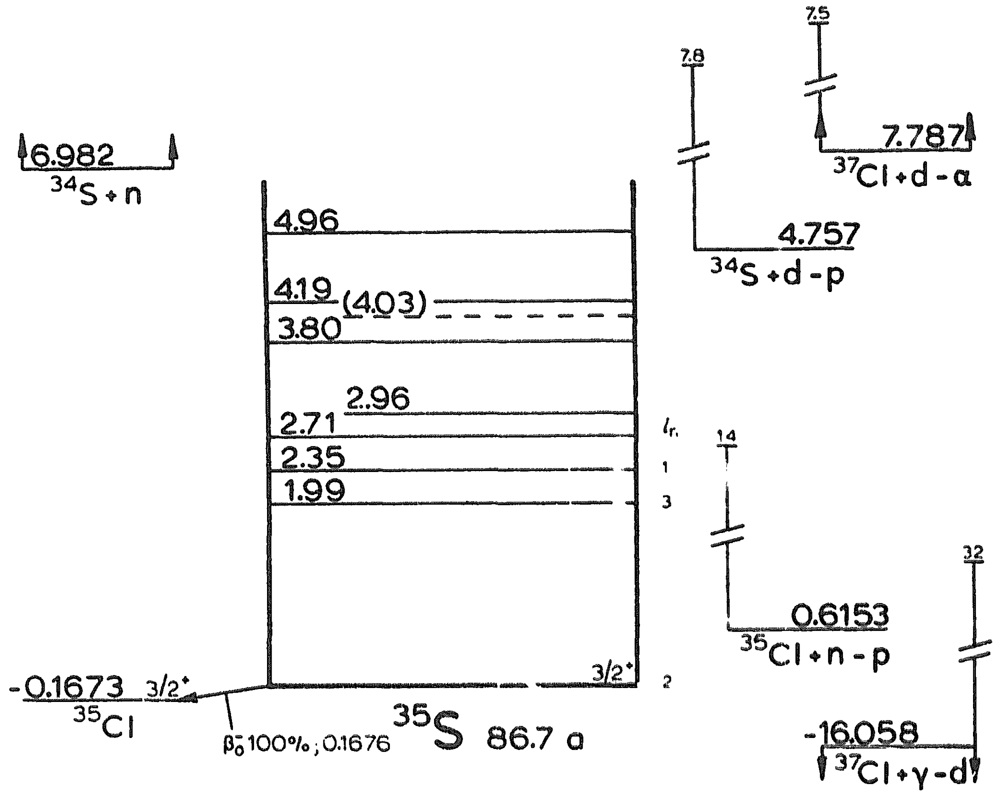

Fig. 35.1. Energy levels of ^{35}S.

TABLE 35.1

Energy levels of ^{35}S

E_x (MeV ± keV)	J^π	$\tau_{\frac{1}{2}}$	Decay	Reactions
0	$\frac{3}{2}^+$	86.73 ± 0.27 days	β^-	A, C, D, E, F
1.992 ± 6	$(\frac{5}{2}, \frac{7}{2})^-$			C, F
2.347 ± 6	$(\frac{1}{2}, \frac{3}{2})^-$			C, F
2.714 ± 10				F
2.955 ± 10				F
3.803 ± 10				C
(4.025 ± 10)				F
4.192 ± 10				C
4.961 ± 10				C

1.992 ± 0.008, 2.346 ± 0.008, 3.803 ± 0.010, 4.192 ± 0.010, and 4.961 ± 0.010 MeV; $Q_0 = 4.757 \pm 0.010$ MeV (En 58). At $E_d = 7.77$ MeV, angular distribution measurements of the groups to $^{35}S^* = 0$, 1.992, and 2.346 MeV, yield $l_n = 2$, 3, and 1, respectively, and $(2J+1)\theta_n^2 = 1.5$, 11.0, and 5.7 (relative), Ja 61b.

D. ^{35}Cl(n, p)^{35}S $Q_m = 615.27 \pm 0.44$

The thermal neutron cross section is 0.19 ± 0.05 b (Hu 58). See also Be 55c. Cross section at 14 MeV, Al 61.

From measurements with thermal and D(d, n) neutrons, $Q_0 = 0.52 \pm 0.04$ MeV (Gi 44).

For resonances, see ^{36}Cl.

E. ^{37}Cl(γ, d)^{35}S $Q_m = -16058.4 \pm 3.2$

Cross section for 32 MeV bremsstrahlung, Er 57.

F. ^{37}Cl(d, α)^{35}S $Q_m = 7787.2 \pm 3.2$

From bombardment of targets containing natural chlorine, at several deuteron energies between 3.0 and 7.5 MeV, $Q_0 = 7.783 \pm 0.012$ MeV has been determined by magnetic analysis. Levels in ^{35}S have been observed at (1.992), (2.348), 2.714, and (4.025) MeV, all ± 0.010 MeV (Pa 55c). An additional α-particle group which had been assigned to the ^{35}Cl(d, α)^{33}S reaction, actually has to be ascribed to ^{37}Cl(d, α)^{35}S, leading to a ^{35}S level at 2.955 ± 0.010 MeV (En 58).

G. Not reported:

^{33}S(t, p)^{35}S	$Q_m = 9920.3 \pm 3.6$
^{34}S(t, d)^{35}S	$Q_m = 724.2 \pm 3.7$
^{34}S(α, ^{3}He)^{35}S	$Q_m = -13595.3 \pm 3.8$
^{35}Cl(t, ^{3}He)^{35}S	$Q_m = -149.21 \pm 0.20$
^{36}S(p, d)^{35}S	$Q_m = -7657 \pm 9$
^{36}S(d, t)^{35}S	$Q_m = -3624 \pm 9$
^{36}S(^{3}He, α)^{35}S	$Q_m = 10695 \pm 9$
^{37}Cl(n, t)^{35}S	$Q_m = -9800.8 \pm 3.2$
^{37}Cl(p, ^{3}He)^{35}S	$Q_m = -10565.3 \pm 3.2$
^{38}Ar(n, α)^{35}S	$Q_m = -230.8 \pm 3.4$

^{35}Cl

(Fig. 35.2, p. 204; table 35.2, p. 205)

A. ^{32}S(α, p)^{35}Cl $Q_m = -1865.1 \pm 2.6$

At $E_\alpha = 8$ MeV, proton groups have been observed to ^{35}Cl* = 0, (0.7), 1.1, and (1.7) MeV; $Q_0 = -2.3$ MeV (Pi 55). For work with α particles from natural radioactive sources, see En 54a.

B. ^{34}S(p, γ)^{35}Cl $Q_m = 6366.6 \pm 3.7$

With enriched targets, 44 resonances have been found in the $E_p = 0.6$–1.9 MeV region; see table 35.3 for resonance energies, corresponding ^{35}Cl excitation energies, J^π values, widths, and yields (An 60a, An 61c). For branching ratios

D. Not reported:

^{33}S(^{3}He, n)^{35}Ar	$Q_m = 3317 \pm 30$
^{35}Cl(^{3}He, t)^{35}Ar	$Q_m = -5988 \pm 30$
^{36}Ar(p, d)^{35}Ar	$Q_m = -13033 \pm 30$
^{36}Ar(d, t)^{35}Ar	$Q_m = -9001 \pm 30$
^{36}Ar(^{3}He, α)^{35}Ar	$Q_m = 5319 \pm 30$

^{36}S

(Not illustrated)

A. ^{36}Cl(EC)^{36}S $Q_m = 1137 \pm 10$

See ^{36}Cl.

B. ^{40}Ar(γ, α)^{36}S $Q_m = -6809 \pm 9$

Observed at $E_\gamma = 23$, 26, and 30 MeV (Em 59; see also Wi 51).

C. Not reported:

^{34}S(t, p)^{36}S	$Q_m = 8381 \pm 9$
^{37}Cl(n, d)^{36}S	$Q_m = -6177 \pm 9$
^{37}Cl(d, ^{3}He)^{36}S	$Q_m = -2908 \pm 9$
^{37}Cl(t, α)^{36}S	$Q_m = 11411 \pm 9$
^{38}Ar(n, ^{3}He)^{36}S	$Q_m = -10926 \pm 9$

^{36}Cl

(Fig. 36.1, p. 209; table 36.1, p. 210)

A. (a) ^{36}Cl(β^-)^{36}Ar $Q_m = 711.5 \pm 4.3$
(b) ^{36}Cl(EC)^{36}S $Q_m = 1137 \pm 10$

The half-life has been measured by absolute β^- counting, using samples of known ^{36}Cl content, as $(4.4 \pm 0.5) \times 10^5$ yr (Wu 49), $(3.08 \pm 0.03) \times 10^5$ yr (Ba 55a), and $(2.5 \pm 0.4) \times 10^5$ yr (Wr 57).

The end point of the β^- spectrum is 0.714 ± 0.005 MeV (Fe 52). For a discussion of the *ft*-value (log *ft* = 13.4), see Fo 54, Jo 56. The shape of the β^- spectrum is consistent with a $\Delta J = 2$, no, transition (Wu 50, Fu 51, Fe 52, Jo 56).

The number of positons is less than 10^{-4} times the number of electrons (Wu 49, Jo 49); no γ rays are present with $E_\gamma > 20$ keV and with an intensity of more than 5% (Wu 49, Dr 55). Through observation of K quanta, it has been shown that ^{36}Cl also decays by K capture to ^{36}S with $K/\beta^- = (1.7 \pm 0.1)\%$; log *ft* = 13.5 (Dr 55).

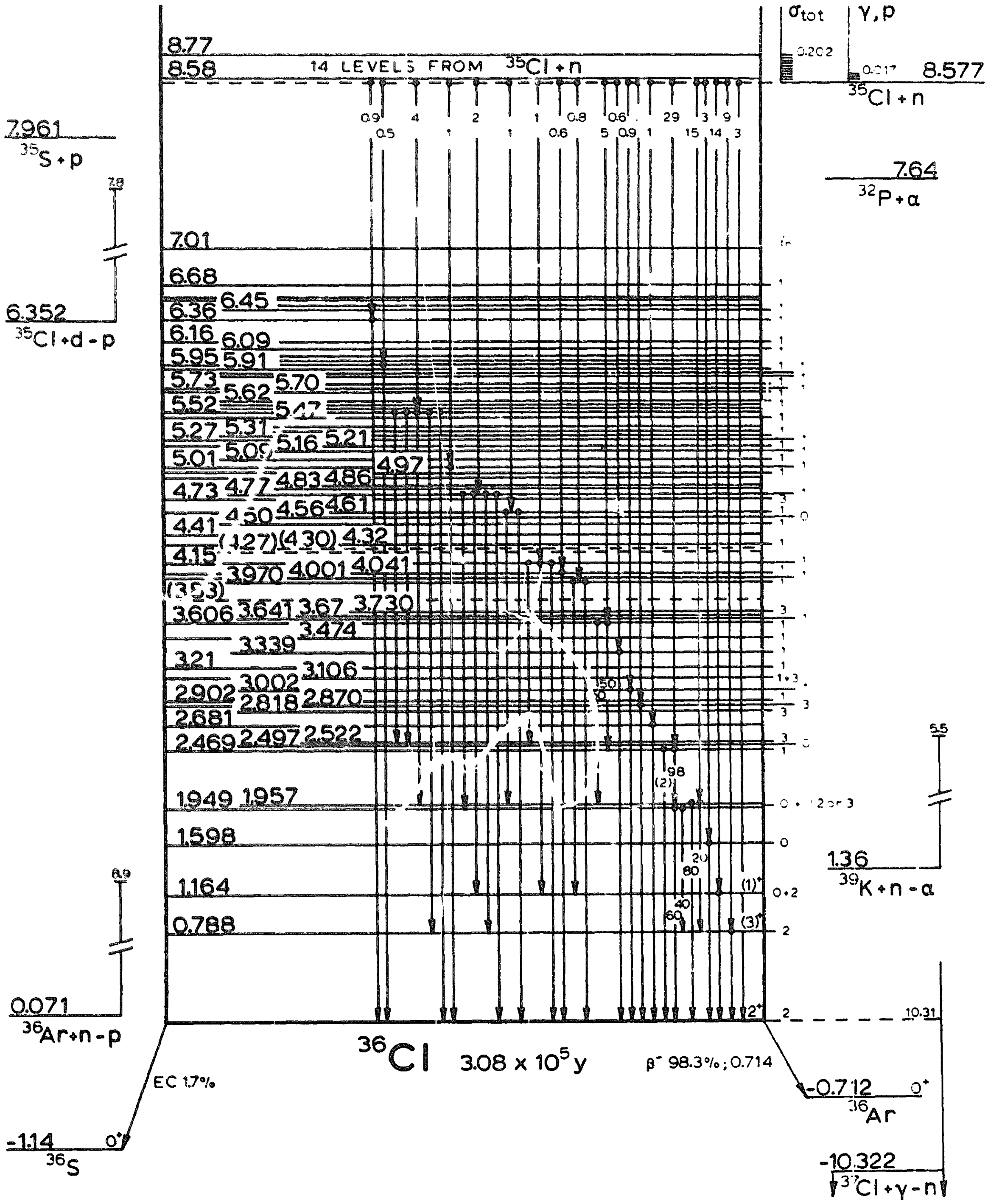

Fig. 36.1. Energy levels of ^{36}Cl.

B. $^{35}Cl(n, \gamma)^{36}Cl$ $\qquad Q_m = 8576.7 \pm 4.5$

From the thermal-neutron absorption cross section of natural chlorine, 33.6 ± 1.1 b, and the capture cross section of ^{37}Cl, 0.56 ± 0.12 b (Hu 58), and the ^{35}Cl and ^{37}Cl abundances, it follows that less than 1% of the thermal-neutron captures in natural chlorine occur in ^{37}Cl.

TABLE 36.1

Energy levels of ^{36}Cl

E_x (MeV ± keV)	J^π	$\tau_{\frac{1}{2}}$	Decay	Reactions
0	2+	(3.08 ± 0.03) × 10^5 yr	β^-, EC	many
0.788 ± 2	(3)+		γ	B, E, F, H
1.164 ± 2	(1)+		γ	B, E, F
1.598 ± 3	(1, 2)+		γ	B, E, F
1.949 ± 3	(1, 2)+		γ	B, E
1.957 ± 3			γ	B, E
2.469 ± 3	(≤ 3)$^-$		γ	B, E
2.497 ± 5	(1, 2)+		γ	B, E
2.522 ± 5	(≤ 5)$^-$		γ	B, E
2.681 ± 5			γ	B, E
2.818 ± 5	(≤ 5)$^-$		γ	B, E
2.870 ± 5	(≤ 5)$^-$		γ	B, E
2.902 ± 5	(≤ 3)$^-$		γ	B, E
3.002 ± 5	(≤ 3)$^-$		γ	B, E
3.106 ± 5	(≤ 3)$^-$		γ	B, E
3.213 ± 6	(≤ 3)$^-$		γ	B, E
3.339 ± 5	(≤ 3)$^-$		γ	B, E
3.474 ± 5	(≤ 3)$^-$			E
3.606 ± 5	(≤ 3)$^-$		γ	B, E
3.641 ± 5	(≤ 3)$^-$		γ	B, E
3.671 ± 6				E
3.730 ± 5	(≤ 5)$^-$		γ	B, E
(3.831)				E
3.970 ± 5	(≤ 3)$^-$		γ	B, E
4.001 ± 5	(≤ 3)$^-$			E
4.041 ± 5	(≤ 3)$^-$		γ	B, E
4.146 ± 7	(≤ 3)$^-$		γ	B, E
4.269–7.007; 45 levels, see table 36.5 and reaction				E (and B)
8.576–8.773; 14 levels, see tables 36.3 and 36.4 and reactions				B, C, D

Gamma rays from thermal neutron capture in natural chlorine, observed with a Compton spectrometer, are listed in table 36.2, with the intensities in photons per 100 captured neutrons in natural chlorine, and the levels between which they are assumed to occur (Gr 60a). Previous lower resolution work, reported in Ki 52 (as corrected in Ba 58c), Br 56e, and Dr 60, is in agreement with these results, except for the intensities of the three lowest energy γ rays (Br 56e) and of most of the higher energy γ rays (Ba 58c). See also Ur 59.

Assignments of the most intensive γ rays to transitions in ^{36}Cl are based on coincidence measurements with a three-crystal pair spectrometer. These measurements also yield the branching of the 1.95, 2.47, (2.87), and 3.60 MeV levels; see fig. 36.1 (Se 59). Sum-coincidence measurements confirm the two-step cascades through ^{36}Cl* = 0.79, 1.16, (1.60), 1.96, and 2.87 MeV (Bu 59b), and through ^{36}Cl* = 0.79, 1.60, 1.96, 2.68, 2.87, (3.00), (5.52), 5.95, and 6.36 MeV (Dr 61). See also Re 54. The branching fractions of these intermediate states

TABLE 36.2

Gamma rays from ^{35}Cl(n, γ)^{36}Cl (Gr 60a)

E_γ (MeV ± keV)	I_γ[a]	Assignment[b]	E_γ (MeV ± keV)	I_γ[a]	Assignment[b]
8.573 ± 4[d]	3.1	C → 0	3.742 ± 6	0.4	(3.73 → 0)
7.786 ± 5	8.2	C → 0.79(c)	3.596 ± 5	0.5	4.77 → 1.16
7.410 ± 5	12.7	C → 1.16(c)	3.566 ± 4	1.2	C → 5.01(t); 5.52 → 1.95
6.974 ± 5	2.7	C → 1.60(c)	3.510 ± 4	0.8	(4.30 → 0.79)
6.621 ± 5	13.6	C → 1.96(c)	3.435 ± 4	1.0	(4.61 → 1.16)
6.423 ± 8	0.3		3.383 ± 4	0.5	(4.56 → 1.16)
6.344 ± 8	0.3	6.36 → 0(c)	3.338 ± 5	0.8	3.34 → 0(c)
6.266 ± 6	0.6		3.121 ± 4	0.9	(3.11 → 0)
6.110 ± 5	25.2	C → 2.47(c)	3.067 ± 4	3.6	C → 5.52(c)
5.959 ± 6	0.3	5.95 → 0(c)	3.024 ± 4	0.8	5.52 → 2.50
5.902 ± 5	1.3	C → 2.68(c)	3.002 ± 5	1.4	3.00 → 0(c); 5.52 → 2.52
5.715 ± 4	6.1	C → 2.87(c)	2.980 ± 5	1.4	4.15 → 1.16
5.585 ± 5	0.8	C → 3.00(c)	2.896 ± 3	0.6	(2.90 → 0)
5.516 ± 4	1.5	5.52 → 0(c)	2.868 ± 3	5.9	2.87 → 0(c)
5.246 ± 5	0.6	C → 3.34(c)	2.852 ± 4	0.8	(3.64 → 0.79)
5.016 ± 4	0.6	5.01 → 0(t)	2.810 ± 4	0.7	4.77 → 1.96; 3.97 → 1.16
4.981 ± 4	4.2	C → 3.61(c)	2.681 ± 3	1.5	2.68 → 0(c)
4.757 ± 5	0.3	4.77 → 0(t)	2.628 ± 4	0.5	C → 5.95(c)
4.732 ± 4	1.0	5.52 → 0.79	2.535 ± 7	0.7	
4.613 ± 4	0.7	C → 3.97(t)	2.498 ± 3	0.5	2.50 → 0
4.589 ± 5	0.3	4.61 → 0(t)	2.477 ± 3	0.5	2.47 → 0
4.547 ± 8	0.4	(4.56 → 0)	2.422 ± 4	0.5	(3.21 → 0.79)
4.522 ± 5	0.6	C → 4.04(t)	2.235 ± 3	0.8	C → 6.36(c)
4.444 ± 4	1.1	C → 4.15(t)	2.033 ± 7	1.2	(2.82 → 0.79)
4.417 ± 6	0.5	(4.41 → 0)	1.957 ± 3	10.0	1.96 → 0(c)
4.298 ± 4	0.5	(4.30 → 0)	1.949 ± 3	18.5	1.95 → 0(c)
4.203 ± 5	0.2	(5.38 → 1.16)	1.636 ± 3	1.1	3.61 → 1.96, 1.95(c); 4.15 → 2.50
4.138 ± 8	0.2	4.15 → 0(t)	1.597 ± 3	3.2	1.60 → 0(c)
4.080 ± 4	0.7	(4.86 → 0.79)	1.329 ± 2	1.3	2.50 → 1.16
4.053 ± 4	0.7	4.04 → 0(t)	1.165 ± 2	27.5	1.16 → 0(c); 1.96, 1.95 → 0.79(c)
3.980 ± 4	1.2	C → 4.61(t)	1.13[e]		3.61 → 2.47(c)
3.957 ± 7	0.3	3.97 → 0(t)	0.792 ± 2	18.0	0.79 → 0(c)
3.822 ± 4	1.8	C → 4.77(t)	0.518 ± 2	≈ 20	2.47 → 1.95(c)

[a] Intensities per 100 neutrons captured in natural chlorine; the errors in the intensities are 10% for the strong lines, and up to 50% for the weak lines.

[b] The capturing state is indicated by C; excitation energies in MeV.
Assignments marked (c) are based on coincidence measurements (Bu 59b, Se 59, Dr 61). The remaining γ rays are fitted between levels known from Ho 61b; two-step cascades are marked (t). Gamma rays de-exciting levels of which the mode of population is unknown, are bracketed; these transitions are not included in fig. 36.1.

[d] Calibration line; energy calculated from masses.

[e] Se 59.

to the ground state are 1, 0.91±0.09, 1.07±0.15, 0.89±0.09, 1.2±0.2, 0.84±0.15, 0.45±0.1, 0.45±0.1, ≤ 1, and ≤ 0.55, respectively (Dr 61). For a discussion of spins and parities of ^{36}Cl levels with $E_x < 3$ MeV, based on the intensities of the cascades, see Dr 61.

The assignments based on coincidence measurements are marked as such in table 36.2. See also Bu 59c. Using the precision energy measurements and the intensities, most of the remaining γ rays can be fitted in the ^{36}Cl level scheme known from the ^{35}Cl(d, p)^{36}Cl reaction. Gamma-ray pairs with energies adding up to the neutron binding energy indicate two-step cascades through new levels at 4.138, 4.589, 4.757, 5.016, 5.516, and 6.344 MeV (Gr 60a). The existence of these levels has later been confirmed from the ^{35}Cl(d, p)^{36}Cl reaction (Ho 61b).

The doublet character of the 1.95 MeV level is indicated by the fact that the branching of this level depends on the method of its population (Se 59); later, this doublet has been resolved in 1.957 ± 0.003 and 1.949 ± 0.003 MeV levels. The 2.47 MeV level decays to the lowest of these two levels by a 518 ± 2 keV γ ray. Using the assignments based on coincidence measurements, the γ-ray energies yield the excitation energies of the six lowest ^{36}Cl levels with good precision: ^{36}Cl* $= 0.787 \pm 0.002$, 1.165 ± 0.002, 1.597 ± 0.003, 1.949 ± 0.003, 1.957 ± 0.003, and 2.467 ± 0.003 MeV (Gr 60a).

For resonances, see table 36.3.

C. ^{35}Cl(n, p)^{35}S $\qquad Q_m = 615.27 \pm 0.44 \qquad E_b = 8576.7 \pm 4.5$

For resonances, see table 36.3. For non-resonance data, see ^{35}S.

TABLE 36.3

Resonances in the ^{35}Cl(n, γ)^{36}Cl and ^{35}Cl(n, p)^{35}S cross sections (Po 61b)

E_n (keV)	^{36}Cl* (MeV)	Γ_γ (eV)	Γ_p (meV)	Γ_n (meV)	l_n
-0.21 ± 0.01[a]	8.576	0.50 ± 0.01	2.4 ± 0.8		0
0.405 (datum)	8.577		70 ± 22	26 – 65[b]	1[c]
1.1 ± 0.2	8.578		≈ 50	4 – 30[b]	1
4.3 ± 0.3	8.581		35 ± 15	250 – 700[b]	1
15	8.592		≈ 100	65×10^3	0
17	8.594				

[a] Already suggested in Br 56c.
[b] Value depending on resonance spin.
[c] In Hu 58 $l_n = 0$ is given.

TABLE 36.4

Resonances in the ^{35}Cl – n total cross section (Hu 58)

E_n (keV)	^{36}Cl* (MeV)	l_n	Γ_n (keV)	E_n (keV)	^{36}Cl* (MeV)	Γ_n (keV)
0.405 ± 0.006	8.577	0	0.00014	134	8.707	0.51
15	8.591		≈ 0.03	144	8.717	0.51
27	8.603		0.13	184	8.756	1.7
104	8.678		0.30	190	8.762	1.2
114	8.688		0.40	202	8.773	2.8

TABLE 36.5

Energy levels of ^{36}Cl from $^{35}Cl(d, p)^{36}Cl$

$^{36}Cl^{*}$ [a] (MeV ± keV)	$^{36}Cl^{*}$ [b] (MeV ± keV)	l_n [a]	$(2J+1)\theta_n^2$ [a] × 10^3	$^{36}Cl^{*}$ [a] (MeV)	l_n [a]	$(2J+1)\theta_n^2$ [a] × 10^3
0	0	2 (+0) [c, d, e]	41 (≤ 2)	4.834		
0.789 ± 4	0.790 ± 5	2 [c, e]	16	4.857		
1.163 ± 4	1.163 ± 6	{ 0 [c]	5.3	4.887		
		{ 2	7.4	4.919		
1.599 ± 5	1.600 ± 7	0 [c]	2.7	4.965	1	14
1.954 ± 5	1.952 ± 7	{ 0 [c]	13	5.008 [f]	1	18
		{ 2 or 3 [c]	≤ 30 or ≤ 60	5.090	1	6
2.472 ± 6	2.473 ± 7	1	43	5.169	1	13
2.497 ± 6	2.498 ± 7	0	3.4	5.213	1	79
2.522 ± 6	2.523 ± 7	3	133	5.269	1	36
2.679 ± 6	2.684 ± 7			5.314	1	35
2.816 ± 6	2.820 ± 7	3	56	5.339		
2.868 ± 6	2.872 ± 7	3	22	5.376		
2.900 ± 6	2.905 ± 7	1	55	5.469	1	56
3.000 ± 6	3.004 ± 7	1	35	5.518 [f]		
3.103 ± 7	3.110 ± 8	{ 1	2	5.550		
		{ 3	22	5.584		
3.212 ± 8	3.214 ± 8	1	22	5.622	1	3.0
3.338 ± 6	3.341 ± 8	1	77	5.701	1	12
3.474 ± 7	3.474 ± 8	1	2.1	5.731	1	8.0
3.606 ± 7	3.606 ± 8	1	3.6	5.766	1	12
3.640 ± 6	3.644 ± 8	1	22	5.836	1	7.1
3.670 ± 8	(3.673 ± 8)			5.871	1	7.6
3.728 ± 7	3.732 ± 8	3	23	5.906	1	62
(3.831)				5.952		
3.970 ± 7	3.970 ± 8	1	27	5.972		
4.000 ± 7	4.003 ± 8	1	45	6.032		
4.040 ± 7	4.043 ± 8	1	42	6.090	1	64
4.146 ± 7	[f]	1	17	6.155	1	17
(4.269)				6.356 [f]	1	
(4.300)				6.445	1	
4.323 ± 7		1	19	6.474		
4.413 ± 8				6.510		
4.504 ± 7		1	46	6.546		
4.560 ± 8		0	3	6.680	1	
4.607 ± 8	[f]	1	39	7.007		
4.734 ± 8		3	12	all ± 8 keV		
4.765 ± 8	[f]	1	9.2			

[a] Ho 61b; E_d = 7.5 MeV.
[b] Pa 55c; E_d = 3.0–7.5 MeV.
[c] Also Te 56b; E_d = 4 MeV.
[d] Also Ki 52a, Ki 53b, E_d = 6.9 and 7.8 MeV.
[e] Se 61; E_d = 7.77 MeV.
[f] See also reaction B (Gr 60a).

D. $^{35}Cl(n, n)^{35}Cl$ $E_b = 8576.7 \pm 4.5$

Resonances observed with enriched material are listed in table 36.4 (Hu 58; see also Br 56c, Bi 61). For cross section, see Hu 58.

For non-resonance information, see ^{35}Cl.

E. ^{35}Cl(d, p)^{36}Cl $Q_m = 6352.0 \pm 4.5$

Magnetic analysis of (d, p) reactions with natural chlorine targets yields $Q_0 = 6.354 \pm 0.008$ MeV (Pa 55c and Ho 61b). Seventy levels are listed in table 36.5 (Pa 55c, Ho 61b; for low-resolution work, see En 51b, Te 56b) with l_n values and reduced widths (Ho 61b, Se 61, Te 56b). The $l_n = 2$ ground-state group has less than 4% admixture of $l_n = 0$ (Ki 52a, Ki 53b). The reduced widths of the lowest three states are in agreement with the results of a jj-coupling computation, assuming $J^\pi = 2^+, 3^+$, and 1^+, for ^{36}Cl(0), (1), and (2), respectively (Ho 61b). See also Me 59. The $l_n = 0+3$ value of the 1.95 MeV level suggests a doublet character (see ^{36}Cl, reaction B) (Te 56b, Gr 60a).

F. ^{36}Ar(n, p)^{36}Cl $Q_m = 71.2 \pm 4.3$

At $E_n = 1.32$–8.94 MeV, cross sections have been measured for proton groups to the ^{36}Cl ground state and the first three excited states (Da 60, Da 61b).
Resonances, see ^{37}Ar.

G. ^{37}Cl(γ, n)^{36}Cl $Q_m = -10322 \pm 5$

The photo-neutron threshold is 10.307 ± 0.037 MeV (Ge 60a). See also Sh 51a. Cross section measurements, Go 54a.

H. ^{39}K(n, α)^{36}Cl $Q_m = 1364 \pm 6$

Irradiation of KI crystals with D(d, n) neutrons and pulse-height analysis of the scintillation spectrum, yields $Q_0 = 1.25 \pm 0.2$ MeV. A transition to ^{36}Cl* $= 0.87 \pm 0.1$ MeV is also observed (Sc 56a). For cross section measurements, see Li 58d, Bo 60d, Ba 61g, Di 61.
For resonances, see ^{40}K.

I. Not reported:

^{33}S(α, p)^{36}Cl	$Q_m = -1931 \pm 6$
^{34}S(t, n)^{36}Cl	$Q_m = 6461 \pm 6$
^{34}S(^{3}He, p)^{36}Cl	$Q_m = 7225 \pm 6$
^{34}S(α, d)^{36}Cl	$Q_m = -11127 \pm 6$
^{35}Cl(t, d)^{36}Cl	$Q_m = 2319.1 \pm 4.5$
^{35}Cl(α, ^{3}He)^{36}Cl	$Q_m = -12000.4 \pm 4.5$
^{36}S(p, n)^{36}Cl	$Q_m = -1920 \pm 10$
^{36}S(^{3}He, t)^{36}Cl	$Q_m = -1156 \pm 10$
^{36}Ar(t, ^{3}He)^{36}Cl	$Q_m = -693.3 \pm 4.3$
^{37}Cl(p, d)^{36}Cl	$Q_m = -8097 \pm 5$
^{37}Cl(d, t)^{36}Cl	$Q_m = -4064 \pm 5$
^{37}Cl(^{3}He, α)^{36}Cl	$Q_m = 10255 \pm 5$
^{38}Ar(n, t) ^{36}Cl	$Q_m = -12082 \pm 6$
^{38}Ar(p, ^{3}He)^{36}Cl	$Q_m = -12847 \pm 6$
^{38}Ar(d, α)^{36}Cl	$Q_m = 5506 \pm 6$

REMARKS

Pure *jj* coupling predicts a linear relation between excitation energies of ($d_{\frac{3}{2}}$, $d_{\frac{3}{2}}^{-1}$) levels in ^{36}Cl and those of ($d_{\frac{3}{2}}^{-1}$, $d_{\frac{3}{2}}^{-1}$) levels in ^{38}K. Using this relation $J^{\pi} = 2^+$, 3^+, and 1^+ has been calculated for ^{36}Cl* = 0, 0.79, and 1.60 MeV (Pa 61b).

For a theoretical discussion of the ^{36}Cl ground-state configuration, see Ku 53, De 53a, Hi 54, Sc 54c.

^{36}Ar

(Fig. 36.2, p. 216; table 36.6, p. 217)

A. ^{35}Cl(p, γ)^{36}Ar $Q_n = 8505.6 \pm 2.1$

The γ ray yield from targets containing natural chlorine bombarded with protons in the energy range $E_p = 500$–2150 keV shows 86 resonances (not tabulated), Br 51. The resonances assigned to ^{35}Cl by the use of isotopically enriched targets and/or by the energies of the γ rays emitted, are listed in table 36.7 together with the observed resonance strengths, the corresponding ^{36}Ar excitation energies, and a qualitative indication of the decay (Ku 61, Li 60b, Wa 60, To 57, Br 51, Ta 46).

Using single counter and coincidence techniques, the decay schemes of six resonance levels and of the lower levels at 1.97 ± 0.02, 4.17 ± 0.03, 4.45 ± 0.05, 4.94 ± 0.03, 5.85 ± 0.03, and 6.85 ± 0.03 MeV have been measured; see fig. 36.2 (Li 60b). A few discrepancies with measurements reported in Ku 61 and To 57 are given in the figure caption.

Angular distribution measurements at $E_p = 861$ keV indicate $J^{\pi} = 2^{(+)}$, $3^{(-)}$, and $3^{(+)}$ for ^{36}Ar* = 1.95, and 4.1 MeV, and the resonance state, respectively (Be 57b). At $E_p = 735$ and 861 keV, the angular distributions are consistent with $J = 3$ for ^{36}Ar* = 4.17 MeV, but $J = 2$ cannot be excluded. The assignment $J = (2,4)$ to the 4.94 MeV level is tentative (Li 60b).

B. ^{35}Cl(p, p')^{35}Cl $E_b = 8505.6 \pm 2.1$

Resonances (not tabulated) in the excitation curve for inelastic proton scattering, observed by measuring the γ-ray yield from ^{35}Cl(1), have a spacing of 18 keV at an average proton energy of 2.8 MeV (Pr 58a). The excitation function for $E_{\gamma} = 1.22$ and 1.76 MeV shows 31 resonances in the $E_p = 2.30$–3.25 MeV range (St 61b); for energies and widths, see table 36.8. With natural chlorine targets weak p_0 resonances have been observed at $E_p = 1.496$ and 1.96 MeV, with $\Gamma = 20$ and 70 keV, respectively (Ru 59).

For non-resonance data, see ^{35}Cl.

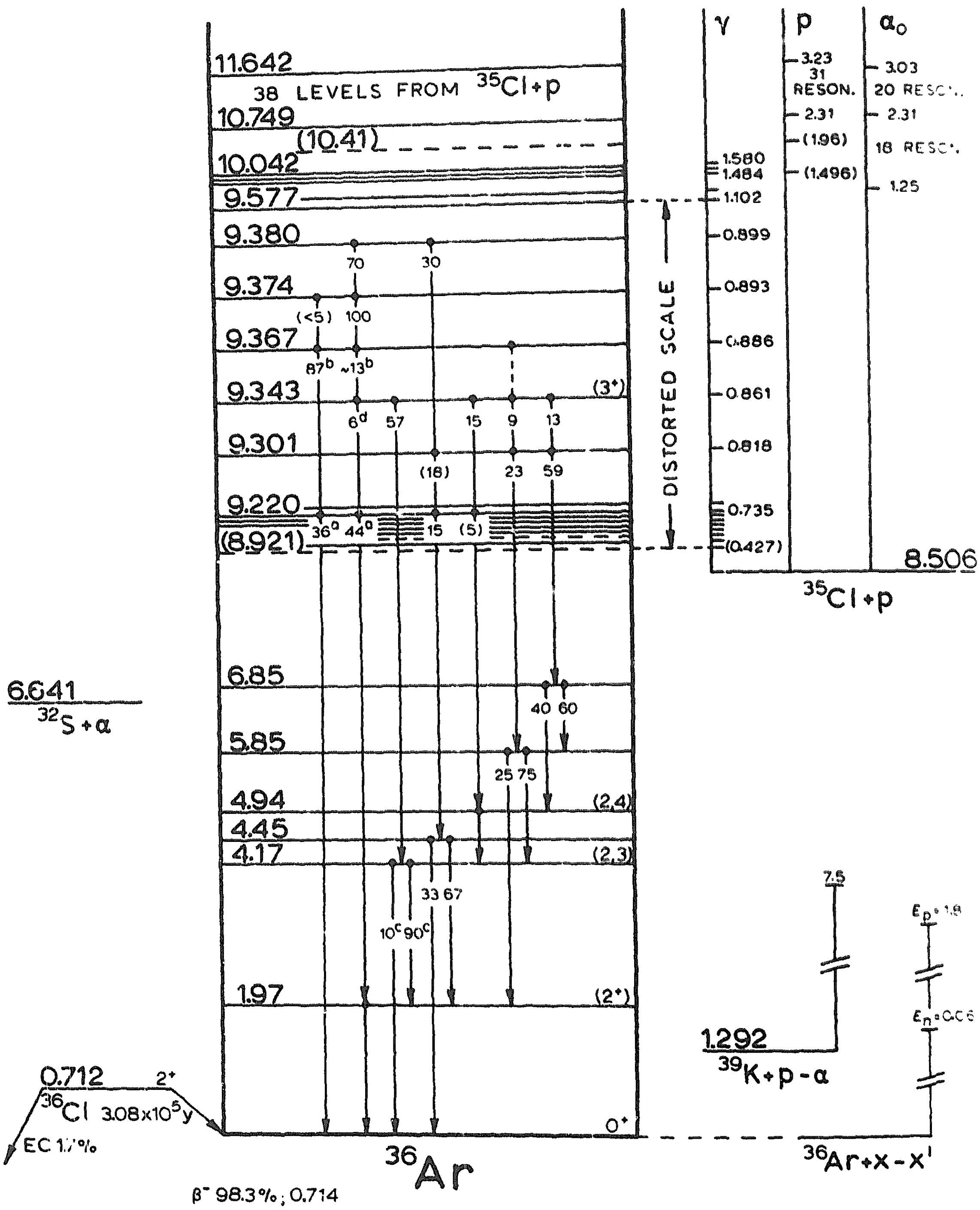

Fig. 36.2. Energy levels of ^{36}Ar. Gamma decay as reported in Li 60b. The branchings are in agreement with the indications given in Ku 61, To 57, Be 57b, except for the annotated transitions: [a] intensity ratio $\gamma_1/\gamma_0 = 3$ (Ku 61); [b] decay proceeds to 1.97 level, ground-state transition not observed (Ku 61); [c] intensity ratio $\gamma_1/\gamma_0 = 4$ (Be 57b); [d] intensity $\gamma_1 \gtrsim 3$ (To 57).

C. ^{35}Cl(p, α)^{32}S $\quad Q_m = 1865.1 \pm 2.6 \quad E_b = 8505.6 \pm 2.1$

Thirty-eight resonances (not tabulated) have been observed in the energy range $E_p = 1.25$–3.1 MeV. For a discussion of level spacing, strength function,

TABLE 36.6

Energy levels of ^{36}Ar

E_x (MeV ± keV)	J^π	Decay	Reactions
0	0^+	stable	A, D, E, F, G
1.973 ± 7	(2^+)	γ	A, C
4.17 ± 30	(2, 3)	γ	A
4.45 ± 50		γ	A
4.94 ± 30	(2, 4)	γ	A
5.85 ± 30		γ	A
6.85 ± 30		γ	A
8.921–10.042; 19 levels, see table 36.7 and reaction			A
9.948		γ, p	A, B
(10.41)		p	B
10.749—11.642; 38 levels, see table 36.8 and reactions			B, C

TABLE 36.7

Resonances in the reaction $^{35}Cl(p, \gamma)^{36}Ar$

E_p keV)			$^{36}Ar^*$	$(2J+1)\,\Gamma_\gamma\Gamma_p/\Gamma$	Decay[a]
Ku 61	Wa 60	Ta 46	(MeV)	(meV)	
		427[b]	(8.921)		
445.9 ± 1.5	443.9 ± 0.4	447	8.939	3[f]	γ_1
		500[c]	(8.992)		
533.8 ± 1.5		532	9.025	8[f]	γ_1
575.9 ± 1.5			9.066	7[f]	
644.2 ± 1.5			9.132	4[f]	γ_1
656.8 ± 1.5	Li 60b[h]	Br 51	9.144	3[f]	γ_1
734.6 ± 1.5	736		9.220	20[f]	see fig. 36.3
755.4 ± 1.5			9.240	4[f]	γ_1
818.2 ± 1.5	819		9.301	3[f]	see fig. 36.3
861.4 ± 1.5	861	858	9.343	100[f]; 9600[g]	see fig. 36.3
885.7 ± 1.5	883	888	9.367	20[f]	see fig. 36.3
893.0 ± 1.5	890		9.374	40[f]	see fig. 36.3
899.2 ± 1.5	896		9.380		see fig. 36.3
	all ± 5	1102	9.577		
To 57		1258	9.729		
1484		1484[d]	9.948	8000[g]	γ_0
1510		1510[d]	9.974	32000[g]	γ_0
1580			10.042	22000[g]	γ_0
			(10.41)[e]		

[a] The γ_0 indicates a transition to the ground state (To 57); observation of this transition implies $J^\pi = (1^\pm, 2^+)$ for the resonance level. The γ_1 indicates a transition to $^{36}Ar = 1.95 \pm 0.02$ MeV (Ku 61).
[b] Possibly due to ^{15}N contamination (Ku 61).
[c] Not observed in Ku 61.
[d] At $E_p = 1496$ keV, a resonance is reported in the reaction Cl(p, p)Cl, with $\Gamma \approx 20$ keV, Ru 59.
[e] This level corresponds to a 1960 keV resonance in the reaction Cl(p, p)Cl; $\Gamma = 70$ keV, Ru 59.
[f] Ku 61.
[g] To 57; the yields given here are apparently about 100 times higher than those given in Ku 61.
[h] $\Gamma \leqslant 5$ keV for these resonances.

and reduced α-particle and proton widths, see Cl 60. The resonances above 2.3 MeV are quoted in St 61b; see table 36.8.

For non-resonance data, see ^{32}S.

D. ^{36}Cl(β^-)^{36}Ar $\qquad Q_m = 711.5 \pm 4.3$

See ^{36}Cl.

E. ^{36}Ar(n, n)^{36}Ar

See ^{37}Ar for cross section and resonances.

TABLE 36.8

Levels in ^{36}Ar from the ^{35}Cl(p, p′γ)^{35}Cl and ^{35}Cl(p, α_0)^{32}S reactions

Cl 60[c] (p, α_0) E_p (MeV)	St 61b[a] (p, p′γ) E_p (MeV)	Γ (keV)	^{36}Ar* (MeV)	Cl 60[c] (p, α_0) E_p (MeV)	St 61b[a] (p, p′γ) E_p (MeV)	Γ (keV)	^{36}Ar* (MeV)
2.307			10.749	2.830	2.826		11.256
2.325			10.767		2.838	5	11.265
	2.345	6	10.786	2.867			11.294
2.400			10.840	2.892	2.892	5	11.318
2.450	2.460	8	10.893	2.910	2.907	10	11.334
2.505			10.942		2.921		11.346
	2.530	11	10.966		2.933	≈ 5	11.358
2.545	2.545	6	10.980	2.978	2.980[b]	8	11.402
	2.560	≈ 7	10.995		2.993	≈ 9	11.416
2.572	2.572	< 3	11.007	3.03	3.020	5	11.442
2.602	2.606	8	11.038		3.065[b]	9	11.486
	2.650	7	11.083		3.093[b]	14	11.513
2.682	2.683	< 4	11.115		3.115[b]	≈ 4	11.535
2.718	2.724	≈ 4	11.152		3.135[b]	≈ 4	11.554
2.730	2.733		11.163		3.154	23	11.573
2.757			11.187		3.159[b]		11.578
2.772			11.201		3.182	< 10	11.600
2.800	2.807	8	11.232		3.205[b]	< 8	11.622
	2.818		11.246		3.225	< 12	11.642
	all ±0.005				all ±0.005		

[a] The yield was measured of E_γ = 1.22 and 1.76 MeV.
[b] At these resonances the 1.76 MeV γ ray is strong.
[c] As quoted in St 61b.

F. ^{36}Ar(p, p)^{36}Ar

For cross section and resonances, see ^{37}K.

G. ^{39}K(p, α)^{36}Ar $\qquad Q_m = 1292.3 \pm 3.9$

Magnetic analysis at E_p = 7.0–7.5 MeV yields an α-particle group to the ground state, $Q_0 = 1.286 \pm 0.007$ MeV, and one to an excited state at 1.977 ± 0.008 MeV (Sp 58). At E_p = 1.9 MeV, $Q_0 = 1.267 \pm 0.020$ MeV (Cl 60).

For resonances, see ^{40}Ca.

H. Not reported:

^{33}S(α, n)^{36}Ar	$Q_m = -\ 2002.1 \pm 4.1$
^{34}S(^{3}He, n)^{36}Ar	$Q_m = \ 7154.3 \pm 4.2$
^{35}Cl(d, n)^{36}Ar	$Q_m = \ 6280.9 \pm 2.1$
^{35}Cl(^{3}He, d)^{36}Ar	$Q_m = \ 3012.4 \pm 2.1$
^{35}Cl(α, t)^{36}Ar	$Q_m = -11307.1 \pm 2.1$
^{38}Ar(p, t)^{36}Ar	$Q_m = -12153.2 \pm 3.8$

REMARKS

Recalculation of the excitation energy of the lowest $T = 1$ state in ^{36}Ar, computed in Wi 56a, yields $E_x = 6.68$ MeV (Gl 61b).

^{37}S

(Fig. 37.1, p. 219; table 37.1, p. 220)

A. ^{37}S(β^-)^{37}Cl $Q_m = 4790 \pm 90$

The half-life is 5.07 ± 0.01 min (El 59), 5.04 ± 0.02 min (Bl 46). The β^- spectrum, measured by Al absorption, consists of two components with the follow-

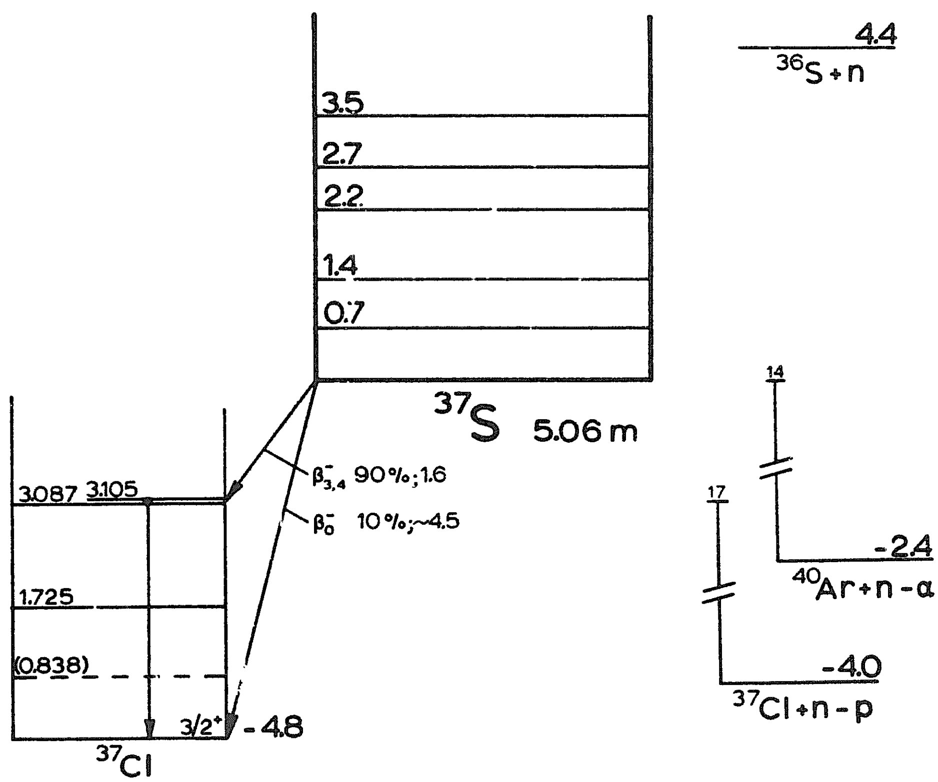

Fig. 37.1. Energy levels of ^{37}S.

ing end points and relative intensities: 4.3 ± 0.3 MeV (10%) and 1.6 ± 0.1 MeV (90%). The second component is in coincidence with a 2.7 ± 0.2 MeV γ ray (Bl 46).

Essentially the same results have been obtained by scintillation spectrometer: $E_\beta \approx 4.7$ MeV (10%) and 1.6 MeV (90%), respectively, and $E_\gamma = 3.1$ MeV. No other γ ray with more than 1% intensity has been observed (Mo 56). The energy of the γ ray has more accurately been determined as 3.09 ± 0.03 MeV (St 56a).

The β^- ground-state transition is evidently forbidden: log $ft = 7.2$ and $\log (W_0^2-1)\, ft = 9.2$, while the transition to the 3.1 MeV level in ^{37}Cl is allowed (log $ft = 4.2$).

TABLE 37.1

Energy levels of ^{37}S

E_x (MeV$\pm$keV)	$\tau_{\frac{1}{2}}$	Decay	Reactions
0	5.06 ± 0.01 min	β^-	A, B, C, D
0.65 ± 60			D
1.39 ± 70			D
2.19 ± 90			D
2.7 ± 100			D
3.5 ± 200			D

B. $^{36}S(n, \gamma)^{37}S$ $Q_m = 4390 \pm 90$

The thermal neutron cross section is 0.14 ± 0.04 b (Hu 58).

C. $^{37}Cl(n, p)^{37}S$ $Q_m = -4010 \pm 90$

For cross section, see Hu 58, Ma 60c.

D. $^{40}Ar(n, \alpha)^{37}S$ $Q_m = -2420 \pm 90$

At $E_n = 14$ MeV, ionization-chamber pulse-height analysis yields α-particle groups to $^{37}S^* = 0$, 1.3 ± 0.05, 2.2 ± 0.1, 2.7 ± 0.1, and 3.5 ± 0.2 MeV; $Q_0 = -2.5 \pm 0.1$ MeV (Be 55a). At $E_n = 1.3$–8.9 MeV, groups have been observed to $^{37}S^* = 0$, 0.65 ± 0.06, 1.39 ± 0.07, 2.19 ± 0.09, and (2.8 ± 0.2) MeV; $Q_0 = -2.49 \pm 0.05$ MeV (Da 60, Da 61b).

For resonances, see ^{41}Ar.

E. Not reported:

$^{36}S(d, p)^{37}S$	$Q_m = 2170 \pm 90$
$^{36}S(t, d)^{37}S$	$Q_m = -1860 \pm 90$
$^{36}S(\alpha, {}^3He)^{37}S$	$Q_m = -16180 \pm 90$
$^{37}Cl(t, {}^3He)^{37}S$	$Q_m = -4770 \pm 90$

^{37}Cl

(Fig. 37.2, p. 221; table 37.2, p. 221)

A. $^{36}Cl(n, \gamma)^{37}Cl$ $Q_m = 10322 \pm 5$

The thermal neutron capture cross section is 90 ± 30 b, Hu 58.

B. $^{37}S(\beta^-)^{37}Cl$ $Q_m = 4790 \pm 90$

See ^{37}S.

C. $^{37}Cl(p, p')^{37}Cl$

At $E_p = 7.0$ MeV, magnetic analysis yields proton groups to $^{37}Cl^* = 0.838$, 1.728, 3.087, and 3.105 MeV, all ± 0.005 MeV (En 56c). With enriched ^{37}Cl

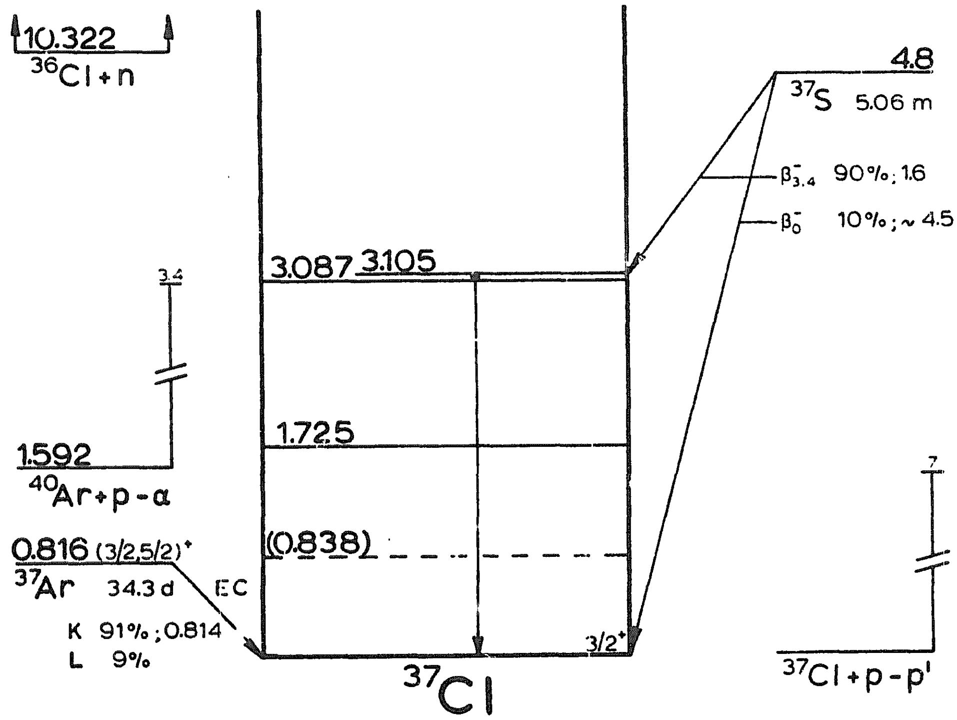

Fig. 37.2. Energy levels of ^{37}Cl.

TABLE 37.2

Energy levels of ^{37}Cl

E_x (MeV ± keV)	J^π	Decay	Reactions
0	$\frac{3}{2}^+$	stable	A, B, C, D
(0.838 ± 5)			C
1.725 ± 5			C
3.087 ± 5			B, C
3.105 ± 5			B, C

targets, however, only one level below $E_x = 2$ MeV has been found: $^{37}Cl^* = 1.713 \pm 0.010$ MeV (Sc 56c; $E_p = 4.6$–5.6 MeV).

For resonances, see ^{38}Ar.

D. ^{37}Ar(EC)^{37}Cl $Q_m = 816.0 \pm 1.5$

See ^{37}Ar.

E. ^{40}Ar(p, α)^{37}Cl $Q_m = 1592.3 \pm 2.2$

For resonances, see ^{41}K.

F. Not reported:

^{36}S(p, γ)^{37}Cl	$Q_m = 8401 \pm 9$
^{36}S(d, n)^{37}Cl	$Q_m = 6177 \pm 9$
^{36}S(^{3}He, d)^{37}Cl	$Q_m = 2908 \pm 9$
^{36}S(α, t)^{37}Cl	$Q_m = -11411 \pm 9$
^{38}Ar(n, d)^{37}Cl	$Q_m = -8018.0 \pm 1.0$
^{38}Ar(d, ^{3}He)^{37}Cl	$Q_m = -4749.5 \pm 0.9$
^{38}Ar(t, α)^{37}Cl	$Q_m = 9570.0 \pm 1.0$
^{39}K(n, ^{3}He)^{37}Cl	$Q_m = -8892.0 \pm 3.5$

^{37}Ar

(Fig. 37.3, p. 223; table 37.3, p. 224)

A. ^{37}Ar(EC)^{37}Cl $Q_m = 816.0 \pm 1.5$

The weighted mean half-life is 34.33 ± 0.15 days (Ki 59, Mi 52a, We 44); $\log ft = 5.0$. Shape and intensity of the internal bremsstrahlung spectrum have been investigated by several authors (An 53, Em 54, Li 55b, Sa 56). The results are in agreement with theory, taking account of capture from P states (Gl 56). The end point is in agreement with the decay energy computed from the threshold for the ^{37}Cl(p, n)^{37}Ar reaction. The decay energy has also been obtained from recoil measurements as 814 ± 2 keV (Sn 55) and 812 ± 8 keV (Ko 54b; also Ru 55b). The L- to K-capture ratio is 0.102 ± 0.003 (weighted mean of Sa 60b, Ki 59, La 56b; see also Po 49a). For other small effects (e.g. the production of double holes in the K shell), see Mi 54, Wo 54a, Ki 59. Theoretical discussion of the matrix element, Go 56b, Gr 56c.

The circular polarization of the internal bremsstrahlung has been measured as $P = 0.97 \pm 0.15$ (Ma 58c, d) and 1.03 ± 0.04 (Ha 58b, Ha 59d).

The cross section of the inverse reaction ^{37}Cl($\bar{\nu}$, e$^-$)^{37}Ar is smaller than 2.5×10^{-46} cm^2 (Da 59).

B. ^{34}S(α, n)^{37}Ar $Q_m = -4628.7 \pm 3.4$

For threshold measurement, see Ne 61.

C. ^{36}Ar(n, γ)^{37}Ar $Q_m = 8794.2 \pm 4.0$

The thermal neutron activation cross section is 6 ± 2 b (Hu 58).

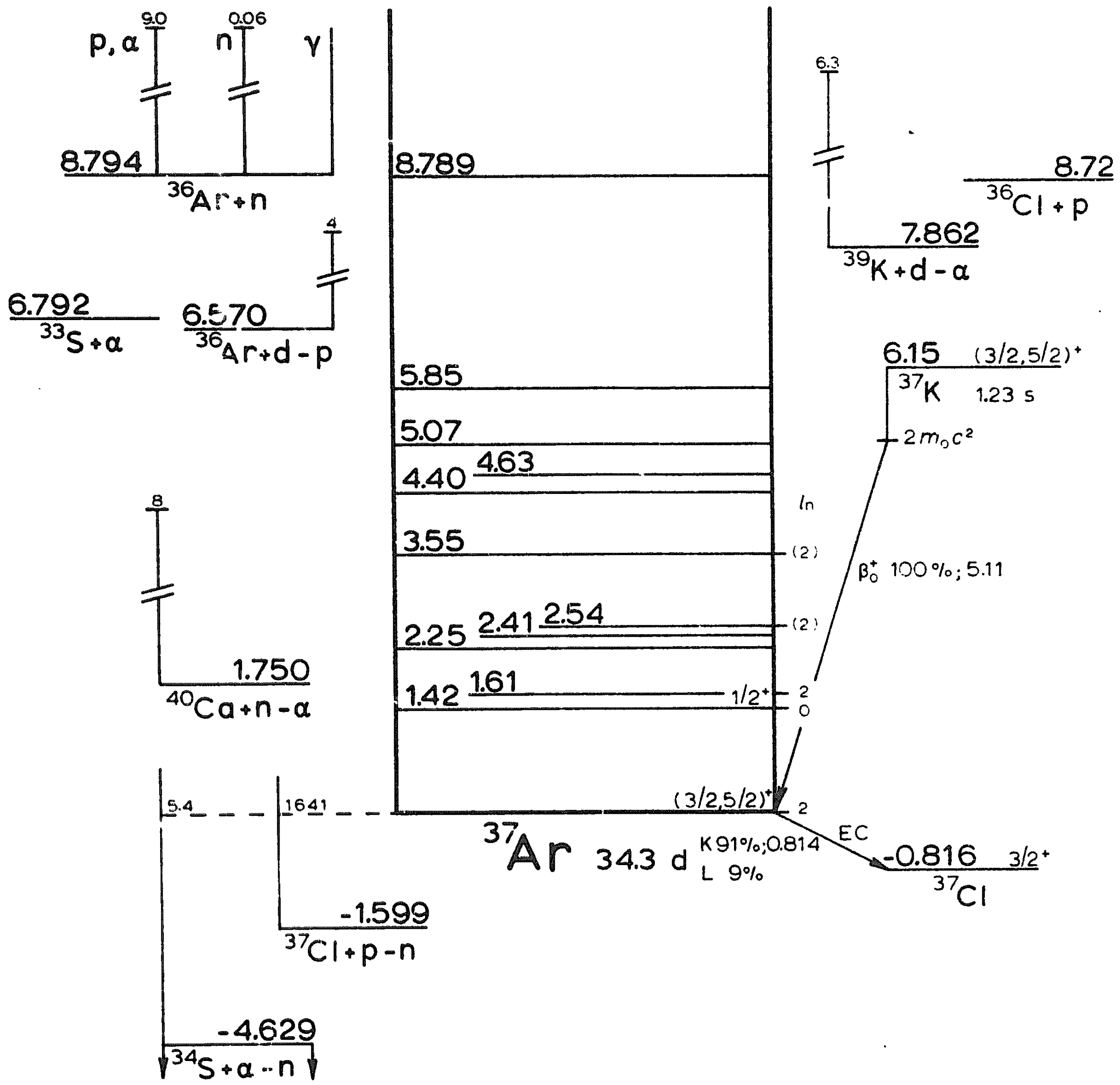

Fig. 37.3. Energy levels of ^{37}Ar.

D. ^{36}Ar(n, n)^{36}Ar $\qquad E_b = 8794.2 \pm 4.0$

Analysis of the scattering cross section measured in the $E_n = 0.1$–6×10^4 eV range, yields a resonance at $E_n = -5.4$ keV, with $\Gamma_n = 50$ eV, and $\Gamma_\gamma = 1.0$ eV (Ch 60). See also He 57a.

E. (a) ^{36}Ar(n, p)^{36}Cl $\qquad Q_m = 71.2 \pm 4.3 \qquad E_b = 8794.2 \pm 4.0$

(b) ^{36}Ar(n, α)^{33}S $\qquad Q_m = 2002.1 \pm 4.1 \qquad E_b = 8794.2 \pm 4.0$

Pronounced resonance structure has been observed in the $E_n = 1.2$–9.0 MeV region (Da 61b). For non-resonance data, see ^{33}S and ^{36}Cl.

F. ^{36}Ar(d, p)^{37}Ar $\qquad Q_m = 6569.5 \pm 4.0$

Deuteron bombardment of argon gas enriched in ^{36}Ar content yields the

TABLE 37.3

Energy levels of ^{37}Ar

E_x (MeV ±keV)	J^π	$\tau_{\frac{1}{2}}$ or Γ	Decay	Reactions
0	$(\frac{3}{2}, \frac{5}{2})^+$	34.33±0.15 days	EC	many
1.42 ±10	$\frac{1}{2}^+$			F, G
1.61 ±10	$(\frac{3}{2}, \frac{5}{2})^+$			F, G
2.25 ±10				F, G
2.41 ±10				G
2.54 ±50				F
3.55 ±50				F
4.40				F
4.63				F
5.07				F
5.85				F
8.789± 4		50 eV	n	D

TABLE 37.4

Levels in ^{37}Ar from the ^{36}Ar(d, p)^{37}Ar reaction

^{37}Ar* [a] (MeV)	^{37}Ar* [b] (MeV)	^{37}Ar* [c] (MeV)	l_n [c]
0	0	0	2 [d]
1.53	1.44	1.39±0.06	0
1.67		1.63±0.06	2
2.27			
2.56	2.56	2.54±0.05	(2)
3.46	3.54	3.55±0.05	(2)
	4.40		
	4.63		
5.01	5.07		
	5.85		

[a] Da 49; E_d = 3.4 MeV.
[b] Zu 50; E_d = 3.9 MeV.
[c] Ya 61; E_d = 3.85 MeV.
[d] Also Su 59a; E_d = 4 MeV.

^{37}Ar excitation energies and l_n values listed in table 37.4; $Q_0 = 6.59\pm0.03$ MeV (Da 49), 6.49±0.08 MeV (Zu 50), 6.55±0.05 MeV (Ya 61).

G. ^{37}Cl(p, n)^{37}Ar $\qquad Q_m = -1598.6\pm1.5$

The threshold has been measured as $E_p = 1640\pm4$ keV (Ri 50), 1641±2 keV (Sc 52a). Neutron groups have been observed to ^{37}Ar* = 1.42, 1.61, 2.25, and 2.41 MeV, all ±0.01 MeV; $Q_0 = -1.64$ MeV (Fe 59; see also St 52a, Gr 50c).

Cross section, Jo 58, Sc 58a. For resonances, see ^{38}Ar.

H. ^{37}K(β^+)^{37}Ar $\qquad Q_m = 6150\pm50$

See ^{37}K.

I. ^{39}K(d, α)^{37}Ar $Q_m = 7861.9 \pm 3.8$

Observed, We 44.

J. ^{40}Ca(n, α)^{37}Ar $Q_m = 1750.2 \pm 4.3$

Cross section measurements, Ba 60c, Mu 58a. With emulsion techniques, $Q_0 = 2.0 \pm 0.44$ MeV has been found (Mu 58a).

K. Not reported:

^{35}Cl(t, n)^{37}Ar	$Q_m = 8817.5 \pm 3.5$
^{35}Cl(^{3}He, p)^{37}Ar	$Q_m = 9581.9 \pm 3.5$
^{35}Cl(α, d)^{37}Ar	$Q_m = -8770.5 \pm 3.5$
^{36}Ar(t, d)^{37}Ar	$Q_m = 2536.6 \pm 4.0$
^{36}Ar(α, ^{3}He)^{37}Ar	$Q_m = -11783.0 \pm 4.0$
^{37}Cl(^{3}He, t)^{37}Ar	$Q_m = -834.1 \pm 1.5$
^{38}Ar(p, d)^{37}Ar	$Q_m = -9616.6 \pm 1.7$
^{38}Ar(d, t)^{37}Ar	$Q_m = -5583.7 \pm 1.8$
^{38}Ar(^{3}He, α)^{37}Ar	$Q_m = 8735.9 \pm 1.8$
^{39}K(n, t)^{37}Ar	$Q_m = -9726.1 \pm 3.8$
^{39}K(p, ^{3}He)^{37}Ar	$Q_m = -10490.6 \pm 3.7$

^{37}K

(Fig. 37.4, p. 226; table 37.5, p. 226)

A. ^{37}K(β^+)^{37}Ar $Q_m = 6150 \pm 50$

The half-life is 1.23 ± 0.02 sec (weighted mean of Sc 58b, Su 58, Wa 60a, Bo 51, La 48). The β^+ end point is 5.15 ± 0.07 MeV (Wa 60a), 5.10 ± 0.07 MeV (Su 58), 5.06 ± 0.11 MeV (Ki 54b). The transition is super-allowed, with $\log ft = 3.6$.

B. ^{36}Ar(p, γ)^{37}K $Q_m = 1860 \pm 50$

No resonances have been found in the range $E_p = 0.5$–1.8 MeV with targets containing separated ^{36}Ar (Br 48a).

C. ^{36}Ar(p, p)^{36}Ar $E_b = 1860 \pm 50$

The elastic scattering differential cross section has been measured in the $E_p = 1.0$–1.8 MeV region; an anomaly at $E_p = 1.494$ MeV corresponds with ^{37}K* $= 3.31$ MeV; $J = \frac{1}{2}$ (Ki 61a).

D. ^{36}Ar(d, n)^{37}K $Q_m = -360 \pm 50$

At $E_d = 3.85$ MeV, two neutron groups have been observed with $Q = -0.32 \pm 0.10$ and -1.78 ± 0.10 MeV, corresponding to the ground state and a ^{37}K level (or doublet) at 1.46 ± 0.10 MeV; angular distribution measurement yields $l_p = 2$ and $0+2$, respectively (Ya 61).

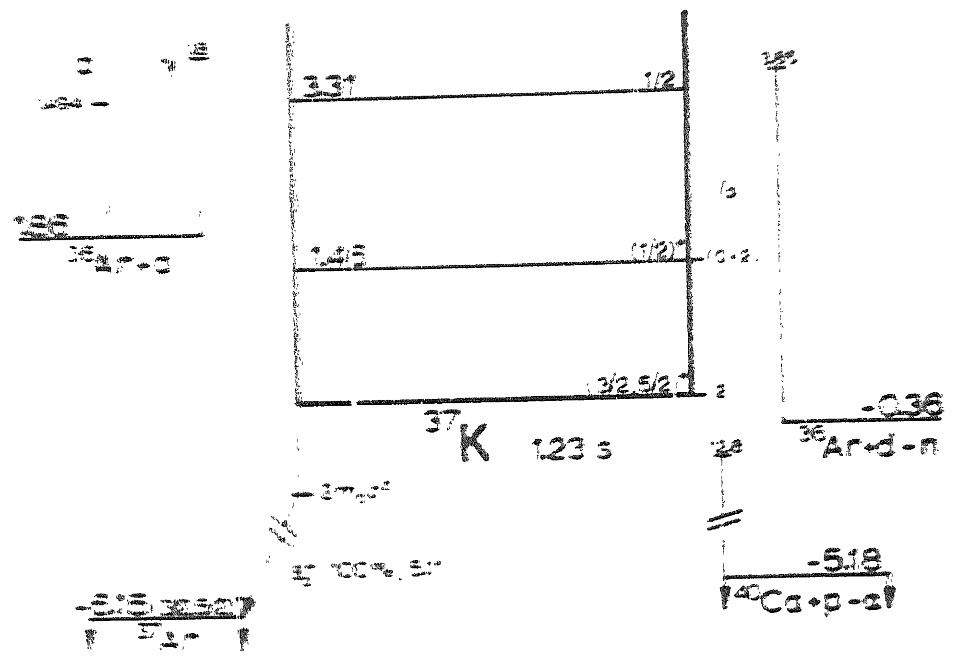

Fig. 37.4. Energy levels of ^{37}K.

TABLE 37.4

Energy levels of ^{37}K

E_x (MeV)	J^π	τ_m	Decay	Reactions
0	$(\frac{3}{2}, \frac{5}{2})^+$	1.23 ± 0.02 sec	β^+	A, B
1.46 ± 0.03	$(\frac{1}{2})^+$	unbound		B
3.31	$\frac{1}{2}$		p	C

E. [illegible] $Q_m = -5180 \pm 30$

At E_p = [illegible] MeV ^{37}K has been produced (Su 58).

F. Not reported

[illegible] $Q_m = 2550 \pm 50$

[illegible] $Q_m = -3630 \pm 50$

[illegible] $Q_m = -17950 \pm 50$

[illegible] $Q_m = -16660 \pm 50$

^{38}S

(Not illustrated; see fig. 38.1, p. 228)

A. $^{38}S(\beta^-)^{38}Cl$ $Q_m = 3000 \pm 150$

At E_α = 44 MeV, ^{38}S has been produced in the reaction $^{37}Cl(\alpha, 3p)^{38}S$. The half-life is 172 ± 1 min. The main β^- branch ($\approx 95\%$), with end point 1.1 ± 0.1 MeV proceeds to a 1.88 MeV level of ^{38}Cl. The 1.88 MeV γ ray has been observed in coincidence with β^-. The transition is allowed (log ft = 5.0), giving $J^\pi = 1^+(0^+)$ for ^{38}Cl(1.88). A (5±3)% β^- branch, with end point 3.0±0.2 MeV, proceeds to ^{38}Cl(0). This once-forbidden $0^+ \to 2^-$ transition has log ft = 8.2, log $(W_0^2-1)\,ft$ = 9.9 (Ne 58).

B. Not reported:

^{36}S(t, p)^{38}S	Q_m = 3810±150
^{40}Ar(n, ^{3}He)^{38}S	Q_m = −15090±150

^{38}Cl

(Fig. 38.1, p. 228; table 38.1, p. 228)

A. ^{38}Cl(β^-)^{38}Ar $\quad Q_m$ = 4916±8

The half-life is 37.29±0.04 min (Co 50a; see also Ma 55b, En 54a).

The decay is complex. Three β^- branches and two γ rays have been observed; see table 38.2 for energies and relative intensities. The intensity of a potential 3.78 MeV cross-over γ ray is less than 0.3% per β^- particle (My 49). The shape of the high-energy β^- spectrum and its ft value, log ft = 7.5 and log $(W_0^2-1)\,ft$ = 9.5, are characteristic for unique once-forbidden transitions, thus $J^\pi(^{38}\text{Cl}) = 2^-$ (La 50a, Wu 50; theory Ko 58). The β^- transition to the 2.16 MeV level is also forbidden (log ft = 6.9), while that to the 3.78 MeV level is allowed (log ft = 4.9). From the data given above and from the measured γ-γ angular correlation (Wa 41, St 50, Kr 54a) and γ polarization (Br 58d), $J^\pi = 2^+$ and 3^- follow for ^{38}A* = 2.16 and 3.78 MeV, respectively. For β-γ angular correlation, see Ma 55b.

B. ^{37}Cl(n, γ)^{38}Cl $\quad Q_m$ = 6110±8

The thermal neutron capture cross section is 0.56±0.12 b (Hu 58). For the cross section at E_n = 25 keV, see Ko 58d.

From thermal neutron capture in separated ^{37}Cl, an isomeric state has been found emitting 660±20 keV γ rays with a half-life of 1.0±0.2 sec (Sc 54). In Po 59a are reported: E_γ = 663±12 keV and $\tau_{\frac{1}{2}}$ = 1.5±0.8 sec. The thermal neutron cross section for formation of ^{37}Cl^m is 5±3 mb (Hu 58).

C. ^{37}Cl(n, n)^{37}Cl $\quad E_b$ = 6110±8

With enriched material, resonances in the total neutron cross section have been observed at E_n = 8.8, 26.5, 47.4, 55.5, 65.0, and 94.2 keV, with Γ_n = 0.09, 0.33, 0.20, 0.18, 0.18, and 0.80 keV, respectively (Hu 58).

See also Bi 61.

D. ^{37}Cl(d, p)^{38}Cl $\quad Q_m$ = 3885±8

At E_d = 3.0 and 7.5 MeV, ten proton groups have been observed. The excitation energies of ^{38}Cl levels, the reduced widths, and l_n values are listed

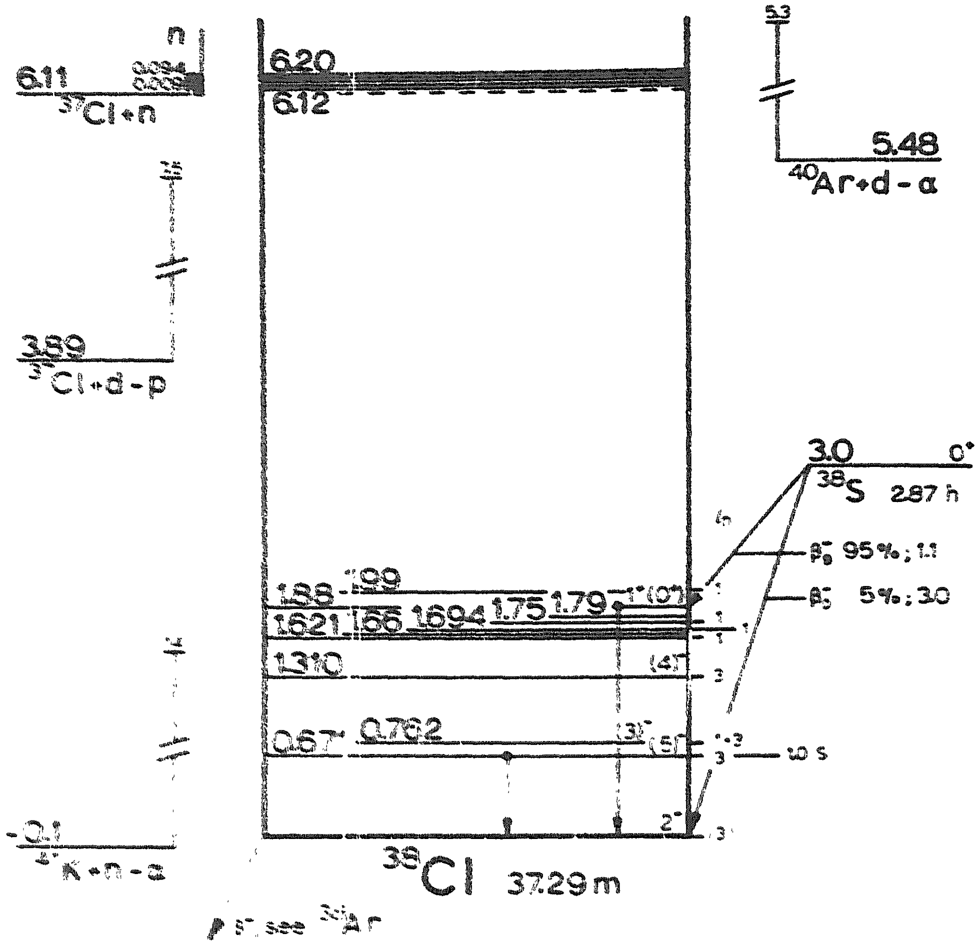

Fig. 38.1. Energy levels of ^{38}Cl.

TABLE 38.1

Energy levels of ^{38}Cl

E_x MeV ± keV	J^{π}	$\tau_{\frac{1}{2}}$	Decay	Reactions
0	2⁻	37.29 ± 0.04 min	β^-	A, D, E, F, G, H
0.671 ± 3	5⁻	1.0 ± 0.2 sec	γ	B, D
0.762 ± 4	3⁻			D
1.310 ± 4	4⁻			D
1.621 ± 5	≤ 3⁻			D
1.656 ± 7				D
1.694 ± 7	≤ 3⁻			D
1.745 ± 7	≤ 3⁻			D
1.784 ± 8				D
1.88	1⁻ 0⁻		γ	E
1.985 ± 7	≤ 3⁻			D
6.119 ± [illegible]			n	C
6.136 ± [illegible]			n	C
6.158 ± [illegible]			n	C
6.164 ± [illegible]			n	C
6.179 ± [illegible]			n	C
6.202 ± [illegible]			n	C

TABLE 38.2

Beta decay of ^{38}Cl

E_{β_0} (MeV)	E_{β_1} (MeV)	E_{β_2} (MeV)	E_{γ_1} (MeV)	E_{γ_2} (MeV)	Ref.
4.99±0.06		1.08±0.06			Wa 39
			2.15 (57%)	1.65 (43%)	Cu 40
			2.19±0.03 (53%)	1.64±0.02 (47%)	It 41
5.2 (53%)	2.70 (11%)	1.19 (36%)	2.15 (57%)	1.60 (43%)	Ho 46
4.81±0.05 (53.4%)	2.77±0.05 (15.8%)	1.11±0.01 (30.8%)			Lo 50a

TABLE 38.3

Levels of ^{38}Cl from ^{37}Cl(d, p)^{38}Cl

^{38}Cl* [a] (MeV±keV)	^{38}Cl* [b] (MeV±keV)	l_n [b]	$(2J+1)\theta_n^2$ [b] × 10^3
0	0	– [c]	– [c]
0.672±5	0.671±5	3	200
0.762±5	0.761±5	1, 3	24, 70
1.312±6	1.309±6	3	110
1.620±7	1.622±6	1	39
1.658±7			
1.693±7	1.695±6	1	79
	1.748±7	1	32
	1.789±8		
	1.986±7	1	102

[a] Pa 55c; E_d = 3.0 and 7.5 MeV.
[b] Ho 61b; E_d = 7.5 MeV.
[c] Angular distribution incomplete because of interference with a ^{35}Cl(d, p)^{36}Cl group.

in table 38.3; Q_0 = 3.877±0.008 MeV (Pa 55c), 3.878±0.008 MeV (Ho 61b). The intensity ratio of the proton groups leading to ^{38}Cl(0) and (1) is 0.43±0.04, as measured at E_d = 5.6 MeV, in agreement with $J^\pi = 2^-$ and 5^- assignments, respectively (Pa 55c).

E. ^{38}S(β^-)^{38}Cl $\qquad$ Q_m = 3000±150

See ^{38}S.

F. ^{40}Ar(γ, np)^{38}Cl $\qquad$ Q_m = −20593±8

Cross section for E_γ = 20–45 MeV, Pe 59.

G. ^{40}Ar(d, α)^{38}Cl $\qquad$ Q_m = 5477±8

Perhaps observed, En 54a.

H. ^{41}K(n, α)^{38}Cl $\qquad$ Q_m = −98±9

Cross-section measurements at E_n = 14 MeV, Pa 53, Bo 60d.

I. Not reported:

^{34}S(t, n)^{36}Cl	$Q_m = 6029\pm12$
^{34}S(^{3}He, p)^{36}Cl	$Q_m = 6793\pm12$
^{36}S(α, d)^{38}Cl	$Q_m = -11559\pm12$
^{37}Cl(t, d)^{38}Cl	$Q_m = -148\pm8$
^{37}Cl(α, ^{3}He)^{38}Cl	$Q_m = -14467\pm8$
^{38}Ar(n, p)^{38}Cl	$Q_m = -4133\pm8$
^{38}Ar(t, ^{3}He)^{38}Cl	$Q_m = -4897\pm8$
^{40}Ar(n, t)^{38}Cl	$Q_m = -12111\pm8$
^{40}Ar(p, ^{3}He)^{38}Cl	$Q_m = -12875\pm8$

REMARKS

For pure *jj* coupling, a linear relation can be derived between excitation energies of $(d_{\frac{3}{2}}, f_{\frac{7}{2}})$ states in ^{38}Cl and those of $(d_{\frac{3}{2}}^{-1}, f_{\frac{7}{2}})$ states in ^{40}K. From known excitation energies and spins in ^{40}K calculation yields ^{38}Cl levels at 0, 0.702, 0.751, and 1.328 MeV, with $J^\pi = 2^-, 5^-, 3^-$, and 4^-, respectively (Go 56a, Pa 56a, Pa 57a), in very good agreement with experiment.

^{38}Ar

(Fig. 38.2, p. 231; table 38.4, p. 231)

A. ^{35}Cl(α, p)^{38}Ar $\qquad Q_m = 846.1\pm3.4$

At $E_\alpha = 7.5$ MeV, bombardment of enriched ^{35}Cl targets yields proton groups to ^{38}Ar* $= 2.13\pm0.04$ and 3.73 ± 0.04 MeV; $Q_0 = 0.81\pm0.08$ MeV (Kr 53).

B. (a) ^{37}Cl(p, γ)^{38}Ar $\qquad Q_m = 10242.7\pm0.9$

(b) ^{37}Cl(p, p)^{37}Cl $\qquad E_b = 10242.7\pm0.9$

Resonances found with enriched ^{37}Cl targets in the range $E_p = 0.3$–0.9 MeV (Ku 61), 0.5–1.0 MeV (Li 60b), and 0.8–1.8 MeV (To 57) are listed in table 38.5, with the excitation energies of corresponding ^{38}Ar levels, widths, and main modes of decay. See fig. 38.2 for the decay of the intermediate states.

Older work with natural chlorine targets, Br 51, Ta 46, Cu 39. For the reaction Cl(p, p), see also Ru 59.

For non-resonance data, see ^{37}Cl.

C. ^{37}Cl(p, n)^{37}Ar $\qquad Q_m = -1598.6\pm1.5 \quad E_b = 10242.7\pm0.9$

From threshold ($E_p = 1641\pm2$ keV) to 2150 keV, 130 resonances have been found; for energies (±0.1%), widths (resolution 1.4 keV at $E_p = 1800$ keV) and relative intensities, see Sc 52a. See also Bl 51, Br 51, Jo 58. The 150 resonances (not tabulated) observed in the range $E_p = 1.64$–2.9 MeV form two distinct groups which may be associated with giant resonance splitting (Ma 61).

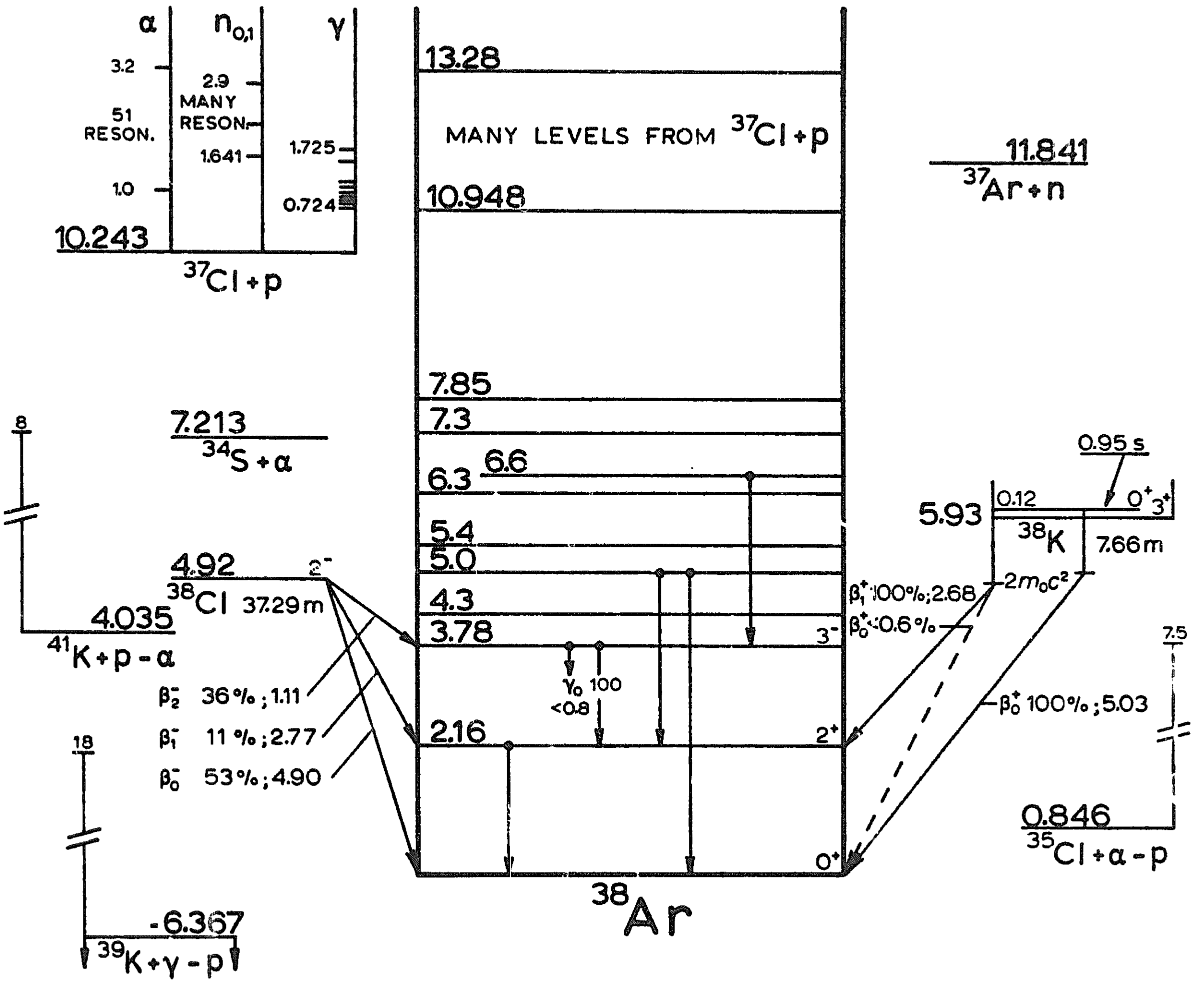

Fig. 38.2. Energy levels of ^{38}Ar.

TABLE 38.4

Energy levels of ^{38}Ar

E_x (MeV ± keV)	J^π	Decay	Reactions
0	0^+	stable	A, B, E, F, G, H
2.158 ± 13	2^+	γ	A, B, E, F, G, H
3.78 ± 20	3^-	γ	A, B, E, G
4.3			G
5.0		γ	B, G
5.4			G
6.3			G
6.6		γ	B, G
7.3			G
7.85			G
10.948–11.923; 10 levels, see table 38.5 and reaction			B
For levels with $E_x > 11$ MeV, see also reactions			C, D

Table [illegible]

Resonances in ^{37}Cl(p, γ)^{38}Ar

E_p keV	^{38}Ar* MeV	$(2J+1)\Gamma_p\Gamma_\gamma/\Gamma$ meV	Decay[d] γ_0	γ_1	γ_2	γ_6	γ_7
[illegible] ± [illegible][b]	[illegible]	[illegible][a]		✓	✓		
[illegible] ± [illegible][b]	[illegible]	[illegible][a]		✓	(✓[e])		
[illegible] ± [illegible][b]	[illegible]	[illegible][a]		✓	✓		
[illegible] ± [illegible][b]	[illegible]	[illegible][a]	✓	✓	✓		
[illegible] ± [illegible][b]	[illegible]	[illegible][a]		✓[e]	✓		
[illegible] ± [illegible][a]	[illegible]	[illegible][a]		✓			
[illegible] ± [illegible]	[illegible]	[illegible] × [illegible][c]		✓	✓	✓	
[illegible] ± [illegible]	[illegible]	[illegible] × [illegible][c]		✓	✓	✓	
[illegible] ± [illegible][f]	[illegible]	[illegible] × [illegible][c]		✓		✓	
[illegible] ± [illegible]	[illegible]						✓

[a] [illegible]

[b] Resonance energies (with [illegible] keV errors) reported in [illegible] are in agreement with the energies listed.

[c] [illegible]

[d] The γ_0, γ_1, γ_2, γ_6 and γ_7 stand for transitions to ^{38}Ar* = 0, 2.16, 3.75, 5.0, and 6.6 MeV, respectively. For resonances with E_p < 1000 keV, see [illegible]; for E_p > 1000 keV, see To 57.

[e] Not reported in [illegible].

[f] Angular distribution of γ_1, [illegible].

The yield of [illegible] shows broad maxima similar to those in the yield of ground-state neutrons ([illegible]).

For threshold measurements and neutron groups, see ^{37}Ar.

D. ^{37}Cl(p, α)^{34}S $\quad Q_m = 3030.1 \pm 3.1 \quad E_b = 10242.7 \pm 0.9$

In the range E_p = 1.[illegible]–3.12 MeV, 51 resonances (not tabulated) have been observed. For a discussion of the widths, strengths, and level spacing, see Cl 60. See also Br 51.

For Q_0 value and α-particle groups, see ^{34}S.

E. ^{38}Cl(β⁻)^{38}Ar $\quad Q_m = 4916 \pm 8$

See ^{38}Cl.

F. ^{38}K(β⁺)^{38}Ar $\quad Q_m = 5929 \pm 11$

See ^{38}K.

G. ^{39}K(γ, p)^{38}Ar $\quad Q_m = -6367.2 \pm 3.6$

Proton groups to ^{38}Ar* = 0, 2.16, 3.75, 4.5, 5.0, 5.4, 6.3, 6.6, 7.3, and 7.85 MeV have been observed at E_γ = 17.6 MeV (Op 58).

Cross section, Ka 56a.

H. ^{41}K(p, α)^{38}Ar $\quad Q_m = 4035.2 \pm 4.8$

Magnetic analysis at E_p = 1.9 MeV gives $Q_0 = 4.002 \pm 0.020$ MeV (Cl 60); at E_p = 7 and 4 MeV $Q_0 = 4.008 \pm 0.008$ MeV (Bi 59). In the range E_p = 2.5–3.5 MeV, a 2.16 MeV γ ray has been observed in coincidence with α-particles; its angular distribution is isotropic (Sh 58c, Sh 59a, Sh 61).

For resonances, see ^{42}Ca.

I. Not reported:

^{36}S(^{3}He, n)^{38}Ar	$Q_m =$ 10926 ± 9
^{36}Ar(t, p)^{38}Ar	$Q_m =$ 12153.2 ± 3.8
^{37}Cl(d, n)^{38}Ar	$Q_m =$ 8018.0 ± 1.0
^{37}Cl(^{3}He, d)^{38}Ar	$Q_m =$ 4749.5 ± 0.9
^{37}Cl(α, t)^{38}Ar	$Q_m = -$ 9570.0 ± 1.0
^{39}K(n, d)^{38}Ar	$Q_m = -$ 4142.4 ± 3.6
^{39}K(d, ^{3}He)^{38}Ar	$Q_m = -$ 374.0 ± 3.6
^{39}K(t, α)^{38}Ar	$Q_m =$ 13445.5 ± 3.6
^{40}Ar(p, t)^{38}Ar	$Q_m = -$ 7977.7 ± 2.3
^{40}Ca(n, ^{3}He)^{38}Ar	$Q_m = -$ 6985.7 ± 4.1

REMARKS

Theoretical discussions on low-lying excited states in ^{38}Ar, Th 56, Ta 54.

^{38}K

(Fig. 38.3, p. 234; table 38.6, p. 234)

A. (a) ^{38}K(β^+)^{38}Ar $\quad Q_m = 5929 \pm 11$

The weighted mean of the half-life measurements for which errors have been given is 7.66 $\pm$ 0.03 min (Ri 37, He 37a, Hu 37, Gr 56, Cl 57).

The β^+ spectrum has the allowed shape, with a 2.68 $\pm$ 0.03 MeV end point; log ft = 5.0. The β^+ decay is followed by a 2.16 $\pm$ 0.03 MeV γ ray (Ti 51). The intensity of a possible higher energy β^+ transition is less than 0.6% of the main transition (Gr 56). These results yield J^π(^{38}K) = (2,3)$^+$.

For a jj-coupling calculation of the β^+ matrix element, see Gr 56c.

(b) ^{38}K^m(β^+)^{38}Ar $\quad Q_m = 6052 \pm 14$

The half-life is 0.946 $\pm$ 0.005 sec (weighted mean of St 53b, Kl 54b, Cl 57, Mi 58, Ja 60a, Li 60a). The β^+ end point is 5.00 $\pm$ 0.10 MeV (Ju 61), 5.06 $\pm$ 0.11 MeV (Hu 54a). The super-allowed (log ft = 3.5) character of this transition yields a $J^\pi = 0^+$, $T = 1$ assignment to the isomeric state. The occurrence of isomerism requires a spin difference with the ground state of at least 3, which determines, with the results mentioned above, J^π(^{38}K) = 3$^+$. For theoretical discussions concerning the isobaric spin of levels in ^{38}K, see Mo 54, Ta 54, Wi 56a.

The absence of ^{38}K in meteorites contradicts the hypothesis of a long-lived ^{38}K isomeric state (Vo 59).

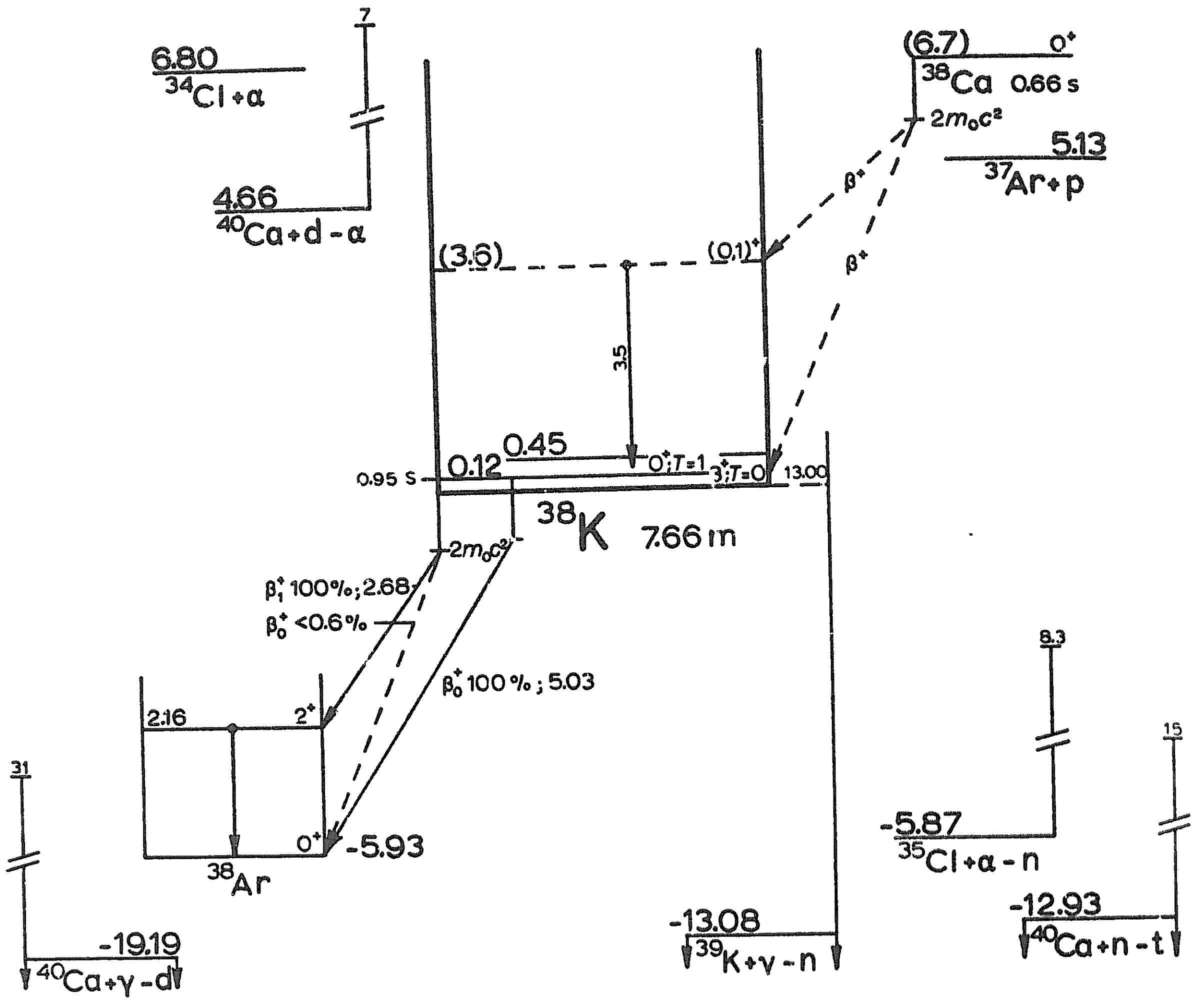

Fig. 38.3. Energy levels of ³⁸K.

TABLE 38.6

Energy levels of ³⁸K

E_x (MeV ± keV)	J^π; T	$\tau_{\frac{1}{2}}$	Decay	Reactions
0	3+; 0	7.66 ±0.03 min	β^+	A, B, D, E, F, G
0.123± 8	0+; 1	0.946±0.005 sec	β^+	A, C, D, G
0.45 ±10				G
(3.6)	(0, 1)+		γ	C

B. ^{35}Cl(α, n)^{38}K $Q_m = -5866 \pm 11$

The ground-state Q value has been measured as $Q_0 = -5.89 \pm 0.06$ MeV (Sm. 61).

C. ^{38}Ca(β^+)^{38}K $Q_{\text{estimated}} = 6700$

See ³⁸Ca.

D. (a) $^{39}K(\gamma, n)^{38}K$ $Q_m = -13079 \pm 11$
(b) $^{39}K(\gamma, n)^{38}K^m$ $Q_m = -13202 \pm 14$

The threshold for the production of the 7.7 min activity has been measured as $\leq 13.125 \pm 0.038$ MeV (Ge 60a), 13.2 ± 0.2 MeV (Mc 49), and 13.00 MeV (De 55). Cross-section measurements, see Wa 48, Mc 50, Ed 52. See also Em 59a.

Production of $^{38}K^m$, see Cl 57.

E. $^{40}Ca(\gamma, d)^{38}K$ $Q_m = -19191 \pm 10$

Cross section, Fe 60.

F. $^{40}Ca(n, t)^{38}K$ $Q_m = -12933 \pm 10$

Upper limit of the cross section at $E_n = 14.6$ MeV, Ba 61f.

G. $^{40}Ca(d, \alpha)^{38}K$ $Q_m = 4655 \pm 10$

At deuteron energies up to 7 MeV, two α-particle groups have been observed, to $^{38}K^* = 0$ and 0.45 ± 0.01 MeV; $Q_0 = 4.650 \pm 0.010$ MeV (Br 56f). A new group, corresponding to $^{38}K^* = 0.123 \pm 0.008$ MeV, with about one tenth of the intensity of the two known groups, has been found at $E_d = 3.2$–4.1 MeV. This level presumably is the $T = 1$, $J = 0^+$ state expected at about this energy (Ha 59c). For a discussion of the relative intensities of the groups, see Ha 59c.

H. Not reported:

$^{36}Ar(t, n)^{38}K$	$Q_m = 5441 \pm 11$
$^{36}Ar(^3He, p)^{38}K$	$Q_m = 6206 \pm 11$
$^{36}Ar(\alpha, d)^{38}K$	$Q_m = -12147 \pm 11$
$^{38}Ar(p, n)^{38}K$	$Q_m = -6712 \pm 11$
$^{38}Ar(^3He, t)^{38}K$	$Q_m = -5947 \pm 11$
$^{39}K(p, d)^{38}K$	$Q_m = -10854 \pm 11$
$^{39}K(d, t)^{38}K$	$Q_m = -6821 \pm 11$
$^{39}K(^3He, \alpha)^{38}K$	$Q_m = 7498 \pm 11$
$^{40}Ca(p, ^3He)^{38}K$	$Q_m = -13697 \pm 10$

REMARKS

For a theoretical discussion of $(d_{\frac{3}{2}}^{-1}, d_{\frac{3}{2}}^{-1})$ levels, see Pa 61b.

^{38}Ca

(Not illustrated; see fig. 38.3, p. 234)

A. $^{38}Ca(\beta^+)^{38}K$ $Q_{estimated} = 6700$

Calcium targets irradiated with 85 MeV bremsstrahlung yield 3.5 ± 0.1 MeV γ rays with a half-life of 0.66 ± 0.05 sec. This activity is interpreted as a transition in ^{38}K (presumably to $^{38}K^* = 0$ or 0.12 MeV) following a branching of the β^+ decay of ^{38}Ca, produced in the $^{40}Ca(\gamma, 2n)^{38}$Ca reaction.

The occurence of this β^+ branch (only γ rays have been observed) in competition with a super-allowed transition to $^{38}K^* = 0.12$ MeV (not observed since other β^+ transitions with about the same end point occur simultaneously) suggests a $J^\pi = 1^+$, $T = 0$ assignment to $^{38}K^* = 3.6$ MeV, but $J^\pi = 0^+, T = 1$ is also possible (Cl 57); in the latter case, the 3.5 MeV γ ray probably would not feed the ground state or 0.12 MeV level, but the 0.45 MeV level (presumably $J^\pi = 1^+$).

An estimate of the ^{38}Ca mass excess from Coulomb energy systematics yields the Q values for reactions A and B.

B. Not reported:

$^{36}Ar(^3He, n)^{38}$Ca $Q_{\text{estimated}} = -1300$

^{39}Cl

(Not illustrated; see fig. 39.1, p. 238; table 39.1, p. 236)

A. $^{39}Cl(\beta^-)^{39}$Ar $Q_m = 3430 \pm 21$

The half-life is 55.5 ± 0.2 min (Ha 50a), 56.5 min (Ru 52).

The decay is complex. By magnetic spectrometer, three branches are observed with the following end points and intensities: 3.45 ± 0.02 MeV (7 ± 2)%, 2.18 MeV (8 ± 4)%, and 1.91 ± 0.02 MeV (85 ± 6)%. The shape of the high-energy branch is characteristic of unique, once-forbidden transitions ($\Delta J = 2$, yes).

TABLE 39.1

Energy levels of ^{39}Cl

E_x (MeV)	J^π	$\tau_{\frac{1}{2}}$	Decay	Reactions
0	$\frac{3}{2}^+$	55.5 ± 0.2 min	β^-	A, B, C, D
0.364 ± 0.030				D
(0.8 ± 0.2)	$(\frac{1}{2}^+)$			C

Three γ rays are observd with the following energies and relative intensities: $E_{\gamma_1} = 0.246 \pm 0.003$ MeV (0.9 ± 0.1), $E_{\gamma_2} = 1.266 \pm 0.010$ MeV (1), $E_{\gamma_3} = 1.520 \pm 0.010$ MeV (0.85 ± 0.05). Upper limits of 2.1×10^{-3}, 1.6×10^{-3}, and 3.2×10^{-3} are given for the conversion coefficients of γ_1, γ_2, and γ_3, respectively. Coincidence measurements yield the decay scheme given in fig. 39.1. From β_2–γ coincidences a half-life of $(9.5 \pm 0.5) \times 10^{-10}$ sec is found for $^{39}Ar^* = 1.52$ MeV. The log ft values for the β^- transitions to $^{39}Ar^* = 0, 1.27$, and 1.52 MeV, are 8.3, 6.8, and 5.6, respectively.

All data are in agreement with the assignments $J^\pi = \frac{3}{2}^+$ to ^{39}Cl, and $J^\pi = \frac{7}{2}^-$, $(\frac{3}{2}, \frac{5}{2})^-$, and $\frac{3}{2}^+$ to $^{39}Ar^* = 0$, 1.27, and 1.52 MeV, respectively (Pe 56). See also Ha 50a.

For a jj-coupling computation of the β^- matrix element, see Gr 56c.

B. $^{36}S(\alpha, p)^{39}Cl$ $\qquad Q_m = -5714 \pm 23$

A 1.1 hr activity has been observed from the bombardment of sulphur by 16 MeV α particles (Ki 39a).

C. $^{40}Ar(\gamma, p)^{39}Cl$ $\qquad Q_m = -12523 \pm 22$

A threshold measurement yields $E_\gamma = 14.2 \pm 0.2$ MeV, not corrected for penetration of protons through the Coulomb barrier (Ha 50a).

For proton energy spectrum, see Wi 51 ($E_\gamma = 17.6$ MeV), Gu 58 ($E_\gamma = 15$ MeV). The proton angular distribution indicates the possible existence of a 0.8 ± 0.2 MeV excited state in ^{39}Cl, with $J^\pi = \frac{1}{2}^+$ (Gu 58). See also Em 59, Sp 55a, Ko 56.

Cross section, Mc 54a, Ia 58, Br 59e, Pe 59, Do 60a, Go 60.

D. $^{40}Ar(t, \alpha)^{39}Cl$ $\qquad Q_m = 7290 \pm 22$

Magnetic analysis at $E_t = 2.6$ MeV, yields α-particle groups to ^{39}Cl(0). $Q_0 = 7.259 \pm 0.040$, and to a level at 0.364 ± 0.030 MeV (Ja 61d).

E. Not reported:

$^{37}Cl(t, p)^{39}Cl$	$Q_m = 5698 \pm 22$
$^{40}Ar(n, d)^{39}Cl$	$Q_m = -10298 \pm 22$
$^{40}Ar(d, {}^3He)^{39}Cl$	$Q_m = -7030 \pm 22$
$^{41}K(n, {}^3He)^{39}Cl$	$Q_m = -12605 \pm 22$

^{39}Ar

(Fig. 39.1, p. 238; table 39.2, p. 238)

A. $^{39}Ar(\beta^-)^{39}K$ $\qquad Q_m = 565 \pm 5$

The half-life is 265 ± 30 yr (Ze 52).

The shape of the β^- spectrum, with end point 565 ± 5 keV is unique first forbidden ($\Delta J = 2$, yes) which agrees with the ft value; log $ft = 9.9$ and log $(W_0^2 - 1)\ ft = 10.4$ (Br 50) Gamma rays have not been observed (Br 50, An 52).

B. $^{38}Ar(n, \gamma)^{39}Ar$ $\qquad Q_m = 6585 \pm 6$

The thermal neutron activation cross section is 0.8 ± 0.2 b (Hu 58).

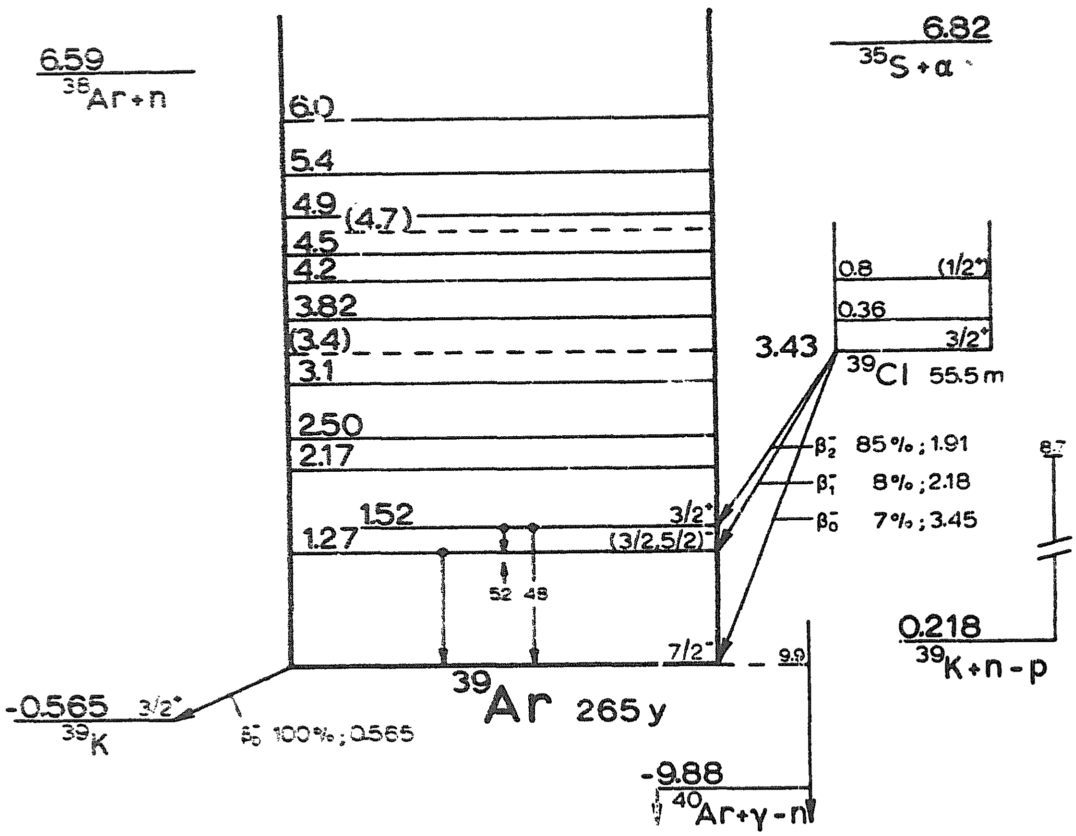

Fig. 39.1. Energy levels of ^{39}Ar.

TABLE 39.2

Energy levels of ^{39}Ar

E_x (MeV ± keV)	J^π	$\tau_{\frac{1}{2}}$	Decay	Reactions
0	$\frac{7}{2}^-$	265 ± 30 yr	β^-	A, C, D, E
1.270 ± 9	$(\frac{3}{2}, \frac{5}{2})^-$		γ	C, D
1.516 ± 9	$\frac{3}{2}^-$	(9.5 ± 0.5) × 10^{-10} sec	γ	C, D
2.17 ± 60				D
2.50 ± 40				D
3.10 ± 100				D
3.45 ± 100				D
3.82 ± 50				D
4.25 ± 100				D
4.52 ± 100				D
4.75 ± 100				D
4.94 ± 100				D
5.40 ± 100				D
6.0[illegible] ± 100				D

C. ^{39}Cl(β^-)^{39}Ar $\qquad Q_m = 3430 \pm 21$

See ^{39}Cl.

D. ^{39}K(n, p)^{39}Ar $\qquad Q_m = 218 \pm 5$

Bombardment of a KI scintillation crystal with monoenergetic neutrons in the range $E_n = 2.4$–8.7 MeV, yields proton groups leading to ^{39}Ar* = 0, 1.32, 1.57, 2.17, 2.52, all ± 0.05, 3.10 ± 0.10, (3.45 ± 0.10), 3.82 ± 0.05, 4.25, 4.52, (4.75), 4.94, 5.40, and 6.00, all ± 0.10 MeV. The groups to ^{39}Ar* = 1.32, 2.52, 3.82, and 5.40 MeV are strong (Ba 61g). In the range $E_n = 2.0$–5.5 MeV, pulse height analysis yields proton groups to ^{39}Ar* = 1.24 ± 0.05 and 2.46 ± 0.10 MeV, if $Q_0 = 0.20$ MeV is assumed (Sc 56a).

For cross section, see Li 58d, Bo 60d, Ba 61g, Di 61.

For resonances, see ^{40}K.

E. ^{40}Ar(γ, n)^{39}Ar $\qquad Q_m = -9875 \pm 6$

The threshold is 9.85 ± 0.15 MeV (Ha 54). For cross section, see Fe 54, Mc 54a, Ja 58, Fa 60.

F. Not reported:

^{36}S(α, n)^{39}Ar	$Q_m = -\ 3066 \pm 11$
^{37}Cl(t, n)^{39}Ar	$Q_m = \ 8345 \pm 6$
^{37}Cl(^{3}He, p)^{39}Ar	$Q_m = \ 9110 \pm 6$
^{37}Cl(α, d)^{39}Ar	$Q_m = -\ 9243 \pm 6$
^{38}Ar(d, p)^{39}Ar	$Q_m = \ 4360 \pm 6$
^{38}Ar(t, d)^{39}Ar	$Q_m = \ 327 \pm 6$
^{38}Ar(α, ^{3}He)^{39}Ar	$Q_m = -13992 \pm 6$
^{39}K(t, ^{3}He)^{39}Ar	$Q_m = -\ 547 \pm 5$
^{40}Ar(p, d)^{39}Ar	$Q_m = -\ 7651 \pm 6$
^{40}Ar(d, t)^{39}Ar	$Q_m = -\ 3618 \pm 6$
^{40}Ar(^{3}He, α)^{39}Ar	$Q_m = \ 10702 \pm 6$
^{41}K(n, t)^{39}Ar	$Q_m = -\ 9193 \pm 7$
^{41}K(p, ^{3}He)^{39}Ar	$Q_m = -\ 9957 \pm 7$
^{41}K(d, α)^{39}Ar	$Q_m = \ 8395 \pm 7$
^{42}Ca(n, α)^{39}Ar	$Q_m = \ 344 \pm 7$

^{39}K

(Fig. 39.2, p. 240; table 39.3, p. 240)

A. ^{36}Ar(α, p)^{39}K $\qquad Q_m = -1292.3 \pm 3.9$

At $E_\alpha = 7.4$ MeV, with enriched targets, Q values are observed of -1.28 ± 0.03, -3.78 ± 0.06, and -4.15 ± 0.04 MeV, corresponding to transitions to ^{39}K* = 0, 2.50, and 2.87 MeV (Sc 56b).

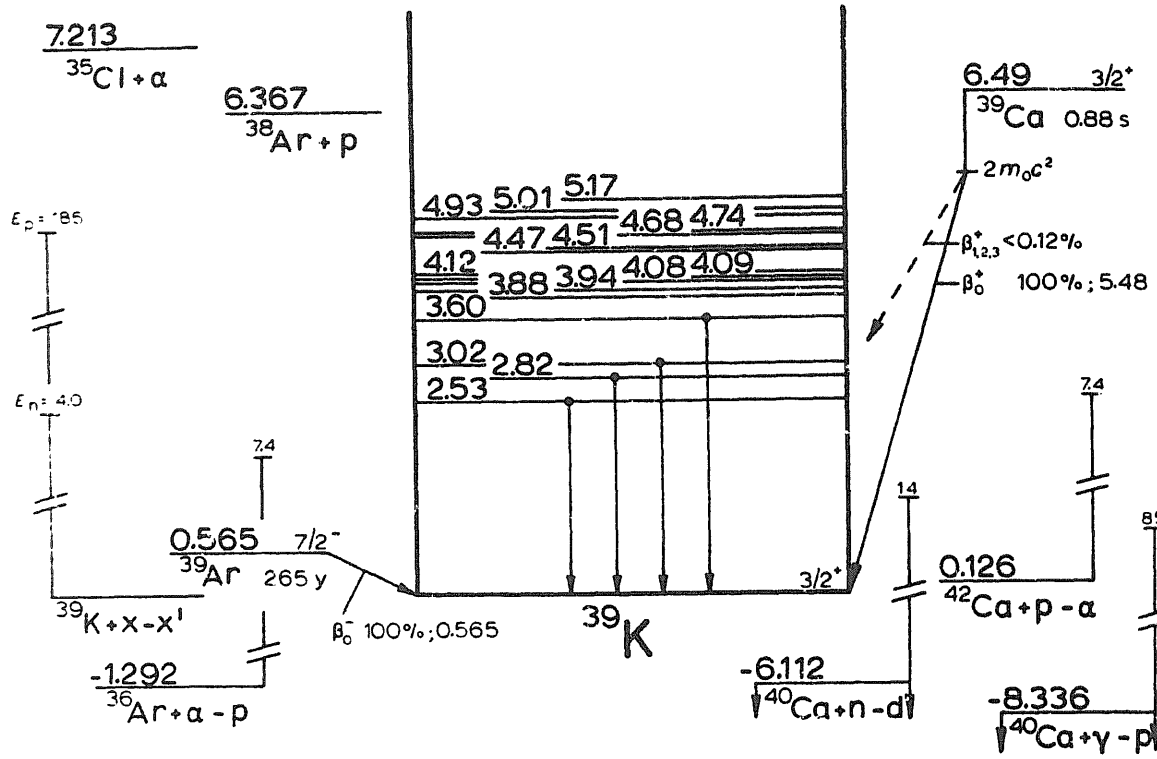

Fig. 39.2. Energy levels of ^{39}K.

TABLE 39.3

Energy levels of ^{39}K

E_x (MeV ± keV)	J^π	Decay	Reactions
0	$\frac{3}{2}^+$	stable	A, B, C, D, E, F, G, H
2.526±7		γ	A, C, D
2.817±7		γ	A, C, D
3.021±7		γ	C, D
3.603±7		γ	C, D
3.879–5.168; 12 levels, see reaction			D

B. ^{39}Ar(β^-)^{39}K $\qquad Q_m = 565 \pm 5$

See ^{39}Ar.

C. ^{39}K(n, n′)^{39}K

In the range $E_n = 2.5$–4.0 MeV, the cross section for inelastic neutron scattering to ^{39}K* = 2.52, 2.81, 3.05, and 3.59 MeV has been measured by observation of the γ rays de-exciting these levels to the ground state (Li 61). Angular distribution measurements of elastically scattered neutrons in the range $E_n = 60$–1800 keV, see La 57b.

For resonances, see ^{40}K.

D. ^{39}K(p, p')^{39}K

Magnetic analysis at several angles of observation at $E_p = 7.0–7.5$ MeV, yields proton groups to ^{39}K* = 2.526, 2.817, 3.021, 3.603, 3.879, and 3.935 MeV, all ±0.007 MeV, and 4.078, 4.092, 4.122, 4.472, 4.511, 4.678, 4.737, 4.928, 5.010, and 5.168 MeV, all ±0.008 MeV (Sp 58). The absence of levels below $E_x = 2$ MeV has been confirmed (Sc 56c). Inelastic scattering at $E_p = 185$ MeV, see Ty 58.

For resonances, see ^{40}Ca.

E. ^{39}Ca(β^+)^{39}K $\qquad Q_m = 6490 \pm 40$

See ^{39}Ca.

F. ^{40}Ca(γ, p)^{39}K $\qquad Q_m = -8336.4 \pm 4.3$

At $E_\gamma = 85$ MeV, some structure has been observed in the proton spectrum (Ko 59). Cross section, Jo 55, Mo 55a.

G. ^{40}Ca(n, d)^{39}K $\qquad Q_m = -6111.7 \pm 4.4$

A ground-state group and some unresolved groups have been observed at $E_n = 14$ MeV (Co 59b).

H. ^{42}Ca(p, α)^{39}K $\qquad Q_m = 126.0 \pm 4.4$

Magnetic analysis at $E_p = 6.5$ and 7.4 MeV yields $Q_0 = 0.118 \pm 0.005$ MeV (Br 56f).

I. Not reported:

^{37}Cl(^{3}He, n)^{39}K	$Q_m = 8892.0 \pm 3.5$
^{38}Ar(p, γ)^{39}K	$Q_m = 6367.2 \pm 3.6$
^{38}Ar(d, n)^{39}K	$Q_m = 4142.4 \pm 3.6$
^{38}Ar(^{3}He, d)^{39}K	$Q_m = 874.0 \pm 3.6$
^{38}Ar(α, t)^{39}K	$Q_m = -13445.5 \pm 3.6$
^{40}Ca(d, ^{3}He)^{39}K	$Q_m = -2843.3 \pm 4.3$
^{40}Ca(t, α)^{39}K	$Q_m = 11476.3 \pm 4.4$
^{41}K(p, t)^{39}K	$Q_m = -9410 \pm 5$

^{39}Ca

(Fig. 39.3, p. 242; table 39.4, p. 242)

A. ^{39}Ca (β^+)^{39}K $\qquad Q_m = 6490 \pm 40$

The half-life is 0.877 ± 0.006 sec (weighted mean of Li 60a, Cl 58, Ki 58, Mi 58, Kl 54b; see also Wa 60a, Br 53, Su 53, Bo 51, Hu 43).

Magnetic spectrometer measurements of the end point give 5.43 ± 0.06 MeV (Wa 60a), 5.490 ± 0.025 MeV (Ki 58); see also Br 53, Hu 54. The transition is super-allowed (log ft = 3.6), giving $J^\pi = \frac{3}{2}^+$ for ^{39}Ca.

Potential branches to ^{39}K excited states are very weak. Gamma rays with $E_\gamma = 2.5$–3.5 MeV have an intensity $< 0.12\%$ per disintegration (Ki 58; see also Ta 60c).

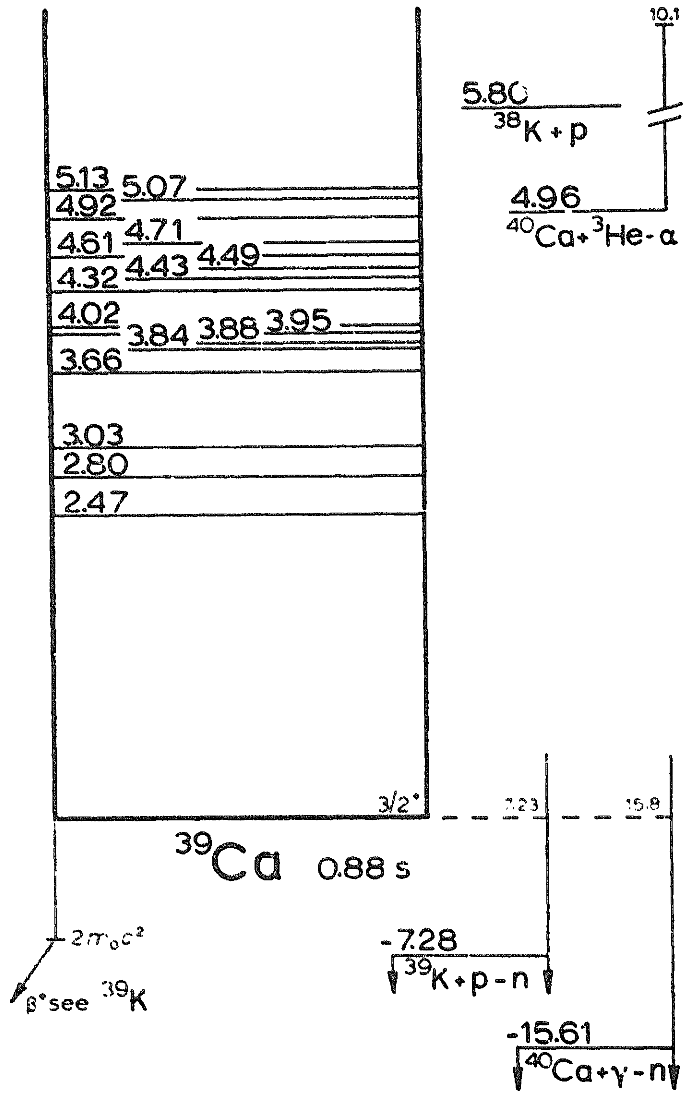

Fig. 39.3. Energy levels of ^{39}Ca.

TABLE 39.4

Energy levels of ^{39}Ca

E_x (MeV)	J^π	$\tau_{\frac{1}{2}}$	Decay	Reactions
0	$\frac{3}{2}^+$	0.877 ± 0.006 sec	β^+	A, B, C, D
2.473–5.13; 16 levels, see reaction				D

B. ^{39}K(p, n)^{39}Ca $\qquad Q_m = -7280 \pm 40$

The threshold has been measured at 7.227 ± 0.070 MeV, giving $Q_0 = -7.044 \pm 0.70$ (Br 59f).

Cross section, Ta 58.

C. ^{40}Ca(γ, n)^{39}Ca $\qquad Q_m = -15610 \pm 40$

The threshold is measured as 15.8 ± 0.1 MeV (Su 53), 15.9 ± 0.4 MeV (Mc 49), and 16.0 ± 0.3 MeV (Be 47). For neutron energy spectra, measured at $E_\gamma = 30$ MeV, see Ag 59, Em 59a.

Cross section, Wa 48, Mc 50, Su 53, Go 54a, Mo 55a, Li 60a, Ne 50c. Theory, see Le 61.

D. ^{40}Ca(^{3}He, α)^{39}Ca. $\qquad Q_m = 4960 \pm 40$

At $E(^3\text{He}) = 10.1$ MeV, magnetic analysis yields seventeen α-particle groups leading to ^{39}Ca* = 0, 2.473, 2.799, 3.032 (all ± 0.010), 3.66, 3.84, 3.88, 3.95, 4.02, 4.32, 4.43, 4.49, 4.61, 4.71, 4.92 (double?), 5.07 and 5.13 MeV (all ± 0.02 MeV) (Hi 60f).

E. Not reported:

^{36}Ar(α, n)^{39}Ca	$Q_m = -\ 8570 \pm 40$
^{39}K(^{3}He, t)^{39}Ca	$Q_m = -\ 6510 \pm 40$
^{40}Ca(p, d)^{39}Ca	$Q_m = -13390 \pm 40$
^{40}Ca(d, t)^{39}Ca	$Q_m = -\ 9350 \pm 40$

^{40}Cl

(Not illustrated; see fig. 40.1, p. 244)

A. ^{40}Cl(β^-)^{40}Ar $\qquad Q_m = 7500 \pm 500$

The half-life is 1.42 ± 0.02 min (Ro 57).

The β^- spectrum has been investigated with a scintillation spectrometer; the end point is 7.5 MeV. A strong β^- transition with end point between 3.0 and 3.5 MeV is also present (Mo 56b). Gamma rays of 0.55, 0.66, 0.96, 1.1, 1.46, 2.80, 3.10, 4.2–4.4, 5.8, and 6.3 MeV, and several more in the $E_\gamma = 2.5$–3.0 MeV range have been observed (Ro 57, Mo 56b). The 1.46 and 2.80 MeV γ rays have about equal intensities. These data suggest a decay scheme as shown in fig. 40.1. They are compatible with the assignment $J^\pi = 2^-$ to ^{40}Cl, and $J^\pi = 0^+$, 2^+, 3^-, and 1^- to ^{40}Ar* = 0, 1.46, 4.2, and 5.8 MeV, respectively (Mo 56b).

B. ^{40}Ar(n, p)^{40}Cl $\qquad Q_m = -6700 \pm 500$

Cross section, Za 59.

C. Not reported:

^{40}Ar(t, ^{3}He)^{40}Cl $\qquad Q_m = -7500 \pm 500$

REMARKS

For a prediction of the excitation energies of $(d_{\frac{3}{2}}, f_{\frac{7}{2}}^3)$ states in ^{40}Cl, see Ta 57a, Pa 57c.

^{40}Ar

(Fig. 40.1, p. 244; table 40.1, p. 245)

A. ^{40}Cl(β^-)^{40}Ar $\qquad Q_m = 7500 \pm 500$

See ^{40}Cl.

B. ^{40}Ar(e, e')^{40}Ar

Magnetic analysis at $E_e = 187$ MeV of inelastically scattered electrons shows levels at 1.46 and 2.4 MeV. The differential cross section leads to tentative assignments $J^\pi = 0^+$ and 2^+, respectively, and to $\Gamma_\gamma = 2.0 \pm 0.4$ meV, $\tau_m = (3.3 \pm 0.6) \times 10^{-13}$ sec, for the 2.4 MeV level (He 56).

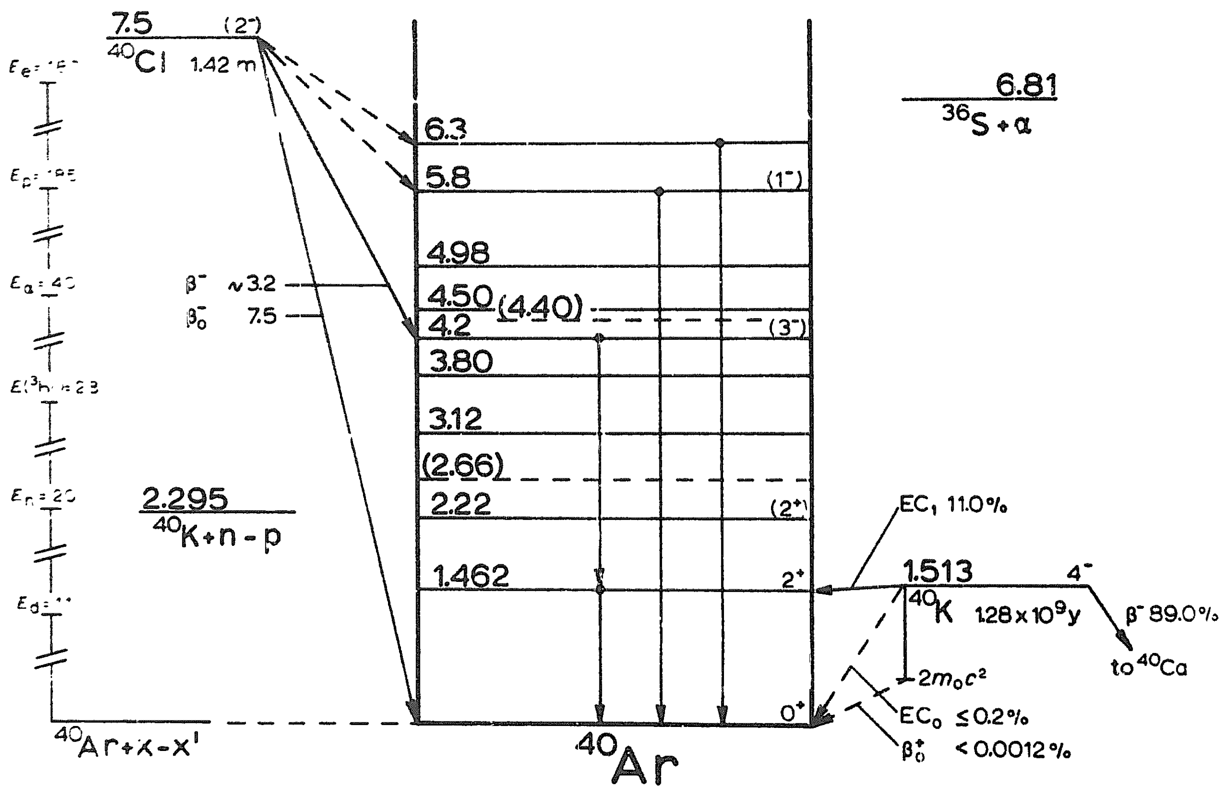

Fig. 40.1. Energy levels of ^{40}Ar.

C. ^{40}Ar(n, n)^{40}Ar

Cross section and resonances, see ^{41}Ar.

D. ^{40}Ar(p, p')^{40}Ar

Inelastic scattering of protons by ^{40}Ar yields groups to ^{40}Ar* $= 1.48 \pm 0.02$ MeV (Fr 54), 1.48 ± 0.02, 2.22 ± 0.04, (2.66), 3.12 ± 0.03, 3.80 ± 0.03, (4.40), 4.50 ± 0.05, and 4.98 ± 0.05 MeV (Va 56e); 1.46, 3.7, and ≈ 4.8 MeV (Od 60). A scintillation spectrometer measurement yields a γ ray with $E_\gamma = 1.442 \pm 0.015$ MeV (Ho 59). Angular distribution of elastically and inelas-

TABLE 40.1
Energy levels of ^{40}Ar

E_x (MeV ± keV)	J^π	τ_m	Decay	Reactions
0	0^+		stable	many
1.462 ± 5	2^+		γ	A, B, D, G, H
2.22 ± 40	(2^+)	$(3.3 \pm 0.6) \times 10^{-13}$ sec		B, D
(2.66)				D
3.12 ± 30				D
3.80 ± 30				D
4.2	(3^-)		γ	A
(4.40)				D
4.50 ± 50				D
4.98 ± 50				D
5.8	(1^-)		γ	A
6.3			γ	A

tically scattered protons, He 47, Fr 54, Hi 55, Bu 56a, Ei 56, Ki 56a, Va 56e, Gi 57, Ty 58, Od 60; theory Me 57a. Polarization measurement of elastically scattered protons, Ro 61c.

For cross section and resonances, see ^{41}K.

E. ^{40}Ar(d, d)^{40}Ar

Differential elastic scattering cross section at $E_d = 11$ MeV, Ta 60e.

F. ^{40}Ar(^{3}He, ^{3}He)^{40}Ar

Differential cross section for elastic and inelastic scattering at $E(^3\text{He}) =$ 28.5 MeV, Ag 60.

G. ^{40}Ar(α, α')^{40}Ar

Differential cross section for elastic scattering and for inelastic scattering to ^{40}Ar* = 1.46 MeV, has been measured at $E_\alpha = 18$ MeV (Se 58a), and 40 MeV (Ya 59). Theoretical analysis, Ig 59, Ro 60b. The angular distribution is consistent with $J^\pi = 2^+$ for ^{40}Ar(1) (Ya 59).

H. ^{40}K(EC)^{40}Ar $\qquad Q_m = 1512.8 \pm 3.4$

See ^{40}K.

I. ^{40}K(n, p)^{40}Ar $\qquad Q_m = 2295.3 \pm 3.4$

Cross section, Ro 58a.

J. Not reported:

^{37}Cl(α, p)^{40}Ar $\qquad Q_m = -\ 1592.3 \pm 2.2$

^{38}Ar(t, p)^{40}Ar $\qquad Q_m = \ 7977.7 \pm 2.3$

^{41}K(n, d)^{40}Ar $\qquad Q_m = -\ 5575.1 \pm 4.3$

^{41}K(d, ^{3}He)^{40}Ar	$Q_m = -\ 2306.7 \pm 4.3$
^{41}K(t, α)^{40}Ar	$Q_m = \ 12012.9 \pm 4.3$
^{42}Ca(n, ^{3}He)^{40}Ar	$Q_m = -10358.2 \pm 4.2$
^{43}Ca(n, α)^{40}Ar	$Q_m = \ 2289.5 \pm 4.5$

REMARKS

Pure jj-coupling theory predicts a $J^\pi = 3^-$ level in ^{40}Ar with $E_x = 2.51$ MeV (Th 57).

^{40}K

(Fig. 40.2, p. 247; table 40.2, p. 248)

A.	(a) ^{40}K(β^-)^{40}Ca	$Q_m = 1321.5 \pm 4.5$
	(b) ^{40}K(EC)^{40}Ar	$Q_m = 1512.8 \pm 3.4$

(a) The number of β^- particles emitted per sec per g of potassium is 27.7 ± 0.3 (weighted average of Gr 48, Fl 49, Ho 50, Sa 5 a, Go 51c, Ko 55, Su 55, Mc 56, Ke 59a, Sa 60c). Together with the abundance of ^{40}K in natural potassium, $(1.178 \pm 0.004) \times 10^{-4}$ (Ni 50, Re 52a, Re 56a), this number gives a partial half-life for β^- decay, $\tau_{\frac{1}{2}}(\beta^-) = (1.439 \pm 0.015) \times 10^9$ yr.

The β^- end point is 1330 ± 9 keV (weighted average of Dz 46, Al 50c, Be 50b, Go 51c, Fe 52, Ko 55, Ke 59a); log $ft = 18.5$. The shape of the spectrum is unique third forbidden (Wu 50, Al 50c, Be 50b, Go 51c, Fe 52, Ma 53c, Ko 55), in agreement with the $J^\pi = 4^-$ assignment to ^{40}K (St 58b), and $J^\pi = 0^+$ to ^{40}Ca.

(b) The decay almost entirely proceeds through electron capture to ^{40}Ar* = 1.46 MeV. The number of 1.46 MeV γ rays emitted per sec per g of potassium is 3.38 ± 0.06 (weighted mean of Sa 49a, Fa 50, Ho 50, Bu 53, Ba 55b, We 57, Sa 60c; see also Su 55). If electron capture and β^+ emission to ^{40}Ar(0) are neglected (see below), this number of γ rays gives a partial half-life $\tau_{\frac{1}{2}}$ (EC) = $(11.8 \pm 0.2) \times 10^9$ yr.

Measurements of the γ-ray energy yield a weighted average of 1.462 ± 0.005 MeV (Gl 47, Be 50c, Be 50d, Ho 50b, Pr 50, Go 51a, Mc 56). The assignment of this γ ray to ^{40}Ar, which follows from the mass-spectroscopic ^{40}K–^{40}Ca and ^{40}K–^{40}Ar mass differences, is confirmed by coincidence measurements between γ quanta and Auger electrons (Pa 52a). Independent experiments (see ^{40}Ar) yield a ^{40}Ar excited state at 1.462 ± 0.012 MeV. Combination of the γ-ray energy with the Q_m value, gives 51 ± 6 keV for the capture energy. With the partial half-life given above, this energy yields log $ft = 10.6$, a rather high value in the class of first-forbidden electron capture transitions.

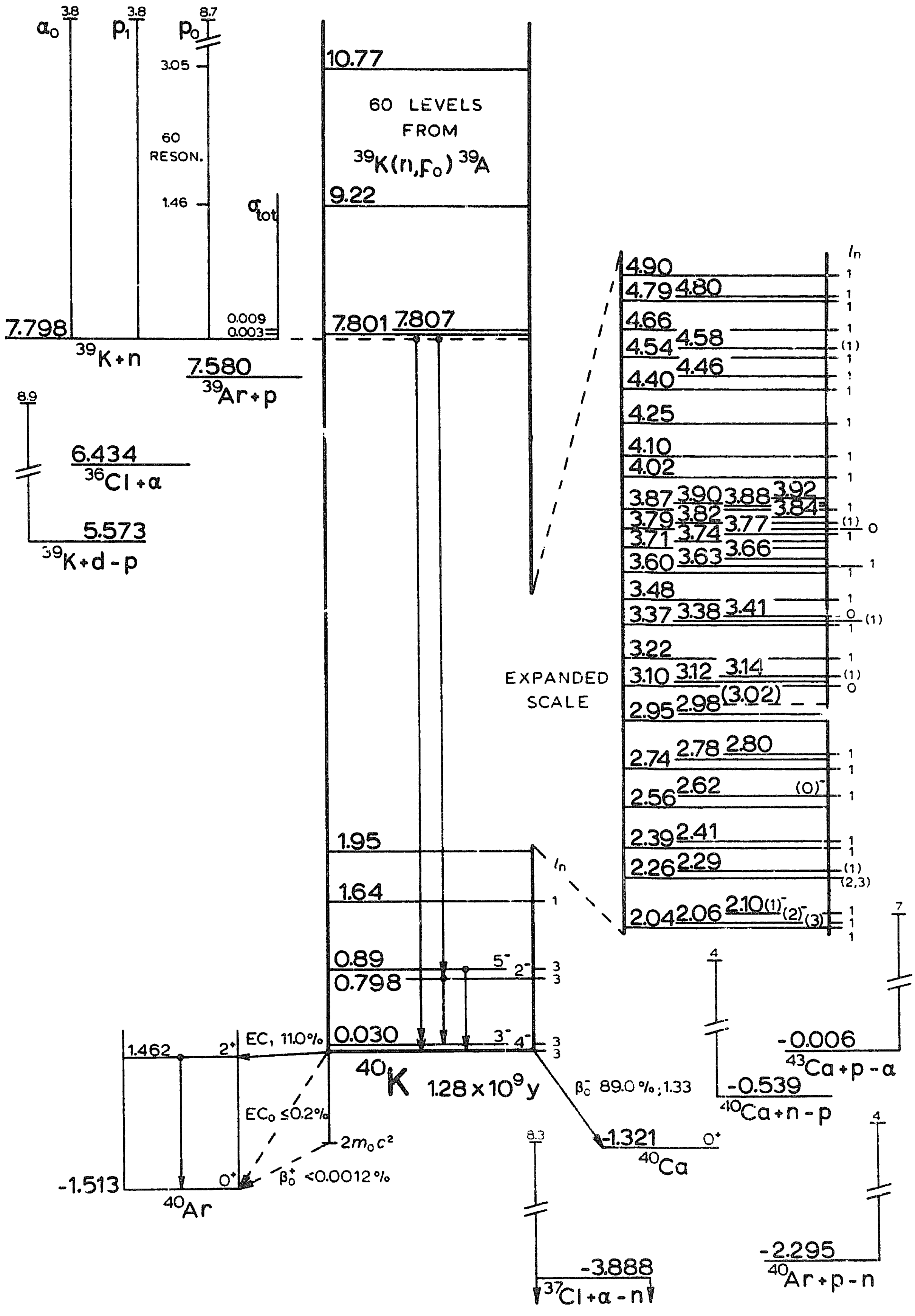

Fig. 40.2. Energy levels of ^{40}K.

TABLE 40.2

Energy levels of ^{40}K

E_x (MeV ± keV)	J^π	$\tau_{\frac{1}{2}}$ or Γ	Decay	Reactions
0	4^-	$(1.282 \pm 0.013) \times 10^9$ yr	β^-, EC	many
0.0297 ± 0.7	3^-	$(3.9 \pm 0.4) \times 10^{-9}$ sec	γ	C, F, G, H, I
0.789 ± 4	2^-		γ	C, F, G, H, I
0.888 ± 6	5^-		γ	C, F, H, I
1.639 ± 8	$(\leqslant 3)^-$			F
1.954 ± 8				F
2.042 ± 8	(3^-)			F
2.064 ± 8	(2^-)			C, F
2.099 ± 8	(1^-)			F
2.256 ± 8				F
2.286 ± 8				F
2.393 ± 8	$(\leqslant 3)^-$			F
2.415 ± 8	$(\leqslant 3)^-$			F
2.565 ± 8				F
2.622 ± 8	(0^-)			F
2.743–4.902; 38 levels, see table 40.4 and reaction				F
7.801 ± 4		12 eV	n	D
7.807 ± 4		60 eV	n	D
9.22–10.77; 60 levels, see reaction				E

The number of K captures per sec per g of potassium, 1.42 ± 0.03 (He 54), and the number of γ quanta adopted above, lead to an LM/K capture ratio 1.35 ± 0.25. The transition energy inferred from this ratio, 20 ± 3 keV, leads to a log *ft* value in the range of the log *ft* values found for the class of first-forbidden electron-capture transitions (Ro 60d).

The number of positons emitted per sec per g potassium is less than $(3.6 \pm 1.8) \times 10^{-4}$ (Ti 59). Thus less than $(0.0012 \pm 0.0006)\%$ of the ^{40}K decay goes by positon emission to ^{40}Ar(0) (see also Be 50d: $< 0.002\%$; Co 51a, Go 51b). Since 1.5 MeV is available for β^+ decay, the ratio of K captures to the ground state over β^+ emissions is expected to be about 200 (Mo 51a). It is not excluded therefore, that a few tenths of a percent of the decay to ^{40}Ar proceeds by electron capture directly to the ground state.

(a) and (b). The most accurate direct measurements of the ratio of the number of γ quanta over the number of electrons yield 0.124 ± 0.002 and 0.121 ± 0.004 (Mc 56). This is to be compared with the ratio 0.122 ± 0.003, which follows from the average values given above for the number of β^- particles and γ quanta emitted per sec per g of potassium. Measurement of the ratio of the number of electron captures over the number of β^- emissions yields 0.135 ± 0.040 (Sa 50a; see also En 54a).

Measurements of the amount of argon in minerals of known age which contain potassium, and mass spectrometer studies of the relative amounts of ^{40}Ar,

^{40}K, and ^{40}Ca in such minerals, yield values for the electron capture to β^- emission branching ratio which generally come out lower than the value deduced from counting experiments (In 50, however, gives 0.126 ± 0.005). A review of geochemical experiments (We 56) shows that several older determinations need upward revision and that geological evidence gives a branching ratio of 0.117 ± 0.015, in good agreement with the value 0.1230 ± 0.0015, deduced from counting experiments.

Other reviews of the ^{40}K decay, We 56, Ro 60d.

Summary: ^{40}K decays by 1.33 MeV β^- emission (89.0%) to ^{40}Ca(0), and by electron capture (11.0%) to ^{40}Ar(1), which in turn decays by γ emission to ^{40}Ar(0). It is not excluded that a few tenths of a percent of the decay proceeds by electron capture directly to ^{40}Ar(0).

The partial half-life for the β^- decay to ^{40}Ca, $\tau_{\frac{1}{2}}(\beta^-) = (1.439 \pm 0.015) \times 10^9$ yr, and for electron capture to ^{40}Ar(1), $\tau_{\frac{1}{2}}$ (EC) $= (11.8 \pm 0.2) \times 10^9$ yr, yield a total half-life $(1.282 \pm 0.013) \times 10^9$ yr.

B. ^{37}Cl(α, n)^{40}K $\qquad Q_m = -3837.6 \pm 3.9$

At $E_\alpha = 8.3$ MeV, nuclear emulsion measurements yield $Q_0 = -3.86 \pm 0.06$ MeV (Sm 61).

C. ^{39}K(n, γ)^{40}K $\qquad Q_m = 7797.6 \pm 3.3$

The thermal neutron absorption cross section of natural potassium is 2.07 ± 0.07 b. The isotopic cross sections of ^{39}K, ^{40}K, and ^{41}K, are 1.94 ± 0.15, 70 ± 20, and 1.24 ± 0.10 b, and their abundances 93.1, 0.012, and 6.91%, respectively. About 95% of the thermal neutron captures in natural potassium should then occur in ^{39}K (Hu 58).

Energies, intensities, and assignments of γ rays resulting from thermal neutron capture in natural potassium are listed in table 40.3. The assignment of the 9.39 and 8.45 MeV γ rays to capture in ^{40}K is based on experiments with potassium enriched in ^{40}K. Some probable transitions in ^{40}K are indicated in table 40.3; several others must also be assigned to capture in ^{39}K because of intensities. In view of the small spacing of several ^{39}K levels, precision measurements of the γ-ray energies are needed to make possible unambiguous assignments of the other γ rays. For a proposed level scheme which accounts for several of the observed γ transitions, see Ad 56, Gr 58c.

For a comparison of the reduced widths from (n, γ) and (d, p) reactions, see Bo 59a.

D. ^{39}K(n, n)^{39}K $\qquad E_b = 7797.6 \pm 3.3$

Cross section, Hu 58.

Resonances have been reported at $E_n = 3.4$ keV ($\Gamma = 12$ eV) and 9.2 keV ($\Gamma = 60$ eV), Go 58a. See also Hu 58, Ma 58, Bl 58b.

TABLE 40.3

Gamma rays from thermal neutron capture in potassium

E_γ [a] (MeV ± keV)	I_γ [b, h]	I_γ [c, h]	E_γ [d] (MeV ± keV)	I_γ [d, h]	Final nucleus	Probable[g] transition
9.39 ±60	0.08	0.02			^{41}K	
8.45 ±20	0.1	0.1			^{41}K	C → 1.67
7.757± 8	4	3.5	7.763±10	4.4	^{40}K	C → 0.03
7.34 ±20	0.4	0.1	7.320±25	0.2		
6.994± 7	2	1.3	7.000±15	1.6	^{40}K	C → 0.80
6.31 ±60	0.4	0.3				
5.740±12	12 (5.740 and 5.66 together)	6	5.725±15	11	^{40}K	C → 2.06
5.66 ±20		4	(5.65 ±40)	≈ 3		
5.50 ±20		2.5	5.51 ±30	≈ 2		
5.38 ±30	6	6	5.40 ±20	6.4		
5.18 ±20		2	5.25 ±50	2.5		
5.06 ±20	4	3	5.02 ±30	4.5		
			4.81 ±40	1.5		
			4.70 ±30	≈ 1		
			4.50 ±40	≈ 1		
4.39 ±30	9	4	4.39 ±20	5		
4.18 ±50	7		4.11 ±30	4		
3.92 ±50	6		3.97 ±30	5		
			3.81 ±50	2		
3.67 ±50	9		3.70 ±30	4		
			3.60 ±30	4		
			3.55 ±50	2		
E_γ [e] (MeV ± keV)	**I_γ [e, h]**					
3.45 ±50	8		3.40 ±50	≈ 4		
			(3.15 ±50)	≈ 1.5		
			3.05 ±30	≈ 3		
2.80 ±30	6		2.75 ±40	≈ 4		
			(2.60 ±40)	≈ 4		
			(2.55 ±40)	≈ 4		
			(2.42 ±30)	≈ 2		
			(2.37 ±30)	≈ 3		
			(2.30 ±30)	≈ 3		
			2.06 ±10	9		
2.03 ±30	13		2.020±15	7		
			1.95 ±20	4		
			1.85 ±20	≈ 3		
			1.75 ±20	≈ 3		
1.61 ±30	5		1.610± 8	13		
			1.51 ±10	5		
			1.40 ±20	≈ 2		
			1.27 ±20	≈ 2		
1.19 ±30	8		1.180±15	7[f]		
			0.900±15	2	^{40}K	0.89 → 0
0.77 ±30	24		0.770± 7	26[f]	^{40}K	0.80 → 0.03
			0.625±10	3		

[a] Ki 52, Ba 53; magnetic pair spectrometer.
[b] Ki 52, as revised in Ba 58c.
[c] Ba 53.
[d] Kd 56, as corrected in Gr 58c; magnetic Compton spectrometer.
[e] Br 56e; 2-crystal scintillation spectrometer.
[f] Also reported in Ur 59; scintillation spectrometer.
[g] The capturing state is indicated by C, the excitation energies are in MeV.
[h] Intensities are given as the number of γ quanta per 100 captures in natural potassium.

E. (a) $^{39}K(n, p)^{39}Ar$ $Q_m = 218 \pm 5$ $E_b = 7797.6 \pm 3.3$
(b) $^{39}K(n, \alpha)^{36}Cl$ $Q_m = 1364 \pm 6$ $E_b = 7797.6 \pm 3.3$

Sixty resonances in p_0 have been observed in the $E_n = 1.46$–3.05 MeV region (10 keV resolution). With 70–150 keV resolution, strong resonance structure in the p_0 yield has also been found in the $E_n = 3.05$–8.7 MeV region, and in the p_1 and α_0 yield in the 2.3–3.8 MeV region (Ba 61g).

F. $^{39}K(d, p)^{40}K$ $Q_m = 5572.8 \pm 3.3$

The excitation energies of 52 levels in the $E_x = 0$–5.0 MeV range are listed in table 40.4, together with l_n values and reduced widths (En 59, Ma 60d). Analogous work, at $E_d = 8.9$ MeV, with lower resolution, is reported in Da 59b. The relative reduced widths in En 59 and Da 59b are in good agreement. At $E_d = 4.8$–5.7 MeV, the excitation energies of the first three levels are given as 0.032 ± 0.002, 0.800 ± 0.010, and 0.893 ± 0.010 MeV (Bu 53a). See also Sa 50, Te 57a. The ground-state Q value is 5.576 ± 0.010 MeV (Bu 53a), 5.569 ± 0.010 MeV (En 59), 5.583 ± 0.010 MeV (Ma 60e).

The states at 0, 0.030, 0.798, and 0.888 MeV all have $l_n = 3$. The ratio of the weighted reduced widths, $(2J+1)\theta_n^2$, is 9.8 : 8.4 : 6.1 : 11. This ratio is in agreement with the theoretical ratio 9 : 7 : 5 : 11, calculated assuming a $J^\pi = 4^-, 3^-, 2^-$, and 5^- sequence for the four levels, the $(d_{\frac{3}{2}}^{-1}, f_{\frac{7}{2}})$ quadruplet, mentioned above. The levels at 2.042, 2.064, and 2.099 MeV, to which strong proton groups have been observed, evidently belong to the $(d_{\frac{3}{2}}^{-1}, p_{\frac{3}{2}})$ quadruplet. The fourth member is probably the level at 2.622 MeV. The relative intensities of the four groups to these levels suggest a spin sequence $J^\pi = 3^-, 2^-, 1^-$, and 0^-. For a theoretical discussion of the observed reduced widths, see Ma 60d.

For a comparison of the (d, p) and (n, γ) reduced widths, see Bo 59a.

G. $^{40}Ar(p, n)^{40}K$ $Q_m = -2295.3 \pm 3.4$

Time-of-flight measurements yield neutron groups to $^{40}K^* = 0.029$ and 0.80 MeV, with $Q = -2.336 \pm 0.010$ and -3.104 ± 0.015 MeV, respectively. With a scintillation spectrometer, thresholds have been measured for the production of 29.4 ± 1.0 keV ($1 \rightarrow 0$) and 771 ± 10 keV ($2 \rightarrow 1$) γ rays, yielding $Q = -2.332 \pm 0.010$ and -3.096 ± 0.010 MeV, respectively. These four Q values, combined with the excitation energies of Bu 53a, yield $Q_0 = -2.304 \pm 0.006$ MeV (Ho 59). The mean life of the 30 keV level, measured by a pulsed-beam technique, is $(5.6 \pm 0.5) \times 10^{-9}$ sec. This supports the assumption that the 30 keV γ ray is mainly M1 (Ly 59).

H. $^{40}Ca(n, p)^{40}K$ $Q_m = -538.9 \pm 4.5$

Gamma rays of 30 ± 2, 767 ± 7, and 877 ± 17 keV, corresponding to the transitions (1) $\rightarrow$ (0), (2) $\rightarrow$ (1), and (3) $\rightarrow$ (0) or (1), respectively, have been found at $E_n = 4$ MeV (Da 56c).

For cross section, see Ba 60c, Al 61; for angular distributions, Co 58d.

TABLE 40.4

Levels in ^{40}K from the ^{39}K(d, p)^{40}K reaction

E_x [a] (MeV)	l_n [a]	$(2J+1)\theta_n^2$ [b] $\times 10^3$	E_x [a] (MeV)	l_n [a]	$(2J+1)\theta_n^2$ [b] $\times 10^3$
0	3	86	3.412	0	0.7
0.028 [c]	3	73	3.479	1	4.9
0.795	3	55	3.599	1	1.4
0.885	3	100	3.629	1	30
1.639	1	0.7	3.657		
1.954			3.715		
2.042	1	86	3.738		
2.064	1	78	3.766	1	2.7
2.099	1	53	3.790	0	1.3
2.256	2 or 3		3.820	(1)	(1.6)
2.286	(1)	(1.6)	3.838		
2.393	1	1.0	3.869	1	17
2.415	1	2.6	3.883		
2.565			3.898		
2.622	1	18	3.920		
2.743	1	6.7	4.017 [d]	1	9.7
2.781			4.102 [d]	1	16
2.802	1	1.8	4.253 [d]	1	33
2.948			4.396 [d]	1	17
2.983			4.462 [d]	1	17
(3.021)			4.539 [d]	1	17
3.104	0	1.0	4.582 [d]	(1)	(6.3)
3.125			4.658 [d]	1	9.4
3.144	(1)	(1.5)	4.788 [d]	1	7.3
3.225	1	22	4.801 [d]	1	12
3.367	1	6.3	4.902 [d]	1	8.9
3.385	(1)	(2.5)	all ±8 keV		
all ±8 keV					

[a] En 59.
[b] En 59, Ma 60d.
[c] ±2 keV.
[d] For $E_x > 4$ MeV, only levels corresponding to strong groups have been tabulated.

I. ^{43}Ca(p, α)^{40}K $\qquad Q_m = -5.9 \pm 4.9$

Magnetic analysis at $E_p = 6.5$ and 7.0 MeV yields $Q_0 = -0.014 \pm 0.008$ MeV (Br 56f).

J. Not reported:

^{38}Ar(t, n)^{40}K	$Q_m = 5682.4 \pm 4.0$
^{38}Ar(^{3}He, p)^{40}K	$Q_m = 6446.8 \pm 4.0$
^{38}Ar(α, d)^{40}K	$Q_m = -11905.6 \pm 4.0$
^{39}K(t, d)^{40}K	$Q_m = 1539.9 \pm 3.3$
^{39}K(α, ^{3}He)^{40}K	$Q_m = -12779.6 \pm 3.4$
^{40}Ar(^{3}He, t)^{40}K	$Q_m = -1530.9 \pm 3.4$

^{40}Ca(t, ^{3}He)^{40}K	$Q_m = -1303.3 \pm 4.5$
^{41}K(p, d)^{40}K	$Q_m = -7870 \pm 5$
^{41}K(d, t)^{40}K	$Q_m = -3838 \pm 5$
^{41}K(^{3}He, α)^{40}K	$Q_m = 10482 \pm 5$
^{42}Ca(n, t)^{40}K	$Q_m = -11889 \pm 5$
^{42}Ca(p, ^{3}He)^{40}K	$Q_m = -12653.6 \pm 4.9$
^{42}Ca(d, α)^{40}K	$Q_m = 5699 \pm 5$

REMARKS

For a discussion of a relation between excitation energies in ^{38}Cl and ^{40}K based on jj-coupling, see ^{38}Cl, Remarks. Theoretical discussion of the ^{40}K ground state configuration, Ku 53, De 53a, Hi 54, Ma 54, Sc 54c, Ta 54a, Pa 56a, Pa 57a, Sh 60, De 61a.

^{40}Ca

(Fig. 40.3, p. 254; table 40.5, p. 255)

A. ^{39}K(p, γ)^{40}Ca $\qquad Q_m = 8336.4 \pm 4.3$

Experimental information on resonance energies, relative γ yields, absolute γ_0 yields, and branching percentages is given in table 40.6. Resonances in the E_p = 2–3 MeV region (not tabulated) have also been observed (Zi 61).

The γ_0 yield measured in the E_p = 9–14 MeV region shows broad resonances at E_p = 10.8, 11.6, and 12.0 MeV (Ta 61b).

From delayed coincidence measurements the half-life of ^{40}Ca(1) has been determined as $\tau_{\frac{1}{2}} = (2.15 \pm 0.08) \times 10^{-9}$ sec (Go 60f).

B. ^{39}K(p, p')^{39}K $\qquad E_b = 8336.4 \pm 4.3$

No elastic scattering resonances have been observed in the E_p = 1.0–2.0 MeV region (Ru 59). Many resonances (not tabulated) are seen in the yield of the E_γ = 2.53 MeV γ ray de-exciting ^{39}K(1). The average distance at an excitation energy of 12.4 MeV in ^{40}Ca is D = 16 keV (Pr 58a).

For non-resonance data, see ^{39}K.

C. ^{39}K(p, α)^{36}Ar $\qquad Q_m = 1292.3 \pm 3.9 \qquad E_b = 8336.4 \pm 4.3$

The α_0 yield has been measured in the E_p = 2.2–3.2 MeV region. Many resonances (not tabulated; yield curve given) are found, at an average distance $D <$ 15 keV (Cl 60).

For non-resonance data, see ^{36}Ar.

D. ^{40}K(β^-)^{40}Ca $\qquad Q_m = 1321.5 \pm 4.5$

See ^{40}K.

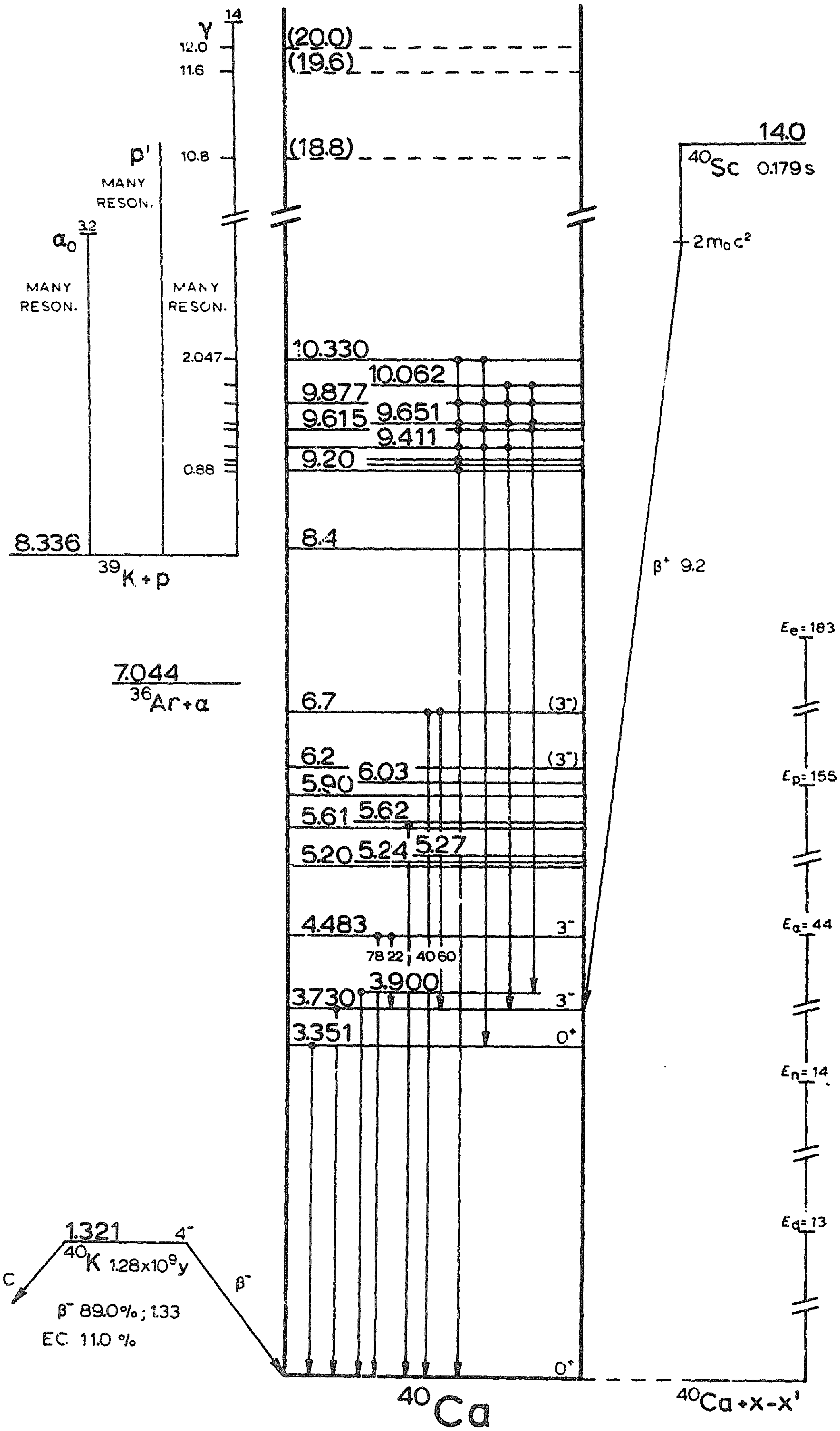

Fig. 40.3. Energy levels of ^{40}Ca.

TABLE 40.5

Energy levels of ^{40}Ca

E_x (MeV ± keV)	J^π	τ_m	Decay	Reactions
0	0^+		stable	many
3.351 ± 3	0^+	$(3.15 \pm 0.10) \times 10^{-9}$ sec	π, e^-	A, F, G
3.730 ± 4	3^-	$(7.1 \pm 0.3) \times 10^{-11}$ sec	γ	A, E, F, G, I, J
3.900 ± 4			γ	A, F, G, I
4.483 ± 5	3^-		γ	A, G, I
5.202 ± 8				G
5.241 ± 6				G
5.272 ± 6				G
5.606 ± 8			γ	G
5.621 ± 8			γ	G
5.901 ± 8				G
6.029 ± 8				G
6.16 ± 70	(3^-)			I
6.74 ± 70	(3^-)		γ	G, I
8.4				I
9.197 ± 11			γ	A
9.238 ± 11			γ	A
9.292 ± 11			γ	A
9.441 ± 5			γ	A
9.615 ± 5			γ	A
9.651 ± 5			γ	A
9.877 ± 5	(doublet)		γ	A
10.062 ± 5			γ	A
10.330 ± 5			γ	A
10.3–13.4; many levels, see reactions				A, B, C
18.8			γ	A
19.6			γ	A
20.0			γ	A

E. $^{40}Ca(e, e')^{40}Ca$

The angular distribution has been measured by magnetic analysis of 183 MeV electrons scattered inelastically from calcium. Both the angular distribution and the cross section, yielding a mean life $\tau_m = (7.1 \pm 0.3) \times 10^{-11}$ sec, support a $J^\pi = 3^-$ assignment to the ^{40}Ca level at 3.73 MeV (Ha 56b, He 56).

F. $^{40}Ca(n, n')^{40}Ca$

Inelastic scattering of 4 MeV neutrons by calcium yields γ rays of $E_\gamma = 3.74 \pm 0.04$ and 3.9 ± 0.1 MeV, in addition to annihilation radiation. The threshold for β^+ production is $E_n = 3.44 \pm 0.05$ MeV, showing that $^{40}Ca(1)$ decays by pair emission (Da 56c). The mean life of $^{40}Ca(1)$ has been measured with a pulsed neutron source, yielding $\tau_m = (3.4 \pm 0.2) \times 10^{-9}$ sec and a reduced E0 matrix element $\varrho = 0.15$ (Kl 59).

TABLE 40.6

Levels in ^{40}Ca from the ^{39}K(p, γ)^{40}Ca reaction

De 57		To 57, Be 57L[a]		Po 61a[b]		^{40}Ca*	Main decay[c] in %				
E_p (keV)	relative yield	E_p (keV)	$(2J+1)\,\Gamma_p\Gamma_{\gamma_0}/\Gamma$ (eV)	E_p (keV)	relative yield	(MeV)	γ_0	γ_1	γ_2	γ_3	γ_4
883 ± 10	1.2					9.197	×				
925 ± 10	1.0					9.238	×				
980 ± 10	small					9.292	×				
1150 ± 10	10	1120 ± 5	0.5	1133.0 ± 1.4	1	9.441	88	8	4		
		1300 ± 5	1.0	1311.7 ± 1.6	1.5	9.615	84	5		6	(≈ 5)
		1338 ± 5		1349.3 ± 1.6	2.5	9.651	< 5		35	65	
		1566 ± 5	1.7	1579.9 ± 1.9	2.2	9.877[d]	70	12	12 (spans γ_2–γ_3)		(6)
				1769.7 ± 2.1	1.8	10.062			×	×	
				≈ 1880 (doublet)	< 3.5			×			
				2046.7 ± 2.5	8.0	10.330[e]	×	×			

[a] The angular distribution of γ_0 at the E_p = 1120, 1300, and 1566 keV resonances has the form $1+a_2P_2$ with a_2 = 0.44 ± 0.03, 0.43 ± 0.03, and − 0.07 ± 0.03, respectively.

[b] The total width of all observed resonances is Γ < 0.5 keV.

[c] Information from De 57, To 57, and Po 61a. The decay modes γ_0 through γ_4 indicate transitions to ^{40}Ca(0) through (4). A cross indicates that the corresponding decay mode has been observed.

[d] This level is a doublet (Zi 61).

[e] A resonance absorption measurement of γ_0 yields Γ_{γ_0} = 3.6 ± 0.24 eV, Γ_p = 5.8 ± 1.8 eV, Γ = 10.3 ± 1.7 eV (Ec 61). Resonance spin J = 2 has been assumed.

Elastic scattering cross section and angular distribution, Cr 55, We 56a, Cr 58, Cr 60, Ke 60, La 61; theory, Cu 56.

For resonances, see ^{41}Ca.

G. ^{40}Ca(p, p')^{40}Ca

Eleven levels in ^{40}Ca (table 40.7) have been found by magnetic analysis at several proton energies between 6 and 8 MeV (Br 56b).

TABLE 40.7

Levels in ^{40}Ca (E_x in MeV ±keV) from the ^{40}Ca(p, p')^{40}Ca reaction (Br 56b)

3.348±4	4.483±5	5.272±6	5.901±8
3.730±4	5.202±8	5.606±8	6.029±8
3.900±4	5.241±6	5.621±8	

The first level in ^{40}Ca has been found to decay by internal pair formation; the sum of e^+ and e^- energies leads to $E_x = 3.46 \pm 0.10$ MeV (Be 55b). The e^+–e^- angular correlation establishes the transition as E0 (Go 58g, Ch 59a). The corresponding e^- conversion line has also been observed; the measured energy leads to ^{40}Ca*(1) = 3.353±0.003 MeV; the intensity relative to pair emission is $(6.94 \pm 0.20) \times 10^{-3}$ (Ne 59a, Ne 60e). The intensity of 2-photon decay relative to pair emission is at most 1.4×10^{-2} (De 61, also Ne 59). Resonances in the yield of e^+–e^- pairs, Be 58a.

Resonances have been observed in the yield of elastically scattered protons (Da 57a, Jo 59a), and in the yield of protons exciting ^{40}Ca(1) and (2). The $l_p = 0$ resonances decay to (1), the $l_p = 2$ resonances decay with equal intensity to (1) and (2), one $l_p = 3$ resonance decays only to (2) (Jo 59).

Angular distribution of elastic scattering, Jo 61b, and of inelastically scattered protons exciting ^{40}Ca(1) and (2) (unresolved), Ha 52c. Energy spectrum of inelastically scattered protons at $E_p = 11$ MeV, Sh 59. Angular distribution of $E_\gamma = 3.73$ and 3.90 MeV (unresolved), Hi 58b. Gamma spectrum at $E_p = 10$ and 14 MeV, Wa 60c. Polarization of p_0 and p_1 proton groups, Al 57d, Ro 61c.

From p'–γ angular correlation measurements at $E_p = 150$ MeV, branchings (see fig. 40.3) have been obtained of the levels at 3.73 MeV ($J^\pi = 3^-$), 4.48 MeV ($J^\pi = 3^-$), ≈ 5.6, and ≈ 6.8 MeV (Ro 61e).

H. ^{40}Ca(d, d)^{40}Ca

Differential cross section for elastic scattering at $E_d = 11$ MeV, Ta 60e; at $E_d = 13$ MeV, Fr 61.

I. ^{40}Ca(α, α')^{40}Ca

At $E_\alpha = 43$ MeV, α-particle groups have been observed exciting ^{40}Ca(4.48) and a new level at 8.4±0.2 MeV. The 4.48 MeV level decays to ^{40}Ca(2) or (3).

The α' angular distribution and the α'–γ ($E_\gamma = 3.8$ MeV) angular correlation yield $J^\pi = 1^-$ or 3^- for ^{40}Ca(4.48), and 2^+ or 3^- for ^{40}Ca(2) or (3) (Sh 59). At $E_\alpha = 44$ MeV, ^{40}Ca levels at 3.78, 4.47, 6.16 and 6.74 MeV, all ± 0.07 MeV, are excited; the α' angular distribution points to odd parity for all these states, and to spins $J = 3$, 5 (or 1), (3), and (3), respectively (Be 61e, Sa 61a). In Bl 59a, the α' angular distribution measurements given in Sh 59 are re-analysed, with diffraction scattering theory, yielding $J^\pi = 3^-$ for ^{40}Ca(4.48 MeV). See also Ko 60b.

J. ^{40}Sc(β^+)^{40}Ca $\qquad Q_m = 13950 \pm 200$

The half-life has been measured as 0.35 sec (Ty 54), 0.22 ± 0.03 sec (Gl 55), 0.179 ± 0.002 sec (Sc 59c). The β^+ end point is 9.0 ± 0.4 MeV (Gl 55), 9.2 ± 0.2 MeV ($\log ft = 4.1$) (Sc 59c). A γ ray ($E_\gamma = 3.75 \pm 0.04$ MeV) has been observed. No delayed α particles are found (Gl 55). Discussion of a possible β^+ transition to the lowest $T = 1$ state in ^{40}Ca, expected at 7.5 MeV, Bo 55, Wi 56a.

K. Not reported:

^{38}Ar(^{3}He, n)^{40}Ca	$Q_m = 6985.7 \pm 4.1$
^{39}K(d, n)^{40}Ca	$Q_m = 6111.7 \pm 4.4$
^{39}K(^{3}He, d)^{40}Ca	$Q_m = 2843.3 \pm 4.3$
^{39}K(α, t)^{40}Ca	$Q_m = -11476.3 \pm 4.4$
^{42}Ca(p, t)^{40}Ca	$Q_m = -11350 \pm 5$

REMARKS

For theoretical discussions of ^{40}Ca states, see Da 59a, Sh 60. A discussion of vibrational 3^- states in ^{40}Ca is given in Br 61f, La 60.

^{41}Ar

(Fig. 41.1, p. 259; table 41.1, p. 260)

A. ^{41}Ar(β^-)^{41}K $\qquad Q_m = 2490 \pm 10$

The half-life measurement with the lowest stated error, yielding 109.6 ± 0.4 min (Ha 51a), is in good agreement with older measurements with larger errors (En 54a).

The β^- decay proceeds by two branches. The end point of the ground-state transition has been measured by magnetic spectrometer as 2.48 ± 0.04 MeV (intensity 0.88%) (Sc 56), and 2.485 ± 0.010 MeV (intensity 0.78%) (Ka 61b), yielding $\log ft = 8.5$, $\log (W_0^2-1) ft = 10.0$. The shape of the spectrum is unique once-forbidden ($\Delta J = 2$, yes) (Sc 56). The end point of the main branch has been measured by magnetic spectrometer as 1.245 ± 0.005 MeV (Br 50a), 1.199 ± 0.008 MeV (Sc 56), and 1.195 ± 0.008 MeV (Ka 61b). The spectrum has an allowed shape (Br 50a, Sc 56, Ka 61b). Log $ft = 5.1$.

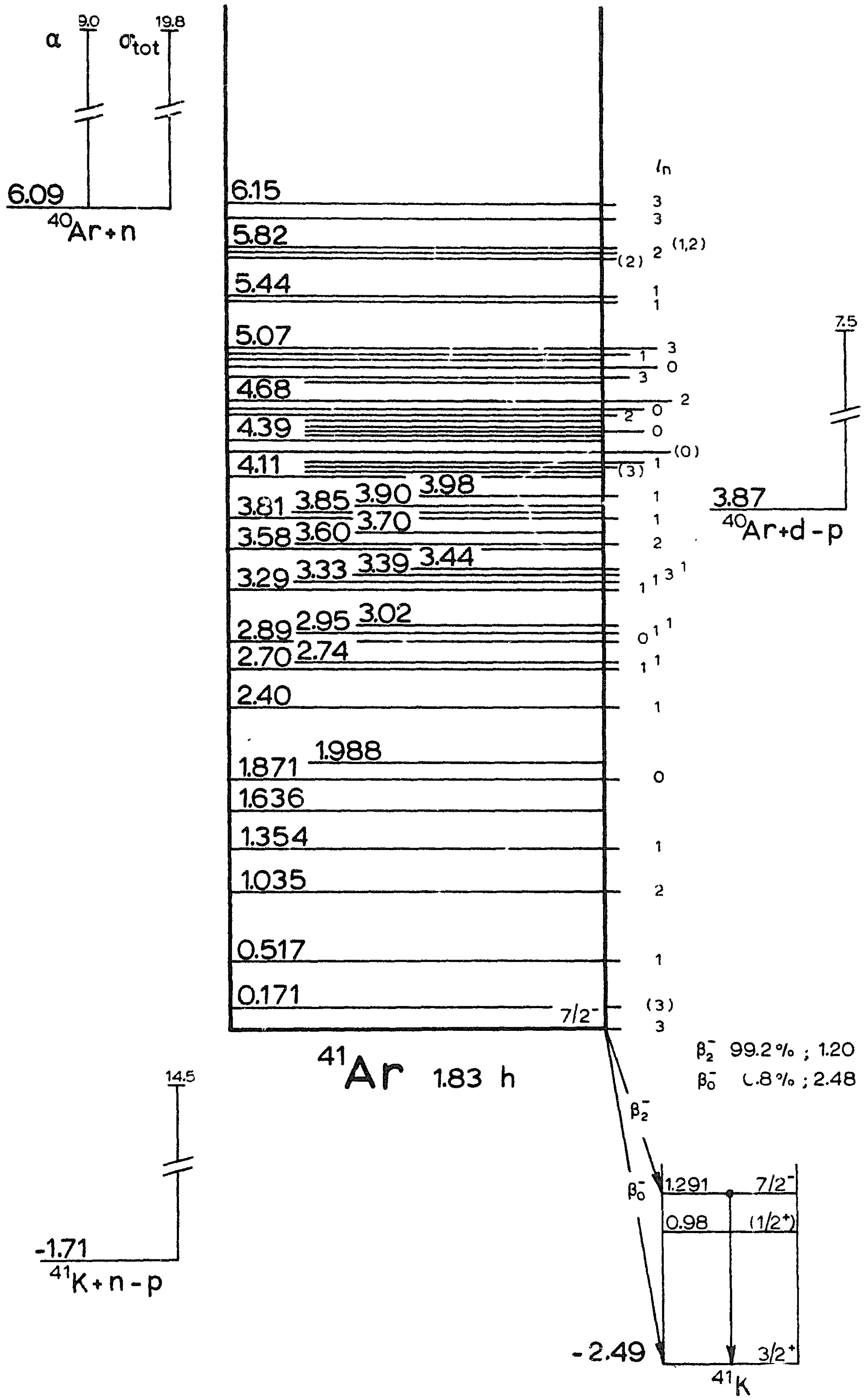

Fig. 41.1. Energy levels of ^{41}Ar.

TABLE 41.1

Energy levels of ^{41}Ar

E_x (MeV)	J^π	$\tau_{\frac{1}{2}}$	Decay	Reactions
0	$\frac{7}{2}^-$	109.6±0.4 min	β^-	A, B, E, F
0.171–6.146; 50 levels, see table 41.2 and reaction				E

The energy of the γ ray following the main β^- branch has been measured by scintillation spectrometer as 1.298±0.010 MeV (Kl 55), and 1.290±0.005 MeV (Sc 56), and by magnetic spectrometer as 1.290±0.004 MeV (Ka 61b). The conversion coefficient is (6.8±0.9) × 10^{-5}, indicating an M2 transition (Ka 61b).

By β–γ delayed coincidence measurements the half-life of the 1.29 MeV level in ^{41}K has been established as (6.7±0.5) × 10^{-9} sec (El 52), and 6.6 × 10^{-9} sec (En 53), which is 60 times slower than the single particle estimate for an M2 transition.

Two measurements of the β–γ circular polarization correlation are contradictory as to the existence of a Fermi contribution in the β^- matrix element (Ma 59e; Bl 60c, Bl 61c). Theoretically, this contribution should be quite small (Bo 61a).

A measurement of the β–γ angular correlation shows that the parity non-conserving relative amplitude in the γ decay is smaller than 6 × 10^{-5} (Bo 60).

For a jj-coupling computation of the β^- matrix element, see Gr 56c.

B. ^{40}Ar(n, γ)^{41}Ar $\qquad Q_m = 6092 \pm 11$

The thermal neutron capture cross section is 0.53±0.02 b (Hu 58). For the cross section at $E_n \approx 1$ MeV, see Hu 58.

C. ^{40}Ar(n, n)^{40}Ar $\qquad E_b = 6092 \pm 11$

There are no resonances in the total cross section beneath $E_n = 10$ keV (Hu 58). See also He 57a, Sp 60. Pronounced resonance structure has been observed in the $E_n = 0.4$–1.1 MeV region (Gu 53). For the $E_n = 0.12$–6.2 MeV and 12.1–19.8 MeV regions, see Va 60c.

D. ^{40}Ar(n, α)^{37}S $\qquad Q_m = -2420 \pm 90 \qquad E_b = 6092 \pm 11$

Pronounced resonance structure has been observed in the 5.8–9.0 MeV region (Da 61b). For non-resonance data, see ^{37}S.

E. ^{40}Ar(d, p)^{41}Ar $\qquad Q_m = 3868 \pm 11$

The ground-state Q value has been measured as 3.874±0.004 MeV. High resolution angular distribution measurements have been performed at $E_d = 7.5$ MeV. Excitation energies of 56 ^{41}Ar levels, l_n values, and reduced widths are listed in table 41.2 (Ka 61a). For earlier measurements at low resolution, see En 57. The reduced widths from the older work, as analysed in

TABLE 41.2

Levels in ^{41}Ar from the ^{40}Ar(d, p)^{41}Ar reaction (Ka 61a)

^{41}Ar* [a] (MeV)	l_n	$(2J+1)\theta_n^2 \times 10^3$	^{41}Ar* [a] (MeV)	l_n	$(2J+1)\theta_n^2 \times 10^3$
0	3	68	4.135		
0.171	(3)	weak	4.163	(3)	
0.517	1	16	4.180	1	3.0
1.035	2	4.9	4.305	(0)	
1.354	1	68	4.395		
1.636		weak	4.414		
1.871	0	3.4	4.447	0	0.37
1.988		weak	4.487		
2.402	1	11.2	4.526	isotropic	weak
2.701	1	1.3	4.577	2	4.4
2.740	1	11.3	4.613	0	0.53
2.895	0	0.4	4.676	2	7.2
2.955	1	7.5	6.816	isotropic	weak
3.017	1	3.4	4.840	3	8.7
3.293	1	0.83	4.935	0	1.3
3.335	1	19	4.977		
3.393	3	2.9	5.018	1	3.3
3.438	1	1.6	5.070	3	16
3.577	isotropic		5.407	1	2.8
3.601	2	0.9	5.440	1	1.3
3.705	isotropic		5.754	(2)	2.5
3.808	1	1.7	5.790	2	1.8
3.847	isotropic	weak	5.825	(1, 2)	
3.900		weak	6.041	3	9
3.979	1	17	6.146	3	15
4.108					

[a] Errors in excitation energies range from 2 keV for the 0.171 MeV level to 9 keV for all levels above 4.5 MeV. For $E_x > 5.07$ MeV only the levels with relatively high yields have been included.

Ma 60d, are in fair agreement with those given in Ka 61a. See also Ma 60d for theoretical remarks on the observed widths. See also Ra 56a.

F. ^{41}K(n, p)^{41}Ar $\qquad Q_m = -1707 \pm 10$

For the cross section at $E_n = 14.5$ MeV, see Pa 53.

G. Not reported:

^{40}Ar(t, d)^{41}Ar $\qquad Q_m = -165 \pm 11$

^{40}Ar(α, ^{3}He)^{41}Ar $\qquad Q_m = -14485 \pm 11$

^{41}K(t, ^{3}He)^{41}Ar $\qquad Q_m = -2472 \pm 10$

^{43}Ca(n, ^{3}He)^{41}Ar $\qquad Q_m = -12195 \pm 12$

^{44}Ca(n, α)^{41}Ar $\qquad Q_m = -2754 \pm 11$

^{41}K

(Fig. 41.2, p. 263; table 41.3, p. 264)

A. ^{40}Ar(p, γ)^{41}K $Q_m = 7799.8 \pm 4.3$

Fifty seven resonances have been found in the $E_p = 0.7$–1.4 MeV range (Ar 61, Va 60e). See table 41.4. Gamma-ray spectra have been investigated at the 1086 and 1101 keV resonances, yielding a.o. $E_\gamma = 1.59$, 1.29, 0.98, and 0.60 MeV (Va 60e). The first three are probably ground-state transitions, the last a transition from ^{41}K(1.58) to ^{41}K(0.98). See also Br 48a.

B. ^{40}Ar(p, p)^{40}Ar $E_b = 7799.8 \pm 4.3$

Strong resonances for elastic scattering have been observed at 1.90 and 2.48 MeV (Fr 58), 1.86 and 2.45 MeV (Va 59b), 1.88, 2.45, and 3.4 MeV (Ba 60d). The 1.86 MeV resonance is at least double; the 2.45 MeV resonance has $l_p = 0$ ($J^\pi = \frac{1}{2}^-$) (Va 59b).

For non-resonance data, see ^{40}Ar.

C. ^{40}Ar(p, α)^{37}Cl $Q_m = 1592.3 \pm 2.2$ $E_p = 7799.8 \pm 4.3$

Thirty five resonances (not tabulated) have been observed in the $E_p = 2.4$–3.4 MeV region (Ba 60d).

D. ^{40}Ar(d, n)^{41}K $Q_m = 5575.1 \pm 4.3$

At $E_d = 3.2$ MeV, the ground-state Q value has been measured as 5.97 ± 0.25 MeV, and transitions are observed to ^{41}K* $= 1.34 \pm 0.15$, 3.10, and 4.0 MeV (Wo 50). See also Be 58f.

E. ^{40}K(n, γ)^{41}K $Q_m = 10095 \pm 5$

The thermal neutron absorption cross section is 70 ± 20 b (Hu 58).

Two weak high energy γ rays ($E_\gamma = 9.39 \pm 0.06$ and 8.45 ± 0.02 MeV; see table 40.3), produced by thermal neutron capture in natural potassium, are assigned to ^{40}K on account of their energies, and from experiments with targets enriched in ^{40}K (Ki 52). The first is difficult to fit into the ^{41}K level scheme, the second might excite the 1.67 MeV level.

F. ^{41}Ar(β^-)^{41}K $Q_m = 2490 \pm 10$

See ^{41}Ar.

G. ^{41}K(p, p')^{41}K

Levels found from magnetic analysis at $E_p = 6.5$ MeV are given in table 41.5 (En 58a, Ke 58).

Gamma rays of $E_\gamma = 0.98$, 1.27, and 1.65 MeV have been observed in coincidence with inelastically scattered protons. They might be explained as ground-state transitions. Gamma-ray angular distribution measurements show

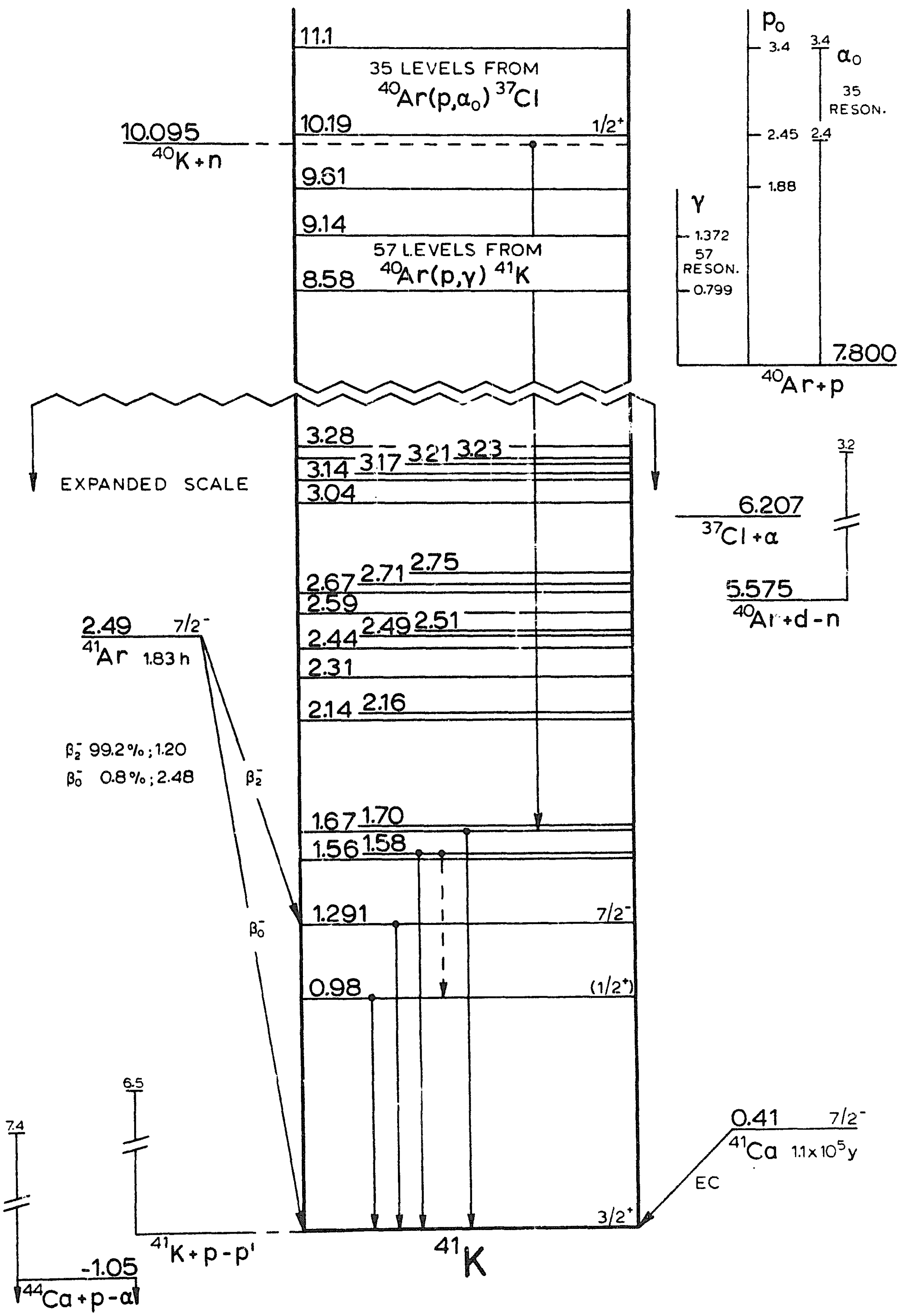

Fig. 41.2. Energy levels of ⁴¹K.

TABLE 41.3

Energy levels of ^{41}K

E_x (MeV ± keV)	J^π	$\tau_{\frac{1}{2}}$	Decay	Reactions
0	$\frac{3}{2}+$		stable	A, D, F, G, H, I
0.978 ± 6	($\frac{1}{2}+$)		γ	A, G
1.291 ± 4	$\frac{7}{2}-$	(6.7 ± 0.5) × 10^{-9} sec	γ	A, D, F, G
1.559 ± 6				G
1.580 ± 6			γ	A, G
1.675 ± 6			γ	E, G
1.696 ± 6				G
2.143–3.279; 16 levels, see table 41.5, reaction				G
8.579–9.139; 57 levels, see table 41.4, reaction				A
9.61 (double)			p	B
10.19	$\frac{1}{2}+$		p	B
10.2–11.1; 35 levels, see reaction				C
11.1			p	B

TABLE 41.4

Levels in ^{41}K from the ^{40}Ar(p, γ)^{41}K reaction (Ar 61)

E_p[a] (keV)	E_x (MeV)	E_p[a] (keV)	E_x (MeV)	E_p[a] (keV)	E_x (MeV)
799	8.579	1068	8.842	1229	8.999
819	8.599	1074	8.848	1240	9.010
856	8.635	1081	8.855	1244	9.014
898[c]	8.676	1086[d]	8.860	1249	9.019
904	8.682	1096	8.869	1258	9.027
911	8.689	1101[d]	8.874	1262	9.031
920	8.698	1108[d]	8.881	1268	9.037
942	8.719	1118[d]	8.891	1279	9.048
950	8.727	1139	8.911	1283	9.052
962[c]	8.739	1152	8.924	1293	9.061
973[b]	8.749	1162[c]	8.934	1303	9.071
985	8.761	1170	8.941	1321	9.089
995	8.771	1179	8.950	1331	9.099
1005	8.781	1186	8.957	1336	9.103
1015[b]	8.790	1194	8.965	1349	9.116
1029	8.804	1200	8.971	1358	9.125
1049	8.823	1207	8.978	1365	9.132
1052	8.826	1217	8.987	1368	9.135
1061	8.835	1222	8.992	1372	9.139

[a] All values ± 1 keV.

[b] Double.

[c] Probably double.

[d] Also observed in Va 60e, at proton energies about 6 keV higher.

TABLE 41.5

Levels in ^{41}K (E_x in MeV) from the ^{41}K(p, p′)^{41}K reaction (En 58a, Ke 58)[a]

0.978	2.143	2.588	3.139
1.291	2.165	2.673	3.173
1.559	2.315	2.709	3.212
1.580	2.438	2.755	3.230
1.675	2.493	3.045	3.279
1.696	2.507	all ±0.006 MeV	

[a] E_p = 6.5 MeV, enriched target, magnetic analysis at two different angles.

that the 0.98 MeV level in ^{41}K is most likely a $\frac{1}{2}^+$ state (Sh 58c, Sh 59a, Sh 61).

For resonances, see ^{42}Ca.

H. ^{41}Ca(EC)^{41}K $\quad Q_m = 413 \pm 9$

See ^{41}Ca.

I. ^{44}Ca(p, α)^{41}K $\quad Q_m = -1047 \pm 6$

By magnetic analysis at $E_p = 6.5$ and 7.4 MeV the ground state Q value is measured as -1.057 ± 0.010 MeV (Br 56f).

J. Not reported:

^{39}K(t, p)^{41}K	$Q_m = 9410 \pm 5$
^{40}Ar(^{3}He, d)^{41}K	$Q_m = 2306.7 \pm 4.3$
^{40}Ar(α, t)^{41}K	$Q_m = -12012.9 \pm 4.3$
^{42}Ca(n, d)^{41}K	$Q_m = -8052 \pm 6$
^{42}Ca(d, ^{3}He)^{41}K	$Q_m = -4783 \pm 6$
^{42}Ca(t, α)^{41}K	$Q_m = 9536 \pm 6$
^{43}Ca(n, t)^{41}K	$Q_m = -9723 \pm 6$
^{43}Ca(p, ^{3}He)^{41}K	$Q_m = -10488 \pm 6$
^{43}Ca(d, α)^{41}K	$Q_m = 7865 \pm 6$

^{41}Ca

(Fig. 41.3, p. 266; table 41.6, p. 267)

A. ^{41}Ca(EC)^{41}K $\quad Q_m = 413 \pm 9$

The half-life is $(1.1 \pm 0.3) \times 10^5$ yr (Br 53a); $\log ft = 10.7$.

B. ^{40}Ca(n, γ)^{41}Ca $\quad Q_m = 8361 \pm 8$

The thermal neutron absorption cross section of natural calcium is 0.44 ± 0.02 b; the main contributions are from ^{40}Ca and ^{42}Ca, with cross sections of 0.22 ± 0.04 and 42 ± 3 b, and abundances of 97% and 0.64%, respectively, indicating that these isotopes contribute about equally to the cross section of natural calcium (Hu 58). For a theoretical estimate of the cross section, see Mo 60a.

Observed γ rays from thermal neutron capture in natural calcium are given

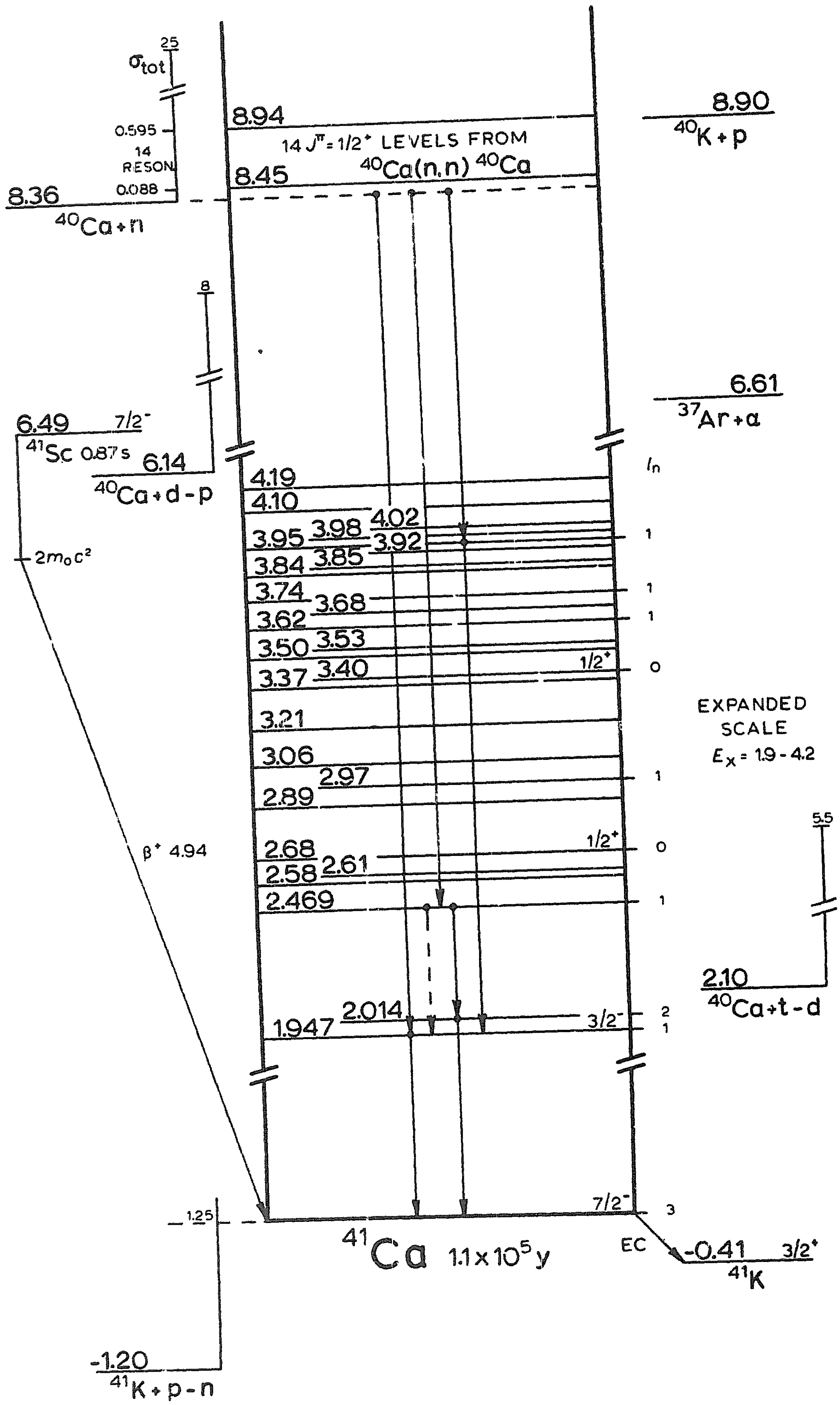

Fig. 41.3. Energy levels of ⁴¹Ca.

TABLE 41.6

Energy levels of ^{41}Ca

E_x (MeV ± keV)	J^π	$\tau_{\frac{1}{2}}$	Decay	Reactions
0	$\frac{7}{2}^-$	$(1.1 \pm 0.3) \times 10^5$ yr	EC	A, B, D, E, F, G
1.947±4	$\frac{3}{2}^-$		γ	B, D
2.014±5			γ	B, D
2.469±5			γ	B, D, E
2.584–4.194; 22 levels, see table 41.9, reaction				D (and B)
8.447–8.942; 14 levels, see table 41.8, reaction				C

TABLE 41.7

Gamma rays from thermal neutron capture in natural calcium

Ad 56, Gr 58c		Ki 52, Ba 58c		Probable transition in ^{41}Ca[b]
Magn. Compton spectrometer		Magn. pair spectrometer		
E_γ (MeV)	Intensity[a]	E_γ (MeV)	Intensity[a]	
		7.83±0.05	0.4	
		7.43±0.05	0.6	
6.406±0.015	22	6.42±0.03	40	C → 1.95
5.90 ±0.03	3.8	5.89±0.03	6	C → 2.47
5.70 ±0.03	1.2	5.66±0.06	3	
5.50 ±0.04	1.2	5.49±0.05	4	^{42}Ca(n, γ)^{43}Ca
5.15 ±0.04	0.9			^{42}Ca(n, γ)^{43}Ca
4.94 ±0.03	2.3	4.95±0.03	5	
4.76 ±0.03	2.5	4.76±0.03	4	
4.418±0.015	12.3	4.45±0.05	18	C → 3.95
3.76 ±0.02	1.8			
3.60 ±0.01	6.4	3.62±0.05	10	
2.81 ±0.03	⩾ 3.6	Br 56e		
2.66 ±0.05	⩾ 2.0	Two-crystal scint. spectrom.		
2.004±0.010	12.7			3.95 → 1.95, 2.01 → 0
1.944±0.008	39	1.93±0.03	45	1.95 → 0
1.844±0.015	6.4			
1.790±0.015	⩾ 3.6			
≈ 1.48	≈ 3.2			
≈ 1.2	≈ 4.8			
(0.532±0.010)	≈ 5			2.47 → 1.95
0.463±0.010	≈ 9	0.48±0.05	15	2.47 → 2.01

[a] Number of photons per 100 captures in natural calcium.
[b] The capturing state is denoted by C.

in table 41.7. By using enriched material it has been made probable that the 5.50 and 5.15 MeV lines result from capture in ^{42}Ca. It is not clear why the observed intensity sum of ^{42}Ca(n, γ) lines is so relatively small (Ad 56). For comparison between (n, γ) and (d, p) intensities, see Gr 58b, Bo 59a.

The circular polarization has been measured of the strong 6.41 MeV γ ray, resulting from capture of polarized thermal neutrons. This yields $J^{\pi} = \frac{3}{2}^{-}$ for the 1.95 MeV level in ^{41}Ca (Tr 57).

Cross section at higher E_n, Hu 58, Be 58e.

C. ^{40}Ca(n, n)^{40}Ca $E_b = 8361 \pm 8$

Observed resonances in the total cross section below $E_n = 600$ keV (Bi 61a, Wi 61) are given in table 41.8. See also Ma 58. Considerable resonance structure has also been observed in the $E_n = 600$–1000 keV region (Wi 61). For total cross section measurements in the $E_n = 1$–25 MeV region, see Hu 58, Co 58, Cr 58, Pe 60.

For non-resonance data, see ^{40}Ca.

TABLE 41.8

Resonances in the ^{40}Ca+n total cross section[a]

E_n (keV)	^{41}Ca* (MeV)	Γ_n (keV)	$\theta_n^2 \times 10^2$
88 ±0.25	8.447	0.148±0.015	0.10
132 ±0.5	8.490	2.54 ±0.12	1.3
144 ±0.5	8.501	0.19 ±0.04	0.09
167 ±1.0	8.524	2.49 ±0.25	1.1
220 ±3	8.576	7.0 ±1.5	2.2
254 ±1[b]	8.609	22.7 ±2[b]	8.3
299 ±2	8.653	2.2 ±0.5	0.90
337.5 ±2	8.690	13.6 ±1.2	4.3
360 ±2	8.712	1.5 ±0.6	0.46
(440)	(8.790)		
447.5 ±2	8.798	13.4 ±1.5	3.7
(485)	(8.834)		
504 ±2	8.853	10.6 ±2.0	2.8
595 ±2	8.942	58 ±4	13.8

[a] Bi 61a for $E_n < 250$ keV; Wi 61 for $E_n > 250$ keV. All resonances are probably s wave ($J^{\pi} = \frac{1}{2}^{+}$). Several weaker resonances might be present.

[b] In Bi 61a $E_n = 250 \pm 4$ keV and $\Gamma_n = 20 \pm 3$ keV is given for this resonance.

D. ^{40}Ca(d, p)^{41}Ca $Q_m = 6136 \pm 8$

The ground-state Q value is 6.140 ± 0.009 MeV (Br 56g). Levels in ^{41}Ca from magnetic analysis, and the results from high resolution angular distribution measurements are given in table 41.9. The latter results are in essential agreement with earlier low resolution results at $E_d = 8.1$ MeV (Ho 53c). See also Te 57a, Za 60. For a discussion of the reduced widths, see Fu 54, Ra 56, Be 58a, Ma 60d.

For measurements of proton polarization, see Hi 58d, Ta 60d, Jo 61; for measurements with polarized deuterons, Hi 60e.

For resonances in the yield of the ground-state group in the $E_d = 1.5$–4.2 MeV region, see Le 57.

E. ^{40}Ca(t, d)^{41}Ca $\qquad Q_m = 2103 \pm 8$

At $E_t = 5.5$ MeV, angular distributions have been measured yielding $l_n = 3$ and 1 for the deuteron groups leading to ^{41}Ca(0) and ^{41}Ca(2.47), respectively (De 61b).

F. ^{41}K(p, n)^{41}Ca $\qquad Q_m = -1196 \pm 9$

The threshold has been observed at $E_p = 1.25 \pm 0.02$ MeV (Ri 50); the Q value is measured as -1.10 ± 0.05 MeV (El 58). Cross section, Sc 58a.

For resonances, see ^{42}Ca.

TABLE 41.9

Levels in ^{41}Ca from the ^{40}Ca(d, p)^{41}Ca reaction[a]

^{41}Ca* (MeV ± keV)	l_n	$(2J+1)\theta_n^2$, $\times 10^3$	^{41}Ca* (MeV ± keV)	l_n	$(2J+1)\theta_n^2$ $\times 10^3$
0	3	114	3.500 ± 7		
1.947 ± 4	1	80	3.531 ± 7		
2.014 ± 5	2[b]	5	3.619 ± 7	1[b]	5
2.469 ± 5	1	27	3.682 ± 7		
2.584 ± 6			3.736 ± 7	1[b]	3
2.612 ± 6			3.837 ± 7		
2.677 ± 6	0	1	3.854 ± 7		
2.890 ± 6			3.921 ± 7		
2.967 ± 6	1	2	3.950 ± 7	1[b]	32
3.056 ± 6			3.982 ± 7		
3.206 ± 6			4.023 ± 7		
3.375 ± 7			4.101 ± 7		
3.405 ± 7	0	1.2	4.194 ± 7		

[a] Excitation energies from Br 56g; angular distribution results ($E_d = 7.0$ MeV) from Bo 57c. Groups for which no l_n and reduced width has been indicated are weak and/or isotropic. Reduced widths in Bo 57c are not absolute; they have roughly been normalized (Ma 60d) with the help of the absolute widths given in Ho 53c.

[b] Two l_n values are indicated in Bo 57c as possible for these groups; for reasons given in Ma 60d, always the lowest l_n value has been taken here.

G. ^{41}Sc(β^+)^{41}Ca $\qquad Q_m = 6495 \pm 13$

The half-life has been measured as 0.87 ± 0.03 sec (El 41), 0.873 sec (Ma 52a), 0.87 ± 0.05 sec (Wa 60a), and 0.628 ± 0.014 sec (Ja 60a). The β^+ end point, as measured by cloud chamber is 4.94 ± 0.07 MeV (El 41). A recent measurement, however, yields 5.65 ± 0.10 MeV (Cl 60b). The transition is superallowed ($\log ft = 3.6$).

H. Not reported:

^{38}Ar(α, n)^{41}Ca	$Q_m = -5231 \pm 9$
^{39}K(t, n)^{41}Ca	$Q_m = 8215 \pm 9$
^{39}K(^{3}He, p)^{41}Ca	$Q_m = 8979 \pm 9$
^{39}K(α, d)^{41}Ca	$Q_m = -9373 \pm 9$

^{40}Ca(α, ^{3}He)^{41}Ca	$Q_m = -12217 \pm 8$
^{41}K(^{3}He, t)^{41}Ca	$Q_m = -\ \ 431 \pm 9$
^{42}Ca(p, d)^{41}Ca	$Q_m = -\ \ 9247 \pm 9$
^{42}Ca(d, t)^{41}Ca	$Q_m = -\ \ 5214 \pm 9$
^{42}Ca(^{3}He, α)^{41}Ca	$Q_m = \ \ 9105 \pm 9$
^{43}Ca(p, t)^{41}Ca	$Q_m = -10919 \pm 9$

REMARKS

For theoretical work on the ^{41}Ca level scheme, see Ni 58, **Kh 59**, **Ab 60**, Sh 60.

^{42}Ar

(Fig. 42.1, p. 270; table 42.1, p. 271)

A. ^{42}Ar(β^-)^{42}K $\qquad Q_m = 583 \pm 45$

Successive capture of two neutrons in ^{40}Ar in a nuclear reactor has produced ^{42}Ar. Its presence has been detected by the observation of the 12.5 hr ^{42}K daughter activity in milkings from irradiated argon gas. From the fact that the

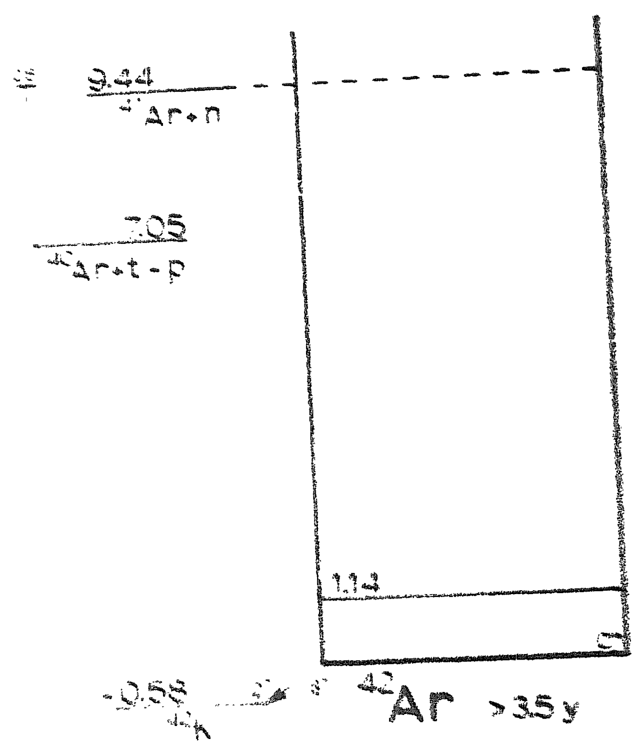

Fig. 42.1. Energy levels of ^{42}Ar.

milkings over a period of 400 days did not show a decrease in activity of m[illegible] than 20%, a lower limit for the ^{42}Ar half-life is obtained of 3.5 yr (Ka [illegible]). Assuming that the β decay is unique first-forbidden (log ft = 10), the half-[illegible] can be estimated from the known decay energy as 300 yr.

TABLE 42.1

Energy levels of ^{42}Ar

E_x (MeV ± keV)	J^π	$\tau_{\frac{1}{2}}$	Decay	Reactions
0	0^+	> 3.5 yr	β^-	A, B, C
1.138 ± 30				B

B. ^{40}Ar(t, p)^{42}Ar $\qquad Q_m = 7046 \pm 40$

From magnetic analysis at $E_t = 2.6$ MeV, the ground state Q value has been measured as 7.046 ± 0.040 MeV. The first excited state in ^{42}Ar is at 1.138 ± 0.030 MeV (Ja 61d).

C. ^{41}Ar(n, γ)^{42}Ar $\qquad Q_m = 9436 \pm 41$

The thermal neutron capture cross section is larger than 0.06 b (Ka 52a).

D. Not reported:

^{44}Ca(n, ^{3}He)^{42}Ar $\qquad Q_m = -13896 \pm 40$

^{42}K

(Fig. 42.2, p. 272; table 42.2, p. 271)

A. ^{42}K(β^-)^{42}Ca $\qquad Q_m = 3530 \pm 20$

The measurement of the half-life with the lowest stated error, 12.516 ± 0.007 hr (Bu 53), is in reasonable agreement with older results with larger errors (En 54a), and with more recent measurements, 12.37 ± 0.09 hr (Ma 59g), 12.46 ± 0.07 hr (Wr 57).

TABLE 42.2

Energy levels of ^{42}K

E_x (MeV)	J^π	Γ	Decay	Reactions
0	2^-		β^-	A, B, D, E, F, G, H
0.104–4.842; 55 levels, see table 42.4, reaction				D
7.534		35 eV	n	C
7.545		60 eV	n	C

There are strong β^- transitions to ^{42}Ca(0) and (1). The best measurement of the end points yields 3.545 ± 0.010 and 1.985 ± 0.010 MeV, respectively (Po 56). The intensity of the low-energy branch (in percents of total decay) has been measured as 30% (Bl 47), 25% (Si 47), (20 ± 1)% (Ka 53), 16% (Si 47a), 18.2% (Ko 54), (10.8 ± 0.6)% (Em 55), (18.4 ± 1.4)% (Ma 59g). The average, 18%, yields $\log ft = 7.9$, $\log (W_0^2-1)\, ft = 9.7$, for β_0^-, and $\log ft = 7.5$ for β_1^-.

One strong and many weak γ lines have been observed; see table 42.3. They

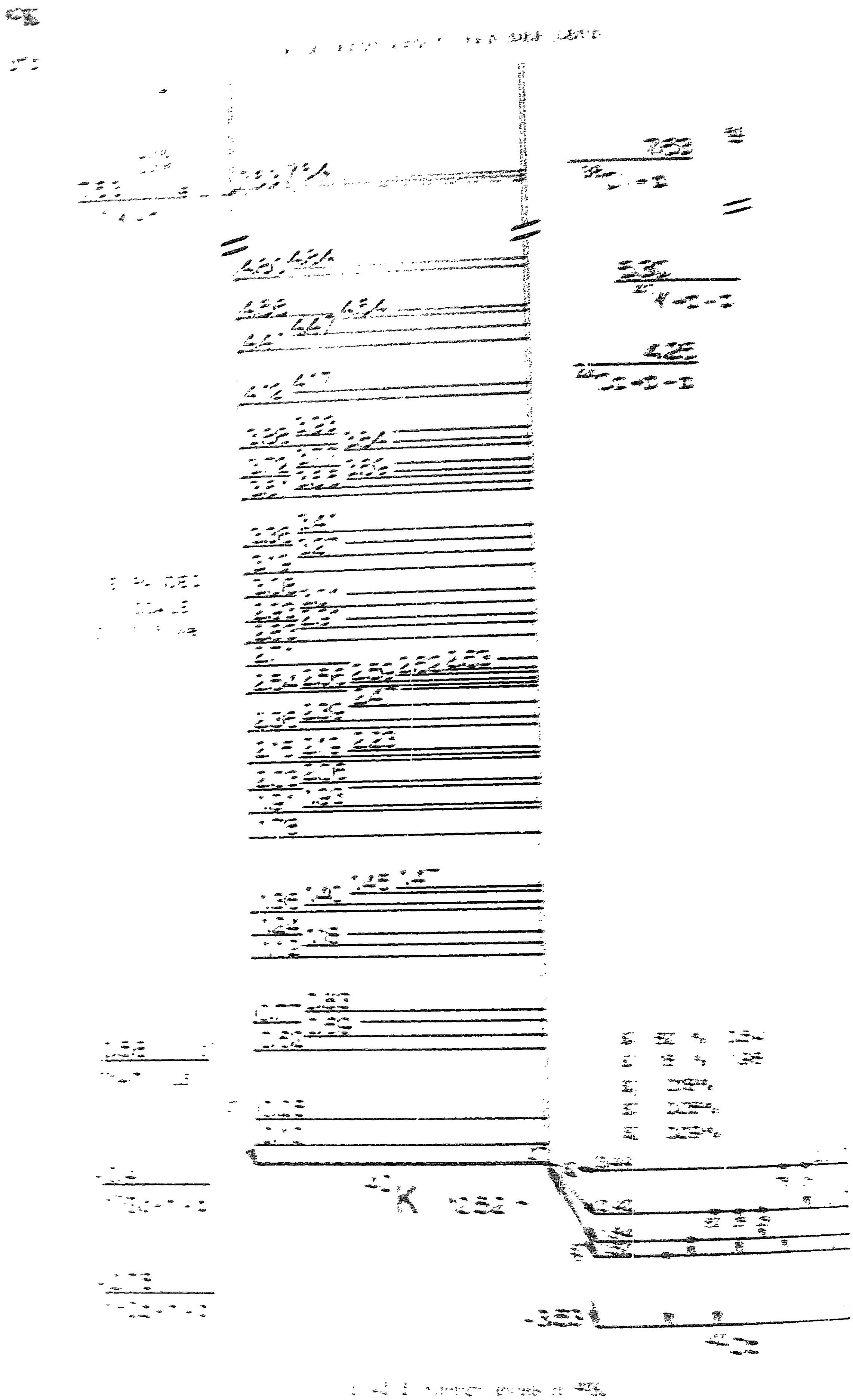

TABLE 42.3

Gamma rays following the $^{42}K(\beta^-)^{42}Ca$ decay[a]

La 54b Scint. spectrom.	Po 56 Magn. spectrom.	Mo 59b Scint. spectrom.	Mc 61 Scint. spectrom.	Probable transition in ^{42}Ca[b]
0.309 (1.5)	0.320±0.005 (0.8)	0.31 (1)[c]	0.31±0.01 (1.1)[c]	1.84 → 1.52
			(0.49±0.02) (< 0.1)	(3.25 → 2.75)
			0.60±0.02 (0.1)[c]	2.42 → 1.84
		0.9 (0.3)[c]	0.90±0.02 (0.1)[c]	2.42 → 1.52
			1.02±0.02 (0.1)[c]	3.44 → 2.42
1.52 (100)	1.53 ±0.01 (100)	1.53 (100)	1.52±0.01 (100)	1.52 → 0
		1.94 (0.3)[c]	1.92±0.01 (0.3)[c]	3.44 → 1.52
		2.42 (0.2)	2.42±0.02 (0.2)	2.42 → 0

[a] Gamma-ray energies in MeV; intensities, in percents of E_γ = 1.52 MeV intensity, in brackets.
[b] Excitation energies of ^{42}Ca levels in MeV.
[c] In coincidence with E_γ = 1.52 MeV.

yield branching ratios of 0.18% (log ft = 9.2), 0.05% (log ft = 8.1), < 0.02% (log ft > 7.9), and 0.09% (log ft = 5.1), for the β^- transitions to the 1.84, 2.42, 3.25, and 3.44 MeV ^{42}Ca levels, respectively (Mc 61).

The shape of the high-energy β^- spectrum is unique first-forbidden (ΔJ = 2, yes), from which a $J^\pi = 2^-$ assignment follows for ^{42}K(0) (Si 47, Sh 49, Ko 54, Po 56; for theory, see De 53a, Sc 54c). The β^- transition to ^{42}Ca(1) has the allowed shape (Ko 54, Po 56); for theory, see Ko 58.

The β–γ (E_γ = 0.31 MeV) angular correlation is not isotropic (Be 50, St 51b, St 61a). For β–γ polarization correlation measurements, see Ha 53a, St 58a.

The γ–γ (E_γ = 0.31–1.52 MeV) angular correlation yields a $J = 0 \to 2 \to 0$ sequence (As 59, Mo 59b), in contradiction to an earlier result (Ca 54). From a delayed coincidence experiment the mean life of ^{42}Ca(2) has been measured as $(4.8\pm0.3)\times10^{-10}$ sec (Si 61).

B. $^{41}K(n, \gamma)^{42}K$ $\qquad Q_m = 7529\pm21$

The thermal neutron absorption cross section is 1.24±0.10 b (Hu 58). For cross section at higher E_n, see Hu 58, Bo 58b, Ko 58d.

None of the γ rays from thermal neutron capture in natural potassium can be assigned to capture in ^{41}K with confidence.

C. $^{41}K(n, n)^{41}K$ $\qquad E_b = 7529\pm21$

Resonances in the total cross section have been observed at E_n = 5.4 keV (Γ = 35 eV), and 16.2 keV (Γ = 60 eV), corresponding to ^{41}K* = 7.534 and 7.545 MeV, respectively (Go 58a).

D. $^{41}K(d, p)^{42}K$ $\qquad Q_m = 5304\pm21$

The ground-state Q value is 5.309±0.012 MeV (Mo 58). Levels in ^{42}K found

TABLE 42.4

Levels in ^{42}K from the ^{41}K(d, p)^{42}K reaction (Mo 58)[a]

0	1.453	*2.470*	*3.195*	*4.123*
0.104	1.472	2.542	*3.275*	*4.174*
0.252	1.776	2.563	3.356	*4.409*
0.623	*1.913*	2.595	*3.408*	*4.474*
0.689	*1.927*	*2.616*	*3.606*	*4.544*
0.772	2.035	*2.633*	*3.650*	*4.561*
0.827	*2.061*	*2.706*	3.691	*4.797*
1.120	2.162	2.832	3.719	*4.842*
1.179	2.189	*2.906*	3.766	
1.242	*2.227*	*2.929*	3.837	
1.363	*2.356*	*3.007*	*3.881*	
1.396	*2.389*	3.076	3.928	

[a] Excitation energies in ^{42}K in MeV. The relatively strong groups are printed in italics. All errors in Q values are 12 keV. There are unresolved levels in the $E_x = 2.74$–2.80 MeV region.

at $E_d = 6.0$ MeV by magnetic analysis at three angles are given in table 42.4. See also Sa 50.

E. ^{42}Ar(β^-)^{42}K $Q_m = 583 \pm 45$

See ^{42}Ar.

F. ^{42}Ca(n, p)^{42}K $Q_m = -2747 \pm 20$

Cross section, Le 57b.

G. ^{44}Ca(d, α)^{42}K $Q_m = 4257 \pm 21$

Weak ^{42}K activity observed, En 54a.

H. ^{45}Sc(n, α)^{42}K $Q_m = -407 \pm 21$

Cross section, Ba 61b.

I. Not reported:

^{40}Ar(t, n)^{42}Ca	$Q_m = 6846 \pm 20$
^{40}Ar(^{3}He, p)^{42}K	$Q_m = 7611 \pm 20$
^{40}Ar(α, d)^{42}K	$Q_m = -10742 \pm 20$
^{41}K(t, d)^{42}K	$Q_m = 1271 \pm 21$
^{41}K(α, ^{3}He)^{42}K	$Q_m = -13048 \pm 21$
^{42}Ca(t, ^{3}He)^{42}K	$Q_m = -3512 \pm 20$
^{43}Ca(n, d)^{42}K	$Q_m = -8452 \pm 21$
^{43}Ca(d, ^{3}He)^{42}K	$Q_m = -5184 \pm 21$
^{43}Ca(t, α)^{42}K	$Q_m = 9136 \pm 21$
^{44}Ca(n, t)^{42}K	$Q_m = -13331 \pm 21$
^{44}Ca(p, ^{3}He)^{42}K	$Q_m = -14095 \pm 21$

REMARKS

For a theoretical discussion of the ^{42}K level scheme, see Pa 57c, Go 57c.

^{42}Ca

(Fig. 42.3, p. 275; table 42.5, p. 276)

A. ^{39}K(α, p)^{42}Ca $\qquad Q_m = -126.0 \pm 4.4$

At $E_\alpha = 8.2$ MeV, the ground-state Q value was determined by range analysis as -0.19 ± 0.07 MeV, and levels in ^{42}Ca were observed at 1.51 ± 0.05, 1.95 ± 0.07, 2.29 ± 0.05, 2.59 ± 0.07, 3.02 ± 0.05, (3.30 ± 0.10), 3.75 ± 0.07, and (4.09 ± 0.10) MeV (Sc 55).

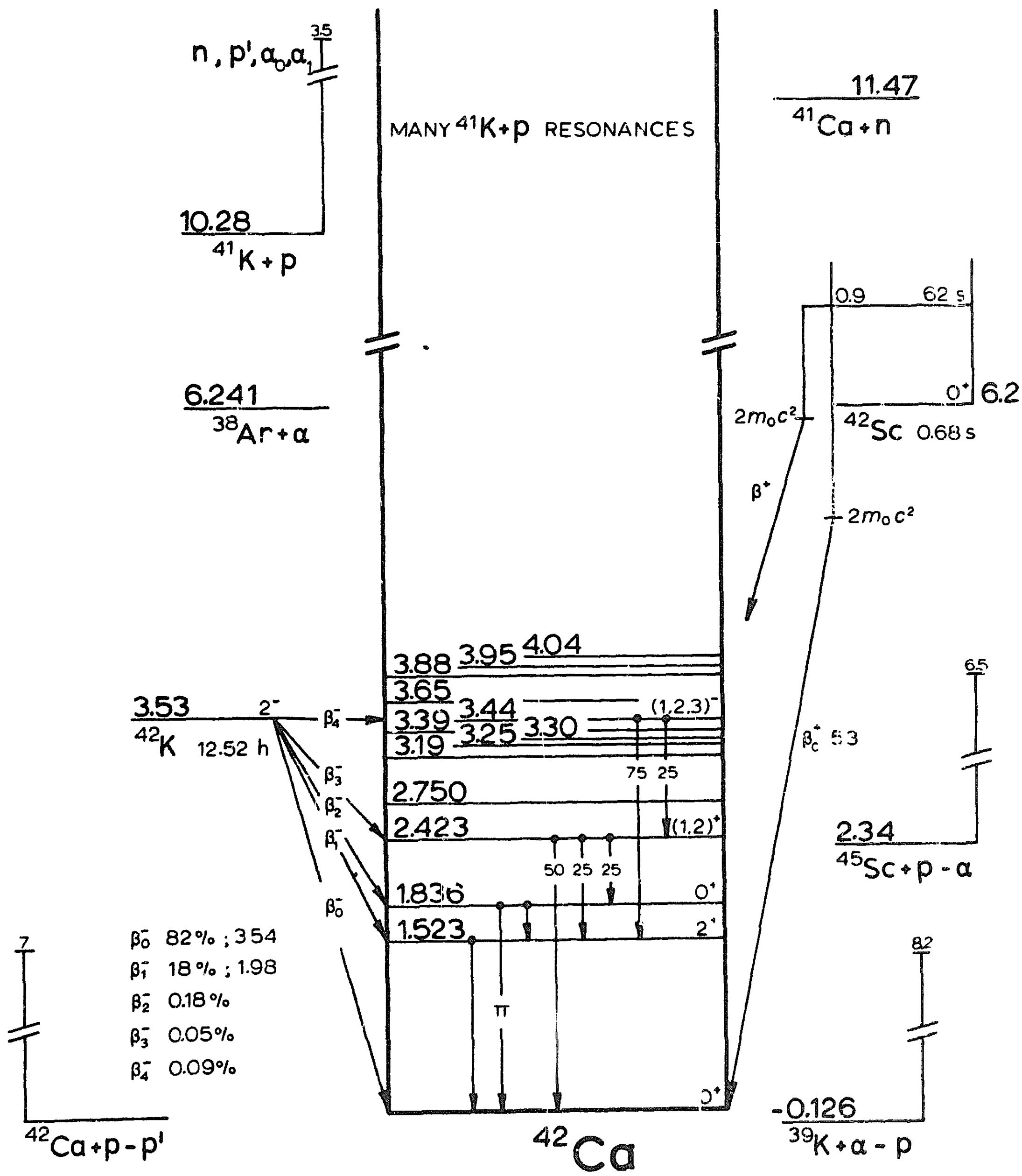

Fig. 42.3. Energy levels of ^{42}Ca.

TABLE 42.5

Energy levels of ^{42}Ca

E_x (MeV ± keV)	J^π	τ_m	Decay	Reactions
0	0^+		stable	many
1.523 ± 4	2^+		γ	A, E, F, G, H
1.836 ± 4	0^+	$(4.8 \pm 0.3) \times 10^{-10}$ sec	γ, e^+–e^-	A, E, F, H
2.423 ± 4	$(1, 2)^+$		γ	A, E, F, H
2.751 ± 4				A, F, H
3.191 ± 8				H
3.252 ± 5				A, F, H
3.297 ± 6				F
3.389 ± 6				F
3.442 ± 6	$(1, 2, 3)^-$		γ	A, E, F
3.651 ± 6				F
3.883 ± 7				F
3.949 ± 7				F
4.043 ± 7				F

B. ^{41}K(p, n)^{41}Ca $\quad Q_m = -1196 \pm 9 \quad E_b = 10276 \pm 6$

Several incompletely resolved resonances are observed in the $E_p = 1.5$–3.5 MeV region (Ri 50). For threshold, see ^{41}Ca.

C. ^{41}K(p, p′)^{41}K $\quad E_b = 10276 \pm 6$

About fifty resonances (not tabulated) in the $E_p = 2.3$–3.5 MeV region have been observed in the yield of the 0.98 MeV γ ray (Sh 58c, Sh 59a, Sh 61).

For non-resonance data, see ^{41}K.

D. ^{41}K(p, α)^{38}Ar $\quad Q_m = 4035.2 \pm 4.8 \quad E_b = 10276 \pm 6$

The α_0 yield has been measured in the $E_p = 1$–3 MeV region. Many resonances (not tabulated) have been seen at an average spacing of 8 keV (Cl 60). For resonances in the yield of the 2.16 MeV γ ray, see Sh 58c, Sh 59a, Sh 61. For Q value, see ^{38}Ar.

E. ^{42}K(β^-)^{42}Ca $\quad Q_m = 3530 \pm 20$

See ^{42}K.

F. ^{42}Ca(p, p′) ^{42}Ca

Magnetic analysis, at 90° and 120°, and at several bombarding energies between 6.5 and 7.0 MeV, gives levels in ^{42}Ca at 1.523 ± 0.004, 1.836 ± 0.004, 2.422 ± 0.005, 2.750 ± 0.005, 3.250 ± 0.006, 3.297 ± 0.006, 3.389 ± 0.006, 3.442 ± 0.006, 3.651 ± 0.006, 3.883 ± 0.007, 3.949 ± 0.007, and 4.043 ± 0.007 (Br 56f).

With a magnetic lens spectrometer, conversion electrons have been observed of 1.834 ± 0.009 and 0.305 ± 0.003 MeV transitions. The relative intensity of the former to the latter is 1.03±0.10. A continuous e^+ distribution with end point at 0.80±0.03 MeV has also been found, originating from e^+–e^- pair formation; the intensity relative to the 1.834 MeV e^- is 9.0±1.8. The shape of the e^+ spectrum and the observed relative intensities confirm the 0^+ assignment to ^{42}Ca(2) (Be 61d).

G. (a) ^{42}Sc(β^+)^{42}Ca $Q_m = 6260 \pm 60$

The half-life is 0.62±0.05 sec (Mo 55c), 0.68±0.01 sec (Cl 57a), 0.695±0.007 sec (Ja 60a). With scintillation detectors the β^+ end point has been measured as 4.8±0.9 MeV (Cl 57a), and 5.32±0.15 MeV (Ju 61). No γ rays have been detected (Cl 57a).

The decay is super-allowed (log ft = 3.4), indicating that the ^{42}Sc ground state presumably has $J^\pi = 0^+$, $T = 1$. See also Mo 54.

(b) ^{42}Sc^m(β^+)^{42}Ca $Q_m = 7130 \pm 40$

Gamma-radiation with E_γ = 0.43(1), 1.21(2), and 1.51(1) MeV (relative intensities in brackets), and annihilation radiation has been observed with a half-life of 62±4 sec. It has been produced from the ^{39}K(α, n)^{42}Sc reaction with a threshold of E_α = 8.86±0.04 MeV. Presumably, a high-spin, $T = 1$, ^{42}Sc state at E_x = 0.88±0.07 MeV is excited, decaying through β^+ emission to a high-spin ^{42}Ca level (Ne 61a). See also Ju 61.

H. ^{45}Sc(p, α)^{42}Ca $Q_m = 2341 \pm 6$

By magnetic analysis at E_p = 5.9 and 6.5 MeV, the ground-state Q value has been measured as 2.341±0.008 MeV, and levels in ^{42}Ca have been observed at E_x = 1.526, 1.836, 2.425, 2.753, 3.191, and 3.255 MeV, all ±0.008 MeV (Ma 58h, Bu 58b).

I. Not reported:

^{40}Ar(^{3}He, n)^{42}Ca	Q_m = 10358.2±4.2
^{40}Ca(t, p)^{42}Ca	Q_m = 11350 ±5
^{41}K(d, n)^{42}Ca	Q_m = 8052 ±6
^{41}K(^{3}He, d)^{42}Ca	Q_m = 4783 ±6
^{41}K(α, t)^{42}Ca	Q_m = − 9536 ±6
^{43}Ca(p, d)^{42}Ca	Q_m = − 5705 ±5
^{43}Ca(d, t)^{42}Ca	Q_m = − 1672 ±5
^{43}Ca(^{3}He, α)^{42}Ca	Q_m = 12648 ±5
^{44}Ca(p, t)^{42}Ca	Q_m = −10583 ±6

REMARKS

For theoretical discussions of the ^{42}Ca level scheme, see Sc 54a, Th 56, Ko 59a, Iw 60, Ab 60, Mi 61.

^{43}K

(Fig. 43.1, p. 278; table 43.1, p. 278)

A. $^{43}K(\beta^-)^{43}Ca$ $Q_m = 1817 \pm 10$

The half-life is 22.4 hr (Ov 49), 21.5 hr (Ru 52), 22.0 hr (Li 54a).

The β^- decay is complex; β^- end points, γ-ray energies, and relative intensities are given in table 43.2. Extensive β–γ, γ–γ, and e^-–γ coincidence measurements have been reported (Ba 57, Ni 57, Be 59a); these all support the decay scheme as given in table 43.2 and fig. 43.1. The β_5^- branch given in Li 54a must be

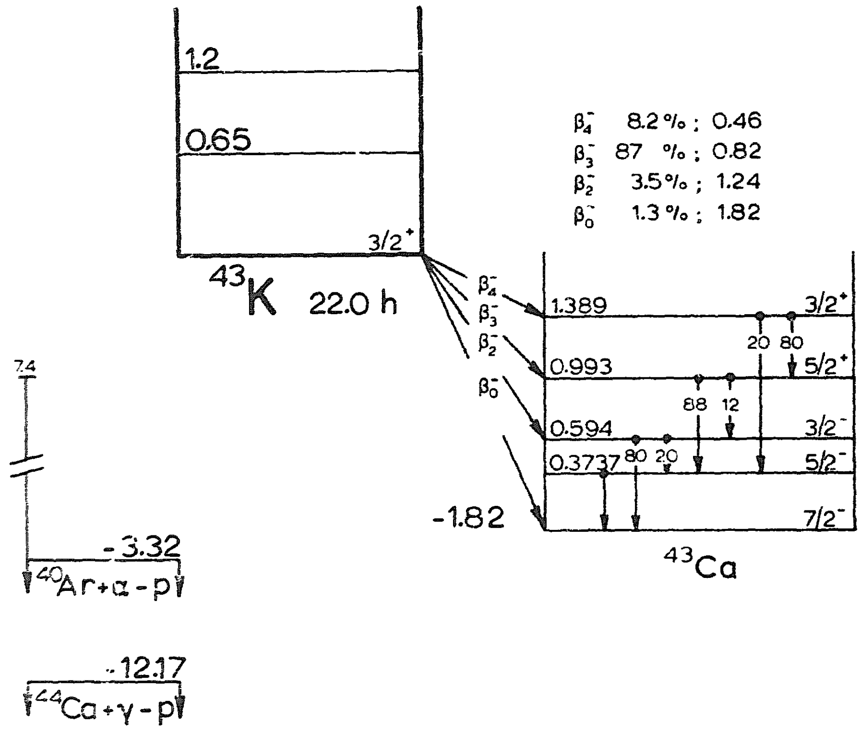

Fig. 43.1. Energy levels of ^{43}K.

TABLE 43.1

Energy levels of ^{43}K

E_x (MeV ± keV)	J^π	$\tau_{\frac{1}{2}}$	Decay	Reactions
0	$\frac{3}{2}^+$	22.0 hr	β^-	A, B, C
0.65 ± 40				B
1.18 ± 70				B

regarded as instrumental. A comparison of the γ-ray energies given in Ba 57 and Be 59a shows that the latter are low by about 0.75%. With this correction the best value found from table 43.2 for the excitation energy of ^{43}Ca(4) is 1384 ± 4 keV, which differs more than the sum of the experimental errors with the value 1394 ± 4 keV found from the ^{42}Ca(d, p)^{43}Ca and ^{43}Ca(p, p')^{43}Ca

TABLE 43.2

The ^{43}K(β^-)^{43}Ca decay[a]

	Li 54a	Ba 57	Ni 57	Be 59a		Probable
	Lens spectrom.	Double foc. sp.[b]	Lens spectrom.	Lens spectrom.[b]	log ft	transition
β_0^-	1839 ± 30 (1.6)			1814 ± 25 (1.3)	8.7	
$\beta_1^- + \beta_2^-$	1218 ± 25 (5.4)			1240 (3.5)	> 7.4	
β_3^-	827 ± 20 (83.1)			825 ± 10 (87)	5.5	
β_4^-	460 ± 20 (5.4)			465 ± 50 (8.2)	5.5	
β_5^-	243 ± 20 (4.5)					
γ_1	219 ± 4 (1)		215 ± 5	220 ± 2 (3)		(2) → (1)
γ_2	369 ± 3 (67)	373.7 ± 0.4	376 ± 4	371 ± 3 (85)		(1) → (0)
γ_3				388 ± 4 (7)		(4) → (3)
γ_4	393 ± 4 (6)			394 ± 4 (11)		(3) → (2)
γ_5				591 ± 6 (13)		(2) → (0)
γ_6	627 ± 6 (100)[c]	618.9 ± 0.6	612 ± 5	614 ± 6 (81)		(3) → (1)
γ_7	1000 ± 20 (4)	1020 ± 10	1015 ± 10	1005 ± 20 (2)		(4) → (1)

[a] Beta-decay end points and γ-ray energies in keV; relative intensities in brackets. All γ-ray energies determined from external conversion spectrum unless otherwise stated.

[b] Energy of γ_7 determined by scintillation spectrometer.

[c] Also internal conversion line observed with $\alpha_K \approx 2 \times 10^{-4}$.

reactions (table 43.2). The best value for the decay energy from the data in table 43.2 is 1.818 ± 0.010 MeV.

The shape of the β_0^- spectrum is unique first-forbidden ($\Delta J = 2$, yes), with log ft = 8.7 and log $(W_0^2-1)\,ft$ = 10.0 (Li 54a, Be 59a).

The γ–γ angular correlation of the (3) → (1) → (0) and the (4) → (1) → (0) cascades has been measured (Li 57c). For conclusions, see ^{43}Ca, Remarks. For theoretical remarks on the β–γ angular correlation, see Ga 57.

B. ^{40}Ar(α, p)^{43}K $\qquad Q_m = -3324 \pm 11$

From nuclear emulsion measurements at $E_\alpha = 7.4$ MeV, the ground state Q value has been measured as −3.36 ± 0.03 MeV, and levels in ^{43}K have been observed at 0.65 ± 0.04 and 1.18 ± 0.07 MeV (Sc 56b). Cross section, Sc 56b, Ta 60f.

C. ^{44}Ca(γ, p)^{43}K $\qquad Q_m = -12170 \pm 12$

Cross section, Br 58a.

D. Not reported:

^{41}K(t, p)^{43}K	$Q_m = 8689 \pm 12$
^{43}Ca(n, p)^{43}K	$Q_m = -1034 \pm 10$
^{43}Ca(t, ^{3}He)^{43}K	$Q_m = -1799 \pm 10$
^{44}Ca(n, d)^{43}K	$Q_m = -9946 \pm 12$
^{44}Ca(d, ^{3}He)^{43}K	$Q_m = -6677 \pm 12$
^{44}Ca(t, α)^{43}K	$Q_m = 7642 \pm 12$
^{45}Sc(n, ^{3}He)^{43}K	$Q_m = -11342 \pm 12$
^{46}Ca(p, α)^{43}K	$Q_m = -1696 \pm 15$

^{43}Ca

(Fig. 43.2, p. 281; table 43.3, p. 282)

A. ^{40}Ar(α, n)^{43}Ca $Q_m = -2289.5 \pm 4.5$

Cross section, Sc 56b. Resonances, ^{44}Ca.

B. ^{42}Ca(n, γ)^{43}Ca $Q_m = 7929 \pm 5$

The thermal neutron absorption cross section is 42 ± 3 b (Hu 58). Thermal neutron capture γ rays of 5.50 ± 0.04 and 5.15 ± 0.04 MeV are assigned to ^{42}Ca (Ad 56).

C. ^{42}Ca(d, p)^{43}Ca $Q_m = 5705 \pm 5$

The ground state Q value has been measured as 5.711 ± 0.010 MeV (Br 57b). Levels in ^{43}Ca from magnetic analysis and results from angular distribution measurements at $E_d = 7.0$ MeV are given in table 43.4. For a theoretical interpretation of the measured angular distributions, see Fr 55, Ra 56, Ma 60d.

D. ^{43}K(β^-)^{43}Ca $Q_m = 1817 \pm 10$

See ^{43}K.

E. ^{43}Ca(p, p')^{43}Ca

Levels in ^{43}Ca found by magnetic analysis are given in table 43.4.

F. ^{43}Sc(β^-)^{43}Ca $Q_m = 2220 \pm 10$

The measurement of the half-life with the smallest stated error, 3.92 ± 0.02 hr (Hi 45), is in reasonable agreement with other measurements with larger errors (En 54a, Li 54).

The β^+ decay proceeds to the lowest two ^{43}Ca states (table 43.5). For theoretical remarks on ft values, see Gr 56c, Bl 57, Ca 58.

G. ^{44}Ca(γ, n)^{43}Ca $Q_m = -11136 \pm 6$

Cross section, Go 54a.

H. Not reported:

^{41}K(t, n)^{43}Ca	$Q_m = 9723 \pm 6$
^{41}K(^{3}He, p)^{43}Ca	$Q_m = 10488 \pm 6$
^{41}K(α, d)^{43}Ca	$Q_m = -7865 \pm 6$
^{42}Ca(t, d)^{43}Ca	$Q_m = 1672 \pm 5$
^{42}Ca(α, ^{3}He)^{43}Ca	$Q_m = -12648 \pm 5$
^{44}Ca(p, d)^{43}Ca	$Q_m = -8911 \pm 6$
^{44}Ca(d, t)^{43}Ca	$Q_m = -4878 \pm 6$
^{44}Ca(^{3}He, α)^{43}Ca	$Q_m = 9441 \pm 6$
^{45}Sc(n, t)^{43}Ca	$Q_m = -9543 \pm 6$
^{45}Sc(p, ^{3}He)^{43}Ca	$Q_m = -10307 \pm 6$
^{45}Sc(d, α)^{43}Ca	$Q_m = 8045 \pm 6$
^{46}Ti(n, α)^{43}Ca	$Q_m = -79 \pm 6$

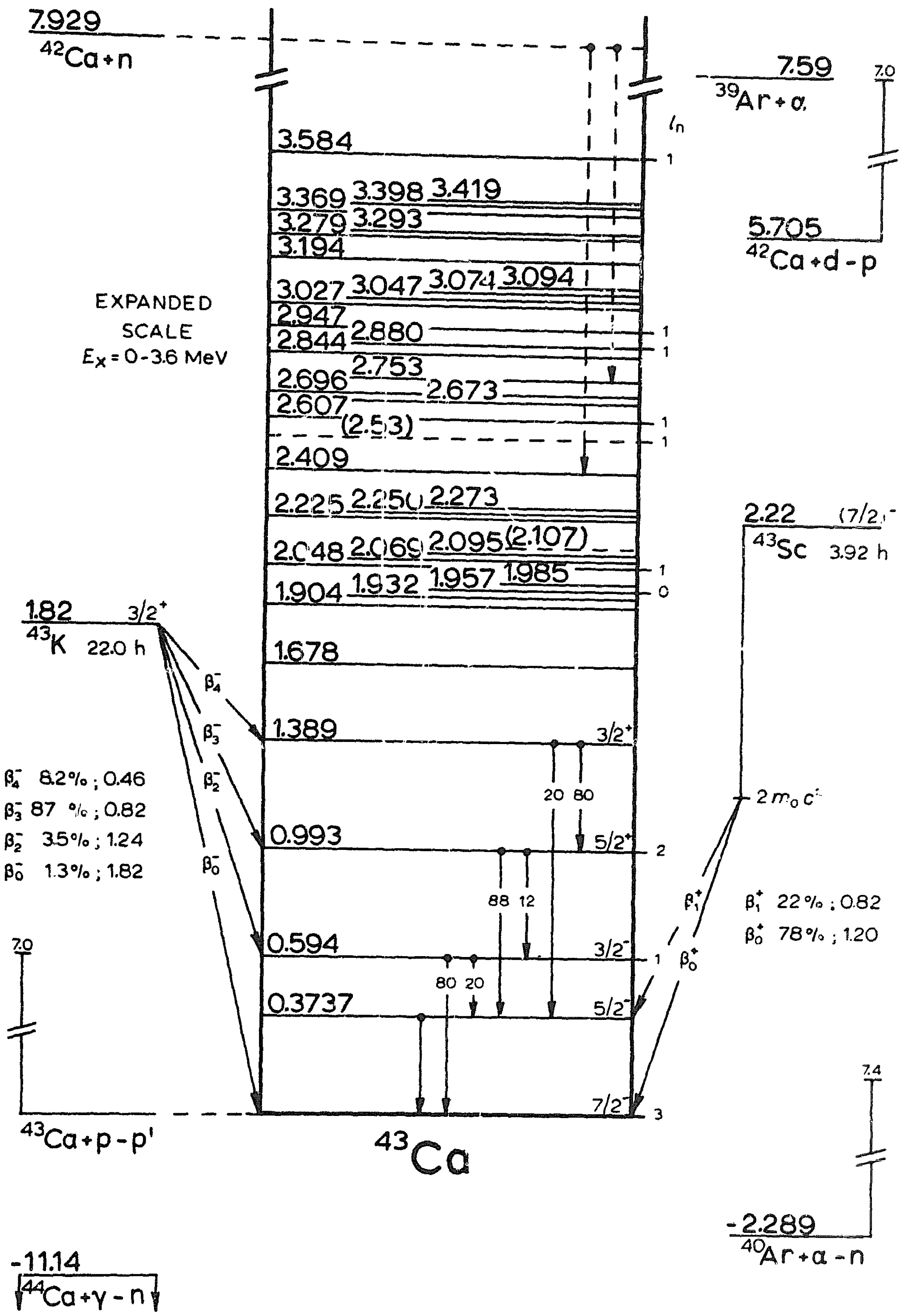

Fig. 43.2. Energy levels of ^{43}Ca.

TABLE 43.3

Energy levels of ^{43}Ca

E_x (MeV ± keV)	J^π	Decay	Reactions
0	$\frac{7}{2}^-$	stable	A, C, D, E, F, G
0.3737 ± 0.4	$\frac{5}{2}^-$	γ	C, D, E, F
0.594 ± 2	$\frac{3}{2}^-$	γ	C, D, E
0.9926 ± 0.7	$\frac{5}{2}^+$	γ	C, D, E
1.389 ± 3	$\frac{3}{2}^+$	γ	C, D, E
1.678–3.584; 32 levels, see table 43.4, reactions			C, E

TABLE 43.4

Levels in ^{43}Ca from the ^{42}Ca(d, p)^{43}Ca and ^{43}Ca(p, p')^{43}Ca reactions

^{43}Ca* [a] (MeV ± keV)	l_n [e]	$(2J+1)\theta_n^2$ [f] × 10^3	^{43}Ca* [a] (MeV ± keV)	l_n [e]	$(2J+1)\theta_n^2$ [f] × 10^3
0 [b, c]	3	82	2.607 ± 5 [b, c]	1	8
0.373 ± 3 [b, c]			2.673 ± 5 [c]		
0.593 ± 3 [b, c]	1	5	2.696 ± 5 [c]		
0.991 ± 3 [b, c]	2	4	2.753 ± 5 [c]		
1.394 ± 4 [b, c]			2.844 ± 5 [b, c]		
1.678 ± 4 [b, c]			2.880 ± 5 [b, c]	1	5
1.904 ± 4 [b, c]			2.947 ± 5 [b, c]	1	5
1.932 ± 4 [b, c]			3.027 ± 6 [c]		
1.957 ± 4 [b, c]	0	2.6	3.047 ± 6 [b, c]		
1.985 ± 5 [b]			3.074 ± 6 [c]		
2.048 ± 5 [b, c]	1	80	3.094 ± 6 [b, c]		
2.069 ± 5 [c]			3.194 ± 6 [c]		
2.095 ± 5 [c]			3.279 ± 6 [c]		
(2.107 ± 5) [c]			3.293 ± 6 [c]		
2.225 ± 5 [b, c]			3.369 ± 6 [c]		
2.250 ± 5 [b, c]			3.398 ± 6 [c]		
2.273 ± 5 [c]			3.419 ± 6 [b, c]		
2.409 ± 5 [c]			3.584 [d]	1	5
(2.53) [d]	1	1			

[a] Listed excitation energies are weighted averages (where possible) of results obtained from the ^{42}Ca(d, p)^{43}Ca and ^{43}Ca(p, p')^{43}Ca reactions.

[b] Observed from the ^{42}Ca(d, p)^{43}Ca reaction at several deuteron energies between 2.9 and 7.0 MeV and at $\vartheta = 90°$ (Br 57b).

[c] Observed from the ^{43}Ca(p, p')^{43}Ca reaction at $E_p = 6.5$ MeV ($\vartheta = 90°$) and $E_p = 7.0$ MeV ($\vartheta = 130°$) (Br 57b).

[d] Additional level observed from the ^{42}Ca(d, p)^{43}Ca reaction (Bo 57).

[e] Angular distribution measurements of the ^{42}Ca(d, p)^{43}Ca reaction at $E_d = 7.0$ MeV (Bo 57). Groups for which no l_n value and reduced width are given, are weak and/or isotropic.

[f] Normalization of reduced widths in Ma 60d. In Bo 57 only relative reduced widths are given; in Bo 57c the yields of the ^{42}Ca(d, p)^{43}Ca and ^{40}Ca(d, p)^{41}Ca reactions are compared.

TABLE 43.5

The ^{43}Sc(β^+)^{43}Ca decay

Method	$E(\beta_0^+)$ (MeV)	$E(\beta_1^+)$ (MeV)	E_γ (MeV)	Reference
magn. spectrom.	1.18±0.02 (72%)	0.77±0.04 (28%)	0.375±0.002	Ha 52d
scint. spectrom.			0.375±0.004 (25±2)%	Nu 53
magn. spectrom.	1.20±0.01 (82%)	0.82±0.02 (18%)	0.369±0.005 (16%)	Li 54[a]
magn. spectrom.			0.374±0.004	Ni 57
log *ft*	5.1	4.7		

[a] Also reported in Li 54 are a β^+ branch of 0.39±0.03 MeV end point (4%), and γ rays of $E_\gamma = 0.25 \pm 0.01$ MeV, 0.627±0.005 MeV (4%), and 0.84±0.02 MeV (weak). The existence of the last two γ rays has not been substantiated in later work (Va 57b). All these transitions seem improbable in view of what is known about ^{43}Ca spins and parities

REMARKS

For theoretical work on the ^{43}Ca level scheme, see Le 55, Ko 59a, Ab 60, Mi 61.

The ^{42}Ca(d, p)^{43}Ca angular distribution measurements (table 43.4) limit J^π of ^{43}Ca(2) and ^{43}Ca(3) to $(\frac{1}{2}, \frac{3}{2})^-$ and $(\frac{3}{2}, \frac{5}{2})^+$, respectively. The observation of a γ transition to the $\frac{7}{2}^-$ ^{43}Ca ground state (γ_5 in table 43.2), then yields for ^{43}Ca(2) the unique assignment $J^\pi = \frac{3}{2}^-$.

The ^{43}Sc ground state very probably has $J^\pi = \frac{7}{2}^-$ ($f_{\frac{7}{2}}$). The allowed character of the ^{43}Sc(β^+)^{43}Ca(1) transition then limits J^π of ^{43}Ca(1) to $(\frac{5}{2}, \frac{7}{2}, \frac{9}{2})^-$; spin $\frac{9}{2}$ can be excluded by the observation of the ^{43}Ca(3) → ^{43}Ca(1) γ transition (γ_6 in table 43.2).

The ^{43}K ground state has $J^\pi = \frac{3}{2}^+$. The allowed character of the β_4^- branch limits J^π of ^{43}Ca(4) to $(\frac{1}{2}, \frac{3}{2}, \frac{5}{2})^+$; the observation of the ^{43}Ca(4) → ^{43}Ca(1) transition (γ_7 in table 43.2) eliminates spin $\frac{1}{2}$.

If ^{43}Ca(1) had $J^\pi = \frac{7}{2}^-$, both ^{43}Ca(3) and ^{43}Ca(4) would have $J^\pi = \frac{5}{2}^+$ (because the observation of γ_6 and γ_7 rules out $\frac{3}{2}^+$). The γ_6–γ_2 and γ_7–γ_2 angular correlations would then have to be identical, of $\frac{5}{2}^+ \xrightarrow{\text{E1}} \frac{7}{2}^- \xrightarrow{\text{M1+E2}} \frac{7}{2}^-$ character. However, they have been measured to be different (Li 57c). Thus, ^{43}Ca(1) has $J^\pi = \frac{5}{2}^-$. The γ–γ angular correlation measurements then yield $J^\pi = \frac{5}{2}^+$ for ^{43}Ca(3) and $\frac{3}{2}^+$ for ^{43}Ca(4), with an E2/M1 amplitude ratio for γ_2 of $x = -0.05$ or $x = -5.4$.

^{44}K

(Not illustrated)

A. ^{44}K(β^-)^{44}Ca $\qquad Q_m = 6100 \pm 200$

Half-life, 18±1 min (Wa 37), 20 min (An 54), 22.0±0.5 min (Co 54), and 22.3 min (Su 60b).

TABLE 44.1

The $^{44}K(\beta^-)^{44}Ca$ decay[a]

References	End points (in MeV) of partial β^- spectra
Co 54	4.9 1.5
Su 60b	4.91 (10%), 3.55, 2.63
	Observed gamma rays (energies in MeV)
Co 54	1.13, 2.07, 2.48, 3.6. Also unresolved γ rays with $E_\gamma < 0.5$ MeV.
Su 60b	0.48, 0.63, 0.74, 0.90 (1), 1.06 (1), 1.16 (100), 1.5, 1.74 (13), 2.08+2.13 (13), 2.55 (12), 3.4, 3.66 (6.2), 4.4, 4.6, 5.0 (0.6).

[a] Scintillation spectrometer, both for β^- and for γ. Relative intensities in brackets.

The β^- decay is complex. End points of partial β^- spectra and observed γ rays are given in table 44.1. The assignment of most of the observed data is obscure. It is uncertain to which of the known ^{44}Ca states the 4.9 MeV β^- branch proceeds; the Q_m value is calculated assuming that this branch proceeds to $^{44}Ca^* = 1.16$ MeV.

B. ^{44}Ca(n, p)^{44}K $\quad Q_m = -5320 \pm 200$

Cross section, Le 57b.

C. Not reported:

^{44}Ca(t, ^{3}He)^{44}K $\quad Q_m = -6080 \pm 200$
^{46}Ca(n, t)^{44}K $\quad Q_m = -14660 \pm 200$
^{46}Ca(p, ^{3}He)^{44}K $\quad Q_m = -15420 \pm 200$
^{46}Ca(d, α)^{44}K $\quad Q_m = 2930 \pm 200$

^{44}Ca

(Fig. 44.1, p. 285; table 44.2, p. 285)

A. ^{40}Ar(α, n)^{43}Ca $\quad Q_m = -2289.5 \pm 4.5 \quad E_b = 8846.6 \pm 4.5$

Resonances observed with Th C′ α particles, Fu 38.

B. ^{41}K(α, p)^{44}Ca $\quad Q_m = 1047 \pm 6$

From range analysis at $E_\alpha = 7.8$ MeV, the ground-state Q value is measured as 0.98 ± 0.10 MeV, and levels in ^{44}Ca are observed at 1.13, 1.92, 2.28, 2.58, 2.97, and 3.17 MeV, all ± 0.05 MeV (Se 55).

C. ^{43}Ca(d, p)^{44}Ca $\quad Q_m = 8911 \pm 6$

From magnetic analysis at $E_d = $ [illegible].0 MeV, the ground-state Q value is measured as 8.913 ± 0.014 MeV. Transitions are also observed to the lowest six ^{44}Ca levels (Br 56f).

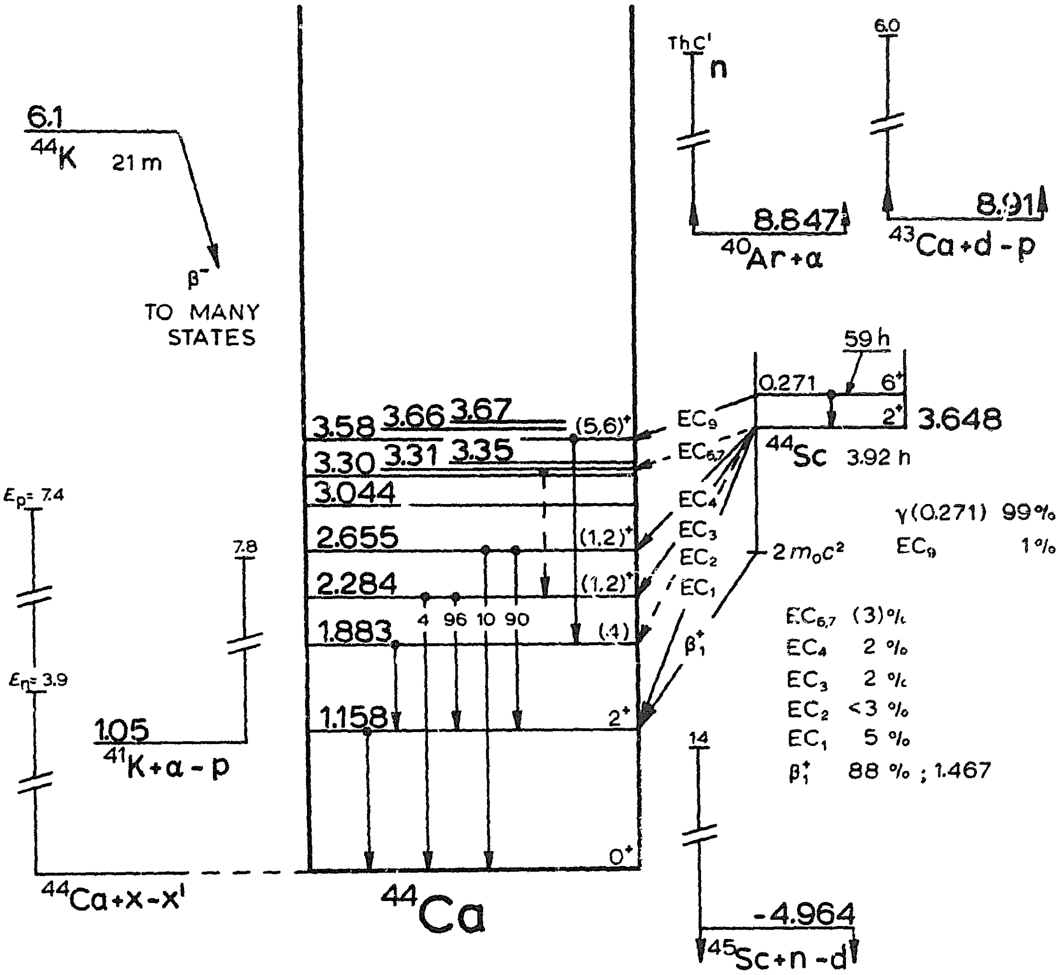

Fig. 44.1. Energy levels of ^{44}Ca.

TABLE 44.2

Energy levels of ^{44}Ca

E_x (MeV ± keV)	J^π	τ_m	Decay	Reactions
0	0^+		stable	many
1.158 ± 3	2^+	$(5.5 \pm 1.1) \times 10^{-12}$ sec	γ	B, C, D, E, F, G, H
1.883 ± 4	(4)		γ	B, C, F, H
2.284 ± 5	$(1, 2)^+$		γ	B, C, F, H
2.655 ± 5	$(1, 2)^+$		γ	B, C, F, H
3.044 ± 5				B, C, F
3.297 ± 6			(γ)	B, C, F, H
3.305 ± 6			(γ)	F, H
3.354 ± 6				F
3.581 ± 6	$(5, 6)^+$		γ	F, H
3.656 ± 6				F
3.671 ± 6				F

D. ^{44}K(β^-)^{44}Ca $Q_m = 6100 \pm 200$

See ^{44}K.

E. ^{44}Ca(n, n')^{44}Ca

From inelastic scattering of 3.9 MeV neutrons on natural calcium, a 1.152 ± 0.020 MeV γ ray has been observed with a scintillation spectrometer (Da 56c).

F. ^{44}Ca(p, p')^{44}Ca

From magnetic analysis at $E_p = 6.5$, 7.0, and 7.4 MeV, levels in ^{44}Ca have been observed at 1.156 ± 0.004, 1.883 ± 0.004, 2.284 ± 0.005, 2.655 ± 0.005, 3.044 ± 0.005, 3.297 ± 0.006, 3.305 ± 0.006, 3.354 ± 0.006, 3.581 ± 0.006, 3.656 ± 0.006, and 3.671 ± 0.006 MeV (Br 56f).

G. ^{44}Ca+heavy ions (^{14}N, ^{20}Ne)

From Coulomb excitation with 16.8 and 21.5 MeV ^{14}N ions and 26.0 MeV ^{20}Ne ions, the ^{44}Ca(1) mean life has been determined as $(5.5 \pm 1.1) \times 10^{-12}$ sec (An 61f).

H. (a) ^{44}Sc(β^+)^{44}Ca $Q_m = 3648 \pm 5$

The half-life has been measured as 3.92 ± 0.03 hr, (Hi 45), in reasonable agreement with other measurements with larger stated errors (En 54a).

TABLE 44.3

Gamma rays in the ^{44}Sc(β^+)^{44}Ca decay (Mc 61)

	E_γ [a] (MeV)	Probable transition in ^{44}Ca (E_x in MeV)		E_γ [a] (MeV)	Probable transition in ^{44}Ca (E_x in MeV)
γ_1	0.68 ± 0.02 (3.2)	1.88 → 1.16	γ_5	1.50 ± 0.02 (1.7)	2.65 → 1.16
γ_2	1.02 ± 0.02 (3.1)	3.30 → 2.28	γ_6	1.72 ± 0.02 (0.8)	3.58 → 1.88
γ_3	1.12 ± 0.02 (4.7)	2.28 → 1.16	γ_7	2.28 ± 0.02 (0.2)	2.28 → 0
γ_4	1.16 ± 0.01 (100)	1.16 → 0	γ_8	2.69 ± 0.02 (0.2)	2.65 → 0

[a] Measurements by scintillation spectrometer. Relative intensities are in brackets. Gamma rays γ_1, γ_2, γ_3, γ_5, and γ_6 are in coincidence with γ_4.

The decay is complex. The end point of the β^+ branch to ^{44}Ca(1), has been measured by magnetic spectrometer as 1.463 ± 0.005 MeV (Br 50b), and 1.471 ± 0.005 MeV (Bl 55). The Kurie plot is straight (Br 50b, Bl 55). The γ ray following the β^+ decay has $E_\gamma = 1.159 \pm 0.003$ MeV. Its conversion coefficient is $(6.3 \pm 0.3) \times 10^{-5}$, establishing this transition as E2 (Bl 55). Electron capture also occurs, with an intensity EC/$\beta^+ = 0.073 \pm 0.016$ (Bl 55), 0.023 ± 0.019 (Ko 58b). See also La 54a. Two measurements of the β–γ circular polarization are contradictory as to the existence of a Fermi contribution in the β^+ matrix element (Bo 58, Bl 61c, Bl 61d, see also Bo 60b).

A number of weak γ rays have been observed, implying electron capture to higher ^{44}Ca states (Mc 61, table 44.3). In this experiment a ^{44}Sc^{m} source was used; the ^{44}Ca 3.58 MeV level probably is excited directly from ^{44}Sc^{m}. The branching percentages to ^{44}Ca states at 1.16, 1.88, 2.28, 2.65, 3.30, and 3.58 MeV are 90.7, < 2.4, 1.8, 1.9, 3.1, and 0.8, with log ft values of 5.4, > 5.6, 5.2, 5.0, 3.8, and 5.3, respectively. The small log ft value found for excitation of the 3.30 MeV level makes the assignment of γ_2 doubtful (Mc 61). See also Bl 55.

For a jj-coupling calculation of the β^+ matrix element, see Gr 56c.

(b) ^{44}Sc^{m}(γ)^{44}Sc $\quad Q_m = 270.6 \pm 0.6$
^{44}Sc^{m}(EC)^{44}Ca $\quad Q_m = 3919 \pm 5$

The half-life is 58.6 ± 0.7 hr (Hi 45). The decay to ^{44}Sc(0) proceeds through a γ ray of energy 269.3 ± 1 keV (Sm 42), 271.3 ± 0.7 keV (Br 50b). The total conversion coefficient is 0.139 ± 0.003, in agreement with the value expected for an E4 transition (Bl 55). Electron capture to ^{44}Ca(3.58) also occurs with an intensity of 0.8%; log $ft = 5.4$ (Mc 61).

I. ^{45}Sc(n, d)^{44}Ca $\quad Q_m = -4664 \pm 5$

Observed, Co 61a.

J. Not reported:

^{42}Ca(t, p)^{44}Ca	$Q_m = 10583 \pm 6$
^{43}Ca(n, γ)^{44}Ca	$Q_m = 11136 \pm 6$
^{43}Ca(t, d)^{44}Ca	$Q_m = 4878 \pm 6$
^{43}Ca(α, ^{3}He)^{44}Ca	$Q_m = -9441 \pm 6$
^{45}Sc(d, ^{3}He)^{44}Ca	$Q_m = -1396 \pm 5$
^{45}Sc(t, α)^{44}Ca	$Q_m = 12924 \pm 5$
^{46}Ca(p, t)^{44}Ca	$Q_m = -9338 \pm 11$
^{46}Ti(n, ^{3}He)^{44}Ca	$Q_m = -9520 \pm 6$
^{47}Ti(n, α)^{44}Ca	$Q_m = 2170 \pm 9$

^{45}K

(Not illustrated)

A 34 min $A = 45$ activity, observed by electromagnetic separation of a vanadium target bombarded by 187 MeV protons, has tentatively been assigned to ^{45}K (An 54).

^{45}Ca

(Fig. 45.1, p. 288; table 45.1, p. 288)

A. ^{45}Ca(β^-)^{45}Sc $\quad Q_m = 252.0 \pm 1.9$

The half-life has been measured as 163.5 ± 4 days (De 53), 153 ± 2 days (Th 57a), 167 ± 3 days (Ca 59a); weighted average 158.2 ± 4.5 days. For older measurements with larger errors, see En 54a.

The β^- spectrum is simple; no γ rays have been observed. The end point has been measured by magnetic spectrometer as 255 ± 4 keV (Ke 50), 254 ± 3 keV (Ma 50b), 261 ± 4 keV (Ma 53). The Kurie plot is straight; log ft = 5.7. Computation of ft value with configurational mixing, Ca 58.

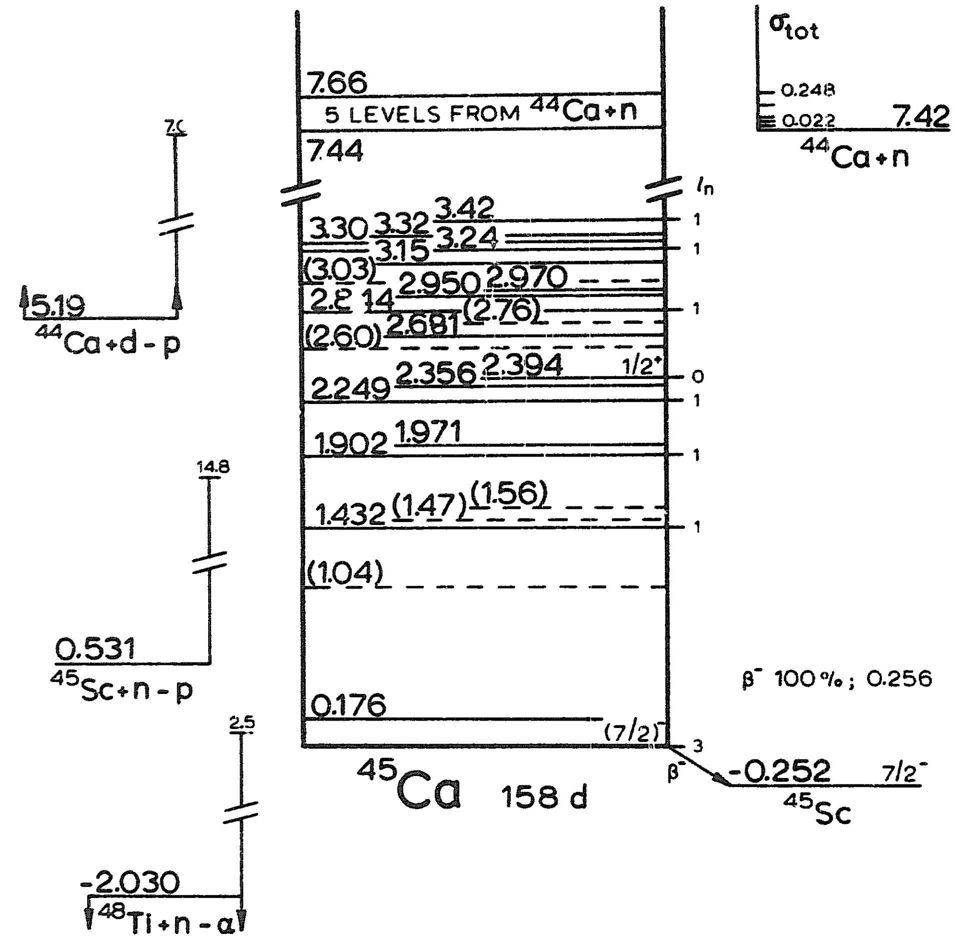

Fig. 45.1. Energy levels of ^{45}Ca.

TABLE 45.1

Energy levels of ^{45}Ca

E_x (MeV)	J^π	$\tau_{\frac{1}{2}}$	Decay	Reactions
0	$(\frac{7}{2})^-$	158.2 ± 4.5 days	β^-	A, B, D, E, F
0.176–3.419; 22 levels, see table 45.3, reaction				D
7.442–7.661; 5 levels, see table 45.2, reaction				C

B. ^{44}Ca(n, γ)^{45}Ca $\qquad Q_m = 7420\pm6$

The thermal neutron capture cross section is 0.67 ± 0.07 b (Hu 58).

C. ^{44}Ca(n, n)^{44}Ca $\qquad E_b = 7420\pm6$

Resonances in the total cross section are given in table 45.2 (Bi 61a).

TABLE 45.2

Resonances in the ^{44}Ca+n total cross section (Bi 61a)[a]

E_n (keV)	^{45}Ca* (MeV)	Γ_n (keV)	Sample
22 ±1	7.442	0.54±0.30	natural calcium
51.5±1	7.470	2.13±0.70	natural calcium
82 ±2	7.500	1.87±1.00	natural calcium
150 ±3	7.567	8.6 ±1.0	enriched
247 ±3	7.661	2.26±0.25	enriched

[a] All resonances are probably s-wave.

TABLE 45.3

Levels in ^{45}Ca from the ^{44}Ca(d, p)^{45}Ca reaction

^{45}Ca*[a] (MeV±keV)	l_n[b]	$(2J+1)\theta_n^2$[b] $\times 10^3$	^{45}Ca*[a] (MeV±keV)	l_n[b]	$(2J+1)\theta_n^2$[b] $\times 10^3$
0	3	45	2.681±5		
0.176± 3			(2.763±5)		
(1.036±10)			2.844±5	1[c]	9
1.432± 4	1	11	2.950±5		
(1.475± 6)			2.970±5		
(1.557±10)			(3.032±6)		
1.902± 4	1	54	3.148±6		
1.971± 4			3.244±6	1[c]	4
2.249± 5	1	9	3.296±6		
2.356± 5			3.319±6		
2.394± 5	0	2.5	3.419±6	1[c]	17
(2.597± 5)					

[a] Br 56f.

[b] Co 57. Only relative reduced widths are given in Co 57. They have been normalized, in Ma 60d, by means of the relative yields of the ^{44}Ca(d, p)^{45}Ca and ^{40}Ca(d, p)^{41}Ca ground-state transitions given in Bo 57c, and by using the absolute reduced width of ^{40}Ca(d, p)^{41}Ca given in Ho 53c.

[c] The lower of two possible l_n values has been chosen, for reasons given in Ma 60d.

D. ^{44}Ca(d, p)^{45}Ca $\quad Q_m = 5195\pm6$

The ground-state Q value is 5.188±0.010 MeV (Br 56f). Levels in ^{45}Ca observed at several deuteron energies between 2.9 and 7.0 MeV (Br 56f), and the results of angular distribution measurements at $E_d = 7.0$ MeV (Co 57), are given in table 45.3. Theoretical remarks, Fr 55, Ra 56, To 59a, Sa 60, Ma 60d.

E. ^{45}Sc(n, p)^{45}Ca $\quad Q_m = 530.6\pm1.9$

Cross section, Za 59, Ba 61b.

F. ^{48}Ti(n, α)^{45}Ca $\quad Q_m = -2030\pm5$

Cross section, He 48.

G. Not reported:

^{44}Ca(t, d)^{45}Ca	$Q_m = 1162 \pm 6$
^{44}Ca(α, ^{3}He)^{45}Ca	$Q_m = -13158 \pm 6$
^{45}Sc(t, ^{3}He)^{45}Ca	$Q_m = -233.9 \pm 1.9$
^{46}Ca(p, d)^{45}Ca	$Q_m = -8176 \pm 11$
^{46}Ca(d, t)^{45}Ca	$Q_m = -4143 \pm 11$
^{46}Ca(^{3}He, α)^{45}Ca	$Q_m = 10177 \pm 11$

^{46}Ca

(Not illustrated)

Not reported:

^{44}Ca(t, p)^{46}Ca	$Q_m = 9338 \pm 11$
^{48}Ca(p, t)^{46}Ca	$Q_m = -8896 \pm 16$
^{49}Ti(n, α)^{46}Ca	$Q_m = 223 \pm 10$

^{47}Ca

(Not illustrated)

A. ^{47}Ca(β^-)^{47}Sc $\qquad Q_m = 1996 \pm 16$

Half-life measurement with lowest stated error: 4.51 ± 0.02 days (Fo 60a). For older measurements, En 57.

The β^- decay is complex. End points of β^- branches, γ-ray energies, and relative intensities are given in table 47.1. The log *ft* values for β_0 and β_2 are 8.5 and 6.0, respectively.

TABLE 47.1

The beta decay of ^{47}Ca

	Co 53[a] magn. spectrom.	Ma 53 magn. spectrom.	Ly 55 Al abs. + scint. spectrom.	Li 56 magn. spectrom. + scint. spectrom.
E_{β_0} (MeV)		2.060 ± 0.020[b] (19%)	1.93 ± 0.2 (24 ± 6)%	1.940 ± 0.020[b] (17%)
E_{β_2} (MeV)		0.685 ± 0.006 (81%)	0.70 ± 0.02 (76 ± 6)%	0.660 ± 0.010[b] (83%)
E_{γ_1} (MeV)	1.303 ± 0.040		1.29 (14.2 ± 1.2)	1.31 ± 0.02[c] (13 ± 2)
E_{γ_2} (MeV)	0.800 ± 0.025		0.182 (1 ± 0.1)	0.83 ± 0.02[c] (1 ± 0.1)
E_{γ_3} (MeV)	0.495 ± 0.015		0.500 (1)	0.48 ± 0.02[c] (1)

[a] Additional γ rays of 234.0 and 149.5 keV reported in Co 53, not observed by others. The β^- end points at 1.4 ± 0.1 MeV (40%) and 0.46 ± 0.02 MeV (60%) do not fit well in the ^{47}Ca decay scheme.

[b] Kurie plot is straight.

[c] Coincidences observed between γ_2 and γ_3; neither γ_2 nor γ_3 coincident with γ_1.

The average energies of γ_1 and of the γ_2–γ_3 cascade (Co 53, Li 56) yield the excitation energy ^{47}Sc* = 1309±14 keV. With the average value for the end point E_{β_2} = 687±10 keV (Ma 53, Ly 55, Li 56) this gives a total decay energy of 1996±16 keV, in agreement with the average end point E_{β_1} = 2000±60 keV (Ma 53, Li 56).

Theoretical remarks, Gr 56c, Ca 58.

B. ^{46}Ca(n, γ)^{47}Ca Q_m = 7269±21

The cross section for thermal neutron capture is 0.25±0.10 b (Hu 58).

C. Not reported:

^{46}Ca(d, p)^{47}Ca	Q_m = 5044±21
^{46}Ca(t, d)^{47}Ca	Q_m = 1012±21
^{46}Ca(α, ^{3}He)^{47}Ca	Q_m = −13308±21
^{48}Ca(p, d)^{47}Ca	Q_m = − 7884±22
^{48}Ca(d, t)^{47}Ca	Q_m = − 3851±22
^{48}Ca(^{3}He, α)^{47}Ca	Q_m = 10469±22
^{49}Ti(n, ^{3}He)^{47}Ca	Q_m = −13085±18
^{50}Ti(n, α)^{47}Ca	Q_m = − 3446±19

^{48}Ca

(Not illustrated; table 48.1, p. 291)

A. ^{48}Ca(β^-)^{48}Sc Q_m = 122±16

This reaction has not been observed. The half-life is longer than 2×10^{16} yr; log *ft* > 21.5 (Jo 52).

B. ^{48}Ca(2β^-)^{48}Ti Q_m = 4112±13

Lower limits of the half-life for double β^- decay are given of 2×10^{18} yr (Aw 56), and 7×10^{18} yr (Do 59). However, in Mc 55 a half-life is reported of

TABLE 48.1

Energy levels of ^{48}Ca

E_x (MeV±keV)	J^π	Decay	Reactions
0	0+	stable	A, B, C
3.825±6			C
4.499±7			C

(1.6±0.7) $\times 10^{17}$ yr and a total kinetic energy of the two electrons of 4.1±0.3 MeV. Theoretical work on double β decay, Me 60. Review paper on double β decay, De 60c.

C. ^{48}Ca(p, p')^{48}Ca

From magnetic analysis at $E_p = 6.5$, 7.0, and 7.4 MeV, levels in ^{48}Ca have been observed at 3.825 ± 0.006 and 4.499 ± 0.007 MeV (Br 56f). A search for de-excitation of the first level by internal pair formation has been unsuccessful (Ek 58).

D. Not reported:

^{46}Ca(t, p)^{48}Ca	$Q_m = 8896 \pm 16$
^{50}Ti(n, ^{3}He)^{48}Ca	$Q_m = -13914 \pm 14$

^{49}Ca

(Fig. 49.1, p. 292; table 49.1, p. 293)

A. ^{49}Ca(β^-)^{49}Sc $Q_m = 5090 \pm 40$

The half-life, averaged from two measurements (Ke 56, Ma 56a) is 8.83 ± 0.14 min.

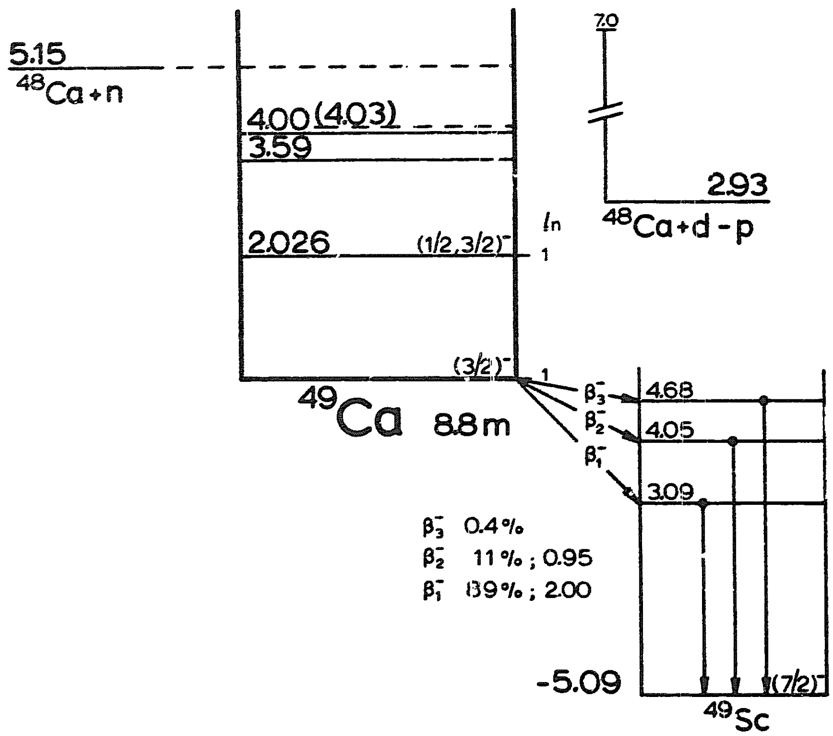

Fig. 49.1. Energy levels of ^{49}Ca.

The β^- decay is complex (table 49.2). Beta transitions with log ft values of 4.9, 4.6, and 4.5 occur to ^{49}Sc levels at 3.09, 4.05, and 4.68 MeV, respectively, which are de-excited by ground-state γ transitions.

B. ^{48}Ca(n, γ)^{49}Ca $Q_m = 5152 \pm 19$

The thermal neutron capture cross section is 1.1 ± 0.1 b (Hu 58).

TABLE 49.1

Energy levels of ^{49}Ca

^{49}Ca* (MeV ± keV)	J^{π}	$\tau_{\frac{1}{2}}$	Decay	Reactions
0	$(\frac{3}{2})^-$	8.83 ± 0.14 min	β^-	A, B, C
2.026 ± 5	$(\frac{1}{2}, \frac{3}{2})^-$			C
3.589 ± 6				C
4.004 ± 7				C
(4.026 ± 10)				C

TABLE 49.2

The beta decay of ^{49}Ca

	Ke 56[a] scint. spectrom.	Ma 56a[b] scint. spectrom.
E_{β_1} (MeV)	1.95 ± 0.05 (88%)	2.12 ± 0.10
E_{β_2} (MeV)	0.95 ± 0.15 (12%)	≈ 1.0
E_{γ_1} (MeV)	3.10 ± 0.03 (90 ± 2%)	3.07 ± 0.05 (89%)
E_{γ_2} (MeV)	4.05 ± 0.05 (10 ± 2%)	4.04 ± 0.06 (10%)
E_{γ_3} (MeV)	4.68 ± 0.05 (0.38 ± 0.1%)	4.7 ± 0.1 (0.8%)

[a] Intensity of a possible 0.95 MeV γ ray is < 2%. No γ–γ coincidences are observed.
[b] Intensity of ground-state β^- transition is < 1%. Intensity of a possible 0.97 MeV γ ray is < 3%.

C. ^{48}Ca(d, p)^{49}Ca $\qquad Q_m = 2927 \pm 19$

The ground state Q value is 2.916 ± 0.006 MeV. By magnetic analysis at $E_d = 6.5$ and 7.0 MeV, levels in ^{49}Ca have been observed as given in table 49.1 (Br 56f). See also Wa 54.

Angular distribution measurements at $E_d = 6.5$ MeV show that ^{49}Ca(0) and (1) are p-states ($l_n = 1$) (Bu 55a).

D. Not reported:

^{48}Ca(t, d)^{49}Ca $\qquad Q_m = -1105 \pm 19$

^{48}Ca(α, ^{3}He)^{49}Ca $\qquad Q_m = -15425 \pm 19$

References

Ab 60 Abraham and Gupta, Nuclear Physics **19** (1960) 496

Ad 53 Adler, Huber, and Hälg, Helv. Phys. Acta **26** (1953) 349

Ad 56 Adyasevich, Groshev, Demidov, and Lysenko, Atomnaya Energiya **1** (1956) 28; J. Nuclear Energy **3** (1956) 325

Ad 56a Adyasevich, Groshev, and Demidov, Atomnaya Energiya **1** (1956) 40; J. Nuclear Energy **3** (1956) 258

Ad 61 Adelson and Waddell, Bull. Amer. Phys. Soc. **6** (1961) 375

Ad 61a Adams, Fox, Heydenburg, and Temmer, Bull. Amer. Phys. Soc. **6** (1961) 250

Ag 50 Agnew, Phys. Rev. **77** (1950) 655

Ag 56 Ager-Hanssen, Lönsjö, and Nordhagen, Phys. Rev. **101** (1956) 1779

Ag 59 Agodi, Cavallaro, Cortini, Emma, Milone, Rinzivillo, Rubbino, and Ferrero, Proc. of the Paris Conf., p. 625 (Dunod, Paris, 1959)

Ag 60 Aguilar, Burcham, England, García, Hodgson, March, McKee, Mosinger, and Toner, Proc. Royal Soc. A **257** (1960) 13

Ag 61 Aguilar, García, England, Hodgson, and Toner, Nuclear Physics **25** (1961) 259

Aj 55 Ajzenberg, Rubin, and Likely, Phys. Rev. **99** (1955) 654(A) and verbal report to Nuclear Data Group

Aj 59 Ajzenberg-Selove and Lauritsen, Nuclear Physics **11** (1959) 1

Aj 60 Ajzenberg-Selove and Dunning, Phys. Rev. **119** (1960) 1681

Aj 60a Ajzenberg-Selove, Cranberg, and Dietrich, Bull. Amer. Phys. Soc. **5** (1960) 493

Aj 61 Ajzenberg-Selove, Cranberg, and Dietrich, Phys. Rev. **124** (1961) 1548

Al 48a Allan and Wilkinson, Proc. Royal Soc. A **194** (1948) 131

Al 48c Albert and Wu, Phys. Rev. **74** (1948) 847(L)

Al 49 Alburger, Phys. Rev. **76** (1949) 435(L)

Al 49a Alburger, Phys. Rev. **75** (1949) 51

Al 50 Alburger and Hafner, Revs. Mod. Phys. **22** (1950) 373

Al 50a Alvarez, Phys. Rev. **80** (1950) 519

Al 50b Alburger, Hughes, and Eggler, Phys. Rev. **78** (1950) 318(A)

Al 50c Alburger, Phys. Rev. **78** (1950) 629(L)

Al 51 Allen, May, and Rall, Phys. Rev. **84** (1951) 1203

Al 55 Allen, Burcham, Chackett, Munday, and Reasbeck, Proc. Phys. Soc. A **68** (1955) 681

Al 55b Allan and Sarma, Proc. Phys. Soc. A **68** (1955) 535

Al 56 Alkhazov, Andreyev, Greenberg, and Lemberg, Physica **22** (1956) 1129; Nuclear Physics **2** (1956) 65; Zh. Eksp. Teor. Fiz. **30** (1956) 809(L); JETP **3** (1957) 964(L)

Al 56a Allen, Collinge, Hird, Maglić, and Orman, Proc. Phys. Soc. A **69** (1956) 705

Al 57 Almqvist, Bromley, Ferguson, Gove, Litherland, and Paul (Chalk River), private communication (1957)

Al 57a Allan, Proc. Phys. Soc. A **70** (1957) 195

Al 57d Alphonce, Johansson, and Tibell, Nuclear Physics **4** (1957) 672

Al 59a Allen, Burman, Herrmannsfeldt, Stähelin, and Braid, Phys. Rev. **116** (1959) 134

Al 59b Alkhazov, Grinberg, Gusinskii, Erokhina, and Lemberg, Zh. Eksp. Teor. Fiz. **37** (1959) 1530; JETP **10** (1960) 1086

Al 60 Almqvist, Bromley, and Kuehner, Phys. Rev. Lett. **4** (1960) 515

Al 60a Alexander and Bredel, Nuclear Physics **17** (1960) 153

Al 60b Almqvist, Bromley, Gove, and Litherland, Nuclear Physics **19** (1960) 1

Al 60c Almqvist, Bromley, and Kuehner, Proc. of the Kingston Conf., p. 258 (Univ. of Toronto Press, 1960)
Al 60d Alekseev, Zherebtsova, Litvin, and Nemilov, Zh. Eksp. Teor. Fiz. **39** (1960) 1508; JETP **12** (1961) 1049
Al 61 Allan, Nuclear Physics **24** (1961) 274
Al 61a Almqvist and Ferguson, as quoted in Mc 61a
Al 61b Albert and Hansen, Phys. Rev. **123** (1961) 1749
Am 52 Ambrosen, Nature **169** (1952) 408(L)
Am 61 Ambrozy, Faudrowicz, Jasinski, Kownacki, Lancman, and Ludziejewski, Proc. Rutherford Jubilee Conf., Manchester (1961)
An 52 Anderson, Wheeler, and Watson, Phys. Rev. **87** (1952) 897(L)
An 53 Anderson, Wheeler, and Watson, Phys. Rev. **90** (1953) 606
An 54 Andersson, Phil. Mag. **45** (1954) 621
An 54a Antenova, Bashilov, Dzhelepov, and Orlov, Izvest. Akad. Nauk, Ser. Fiz. **18** (1954) 93
An 57 Andersen, Holtebekk, Lönsjö, and Tangen, Nuclear Physics **4** (1957) 39
An 57a Anders and Meinke, Nucleonics **15** (1957) No. 12, 68
An 59 Andersen, Bö, Holtebekk, Lönsjö, and Tangen, Nuclear Physics **9** (1959) 509
An 59a Anderson, Gardner, McClure, Nakada, and Wong, Phys. Rev. **115** (1959) 1010
An 59b Andersen, Holtebekk, Lönsjö, and Tangen, Nuclear Physics **13** (1959) 310
An 60 Andreyev, Grinberg, Erokhina, and Lemberg, Nuclear Physics **19** (1960) 400
An 60a Antufev, Valter, Gonchar, Kopanets, Lvov, and Tsytko, Izvest. Akad. Nauk, Ser. Fiz. **24** (1960) 877
An 60b Anders and Meinke, Phys. Rev. **120** (1960) 2114
An 60c Angeli, Közlemények **2** (1960) 199
An 60d Androsenko, Broder, and Lashuk, Atomnaya Energiya **9** (1960) 403
An 61 Andersen, Dörum, Gautvik, and Holtebekk, Nuclear Physics **22** (1961) 245
An 61a Andersen, Haug, Holtebekk, Lönsjö, and Nordhagen (Oslo University), private communication (1961)
An 61b Andersen, Proc. Rutherford Jubilee Conf., Manchester (1961)
An 61c Antufev, Valter, Gonchar, Kopanets, Lvov, and Tsytko, Izvest. Akad. Nauk, Ser. Fiz. **25** (1961) 265
An 61d Antufev, Gonchar, Kopanets, Lvov, and Tsytko, Izvest. Akad. Nauk, Ser. Fiz. **25** (1961) 261
An 61e Andreev, Grinberg, Erokhina, and Lemberg, Izvest. Akad. Nauk, Ser. Fiz. **25** (1961) 70
An 61f Andreev, Vasilev, Gusinskii, Erokhina, and Lemberg, Izvest. Akad. Nauk, Ser. Fiz. **25** (1961) 832
Ap 58 Appel, Schopper, and Bloom, Phys. Rev. **109** (1958) 2211(L)
Ap 59 Appel, Z. Physik **155** (1959) 580
Ar 52 Arthur, Allen, Bender, Hausman, and McDole, Phys. Rev. **88** (1952) 1291
Ar 58 Arnell, Dubois, and Almén, Nuclear Physics **6** (1958) 196
Ar 59 Arns, Sund, and Wiedenbeck, Phys. Rev. Lett. **2** (1959) 50
Ar 60 Artamonova, Gustova, Podkopaev, and Chubinskii, Zh. Eksp. Teor. Fiz. **39** (1960) 1953; JETP **12** (1961) 1109
Ar 61 Arnell, Nuclear Physics **24** (1961) 500
As 59 Asplund and Wiedling, Arkiv f. Fysik **15** (1959) 303; Phys. Rev. **116** (1959) 741
As 61 Ashe, McCrary, Nellis, and Hudson, Bull. Amer. Phys. Soc. **6** (1961) 368
Aw 56 Awschalom, Phys. Rev. **101** (1956) 1041

Ba 40 Barkas, Creutz, Delsasso, Sutton, and White, Phys. Rev. **58** (1940) 383(L)
Ba 46 Baldwin and Klaiber, Phys. Rev. **70** (1946) 259
Ba 49 Baldwin, Phys. Rev. **76** (1949) 182(A)
Ba 52 Baker, Dodd, and Simmons, Phys. Rev. **85** (1952) 1051(L)
Ba 52a Baskova and Kudriavtseva, Zh. Eksp. Teor. Fiz. **23** (1952) 83
Ba 53 Bartholomew and Kinsey, Canadian J. Phys. **31** (1953) 92
Ba 53a Bartholomew, Brown, Howell, Shorey, and Yaffe, Canadian J. Phys. **31** (1953) 714
Ba 54 Batzel and Coleman, Phys. Rev. **93** (1954) 280

Ba 55a Bartholomew, Boyd, Brown, Hawkings, Lounsbury, and Merritt, Canadian J. Phys. **33** (1955) 43

Ba 55b Backenstoss and Goebel, Z. Naturf. **10a** (1955) 920

Ba 56 Baumann, Prosser, Read, and Krone, Phys. Rev. **104** (1956) 376

Ba 57 Bäckström and Lindqvist, Arkiv. f. Fysik **11** (1957) 465

Ba 57a Bazhanov, Volkov, Komar, Kulchitskii, and Chizhov, Dokl. Akad. Nauk **113** (1957) 65; "Doklady" **2** (1957) 107

Ba 57b Basile, Annales de Physique **2** (1957) 267

Ba 58a Barber, Dodge, and Vanhuyse, Bull. Amer. Phys. Soc. **3** (1958) 173; Proc. of the Paris Conf., p. 630 (Dunod, Paris, 1959)

Ba 58c Bartholomew and Higgs, Chalk River Report A.E.C.L. No. 669 (1958)

Ba 59 Bame and Cubitt, Phys. Rev. **113** (1959) 256

Ba 59a Batchelor and Towle, Proc. Phys. Soc. **73** (1959) 307(L)

Ba 59b Barjon, Annales de Physique **4** (1959) 545

Ba 60 Batchelor, Ferguson, Gove, and Litherland, Nuclear Physics **16** (1960) 38

Ba 60b Baart, Green, and Willmott, Proc. Phys. Soc. **75** (1960) 154(L)

Ba 60c Bass, Bonner, and Haenni, Bull. Amer. Phys. Soc. **5** (1960) 248

Ba 60d Barnard and Kim, Bull. Amer. Phys. Soc. **5** (1960) 346

Ba 60f Baart, Green, and Willmott, Proc. of the Kingston Conf., p. 468 (Univ. of Toronto Press, 1960)

Ba 60g Barber, Berthold, Fricke, and Gudden, Phys. Rev. **120** (1960) 2081

Ba 61 Barnard, Bashkin, Broude, and Hornback, Nuclear Physics **23** (1961) 327

Ba 61a Baglin, Thompson, and Spicer, Nuclear Physics **22** (1961) 207 and 216

Ba 61b Bayhurst and Prestwood, Los Alamos Scientific Laboratory Report LA–2493 (1961)

Ba 61c Barker, Phys. Rev. **122** (1961) 572

Ba 61d Bardwick, Tickle, and Parkinson, Bull. Amer. Phys. Soc. **6** (1961) 259

Ba 61e Barnard, Mani, and Forsyth, Bull. Amer. Phys. Soc. **6** (1961) 259

Ba 61f Baerg and Bowes, Canadian J. Chem. **39** (1961) 684

Ba 61g Bass, Häenni, Bonner, and Gabbard, Nuclear Physics **28** (1961) 478

Be 47 Becker, Hanson, and Diven, Phys. Rev. **71** (1947) 466(A)

Be 48 Benson, Phys. Rev. **73** (1948) 7

Be 48b Berggren and Osborne, Phys. Rev. **74** (1948) 1240(A)

Be 50 Beyster and Wiedenbeck, Phys. Rev. **79** (1950) 728(L)

Be 50b Bell, Weaver, and Cassidy, Phys. Rev. **77** (1950) 399(L)

Be 50c Bell and Cassidy, Phys. Rev. **77** (1950) 409(L)

Be 50d Bell and Cassidy, Phys. Rev. **79** (1950) 173(L)

Be 51 Beghian, Bishop, and Halban, Phys. Rev. **83** (1951) 186(L)

Be 55 Bent, Bonner, McCrary, and Ranken, Phys. Rev. **100** (1955) 774

Be 55a Bellamy and Flack, Phil. Mag. **46** (1955) 341

Be 55b Bent, Bonner and McCrary, Phys. Rev. **98** (1955) 1325

Be 55c Berthet and Rossel, Helv. Phys. Acta **28** (1955) 26.

Be 56 Beyster, Walt, and Salmi, Phys. Rev. **104** (1956) 1319

Be 56a Berenbaum, Towle, and Matthews, Proc. Phys. Soc. A **69** (1956) 658(L)

Be 57b Berenbaum and Matthews, Proc. Phys. Soc. A **70** (1957) 445

Be 58a Bent and Kruse, Phys. Rev. **109** (1958) 1240

Be 58b Berko, Whitehead, and Groseclose, Nuclear Physics **6** (1958) 210

Be 58d Bernstein and Lewis, Phys. Rev. **112** (1958) 232

Be 58e Belanova, Zh. Eksp. Teor. Fiz. **34** (1958) 574; JETP **7** (1958) 397

Be 58f Benenson and Shurman, Revs. Sci. Instr. **29** (1958) 1

Be 58g Bennet, Thesis, Princeton University (1958)

Be 59 Berko, Groseclose, Stetson, and Walker, Bull. Amer. Phys. Soc. **4** (1959) 257

Be 59a Benczer-Koller, Schwarzschild, and Wu, Phys. Rev. **115** (1959) 108

Be 61 Benenson and Lidofsky, Phys. Rev. **123** (1961) 939

Be 61a Belote, Kashy, and Risser, Phys. Rev. **122** (1961) 920

Be 61b Bennett, Phys. Rev. **122** (1961) 595

Be 61c Bent and Eidson, Phys. Rev. **122** (1961) 1514

Be 61d Benczer-Koller, Nessin, and Kruse, Phys. Rev. **123** (1961) 262
Be 61e Beurtey, Catillon, Chaminade, Crut, Faraggi, Papineau, and Thirion, Comptes Rendus **252** (1961) 260
Be 61f Beckner, Bramblett, Phillips, and Eastwood, Phys. Rev. **123** (1961) 2100
Bi 50 Bishop, Nilson, and Halban, Phys. Rev. **77** (1950) 416(L)
Bi 52 Birge, Phys. Rev. **85** (1952) 753(A)
Bi 52a Birge, as quoted in Revs. Mod. Phys. **24** (1952) 321
Bi 58a Bizot, Muller, and Bishop, J. Phys. Rad. **19** (1958) 571(L); Proc. of the Paris Conf., p. 344 (Dunod, Paris, 1959)
Bi 59 Bird and Divine, M.I.T., Laboratory for Nuclear Science Progress Report, May 1 (1959) 125
Bi 59a Bishop and Kossanyi-Demay, J. Phys. Rad. **20** (1959) 911
Bi 60 Bishop, Nuclear Physics **14** (1960) 376
Bi 60a Bilaniuk and French, Nuclear Physics **17** (1960) 435
Bi 60b Bisi, Fasana, and Zappa, Nuovo Cimento **16** (1960) 350
Bi 61 Bilpuch, Seth, Bowman, and Newson, Bull. Amer. Phys. Soc. **6** (1961) 69
Bi 61a Bilpuch, Seth, Bowman, Tabony, Smith, and Newson, Annals of Physics **14** (1961) 387
Bl 46 Bleuler and Zünti, Helv. Phys. Acta **19** (1946) 137
Bl 47 Bleuler and Zünti, Helv. Phys. Acta **20** (1947) 195
Bl 51 Blaser, Boehm, Marmier, and Scherrer, Helv. Phys. Acta **24** (1951) 465
Bl 52 Bloom, Phys. Rev. **88** (1952) 312
Bl 53 Black, Phys. Rev. **90** (1953) 381(A)
Bl 55 Blue and Bleuler, Phys. Rev. **100** (1955) 1324
Bl 55a Bleuler and Tendam, Phys. Rev. **99** (1955) 1652(A)
Bl 56a Bleuler, Gailar, Seidlitz, and Tendam, Physica **22** (1956) 1127(A)
Bl 57 Blin-Stoyle and Caine, Phys. Rev. **105** (1957) 1810
Bl 57a Blok and Jonker, Nuovo Cimento **6** (1957) 378
Bl 58 Blair, Bull. Amer. Phys. Soc. **3** (1958) 26
Bl 58a Block, Phys. Rev. **109** (1958) 1217
Bl 58b Block, Haeberli, and Newson, Phys. Rev. **109** (1958) 1620
Bl 59a Blair, Phys. Rev. **115** (1959) 928
Bl 60b Blair, Farwell, and McDaniels, Nuclear Physics **17** (1960) 641
Bl 60c Bloom, Mann and Miskel, Phys. Rev. Lett. **5** (1960) 326
Bl 61 Blachman and Lurio, Bull. Amer. Phys. Soc. **6** (1961) 74
Bl 61a Blair and Hamburger, Phys. Rev. **122** (1961) 566
Bl 61b Blair and Quisenberry, Phys. Rev. **122** (1961) 869
Bl 61c Bloom and Mann, Proc. Rutherford Jubilee Conf. Manchester (1961)
Bl 61d Bloom, Mann, and Nagle, Bull. Amer. Phys. Soc. **6** (1961) 334
Bo 50 Boyer, M.I.T. Laboratory for Nuclear Science Progress Report, July 1 (1950) 166
Bo 51 Boley and Zaffarano, Phys. Rev. **84** (1951) 1059(L)
Bo 55 Bolsterli and Feenberg, Phys. Rev. **97** (1955) 736
Bo 57 Bockelman, Braams, Browne, Buechner, Sharp, and Sperduto, Phys. Rev. **107** (1957) 176
Bo 57a Bostrom, Moore, and Morgan, Bull. Amer. Phys. Soc. **2** (1957) 104
Bo 57c Bockelman, and Buechner, Phys. Rev. **107** (1957) 1366
Bo 58 Boehm and Wapstra, Phys. Rev. **109** (1958) 456
Bo 58a Boley, Thorndike, and Moffet, Phys. Rev. **110** (1958) 915
Bo 58b Booth, Ball, and MacGregor, Phys. Rev. **112** (1958) 226
Bo 59 Booth, Hutchinson, Segar, Shute, and White, Nuclear Physics **11** (1959) 341
Bo 59a Bockelman, Nuclear Physics **13** (1959) 205
Bo 59b Bouchiat, Phys. Rev. Lett. **3** (1959) 516
Bo 60 Boehm and Hauser, Nuclear Physics **14** (1960) 615
Bo 60b Bouchiat, Phys. Rev. **118** (1960) 540
Bo 60d Bormann, Jeremie, Andersson-Lindström, Neuert, and Pollehn, Z. Naturf. **15a** (1960) 200
Bo 60e Bowsher, Dell, and Hausman, Bull. Amer. Phys. Soc. **5** (1960) 406
Bo 60f Booth, Nuclear Physics **19** (1960) 426

Bo 61 Booth and Wright, Bull. Amer. Phys. Soc. **6** (1961) 37
Bo 61a Bouchiat, Proc. Rutherford Jubilee Conf., Manchester (1961)
Bo 61b Bobyr, Grona, and Strizhak, Zh. Eksp. Teor. Fiz. **41** (1961) 24
Bo 61c Boring and McEllistrem, Phys. Rev. **124** (1961) 1531
Br 47 Broström, Huus, and Koch, Nature **160** (1947) 498(L)
Br 47a Broström, Huus, and Tangen, Phys. Rev. **71** (1947) 661
Br 48 Bradner and Gow, Phys. Rev. **74** (1948) 1559(A)
Br 48a Broström, Huus, and Koch, Nature **162** (1948) 695(L)
Br 49 Brolley, Sampson, and Mitchell, Phys. Rev. **76** (1949) 624
Br 50 Brosi, Zeldes, and Ketelle, Phys. Rev. **79** (1950) 902(L)
Br 50a Brown and Perez-Mendez, Phys. Rev. **78** (1950) 649
Br 50b Bruner and Langer, Phys. Rev. **79** (1950) 606
Br 50c Brady and Deutsch, Phys. Rev. **78** (1950) 558
Br 50d Brown and Perez-Mendez, Phys. Rev. **78** (1950) 812(L)
Br 51 Broström, Madsen, and Madsen, Phys. Rev. **83** (1951) 1265(L)
Br 53 Braams and Smith, Phys. Rev. **90** (1953) 995(L)
Br 53a Brown, Yaffe, and Hanna, Proc. Royal Soc. A **220** (1953) 203
Br 53b Brabant, Cochran, and Caswell, Phys. Rev. **91** (1953) 210(A)
Br 54a Breckon, Henrikson, Martin, and Foster, Canadian J. Phys. **32** (1954) 223
Br 54b Browne, Zimmerman, and Buechner, Phys. Rev. **96** (1954) 725
Br 54c Bretscher, Alderman, Elwyn, and Shull, Phys. Rev. **96** (1954) 103
Br 55b Breen and Hertz, Phys. Rev. **98** (1955) 599
Br 56b Braams, Phys. Rev. **101** (1956) 1764
Br 56c Brugger, Evans, Joki, and Shankland, Phys. Rev. **104** (1956) 1054
Br 56e Braid, Phys. Rev. **102** (1956) 1109
Br 56f Braams, Thesis, Univ. of Utrecht (1956)
Br 56g Braams, Phys. Rev. **103** (1956) 1310
Br 56h Broude, Green, Singh, and Willmott (Liverpool Univ.), private communication (1956)
Br 56i Broude, Green, Willmott, and Singh, Physica **22** (1956) 1139(A)
Br 57 Bromley, Gove, Litherland, Paul, and Almqvist, Canadian J. Phys. **35** (1957) 1042
Br 57b Braams, Phys. Rev. **105** (1957) 1023
Br 57c Bromley, Gove and Litherland, Canadian J. Phys. **35** (1957) 1057
Br 57e Brown, Morrison, Muirhead, and Morton, Phil. Mag. **2** (1957) 785
Br 58a Brix, Hegel, Lindenberger, and Quitmann, Z. Physik **150** (1958) 461
Br 58c Broude, Green, and Willmott, Proc. Phys. Soc. **72** (1958) 1097, 1115, and 1122
Br 58d Brazos, Purdue Progress Report AECU-3696, June 15 (1958)
Br 58e Brajovic, Miric, and Popic, Bull. Inst. nat. Sciences "Boris Kidrich" **8** (1958) 145
Br 59 Broude, Green, and Willmott, Proc. of the Paris Conf., p. 724 (Dunod, Paris, 1959)
Br 59a Browne, Phys. Rev. **114** (1959) 807
Br 59b M. Brenner, Soc. Sci. Fennica Comm. Phys. Math. **23** (1959) No. 5
Br 59c Bromley, Kuehner, and Almqvist, Phys. Rev. **115** (1959) 586
Br 59d Browne, Nuclear Physics **12** (1959) 662
Br 59e Brix, Körding, and Lindenberger, Z. Physik **154** (1959) 569
Br 59f Bromley, Ferguson, Gove, Kuehner, Litherland, Almqvist, and Batchelor, Canadian J. Phys. **37** (1959) 1514
Br 60b Broude and Gove, Bull. Amer. Phys. Soc. **5** (1960) 248
Br 60d Browne and Radzyminski, Nuclear Physics **19** (1960) 164
Br 60e Broude and Gove, Proc. of the Kingston Conf., p. 471 (Univ. of Toronto Press, 1960)
Br 60f Brugger, Niewodniczanski, and Steiger, Helv. Phys. Acta **33** (1960) 576
Br 60g Bromley, Kuehner, and Almqvist, Phys. Rev. Lett. **4** (1960) 365
Br 60h Bromley, Kuehner, and Almqvist, Proc. of the Kingston Conf., p. 255 (Univ. of Toronto Press, 1960)
Br 60j Brabec and Vinduška, Czechoslov. J. Phys. **10** (1960) 614
Br 61 Braid, Yntema, and Zeidman, Bull. Amer. Phys. Soc. **6** (1961) 37
Br 61a Brenner, Hoogenboom, and Kashy, Phys. Rev., to be published
Br 61b Broude and Gove, Proc. Phys. Soc. **77** (1961) 1211(L)

Br 61c Braben, Green, and Willmott, Proc. Rutherford Jubilee Conf., Manchester (1961), and private communication
Br 61d Broude and Gove, to be published
Br 61e Brenner (Helsinki Univ.), private communication
Br 61f Brown, Evans, and Thouless, Nuclear Physics **24** (1961) 1
Bu 51 Burkig and Wright, Phys. Rev. **82** (1951) 451
Bu 53 Burch, Nature **172** (1953) 361(L)
Bu 53a Buechner, Sperduto, Browne, and Bockelman, Phys. Rev. **91** (1953) 1502
Bu 55 Budde and Huber, Helv. Phys. Acta **28** (1955) 49
Bu 55a Buechner, Proc. of the Glasgow Conf., p. 52 (Pergamon Press, London, 1955)
Bu 56 Buechner, Mazari, and Sperduto, Phys. Rev. **101** (1956) 188
Bu 56a Burge, Fujimoto, and Hossain, Phil. Mag. **1** (1956) 19
Bu 56c Burton and Williamson, Bull. Amer. Phys. Soc. **1** (1956) 264
Bu 56d Burrows, Green, Hinds, and Middleton, Proc. Phys. Soc. A **69** (1956) 310
Bu 56e Burtov and Danilyan, Izvest. Akad. Nauk, Ser. Fiz. **20** (1956) 941
Bu 57 Buechner and Sperduto, Phys. Rev. **106** (1957) 1008
Bu 57a Butler, Phys. Rev. **106** (1957) 272
Bu 57c Burcham, Encyclopedia of Physics, Springer Verlag, Berlin, **40** (1957) 1
Bu 58b Buechner and Mazari, Revista Mexicana de Fisica **7** (1958) 117
Bu 59a Burgov and Terekhov, Nuclear Physics **10** (1959) 541
Bu 59b Burmistrov, Izvest. Akad. Nauk, Ser. Fiz. **23** (1959) 898
Bu 59c Burmistrov, Atomnaya Energiya **7** (1959) 260; J. Nuclear Energy **12A** (1960) 133
Bu 60 Bussière de Nercy and Langevin, J. Phys. Rad. **21** (1960) 293(A)
Bu 60b Bussière de Nercy, Comptes Rendus **250** (1960) 1252
Bu 60c Bucka, Kopfermann, and Ney, Z. Physik **159** (1960) 49
Bu 61 Buck and Satchler, Bull. Amer. Phys. Soc. **6** (1961) 38
Bu 61a Butler, Phys. Rev. **123** (1961) 873
Bu 61b Butler and Santry, Bull. Amer. Phys. Soc. **6** (1961) 250
Bu 61c Bussière de Nercy, J. Phys. Rad. **22** (1961) 119

Ca 38 Caccapuoti, Nuovo Cimento **15** (1938) 213
Ca 53 Casson, Phys. Rev. **89** (1953) 809
Ca 54 Cappeller and Klingelhöfer, Z. Naturf. **9a** (1954) 1052 (L)
Ca 54a Carlson, Geer, and Nelson, Phys. Rev. **94** (1954) 1311
Ca 55 Calvert, Jaffe, Litherland, and Maslin, Proc. Phys. Soc. A **68** (1955) 1008
Ca 56a Calvert, Jaffe, and Maslin, Phys. Rev. **101** (1956) 501(L)
Ca 57 Calvert, Jaffe, and Maslin, Proc. Phys. Soc. A **70** (1957) 78
Ca 57a Carlson and Henton, Bull. Amer. Phys. Soc. **2** (1957) 358
Ca 57b Campion and Bartholomew, Canadian J. Phys. **35** (1957) 1361
Ca 58 Caine, Proc. Phys. Soc. **71** (1958) 939
Ca 58a Campion and Merritt, Canadian J. Phys. **36** (1958) 983(L)
Ca 59 Campbell and Fettweis, Nuclear Physics **13** (1959) 92
Ca 59a Cali and Lowe, Nucleonics **17** (1959) No. 10, 86
Ca 60 Carroll and Stephens, Phys. Rev. **118** (1960) 1256
Ce 60 Cevolani, Petralia, Righini, Valdrè, and Venturini, Nuovo Cimento **16** (1960) 950
Ch 37 Chang and Szalay, Proc. Royal Soc. A **159** (1937) 72
Ch 50 Charpak and Suzor, J. Phys. Rad. **11** (1950) 633
Ch 54 Charpak and Suzor, J. Phys. Rad. **15** (1954) 378(L)
Ch 55 Charpak, J. Phys. Rad. **16** (1955) 62
Ch 55a Charpak, J. Phys. Rad. **16** (1955) 567
Ch 56 Chick, Evans, Hancock, Hunt, and Pope, Proc. Phys. Soc. A **69** (1956) 624
Ch 58 Chidley, Katz, and Kowalski, Canadian J. Phys. **36** (1958) 407
Ch 58a Chase, Thesis, Stanford Univ. (1958)
Ch 59 Charpak and Suzor, J. Phys. Rad. **20** (1959) 31
Ch 59a Chevallier, Annales de Physique **4** (1959) 1389
Ch 60 Chrien, Jain, and Hughes, Bull. Amer. Phys. Soc. **5** (1960) 19

Ch 60a Chrien and Benade, Phys. Rev. **119** (1960) 748
Ci 38 Cichocki and Soltan, Comptes Rendus **207** (1938) 423(A)
Ci 60 Cindro and Wall, Phys. Rev. **119** (1960) 1340
Ci 60a Cindro, Cerineo, and Strzałkowski, Nuclear Physics **21** (1960) 38
Ci 61 Cindro, Cerineo, and Strzałkowski, Nuclear Physics **24** (1961) 107
Cl 46 Clarke and Irvine, Phys. Rev. **69** (1946) 680(A)
Cl 46a Clarke and Irvine, Phys. Rev. **70** (1946) 893
Cl 51 Cleland, Townsend, and Hughes, Phys. Rev. **84** (1951) 298
Cl 57 Cline and Chagnon, Phys. Rev. **108** (1957) 1495
Cl 57a Cloutier and Henrikson, Canadian J. Phys. **35** (1957) 1190
Cl 58 Cline and Chagnon, Bull. Amer. Phys. Soc. **3** (1958) 206
Cl 60 Clarke, Almqvist, and Paul, Nuclear Physics **14** (1960) 472
Cl 60a Clarke and Cross, Bull. Amer. Phys. Soc. **5** (1960) 245
Cl 60b Class, Farmer, and Cramer, as quoted in Wegner and Hall, Phys. Rev. **119** (1960) 1654
Co 40 Cork and Middleton, Phys. Rev. **58** (1940) 474(L)
Co 48 Cook, Langer, and Price, Phys. Rev. **74** (1948) 548
Co 50a Cobble and Atteberry, Phys. Rev. **80** (1950) 917(L)
Co 51a Colgate, Phys. Rev. **81** (1951) 1063(L)
Co 53 Cork, LeBlanc, Brice, and Nester, Phys. Rev. **92** (1953) 367
Co 54 Cohen, Phys. Rev. **94** (1954) 117
Co 54a Cohen, Reynolds, and Zucker, Phys. Rev. **96** (1954) 1617
Co 54b Cox, Van Loef, and Lind, Phys. Rev. **93** (1954) 925(A)
Co 55a Cohn, Bair, Kington, and Willard, Phys. Rev. **99** (1955) 644 (A), and verbal report to Nuclear Data Group
Co 55b Cohen, Phys. Rev. **98** (1955) 49
Co 55c Coleman, Phil. Mag. **46** (1955) 1135(L)
Co 56 Cohen and White, Nuclear Physics **1** (1956) 73
Co 57 Cobb and Guthe, Phys. Rev. **107** (1957) 181
Co 57a Conzett, Phys. Rev. **105** (1957) 1324
Co 57b Cox and Williamson, Phys. Rev. **105** (1957) 1799
Co 57c Connor and Fairweather, Proc. Phys. Soc. A **70** (1957) 769(L) and 909
Co 57d Colli and Facchini, Nuovo Cimento **5** (1957) 309
Co 58 Conner, Phys. Rev. **109** (1958) 1268
Co 58b Cohen, Davis, Felthauser, and Nicodemus, Phys. Rev. **111** (1958) 250
Co 58d Colli, Facchini, Iori, Marcazzan, Sona, and Pignanelli, Nuovo Cimento **7** (1958) [illegible]
Co 58e Colli, Pignanelli, Rytz, and Zurmühle, Nuovo Cimento **9** (1958) 280
Co 59 Cohen and Rubin, Phys. Rev. **114** (1959) 1143
Co 59a Corelli, Bleuler and Tendam, Phys. Rev. **116** (1959) 1184
Co 59b Colli, Cvelbar, Micheletti, and Pignanelli, Nuovo Cimento **14** (1959) 1120 and 13 (1959) 868
Co 59c Colli, Cvelbar, Micheletti, and Pignanelli, Nuovo Cimento **14** (1959) 81
Co 59d [illegible], Milone, Papa, and Rinzivillo, Nuovo Cimento **14** (1959) 54
Co 59e Cooper and Cotton, Science **129** (1959) 1360
Co 60 Cobb, Funsten, Williamson, and Hereford, Bull. Amer. Phys. Soc. **5** (1960) 288
Co 60a Colli, Marcazzan, Merzari, Sona, and Tonolini, Nuovo Cimento **16** (1960) 991
Co 60b Colli, Iori, Marcazzan, Merzari, Sona, and Sona, Nuovo Cimento **17** (1960) 634
Co 61a Colli, Iori, Micheletti, and Pignanelli, Nuovo Cimento **20** (1961) 94
Co 61b Cohen and Cookson, Nuclear Physics **24** (1961) 529
Co 61c Colli, Marcazzan, Merzari, Sona, and Tomaš, Nuovo Cimento **20** (1961) 928
Co 61d Cohen and Cookson, Nuclear Physics **29** (1962) 604
Cr 40 Creutz, Fox, and Sutton, Phys. Rev. **57** (1940) 567(A)
Cr 55 Cross and Jarvis, Phys. Rev. **99** (1955) 621(A)
Cr 56 Craig, Phys. Rev. **101** (1956) 1479
Cr 56a Cranberg and Levin, Phys. Rev. **103** (1956) 343
Cr 57 Crutchfield, Haeberli, and Newson, Bull. Amer. Phys. Soc. **2** (1957) 33
Cr 58 Cranberg, Seagrave, and Simmons, Bull. Amer. Phys. Soc. **3** (1958) 336

Cr 59 Cross and Clarke, Bull. Amer. Phys. Soc. **4** (1959) 258
Cr 60 Cross and Jarvis, Nuclear Physics **15** (1960) 155
Cr 60a Crut, Sweetman, and Wall, Nuclear Physics **17** (1960) 655
Cs 61 Csongor, Nuclear Physics **23** (1961) 107
Cu 39 Curran and Strothers, Proc. Royal Soc. A **172** (1939) 72
Cu 40 Curran, Dee, and Strothers, Proc. Royal Soc. A **174** (1940) 546
Cu 56 Culler, Fernbach, and Sherman, Phys. Rev. **101** (1956) 1047
Cu 59 Čujec-Dobovišek, Proc. of the Paris Conf., p. **634** (Dunod, Paris, 1959)
Cu 60 Cuzzocrea, Pappalardo, and Ricamo, Nuovo Cimento **16** (1960) 450
Cu 60a Cuperman, Phys. Rev. **117** (1960) 185
Cu 60b Cuzzocrea, Notarrigo, Ricamo, and Vinci, Nuovo Cimento **18** (1960) 671
Cu 61 Cuzzocrea, Notarrigo, and Vinciguerra, Nuovo Cimento **19** suppl. (1961) 310(A)
Cu 61a Cuzzocrea and Pappalardo, Nuovo Cimento **19** suppl. (1961) 311(A)

Da 49 Davison, Buchanan, and Pollard, Phys. Rev. **76** (1949) 890
Da 49a Davison, Phys. Rev. **75** (1949) 757
Da 53 Daniel, Koester, and Mayer-Kuckuk, Z. Naturf. **8a** (1953) 447(L)
Da 54 Dayton, Phys. Rev. **95** (1954) 754
Da 54a Daniel and Bothe, Z. Naturf. **9a** (1954) 402
Da 56a Dayton and Schrank, Phys. Rev. **101** (1956) 1358
Da 56c Day, Phys. Rev. **102** (1956) 767
Da 56d Dawson, Canadian J. Phys. **34** (1956) 1480
Da 57 Dalton, Hinds, and Parry, Proc. Phys. Soc. A **70** (1957) 586
Da 57a Davis, Prosser, Spencer, Young, and Johnson, Bull. Amer. Phys. Soc. **2** (1957) 304
Da 58 Daniel, Nuclear Physics **8** (1958) 191
Da 59 Davis and Harmer, Bull. Amer. Phys. Soc. **4** (1959) 217
Da 59a Davis, Bull. Amer. Phys. Soc. **4** (1959) 387
Da 59b Dalton, Parry, and Scott, Proc. Phys. Soc. **73** (1959) 677 (L)
Da 60 Davis, Bass, Bonner, and Worley, Bull. Amer. Phys. Soc. **5** (1960) 110
Da 60a Daniel and Eakins, Phys. Rev. **117** (1960) 1565
Da 60b Dahl, Costello, and Walters, Nuclear Physics **21** (1960) 106
Da 61a Daum, Bull. Amer. Phys. Soc. **6** (1961) 259 and private communication
Da 61b Davis, Bonner, Worley, and Bass, to be published
De 52 De Vries, Clay, and Veringa, Physica **18** (1952) 1264
De 53 Delaney and Poole, Phys. Rev. **89** (1953) 529 (L)
De 53a De-Shalit, Phys. Rev. **91** (1953) 1479
De 53b De-Shalit and Goldhaber, Phys. Rev. **92** (1953) 1211
De 55 De Souza Santos *et al.*, Geneva Conference Report 8/P/897 (1955)
De 56 Dearnaley, Phil. Mag. **1** (1956) 821
De 57 De Veiga Simão and Sellschop, Phys. Rev. **106** (1957) 98
De 57a Deutsch, Gittelman, Bauer, Grodzins, and Sunyar, Phys. Rev. **107** (1957) 1733(L)
De 57b De Waard and Poppema, Physica **23** (1957) 597(L)
De 58 Delyagin and Shpinel, Dokl. Akad. Nauk **121** (1958) 621; "Doklady" **3** (1958) 789
De 58a De Veiga Simão, Proc. Second Internat. Conf. Peaceful Uses of Atomic Energy, Geneva (1958), Paper No. 1813
De 58b Delyagin and Shpinel, Izvest. Akad. Nauk, Ser. Fiz. **22** (1958) 861
De 58c Deconninck and Martegani, Bull. classe sci. Acad. roy. Belg. **44** (1958) 851
De 59 De S. Barros, Forsyth, Jaffe, and Taylor, Proc. Phys. Soc. **73** (1959) 513(L)
De 59a De S. Barros, Forsyth, Jaffe, and Taylor, Proc. Phys. Soc. **73** (1959) 793
De 60 Deuchars and Dandy, Proc. Phys. Soc. **75** (1960) 855
De 60a Depraz, Legros, and Salin, J. Phys. Rad. **21** (1960) 377(A)
De 60c Dell'Antonio and Fiorini, Nuovo Cimento **17** suppl. (1960) 132
De 61 Dell, Jastram, and Hausman, Bull. Amer. Phys. Soc. **6** (1961) 93
De 61a De-Shalit, Nuclear Physics **22** (1961) 677
De 61b De S. Barros, Forsyth, Jaffe, and Taylor, Proc. Phys. Soc. **77** (1961) 853
De 61c Deuchars and Dandy, Proc. Phys. Soc. **77** (1961) 1197

De 61d Dearnaley and Ferguson, Proc. Rutherford Jubilee Conf., Manchester (1961)
Di 50 Diven and Almy, Phys. Rev. **80** (1950) 407
Di 55 Dixon, McNair, and Curran, J. Phys. Rad. **16** (1955) 538
Di 58 Dickerman, Phys. Rev. **109** (1958) 443
Di 61 Dixon and Aitken, Nuclear Physics **24** (1961) 456
Do 53 Donahue, Jones, McEllistrem, and Richards, Phys. Rev. **89** (1953) 824
Do 56 Doyle and Robbins, Phys. Rev. **101** (1956) 1056
Do 56a Dolan, Fincher, Kenny, Berko, and Whitehead, Bull. Amer. Phys. Soc. **1** (1956) 339
Do 59 Dobrokhotov, Lazarenko, and Luk'yanov, Zh. Eksp. Teor. Fiz. **36** (1959) 76; JETP 9 (1959) 54
Do 60 Doehring, Jahr, and Schmidt-Rohr, Z. Physik **159** (1960) 149
Do 60a Dosch, Lindenberger, and Brix, Nuclear Physics **18** (1960) 615
Dr 55 Drever and Moljk, Phil. Mag. **46** (1955) 1337
Dr 56 Dropesky and Schardt, Phys. Rev. **102** (1956) 426
Dr 60 Draper and Bostrom, Bull. Amer. Phys. Soc. **5** (1960) 17, and verbal report to Nuclear Data Group
Dr 61 Draper and Fleischer, Phys. Rev. **122** (1961) 1585
Du 57 Dulgeroff, Lambe, and Pond, Bull. Amer. Phys. Soc. **2** (1957) 348
Du 60 Durand, Landovitz, and Marr, Phys. Rev. Lett. **4** (1960) 620
Du 61 Du Toit and Bollinger, Phys. Rev. **123** (1961) 629
Du 61a Duquesne, Annales de Physique **6** (1961) 643
Dz 46 Dzelepov, Kopjova, and Vorobjov, Phys. Rev. **69** (1946) 538(L)

Ec 61 Eckert and Shrader, Phys. Rev. **124** (1961) 1541
Ed 52 Edwards and MacMillan, Phys. Rev. **87** (1952) 377(L)
Ed 60 Edakova, Neuchadin, and Romanovskii, Zh. Eksp. Teor. Fiz. **38** (1960) 248(L); JETP **11** (1960) 180(L).
Ei 56 Eisberg and Hintz, Phys. Rev. **103** (1956) 645
Ek 43 Eklund and Hole, Arkiv Mat. Astron. Fys. **29A** (1943) No. 26
Ek 58 Eklund and Bent, Phys. Rev. **112** (1958) 966
Ek 60 Eklund, Columbia Univ. Report CU(PNPL)-196 (1960)
El 41 Elliot and King, Phys. Rev. **60** (1941) 489
El 52 Elliot, Phys. Rev. **85** (1952) 942(L)
El 54 Elbek, Nielsen, and Nielsen, Phys. Rev. **95** (1954) 96
El 55 Elbek, Madsen, and Nathan, Phil. Mag. **46** (1955) 663
El 55a El Bedewi and El Wahab, Proc. Phys. Soc. A **68** (1955) 754
El 56 Elliot, Phys. Rev. **101** (1956) 684
El 56a El Wahab, Thesis, Univ. of Alexandria (1956)
El 57 El Bedewi and El Wahab, Nuclear Physics **3** (1957) 385
El 58 Elwyn, Landon, Oleksa, and Glasoe, Phys. Rev. **112** (1958) 1200
El 59 Elliot and Young, Nuclear Sci. and Eng. **5** (1959) 55
El 60 El Nadi and Wafik, Proc. Phys. Soc. **76** (1960) 185
El 60b Elwyn and Lane Bull. Amer. Phys. Soc. **5** (1960) 410
El 60c El Bedewi and El Wahab, Nuclear Physics **21** (1960) 49
Em 54 Emmerich, Singer, and Kurbatov, Phys. Rev. **94** (1954) 113
Em 55 Emery and Veall, Proc. Phys. Soc. A **68** (1955) 346(L)
Em 59 Emma, Milone, Rinzivillo, and Rubbino, Nuovo Cimento **14** (1959) 62
Em 59a Emma, Milone, and Rinzivillo, Nuovo Cimento **14** (1959) 1149
En 51a Endt, Van Patter, Buechner, and Sperduto, Phys. Rev. **83** (1951) 491
En 51b Ennis, Phys. Rev. **82** (1951) 304(A)
En 52 Endt, Haffner, and Van Patter, Phys. Rev. **86** (1952) 518
En 52a Enge, Buechner, and Sperduto, Phys. Rev. **88** (1952) 963
En 52b Endt, Enge, Haffner, and Buechner, Phys. Rev. **87** (1952) 27
En 53 Engelder, Phys. Rev. **90** (1953) 259
En 54 Enge, Phys. Rev. **94** (1954) 730(L)
En 54a Endt and Kluyver, Revs. Mod. Phys. **26** (1954) 95

En 54b Enge, Universitetet i Bergen Årbok Naturvitenkapelig Rekke (1954) No. 1
En 54c Endt, Kluyver, and Van der Leun, Physica **20** (1954) 1299
En 56 Enge, Angleman, and Jarrell, M.I.T., Laboratory for Nuclear Science Progress Report, May 31 (1956) 118
En 56a Enge, Buechner, Sperduto, and Mazari, Bull. Amer. Phys. Soc. **1** (1956) 212
En 56c Endt, Paris, Sperduto, and Buechner, Phys. Rev. **103** (1956) 961
En 57 Endt and Braams, Revs. Mod. Phys. **29** (1957) 683
En 57a Endt and Paris, Phys. Rev. **106** (1957) 764
En 57d Enge, M.I.T., Laboratory for Nuclear Science Progress Report, Nov. 30 (1956) 47
En 58 Endt and Paris, Phys. Rev. **110** (1958) 89
En 58a Enge, Moore, and Kelly, Bull. Amer. Phys. Soc. **3** (1958) 210
En 59 Enge, Irwin, and Weaner, Phys. Rev. **115** (1959) 949
En 60 Endt and Heyligers, Physica **26** (1960) 230
Er 57 Erdös, Scherrer, and Stoll, Helv. Phys. Acta **30** (1957) 639
Es 56 Estulin, Popov, and Chukreev, Zh. Eksp. Teor. Fiz. **30** (1956) 1052; JETP **3** (1957) 866
Eu 58 Eubank, Peck, and Hassler, Nuclear Physics **9** (1958) 273
Ev 60 Everling, König, Mattauch, and Wapstra, Nuclear Physics **18** (1960) 529
Ev 61 Everling, König, Mattauch, and Wapstra, Nuclear Physics **25** (1961) 177, and private communication
Ev 61a Everling, König, Mattauch, and Wapstra, "1960 Nuclear Data Tables, Part 1", Report of the Nuclear Data Project, U.S. Government Printing Office, Washington 25 D.C. (1961)

Fa 35 Fahlenbrach, Z. Physik **96** (1935) 503
Fa 50 Faust, Phys. Rev. **78** (1950) 624(L)
Fa 57 Farwell and Robison, Cyclotron Res., Univ. of Washington, Annual Progress Report (1957)
Fa 59 Farinelli, Ferrero, Ferroni, Malvano, and Silva, Nuovo Cimento **12** (1959) 89
Fa 60 Fast, Flournoy, Tickle, and Whitehead, Phys. Rev. **118** (1960) 535
Fe 52 Feldman and Wu, Phys. Rev. **87** (1952) 1091
Fe 53 Ferguson and Gove, Phys. Rev. **91** (1953) 439(A)
Fe 54 Ferguson, Halpern, Nathans, and Yergin, Phys. Rev. **95** (1954) 776
Fe 54a Feuvrais and Yuasa, Comptes Rendus **239** (1954) 1627
Fe 55 Feenberg, Phys. Rev. **99** (1955) 71
Fe 58 Ferrero, Malvano, Menardi, and Terracini, Nuclear Physics **9** (1958) 32
Fe 58a Ferguson, Phys. Rev. **112** (1958) 1238
Fe 59 Ferguson and Paul, Nuclear Physics **12** (1959) 426
Fe 59a Ferrero, Ferroni, Malvano, Menardi, and Silva, Nuovo Cimento **11** (1959) 410
Fe 60 Ferrero, Ferroni, Malvano, Menardi, and Silva, Nuclear Physics **15** (1960) 436
Fe 60a Ferguson, Grace, and Newton, Nuclear Physics **17** (1960) 1
Fi 51 Fields and Walt, Phys. Rev. **83** (1951) 479(L)
Fi 54 Fischer, Phys. Rev. **96** (1954) 704
Fi 57 Fisher and Shute, Phil. Mag. **2** (1957) 1255
Fi 58 Fischer, Fischer, Remler, and Tatcher, Phys. Rev. **110** (1958) 286(L)
Fi 58a Fisher, Hadley, and Speers, Phil. Mag. **3** (1958) 163
Fl 49 Floyd and Borst, Phys. Rev. **75** (1949) 1106(L)
Fl 54 Flack, Rutherglen, and Grant, Proc. Phys. Soc. A **67** (1954) 973
Fo 52 Folkierski, Proc. Phys. Soc. A **65** (1952) 1006
Fo 54 Fowler, Proc. Phys. Soc. A **67** (1954) 1005(L)
Fo 60 Forsyth, De S. Barros, Jaffe, Taylor, and Ramavataram, Proc. Phys. Soc. **75** (1960) 291
Fo 60a Foster, Weaver, and Voigt, Iowa State Univ. Report IS–184 (1960)
Fo 60b Fogelström-Fineman and Westermark, Acta Chem. Scand. **14** (1960) 2046
Fo 61 Forkman, Nuclear Physics **23** (1961) 269
Fr 50b Freeman, Proc. Phys. Soc. A **63** (1950) 668(L)
Fr 51 Freeman and Seed, Proc. Phys. Soc. A **64** (1951) 313(L)
Fr 54 Freemantle, Prowse, Hossain, and Rotblat, Phys. Rev. **96** (1954) 1270

Fr 55 French and Raz, Phys. Rev. **98** (1955) 1523(L)

Fr 57 Frauenfelder, Hanson, Levine, Rossi, and DePasquali, Phys. Rev. **107** (1957) 643(L)

Fr 58 Freier, Famularo, Zipoy, and Leigh, Phys. Rev. **110** (1958) 446

Fr 58a Freeman and Montague, Nuclear Physics **9** (1958) 181

Fr 59 Fricke, Kopfermann, Penselin, and Schlüpmann, Z. Physik **156** (1959) 416

Fr 61 Freindl, Niewodniczanski, Nurzynski, Slapa and Strzałkowski, Proc. Rutherford Jubilee Conf., Manchester (1961)

Fu 38 Fünfer, Annalen der Physik **32** (1938) 313

Fu 51 Fulbright and Milton, Phys. Rev. **82** (1951) 274(L)

Fu 54 Fujimoto, Kikuchi, and Yoshida, Prog. in Theor. Phys. **11** (1954) 264

Fu 58 Fulmer and Cohen, Phys. Rev. **112** (1958) 1672

Fu 60 Fulmer and Goodman, Phys. Rev. **117** (1960) 1339

Ga 53 Galonsky, Haeberli, Goldberg, and Douglas, Phys. Rev. **91** (1953) 439(A)

Ga 53a Garrett, Hereford, and Sloope, Phys. Rev. **92** (1953) 1507

Ga 57 Gapanov and Popov, Nuclear Physics **4** (1957) 453

Ga 58 Gailar, Bleuler, and Tendam, Phys. Rev. **112** (1958) 1989

Ga 59 Gaehler, Knipp, and Milne, Bull. Amer. Phys. Soc. **4** (1959) 366

Ga 60b Gabbard, Huffaker, and Kern, Bull. Amer. Phys. Soc. **5** (1960) 442

Ga 61 Gabbard and Loomis, Bull. Amer. Phys. Soc. **6** (1961) 375

Ga 61a Galster, Z. Physik **161** (1961) 46

Ga 61b Gardner and Gugelot, Proc. Rutherford Jubilee Conf., Manchester (1961)

Ge 55 Gerber, Garcia Muñoz, and Maeder, Helv. Phys. Acta **28** (1955) 478(A); Phys. Rev. **101** (1956) 774

Ge 56a Gerstein, Niederer, and Strauch, Bull. Amer. Phys. Soc. **1** (1956) 192

Ge 58a Gerhart, Phys. Rev. **109** (1958) 897

Ge 58b Geiger, Ewan, Graham, and MacKenzie, Phys. Rev. **112** (1958) 1684

Ge 59 Gemmel, Morton, and Smith, Nuclear Physics **10** (1959) 45

Ge 60 Geshkenbein, Zh. Eksp. Teor. Fiz. **38** (1960) 1341; JETP **11** (1960) 965

Ge 60a Geller, Halpern, and Muirhead, Phys. Rev. **118** (1960) 1302

Gi 44 Gibert, Roggen, and Rossel, Helv. Phys. Acta **17** (1944) 97

Gi 57 Gibson, Prowse, and Rotblat, Proc. Royal Soc. A **243** (1957) 237

Gi 59 Gibbons and Macklin, Phys. Rev. **114** (1959) 571

Gl 47 Gleditsch and Graf, Phys. Rev. **72** (1947) 640(L)

Gl 55 Glass and Richardson, Phys. Rev. **98** (1955) 1251

Gl 56 Glauber and Martin, Phys. Rev. **104** (1956) 158

Gl 57 Glassgold and Kellogg, Phys. Rev. **107** (1957) 1372

Gl 61 Glover and Weigold, Nuclear Physics **24** (1961) 630

Gl 61a Glaudemans and Endt, Nuclear Physics **30** (1962) 30

Gl 61b Glaudemans (Utrecht Univ.), private communication (1961)

Gl 61c Glagolev and Yampolsky, Zh. Eksp. Teor. Fiz. **40** (1961) 743; JETP **13** (1961) 520

Gl 61e Glendenning, Nilsson, and Sawicki, Proc. Rutherford Jubilee Conf., Manchester (1961)

Go 51a Good, Phys. Rev. **81** (1951) 891(L)

Go 51b Good, Phys. Rev. **81** (1951) 1058(L)

Go 51c Good, Phys. Rev. **83** (1951) 1054(L)

Go 53 Goldberg, Phys. Rev. **89** (1953) 760

Go 54 Gove, Paul, Bartholomew, and Litherland, Phys. Rev. **94** (1954) 749(A)

Go 54a Goldemberg and Katz, Canadian J. Phys. **32** (1954) 49

Go 54b Goodrich and Payne Phys. Rev. **94** (1954) 405

Go 54c Goldberg, Haeberli, Galonsky, and Douglas, Phys. Rev. **93** (1954) 799

Go 55 Gorodetzky, Muller, and Port, Comptes Rendus **240** (1955) 1704 and 2224

Go 56 Gove, Bartholomew, Paul, and Litherland, Nuclear Physics **2** (1956) 132 and **3** (1957) 344

Go 56a Goldstein and Talmi, Phys. Rev. **102** (1956) 589(L)

Go 56b Goldhammer, Phys. Rev. **101** (1956) 1375

Go 56c Gol'danskii, Zh. Eksp. Teor. Fiz. **30** (1956) 969(L); JETP **3** (1956) 791(L)

Go 57 Gove, Litherland, and Paul, Bull. Amer. Phys. Soc. **2** (1957) 178
Go 57b Gove (Chalk River), private communication (1957)
Go 57c Goldstein and Talmi, Phys. Rev. **105** (1957) 995
Go 57d Gove and Litherland, Phys. Rev. **107** (1957) 1458(L)
Go 58 Gorodetzky, Muller, Port, and Bergdolt, J. Phys. Rad. **19** (1958) 49
Go 58a Good, Neiler, and Gibbons, Phys. Rev. **109** (1958) 926
Go 58d Goldemberg and Marquez, Nuclear Physics **7** (1958) 202
Go 58e Gove, Litherland, Almqvist, and Bromley, Phys. Rev. **111** (1958) 608
Go 58f Gove, Kuehner, Litherland, Almqvist, Bromley, Ferguson, Rose, Bastide, Brooks, and Connor, Phys. Rev. Lett. **1** (1958) 251
Go 58g Gorodetzky, Chevallier, Armbruster, Gallmann, and Sutter, Nuclear Physics **7** (1958) 672
Go 60 Golden, Zaffarano. and Martin, Bull. Amer. Phys. Soc. **5** (1960) 57
Go 60a Gonzales-Vidal, Conzett, and Wade, Bull. Amer. Phys. Soc. **5** (1960) 230
Go 60c Gove, Proc. of the Kingston Conf., p. 438 (Univ. of Toronto Press, 1960)
Go 60d Gove and Broude, Bull. Amer. Phys. Soc. **5** (1960) 473
Go 60e Gonzales-Vidal and Wade, Phys. Rev. **120** (1960) 1354
Go 60f Gorodetzky, Richert, Manquenouille, and Knipper, Comptes Rendus **251** (1960) 944, and private communication
Go 61 Gofman and Nemets, Zh. Eksp. Teor. Fiz. **40** (1961) 477; JETP **13** (1961) 333
Go 61a Gove, private communication, as quoted in Ro 61
Go 61b Gove, Litherland, and Batchelor, Nuclear Physics **26** (1961) 480
Gr 46 Graves and Coon, Phys. Rev. **70** (1946) 101(A)
Gr 48 Graf, Phys. Rev. **74** (1948) 831(L)
Gr 49 Greenlees, Kempton, and Rhoderick, Nature **164** (1949) 663(L)
Gr 50a Grant, Proc. Phys. Soc. A **63** (1950) 1298
Gr 50b Gross and Hamilton, Phys. Rev. **80** (1950) 484(L)
Gr 50c Grosskreutz and Mather, Phys. Rev. **77** (1950) 580
Gr 51 Grove and Cooper, Phys. Rev. **82** (1951) 505
Gr 54 Green, Harris, and Cooper, Phys. Rev. **96** (1954) 817(A)
Gr 55 Greenlees, Proc. Phys. Soc. A **68** (1955) 97
Gr 55a Groshev, Adyasevich, and Demidov, Proc. Internat. Conf. (Geneva, 1955) on Peaceful Uses of Atomic Energy **2** (1956) 39
Gr 55c Green, Singh, and Willmott, Phil. Mag. **46** (1955) 982
Gr 55d Griffith, Phys. Rev. **98** (1955) 579
Gr 55e Grant, Rutherglen, Flack, and Hutchinson, Proc. Phys. Soc. A **68** (1955) 369
Gr 55f Green, Thesis, Univ. of Liverpool (1955)
Gr 56 Green and Richardson, Phys. Rev. **101** (1956) 776
Gr 56b Greenberg and Deutsch, Phys. Rev. **102** (1956) 415
Gr 56c Grayson and Nordheim, Phys. Rev. **102** (1956) 1093
Gr 56e Green, Singh, and Willmott, Proc. Phys. Soc. A **69** (1956) 335
Gr 57 Graetzer and Robbins, Phys. Rev. **105** (1957) 1570
Gr 57a Green, Wiseman, and Milne, Bull. Amer. Phys. Soc. **2** (1957) 377
Gr 57b Greenlees, Haywood, Kuo and Petravić, Proc. Phys. Soc. A **70** (1957) 331
Gr 57c Groshev, Demidov, Lutsenko, and Pelekhov, Atomnaya Energiya **3** (1957) 187; Sov. J. At. Energy **3** (1957) 969
Gr 58a Greenlees, Kuo, Lowe, and Petravić, Proc. Phys. Soc. **71** (1958) 347
Gr 58b Groshev, Demidov, Lutsenko, and Pelekhov, Proc. Second Intern. Conf. Peaceful Uses of Atomic Energy, Geneva **15** (1958) 138
Gr 58c Groshev, Demidov, Lutsenko, and Pelekhov, "Atlas spektrov γ-luchei radiatsionnogo zakhvata teplovykh neitronov" (Moskva, 1958); "Atlas of Gamma-Ray Spectra from Radiative Capture of Thermal Neutrons" (London, Pergamon, 1959)
Gr 58d Grosof, Buck, Lichten, and Rabi, Phys. Rev. Lett. **1** (1958) 214
Gr 59 Greenlees, Kuo, and Petravić, Proc. of the Paris Conf., p. 438 (Dunod, Paris, 1959)
Gr 60 Greenlees and Lowe, Proc. Phys. Soc. **76** (1960) 149
Gr 60a Groshev, Demidov, and Lutsenko, Izvest. Akad. Nauk, Ser. Fiz. **24** (1960) 833

Gr 61 Grüebler and Rossel, Helv. Phys. Acta **34** (1961) 479(A)
Gr 61a Greenlees, Lilley, Rowe, and Hodgson, Nuclear Physics **24** (1961) 334
Gr 61b Green, Willmott, and Kaye, Nuclear Physics **25** (1961) 278
Gu 52 Gugelot, Phys. Rev. **87** (1952) 525(L)
Gu 53 Guernsey and Goodman, Phys. Rev. **92** (1953) 323
Gu 54 Gugelot, Phys. Rev. **93** (1954) 425
Gu 56 Gugelot and Rickey, Phys. Rev. **101** (1956) 1613(L)
Gu 58 Gudden and Eichler, Z. Physik **150** (1958) 436
Gu 58a Gustova, Dzhelepov, Ermolov, and Chubinskii, Izvest. Akad. Nauk, Ser. Fiz. **22** (1958) 211
Gu 58b Gueben and Govaerts, Inst. interuniv. sci. nucléaires (Bruxelles), Monographie No. 2 (1958)

Ha 50a Haslam, Katz, Moody, and Skarsgard, Phys. Rev. **80** (1950) 318
Ha 51 Hanscome and Malich, Phys. Rev. **82** (1951) 304(A)
Ha 51a Hälg, Helv. Phys. Acta **24** (1951) 641(A)
Ha 51b Halpern and Mann, Phys. Rev. **83** (1951) 370
Ha 52 Hausman, Allen, Arthur, Bender, and McDole, Phys. Rev. **88** (1952) 1296
Ha 52a Haslam, Summers-Gill, and Crosby, Canadian J. Phys. **30** (1952) 257
Ha 52c Harvey, Phys. Rev. **88** (1952) 162(A)
Ha 52d Haskins, Duval, Cheng, and Kurbatov, Phys. Rev. **88** (1952) 876
Ha 53 Haeberli, Galonsky, Goldberg, and Douglas, Phys. Rev. **91** (1953) 438(A)
Ha 53a Hamilton, Lemonick, and Pipkin, Phys. Rev. **92** (1953) 1191
Ha 53b Hansen, Kiehn, and Goodman, Phys. Rev. **92** (1953) 652
Ha 54 Halpern, Nathans, and Yergin, Phys. Rev. **95** (1954) 1529
Ha 54a Haslam, Roberts, and Robb, Canadian J. Phys. **32** (1954) 361
Ha 55 Hattori, Hisatake, Mikumo, and Momata, J. Phys. Soc. Japan **10** (1955) 242
Ha 55a Haeberli, Phys. Rev. **99** (1955) 640(A)
Ha 55b Handley and Lyon, Phys. Rev. **99** (1955) 755
Ha 55c Hancock and Verdaguer, Proc. Phys. Soc. A **68** (1955) 1080(L)
Ha 56 Hausman, Monahan, Mooring, and Raboy, Bull. Amer. Phys. Soc. **1** (1956) 56, and verbal report to Nuclear Data Group
Ha 56b Hahn, Ravenhall, and Hofstadter, Phys. Rev. **101** (1956) 1131
Ha 56c Haffner, Phys. Rev. **103** (1956) 1398
Ha 56d Handler and Richardson, Phys. Rev. **102** (1956) 833
Ha 56e Hassler, Steigert, and Pieper, Bull. Amer. Phys. Soc. **1** (1956) 280
Ha 57a Haling, Peck, and Eubank, Phys. Rev. **106** (1957) 971
Ha 58b Hartwig and Schopper, Z. Physik **152** (1958) 314
Ha 58c Hamilton, Langer, and Smith, Phys. Rev. **112** (1958) 2010
Ha 59a Hassler, Zatzick, and Eubank, Bull. Amer. Phys. Soc. **4** (1959) 321
Ha 59c Hashimoto and Alford, Phys. Rev. **116** (1959) 981
Ha 59d Hartwig and Schopper, Bull. Amer. Phys. Soc. **4** (1959) 77
Ha 60a Hamburger, Phys. Rev. **118** (1960) 1271
Ha 60b Hausman, Dell, and Bowsher, Phys. Rev. **118** (1960) 1237
Ha 60c Hamburger and Blair, Phys. Rev. **119** (1960) 777
Ha 61 Hassler, Bull. Amer. Phys. Soc. **6** (1961) 61
Ha 61a Hamburger, Cohen, and Price, Phys. Rev. **121** (1961) 1143
Ha 61b Harris and McCullen, Bull. Amer. Phys. Soc. **6** (1961) 224
Ha 61c Hazewindus (Delft Technol. Univ.), private communication (1961)
He 37a Henderson, Ridenour, White, and Henderson, Phys. Rev. **51** (1937) 1107(L)
He 39 Henderson and Doran, Phys. Rev. **56** (1939) 123(L)
He 43 Hendricks, Bryner, Thomas, and Ivie, J. Phys. Chem. **47** (1943) 469
He 47 Heitler, May, and Powell, Proc. Royal Soc. A **190** (1947) 180
He 48 Hein and Voigt, Phys. Rev. **74** (1948) 1265(A)
He 51 Heller, Sturcken, and Weber, Phys. Rev. **83** (1951) 848(L)
He 52 Hedgran and Lind, Arkiv f. Fysik **5** (1952) 177

He 54 Heintze, Z. Naturf. **9a** (1954) 469
He 54b Heydenburg and Temmer, Phys. Rev. **94** (1954) 1252
He 56 Helm, Phys. Rev. **104** (1956) 1466
He 57a Henshaw, Phys. Rev. **105** (1957) 976
He 61 Heyligers (Utrecht Univ.), private communication (1961)
Hi 45 Hibdon, Pool, and Kurbatov, Phys. Rev. **67** (1945) 289
Hi 47 Hirzel and Wäffler, Helv. Phys. Acta **20** (1947) 373
Hi 52a Hintz and Ramsey, Phys. Rev. **88** (1952) 19
Hi 54 Hitchcock, Phil. Mag. **45** (1954) 379 and 385
Hi 54a Hird, Whitehead, Butler, and Collie, Phys. Rev. **96** (1954) 702
Hi 55 Hintz, Phys. Rev. **100** (1955) 1794(A)
Hi 56b Hinds and Middleton, Proc. Phys. Soc. A **69** (1956) 347(L)
Hi 57b Hinds, Middleton, and Parry, Proc. Phys. Soc. A **70** (1957) 900(L)
Hi 58 Hinds, Middleton, and Parry, Proc. Phys. Soc. **71** (1958) 49
Hi 58a Hill, Phys. Rev. **109** (1958) 2105
Hi 58b Hirao, Okada, Miura, and Wakatsuki, J. Phys. Soc. Japan **13** (1958) 233
Hi 58c Hill and Blair, Phys. Rev. **111** (1958) 1142
Hi 58d Hird, Cookson, and Bokhari, Proc. Phys. Soc. **72** (1958) 489
Hi 59 Hibdon, Phys. Rev. **114** (1959) 179
Hi 59a Hinds and Middleton, Proc. Phys. Soc. **73** (1959) 727
Hi 59b Hinds and Middleton, Proc. Phys. Soc. **73** (1959) 501
Hi 60b Hibdon, Phys. Rev. **118** (1960) 514
Hi 60c Hinds and Middleton, Proc. Phys. Soc. **75** (1960) 444
Hi 60d Hinds and Middleton, Proc. Phys. Soc. **76** (1960) 545
Hi 60e Hird and Strzałkowski, Proc. Phys. Soc. **75** (1960) 868
Hi 60f Hinds and Middleton, Proc. of the Kingston Conf., p. 946 (Univ. of Toronto Press, 1960), and private communication
Hi 60i Hinds and Middleton, Proc. Phys. Soc. **76** (1960) 553
Hi 60k Hinds and Middleton, as quoted in Ma 60, Proc. Phys. Soc. **76** (1960) 56
Hi 60l Hisatake, Ishizaki, Isoya, Nakamura, Nakano, Saheki, Saji, and Yuasa, J. Phys. Soc. Japan **15** (1960) 741
Hi 61 Hinds, Middleton, and Litherland, Proc. Phys. Soc. **77** (1961) 1210(L)
Hi 61a Hinds and Middleton, Proc. Rutherford Jubilee Conf., Manchester (1961)
Hi 61b Hibdon, Phys. Rev. **122** (1961) 1235
Hi 61c Hintz, Lee, and Stovall, Bull. Amer. Phys. Soc. **6** (1961) 260
Hi 61d Hinds, Middleton, and Litherland, Nuclear Physics **24** (1961) 510
Hi 61e Hinds, Middleton, and Litherland, Proc. Rutherford Jubilee Conf., Manchester (1961)
Hi 61f Hinds, Litherland, and Middleton (Aldermaston), private communication (1961)
Hi 61g Hinds, Marchant, and Middleton (Aldermaston), private communication (1961)
Hi 61h Hinds, Marchant, and Middleton, Proc. Phys. Soc. **78** (1961) 473
Hi 61i Hibdon, Phys. Rev. **124** (1961) 500
Ho 40 Hoag, Phys. Rev. **57** (1940) 937(L)
Ho 46 Hole and Siegbahn, Arkiv Mat. Astron. Fys. **33 A** (1946) No. 9
Ho 49 Holt and Young, Nature **164** (1949) 1000(L)
Ho 50 Houtermans, Haxel, and Heintze, Z. Physik **128** (1950) 657
Ho 50b Hofstadter and McIntyre, Phys. Rev. **80** (1950) 631
Ho 53 Holt and Marsham, Proc. Phys. Soc. A **66** (1953) 258
Ho 53a Holt and Marsham, Phys. Rev. **89** (1953) 665(L)
Ho 53b Hornyak and Coor, Phys. Rev. **92** (1953) 675
Ho 53c Holt and Marsham, Proc. Phys. Soc. A **66** (1953) 565
Ho 53d Holt and Marsham, Proc. Phys. Soc. A **66** (1953) 467
Ho 53e Holt and Marsham, Proc. Phys. Soc. A **66** (1953) 249
Ho 58b Holland and Lynch, Bull. Amer. Phys. Soc. **3** (1958) 380
Ho 58c Hoogenboom, Thesis, Utrecht Univ. (1958)
Ho 59 Holland and Lynch, Phys. Rev. **113** (1959) 903
Ho 59a Hosoe and Suzuki, J. Phys. Soc. Japan **14** (1959) 699

Ho 61 Holtebekk, Bull. Amer. Phys. Soc. **6** (1961) 259 and private communication

Ho 61a Hoare, Robbins, and Greenlees, Proc. Phys. Soc. **77** (1961) 830

Ho 61b Hoogenboom, Kashy, and Buechner, Proc. Rutherford Jubilee Conf., Manchester (1961), and private communication

Hu 37 Hurst and Walke, Phys. Rev. **51** (1937) 1033

Hu 41 Huber, Helv. Phys. Acta **14** (1941) 163

Hu 43 Huber, Lienhard, Scherrer, and Wäffler, Helv. Phys. Acta **16** (1943) 33

Hu 44 Huber, Lienhard, Scherrer, and Wäffler, Helv. Phys. Acta **17** (1944) 139

Hu 45 Huber, Lienhard, Scherrer, and Wäffler, Helv. Phys. Acta **18** (1945) 221

Hu 53 Hunt and Jones, Phys. Rev. **89** (1953) 1283

Hu 54 Hunt, Kline, and Zaffarano, Phys. Rev. **95** (1954) 611(A)

Hu 54a Hunt and Zaffarano, Iowa State College Report ISC–469 (1954)

Hu 54b Hunt, Jones, Churchill, and Hancock, Proc. Phys. Soc. A **67** (1954) 443

Hu 54c Hunt, Jones, and Churchill, Proc. Phys. Soc. A **67** (1954) 479(L)

Hu 55 Hunt and Hancock, Phys. Rev. **97** (1955) 567(L)

Hu 55b Huby and Newns, Proc. Phys. Soc. A **68** (1955) 758

Hu 56 Hughes and Sinclair, Proc. Phys. Soc. A **69** (1956) 125

Hu 56a Huang, Phys. Rev. **102** (1956) 422

Hu 58 Hughes and Schwartz, "Neutron Cross Sections", 2nd edition, Brookhaven National Laboratory Report BNL-325 (1958)

Hu 59 Hudson and Morgan, Bull. Amer. Phys. Soc. **4** (1959) 97

Hu 59a Hunting and Wall, Phys. Rev. **115** (1959) 956

Hu 60a Hu, J. Phys. Soc. Japan **15** (1960) 1741

Ia 58 Iavor, Zh. Eksp. Teor. Fiz. **34** (1958) 1420; JETP **7** (1958) 983

Ib 58 Iben, Phys. Rev. **109** (1958) 2059

Ig 56 Igo, Wegner, and Eisberg, Phys. Rev. **101** (1956) 1508

Ig 57 Igo, Phys. Rev. **106** (1957) 256

Ig 59 Igo, Phys. Rev. **115** (1959) 1665

Ig 60 Igo, Gonzales-Vidal, and Markowitz, Bull. Amer. Phys. Soc. **5** (1960) 229

Ig 61 Igo, Lorenz, and Schmidt-Rohr, Phys. Rev. **124** (1961) 832

In 50 Inghram, Brown, Patterson, and Hess, Phys. Rev. **80** (1950) 916(L)

In 53 Inglis, Revs. Mod. Phys. **25** (1953) 390

Is 61 Ishizaki, J. Phys. Soc. Japan **16** (1961) 1056

Is 61a Isoya, Micheletti, Marrone, and Reber, Proc. Rutherford Jubilee Conf., Manchester (1961)

It 41 Itoh, Proc. Phys. Math. Soc. Japan **23** (1941) 605

Iw 53 Iwersen, Koski, and Rasetti, Phys. Rev. **91** (1953) 1229

Iw 55 Iwersen and Koski, Phys. Rev. **98** (1955) 1307

Iw 60 Iwao, Bull. Amer. Phys. Soc. **5** (1960) 29

Ja 60 Jack and Ward, Proc. Phys. Soc. **75** (1960) 833

Ja 60a Jänecke, Z. Naturf. **15a** (1960) 593

Ja 60b Jaffe, De S. Barros, Forsyth, Muto, Taylor, and Ramavataram, Proc. Phys. Soc. **76** (1960) 914

Ja 61 Jastram, Skeel, and Ramaswamy, Bull. Amer. Phys. Soc. **6** (1961) 38

Ja 61a Jaider, Lopez, Mazari, and Dominguez, Revista Mexicana de Fisica **10** (1961) 247

Ja 61b Jänecke, Bull. Amer. Phys. Soc. **6** (1961) 259, and private communication

Ja 61c Jahr, Müller, Oswald, and Schmidt-Rohr, Z. Physik **161** (1961) 509

Ja 61d Jarmie and Silbert, Phys. Rev. **123** (1961) 909

Je 52 Jensen, Nichols, Clement, and Pohm, Phys. Rev. **85** (1952) 112

Jo 49 Johnston and Willard, Phys. Rev. **75** (1949) 528(L)

Jo 52 Jones and Kohman, Phys. Rev. **85** (1952) 941(L)

Jo 53 Jones and Kohman, Phys. Rev. **90** (1953) 495(L)

Jo 55 Johansson, Phys. Rev. **97** (1955) 1186(L)

Jo 56 Johnson, Johnson, and Langer, Phys. Rev. **102** (1956) 1142
Jo 57 Johnson and Moffat, Bull. Amer. Phys. Soc. **2** (1957) 230
Jo 58 Johnson, Galonsky, and Ulrich, Phys. Rev. **109** (1958) 1243
Jo 58a Johnson, Johnson, and Langer, Phys. Rev. **112** (1958) 2004
Jo 59 Johnson and Class, Bull. Amer. Phys. Soc. **4** (1959) 97
Jo 59a Johnson and Class, Bull. Amer. Phys. Soc. **4** (1959) 255
Jo 60 Johnson, Chase, and Imhof, Bull. Amer. Phys. Soc. **5** (1960) 406
Jo 60a Johnson, as quoted in Nuclear Physics **17** (1960) 116
Jo 61 Johnson and Miller, Phys. Rev. **124** (1961) 1190
Jo 61b Johansson, Svanberg, and Hodgson, Arkiv f. Fysik **19** (1961) 541
Ju 58 Juveland and Jentschke, Phys. Rev. **110** (1958) 456
Ju 61 Jung and Jänecke, Bull. Amer. Phys. Soc. **6** (1961) 228

Ka 51 Katz and Cameron, Phys. Rev. **84** (1951) 1115
Ka 51a Katz and Penfold, Phys. Rev. **81** (1951) 815
Ka 51c Katz and Cameron, Canadian J. Phys. **29** (1951) 518
Ka 52 Kaufmann, Goldberg, Koester, and Mooring, Phys. Rev. **88** (1952) 673
Ka 52a Katcoff, Phys. Rev. **87** (1952) 886
Ka 53 Kahn and Lyon, Phys. Rev. **91** (1953) 1212
Ka 54 Katz, Haslam, Goldemberg, and Taylor, Canadian J. Phys. **32** (1954) 580
Ka 55 Kavanagh, Mills, and Sherr, Phys. Rev. **97** (1955) 248(L)
Ka 61 Kantele, Bull. Amer. Phys. Soc. **6** (1961) 252
Ka 61a Kashy, Hoogenboom, and Buechner, Phys. Rev. **124** (1961) 1917
Ka 61b Kartashov, Burgov, and Davydov, Izvest. Akad. Nauk, Ser. Fiz. **25** (1961) 189
Ke 50 Ketelle, Phys. Rev. **80** (1950) 758(L)
Ke 51 Keller, Phys. Rev. **84** (1951) 884
Ke 56 O'Kelley, Lazar, and Eichler, Phys. Rev. **101** (1956) 1059
Ke 56a Kern and Cochran, Phys. Rev. **104** (1956) 711
Ke 58 Kelley, Moore, and Enge, M.I.T., Laboratory for Nuclear Science Progress Report, May 31 (1958) 111
Ke 58a Keszthelyi and Erö, Nuclear Physics **8** (1958) 650
Ke 59 Kern, Thompson, and Ferguson, Nuclear Physics **10** (1959) 226
Ke 59a Kelly, Beard, and Peters, Nuclear Physics **11** (1959) 492
Ke 59b Kern, Bull. Amer. Phys. Soc. **4** (1959) 414
Ke 59c Ketelle, Brosi, Galonsky, and Willard, Bull. Amer Phys. Soc. **4** (1959) 76
Ke 60 Kent, Puri, Bucher, and Snowdon, Bull. Amer. Phys. Soc. **5** (1960) 369
Kh 59 Khanna and Green, Bull. Amer. Phys. Soc. **4** (1959) 387
Kh 59a Khurana and Hans, Nuclear Physics **13** (1959) 88
Ki 39a King, Henderson, and Risser, Phys. Rev. **55** (1939) 1118(A)
Ki 51 Kinsey, Bartholomew, and Walker, Phys. Rev. **83** (1951) 519
Ki 52 Kinsey, Bartholomew, and Walker, Phys. Rev. **85** (1952) 1012
Ki 52a King and Parkinson, Phys. Rev. **88** (1952) 141(L)
Ki 52b Kinsey and Bartholomew, Physica **18** (1952) 1112
Ki 53a Kinsey and Bartholomew, Canadian J. Phys. **31** (1953) 901(L)
Ki 53b King and Beach, Phys. Rev. **90** (1953) 381(A)
Ki 53c Kinsey and Bartholomew, Canadian J. Phys. **31** (1953) 537
Ki 54 Kiehn and Goodman, Phys. Rev. **95** (1954) 989
Ki 54a Kinsey and Bartholomew, Phys. Rev. **93** (1954) 1260
Ki 54b King, Revs. Mod. Phys. **26** (1954) 327
Ki 55 King, Phys. Rev. **99** (1955) 67
Ki 55a Kington, Bair, Cohn, and Willard, Phys. Rev. **99** (1955) 1393
Ki 56 Kistner, Schwarzschild, and Rustad, Phys. Rev. **104** (1956) 154
Ki 56a Kinsey and Stone, Phys. Rev. **103** (1956) 975
Ki 58 Kistner and Rustad, Phys. Rev. **112** (1958) 1972
Ki 59 Kiser and Johnston, J. Amer. Chem. Soc. **81** (1959) 1810
Ki 60 King and McDonald, Nuclear Physics **19** (1960) 94

Ki 61 Kimura, Shoda, Mutsuro, Tohei, Sato, Kuroda, Kuriyama, and Akiba, Nuclear Physics **23** (1961) 338; J. Phys. Soc. Japan **15** (1960) 1128
Ki 61a Kim and Barnard, Bull. Amer. Phys. Soc. **6** (1961) 259
Kl 48 Klema and Hanson, Phys. Rev. **73** (1948) 106
Kl 54 Kluyver, Van der Leun, and Endt, Physica **20** (1954) 1287
Kl 54b Kline and Zaffarano, Phys. Rev. **96** (1954) 1620
Kl 55 Kluyver and Van der Leun, Physica **21** (1955) 604(L)
Kl 59 Kloepper, Day, and Lind, Phys. Rev. **114** (1959) 240
Kn 59 Knowles, Canadian J. Phys. **37** (1959) 203
Ko 52 Koester, Phys. Rev. **85** (1952) 643
Ko 54 Koerts, Schwarzschild, Gold, and Wu, Phys. Rev. **95** (1954) 612(A)
Ko 54a Koester, Z. Naturf. **9a** (1954) 104
Ko 54b Kofoed-Hansen, Phys. Rev. **96** (1954) 1045
Ko 55 Kono, J. Phys. Soc. Japan **10** (1955) 495
Ko 56 Komar and Iavor, Zh. Eksp. Teor. Fiz. **31** (1956) 531(L); JETP **4** (1957) 432(L)
Ko 58 Kotani and Ross, Phys. Rev. Lett. **1** (1958) 140
Ko 58b Konijn, Van Nooyen, Hagedoorn, and Wapstra, Nuclear Physics **9** (1958) 296
Ko 58c Kopaleishvili and Mamasakhlisov, Zh. Eksp. Teor. Fiz. **35** (1958) 1017; JETP **8** (1959) 711
Ko 58d Kononov, Stavisskii, and Tolstikov, Atomnaya Energiya **5** (1958) 564; J. Nuclear Energy **11A** (1959) 46
Ko 59 Komar and Dragnev, Dokl. Akad. Nauk **126** (1959) 1234; "Doklady" **4** (1959) 653
Ko 59a Komoda, Prog. in Theor. Phys. **22** (1959) 891(L)
Ko 60 Korotkov and Chernikov, Izvest. Akad. Nauk, Ser. Fiz. **24** (1960) 899
Ko 61 Kondo, Yamazaki, and Yamabe, J. Phys. Soc. Japan **16** (1961) 1091
Ko 61a Konstantinova, Myakinin, Romanov, and Tsaryova, Zh. Eksp. Teor. Fiz. **41** (1961) 49
Kr 53 Kranz and Watson, Phys. Rev. **91** (1953) 1472
Kr 54 Kreger, Phys. Rev. **96** (1954) 1554
Kr 54a Kraushaar, Mihelich, and Sunyar, Phys. Rev. **95** (1954) 456
Kr 55 Kromchenko, Izvest. Akad. Nauk, Ser. Fiz. **19** (1955) 277
Kr 56 Krone, Everett, and Hanna, Bull. Amer. Phys. Soc. **1** (1956) 329
Kr 56a Kromchenko, Zh. Eksp. Teor. Fiz. **30** (1956) 681; JETP **3** (1956) 531
Kr 60 Krone and Singh, Phys. Rev. **117** (1960) 1562
Kr 60a Kruse, Bent, and Lidofsky, Phys. Rev. **119** (1960) 289
Ku 53 Kurath, Phys. Rev. **91** (1953) 1430
Ku 57 Kumabe, Takekoshi, Ogata, Tsuneoka, and Oki, Phys. Rev. **106** (1957) 155
Ku 57a Kuščer, Mihailović, and Park, Phil. Mag. **2** (1957) 998
Ku 59 Kumabe, Wang, Kawashima, Yada, and Ogata, J. Phys. Soc. Japan **14** (1959) 713
Ku 59a Kuperus, Smulders, and Endt, Physica **25** (1959) 600
Ku 59b Kulchitskii and Presperin, Zh. Eksp. Teor. Fiz. **37** (1959) 1524; JETP **10** (1960) 1082
Ku 59c Kuchowicz, Bull. Acad. Polon. Sci. Ser. Sci. Math. Astron. Phys. **7** (1959) 509
Ku 60d Kuehner, Almqvist, and Bromley, Nuclear Physics **19** (1960) 614
Ku 60e Kuehner, Almqvist, and Bromley, Nuclear Physics **21** (1960) 555
Ku 60f Kuehner, Whalen, Almqvist, and Bromley, Proc. of the Kingston Conf., p. 261 (Univ. of Toronto Press, 1960)
Ku 60g Kuperus and Smith, Physica **26** (1960) 954
Ku 61 Kuperus, Physica **27** (1961) 273

La 37 Laslett, Phys. Rev. **52** (1937) 529
La 39a Lawson, Phys. Rev. **56** (1939) 131
La 48 Langmuir, Phys. Rev. **74** (1948) 1559(A)
La 49 Langer and Price, Phys. Rev. **76** (1949) 641
La 50 Langer, Motz, and Price, Phys. Rev. **77** (1950) 798
La 50a Langer, Phys. Rev. **77** (1950) 50
La 51 Landon, Phys. Rev. **83** (1951) 1081
La 54 Langevin, Yuasa, and Mérinis, J. Phys. Rad. **15** (1954) 778(L)

La 54a Langevin and Marty, J. Phys. Rad. **15** (1954) 127(L)
La 54b Lazar and Bell, Phys. Rev. **95** (1954) 612(A)
La 55 Laubitz, Proc. Phys. Soc. A **68** (1955) 1033
La 56a Lane and Monahan, Bull. Amer. Phys. Soc. **1** (1956) 346
La 56b Laberrigue-Frolow, Radvanyi, and Langevin, J. Phys. Rad. **17** (1956) 530
La 57a Lawson and Uretsky, Phys. Rev. **108** (1957) 1300
La 57b Langsdorf, Lane, and Monahan, Phys. Rev. **107** (1957) 1077
La 58 Langevin-Joliot and Marty, J. Phys. Rad. **19** (1958) 28; Comptes Rendus **245** (1957) 670
La 58a Lawson, Bull. Amer. Phys. Soc. **3** (1958) 223
La 59 Lackner, Dell, and Hausman, Phys. Rev. **114** (1959) 560
La 59a Lal, Goldberg, and Koide, Phys. Rev. Lett. **3** (1959) 380
La 60 Lane and Pendlebury, Nuclear Physics **15** (1960) 39
La 60a Lane and Monahan, Phys. Rev. **118** (1960) 533
La 60b Lane, Revs. Mod. Phys. **32** (1960) 519
La 61 Lane, Langsdorf, Monahan, and Elwyn, Annals of Physics **12** (1961) 135
Le 54 Leamer and Hinman, Phys. Rev. **96** (1954) 1607
Le 55 Levinson and Ford, Phys. Rev. **100** (1955) 13
Le 56a Lewis and Joyner, Bull. Amer. Phys. Soc. **1** (1956) 280
Le 56b Lee and Mooring, Phys. Rev. **104** (1956) 1342
Le 57 Lee and Schiffer, Phys. Rev. **107** (1957) 1340
Le 57a Lewis and Ford, Phys. Rev. **107** (1957) 756
Le 57b Levkovskii, Zh. Eksp. Teor. Fiz. **33** (1957) 1520; JETP **6** (1958) 1174
Le 61 Lee, Bull. Amer. Phys. Soc. **6** (1961) 79
Le 61a Lehar, Palečková, Skřivánek, and Veselá, Czechslov. J. Phys. **11** (1961) 229
Le 61b Leutz, Z. Physik **164** (1961) 78
Li 37 Livingston and Bethe, Revs. Mod. Phys. **9** (1937) 245
Li 53 Lindner, Phys. Rev. **89** (1953) 1150(L)
Li 53a Lindner, Phys. Rev. **91** (1953) 642
Li 54 Lindqvist and Mitchell, Phys. Rev. **95** (1954) 1535
Li 54a Lindqvist and Mitchell, Phys. Rev. **95** (1954) 444
Li 55 Lidén and Starfelt, Phys. Rev. **97** (1955) 419
Li 55a Little, Leonard, Prud'Homme, and Vincent, Phys. Rev. **98** (1955) 634
Li 55b Lindqvist and Wu, Phys. Rev. **100** (1955) 145
Li 56 Lidofsky and Fischer, Phys. Rev. **104** (1956) 759
Li 56a Litherland, Paul, Bartholomew, and Gove, Phys. Rev. **102** (1956) 208
Li 57b Lidofsky, Revs. Mod. Phys. **29** (1957) 773
Li 57c Lindqvist, Arkiv. f. Fysik **12** (1957) 495
Li 58a Litherland and Gove (Chalk River), private communication (1958)
Li 58b Litherland and Gove, Bull. Amer. Phys. Soc. **3** (1958) 200
Li 58c Litherland, McManus, Paul, Bromley, and Gove, Canadian J. Phys. **36** (1958) 378
Li 58d Lindström and Neuert, Z. Naturf. **13a** (1958) 826
Li 59 Litherland, Paul, Bartholomew, and Gove, Canadian J. Phys. **37** (1959) 53
Li 59a Litherland, Gove and Ferguson, Phys. Rev. **114** (1959) 1312
Li 60 Litherland and McCallum, Canadian J. Phys. **38** (1960) 927
Li 60a Lindenberger and Scheer, Z. Physik **158** (1960) 111
Li 60b Lisle and Shaw, Proc. Phys. Soc. **76** (1960) 929
Li 61 Lind and Day, Annals of Physics **12** (1961) 485
Lo 53 Lockett and Thomas, Nucleonics **11** (1953) No. 3, 14
Lo 59 Longuequeue, J. Phys. Rad. **20** (1959) 37(A)
Lo 60 Lovchikova, Zh. Eksp. Teor. Fiz. **38** (1960) 1434; JETP **11** (1960) 1036
Lo 61 Lönsjö (Oslo Univ.), private communication (1961)
Lu 50 Lüscher, Ricamo, Scherrer, and Zünti, Helv. Phys. Acta **23** (1950) 561
Lu 61 Lubitz and Goldman, Bull. Amer. Phys. Soc. **6** (1961) 295
Ly 37 Lyman, Phys. Rev. **51** (1937) 1
Ly 54 Lyon and Manning, Phys. Rev. **93** (1954) 501
Ly 55 Lyon and Handley, Phys. Rev. **100** (1955) 1280

Ly 56 Lyon and Lazar, Phys. Rev. **101** (1956) 1524
Ly 58 Lynn, Firk, and Moxon, Nuclear Physics **5** (1958) 603
Ly 59 Lynch and Holland, Phys. Rev. **114** (1959) 825
Ly 59a Lyon and Macklin, Phys. Rev. **114** (1959) 1619

Ma 50a Macklin, Lidofsky, and Wu, Phys. Rev. **78** (1950) 318(A)
Ma 50b Macklin, Feldman, Lidofsky, and Wu, Phys. Rev. **77** (1950) 137(L)
Ma 52 Mandeville, Swann, Chatterjee, and Van Patter, Phys. Rev **85** (1952) 193
Ma 52a Martin and Breckon, Canadian J. Phys. **30** (1952) 643
Ma 53 Marquez, Phys. Rev. **92** (1953) 1511
Ma 53a Marquez, Phys. Rev. **90** (1953) 330(L)
Ma 53b May and Foster, Phys. Rev. **90** (1953) 243
Ma 53c Marshall, Phys. Rev. **91** (1953) 905
Ma 54 Marty, Nataf, and Prentki, J. Phys. Rad. **15** (1954) 134
Ma 54a Mayer-Kuckuk, Z. Naturf. **9a** (1954) 338
Ma 54c Maeder, Müller, and Wintersteiger, Helv. Phys. Acta **27** (1954) 3
Ma 55 Maeder and Stähelin, Helv. Phys. Acta **28** (1955) 193
Ma 55b Macq, Bull. classe sci. Acad. roy. Belg. **41** (1955) 467
Ma 55c Marion, Bonner, and Cook, Phys. Rev. **100** (1955) 91, and private communication
Ma 56a Martin, Cork, and Burson, Phys. Rev. **102** (1956) 457
Ma 56b Marion, Slattery, and Chapman, Phys. Rev. **103** (1956) 676
Ma 57 MacGregor, Ball, and Booth, Phys. Rev. **108** (1957) 726
Ma 57a Marin, Movchet, and Poupaud, J. Phys. Rad. **18** (1957) 693(L)
Ma 58 Magleby, Bull. Amer. Phys. Soc. **3** (1958) 19
Ma 58c Mann, Miskel, and Bloom, Phys. Rev. Lett. **1** (1958) 34
Ma 58d Mann, Miskel, and Bloom, Bull. Amer. Phys. Soc. **3** (1958) 326
Ma 58e MacDonald, Phys. Rev. **110** (1958) 1420
Ma 58f MacGregor, Ball, and Booth, Phys. Rev. **111** (1958) 1155
Ma 58g March and Morton, Phil. Mag. **3** (1958) 1256
Ma 58h Mazari, M.I.T., Laboratory for Nuclear Science Progress Report, May 31 (1958) 109
Ma 59 Mayer-Kuckuk and Nierhaus, Z. Physik **154** (1959) 383
Ma 59a MacGregor, Proc. of the Paris Conf., p. 609 and 612 (Dunod, Paris, 1959)
Ma 59b Machwe, Kent, and Snowdon, Phys. Rev. **114** (1959) 1563
Ma 59c Manning and Bartholomew, Phys. Rev. **115** (1959) 401
Ma 59e Mayer-Kuckuk, Nierhaus, and Schmidt-Rohr, Z. Physik **157** (1959) 586
Ma 59f Mamasakhlisov and Kopaleishvili, Zh. Eksp. Teor. Fiz. **37** (1959) 131; JETP **10** (1960) 93
Ma 59g Mackin and Love, J. Inorganic Nuclear Chem. **10** (1959) 17
Ma 60 Macefield and Towle, Proc. Phys. Soc. **76** (1960) 56
Ma 60a Martin, Quisenberry, and Low, Phys. Rev. **120** (1960) 492
Ma 60b Mani, McCallum, and Ferguson, Nuclear Physics **19** (1960) 535
Ma 60c Mani, Tombrello, and Rao, Nuclear Physics **21** (1960) 344
Ma 60d Macfarlane and French, Revs. Mod. Phys. **32** (1960) 567
Ma 60e Mazari, Dominguez, Jaidar, Rickards, Alba, Lopez, and Ortiz de Lopez, Proc. Internat. Conf. Nuclidic Masses, Hamilton (1960)
Ma 61 Mani, Barnard, Tombrello, and Rao, Bull. Amer. Phys. Soc. **6** (1961) 38
Ma 61b MacDonald and Douglas, Nuclear Physics **24** (1961) 614
Ma 61c Macefield, Towle, and Gilboy, Proc. Phys. Soc. **77** (1961) 1050
Ma 61d Marion, Revs. Mod. Phys. **33** (1961) 139 and **33** (1961) 623 (Errata)
Mc 49 McElhinney, Hanson, Becker, Duffield, and Diven, Phys. Rev. **75** (1949) 542
Mc 50 McDaniel, Walker, and Stearns, Phys. Rev. **80** (1950) 807
Mc 54 McClure, Phys. Rev. **94** (1954) 1637
Mc 54a McPherson, Pederson, and Katz, Canadian J. Phys. **32** (1954) 593
Mc 55 McCarthy, Phys. Rev. **97** (1955) 1234
Mc 56 McNair, Glover, and Wilson, Phil. Mag. **1** (1956) 199
Mc 57 McCormac, Steuer, Bond, and Hereford, Phys. Rev. **108** (1957) 116

Mc 60b McCallum, Mani, and Ferguson, Nuclear Physics **16** (1960) 313
Mc 61 McCullen and Kraushaar, Phys. Rev. **122** (1961) 555
Mc 61a McCallum, Phys. Rev. **123** (1961) 568
Me 37 Meye, Z. Physik **105** (1937) 232
Me 48 Metzger, Alder, and Huber, Helv. Phys. Acta **21** (1948) 278
Me 51 Meadows and Holt, Phys. Rev. **83** (1951) 1257(L)
Me 54 Meyerhof and Lindstrom, Phys. Rev. **93** (1954) 949(A)
Me 57 Merritt, Campion, and Hawkings, Canadian J. Phys. **35** (1957) 16
Me 57a Melkanoff, Nodvik, Saxon, and Woods, Phys. Rev. **106** (1957) 793
Me 59 Mehta and Warke, Nuclear Physics **13** (1959) 451
Me 59a Merzbacher, Crutchfield, and Newson, Annals of Physics **8** (1959) 194
Me 60 Meichsner, Phys. Rev. **117** (1960) 489
Me 60b Metzger, Swann, and Rasmussen, Nuclear Physics **16** (1960) 568
Me 60c Meyer and Hintz, Phys. Rev. Lett. **5** (1960) 207
Mi 50a Mims, Halban, and Wilson, Nature **166** (1950) 1027(L)
Mi 52 Mileikowsky and Whaling, Phys. Rev. **88** (1952) 1254
Mi 52a Miskel and Perlman, Phys. Rev. **87** (1952) 543(L)
Mi 53 Middleton, El-Bedewi, and Tai, Proc. Phys. Soc. A **66** (1953) 95
Mi 53a Mize and Zaffarano, Phys. Rev. **89** (1953) 902(A)
Mi 54 Miskel and Perlman, Phys. Rev. **94** (1954) 1683
Mi 54a Michalowicz, J. Phys. Rad. **15** (1954) 156
Mi 55 Milani, Cooper, and Harris, Phys. Rev. **99** (1955) 645(A), and verbal report to Nuclear Data Group
Mi 56 Milojević, Bull. Inst. nat. Sciences "Boris Kidrich" **6** (1956) 21
Mi 57 Milone, Ricamo, and Rubbino, Nuovo Cimento **5** (1957) 528
Mi 58 Mihailović and Povh, Nuclear Physics **7** (1958) 296
Mi 59 Mihailović, Pregl, Kernel, and Kregar, Phys. Rev. **114** (1959) 1621
Mi 59a Mikaélyan and Spivak, Zh. Eksp. Teor. Fiz. **37** (1959) 1168; JETP **10** (1960) 831
Mi 59b Miura, Wakatsuki, Hirao, and Okada, J. Phys. Soc. Japan **14** (1959) 239
Mi 59c Milman, Amsel, and Loyau, J. Phys. Rad. **20** (1959) 51
Mi 60a Mizobuchi, Katoh, and Ruan, J. Phys. Soc. Japan **15** (1960) 1737
Mi 61 Mitler, Nuclear Physics **23** (1961) 200
Mi 61a Middleton and Hinds, Proc. Rutherford Jubilee Conf., Manchester (1961), and Nuclear Physics (to be published)
Mo 49 Morganstern and Wolf, Phys. Rev. **76** (1949) 1261(L)
Mo 50 Motz and Humphreys, Phys. Rev. **80** (1950) 595
Mo 51 Mooring, Koester, Goldberg, Saxon, and Kaufmann, Phys. Rev. **84** (1951) 703
Mo 51a Morrison, Phys. Rev. **82** (1951) 209
Mo 52 Motz and Alburger, Phys. Rev. **86** (1952) 165
Mo 52a Motz, Phys. Rev. **85** (1952) 501(L)
Mo 53a Montalbetti, Katz, and Goldemberg, Phys. Rev. **91** (1953) 659
Mo 54 Moszkowski and Peaslee, Phys. Rev. **93** (1954) 455
Mo 54a Moljk and Curran, Phys. Rev. **96** (1954) 395
Mo 55 Morinaga, Phys. Rev. **97** (1955) 444
Mo 55a Morinaga, Phys. Rev. **97** (1955) 1185(L)
Mo 55c Morinaga, Phys. Rev. **100** (1955) 431(L)
Mo 56 Morinaga and Bleuler, Bull. Amer. Phys. Soc. **1** (1956) 30, and verbal report to Nuclear Data Group
Mo 56a Motz, Phys. Rev. **104** (1956) 1353
Mo 56b Morinaga, Phys. Rev. **103** (1956) 504(L)
Mo 56c Morgan, Phys. Rev. **103** (1956) 1031, and verbal report to Nuclear Data Group
Mo 56d Morinaga and Bleuler, Phys. Rev. **103** (1956) 1423
Mo 58 Moore, Kelley, and Enge, M.I.T., Laboratory for Nuclear Science Progress Report, May 31 (1958) 114
Mo 59 Moore, Krumwiede, and Milne, Bull. Amer. Phys. Soc. **4** (1959) 366
Mo 59a Morpurgo, Phys. Rev. **114** (1959) 1075

Mo 59b Morinaga, Mutsuro, and Sugawara, Phys. Rev. **114** (1959) 1146
Mo 59c Motz, Carter and Fisher, Bull. Amer. Phys. Soc. **4** (1959) 477, and private communication to Nuclear Data Group
Mo 60 Mouton and Smith, Nuclear Physics **16** (1960) 206
Mo 60a Morinaga and Ishii, Prog. in Theor. Phys. **23** (1960) 161
Mo 61 Monaro, Vingiani, and Van Lieshout, Physica **27** (1961) 985
Mu 40 Mulder, Hoeksema, and Sizoo, Physica **7** (1940) 849
Mu 58 Muller, Gelsema, and Endt, Physica **24** (1958) 577
Mu 58a Münnich, Z. Physik **153** (1958) 106
Mu 58b Muller, Annales de Physique **3** (1958) 739
Mu 60 Muto, J. Phys. Soc. Japan **15** (1960) 17
Mu 61 Mukherjee, Ganguly, and Majumder, Proc. Phys. Soc. **77** (1961) 508
My 49 Myers and Wattenberg, Phys. Rev. **75** (1949) 992(L)

Na 53 Nahmias and Yuasa, Comptes Rendus **236** (1953) 2399
Na 53a Nagy, Acta Physica Acad. Sci. Hung. **3** (1953) 15
Na 54 Nathans and Halpern, Phys. Rev. **93** (1954) 437
Na 54a Nahmias, J. Phys. Rad. **15** (1954) 568
Na 54b Nahmias and Yuasa, Comptes Rendus **239** (1954) 47
Na 54c Nahmias and Wapstra, J. Phys. Rad. **15** (1954) 570
Na 55 Nathans and Yergin, Phys. Rev. **98** (1955) 1296
Na 56 Nahmias and Yuasa, J. Phys. Rad. **17** (1956) 373(L)
Na 57 Nakada, Anderson, Gardner, and Wong, Bull. Amer. Phys. Soc. **2** (1957) 32
Na 61 Nair, Iyengar, and Ramanna, Nuclear Physics **26** (1961) 193
Ne 54 Newton, Phys. Rev. **96** (1954) 241(L)
Ne 56 Nemilov, Zherebtsova, and Funstein, Physica **22** (1956) 1155(A)
Ne 56a Nemilov and Litvin, Zh. Eksp. Teor. Fiz. **30** (1956) 686; JETP **3** (1956) 523
Ne 56b Nemilov and Litvin, Zh. Eksp. Teor. Fiz. **31** (1956) 719 (L); JETP **4** (1957) 606(L)
Ne 58 Nethaway and Caretto, Phys. Rev. **109** (1958) 504
Ne 59 Nessin, Eklund, and Kruse, Bull. Amer. Phys. Soc. **4** (1959) 18
Ne 59a Nessin, Eklund, and Kruse, Bull. Amer. Phys. Soc. **4** (1959) 278
Ne 59b Neuchadin, Teplov, and Tulinov, Zh. Eksp. Teor. Fiz. **37** (1959) 548; JETP **10** (1960) 387
Ne 59c Newson, Block, Nichols, Taylor, Furr, and Merzbacher, Annals of Physics **8** (1959) 211
Ne 60 Nemets and Prokopets, Zh. Eksp. Teor. Fiz. **38** (1960) 693; JETP **11** (1960) 499
Ne 60b Nemets and Prokopets, Izvest. Akad. Nauk, Ser. Fiz. **24** (1960) 869
Ne 60c Neudachin Shevchenko, and Yudin, Zh. Eksp. Teor. Fiz. **39** (1960) 108; JETP **12** (1961) 79
Ne 60d Newton, Nuclear Physics **21** (1960) 529
Ne 60e Nessin, Thesis, Columbia Univ. (1960)
Ne 61 Nelson, Carter, Mitchell, and Davis, Bull. Amer. Phys. Soc. **6** (1961) 235
Ne 61a Nelson, Plendl, and Oberholtzer, Proc. Rutherford Jubilee Conf., Manchester (1961)
Ni 50 Nier, Phys. Rev. **77** (1950) 789
Ni 52 Nilsson, Trans. Chalmers Univ. Techn., Gothenburg, No. 125 (1952)
Ni 54 Nichols and Jensen, Phys. Rev. **94** (1954) 369
Ni 57 Nielsen and Sheline, Bull. Amer. Phys. Soc. **2** (1957) 260
Ni 58 Nigam and Sundaresan, Canadian J. Phys. **36** (1958) 571
Ni 61 Nichols, McAdams, and Jensen, Phys. Rev. **122** (1961) 172
Ni 61a Nichols, McAdams, and Jensen, Phys. Rev. (to be published)
No 60 Nordhagen (Oslo Univ.), private communication (1960)
No 61 Nordhagen, Nuclear Instr. and Methods **12** (1961) 291, and private communication
No 61a Nordhagen, Nuclear Physics **27** (1961) 112
No 61b Nordhagen and Smith (Utrecht Univ.), private communication (1961)
Nu 53 Nussbaum, Van Lieshout, and Wapstra, Phys. Rev. **92** (1953) 207(L)
Nu 58 Nurmia and Fink, Nuclear Physics **8** (1958) 139
Ny 55 Nybö and Grotdal, Nature **175** (1955) 130(L)
Ny 60 Nysten, Proc. of the Kingston Conf., p. 961 (Univ. of Toronto Press, 1960)

Od 59 Oda, Takeda, Hu, and Kato, J. Phys. Soc. Japan **14** (1959) 1255
Od 59a Oda, Takeda, Hu, and Kato, J. Phys. Soc. Japan **14** (1959) 396
Od 60 Oda, Takeda, Takano, Yamazaki, Hu, Kikuchi, Kobayashi, Matsuda, and Nagahara, J. Phys. Soc. Japan **15** (1960) 760
Of 59 Ofer and Schwarzschild, Phys. Rev. Lett. **3** (1959) 384
Og 60 Ogata, Itoh, Masuda, Takamatsu, Kawashima, Masaike, and Kumabe, J. Phys. Soc. Japan **15** (1960) 1719
Oh 61 Ohmura, Ejiri, Nakajima, Horie, Etoh, Ohuchi, and Nogami, J. Phys. Soc. Japan **16** (1961) 593
Ok 58 Okada, Miura, Wakatsuki, and Hirao, J. Phys. Soc. Japan **13** (1958) 541
Ok 60 Okano, J. Phys. Soc. Japan **15** (1960) 28
Ok 60a Okano, Tabata, Fukuda, and Muto, J. Phys. Soc. Japan **15** (1960) 1556
Ok 60b Okamoto, Proc. of the Japanese Conf. on Low Energy Nuclear Physics, JAERI, p. 57 (1960)
Ol 51 Ollano and Roy, Nuovo Cimento **8** (1951) 77
Ol 54 Olsen and O'Kelly, Phys. Rev. **93** (1954) 1125(L)
Ol 55 Olness and Lewis, Phys. Rev. **99** (1955) 654(A)
Ol 58 Olness, Haeberli, and Lewis, Phys. Rev. **112** (1958) 1702
Ol 60 Olness and Parker, Bull. Amer. Phys. Soc. **5** (1960) 56
Op 58 Ophel, Proc. Phys. Soc. **72** (1958) 321
Ov 49 Overstreet, Jacobson, and Stout, Phys. Rev. **75** (1949) 231
Ov 56 Ovchinnikov, Nemilov, Aleksandrova, and Lomonosov, Izvest. Akad. Nauk, Ser. Fiz. **20** (1956) 1417
Ov 59 Overseth and Peck, Phys. Rev. **115** (1959) 993

Pa 52a Paganelli and Quareni, Phys. Rev. **86** (1952) 423(L)
Pa 53 Paul and Clarke, Canadian J. Phys. **31** (1953) 267
Pa 54 Paul, Gove, Bartholomew, and Litherland, Phys. Rev. **94** (1954) 749(A)
Pa 55 Pasechnik, Geneva Conference Report 8/P/714 (1955)
Pa 55a Paul, Gove, Litherland, and Bartholomew, Phys. Rev. **99** (1955) 1339
Pa 55b Patterson, Newson, and Merzbacher, Phys. Rev. **99** (1955) 1625(A)
Pa 55c Paris, Buechner, and Endt, Phys. Rev. **100** (1955) 1317
Pa 56 Paul, Bartholomew, Gove, and Litherland, Bull. Amer. Phys. Soc. **1** (1956) 39
Pa 56a Pandya, Phys. Rev. **103** (1956) 956
Pa 57a Pandya and French, Bull. Amer. Phys. Soc. **2** (1957) 27
Pa 57b Page and Heinberg, Phys. Rev. **106** (1957) 1220
Pa 57c Pandya, Phys. Rev. **108** (1957) 1312
Pa 57d Pandya, Prog. in Theor. Phys. **18** (1957) 668(L)
Pa 58 Parkinson, Phys. Rev. **110** (1958) 485
Pa 58a Paul and Montague, Nuclear Physics **8** (1958) 61
Pa 61 Parkinson, Bull. Amer. Phys. Soc. **6** (1961) 259, and private communication
Pa 61a Parry, Scott, and Swierszczewski, Proc. Phys. Soc. **77** (1961) 230
Pa 61b Pandya and Shah, Nuclear Physics **24** (1961) 326
Pa 61c Parry, Scott, and Swierszczewski, Proc. Phys. Soc. **77** (1961) 1024
Pa 61d Paul, Evans and Montague, Proc. Rutherford Jubilee Conf., Manchester (1961)
Pe 48 Peck, Phys. Rev. **73** (1948) 947
Pe 48a Perlman and Friedlander, Phys. Rev. **74** (1948) 442
Pe 53 Peaslee, Nuovo Cimento **10** (1953) 1349(L)
Pe 56 Penning, Maltrud, Hopkins, and Schmidt, Phys. Rev. **104** (1956) 740
Pe 57 Penning and Schmidt, Phys. Rev. **105** (1957) 647
Pe 57a Peker, Gustova, and Chubinskii, Izvest. Akad. Nauk, Ser. Fiz. **21** (1957) 1013
Pe 59 Penfold and Garwin, Phys. Rev. **114** (1959) 1139
Pe 59a Persson and Johansson, Nuclear Physics **12** (1959) 432
Pe 59b Petersen, Ehlers, Ewbank, Marino, and Shugart, Phys. Rev. **116** (1959) 734
Pe 60 Peterson, Bratenahl, and Stoering, Phys. Rev. **120** (1960) 521
Pe 61 Pellegrini, Nuclear Physics **24** (1961) 372

Ph 53 Phipps and Zaffarano, Report Iowa State College (1953) 443
Pi 55 Pieper, Stanford, and Von Herrmann, Phys. Rev. **98** (1955) 1185(A)
Pi 57 Pixley, Hester, and Lamb, Bull. Amer. Phys. Soc. **2** (1957) 377
Pi 60 Piraino, Paris, and Buechner, Phys. Rev. **119** (1960) 732
Pl 40 Plain, Herb, Hudson, and Warren, Phys. Rev. **57** (1940) 187
Pl 60 Ploughe, Bleuler, and Tendam, Bull. Amer. Phys. Soc. **5** (1960) 247
Pl 61 Ploughe, Bleuler, and Tendam, Phys. Rev. **124** (1961) 818
Po 37 Pollard and Brasefield, Phys. Rev. **51** (1937) 8
Po 49a Pontecorvo, Kirkwood, and Hanna, Phys. Rev. **75** (1949) 982(L)
Po 52b Pool, Physica **18** (1952) 1304
Po 53 Pool and Kundu, Phys. Rev. **91** (1953) 462(A)
Po 56 Pohm, Waddell, and Jensen, Phys. Rev. **101** (1956) 1315
Po 57 Porter, Wagner, and Freedman, Phys. Rev. **107** (1957) 135
Po 59 Poularikas and Fink, Phys. Rev. **115** (1959) 989
Po 59a Poelz and Schmidt-Rohr, Physikalisch Verhandlungen **10** (1959) 78
Po 61 Pollehn and Neuert, Z. Naturf. **16a** (1961) 227
Po 61a Pope, Freck, and Evans, Nuclear Physics **24** (1961) 657
Po 61b Popov and Shapiro, Zh. Eksp. Teor. Fiz. **40** (1961) 1610; JETP **13** (1961) 1132
Pr 50 Pringle, Standil, and Roulston, Phys. Rev. **77** (1950) 841(L)
Pr 56 Prosser, Baumann, Brice, Read, and Krone, Phys. Rev. **104** (1956) 369
Pr 58 Preston and Hanna, Phys. Rev. **110** (1958) 1406
Pr 58a Preston, Schiffer, Lee, and Rosenzweig, Bull. Amer. Phys. Soc. **3** (1958) 380
Pr 60 Prosser and Sellers, Bull. Amer. Phys. Soc. **5** (1960) 108
Pr 60a Prêtre, Brugger, and Steiger, Helv. Phys. Acta **33** (1960) 583(A)
Pr 61 Prosser, Neher, and Krone, Bull. Amer. Phys. Soc. **6** (1961) 250
Pr 61a Presperin and Kulchitsky, Zh. Eksp. Teor. Fiz. **41** (1961) 60

Qu 56 Quinton and Doyle, Phys. Rev. **101** (1956) 669

Ra 49 Rae, Phil. Mag. **40** (1949) 1155
Ra 55 Rayburn, Lafferty, and Hahn, Phys. Rev. **98** (1955) 701
Ra 55a Ramanna, Veeraraghavan, and Iyengar, Nuovo Cimento **1** (1955) 623
Ra 56 Raz and French, Bull. Amer. Phys. Soc. **1** (1956) 223
Ra 56a Raz, Bull. Amer. Phys. Soc. **1** (1956) 336
Ra 57 Rakavy, Nuclear Physics **4** (1957) 375
Ra 58 Ranken, Bonner, Castillo-Bahena, Harlow, and Rabson, Phys. Rev. **112** (1958) 239
Ra 59a Rasmussen, Metzger, and Swann, Nuclear Physics **13** (1959) 95
Ra 60 Rabson, Bonner, Castillo-Bahena, Harlow, Haenni, and Ranken, Nuclear Physics **19** (1960) 314
Ra 61a Rasmussen, Metzger, and Swann, Phys. Rev. **123** (1961) 1386
Re 52 Reilley, Allen, Arthur, Bender, Ely, and Hausman, Phys. Rev. **86** (1952) 857
Re 52a Reuterswärd, Arkiv. f. Fysik **4** (1952) 203
Re 54 Recksiedler and Hamermesh, Phys. Rev. **96** (1954) 109
Re 55 Renard, J. Phys. Rad. **16** (1955) 575
Re 56 Reynolds and Standing, Phys. Rev. **101** (1956) 158
Re 56a Reuterswärd, Arkiv. f. Fysik **11** (1956) 1
Re 56b Read and Krone, Phys. Rev. **104** (1956) 1018
Re 57 Renard, J. Phys. Rad. **18** (1957) 681
Rh 50 Rhoderick, Proc. Royal Soc. A **201** (1950) 348
Ri 37 Ridenour and Henderson, Phys. Rev. **52** (1937) 889
Ri 44 Riezler, Phys. Z. **45** (1944) 191
Ri 50 Richards, Smith, and Browne, Phys. Rev. **80** (1950) 524
Ri 51 Ricamo, Nuovo Cimento **8** (1951) 383
Ri 55 Ring, Phys. Rev. **99** (1955) 137
Ri 58 Ridley, Nuclear Physics **6** (1958) 34
Ri 58b Rightmire, Kohman, and Hintenberger, Z. Naturf. **13a** (1958) 847

Ri 59 Rightmire, Simanton, and Kohman, Phys. Rev. **113** (1959) 1069
Ri 59a Risti and Grotdal, Univ. i. Bergen Årbok Naturvitenskapelig Rekke No. 14 (1958)
Ri 60 Ricamo, Helv. Phys. Acta **33** (1960) 997(A)
Ro 55 Roderick, Lönsjö, and Meyerhof, Phys. Rev. **97** (1955) 97
Ro 55a Rothman, Hans, and Mandeville, Phys. Rev. **100** (1955) 83
Ro 57 Robinson, Purdue University, Nuclear Physics Progress Report AECU-3515 (1957)
Ro 58a Rossel and Weber, Helv. Phys. Acta **31** (1958) 727
Ro 59 Robert, Annales de Physique **4** (1959) 89
Ro 60 Robbins and Greenlees, Phys. Rev. **118** (1960) 803
Ro 60a Robinson and Johnson, Phys. Rev. **120** (1960) 1321
Ro 60b Rost and Austern, Phys. Rev. **120** (1960) 1375
Ro 60c Romanov, Zh. Eksp. Teor. Fiz. **39** (1960) 1540; JETP **12** (1961) 1072
Ro 60d Robinson and Fink, Revs. Mod. Phys. **32** (1960) 117
Ro 61 Robinson and Johnson, Phys. Rev. **123** (1961) 1349
Ro 61a Robinson, Rhode, and Johnson, Phys. Rev. **122** (1961) 879
Ro 61b Robinson, Lucas, and Johnson, Phys. Rev. **122** (1961) 202
Ro 61c Rosen, Brolley, and Stewart, Phys. Rev. **121** (1961) 1423
Ro 61d Rost, Austern, and Satchler, Bull. Amer. Phys. Soc. **6** (1961) 249
Ro 61e Rowe, Clegg, Salmon, and Newton, Proc. Rutherford Jubilee Conf., Manchester (1961)
Ru 51 Ruby and Richardson, Phys. Rev. **83** (1951) 698
Ru 52 Rudstam, Stevenson, and Folger, Phys. Rev. **87** (1952) 358
Ru 53 Rutherglen and Smith, Proc. Phys. Soc. A **66** (1953) 800
Ru 54 Rutherglen, Grant, Flack, and Deuchars, Proc. Phys. Soc. A **67** (1954) 101
Ru 54a Russel, Taylor, and Cooper, Phys. Rev. **95** (1954) 99
Ru 54b Rubinson and Howland, Phys. Rev. **96** (1954) 1610
Ru 55b Rubenstein and Snyder, Phys. Rev. **99** (1955) 189
Ru 56 Rubin, Ajzenberg-Selove, and Mark, Phys. Rev. **104** (1956) 727
Ru 56a Rudstam, Thesis, Univ. of Uppsala (1956)
Ru 56b Rubin, Johnson, and Reynolds, Phys. Rev. **104** (1956) 1444
Ru 57 Rubin, Phys. Rev. **108** (1957) 62
Ru 58 Russel, Bull. Amer. Phys. Soc. **3** (1958) 61
Ru 59 Rubin, Bailey, and Passel, Phys. Rev. **114** (1959) 1110
Ry 61 Rytz, Staub, Winkler, and Zych, Proc. Rutherford Jubilee Conf., Manchester (1961)

Sa 36 Sagane, Phys. Rev. **50** (1936) 1141
Sa 49a Sawyer and Wiedenbeck, Phys. Rev. **76** (1949) 1535(L)
Sa 50 Sailor, Phys. Rev. **77** (1950) 794
Sa 50a Sawyer and Wiedenbeck, Phys. Rev. **79** (1950) 490
Sa 53 Sargent, Yaffe, and Gray, Canadian J. Phy **31** (1953) 235
Sa 56 Saraf, Phys. Rev. **102** (1956) 466
Sa 56a Sawicki, Physica **22** (1956) 1180(A)
Sa 58 Sawicki and Satchler, Nuclear Physics **7** (1958) 289
Sa 58a Sawicki, Nuclear Physics **7** (1958) 503
Sa 60 Satchler and Tobocman, Phys. Rev. **118** (1960) 1566
Sa 60a Saladin and Marmier, Helv. Phys. Acta **33** (1960) 299
Sa 60b Santos-Ocampo and Conway, Phys. Rev. **120** (1960) 2196
Sa 60c Saha and Gupta, Proc. Nat. Inst. Sci. India A **26** (1960) 486
Sa 61 Sadeh, Phys. Rev. **123** (1961) 855
Sa 61a Saudinos, Beurty, Catillon, Chaminade, Crut, Faraggi, Papineau, and Thirion, Comptes Rendus **252** (1961) 260
Sc 48 Schelberg, Sampson, and Mitchell, Rev. Sci. Instr. **19** (1948) 458
Sc 50 Schelberg, Sampson, and Cochran, Phys. Rev. **80** (1950) 574
Sc 52 Schrank and Richardson, Phys. Rev. **86** (1952) 248(L)
Sc 52a Schoenfeld, Duborg, Preston, and Goodman, Phys. Rev. **85** (1952) 873
Sc 54 Scharff-Goldhaber and McKeown, Phys. Rev. **95** (1954) 613(A)
Sc 54a Schwartz and De-Shalit, Phys. Rev. **94** (1954) 1257

Sc 54b Schneider, Martin, Sempert, and Sutter. Helv. Phys. Acta **27** (1954) 172(A)
Sc 54c Schwartz, Phys. Rev. **94** (1954) 95
Sc 54d Scherrer, Allison, and Faust, Phys. Rev. **96** (1954) 386
Sc 55 Schiffer, Phys. Rev. **97** (1954) 428
Sc 56 Schwarzschild, Rustad, and Wu, Phys. Rev. **103** (1956) 1796
Sc 56a Scott and Segel, Phys. Rev. **102** (1956) 1557
Sc 56b Schwartz, Corbett, and Watson, Phys. Rev. **101** (1956) 1370
Sc 56c Schiffer, Gossett, Philips, and Young, Phys. Rev. **103** (1956) 134
Sc 57 Schopper, Phil. Mag. **2** (1957) 710
Sc 58 Schmitt, Bull. Amer. Phys. Soc. **3** (1958) 37
Sc 58a Schiffer and Lee, Phys. Rev. **109** (1958) 2098
Sc 58b Schweizer, Phys. Rev. **110** (1958) 1414
Sc 59a Schrank and Warburton, Bull. Amer. Phys. Soc. **4** (1959) 220
Sc 59c Schweizer and Richardson, Bull. Amer. Phys. Soc. **4** (1959) 459, and private communication
Sc 61 Schmitt and Halperin, Phys. Rev. **121** (1961) 827
Sc 61a Scott, Nuclear Physics **27** (1961) 490
Sc 61b Schardt, Phys. Rev. **122** (1961) 1871
Sc 61c Schlenker, Thesis, Iowa State Univ. (1961)
Se 49 Seidlitz, Bleuler, and Tendam, Phys. Rev. **76** (1949) 861(L)
Se 53 Seed, Phil. Mag. **44** (1953) 921(L)
Se 54 Sehr, Z. Physik **137** (1954) 523
Se 55 Seiler, Cooper, and Harris, Phys. Rev. **99** (1955) 340(A)
Se 56 Selove, Phys. Rev. **101** (1956) 231
Se 56a Severiens and Hanna, Phys. Rev. **104** (1956) 1612
Se 58a Seidlitz, Bleuler, and Tendam, Phys. Rev. **110** (1958) 682
Se 58b Seliger, Mann, and Cavallo, J. Research Nat. Bur. Standards **60** (1958) 447
Se 59 Segel, Phys. Rev. **113** (1959) 844
Se 59a Seward, Phys. Rev. **11**[illegible] (1959) 514
Se 60 Seward, Koch, Shafer, and Fultz, Bull. Amer. Phys. Soc. **5** (1960) 68
Se 60a Seagondollar, Harris, and Rangan, Phys. Rev. **120** (1960) 251
Se 61 Sevcik (Univ. of Michigan, Ann Arbor), private communication (1961)
Sh 40 Sherr, Phys. Rev. **57** (1940) 937(L)
Sh 49 Shull and Feenberg, Phys. Rev. **75** (1949) 1768(L)
Sh 51 Shoemaker, Faulkner, Bouricius, Kaufmann and Moering, Phys. Rev. **83** (1951) 1011
Sh 51a Sher, Halpern, and Mann, Phys. Rev. **84** (1951) 387
Sh 51b Sheline, Phys. Rev. **82** (1951) 954(L)
Sh 51c Sheline, Holtzmark, and Fan, Phys. Rev. **83** (1951) 919
Sh 54 Shapiro, Phys. Rev. **93** (1954) 290
Sh 54b Sherr and Miller, Phys. Rev. **93** (1954) 1076
Sh 54c Sherr, Li, and Christy, Phys. Rev. **96** (1954) 1258
Sh 54d Sheline, Johnson, Bell, Davis, and McGowan, Phys. Rev. **94** (1954) 1642
Sh 56 Shaw, Conzett, Slobodrian, and Summers-Gill, Bull. Amer. Phys. Soc. **1** (1956) 253
Sh 56a Sheline, Nuclear Physics **2** (1956) 382
Sh 57b Shimanskaia, Zh. Eksp. Teor. Fiz. **31** (1956) 393; JETP **4** (1957) 355
Sh 58 Shafroth, Strait, and Levesque, Bull. Amer. Phys. Soc. **3** (1958) 37
Sh 58a Shute and Fisher, Phil. Mag. **3** (1958) 726
Sh 58c Sharp, Friedman, and Chase, Bull. Amer. Phys. Soc. **3** (1958) 419
Sh 59 Shook, Phys. Rev. **114** (1959) 310
Sh 59a Sharp, Chase, and Friedman, Bull. Amer. Phys. Soc. **4** (1959) 366
Sh 59b Shipley, Owen, and Madansky, Phys. Rev. **115** (1959) 122
Sh 59c Sheline, Nielsen, and Sperduto, Nuclear Physics **14** (1959) 140
Sh 60 Sheline and Wildermuth, Nuclear Physics **21** (1960) 196
Sh 61 Sharp, Chase, Warburton, and Friedman, Bull. Amer. Phys. Soc. **6** (1961) 46
Sh 61a Sheline and Harlan, Bull. Amer. Phys. Soc. **6** (1961) 249
Sh 61b Shoda, Kobayashi, Siina, Abe, and Kimura, J. Phys. Soc. Japan **16** (1961) 1031

Si 36 Sizoo and Koene, Physica **3** (1936) 1053
Si 46 Siegbahn, Phys. Rev. **70** (1946) 127
Si 47 Siegbahn, Arkiv Mat. Astron. Fysik **34B** (1947) No. 4
Si 47a Siegbahn and Johansson, Arkiv Mat. Astron. Fysik **34A** (1947) No. 10
Si 50 Siegbahn and Du Toit, Arkiv f. Fysik **2** (1950) 211(A)
Si 51 Sinclair and Holloway, Nature **167** (1951) 365(L)
Si 52 Siegbahn, Arkiv f. Fysik **4** (1952) 223
Si 54 Simanton, Rightmire, Long, and Kohman, Phys. Rev. **96** (1954) 1711(L)
Si 57 Sinclair, Phys. Rev. **107** (1957) 1306
Si 59 Singh, Davis, and Krone, Bull. Amer. Phys. Soc. **4** (1959) 17
Si 59a Simons, Nuclear Physics **10** (1959) 215
Si 59b Simons, Soc. Sci. Fennica Comm. Phys. Math. **23** (1959) No. 3
Si 59c Simons, Phys. Rev. **114** (1959) 569
Si 59d Singh, Phys. Rev. **115** (1959) 445
Si 59e Singh, Davis, and Krone, Phys. Rev. **115** (1959) 170
Si 59f Singh, Phys. Rev. **115** (1959) 1015
Si 59g Singh, Dosso, and Griffiths, Canadian J. Phys. **37** (1959) 1055 (L)
Si 61 Simms, Benczer-Koller, and Wu, Phys. Rev. **121** (1961) 1169
Sl 52 Slätis and Siegbahn, Arkiv f. Fysik **4** (1952) 485
Sl 59 Slaus and Alford, Phys. Rev. **114** (1959) 1054
Sm 42 Smith, Phys. Rev. **61** (1942) 578
Sm 51 Smith and Anderson, Nature **168** (1951) 429(L)
Sm 54 Smith, Cooper, and Harris, Phys. Rev. **94** (1954) 749(A), and verbal report to Nuclear Data Group
Sm 57 Smith and Breitenbecher, Bull Amer. Phys. Soc. **2** (1957) 59
Sm 58 Smith and Endt, Phys. Rev. **110** (1958) 397
Sm 58a Smith and Endt, Phys. Rev. **110** (1958) 1442
Sm 59 Smith, Proc. of the Paris Conf., p. 655 (Dunod, Paris, 1959)
Sm 60 Smith and Kuperus, Physica **26** (1960) 631(L)
Sm 60a Smulders, Smith, and Endt, Proc. of the Kingston Conf., p. 516 (Univ. of Toronto Press, 1960)
Sm 61 Smith and Steigert, Phys. Rev. **122** (1961) 1527
Sm 61a Smulders (Utrecht Univ.), private communication (1961)
Sm 61b Smith and Van Rinsvelt (Utrecht Univ.), private communication (1961)
Sm 61c Smith, "Charged particle cross sections", Los Alamos Report LA-2424 (1961)
Sn 55 Snell and Pleasonton, Phys. Rev. **100** (1955) 1396
So 50 Solomon, Phys. Rev. **79** (1950) 403(L)
So 58 Sorokin, Valter, Malakhov, and Taranov, Zh Eksp. Teor. Fiz. **35** (1958) 1386; JETP **8** (1959) 969
So 61 Sorokin, Popov, Storizhko, and Taranov, Zh. Eksp. Teor. Fiz. **40** (1961) 1253; JETP **13** (1961) 883
So 61a Sosnowski, Wilhelmi, and Wojtkowska, Nuclear Physics **26** (1961) 280
Sp 52 Sperduto and Buechner, Phys. Rev. **88** (1952) 574
Sp 55a Spicer, Phys. Rev. **100** (1955) 791
Sp 58 Sperduto and Buechner, Phys. Rev. **109** (1958) 462
Sp 60 Springer and Wiedemann, Z. Naturf. **15a** (1960) 828
Sp 60a Spivak and Mikaélyan, Zh. Eksp. Teor. Fiz. **39** (1960) 574; JETP **12** (1961) 404
Sp 61 Spivak, Mikaélyan, Kutikov, and Apalin, Nuclear Physics **23** (1961) 169
Sr 51 Sreb, Phys. Rev. **81** (1951) 469(L)
St 50 Steffen, Phys. Rev. **80** (1950) 115(L)
St 51 Strait, Van Patter, Buechner, and Sperduto, Phys. Rev. **81** (1951) 747
St 51a Stevenson and Deutsch, Phys. Rev. **83** (1951) 1202
St 51b Stevenson and Deutsch, Phys. Rev. **84** (1951) 1071(L)
St 52 Stoddart and Gove, Phys. Rev. **87** (1952) 262
St 52a Stelson and Preston, Phys. Rev. **86** (1952) 807(L)
St 53 Stähelin and Preiswerk, Nuovo Cimento **10** (1953) 1219

St 53a Stähelin, Phys. Rev. **92** (1953) 1076(L)
St 53b Stähelin, Helv. Phys. Acta **26** (1953) 691
St 54 Stelson and Preston, Phys. Rev. **95** (1954) 974
St 54a Stelson, Phys. Rev. **96** (1954) 1584
St 55 Starfelt and Svantesson, Phys. Rev. **97** (1955) 708
St 56 Stribel, Z. Naturf. **11a** (1956) 166(L)
St 56a Stribel, Z. Naturf. **11a** (1956) 254(L)
St 56b Stanford and Pieper, Phys. Rev. **103** (1956) 637
St 58a Steffen, Purdue University, Nuclear Physics Progress Report AECU–3696 (1958)
St 58b Strominger, Hollander, and Seaborg, Revs. Mod. Phys. **30** (1958) 585
St 59 Stuart, Anderson, Gardner, McClure, Nakada, and Wong, Bull. Amer. Phys. Soc. 4 (1959) 257
St 59a Steffen, Phys. Rev. Lett. **3** (1959) 277
St 59b Steffen, Phys. Rev. **115** (1959) 980
St 59c St. Pierre, Machwe, and Lorrain, Phys. Rev. **115** (1959) 999
St 59d Storey and McNeill, Canadian J. Phys. **37** (1959) 1072(L)
St 60 Stelson and McGowan, Bull. Amer. Phys. Soc. **5** (1960) 76
St 60a Storey, Jack, and Ward, Proc. Phys. Soc. **75** (1960) 526
St 61a Steffen, Phys. Rev. **123** (1961) 1787
St 61b Storey and Oleksiuk, Canadian J. Phys. **39** (1961) 917
Su 53 Summers-Gill, Haslam, and Katz, Canadian J. Phys. **31** (1953) 70
Su 55 Suttle and Libby, Anal. Chem. **27** (1955) 921
Su 58 Sun and Wright, Phys. Rev. **109** (1958) 109
Su 59 Suzor and Charpak, J. Phys. Rad. **20** (1959) 25
Su 59a Sukharevskii, Zh. Eksp. Teor. Fiz. **36** (1959) 1377; JETP **9** (1959) 981
Su 59b Sukharevskii, Zh. Eksp. Teor. Fiz. **36** (1959) 52; JETP **9** (1959) 37
Su 60 Sukharevskii, Zh. Eksp. Teor. Fiz. **38** (1960) 219; JETP **11** (1960) 159
Su 60b Sugiyama, Tohei, Sugawara, Dazai, and Kanda, J. Phys. Soc. Japan **15** (1960) 1909
Su 60c Suffert, Endt, and Hoogenboom, Physica **25** (1960) 659
Su 61 Subba Rao, Nuovo Cimento **20** (1961) 178
Sw 50 Swann, Mandeville, and Whitehead, Phys. Rev. **79** (1950) 598
Sw 52 Swann and Mandeville, Phys. Rev. **87** (1952) 215(A)
Sw 56 Swann and Porter, Bull. Amer. Phys. Soc. **1** (1956) 29
Sw 61 Swenson and Cindro, Phys. Rev. **123** (1961) 910
Sz 39 Szalay, Z. Physik **112** (1939) 29
Sz 60 Szilvasi, Geiger, and Dixon, J. Nuclear Energy **11A** (1960) 131

Ta 46 Tangen, Det Kgl. Norske Videnskabers Selskabs Skrifter (1946) No.1
Ta 53 Takemoto, Dazai, and Chiba, Phys. Rev. **91** (1953) 1024(L)
Ta 54 Tauber and Wu, Phys. Rev. **93** (1954) 295
Ta 54a Tauber and Wu, Phys. Rev. **94** (1954) 1307
Ta 54b Taylor, Russell, and Cooper, Phys. Rev. **93** (1954) 1056
Ta 57 Talmi, Phys. Rev. **107** (1957) 326(L)
Ta 57a Talmi, Phys. Rev. **107** (1957) 1601
Ta 58 Tai, Millburn, Kaplan, and Moyer, Phys. Rev. **109** (1958) 2086
Ta 59 Tanner, Phys. Rev. **114** (1959) 1060
Ta 60b Taylor, De S. Barros, Forsyth, Jaffe, and Ramavataram, Proc. Phys. Soc. **75** (1960) 772
Ta 60c Talbert and Stewart, Phys. Rev. **119** (1960) 272
Ta 60d Takeda, Kato, Hu, and Takahashi, Proc. of the Kingston Conf., p. 400 (Univ. of Toronto Press, 1960)
Ta 60e Takeda, J. Phys. Soc. Japan **15** (1960) 557
Ta 60f Tanaka, Furukawa, Mikumo, Iwata, Yagi, and Amano, J. Phys. Soc. Japan **15** (1960) 952
Ta 61 Takeetani and Alford, Bull. Amer. Phys. Soc. **6** (1961) 38
Ta 61a Taylor and Wood, Nuclear Physics **25** (1961) 642
Ta 61b Tanner, Thomas, and Earle, Proc. Rutherford Jubilee Conf., Manchester (1961)

Te 54 Temmer and Heydenburg, Phys. Rev. **96** (1954) 426
Te 54a Teener, Seagondollar, and Krone, Phys. Rev. **93** (1954) 1035
Te 56 Temmer and Heydenburg, Phys. Rev. **104** (1956) 989
Te 56b Teplov, Zh. Eksp. Teor. Fiz. **31** (1956) 25; JETP **4** (1957) 31
Te 57 Teplov, Iurev, and Markelova, Zh. Eksp. Teor. Fiz. **32** (1957) 156; JETP **5** (1957) 156
Te 57a Teplov and Iurev, Zh. Eksp. Teor. Fiz **33** (1957) 1313; JETP **6** (1958) 1011
Te 58 Temmer and Heydenburg, Phys. Rev. **111** (1958) 1303
Te 58a Teplov and Iurev, Zh. Eksp. Teor. Fiz. **34** (1958) 334; JETP **7** (1958) 233
Te 61 Tejera, Mazari, Jaidar, and Lopez, Revista Mexicana de Fisica **10** (1961) 229
Th 54 Thompson, Phys. Rev. **96** (1954) 369
Th 56 Thieberger and Talmi, Phys. Rev. **102** (1956) 923(L)
Th 57 Thieberger and De-Shalit, Nuclear Physics **4** (1957) 469
Th 57a Thiry, Bull. Soc. Roy. Sci. Liège **26** (1957) 29
Th 58 Thornton, Meads, and Collie, Phys. Rev. **109** (1958) 480
Th 58b Thomson, Cranberg, and Levin, Bull. Amer. Phys. Soc. **3** (1958) 365
Th 60 Thomas and Tanner, Proc. Phys. Soc. **75** (1960) 498
Th 60a Thankappan and Pandya, Nuclear Physics **19** (1960) 303
Ti 51 Ticho, Phys. Rev. **84** (1951) 847(L)
Ti 59 Tilley and Madansky, Phys. Rev. **116** (1959) 413
Ti 61 Tickle and Hecht, Bull. Amer. Phys. Soc. **6** (1961) 259, and private communication
To 51 Toms and Stephans, Phys. Rev. **82** (1951) 709
To 52 Toops, Sampson, and Steigert, Phys. Rev. **85** (1952) 280
To 53 Toppel and Bloom, Phys. Rev. **91** (1953) 473(A)
To 55a Toller, Newson, and Merzbacher, Phys. Rev. **99** (1955) 1625(A)
To 55b Tomnovec and Cook, Phys. Rev. **100** (1955) 1254(A)
To 55c Tobailem, J. Phys. Rad. **16** (1955) 48
To 57 Towle, Berenbaum, and Matthews, Proc. Phys. Soc. A **70** (1957) 84
To 58 Toms and McElhinney, Phys. Rev. **111** (1958) 561
To 59 Torki, Proc. of the Paris Conf., p. 557 (Dunod, Paris, 1959)
To 59a Tobocman, Phys. Rev. **115** (1959) 98
To 60 Tobin, Phys. Rev. **120** (1960) 175
To 60a Tohei, J. Phys. Soc. Japan **15** (1960) 372
Tr 56 Trumpy and Graue, Physica **22** (1956) 1155(A)
Tr 57 Trumpy, Nuclear Physics **2** (1957) 664
Ts 56 Tsytko and Antufev, Zh. Eksp. Teor. Fiz. **30** (1956) 1171; JETP **3** (1957) 993
Tu 51 Turner and Cavanagh, Phil. Mag. **42** (1951) 636
Tu 53 Turner, Australian J. Phys. **6** (1953) 380
Tu 54 Turkevich and Samuels, Phys. Rev. **94** (1954) 364
Tu 57 Tutakin, Tsytko, Lvov, Valter, and Gonchar, Atomnaya Energiya **3** (1957) 336; J. Nuclear Energy **8** (1958) 253
Ty 54 Tyrén and Tove, Phys. Rev. **96** (1954) 773
Ty 58 Tyrén and Maris, Nuclear Physics **6** (1958) 446

Ul 61 Uhlmann, Frauenfelder, Lipkin, and Rossi, Phys. Rev. **122** (1961) 536
Ur 59 Urbanec, Kopecký, and Kajfosz, Czechoslov. J. Phys. **9** (1959) 544

Va 52 Van Patter and Buechner, Phys. Rev. **87** (1952) 51
Va 52a Van Patter, Sperduto, Endt, Buechner, and Enge, Phys. Rev. **85** (1952) 142(L)
Va 52b Van Patter, Endt, Sperduto, and Buechner, Phys. Rev. **86** (1952) 502
Va 53 Van Loef (Univ. of Wisconsin, Madison), private communication (1953)
Va 56 Van Patter, Swann, Porter, and Mandeville, Phys. Rev. **103** (1956) 656
Va 56b Varma, Proc. Phys. Soc. A **69** (1956) 641(L)
Va 56d Van der Leun, Endt, Kluyver, and Vrenken, Physica **22** (1956) 1223
Va 56e Van Heerden and Prowse, Phil. Mag. **1** (1956) 967(L)
Va 57a Van Patter, Rothman, Porter, and Mandeville, Phys. Rev. **107** (1957) 171
Va 57b Van Lieshout and Hayward (I.K.O., Amsterdam), private communication (1957)

Va 57d Van Patter, Porter, and Rothman, Phys. Rev. **106** (1957) 1016
Va 58 Varma and Jack, Proc. Phys. Soc. **71** (1958) 100
Va 58a Van der Leun and Endt, Phys. Rev. **110** (1958) 96
Va 58d Van der Leun, Thesis, Univ. of Utrecht (1958)
Va 58e Van der Leun and Endt, Physica **24** (1958) 1095
Va 58f Vasilev and Shavtvalov, Izvest. Akad. Nauk, Ser. Fiz. **22** (1958) 788
Va 58g Valter, Malakhov, Sorokin, and Taranov, Izvest. Akad. Nauk, Ser. Fiz. **22** (1958) 871
Va 59 Vashakidze, Kopaleishvili, and Chilashvili, Zh. Eksp. Teor. Fiz. **37** (1959) 750; JETP **10** (1960) 535
Va 59a Valter, Goncharov, Lvov, and Tsytko, Izvest. Akad. Nauk, Ser. Fiz. **23** (1959) 835
Va 59b Valter, Malakhov, Sorokin, and Taranov, Izvest. Akad. Nauk, Ser. Fiz. **23** (1959) 846
Va 60 Van Oostrum, Thesis, Delft (1960)
Va 60a Vanhuyse and Vanpraet, J. Phys. Rad. **21** (1960) 290
Va 60c Vaughn, Imhof, Johnson, and Walt, Phys. Rev. **118** (1960) 683
Va 60d Valter, Deineko, Sorokin, and Taranov, Izvest. Akad. Nauk, Ser. Fiz. **24** (1960) 884
Va 60e Valter, Antufev, Gonchar, Lvov, Kopanets, and Tsytko, Izvest. Akad. Nauk, Ser. Fiz. **24** (1960) 891
Va 60f Vasilev and Shavtvalov, Zh. Eksp. Teor. Fiz. **39** (1960) 1221; JETP **12** (1961) 851
Va 61 Van Oostrum, Hazewindus, Wapstra, Olness, and Parker, Nuclear Physics **25** (1961) 409
Va 61a Vasilev, Romanovskii, and Timushev, Zh. Eksp. Teor. Fiz. **40** (1961) 972(L); JETP **13** (1961) 678(L)
Va 61c Valerio, Thesis, Iowa State Univ. (1961)
Va 61d Valter, Tsytko, Antufev, Kopanets, and Lvov, Izvest. Akad. Nauk, Ser. Fiz. **25** (1961) 854
Ve 56 Vegors and Axel, Phys. Rev. **101** (1956) 1067
Ve 56a Vegors and Duffield, Bull. Amer. Phys. Soc. **1** (1956) 206
Ve 57 Verbinski, Hurlimann, Stephens, and Winhold, Phys. Rev. **108** (1957) 779
Ve 59 Vervier, Nuclear Physics **9** (1959) 569
Ve 60a Velyukhov, Prokofev, and Starodubtsev, Zh. Eksp. Teor. Fiz. **39** (1960) 563; JETP **12** (1961) 395
Ve 61 Vervier, Nuclear Physics **26** (1961) 10
Vl 59 Vlasov, Kalinin, Ogloblin, and Chuev, Zh. Eksp. Teor. Fiz. **37** (1959) 1187; JETP **10** (1960) 844
Vl 60 Vlasov, Kalinin, Ogloblin, and Chuev, Zh. Eksp. Teor. Fiz. **39** (1960) 1468(L); JETP **12** (1961) 1020(L)
Vl 61 Vlasov, Kalinin, Ogloblin, and Chuev, Izvest. Akad. Nauk, Ser. Fiz. **25** (1961) 115
Vo 57a Von Herrmann and Pieper, Phys. Rev. **105** (1957) 1556
Vo 58 Vogelsang and McGruer, Phys. Rev. **109** (1958) 1663
Vo 59 Voshage and Hintenberger, Z. Naturf. **14a** (1959) 194 (L)
Vo 59a Vorona, Olness, Haeberli, and Lewis, Phys. Rev. **116** (1959) 1563
Vo 60 Vogt and McManus, Phys. Rev. Lett. **4** (1960) 518

Wa 37 Walke, Phys. Rev. **52** (1937) 663(L)
Wa 39 Watase and Itoh, Proc. Phys. Math. Soc. Japan **21** (1939) 626
Wa 41 Watase, Proc. Phys. Math. Soc. Japan **23** (1941) 618
Wa 48 Wäffler and Hirzel, Helv. Phys. Acta **21** (1948) 200
Wa 50 Warshaw, Chen, and Appleton, Phys. Rev. **80** (1950) 288(L)
Wa 52 Wapstra, Phys. Rev. **86** (1952) 561(L), and Arkiv f. Fysik **6** (1953) 263
Wa 53 Wapstra and Veenendaal, Phys. Rev. **91** (1953) 426(L)
Wa 54 Wall, Phys. Rev. **96** (1954) 664
Wa 56 Wäffler and Heinrich, Physica **22** (1956) 1146(A)
Wa 56a Watters, Phys. Rev. **103** (1956) 1763
Wa 57 Waldorf and Wall, Phys. Rev. **107** (1957) 1602
Wa 57a Wade, Conzett, and Gonzalez-Vidal, Bull. Amer. Phys. Soc. **2** (1957) 386
Wa 59 Warner and Alford, Phys. Rev. **114** (1959) 1338
Wa 59a Wagner and Heitzmann, Z. Naturf. **14a** (1959) 784

Wa 60 Wagner and Heitzmann, Z. Naturf. **15a** (1960) 74

Wa 60a Wallace and Welch, Phys. Rev. **117** (1960) 1297

Wa 60b Wakatsuki, Hirao, Okada, and Miura, Progr. in Theor. Phys. **24** (1960) 918

Wa 60c Wakatsuki, Hirao, Okada, Miura, Sugimoto, and Mizobuchi, J. Phys. Soc. Japan **15** (1960) 1141

Wa 60d Wakatsuki, Hirao, Okada, and Miura, Proc. of the Kingston Conf., p. 971 (Univ. of Toronto Press, 1960)

We 44 Weimer, Kurbatov, and Pool, Phys. Rev. **66** (1944) 209

We 51 Wennerblom, Zimen, and Ehn, Svensk. Kem. Tid. **63** (1951) 207

We 52 Westermark, Phys. Rev. **88** (1952) 573

We 54 Weinzierl, Z. Naturf. **9a** (1954) 69

We 56 Wetherill, Wasserburg, Aldrich, Tilton, and Hayden, Phys. Rev. **103** (1956) 987

We 56a Weddell, Phys. Rev. **104** (1956) 1069

We 57 Wetherill, Science **126** (1957) 545

Wh 39 White, Delsasso, Fox, and Creutz, Phys. Rev. **56** (1939) 512

Wh 41 White, Creutz, Delsasso, and Wilson, Phys. Rev. **59** (1941) 63

Wh 60 White and Buechner, Phys. Rev. **118** (1960) 1331

Wh 60a White, Phys. Rev. **119** (1960) 767

Wi 41 Wilkins, Phys. Rev. **60** (1941) 365

Wi 41a Witcher, Phys. Rev. **60** (1941) 32

Wi 49 Wilson and Bishop, Proc. Phys. Soc. A **62** (1949) 457(L)

Wi 51 Wilkinson and Carver, Phys. Rev. **83** (1951) 466(L)

Wi 56 Willard, Bair, Cohn, and Kingston, Bull. Amer. Phys. Soc. **1** (1956) 264

Wi 56a Wilkinson, Phil. Mag. **1** (1956) 1031

Wi 57 Williamson and Burton, Bull. Amer. Phys. Soc. **2** (1957) 182

Wi 57a Winterberg, Z. Naturf. **12a** (1957) 271

Wi 58 Williamson, Hudspeth, Morgan, and Moore, Phys. Rev. **110** (1958) 139

Wi 60 Williamson, Katman, and Burton, Phys. Rev. **117** (1960) 1325

Wi 61 Wilenzick, Mitchell, Seth, and Lewis, Phys. Rev. **121** (1961) 1150

Wo 50 Worth, Phys. Rev. **78** (1950) 378

Wo 54 Wong, Phys. Rev. **95** (1954) 761

Wo 54a Wolfsberg, Phys. Rev. **96** (1954) 1712(L)

Wo 56 Wolf, Phil. Mag. **1** (1956) 102(L)

Wo 60 Wolf, Nukleonik **2** (1960) 255

Wr 53 Wright, Phys. Rev. **90** (1953) 159(L)

Wr 57 Wright, Wyatt, Reynolds, Lyon, and Handley, Nuclear Sci. and Eng. **2** (1957) 427

Wu 49 Wu, Townes, and Feldman, Phys. Rev. **76** (1949) 692(L)

Wu 50 Wu, Revs. Mod. Phys. **22** (1950) 386

Ya 51 Yaffe and Brown, Phys. Rev. **82** (1951) 332(A)

Ya 58 Yamabe, J. Phys. Soc. Japan **13** (1958) 237

Ya 58a Yamabe, Yamazaki, and Toi, J. Phys. Soc. Japan **13** (1958) 777

Ya 59 Yavin and Farwell, Nuclear Physics **12** (1959) 1

Ya 60 Yamamoto and Steigert, Phys. Rev. **117** (1960) 535

Ya 60a Yamabe, Kondo, Kato, Yamazaki, and Ruan, J. Phys. Soc. Japan **15** (1960) 2154

Ya 60b Yamaguchi, Nonaka, Mikumo, Hitaka, Umeda, and Tabata (Tokyo Univ.), as quoted in Nuclear Sci. Abstr. **15** (1961) 1545

Ya 61 Yamamoto and Steigert, Phys. Rev **121** (1961) 600

Ye 56 Yergin, Phys. Rev. **104** (1956) 1340

Yn 60 Yntema, Zeidman, and Raz, Phys. Rev. **117** (1960) 801

Yo 60 Yoshiki, Phys. Rev. **117** (1960) 773

Yu 59 Yuasa, Proc. of the Paris Conf., p. 571 (Dunod, Paris, 1959)

Za 59 Zatzick and Eubank, Bull. Amer. Phys. Soc. **4** (1959) 141

Za 59a Zaika and Nemets, Izvest. Akad. Nauk, Ser. Fiz. **23** (1959) 1460

Za 60 Zaika, Nemets, and Prokopenko, Zh. Eksp. Teor. Fiz. **38** (1960) 287(L); JETP **11** (1960) 208; Izvest. Akad. Nauk, Ser. Fiz. **24** (1960) 872
Za 61 Zatzick and Maxson, Bull. Amer. Phys. Soc. **6** (1961) 237
Ze 52 Zeldes, Ketelle, Brosi, Fultz, and Hibbs, Phys. Rev. **86** (1952) 811(L)
Zi 60 Ziegler, Nuclear Physics **17** (1960) 238
Zi 61 Zimmerman and Moe, Bull. Amer. Phys. Soc. **6** (1961) 47
Zu 50 Zucker and Watson, Phys. Rev. **80** (1950) 966